



**HAL**  
open science

## Enantioselective Radical Reactions Using Chiral Catalysts

Shovan Mondal, Frédéric Dumur, Didier Gimes, Mukund Sibi, Michèle Bertrand, Malek Nechab

► **To cite this version:**

Shovan Mondal, Frédéric Dumur, Didier Gimes, Mukund Sibi, Michèle Bertrand, et al.. Enantioselective Radical Reactions Using Chiral Catalysts. *Chemical Reviews*, 2022, 122 (6), pp.5842-5976. 10.1021/acs.chemrev.1c00582 . hal-03639964

**HAL Id: hal-03639964**

**<https://hal.science/hal-03639964v1>**

Submitted on 13 Apr 2022

**HAL** is a multi-disciplinary open access archive for the deposit and dissemination of scientific research documents, whether they are published or not. The documents may come from teaching and research institutions in France or abroad, or from public or private research centers.

L'archive ouverte pluridisciplinaire **HAL**, est destinée au dépôt et à la diffusion de documents scientifiques de niveau recherche, publiés ou non, émanant des établissements d'enseignement et de recherche français ou étrangers, des laboratoires publics ou privés.

SHOVAN MONDAL,<sup>A</sup> FRÉDÉRIC DUMUR,<sup>B</sup> DIDIER GIGMES,<sup>B</sup> MUKUND SIBI,<sup>\*C</sup> MICHÈLE P. BERTRAND <sup>\*B</sup> AND MALEK NECHAB<sup>\*B</sup>

## Enantioselective Radical Reactions Using Chiral Catalysts

(a) Department of Chemistry, Syamsundar College, Shyamsundar 713424, West Bengal, India

(b) Aix Marseille Univ, CNRS, Institut de Chimie Radicalaire UMR 7273, F-13390 Marseille, France

(c) North Dakota State University, Fargo, ND 58108, USA

\* Corresponding authors

[mukund.sibi@ndsu.edu](mailto:mukund.sibi@ndsu.edu)

[michele.bertrand@univ-amu.fr](mailto:michele.bertrand@univ-amu.fr)

[malek.nechab@univ-amu.fr](mailto:malek.nechab@univ-amu.fr)

<b>1. INTRODUCTION</b> .....	<b>3</b>
<b>2. ORGANOCATALYZED ENANTIOSELECTIVE RADICAL REACTIONS</b> .....	<b>8</b>
<b>2.1. COVALENT-BASED MODE OF ACTIVATION</b> .....	<b>8</b>
2.1.1. <i>Aminocatalysis</i> .....	8
2.1.1.1 <i>Iminium/enamine catalysis involving stoichiometric oxidant</i> .....	11
2.1.1.2 <i>Merging aminocatalysis and metallaphotoredox catalysis</i> .....	21
2.1.1.3 <i>Metal free enantioselective photosensitized aminocatalysis</i> .....	30
2.1.2. <i>NHC-catalyzed coupling reactions using single electron transfer</i> .....	50
2.1.3 <i>Asymmetric catalysis involving chiral thiyl and stannyl radicals</i> .....	57
<b>2.2. NON-COVALENT-BASED MODE OF ACTIVATION</b> .....	<b>60</b>
2.2.1. <i>Hydrogen-bonding mediated organocatalyzed radical reactions</i> .....	60
2.2.2. <i>Merging Photoredox and chiral Brønsted acids</i> .....	81
2.2.2 <i>Lewis Acid Catalyzed Reactions</i> .....	90
2.2.3. <i>Ion-pairing assisted radical transformations</i> .....	95
<b>3. ASYMMETRIC RADICAL PROCESSES WITH CHIRAL TRANSITION METAL-CATALYZED</b> .....	<b>98</b>
<b>3.1 TITANOCENE AND CHROMIUM-CATALYZED ENANTIOSELECTIVE RADICAL REACTIONS</b> .....	<b>99</b>
3.1.1 <i>Titanocene asymmetric radical chemistry</i> .....	99
3.1.2 <i>Chromium-mediated enantioselective radical polar cross over reactions</i> .....	114
<b>3.2. IRON AND MANGANESE-CATALYZED ENANTIOSELECTIVE REACTIONS</b> .....	<b>119</b>
3.2.1. <i>Enantioselective homocoupling of 2-naphthols</i> .....	119

3.2.2. <i>Kumada and Suzuki-Miyaura enantioselective couplings</i> .....	121
3.2.3. <i>Iron and Manganese Bio-inspired Enantioselective Hydroxylation and Oxidation</i> .....	124
<b>3.3. ASYMMETRIC COBALT-CATALYZED RADICAL REACTIONS</b> .....	<b>134</b>
3.3.1 <i>Cobalt metalloradical catalysis</i> .....	134
3.3.1.1 <i>Cyclopropanation reactions</i> .....	134
3.3.1.2 <i>Aziridination reactions</i> .....	141
3.3.1.3. <i>Aminations via C–H activation</i> .....	143
3.3.1.4. <i>Intramolecular C–H alkylation</i> .....	148
3.3.2 <i>Cobalt-Catalyzed Miscellaneous Reactions</i> .....	150
<b>3.4. NICKEL CATALYZED RADICAL REACTION</b> .....	<b>153</b>
3.4.1 <i>Ni-Catalyzed enantioconvergent coupling of organic halides with stoichiometric organometallic nucleophiles</i> .....	153
3.4.2 <i>Reductive cross-coupling in the presence of stoichiometric reductant (Mn(0), Zn(0), TDAE) ....</i>	158
3.4.3 <i>Processes involving photocatalytic generation of alkyl radicals, where chirality is controlled by chiral Ni-complexes templating effects</i> .....	160
3.4.4 <i>Dual Ni/Metallaphotoredox catalysis</i> .....	163
3.4.5 <i>Dual photocatalytic reactions involving organic photocatalysts</i> .....	167
<b>3.5. ENANTIOSELECTIVE COPPER-CATALYZED RADICAL REACTIONS</b> .....	<b>171</b>
3.5.1 <i>Chiral Lewis acidic Cu(II) complexes-mediated radical reactions</i> .....	173
3.5.2 <i>Cu-mediated enantioselective functionalization of alkyl radicals</i> .....	175
3.5.3 <i>Enantioselective functionalization of radicals necessitating dual Cu/photocatalysis</i> .....	181
3.5.4 <i>Enantioselective Copper-catalyzed radical functionalization after intercalation of radical addition, ring-opening or 1,5-HAT rearrangement</i> .....	185
3.5.5 <i>Synthesis of heterocyclic compounds through polar/radical cyclization</i> .....	209
<b>3.6. PHOTOREDOX REACTIONS USING CHIRAL LEWIS ACIDS</b> .....	<b>217</b>
3.6.1 <i>Merging Photoredox Catalysts with Rare Earth Elements</i> .....	217
3.6.2 <i>Photoredox reactions using chiral-at-metal complexes as Lewis acid catalyst</i> .....	221
<b>4. ENZYME-CATALYZED RADICAL REACTIONS</b> .....	<b>237</b>
<b>5. CONCLUSION AND OUTLOOK</b> .....	<b>249</b>

## 1. Introduction

Radicals are highly reactive intermediates, although their existence was suspected before the beginning of twentieth century, they have long been considered as intriguing and uncontrollable species. The decisive turn in the development of radical chemistry started in the 1950s when physical chemists became interested in measuring rate constants of radical reactions in solution with the concomitant emergence of electron spin resonance (ESR) technology that enabled the detection and the direct observation of these elusive species.

A brief discussion of radical stability is appropriate for the theme of this review: enantioselective catalyzed radical reactions. In broad terms, radical stability is of two types: thermodynamic or kinetic stability. Thermochemical data, i.e., bond dissociation energies (BDEs) are generally used to define the “relative thermodynamic stability” of different carbon-centered radicals.<sup>1</sup> Scales of Relative Stabilization Energy (RSE) have been determined from BDE measurements or theoretical calculations. Electronic effects and hyperconjugation of substituents influence thermodynamic stability mainly by their ability to delocalize the unpaired electron. RSE scales have similarly been established in the same way for heteroatom-centered radicals.<sup>2,3</sup>

Radical stability can also refer to its kinetic stability. The relative stability is then defined by monitoring the rate of disappearance of radicals. In this approach, the stability of a radical is related to its half-lifetime, that is determined by measuring the rate of its decay by spectroscopic techniques (ESR, or ultrafast time-resolved UV or visible absorptions).

The problem of the misleading use of “stability” terminology was addressed by Ingold and Griller.<sup>4</sup> These authors proposed a new classification of radicals calling them: “stabilized”, “transient/persistent”, or “stable”. Accordingly, long lived radicals were defined as “persistent”, in contrast to short lived ones called “transient” (typical lifetime less than one millisecond). Most electronically stabilized radicals are in fact transient species. However, the number of

recorded persistent or even air stable radicals has increased exponentially due to their outstanding applications.<sup>5,6</sup> They include both carbon-centered and heteroatom radicals.

The understanding of radical mechanisms and data banks of rate constants allowed radicals to be domesticated so that radical reactions became easy to plan. Radicals considered often react with extremely high rates, typically at diffusion-controlled rates. Despite the high reactivity of radical species, stereochemical concepts are still valid in radical transformations. Early work established near perfect control of chemoselectivity in radical reactions. A better understanding of stereocontrol and parameters governing the approach of a radical to an acceptor enabled the development of incredibly sophisticated radical processes and chemists conquered issues related to diastereoselectivity<sup>7</sup> and eventually the “holy grail” of enantioselectivity. Early work on diastereoselective radical reactions relied on chiral auxiliaries covalently linked either to the radical or to the radical acceptor to control the preferential geometry of irreversible reactions lowest energy diastereomeric transition state. A new level was reached by introducing conformational control by complexation with a Lewis acid. The seminal research on chiral auxiliaries in polar chemistry inspired Porter, Sibi and others in transposing the concept to radical chemistry which eventually led to the discovery of chiral Lewis acid mediated highly enantioselective radical reactions. A variety of enantioselective radical reactions were reported from 1995-2007 mostly using chiral Lewis acid catalysis.

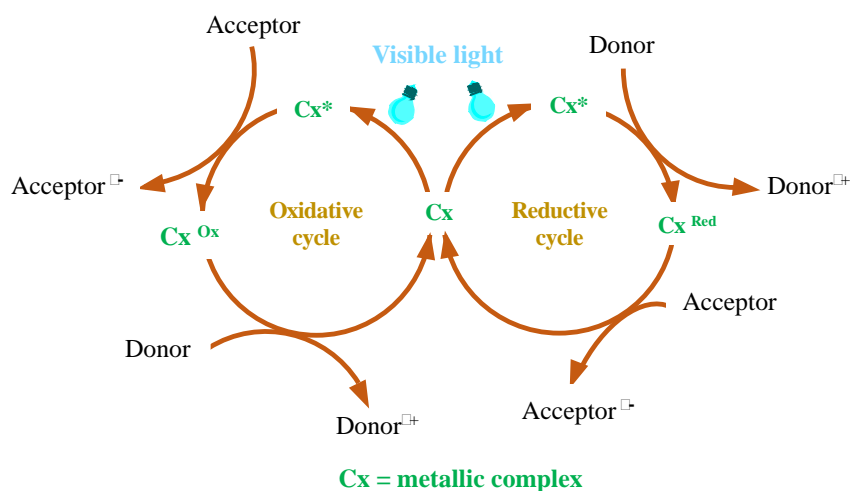
Although chiral Lewis Acid mediated radical reactions were groundbreaking, they have several drawbacks: (1) high catalyst loadings, (2) the need for a large excess of radical precursor, (3) potential toxicity of the Lewis acid, (4) large amounts of the radical initiator, (5) use of tin hydride as the H-atom source and its related toxicity, and (6) most of the enantioselective radical reactions are with a chiral acceptor and a radical donor.

The 21<sup>st</sup> century has seen an unprecedented and spectacular advance in the development of enantioselective radical reactions. Important innovations in the use of different chiral

organocatalysts such as amine catalysts, hydrogen-bonding catalysts, and Bronsted acids has been the major contributor in the development of enantioselective radical reactions. In many of these transformations, the limitations noted above for chiral Lewis acid mediated reactions have been overcome to a certain extent. Additionally, numerous elegant transformations have emerged with the renewed use of photochemistry, enabling visible light induced electron transfer, making use of organo-photocatalysts<sup>8,9,10</sup> and transition metal-photocatalysts<sup>11</sup> that provide access to radical intermediates under mild sustainable experimental conditions. There is currently no clear-cut frontier between organometallic and radical chemistry. The coordination chemistry of radicals is manifold in view of the number of events that can happen when a radical reacts with a metal complex.<sup>12</sup> The two domains have established so strong and complex interplays, that numerous advances in one field have necessarily an impact on the other. This is especially true of course for the top level reached by asymmetric transition metal catalysis. However, due to their sticky reputation of being highly reactive species difficult to control, enantioselective radical reactions have long remained a challenging field.

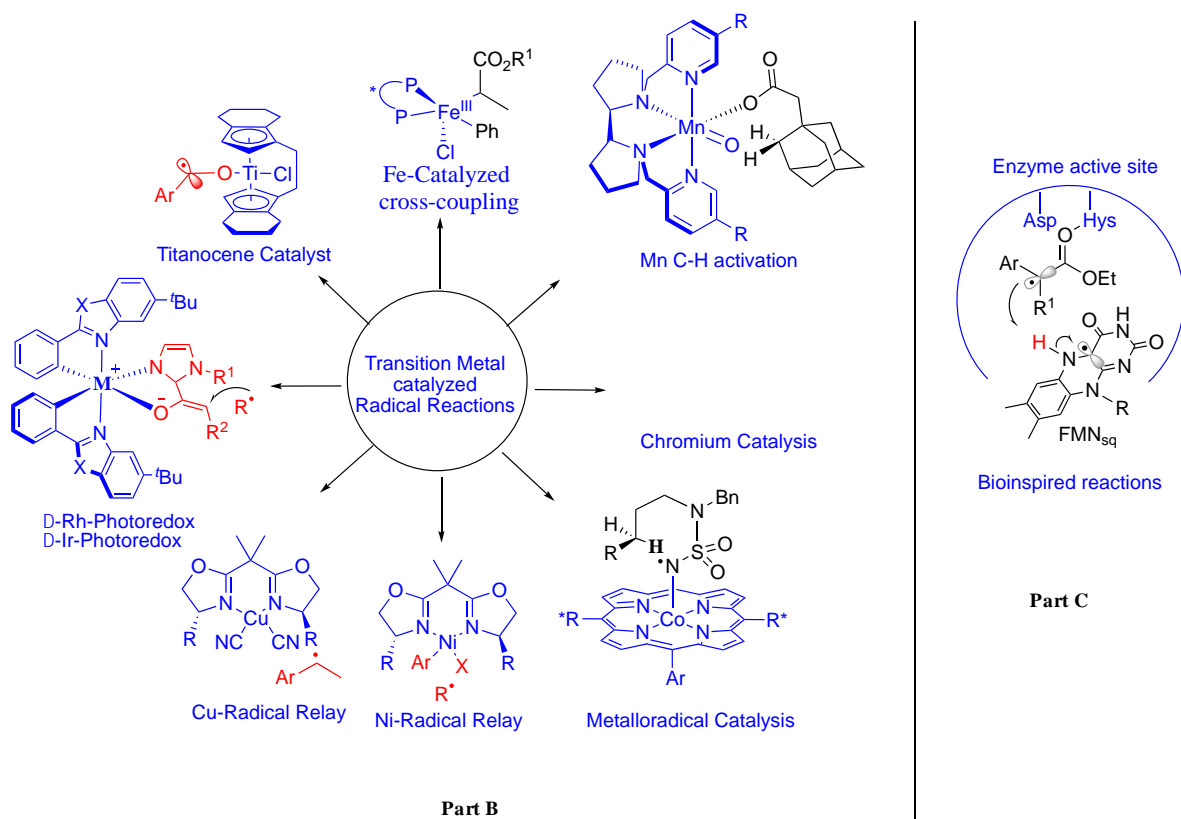
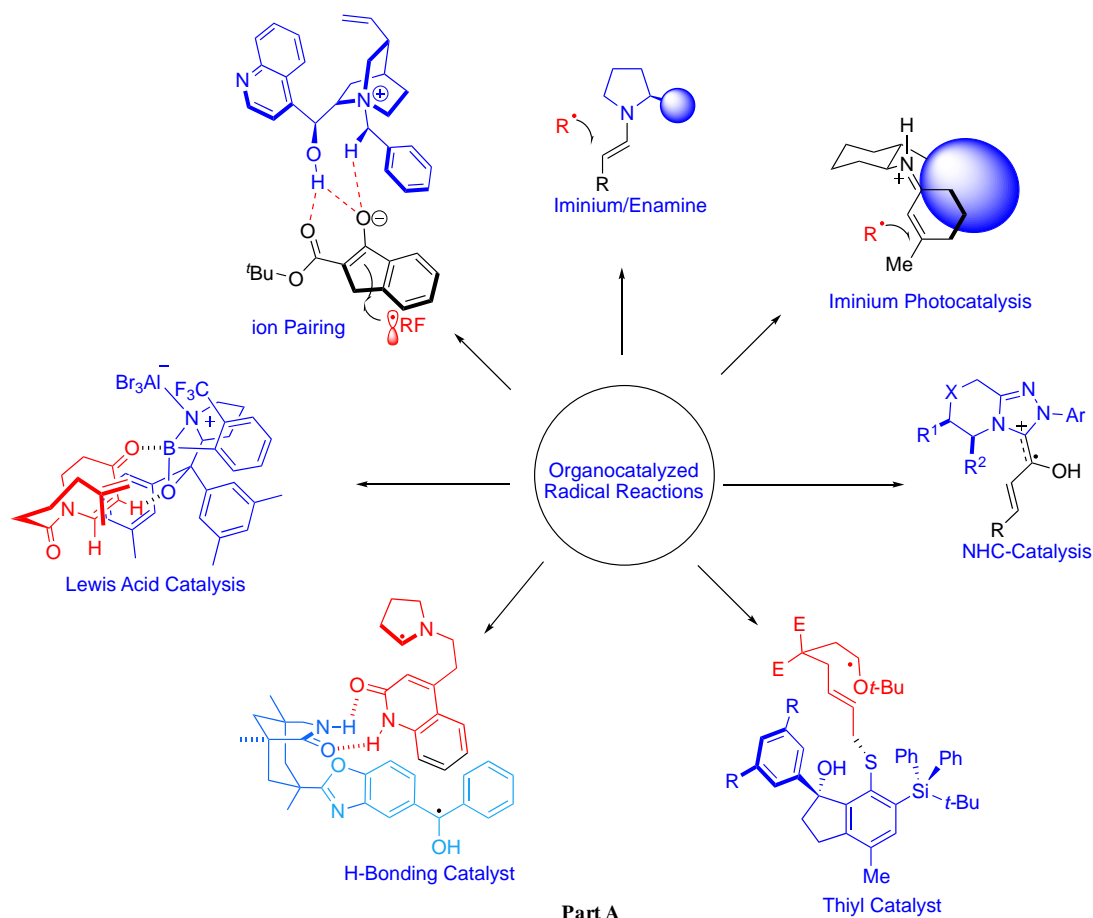
The use of visible light to bring a metal from its ground state to an excited state has been recognized as a new opportunity to generate highly reactive radical species. Excellent tutorial and critical reviews covering the literature from the past two decades have been published. In this SET process, the photoredox metal catalyst could be considered as a radical initiator where the photoexcited metal engages oxidation or reduction of an appropriate substrate. Under suitable photoredox conditions, net oxidative, net reductive or redox-neutral process can be considered (Figure 1). The main advantages of photoredox catalysis are the use of extremely mild conditions, absence of stoichiometric oxidant, and a high tolerance for functional groups.

**Figure 1 Photoredox Mediated Radical Generation**



This review describes the most recent progresses in enantioselective radical reactions resulting from the encounter of reactive radical species with chiral organocatalysts (across covalent or non-covalent interactions) and chiral transition metal-catalysts, putting forward, whenever they get involved, the role of photoexcited states. Figure 2 details the major types of activation involved in the enantioselective radical reactions. In the first section, radical reactions catalyzed by different chiral organocatalysts are discussed (part A, Figure 2). This section also includes the combination of chiral organocatalyst with photoredox radical generation using achiral photocatalyst. The second part of this review aims at detailing how commonplace the transition metal-catalyzed enantioselective reactions proceeding via radical relay have become (part B, Figure 2). Progress due to additional merging of visible light photocatalysis, using chiral-at-metal catalysts, are also covered. The atomic number of the metal has been selected to structure this section. In the third section (part C, Figure 2), we discuss bio-inspired enantioselective radical reactions using enzyme catalysis. The review covers literature till January 2021.

**Figure 2 Different Modes of Activation for Asymmetric Radical Transformations**





## **2. Organocatalyzed enantioselective radical reactions**

Asymmetric organocatalysis, which involves the use of a chiral organic molecule as a catalyst in the absence of any metal (or at least not part of the catalytic cycle), was popularized towards the end of the last century.<sup>13,14</sup> This area of research has blossomed in the beginning of 21<sup>st</sup> century and allowed for the development of a plethora of applications, representing nowadays one of the most employed mode of activation in organic synthesis.

Covalent (as well as non-covalent interactions) are ubiquitous in nature where their involvement in biological mechanisms has been demonstrated. By imitating nature, organic chemists have transposed the concept to provide high stereocontrol in many organic transformations so that this field became an independent area of research. Different types of covalent organocatalysts which include pyrrolidines,<sup>15</sup> imidazolidinones, Cinchona-based catalysts, carbenes have been successfully used. This mode of activation forms an intermediate in which the substrate and catalyst bond covalently together giving a chiral transition state.

In the non-covalent interactions, the catalyst-substrate cooperation can originate from hydrogen-bonding (Brønsted acids, Lewis acids, amide catalysts, thioureas) or electrostatic interactions (phase transfer catalysis, ion pairing catalysts) delivering a weak temporary bond in the organized chiral transition state which ensures a high degree of enantiocontrol.<sup>16</sup>

### **2.1. Covalent-based mode of activation**

#### **2.1.1. Aminocatalysis**

The synergetic intersection between radicals and organocatalysts has led to prolific applications that have been developed because chemists pushed their imagination beyond limits. Inspired by aminocatalytic activation in enzymatic catalysis, chemists exploited the benefit of aminocatalysis to meet the great demand for enantiopure chiral compounds. Aminocatalysis - a subclass of organocatalysis - using chiral secondary amines involves a covalent bond formation with the substrate -a carbonyl derivative- resulting in a chiral iminium intermediate

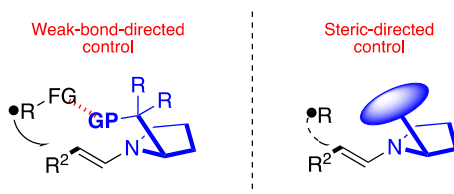
which is in equilibrium with the enamine form (Indeed, *in situ* formed radical can add (intra- or intermolecularly) to an alkene to generate new radical  $\alpha$  to the amine (path (a), Scheme 1A). This step is exothermic because a single bond is formed at the expense of a double bond. Moreover, the formation of a nucleophilic (electron rich) radical stabilized by resonance effect is a favorable step, particularly when R3 is an electron withdrawing group (i.e., electrophilic radical) which allows a polarity-matched radical addition. After an oxidation step followed by hydrolysis of the resulting iminium, the catalyst will be released.

Single Electron Transfer (SET) from the electron rich enamine **2.1.2** to an oxidant (typically a transition metal) could also take place and generate an iminium radical (**Scheme 1, path b**).

**The mesomeric** enamine radical cation then engages in classical radical reactions (addition-path (c), radical-radical coupling-path (d), addition/ $\beta$ -fragmentation, Hydrogen Atom Transfer (HAT), cyclization...). In all these steps, the stereocontrol is governed by the steric/electronic or weak-bond interactions with the covalently installed amine catalyst.

Scheme 1A).<sup>17</sup> The critical aspect for enantiocontrol resides in the facial approach of the reactant through C-C or C-heteroatom bond formation releasing an enantio-enriched product and the catalyst. These fundamentals valuable for polar reactions still apply radical reactions. Stereoelectronic interactions through weak-bond-directed control or steric bias induce  $\pi$ -facial discrimination of the approaching radical, Figure 3 shows the two scenarios.

**Figure 3 weak-bond or steric-directed control in radical addition to enamine**

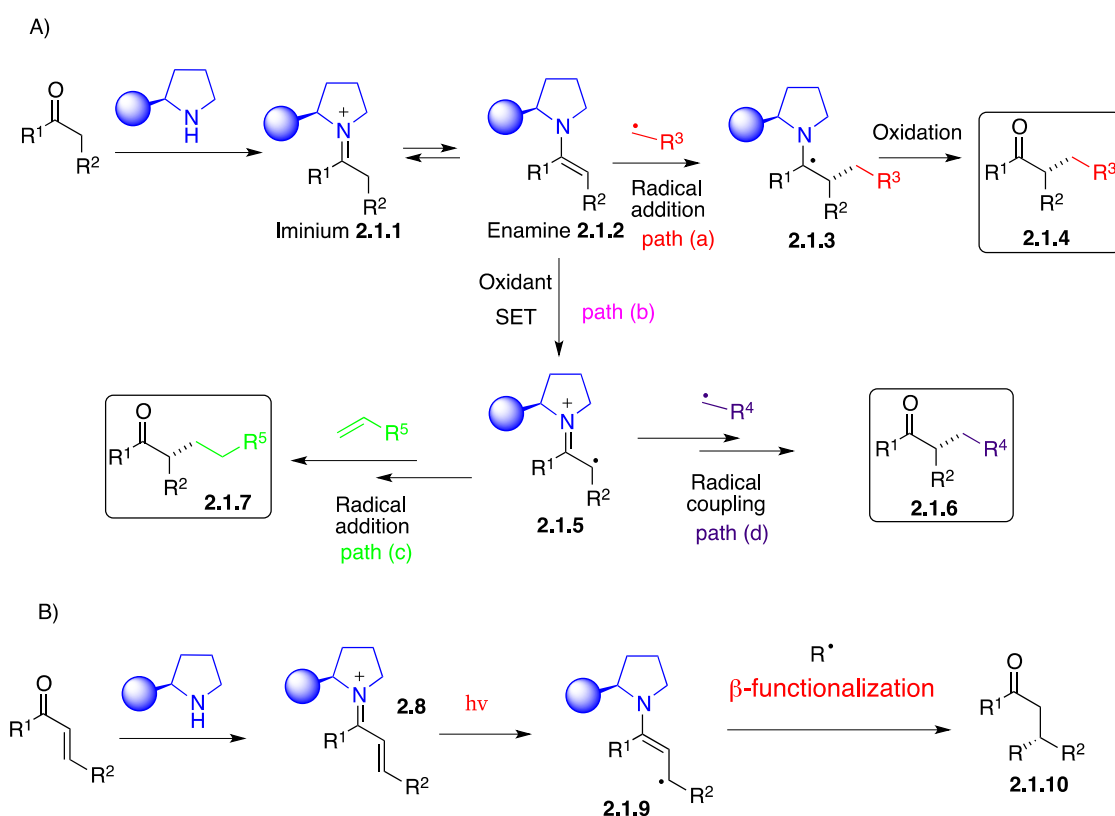


Indeed, *in situ* formed radical can add (intra- or intermolecularly) to an alkene to generate new radical  $\alpha$  to the amine (path (a), Scheme 1A). This step is exothermic because a single bond is formed at the expense of a double bond. Moreover, the formation of a nucleophilic (electron

rich) radical stabilized by resonance effect is a favorable step, particularly when  $R^3$  is an electron withdrawing group (i.e., electrophilic radical) which allows a polarity-matched radical addition. After an oxidation step followed by hydrolysis of the resulting iminium, the catalyst will be released.

Single Electron Transfer (SET) from the electron rich enamine **2.1.2** to an oxidant (typically a transition metal) could also take place and generate an iminium radical (Scheme 1, path b). The mesomeric enamine radical cation then engages in classical radical reactions (addition-path (c), radical-radical coupling-path (d), addition/ $\beta$ -fragmentation, Hydrogen Atom Transfer (HAT), cyclization...). In all these steps, the stereocontrol is governed by the steric/electronic or weak-bond interactions with the covalently installed amine catalyst.

### Scheme 1 Basic Principles of Aminocatalysis



$\alpha,\beta$ -Unsaturated carbonyl compounds are also good candidates for aminocatalysis since they offer the possibility for  $\beta$ -functionalization upon photoactivation (Scheme 1B).

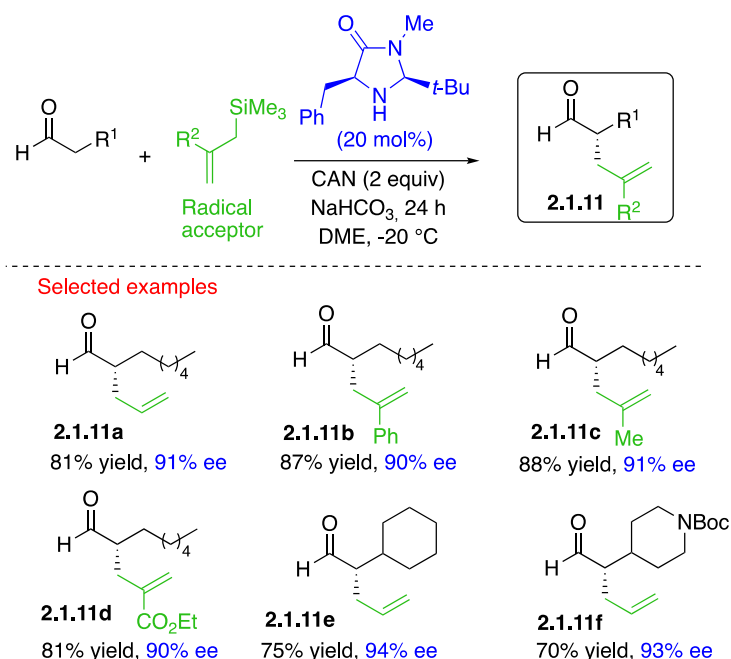
The terminology of Singly Occupied Molecular Orbital (SOMO) activation was introduced by MacMillan in 2007.<sup>18</sup> This strategy has linked the radical chemistry to organocatalysis and opened a range of enantioselective catalytic transformations.<sup>19,20</sup>

### 2.1.1.1 Iminium/enamine catalysis involving stoichiometric oxidant

As already mentioned, the formation of iminium radical through a SET activation necessitates an oxidant. The pioneering work from MacMillan<sup>18</sup> and Sibi<sup>21</sup> using Ceric ammonium nitrate (CAN) and Fe/NaNO<sub>2</sub> respectively, was a breakthrough in asymmetric catalyzed radical reactions.

MacMillan group used CAN in stoichiometric amount and allylsilanes as radical acceptors, good yields were obtained with high ee's using the chiral imidazolidinone catalyst. The reaction is tolerant to the variation of both partners delivering compounds **2.1.11a-f** with 90-94% ee (Scheme 2).

#### Scheme 2 Early Examples of Aminocatalysis in Radical Reactions

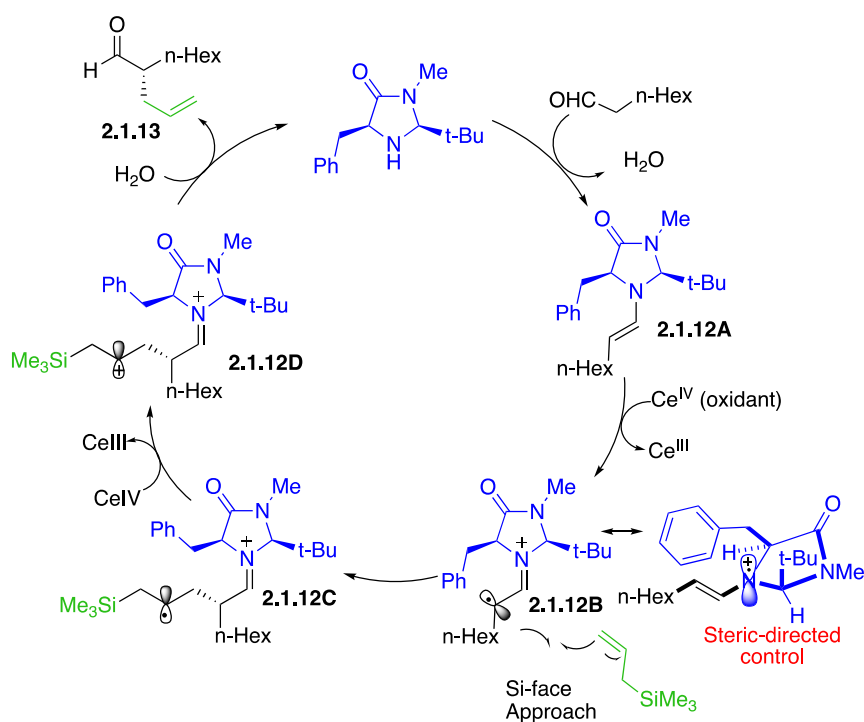


The catalytic cycle is represented in Scheme 3. After enamine **2.1.12A** formation, selective oxidation of the latter, at the expense of the aldehyde and the imidazolidinone catalyst, affords the radical cation intermediate **2.1.12B**. This selective oxidation is critical to establish a catalytic system. Indeed, ionization potential for the enamine is 7.2 eV, lower than that of

aldehyde (9.8 eV). Because of steric considerations the *Re*-face approach is shielded leaving the *Si*-face exposed to the addition to the allylsilane substrate which furnishes  $\beta$ -silyl radical **2.1.12C** with high enantiocontrol. A second equivalent of CAN will then allow an oxidation to form  $\beta$ -silyl cation **2.1.12D**, stabilized through  $\beta$ -effect.  $\beta$ -Elimination and hydrolysis of the iminium intermediate provides the product **2.1.13** with regeneration of the chiral imidazolidinone catalyst.

The SOMO-organocatalyzed  $\alpha$ -allylation of ketones has also been reported but requires a modified imidazolidinone catalyst. This change is due to the difference in electronic and steric interactions between ketones and the amine catalyst when compared to an aldehyde partner discussed above.<sup>22</sup>

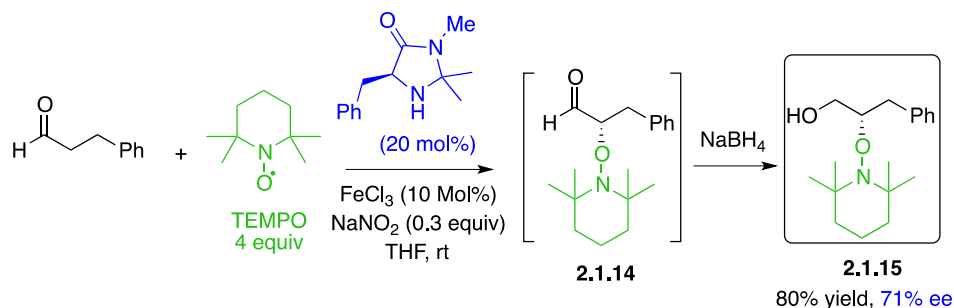
### Scheme 3 $\alpha$ -Allylation of Aldehydes



The Sibi's strategy for  $\alpha$ -functionalization uses FeCl<sub>3</sub> as the oxidant but in catalytic amount and in the presence of NaNO<sub>2</sub>/O<sub>2</sub> as co-oxidant yielding the  $\alpha$ -oxygenated product **2.1.15** with 71% ee (Scheme 4). The reaction is also tolerant to the variation of the aldehyde. The authors

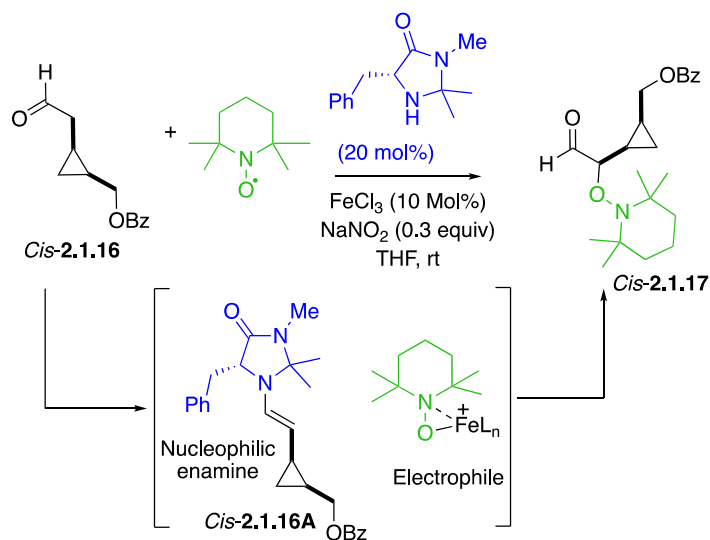
indicated that the use of proline as a catalyst can afford the desired product but with only 3% ee.

#### Scheme 4 $\alpha$ -Hydroxylation of Aldehydes



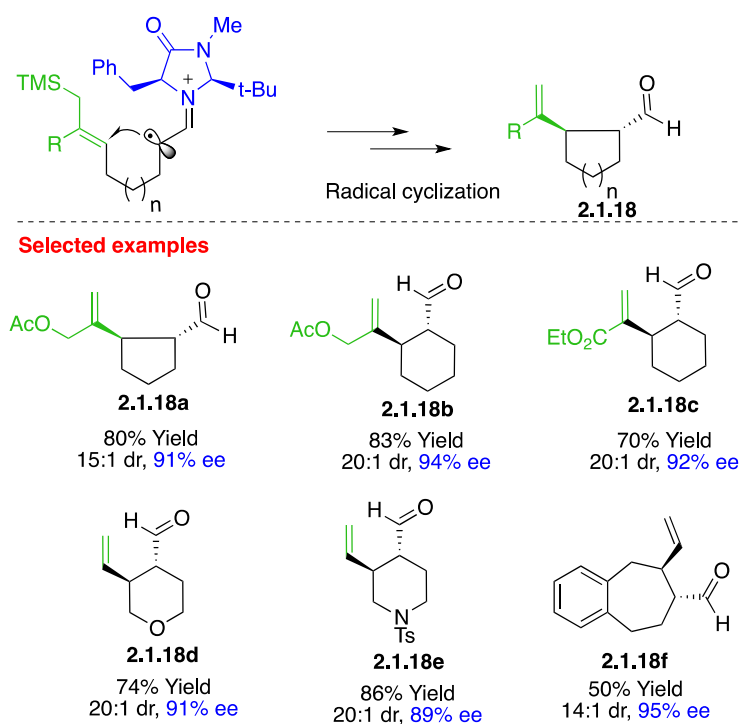
In 2010, the MacMillan group attempted to apply the Sibi oxidative conditions ( $\text{FeCl}_3$ ,  $\text{NaNO}_2/\text{O}_2$ ) to their system with no success. They therefore conducted mechanistic studies of the Sibi oxidant system.<sup>23</sup> The use of cyclopropane-based radical clock *cis*-**2.1.16** afforded the desired product **2.1.17** with low isomerization suggesting, according to the authors, that a closed shell addition into enamine **2.1.16A** would better occur rather than trapping of the radical by TEMPO (Scheme 5). It must be noted that, depending on the concentration of TEMPO and reaction conditions, *cis*/*trans* isomerization occurred which is an argument in favor of a radical mechanism.

#### Scheme 5 MacMillan's Mechanistic Proposal for $\alpha$ -Hydroxylation of Aldehydes



Based on the SOMO activation strategy, the MacMillan group has extended allyl silane radical acceptors to tethered aldehydes in order to trigger intramolecular radical addition and obtain enantioenriched carbocycles and heterocycles **2.1.18** with high diastereomeric and enantiomeric ratios (Scheme 6).<sup>24</sup> Interestingly, the use of *Z*- or *E*-Allyl silane afforded the same *trans* diastereomer in the formation of piperidine product **2.1.18e** suggesting the geometry of the olefin does not affect the diastereoselectivity of the cyclization. Polyene cascade cyclization accessing terpenoidal and steroidal architectures was also reported using the same organocatalyst.<sup>25</sup>

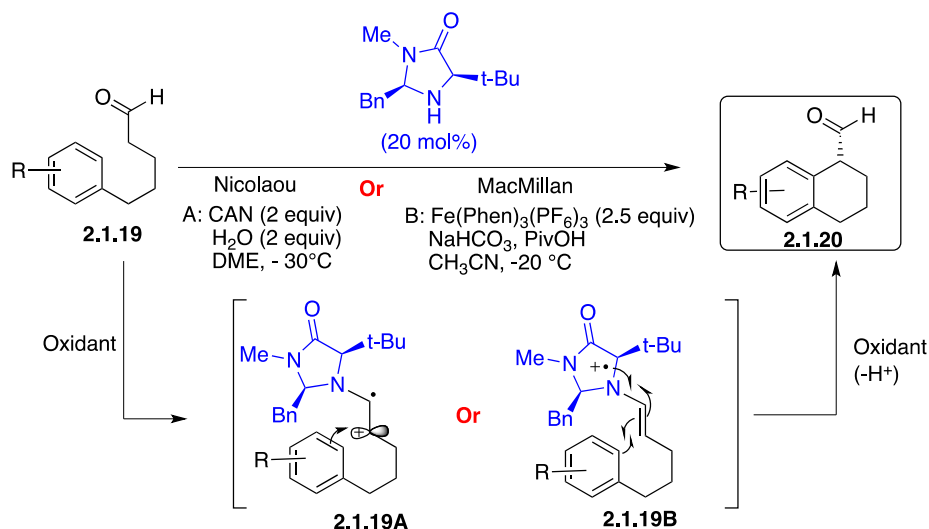
### Scheme 6 Intramolecular Allylation of Aldehydes



Intramolecular  $\alpha$ -arylations of aldehydes **2.1.19** using an imidazolidinone catalyst were independently reported by the Nicolaou (conditions A) and MacMillan (conditions B) groups (Scheme 7). In Nicolaou's work, the authors state that the radical cation intermediate **2.1.19A** evolves through classical Friedel-Crafts rather than a radical mechanism.<sup>26</sup> They applied this strategy to the total synthesis of Demethyl Calamenene. Whereas the MacMillan group insisted on an open shell (radical based) arylation mechanism through intermediate **2.1.19B**.<sup>27</sup> They

supported this hypothesis based on their previous radical clock probe,<sup>18</sup> theoretical calculations<sup>28</sup> and on the exclusive ortho regioselectivity of the reaction when 1,3-disubstituted aryl rings were used. A wide range of electron-rich aryl and heteroaryl ring systems were competent in this cyclization.

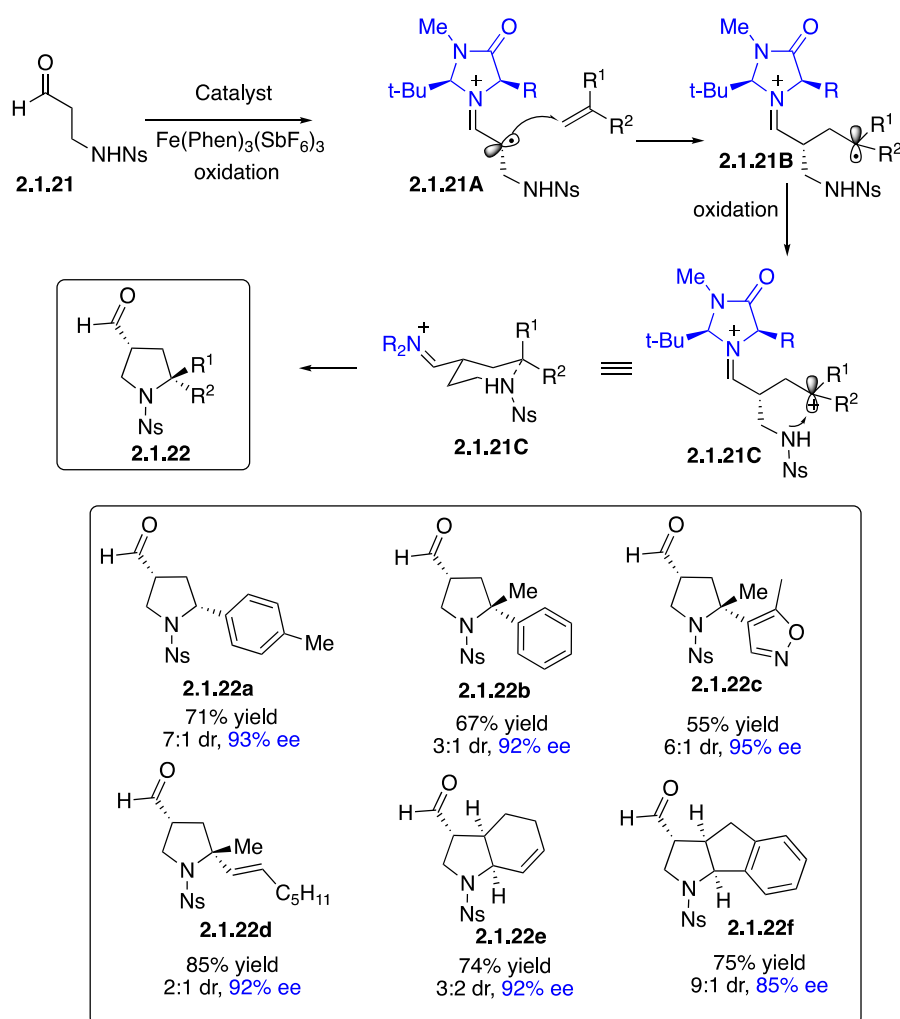
### Scheme 7 Nicolaou and MacMillan's Intramolecular $\alpha$ -Arylation of Aldehydes



Radical/Polar Crossover Cyclization has also been designed by the MacMillan group in 2012.<sup>29</sup> Indeed, nucleophilic amine-connected formaldehyde **2.1.21** in the presence of styrene derivatives allowed the construction of chiral pyrrolidines **2.1.22** (Scheme 8). This enantioselective formal [3+2] cyclization is based on the use of easily oxidable benzylic radical to generate a benzylic carbocation **2.1.21C** which is trapped by the internal nucleophilic amine. The control of the enantioselectivity is likely to be addressed by the benzyl or methyl substituted imidazolidine catalyst. The observed diastereoselectivity can be rationalized by a 6-membered chair transition state where the less hindered substituent occupies a pre-axial position. Overall, high enantiomeric excesses and moderate diastereoselectivities were obtained in this reaction. Interestingly, challenging construction of tetrasubstituted stereocenters was also demonstrated in this work.

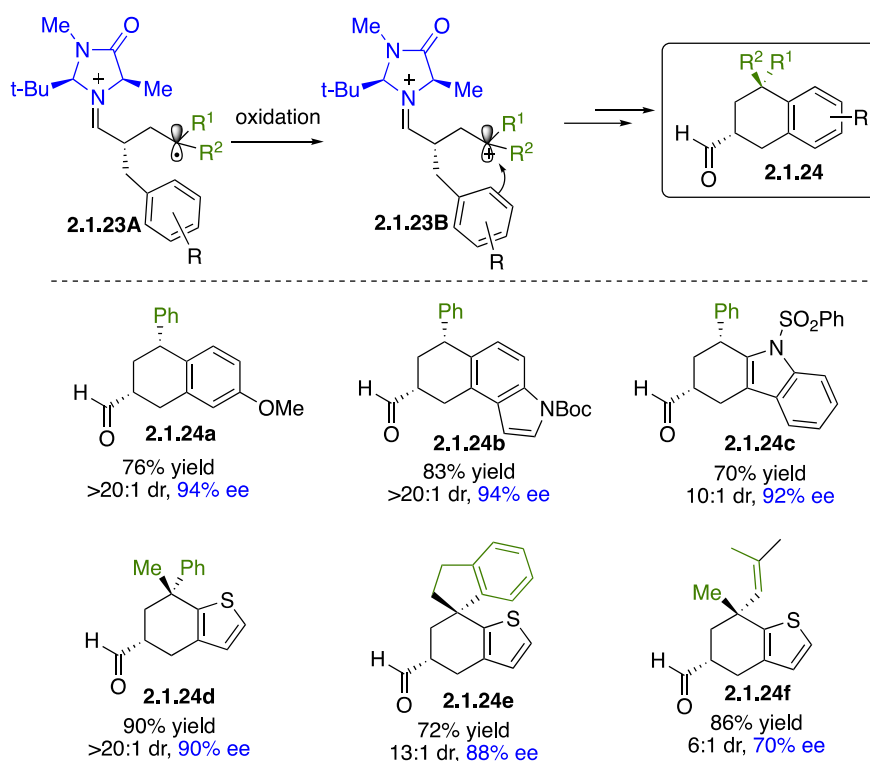


## Scheme 8 Radical/Polar Crossover Cyclization



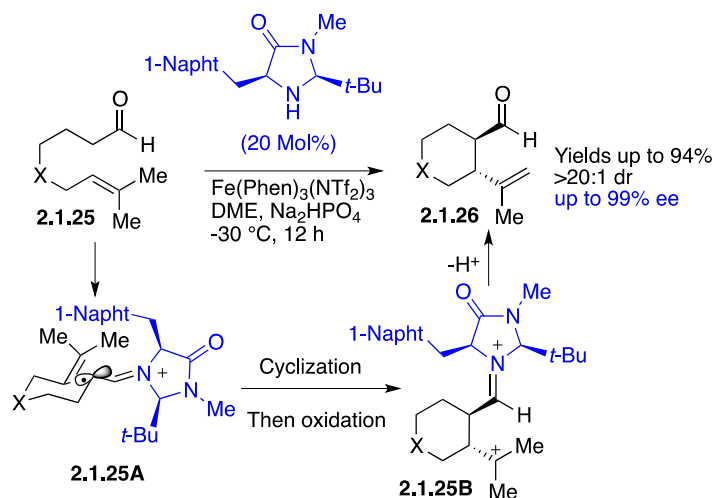
Based on the same approach, a benzylic cation was also intercepted by an internal electron-rich aryl group - through an intramolecular Friedel-Crafts reaction - to provide chiral carbo- and heterocycles **2.1.24** (Scheme 9).<sup>30</sup> This formal [4+2] cycloaddition allowed for better diastereocontrol than C-N bond ring closure. Enantiomeric excesses from 70 to 94% and dr up to 20:1 was observed even in molecules possessing chiral quaternary carbons. This is a nice alternative to the Pd-mediated  $\alpha$ -arylation of aldehydes.<sup>31</sup>

## Scheme 9 Intramolecular Friedel-Crafts Cyclizations



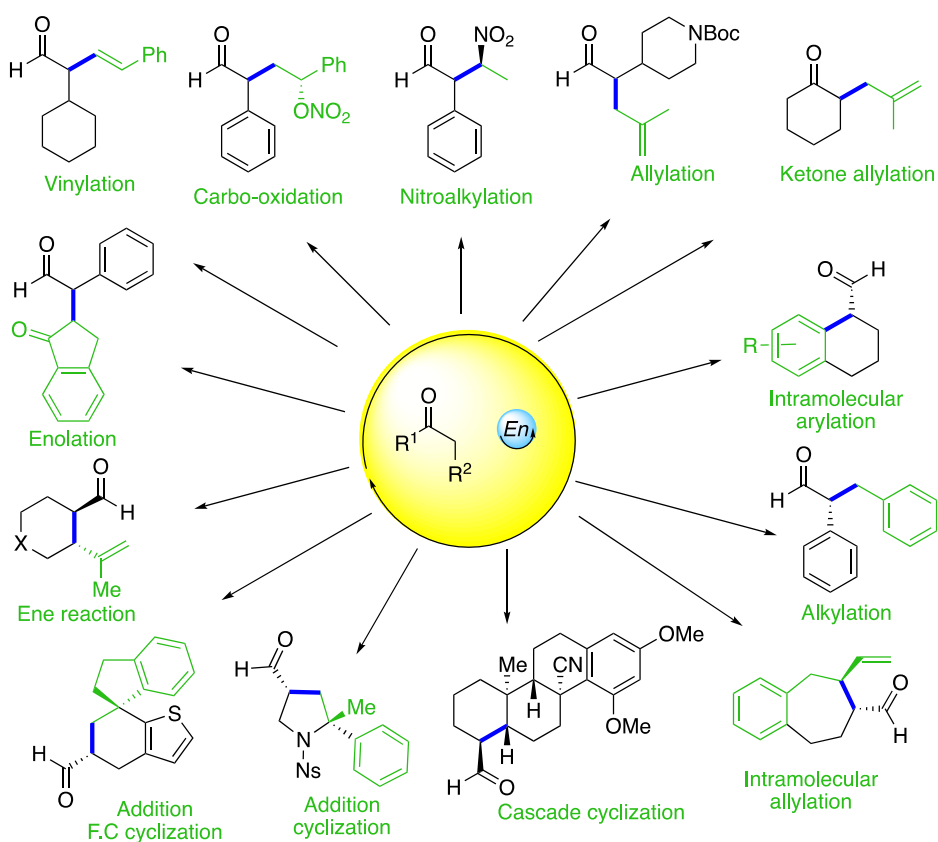
In 2013, an intramolecular alkylation with tethered enophile **2.1.25** as a radical acceptor was reported to afford a homo-ene product **2.1.26**.<sup>32</sup> Group like isopropylidene is an excellent partner for both cascading steps, a favorable radical addition affording a tertiary radical is followed by a second oxidation which furnishes the stabilized tertiary carbocation intermediate **2.1.25B**. Selective loss of proton furnishes the *trans*-diastereomer in good yields, high enantio- and diastereoselectivities. The enantioselective radical addition to the pendant alkene is again directed by the steric considerations due to the presence of the bulky catalyst. Six-membered chair-like transition state will place the alkylidene and radical cation in *trans* di-equatorial positions explaining the observed relative stereochemistry in the product (Scheme 10). Varying the nature of the olefin as well as the core of the molecule afforded a significant scope for this reaction.

## Scheme 10 Intramolecular Alkylation of Aldehydes

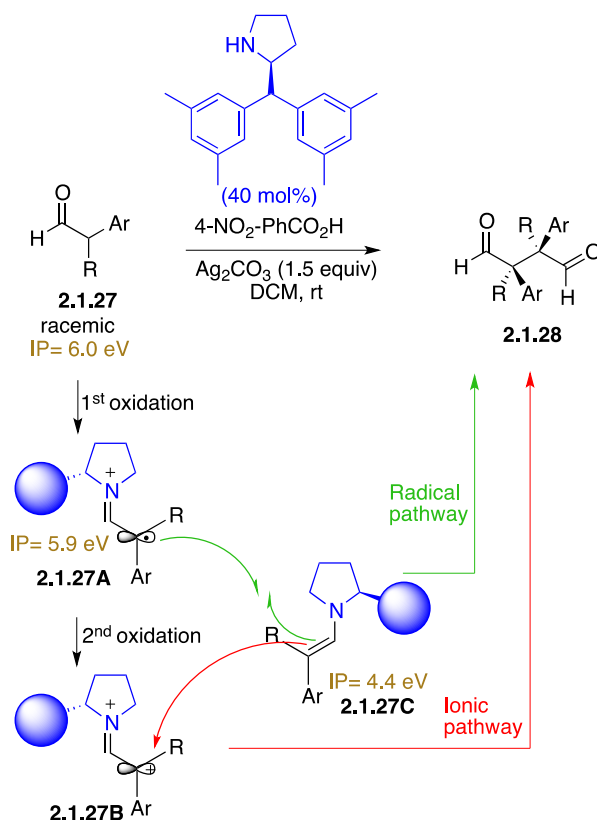


This catalytic activation mode was also efficiently employed in vinylation,<sup>33</sup> enolation,<sup>34,35</sup> carbo-oxidation,<sup>36</sup> nitroalkylation,<sup>37</sup>  $\alpha$ -chlorination.<sup>38</sup> An overview on the potential of this reaction is presented in Scheme 11.

## Scheme 11 Examples of different Alkylation of Aldehydes



## Scheme 12 Oxidative Homocoupling of Aldehydes

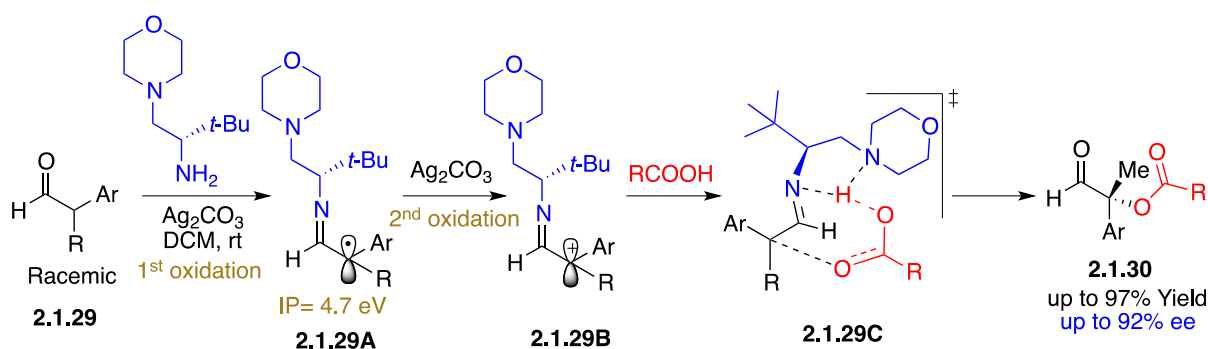


More recently and following their initial finding,<sup>39</sup> Jørgensen reported an oxidative homocoupling of aldehydes **2.1.27**.<sup>40</sup> Using silver carbonate as oxidant, proline derived enamine is oxidized to afford a radical cation **2.1.27A**. The latter undergoes a radical addition to form a C-C bond to afford enantioenriched 1,4-dialdehydes **2.1.28** possessing vicinal quaternary stereocenters (Scheme 12). Calculated ionization potentials of the intermediates revealed that the enamine (IP= 4.4 eV)<sup>41,42</sup> is more susceptible to oxidation which is consistent with MacMillan's results.<sup>18</sup> After the oxidative formation of the iminium radical, competitive pathways could then take place. A highly energetic second oxidation of the latter (IP of 5.9 eV) to afford dicationic species **2.1.27B** followed by ionic addition of the *in situ* formed enamine would deliver the dialdehyde, after hydrolysis. The second path requires a radical addition to enamine that would deliver the product after a second SET and hydrolysis. Kinetic analysis made with competitive reactions and Hammett-type plots convinced the authors to prefer a radical pathway. A third path in which two radicals would recombine has been excluded by the

authors. According to the authors, persistent radical effect (PRE) of this species may prevent dimerization.<sup>43</sup> High enantiomeric and diastereomeric ratios were obtained when electron rich substituted aromatic aldehydes were used. This methodology suffers from a high catalyst loading (40 mol %). Electron poor substrates afforded lower yields because of higher ionization potentials. However, no explanation for the low ee's observed with these aldehydes was provided.

Importantly, in another report,<sup>44</sup> in the presence of primary amine catalyst, the IP of the generated radical is lowered which allows a facile oxidation to carbocation species **2.1.29B**. The latter is then trapped by carboxylic acids to deliver  $\alpha$ -tetrasubstituted aldehydes **2.1.30** with moderate to good yields and ee's (Scheme 13). However, it is surprising to see when only 1.5 equivalent of oxidant is used, the yield could reach 97%. Thanks to X-ray analysis, the absolute configuration was determined to be *R*. The authors propose a transition state where a *Re*-face attack of the carboxylic acid is facilitated by N–H–O hydrogen bonding.

### Scheme 13 Alkylation of Aldehydes: Synthesis of Chiral Tertiary Center



In the previous decade, after extensive development of enamine's HOMO-activation which act as nucleophilic species for traditional ionic reactivity with electrophiles, MacMillan and co-workers have expanded the scope of this methodology to new opportunities in SOMO-catalysis with different radical acceptors. More recently, Jørgensen exploited the electrophilic character through a double oxidation process allowing reactions with nucleophiles, closing therefore the

ring of Iminium/enamine organocatalysis. We are convinced that this umpolung oxidative strategy has a bright future.<sup>45,46</sup>

However, these oxidative strategies have a limitation in the use of excess of oxidant. Fortunately, improvements have been realized through a photoredox activation method using transition metal initiators (section 2.1.1.2) or direct photoexcitation of colored iminium intermediates and organic electron donor acceptor (EDA) complex (section 2.1.1.3).

### **2.1.1.2 Merging aminocatalysis and metallaphotoredox catalysis**

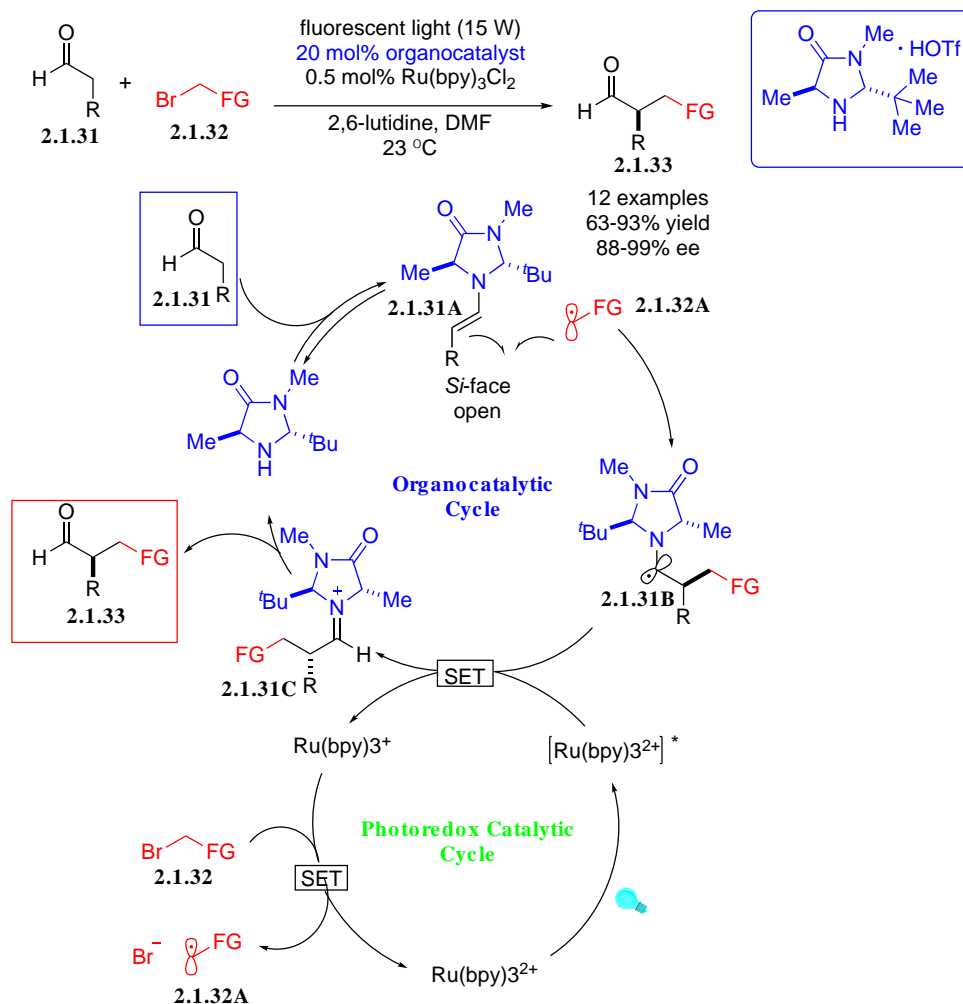
Single electron transfer processes are fundamental in radical reactions. Radical chemistry relies on transition metal catalysis to trigger SET that enables radical initiation. Significant advances were made to explore stereocontrol through chiral complex intermediates using transition metals. The initial work of Cano-Yalo and Deronzier on non-asymmetric photoredox application,<sup>47,48</sup> catalysis paved the way for the advent of enantioselective photoredox radical reactions.

Given its ability to mediate electron transfer, ruthenium catalysts have emerged as go to reagents with compatible enantioselective process, like SOMO catalysis and chiral Lewis acids catalysts, to perform challenging asymmetric chemical reactions. To overcome competing racemic photoreactions, many researchers focused on the different absorption capacity of colorless substrates in the visible region and ruthenium chromophores that absorb intensely.

MacMillan and co-workers showed a new direction for the enantioselective intermolecular  $\alpha$ -alkylation of aldehydes by synergistic merging of photoredox catalysis (using  $\text{Ru}(\text{bpy})_3\text{Cl}_2$  as photoredox catalyst) with organocatalysis (SOMO organocatalyst).<sup>49,50</sup> For example, when aldehydes **2.1.31** were treated with  $\alpha$ -bromocarbonyl **2.1.32** along with a combination of catalysts  $\text{Ru}(\text{bpy})_3\text{Cl}_2$  and imidazolidinone under 15W fluorescent light irradiation, the enantioenriched  $\alpha$ -alkylated aldehydes **2.1.33** were obtained in good yields (Scheme 14).

## Scheme 14 Enantioselective $\alpha$ -Alkylation of Aldehydes by Merging Photoredox Radical

### Initiation with Organocatalysis

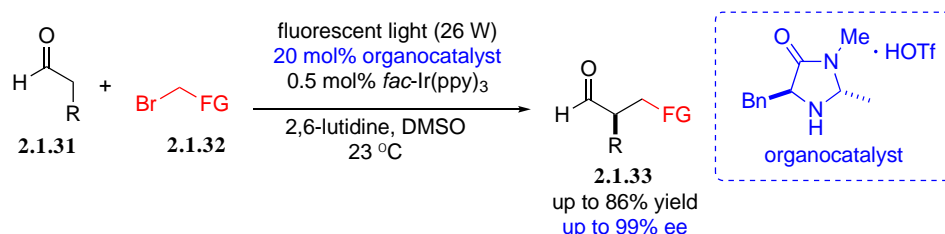


According to the proposed mechanism depicted in Scheme 14, the electron-rich Ru(bpy)<sub>3</sub><sup>3+</sup> generated from photocatalyst Ru(bpy)<sub>3</sub><sup>2+</sup> via photoredox catalytic cycle, can act as a potent reductant and take part in single-electron transfer (SET) to the  $\alpha$ -bromocarbonyl **2.1.32** to furnish the electron-deficient alkyl radical **2.1.32A**. The other catalytic cycle i.e., organocatalytic cycle would generate enamine **2.1.31A** by the condensation between the imidazolidinone catalyst and aldehyde **2.1.31**. The key alkylation step would then occur via addition of the SOMO-philic enamine to the electron-deficient alkyl radical and thereby formation of electron-rich  $\alpha$ -amino radical **2.1.31B** which would readily produce iminium ion

**2.1.31C** via SET process. The origin of enantioselectivity in the asymmetric radical addition of **2.1.32A** to the enamine **2.1.31A** is mainly controlled by the steric effects which was theoretically investigated by Xue and co-workers.<sup>51</sup> Finally, hydrolysis of the iminium ion would deliver the targeted  $\alpha$ -alkylated aldehyde **2.1.33** with the regeneration of catalyst.

After developing ruthenium photoredox organocatalysis, MacMillan advanced enantioselective  $\alpha$ -trifluoromethylation of aldehydes via iridium/enamine dual catalysis (Scheme 15). Electrophilic trifluoromethyl radical was generated with a SET process from excited  $^*Ir(ppy)_2(dtbbpy)^+$  and trifluoromethyl iodide. Addition of this radical to the electron rich  $\pi$ -sophile chiral enamine ensures the stereocontrol guided by the facially biased chiral conformer.<sup>52</sup> The initiation step resides in SET from a sacrificial amount of enamine. The excited photoredox catalyst acts as an oxidant with respect to the  $\alpha$ -aminyl radical delivering the  $Ir(ppy)_2(dtbbpy)$  which plays a role of strong reductant ( $E_{red} = -1.51V$  vs. SCE in  $CH_3CN$ ) for reduction of alkyl halide ( $E_{red} = -1.22V$  vs. SCE in DMF).

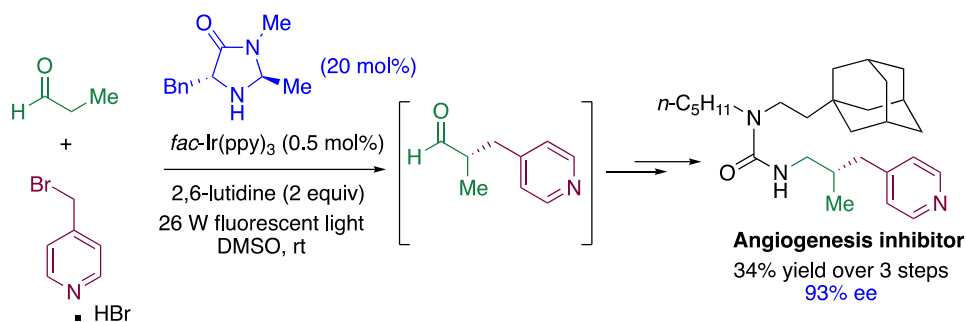
### Scheme 15 $\alpha$ -Trifluoromethylation of Aldehydes



$\alpha$ -Benzylation of aldehydes via iridium/enamine dual catalysis has also been reported by the same group.<sup>53</sup> An elegant short synthesis of an angiogenesis inhibitor could be targeted using this concept in 34% yield over three steps with 93% ee (Scheme 16).

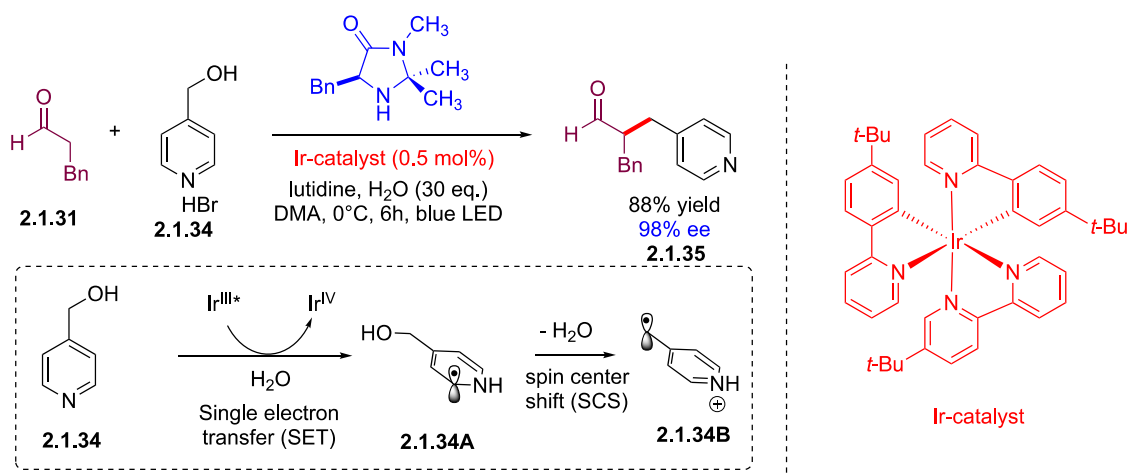
### Scheme 16 $\alpha$ -Benylation of Aldehydes: Synthesis of an Angiogenesis Inhibitor





Inspired by the DNA biosynthesis making use of alcohols as alkylation agents, MacMillan and co-workers succeeded in 2018 to use heterobenzylic alcohols **2.1.34** as alkylating agents for the enantioselective  $\alpha$ -benzylation of aldehydes by means of a radical-mediated spin center-shift (SCS) mechanism.<sup>54</sup> To facilitate the reaction, 4-(hydroxymethyl)pyridine ( $E_{\text{red}} = 1.29$  V) was selected so that it could be reduced by the excited state of the photoredox catalyst Ir(ppy)<sub>3</sub>\* ( $E_{\text{red}} = -1.81$  V). After generation of the electron-rich radical **2.1.34A**, this iridium catalyst could undergo a spin-center shift after proton transfer from water to provide electron-poor radical **2.1.34B** (Scheme 17).

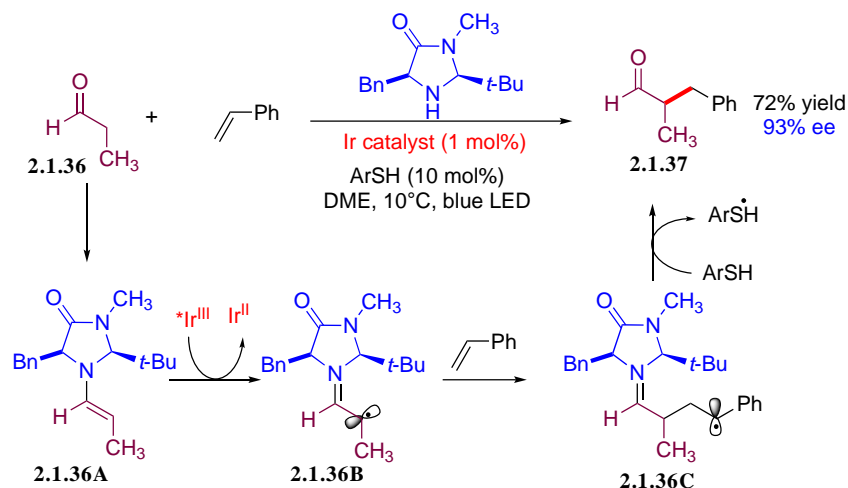
### Scheme 17 $\alpha$ -Benzylation of Aldehydes by Spin Center-Shift (SPS) Mechanism



Reversing the reactivity of the enamine intermediate as the reductant in the presence of \*Ir<sup>III</sup> as an oxidant provides a nice opportunity for addition of styrene to aldehyde **3.1.36** (Scheme 18).<sup>55</sup> Three synergetic catalysts (imidazolidinone, iridium and thiol) are operating in this system. After stereoselective radical addition of the enamynyl radical **2.1.36B** to the olefin, additional

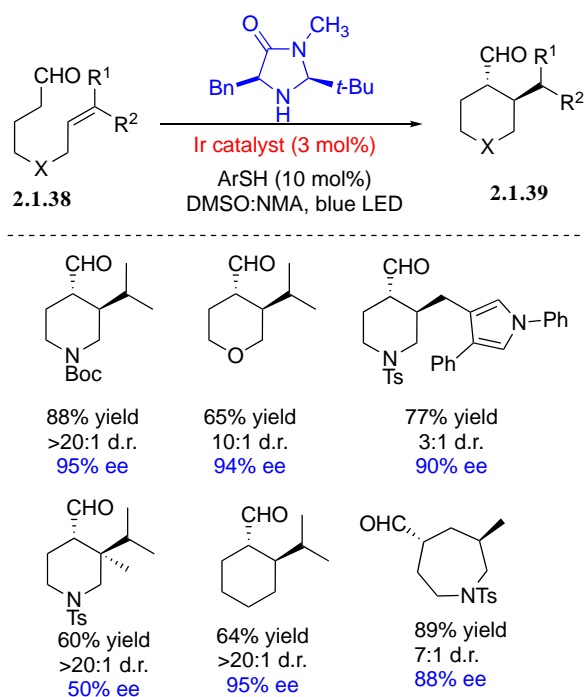
HAT process with thiol catalyst enables the regeneration of the amine catalyst and the release of the product **2.1.37**.

### Scheme 18 $\alpha$ -Alkylation of Aldehydes using Olefins



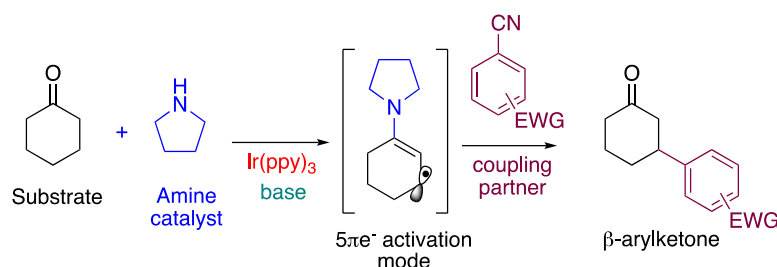
Interestingly, the use of tethered aldehydic olefins **2.1.38** allows for the formation of *trans*-disubstituted carbo or heterocyclic compounds **2.1.39** by intramolecular alkylation in a diastereo- and enantioselective manner. This multicatalytic system allows the construction of five-, six- and seven-membered cycles (Scheme 19).

### Scheme 19 Intramolecular Alkylation of Aldehydes



The direct radical  $\beta$ -functionalization of saturated carbonyl compounds is a challenging endeavor in organic synthesis, and this topic has been the subject of numerous efforts.<sup>56</sup> In 2013, MacMillan and co-workers developed an unprecedented protocol merging photoredox and organocatalysis, enabling the direct  $\beta$ -arylation of saturated aldehydes and ketones (Scheme 20).<sup>57</sup> By concomitantly generating  $5\pi$ -electron  $\beta$ -enaminyll radicals by the organocatalytic cycle and radical anions by photocatalytic reduction of benzonitrile derivatives by the photoredox catalytic cycle, a broad range of aliphatic aldehydes and ketones could be  $\beta$ -functionalized, using the same procedure.

### Scheme 20 Direct Radical $\beta$ -Functionalization of Saturated Carbonyl Compounds

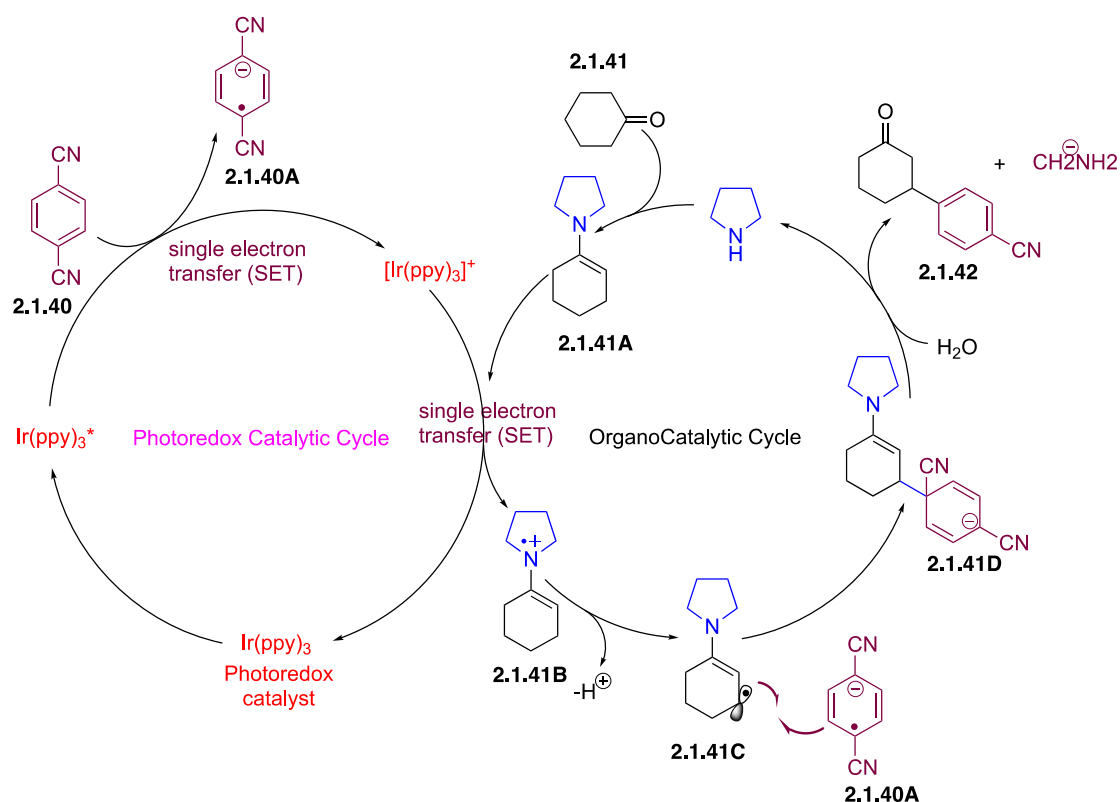


In fact, this dual catalysis possesses several key features. Notably, the radical anion **2.1.40A** formed from benzonitrile derivatives **2.1.40** should be sufficiently stabilized and electron-rich to avoid these radicals to directly react with the intermediate enamine **2.1.41A**. The homocoupling of radical anions should also be unfavorable as it could cause a severe reduction in the yield of the reaction. Concerning the intermediate enamine, several prerequisites have also to be pointed out. Notably, its formation should be highly favorable as well as its oxidation. Finally, the  $5\pi$  electron- intermediate **2.1.41C** formed transiently should be highly reactive towards the coupling with the radical anions. A complete picture of the mechanism is provided in Scheme 21.

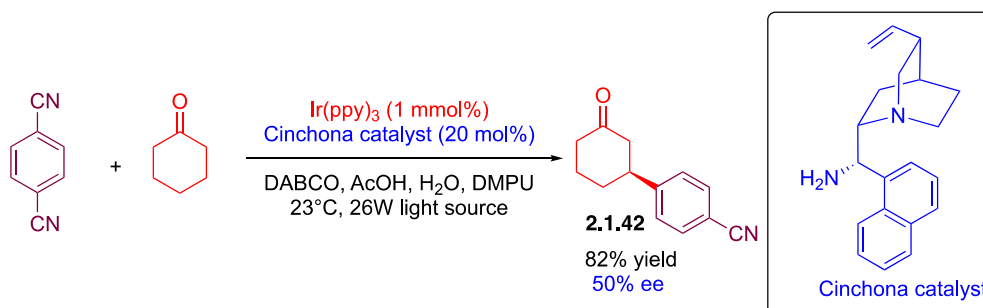
The authors demonstrated in this article that ketones are amenable to  $\beta$ -coupling reactions and azepane was identified as a remarkable amine catalyst. Thus, the  $\beta$ -functionalization of a wide range of cyclohexanones could be successfully realized. The  $\beta$ -functionalization of ketones was

tolerant to a wide range of substituents of different bulkiness (ester, aliphatic, aromatic substituents). Finally, preliminary experiment was also carried out to control the enantioselectivity during the  $\beta$ -coupling reaction. A reaction yield of 82% with 55% ee could be obtained while using a cinchona-based organocatalyst, demonstrating that the  $\beta$ -coupling reaction was amenable to asymmetric catalysis. The use of imidazolidinone chiral catalyst is limited in this case because of the remote stereocontrol needed (Scheme 22).

### Scheme 21 Mechanism of Dual Catalysis Reaction

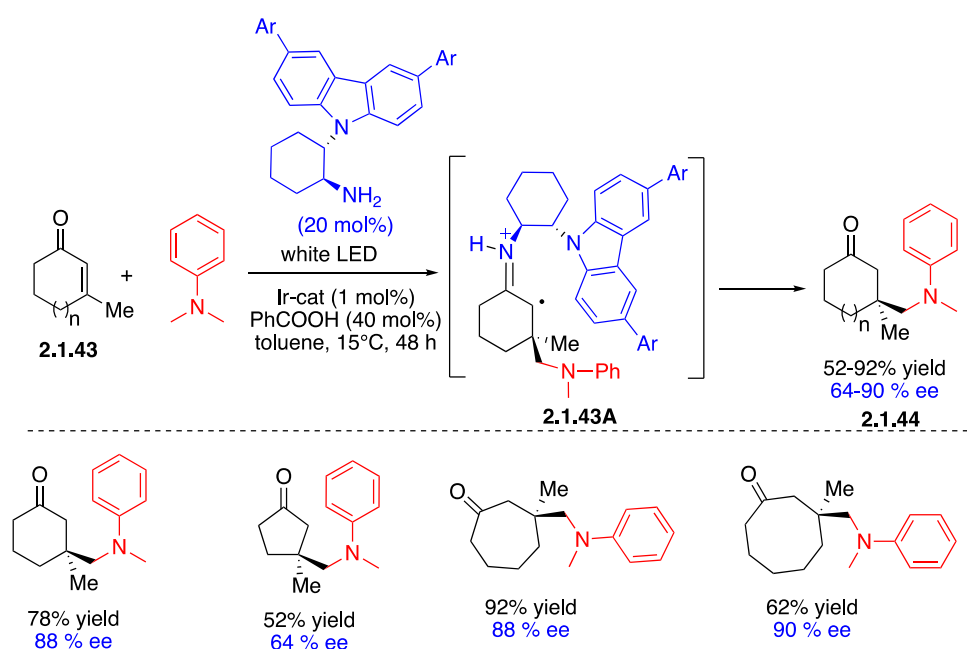


### Scheme 22 Enantioselective Functionalization of the $\beta$ -Carbon of Ketones



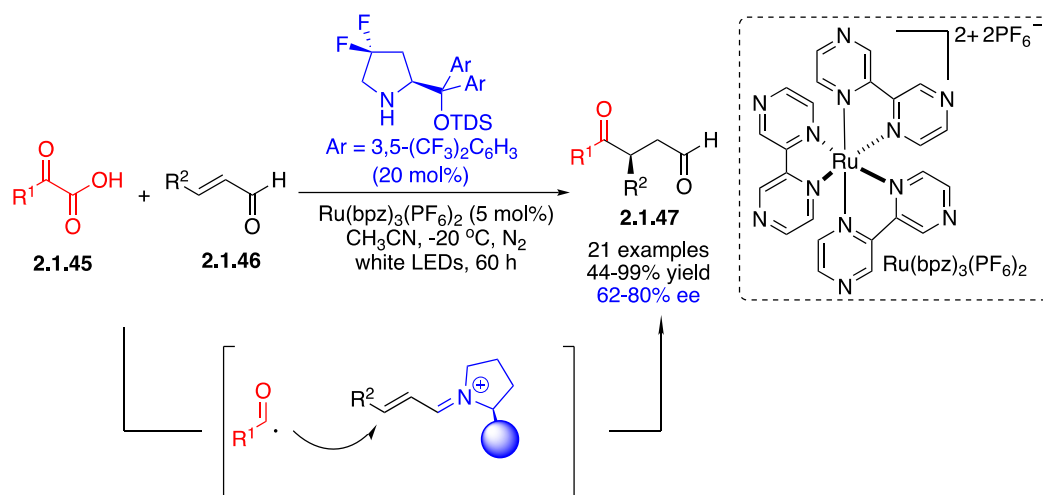
To obtain  $\beta$ -functionalized ketones **2.1.44**, Melchiorre has carried out enantioselective radical conjugated addition (RCA) to  $\beta,\beta$ -disubstituted enones. The authors have also shown that iridium is able generate  $\alpha$ -amino radical from *N*-arylamines. A photoredox asymmetric RCA occurs through iminium activation and enables the construction of chiral quaternary center. This dual metallaphotoredox/organocatalysis allows the formation of ketones with different ring size with a nice level of enantioselectivity (Scheme 23).<sup>58</sup>

### Scheme 23 Enantioselective Conjugate Radical Addition using Dual Catalysis



Yu et al. also carried out a similar strategy, using covalent amine catalysis, for the synthesis of 1,4-dicarbonyl compounds **2.1.47** in an enantioselective fashion via radical hydroacylation of enals **2.1.46** with  $\alpha$ -ketoacids **2.1.45** by merging Ru(bpz)<sub>3</sub>(PF<sub>6</sub>)<sub>2</sub> catalyzed photoredox catalysis with amine catalysis (Scheme 24).<sup>59</sup> Here, acyl radical is generated from  $\alpha$ -ketoacid act as the acylation reagent with the iminium ion which is generated from the enal and amine catalyst by the help of a proton.

**Scheme 24 Enantioselective Radical Hydroacylation of Enals with  $\alpha$ -Ketoacids by Merging Photoredox Catalysis with Amine Catalysis.**

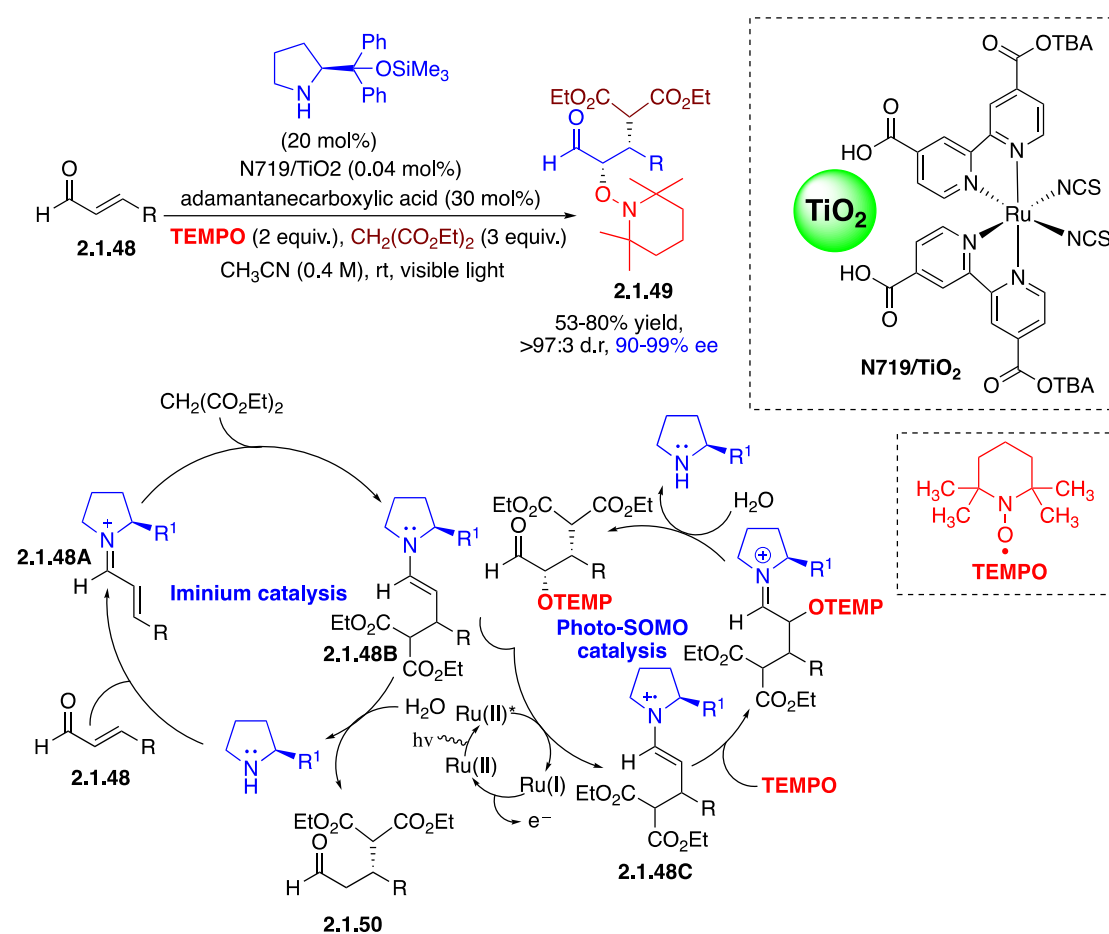


Jang et al. exploited enantioselective tandem Michael addition/oxyamination of  $\alpha,\beta$ -unsaturated aldehydes by combining asymmetric iminium catalysis using organocatalyst with photoinduced SOMO catalysis using N719/ $\text{TiO}_2$ .<sup>60</sup> Here,  $\text{TiO}_2$  acts as a second cooperative photocatalyst along with Ru photocatalyst N719 which bound to the latter, increases the enantio- and diastereoselectivity of the process. Adamantane carboxylic acid (30 mol%) was used as an additive which promotes formation of iminium ion **2.1.48A** from aldehyde **2.1.48** and chiral amine catalyst. This iminium intermediate then reacts with diethyl malonate to provide intermediate **2.1.48B** which either undergoes hydrolysis to form  $\beta$ -substituted aldehyde **2.1.50** or photo-oxidation by the photoexcited Ru(II) dye to form enamine radical **2.1.48C**. Subsequent addition of TEMPO to radical intermediate **2.1.48BC** followed by hydrolysis afforded the desired product **2.1.49** (Scheme 25). This mechanism is obeying to a polar/radical crossover sequence where the first stereocontrol arises from the addition of the malonate.

Recently, Bach group reported promising preliminary results of enantioselective [2+2] photocycloaddition of cinnamaldehyde in the presence of ruthenium photocatalyst and proline derived organocatalyst.<sup>61</sup>

## Scheme 25 Tandem Michael Addition/oxyamination via TiO<sub>2</sub>/N719 Dye-sensitized

### Organophotocatalysis



#### 2.1.1.3. Metal free enantioselective photosensitized aminocatalysis

The success of enantioselective reactions depends on a good balance of issues related to reaction conditions and the appropriate molecular architecture of the catalyst. The two fields of organocatalysis and photocatalysis have grown in parallel until a synergetic interaction of both activation modes has impacted enantioselective radical reactions significantly. The advent of photoredox asymmetric catalysis allowing for the “domestication” of open-shell species has led to a plethora of novel enantioselective methods using radical chemistry. The fundamental radical mechanisms are still applicable to these reactions. Photoredox catalysis can initiate radical formation by two activation modes: (1) use of a transition metal (vide supra) or an organic dye that absorbs light to initiate a radical photoprocess upon excitation. (2) organic

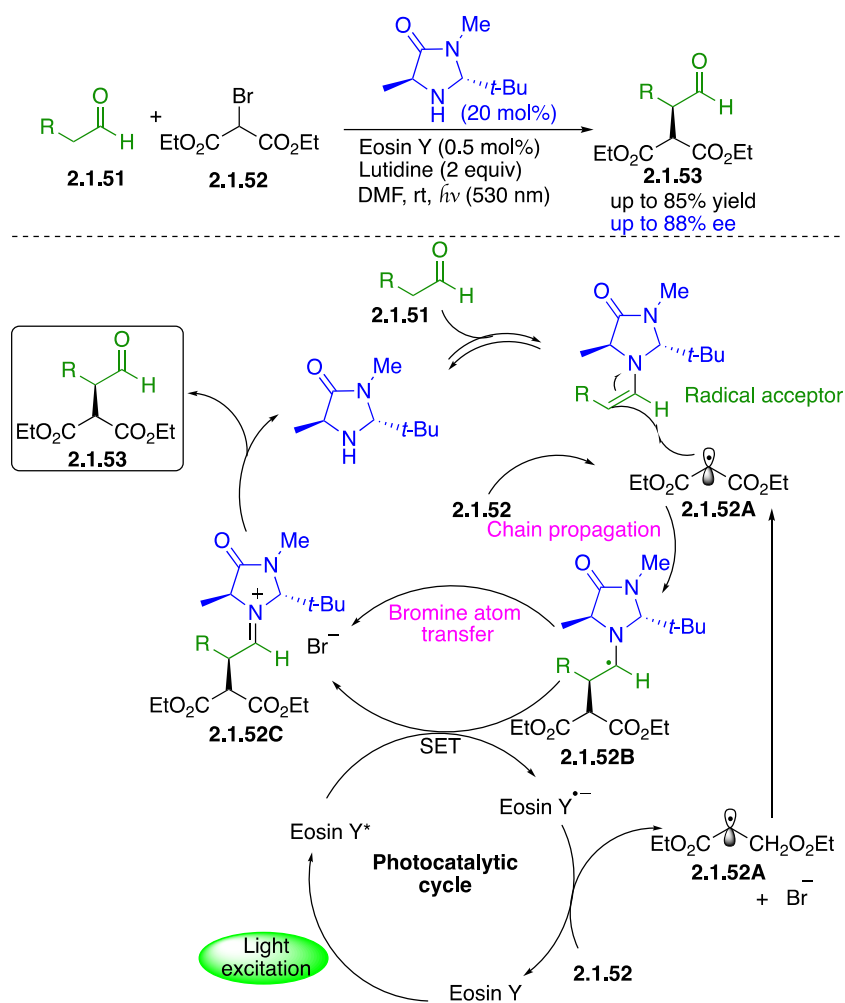
molecule/catalyst absorbing light will display, after excitation, a radical pattern in the absence of an external dye.

In this section, we will limit our discussion to recent advances in metal-free cooperative asymmetric photoredox aminocatalysis.<sup>62</sup> The main advantage offered by this strategy is avoiding the use of stoichiometric metallic oxidants and undoubtedly with an eye towards green chemistry principles and sustainability criteria.

While Nicewicz and MacMillan translated the SOMO strategy by using ruthenium as a photoredox catalyst to achieve enantioselective  $\alpha$ -functionalization,<sup>49</sup> Zeitler and König oriented their work to the use of organic dyes.<sup>63</sup> Eosin derivatives<sup>64</sup> showed remarkable similarities in redox properties with iridium and ruthenium photosensitizers. Indeed, in the presence of imidazolidinone catalyst (20 mol%), 0.5 mol % of eosin Y, 2 equivalents of lutidine and visible light (LED 530 nm), high yielding and enantioselective alkylation and perfluoroalkylation reactions were realized. The authors proposed a mechanism similar to that proposed for ruthenium photoredox reaction in which two independent catalytic cycles are operating.<sup>49</sup> Excitation of the eosin dye allows for reduction of the C-Br bond to afford the corresponding electrophilic radical **2.1.52A** (Scheme 26). The electrophilic radical adds to the electron rich chiral enamine to generate  $\alpha$ -aminyl radical **2.1.52B**. One-electron oxidative path of the  $\alpha$ -aminyl radical - driven by the excited eosin acting as oxidant - is proposed to close the photoredox cycle and releases the iminium intermediate **2.1.52C**. Another path is also viable through innate radical chain propagation where a bromine atom transfer (ATRA) could take place. The  $\alpha$ -aminyl radical **2.1.52B** would thus act as a reducing agent with respect to the alkylbromide substrate. Quantum yield measurements realized on analogous Ru-catalyzed reaction seem to support a chain-propagating pathway.<sup>65</sup> In this scenario, the photocatalysis is therefore acting as a smart initiator.<sup>66</sup>



## Scheme 26 Use of Eosin Y and an Amine Catalyst for $\alpha$ -Alkylation of Aldehydes



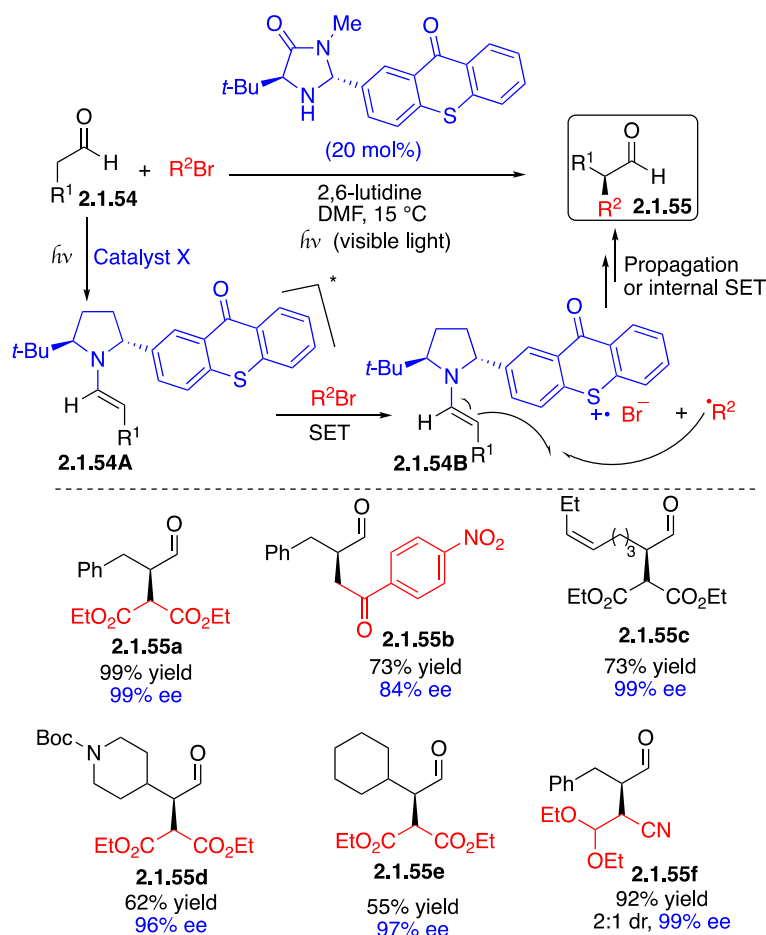
As detailed above, the stereodetermining step is the addition of the malonyl (or perfluoroalkyl) radical to the *in situ* formed chiral enamine acting as a radical acceptor in a highly enantioselective manner (Scheme 26). Hydrolysis of the iminium species **2.1.52C** furnishes the  $\alpha$ -alkylated aldehyde **2.1.53** while releasing the amine catalyst which closes the second catalytic cycle.

The same authors have also reported a visible light promoted stereoselective alkylation under heterogeneous catalysis with MacMillan catalyst.<sup>67</sup>

The use of Rose Bengal is also suitable to achieve the same reaction, the Ferroud group has demonstrated the viability of this dye under the same conditions.<sup>68</sup>

More recently, Rigotti *et al.* incorporated a thioxanthone dye into an organocatalyst having therefore bifunctional utility to work under visible light.<sup>69</sup> The study showed no alteration of the redox properties of the thioxanthone after linkage to imidazolidinone. This offered the possibility to design bifunctional catalysis including photoexcitation and organocatalyzed radical transformation. Under visible light,  $\alpha$ -alkylation of different aldehydes was performed using a variety of alkyl bromides (Scheme 27). Moderate to good yields as well as high enantiomeric excesses were achieved. A tentative creation of a second stereocenter in product **2.1.55f** was not successful since a 2:1 ratio was observed for the diastereomers even though high ee's were obtained for both diastereomers. Some representative examples are shown in Scheme 27.

### Scheme 27 Application of an Amine Catalyst with a Thioxanthone Substituent for $\alpha$ -Alkylation of Aldehydes

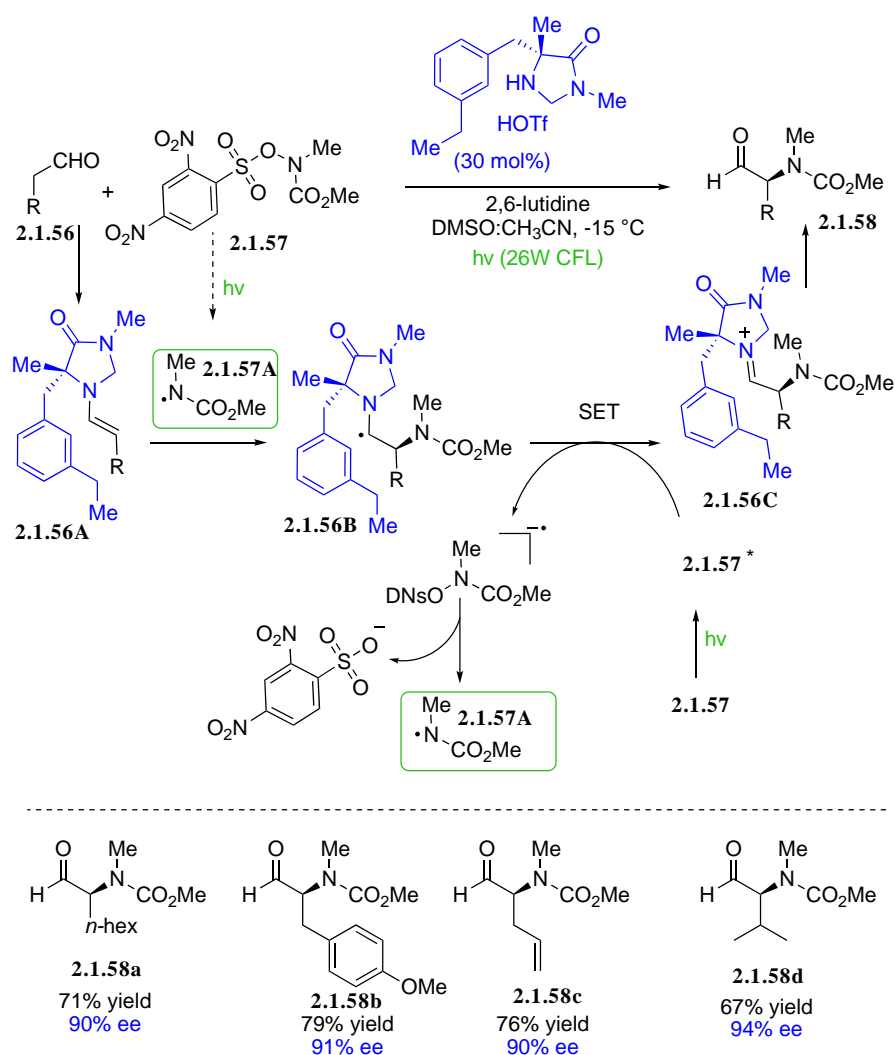


Rigorous mechanistic investigations were conducted and indicated that the dye is crucial for the reaction to proceed. Interestingly, they highlighted that steric effect of organocatalyst affects the SET process. The presence of the thioxanthone in the catalyst has a decreasing tendency for the propagating mechanism (diminution of the quantum yield). With this bifunctional catalyst, internal SET from aminyl radical to xanthone radical cation and a propagation step involving alkylbromide appears to be competing.

The oxyamination reported by Sibi<sup>21</sup> was recently transposed to visible light photoredox/enamine dual catalysis using a proline derived peptide which contained a flavin antenna. However, because of the distal chiral stereocenter from the active site, the reaction was not enantioselective.<sup>70</sup> Nevertheless, the flavin antenna was demonstrated to be efficient to induce a remote SET mechanism.

Nitrogen containing compounds are of prime importance particularly in natural products and pharmaceuticals. In addition to the appeal of the creation of the C–N bond, MacMillan decided to plan  $\alpha$ -amination of aldehyde because due to the protocol, these products can be directly purified without postreaction manipulation and thus are configurationally more stable.<sup>71</sup> To reach this goal, the photogeneration of *N*-centered radical was envisioned using N–O bond reductive cleavage.<sup>72,73</sup> From mechanistic point of view, photoexcitation of the amine bearing dinitrophenylsulfonyloxy (ODNS) photolabile group undergoes mesolytic breaking of the weak N–O bond to generate the *N*-centered radical and sulfonate (Scheme 28). The *N*-centered radical adds to the electron-rich enamine **2.1.56A** with a high level of enantiocontrol to give rise to  $\alpha$ -carbon radical **2.1.56B**, which can be further oxidized to an iminium through a SET pathway by another molecule of amine-ODNS. The robust enantio-discriminating imidazolidinone catalyst has again demonstrated its efficiency. Steric modulation of the catalyst was necessary for high efficacy.

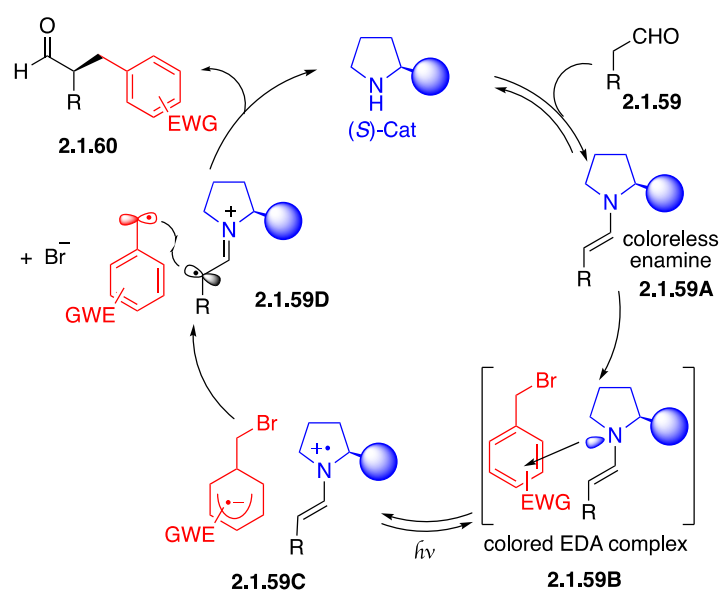
## Scheme 28 $\alpha$ -Amination of Aldehydes



In 2013, Melchiorre exploited the ability of in situ formed colored Electron Donor-Acceptor (EDA) complex **2.1.59B** to trigger electron transfer and generation of radicals with no need for external photosensitizer or oxidant.<sup>74,75</sup> The mechanism relies on the EDA complex formation in the ground state which absorbs in visible region. The association, through  $n \rightarrow \pi^*$  interactions, of electron-deficient benzylbromide and the enamine is responsible for the coloration of this complex. In fact, radical alkylation of enamine was disclosed by Russel and co-worker in 1991 using a Rayonet apparatus (350 nm) in non-enantioselective fashion.<sup>76</sup> Melchiorre succeeded in implementing enantioselective  $\alpha$ -alkylation of aldehydes with Hayashi-Jorgensen type catalyst and visible light irradiation. In the first report, the authors proposed the mechanism depicted in Scheme 29. Electron transfer (ET) occurs producing a chiral radical cation **2.1.59C**

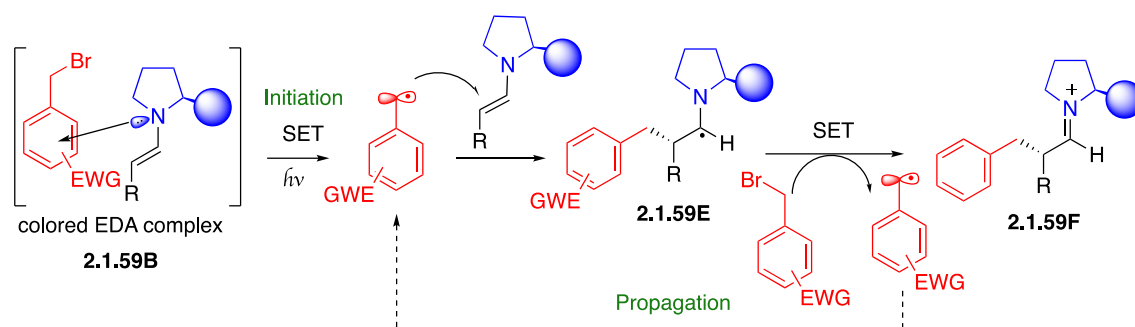
and radical anion pair in close proximity. The success for the reactivity of such species resides in the fragmentation of C–Br bond leaving a stabilized benzylic radical and preventing the reverse ET (Back Electron Transfer (BET)). The two resulting radicals would collapse in enantiocontrolled C–C formation with the assistance of the chiral prolinol catalyst to afford product **2.1.60**.

**Scheme 29 Original Proposed Mechanism for the use of an EDA Complex in Enantioselective  $\alpha$ -Benzylation of Aldehydes**

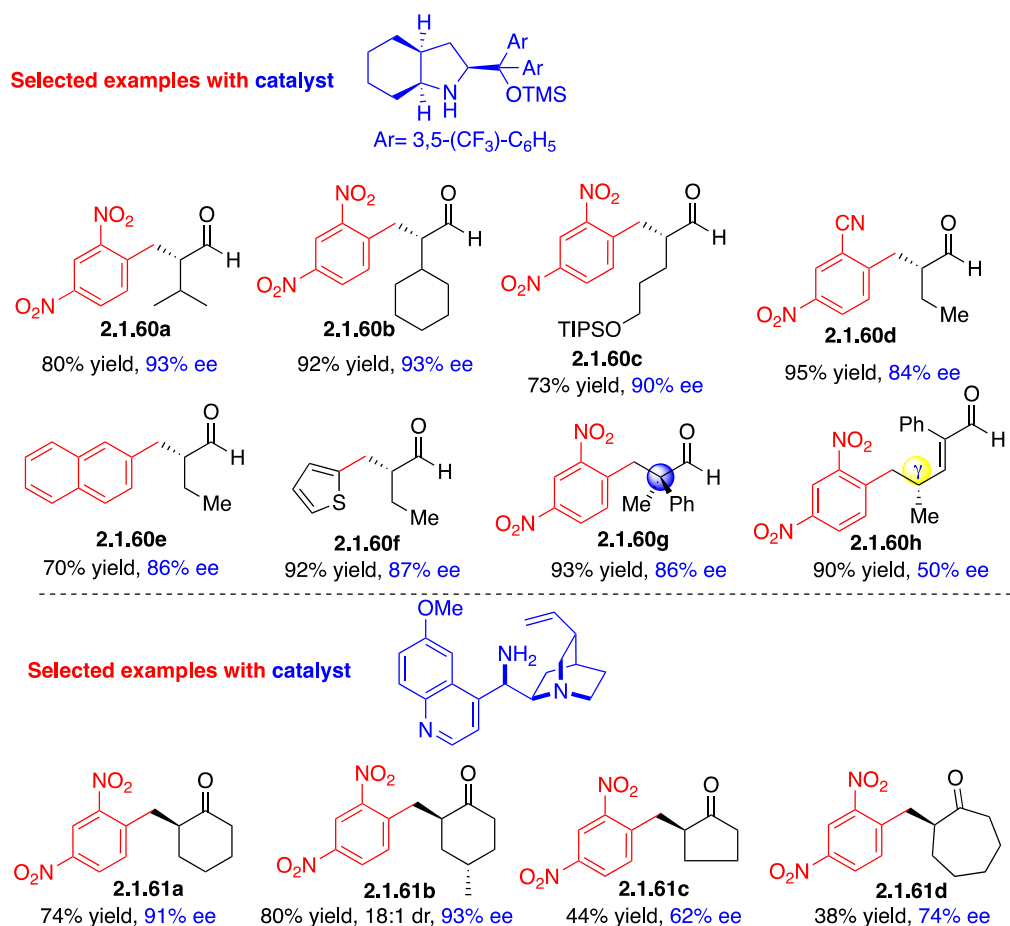


However, a revised mechanism based on further mechanistic studies was published in 2016. These studies suggest that a radical chain mechanism is more likely to be operative.<sup>77</sup> Benzyl radical formation through a photochemical SET is the initiation step. Reductive cleavage of the benzyl bromide with the strong reducing  $\alpha$ -aminoalkylradical **2.1.59E** through an outer-sphere SET produces the iminium **2.1.59F** and the benzyl radical and they participate in the propagating chain process (Scheme 30).

## Scheme 30 Revised Mechanism for the use of EDA Complex in $\alpha$ -Benzylation of Aldehydes



## Scheme 31 Substrate Scope for $\alpha$ -Alkylation of Aldehydes and Ketones

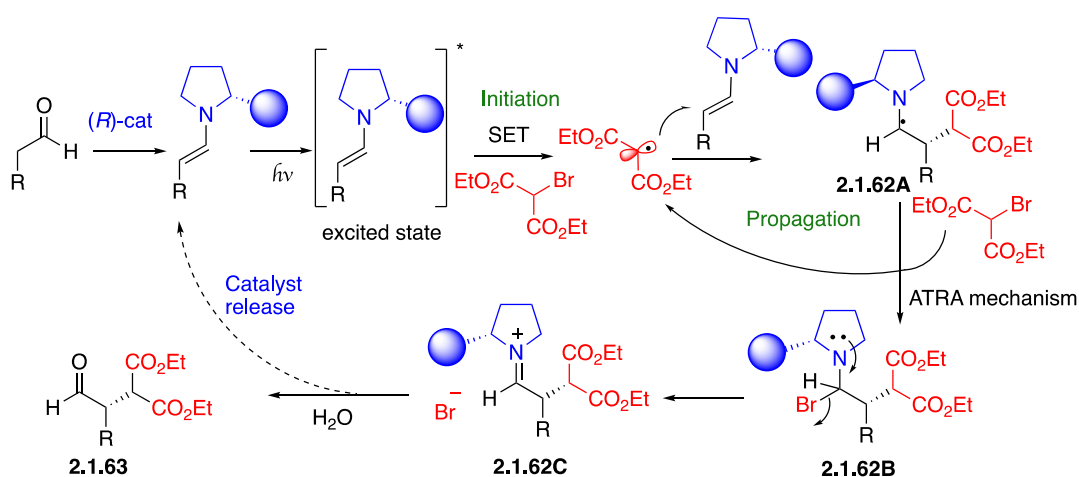


High yields and excellent ee's were observed in the benzylation of aldehydes and later with ketones, with quinidine derived catalyst.<sup>78</sup> Control experiments confirmed that no reaction could occur in the absence of light or catalyst. A wide product scope was obtained including one example of a compound possessing quaternary carbon (**2.1.60g**, Scheme 31). Vinylogous

attempts to induce  $\gamma$ -alkylations from  $\alpha,\beta$ -unsaturated aldehydes were high yielding but with moderate stereoselectivity (**2.1.60h**, Scheme 31).<sup>74</sup> When ketones were used as carbonyl substrates and using cinchona-based catalyst, six-membered carbocycles were formed in good yields and stereoselectivity. Remarkably, when prochiral 4-methylcyclohexanone was used as the substrate, the desymmetrized product **2.1.61b** was obtained with 93% ee and 18:1 diastereomeric ratio.<sup>78</sup> Five and seven-membered cyclic ketones were less efficient in this radical benzylation. It is also important to note that linear ketones present another limitation for this method.

A second strategy based on direct visible light excitation of enamine intermediates was reported by the same group.<sup>79</sup> The reduction potential of bromomalonate of -2.0 V vs Ag/Ag<sup>+</sup> in CH<sub>3</sub>CN allowed for an efficient production of malonyl radical which engages in  $\alpha$ -alkylation of aldehydes. Mechanism of propagation step is provided by an ATRA with malonyl bromide and  $\alpha$ -aminoalkyl radical **2.1.62A** (Scheme 32). This mechanism was proposed on the basis of quantum yield measurements.<sup>77</sup>

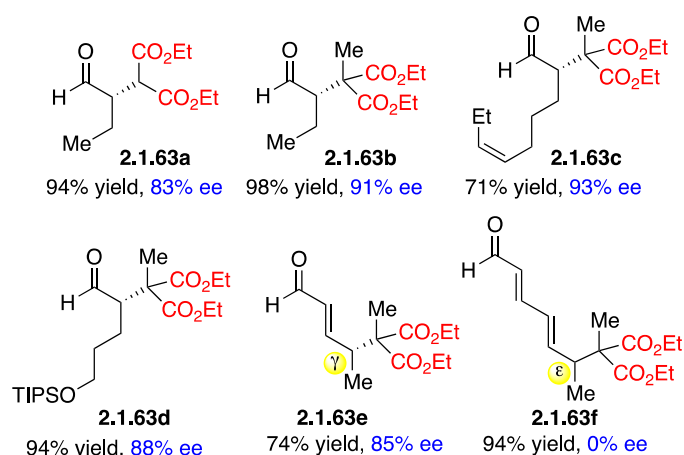
### Scheme 32 Enantioselective $\alpha$ -Alkylation of Aldehydes using Photoexcited Enamines



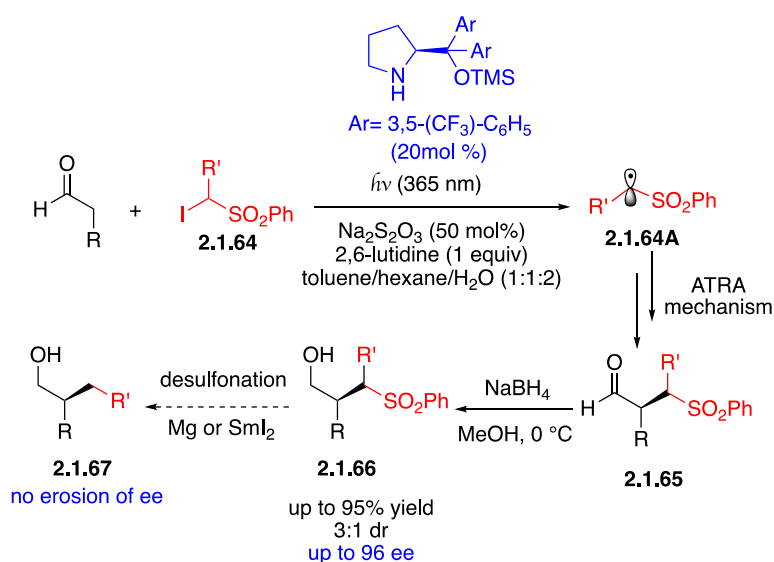
Interestingly, this self-propagating radical chain mechanism enabled  $\gamma$ -malonation, through a dienamine activation, in a more efficacious way than the benzylation in term of enantioselectivity (*vide supra*). However, the more challenging remote stereocontrol to

functionalize  $\epsilon$ -position (trienamine activation) of conjugated dienals was less successful (Scheme 33), high yield for the product was observed but in racemic form (**2.1.42f**). This result is likely due to the long distance between the reactive radical and the chiral proline sites, which reduces enantiofacial discrimination.

### Scheme 33 Self Propagating Radical Chain Reaction for $\gamma$ -Functionalization of Aldehydes



### Scheme 34 Photoexcited Enamines: $\alpha$ -Functionalization of Aldehydes using Phenylsulfonyl Alkyl Radicals

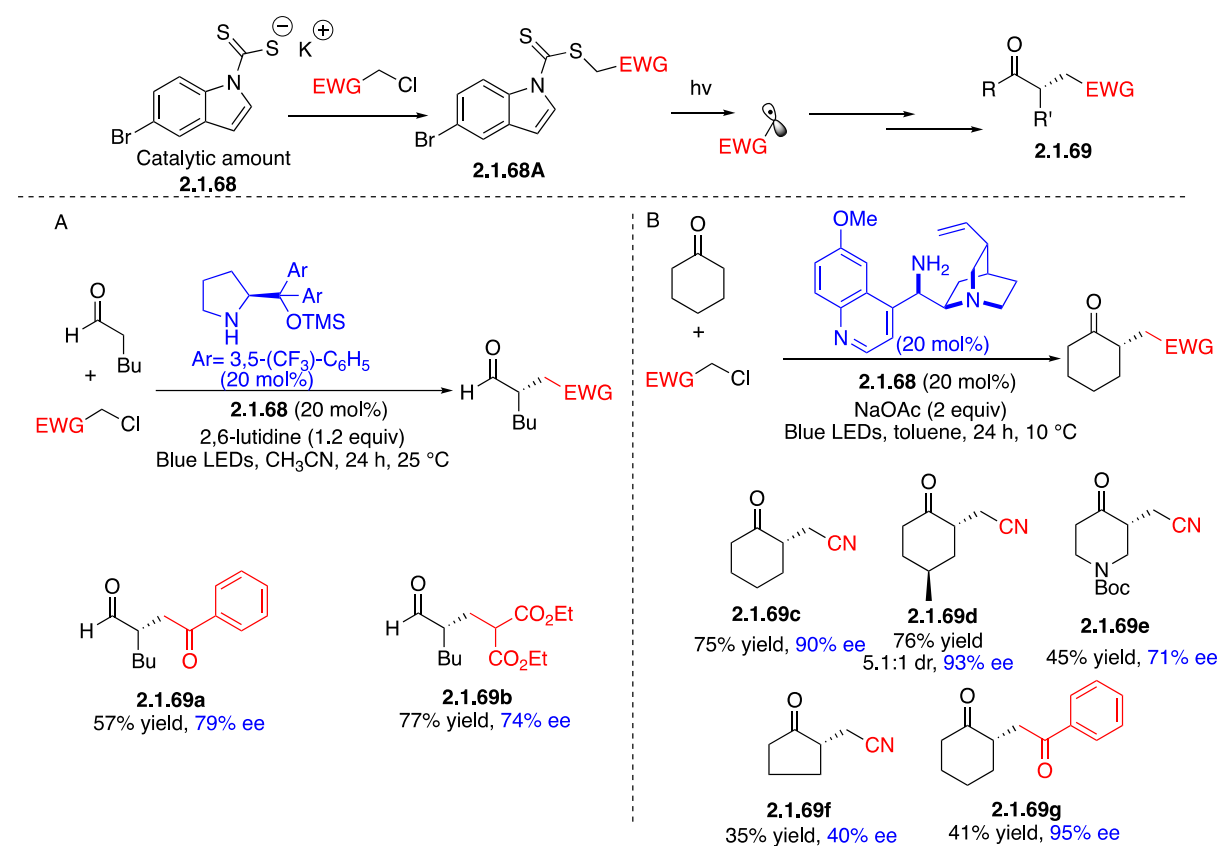


Photoexcited enamine activation strategy was further extended to (phenylsulfonyl)alkyl iodide with high stereochemical control (Scheme 34).<sup>80</sup> Given the propensity of  $\alpha$ -sulfonylalkylated



aldehydes **2.1.65** to racemization, the corresponding alcohols **2.1.66** were obtained, after *in situ* reduction, with good yields, high ee's, and moderate diastereoselectivity. Reductive desulfonation using SmI<sub>2</sub> or magnesium was achieved with no erosion of ee. An identical mechanism (SET and ATRA) as one shown in Scheme 32 has been proposed for the incorporation of (phenylsulfonyl)alkyl groups into aldehyde.

### Scheme 35 $\alpha$ -Functionalization of Aldehydes using Photochemically Generated Radicals from Alkyl Chlorides

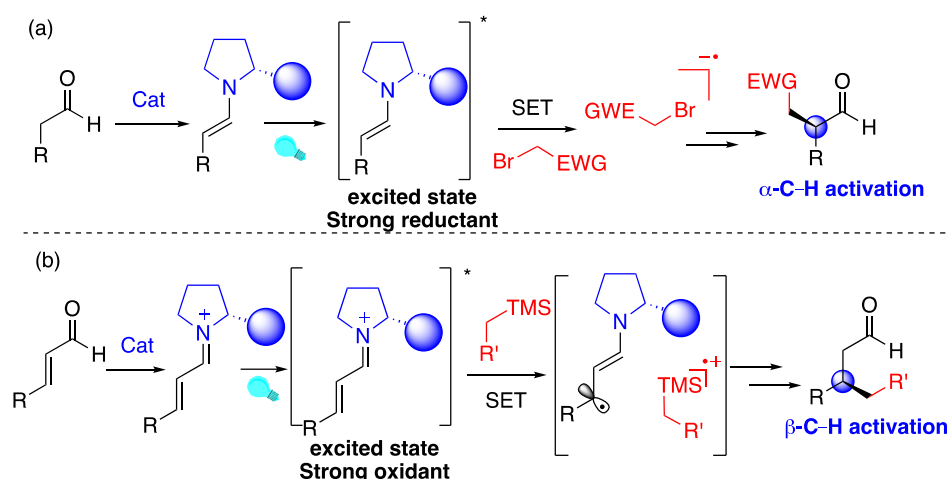


The same group disclosed a photochemical catalytic approach to generate radicals from alkyl chlorides (that are redox inert to generate radicals) using a nucleophilic dithiocarbonyl anion **2.1.68** in catalytic amount. Upon homolytic photocleavage of the *in situ* formed C-S bond in **2.1.86A**, the resulting radical can be incorporated in an enantioselective alkylation of aldehydes (Scheme 35A).<sup>81</sup> With proline derived catalyst, good ee's (up to 79%) were obtained. The authors have also applied this strategy with cyclic ketones. These latter substrates, in the

presence of cinchona-based organocatalyst, are able to give the  $\alpha$ -alkylated ketone **2.1.69c-g** in with enantioselectively, except for cyclopentanone **2.1.69f** (Scheme 35B).<sup>82</sup>

In all of the above examples, the enamine activation involved  $\alpha$ -sp<sup>3</sup> carbon which in turn could be regarded as a C–H activation with electron poor substrates. Activation of C(sp<sup>2</sup>)–H through a radical  $\beta$ -alkylation of enals is more challenging. In 2017, Melchiorre group envisaged a strategy by exploiting the oxidative power of excited conjugated iminium to react with electron rich substrates (Scheme 36).<sup>83</sup> In part b, the SET event may just be an initiation step and then, the nucleophilic radical could add to the iminium and propagate a radical chain with the resulting radical cation oxidizing the silane.

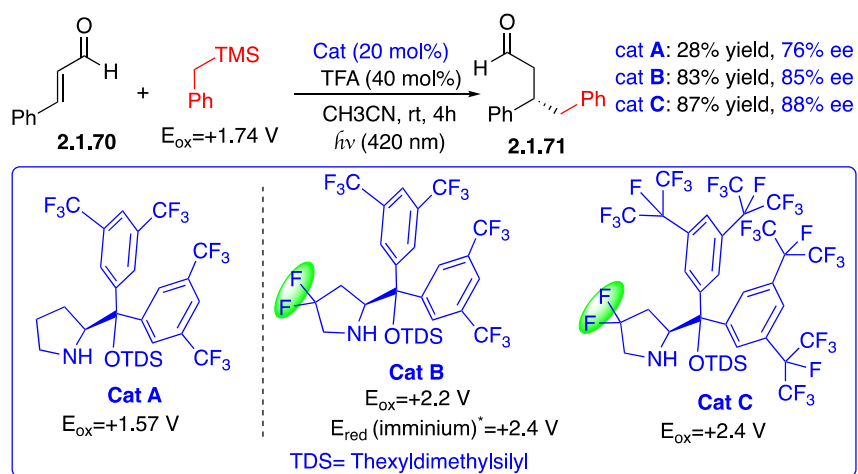
### Scheme 36 $\beta$ -Functionalization of Aldehydes using Conjugated Iminium Ion in the Excited State



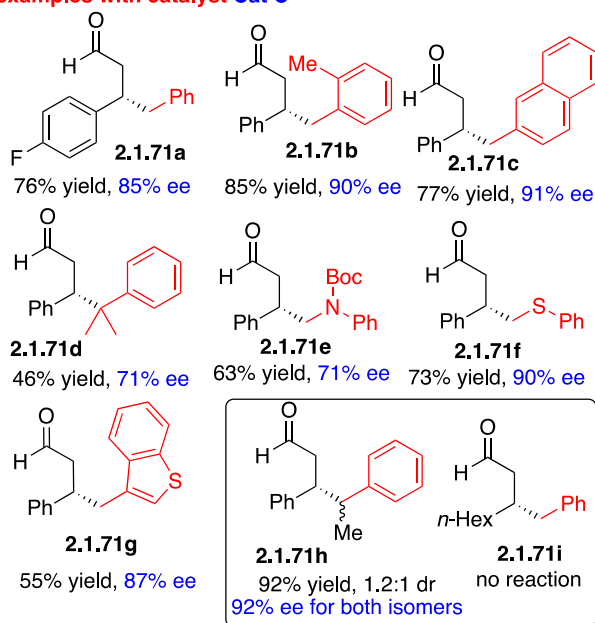
This methodology was elegantly applied for  $\beta$ -alkylation of conjugated enals using alkyl silanes. The low oxidation potential of the silane in addition to a rapid C–Si bond cleavage to afford a benzyl radical after oxidation are central for success of the reaction. To eliminate the competing oxidation of the catalyst by the iminium ion in the excited state,<sup>82</sup> the authors have judiciously incorporated two fluorine atoms into the catalyst. This has a consequence in the enhancement of the  $E_{\text{ox}}$  (2.2 V) for the catalyst preventing its oxidation and leaving the silane substrate with a lower  $E_{\text{ox}}$  to be oxidized.<sup>84</sup> The  $\gamma$ -rule establishes therefore the thermodynamic

feasibility of the SET oxidation between the excited iminium ( $E_{\text{red}} = 2.4 \text{ V}$ ) and the organosilane ( $E_{\text{ox}} = 1.74 \text{ V}$ ). More importantly, the presence of *gem*-fluorine atoms in catalyst **B** induces higher enantiocontrol than the non-fluorinated catalyst **A** (Scheme 37). Moreover, because of  $E_{\text{ox}}$  below that of the substrate, catalyst **A** is degraded through an oxidative path explaining a lower yield (28%) observed in this case. Catalyst **C** gave the best efficiency. Considering the redox potentials of intermediates (endergonic set), a radical chain mechanism has been excluded.

### Scheme 37 $\beta$ -Alkylation of Conjugated Enals using Alkyl Silanes



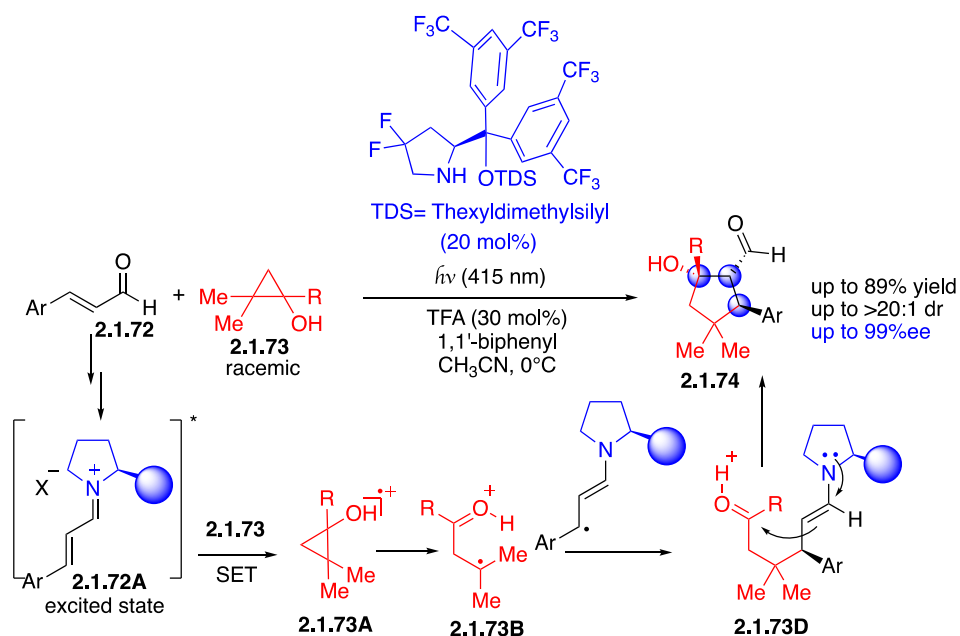
#### Selected examples with catalyst Cat C



A nice diversity is achieved either by changing the nature of the cinnamaldehyde or by modifying the benzyl silane and good enantiomeric ratios and yields were obtained (Scheme 37). However, as is often the case in radical chemistry, a modest diastereoselectivity was observed when two vicinal stereocenters are present in the product like in **2.1.71h**. Another limitation of the method is the use of  $\beta$ -substituted alkyl enal to reach compound **2.1.71i**, where no reaction was observed. Benzyl silanes derived from different aromatics, including heteroaromatics, afforded products in moderate to high yields and ee up to 91%.  $\alpha$ -silyl amine and  $\alpha$ -silyl thioether could also be engaged in the oxidative alkylation process.

As delineated above, the choice of readily fragmentable group is crucial to modulate redox ability of the partners to generate the transient radicals which are ready to recombine. However, as mentioned above in most forthcoming cases, alternative radical chain processes can be imagined.

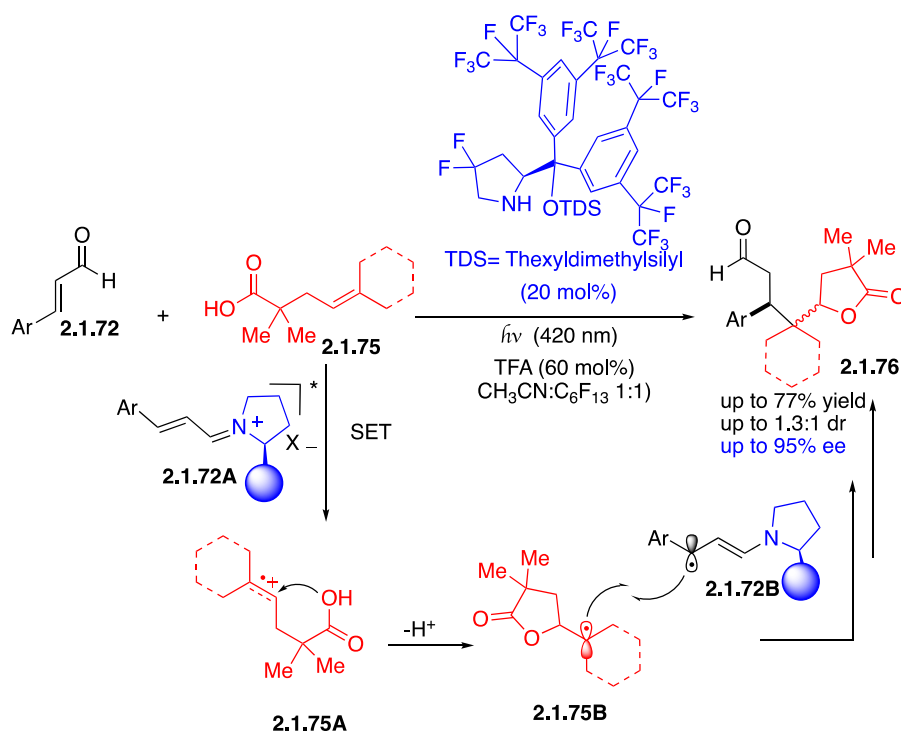
### Scheme 38 Radical Cascades using Cyclopropanols



The Melchiorre group expanded the application of this methodology by varying the nature of the fragmentable group. Successful implementation of the photoexcitation route was achieved in the field of cascading radical reactions. Indeed, constrained skeleton like cyclopropane is

commonly used fragmentable group, notably as a radical clock in mechanistic studies. Thus, cyclopropanols **2.1.73** were selected as SET partners for oxidation to release oxycyclopropyl radical cation **2.1.73A** (Scheme 38). Because of the high tendency for ring opening,<sup>85</sup> the cyclopropyl group delivers a tertiary radical **2.1.73B** able to couple with the  $\beta$ -enaminy radical **2.1.72A** emerging from SET, establishing the first stereocenter. A classic ionic nucleophilic aldol cyclization affords the cyclopentanol **2.1.74**.<sup>86</sup> It is important to note that control experiments demonstrated that this last step obeys a kinetic resolution regime. In this overall radical/polar crossover reaction,<sup>87</sup> the close proximity of the prolinol catalyst delivers the product with three contiguous stereocenters with high enantio- and diastereocontrol. Despite the broad scope of the reaction, a limitation to the method is the requirement of cinnamaldehyde derivatives as starting materials. Another limitation to this method is the need for the presence of *gem*-dimethyl groups in the cyclopropyl moiety that helps the cyclization through a Thorpe-Ingold effect.

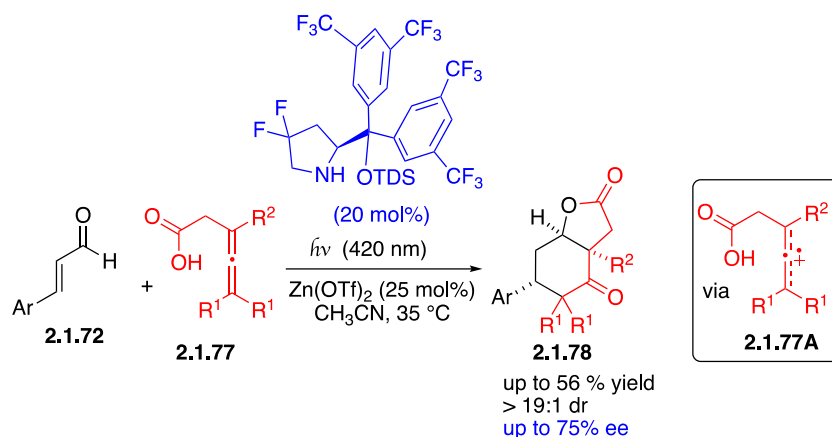
### Scheme 39 Polar/radical Crossover Cascade Reactions



Additional polar/radical crossover cascade reactions were reported in 2018.<sup>88,89</sup> Melchiorre and co-workers found that unactivated olefins tethered to a nucleophilic partner (**2.1.75**) exhibit well-behaved oxidation potential in the range +2.03 to +2.19 V, i.e., within the range of the reduction potential of the excited iminium (2.40 V) as discussed above. Formation of a radical cation through **2.1.75A** a SET offers the possibility to undergo a lactonization followed by radical recombination between **2.1.75B** and **2.1.72B** to furnish the desired product **2.1.76** in good yields, high ee's and modest diastereomeric ratios (Scheme 39). A three-component cascade variant has also been developed.

To overcome the poor diastereoselectivity observed in this cyclization, it has been proposed that the use of tethered allenes **2.1.77** with similar oxidative behavior (passage from a radical cation **2.1.57A**) offers a better opportunity to reach complex scaffolds as single diastereoisomers (Scheme 40).<sup>90</sup>

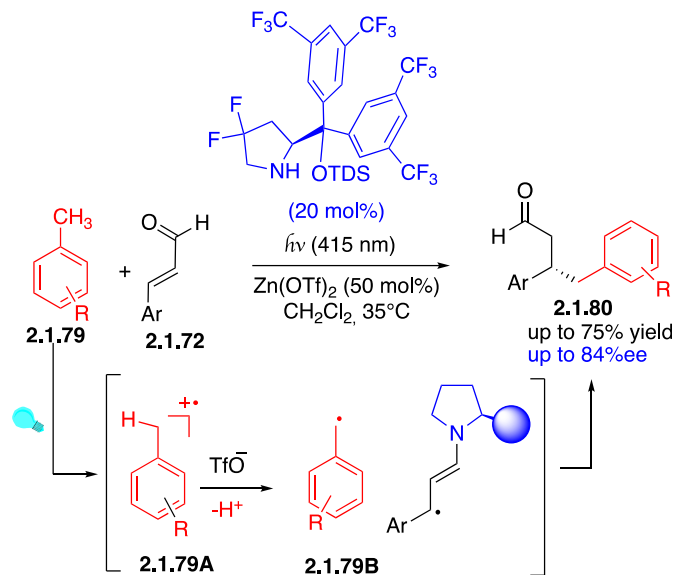
#### Scheme 40 Highly Diastereoselective Radical Cyclization using Allenes



The high oxidation power of excited-state iminium ion was also used to trigger toluene oxidation. It is important to note that these species are difficult to oxidize through electron transfer. Addition of Lewis acid Zn(OTf)<sub>2</sub>, whose conjugated base serves to deprotonate the radical cation of toluene arising from SET, is critical for the generation of benzyl radical and prevent Back-Electron Transfer (BET). Radical-radical coupling with the  $\beta$ -enaminy radical

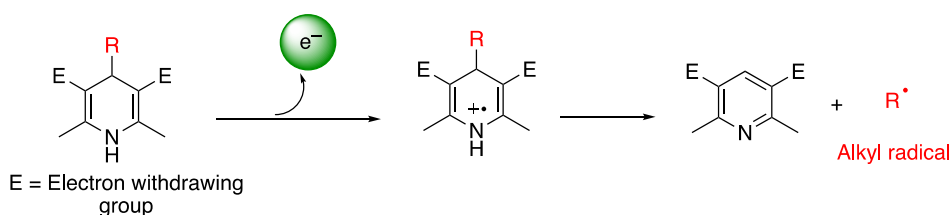
**2.1.79B** provides benzylated product, after hydrolysis of the resulting iminium ion (Scheme 41).<sup>91</sup>

### Scheme 41 Benzyl Radical Coupling with $\beta$ -Enaminy Radical



Melchiorre has continued to develop a range of photochemical radical reactions. With an aim to photogenerate alkyl (or acyl) radicals, 4-alkyl Hantzsch esters (HE) served as precursors for open-shell species.<sup>92</sup> This concept has been previously used to generate radicals and the field has been reviewed recently (Scheme 42).<sup>93</sup>

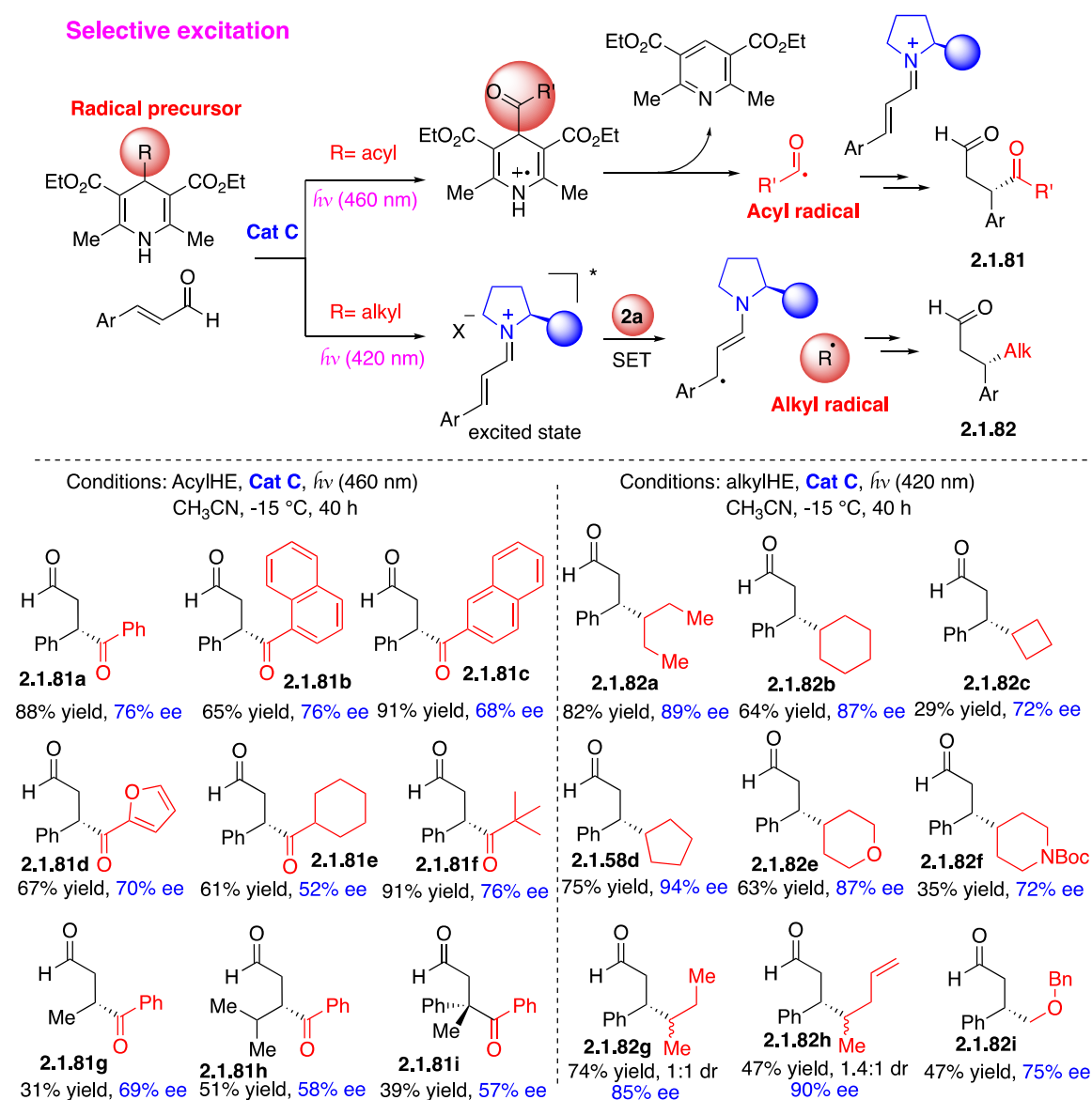
### Scheme 42 Alkyl Hantzsch Esters (HE) as Radical Precursors



The DHP entity bearing an acyl group absorbs in the visible region and it can be excited at 460 nm to serve as the photoexcited partner to give, after decomposition to pyridine derivative, an acyl radical (Scheme 43).<sup>94</sup> Giese-type addition of this acyl radical to the chiral iminium intermediate is the stereodetermining step for the  $\beta$ -acylation of cinnamaldehydes.<sup>95</sup>

## Scheme 43 Giese-type Addition of Acyl and Alkyl Radicals to Chiral Iminium

### Intermediate



The scope of the acylation reaction revealed that a variety of substituents are tolerated (Scheme 43).<sup>94</sup> Aryl, alkyl as well as heteroaryl groups could be introduced from the acyl function with moderate results. Interestingly, the challenging use of enals bearing alkyl fragments instead of cinnamaldehydes is possible, albeit with low yields. The  $\beta,\beta'$ -substituted enal afforded the desired 1,4-dicarbonyls **2.1.81i** possessing a quaternary carbon in 39% yield and 57% ee.

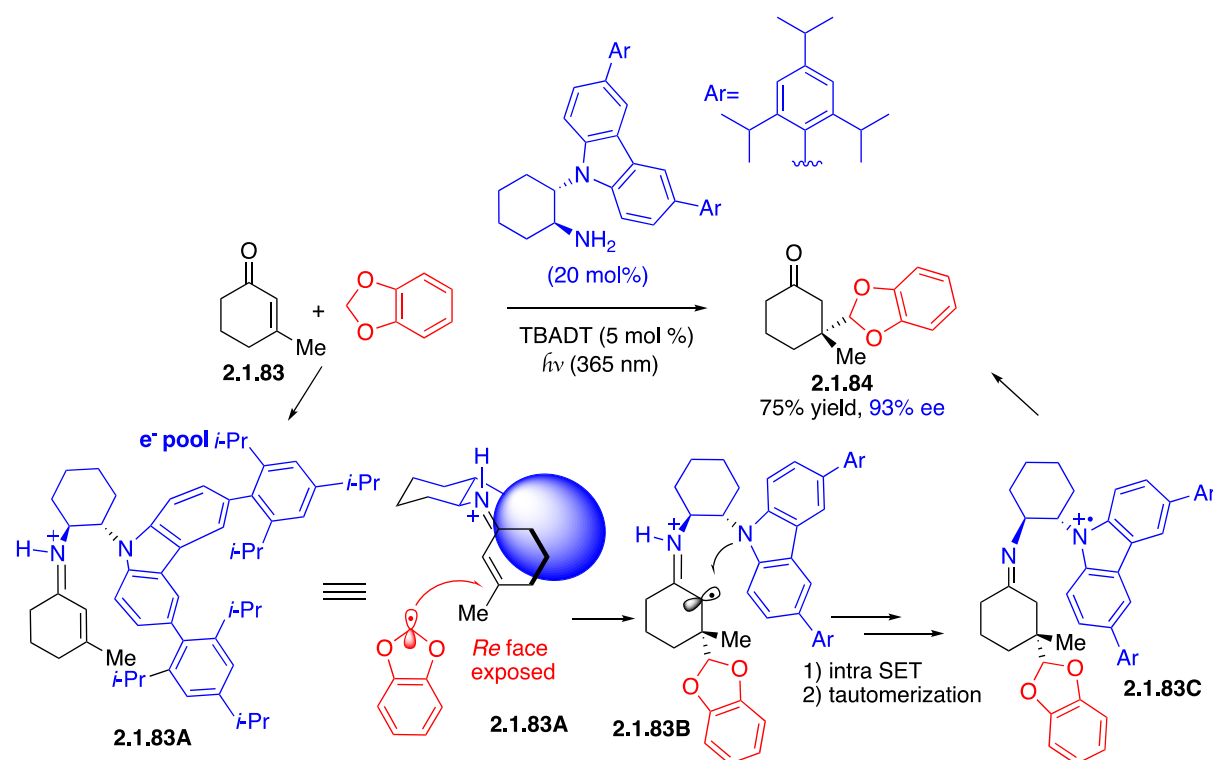
Whereas the alkylation strategy is applicable to only cinnamaldehyde substrates, alkyl-HE allowed a chemical diversity in the product obtained in low to high yields depending on the



nature of the alkylating partner (Scheme 43).<sup>96</sup> For stability reason, primary alkyl group is not suitable except when a stabilizing  $\alpha$ -heteroatom is present. Some limitations were also found in the presence of olefinic substrate (product **2.1.82h**, 47 % yield), this reactive moiety gave side reactions. The cyclobutyl (**2.1.82c**) and piperidinyl DHP (**2.1.82f**) afforded poor yields, 29% and 35%, respectively. As previously mentioned, the low diastereoselectivity observed in the presence of a second stereocenter is also a limitation (**2.1.82h**), suggesting that a radical-radical coupling is involved in the mechanism.<sup>97,98</sup>

## Scheme 44 Functionalization of $\beta,\beta$ -Disubstituted Enones using Radical Conjugate

### Addition with Iminium Activation



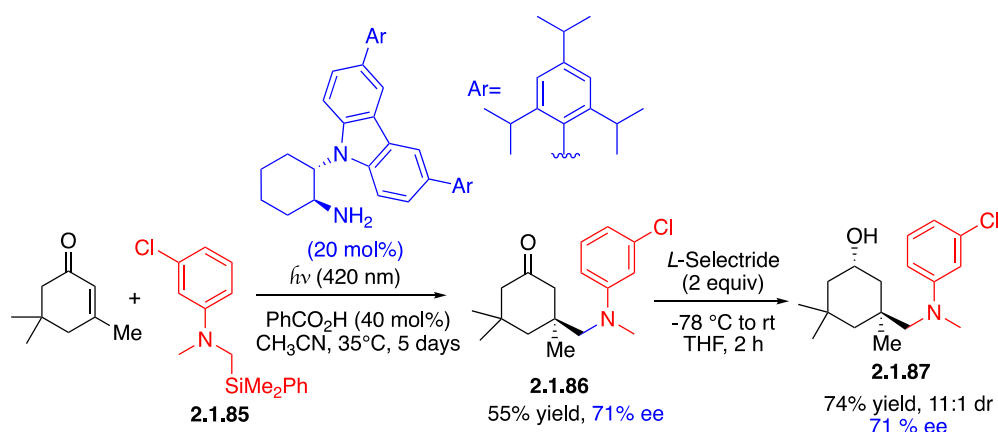
To close this section, we want to highlight the use of primary amines as photocatalysts to realize enantioselective radical conjugate additions (RCA). The first enantioselective RCA was reported in 1996 by Sibi and Porter using chiral Lewis acids to induce the stereoselectivity.<sup>99</sup> However, this methodology is limited to  $\beta$ -substituted enones. Functionalization of  $\beta,\beta$ -disubstituted enones using RCA with iminium activation that would form asymmetric quaternary carbon is therefore challenging. Indeed, the resulting  $\alpha$ -iminyl radical cation has a

tendency to undergo  $\beta$ -scission. Melchiorre has ingeniously envisioned to trap this unstable intermediate through an intramolecular SET using an “electron pool” fixed to the iminium intermediate **2.1.83A** (Scheme 44).<sup>58,100</sup> Electron rich carbazole moiety was envisioned to do this electron relay. The group selected chiral *trans* cyclohexyldiamine possessing a carbazole skeleton for successful organocatalytic RCA.

Nucleophilic radicals were generated first through a HAT from benzodioxole using photoexcited tetrabutylammonium decatungstate (TBADT) as the H-atom abstracting agent. During the addition of the radical, the bulky carbazole scaffold is positioned in a way to shield the *Si* face leaving the *Re* face exposed to the C–C bond formation with high enantiocontrol.

During their mechanistic studies, the authors crystallized the tetrafluoroborate salt of the iminium ion which showed an intense bright-yellow color. The broad absorption band in the visible region is induced by an intramolecular charge-transfer  $\pi$ - $\pi$  interaction. This intramolecular EDA complex was harnessed to generate alkyl radicals from organosilanes **2.1.85**. Using the electron relay mechanism, they succeeded in enantioselective RCA without the need of the external photoredox catalyst TBADT.<sup>101</sup> The authors applied the strategy for the synthesis of an epimer of a compound used for the treatment of influenza (**2.1.87**, Scheme 45). A more general asymmetric radical addition, using iminium-based catalysis, has been reported more recently.<sup>102</sup>

#### Scheme 45 Synthesis of a Compound by Radical Conjugate Addition to Treat Influenza

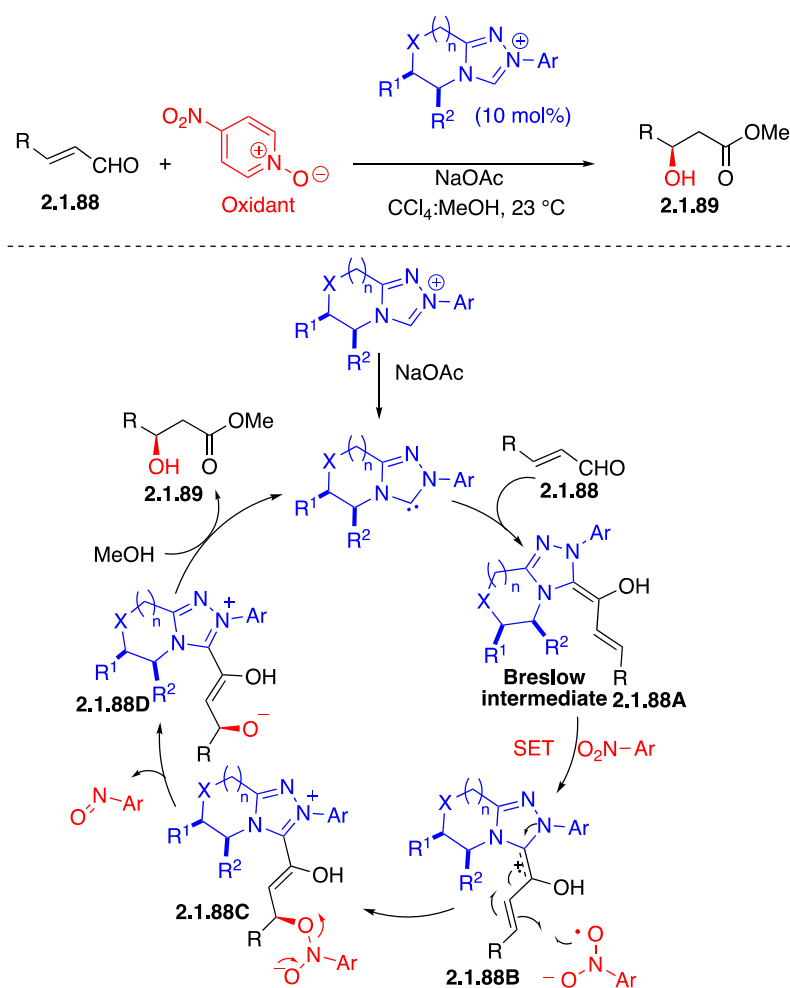


### 2.1.2. NHC-catalyzed coupling reactions using single electron transfer

A carbene is a neutral carbon species possessing six valence electrons. Spectacular advancements have been reported on the use of NHC carbenes as organocatalysts particularly for chemical transformations like benzoin condensation, Stetter reactions and enolate activation reaction using various aldehydes.<sup>103</sup> Great efforts have been exerted to understand the reactivity and stability of these species. Reaction of NHC-based homoenolate using a two-electron pathway is one of the popular transformations advanced in the two last decades. Pioneering work from the Studer group,<sup>104</sup> has demonstrated that reactions involving one-electron intermediates are possible and new achievements have emerged. Inspired by the natural process of pyruvate, Studer planned a SET mechanism between TEMPO and Breslow intermediate to generate a radical cation. In 2014, Rovis and co-workers showed that condensation of enals and NHC involves a  $\beta$ -hydroxylation in the presence of mild oxidant, 4-nitropyridine N-oxide.<sup>105</sup> Even though a SET mechanism is a matter of debate,<sup>106</sup> radical pathway is believed to be a part of this reaction.

The Rovis and Chi groups independently reported the first enantioselective radical reaction involving NHC catalysis.<sup>105,107</sup> The Rovis group used 4-nitropyridine *N*-oxide whereas the Chi group used nitrobenzenesulfonic carbamate. Both authors invoked a SET mechanism from the nitro compound to the Breslow intermediate (formed between enal and NHC catalyst). The homoenolate radical cation **2.1.88B** could evolve, after radical coupling forging the stereocenter and elimination of nitroso by-product, to form the intermediate **2.1.88D**. Protonation and displacement of the catalyst by methanol, releases the desired  $\beta$ -hydroxylated product **2.1.89** and regenerates the NHC catalyst (Scheme 46).

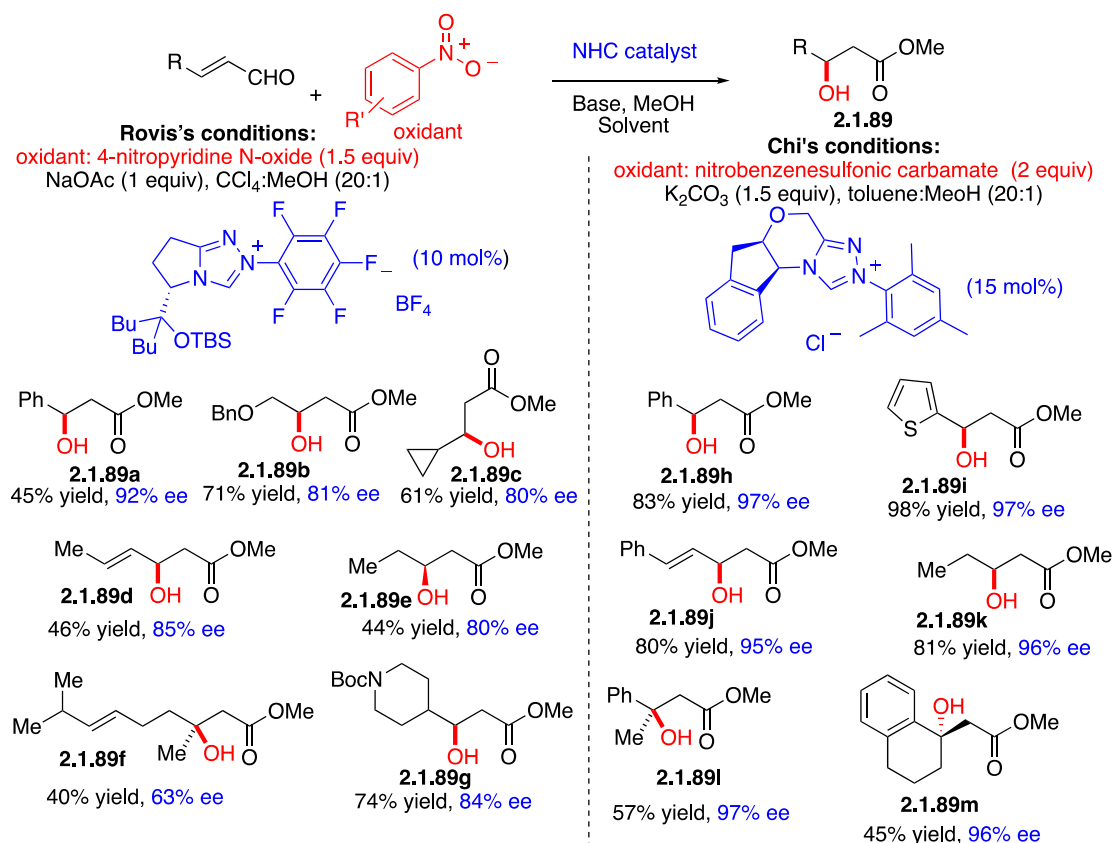
### Scheme 46 Synthesis of Acetate Aldols using Chiral NHC Catalysts



Several control experiments like EPR, spin-trapping with DMPO, cyclic voltammetry, and reaction with *Z*- and *E*-enals, were conducted to support this mechanism. It is important to mention that in both reports, the radical clock reactions did not show ring opening of the cyclopropyl ring suggesting that the radical formed is an  $\alpha$ -aminyl one. This hypothesis is more consistent with the results obtained by Martin and Bertrand.<sup>106</sup>

In this enantioselective  $\beta$ -hydroxylation of enals, the Chi's system is more general in scope and gave higher yields and ee's. Various alkyl and aryl substituted enals were tolerated giving up to 98 and 97% yield and ee, respectively (Scheme 47).

## Scheme 47 Enantioselective $\beta$ -Hydroxylation of Enals

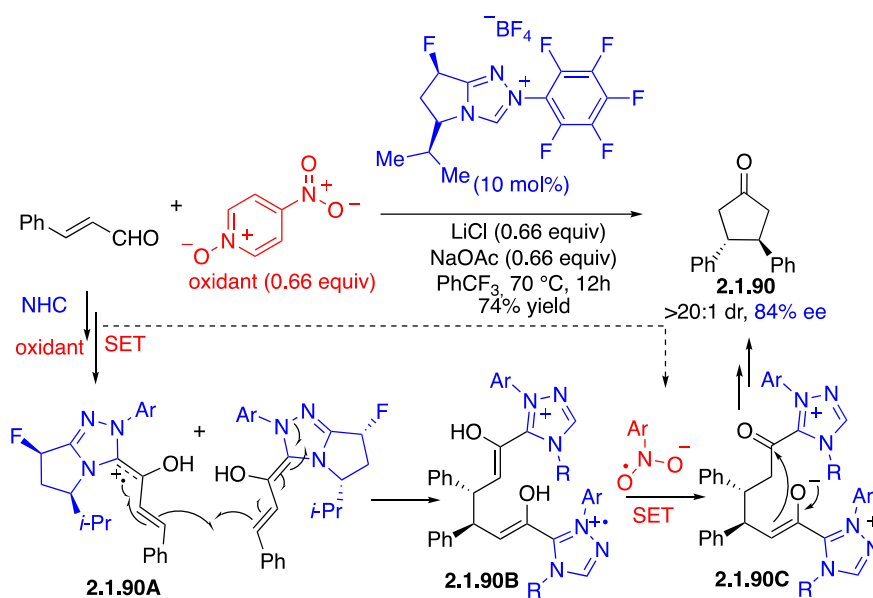


The Chi's group has developed a new class of chiral oxidant containing a nitro group for oxidation and a proline derived sulfonamide as a chiral inductor. Use of chiral NHC catalyst in adapted experimental conditions afforded the  $\beta$ -hydroxy esters in good yields and ee's.<sup>108</sup>

Subsequently, these two groups further extended their findings to other applications. For instance, Rovis demonstrated that homo-coupling of enals is possible.<sup>109</sup> Following the same protocol described above and using only 0.66 equivalent of the oxidant and in the absence of methanol, *trans*-diarylcyclopentanones were obtained in good yields, high diastereomeric ratios and ee's. This is a radical/polar crossover reaction based on a SET process triggered by 4-nitropyridine *N*-oxide. The resulting radical cation intermediate adds - through a conjugate addition - to the Breslow intermediate to generate the *trans* homocoupling intermediate, which undergoes a second SET to form an acyl azolium intermediate. Intramolecular displacement of NHC by the enolate followed by hydrolysis delivers the C<sub>2</sub> symmetric cyclopentanone and

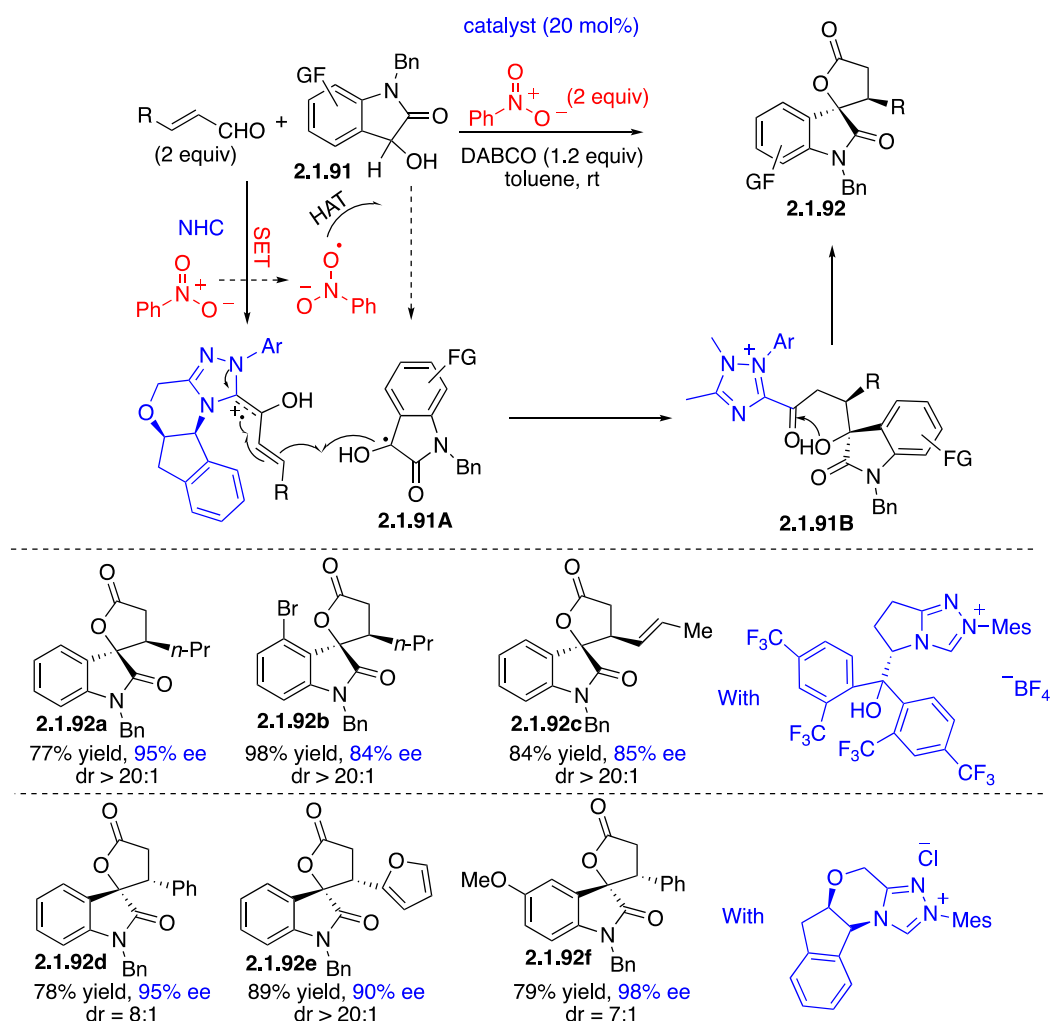
releases the catalyst (Scheme 48). Heterocoupling using mixed cinnamaldehyde analogs was also proven to be effective in this transformation to obtain nonsymmetric 3,4-disubstituted cyclopentenones **2.1.90** in good yields and high ee's.

### Scheme 48 Synthesis of C<sub>2</sub> Symmetric Cyclopentanones using NHC Carbenes



In 2017, Chi and co-workers used polyhalides as an efficient oxidant for NHC-catalyzed radical reactions. Enantioselective synthesis of lactone and lactam products using this strategy was disclosed. They evaluated the potential of CCl<sub>4</sub> and C<sub>2</sub>Cl<sub>6</sub> to initiate two successive single electron transfers and found that C<sub>2</sub>Cl<sub>6</sub> can effectively oxidize the Breslow intermediate to an acyl azolium intermediate. The acyl azolium intermediate undergoes lactonization/lactamization in the presence of 1,3-dicarbonyls or imines.<sup>110</sup> This reaction is more in agreement with two-electron annulation rather than a radical transformation.<sup>111,112</sup> Nevertheless, a formal [3+2] annulation catalyzed by NHC through a radical process has been reported by Ye in 2017.<sup>113</sup> Enantioenriched spirooxindoles could be obtained from enals and dioxindoles using chiral NHC catalyst and nitrobenzene as an oxidant (Scheme 49).

### Scheme 49 Formal [3+2] Annulation Catalyzed by NHC through a Radical Process

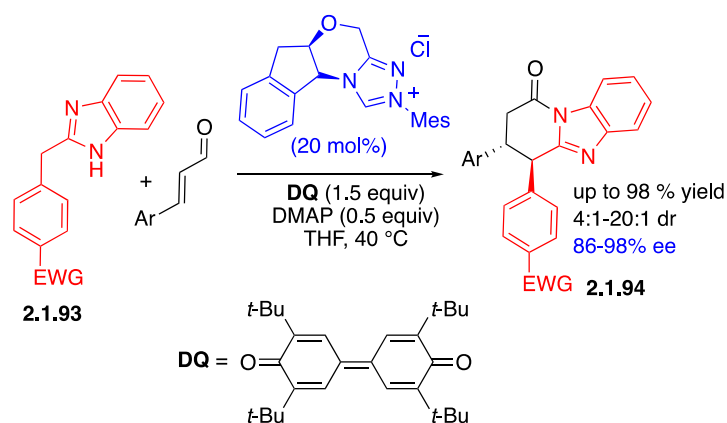


The mechanism is believed to engage a radical/radical cross-coupling between the radical cation and the captodative radical **2.1.91A**. The latter would be obtained from a HAT process between the nitrosyl radical and oxindole. After tautomerization, intramolecular lactonization of the acyl azolium **2.1.91B** gives the spiro cycloadduct **2.1.92**. Evaluation of the scope of this oxidative annulation demonstrated a tolerance for aliphatic, aromatic and heteroaromatic enals as well as oxindole incorporating electron withdrawing and donating groups. The aliphatic enals afforded higher diastereoselectivities than cinnamaldehyde counterparts, in the latter case there was a need for additional DBU (0.2 equiv). Reaction with  $\alpha,\beta,\epsilon$ -unsaturated aldehyde afforded oxindole **2.1.92c** in 84% yield and 85% ee as a single diastereomer, no reference to  $\epsilon$ -side product was reported in this publication. Absolute configurations of the product obtained from

cinnamaldehyde was characterized by X-ray analysis and surprisingly was opposite to that obtained with alkyl enals using the same catalyst. The absolute stereochemistry of the alkyl substituted compound was established by comparison of its the optical rotation with that of the same product obtained in previous work,<sup>114</sup> itself assigned by analogy with analogous spirooxindole. Therefore, a careful attention should be paid when assigning absolute configurations.

According to the careful mechanistic study from Bertrand and Martin, nitrobenzene ( $E_{\text{red}} = -0.9$  V) is not strong enough to engage in a SET reaction with Breslow intermediate. Regarding the presence of a base in the reaction medium, they suggested that the deprotonated form of Breslow intermediate is the SET reductant.<sup>106</sup> Later on, the use of  $\beta,\beta'$ -unsaturated cinnamaldehydes giving spirooxindoles bearing two contiguous tetrasubstituted stereocenters was published by the same group,<sup>115</sup> through a radical reaction.

### Scheme 50 Synthesis of Highly Functionalized Heterocycles using NHC Carbenes



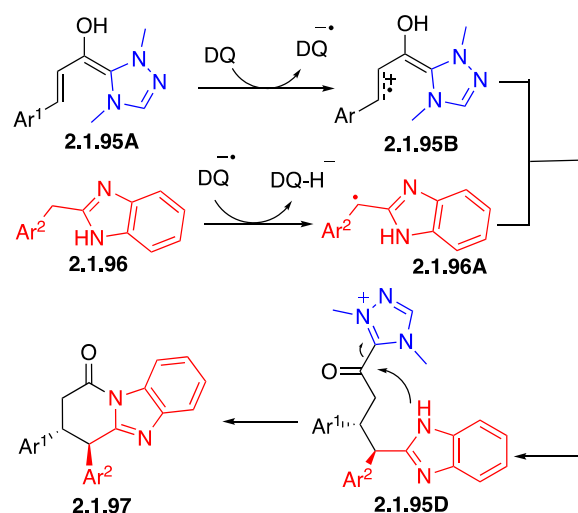
A combination of HAT and SET mechanisms was proposed by Chi to obtain enantioenriched heterocycles fused to benzimidazole through asymmetric NHC-catalysis.<sup>116</sup> Highly functionalized heterocycles were obtained in good to excellent yields and stereoselectivities (Scheme 50).

The reaction comprises of a C-H functionalization of diarylmethane **2.1.96** using enals and 3,3',5,5'-tetra-*tert*-butyl-4,4'-diphenylquinone (DQ) as the oxidant. The diarylmethane

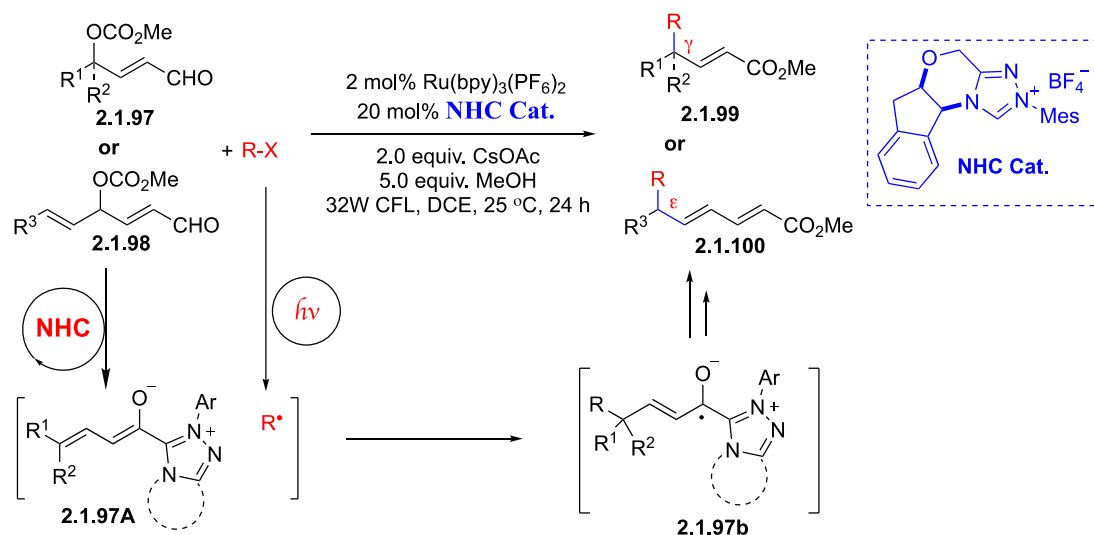


derivative accepts only electron-withdrawing groups to generate a radical, upon HAT from diphenylquinone radical anion (Scheme 51). This requirement suggests that a deprotonation involving a polar mechanism is more likely to proceed. However, other experiments show that a radical pathway cannot be completely ruled out.

**Scheme 51 Mechanism for C-H Functionalization of Diarylmethane using NHC Enals and 3,3',5,5'-tetra-tert-butyl-4,4'-Diphenylquinone (DQ) as the Oxidant**



**Scheme 52 The  $\gamma$ - and  $\epsilon$ -Alkylation of Enals via Dual Catalysis**



Ye et al. developed  $\gamma$ - and  $\epsilon$ -alkylation of enals **2.1.97** or **2.1.98** with alkyl radicals ( $R^\bullet$ ) for the synthesis of  $\gamma$ -multisubstituted- $\alpha,\beta$ -unsaturated esters including vicinal all-carbon quaternary centers **2.1.99** or **2.1.100** by merging photoredox catalysis using  $\text{Ru}(\text{bpy})_3(\text{PF}_6)_2$  photocatalyst

with *N*-heterocyclic carbene (NHC) catalysis (Scheme 52).<sup>117</sup> The stereoselective addition of alkyl radical (R·) to the dienolate **2.1.97A** (or trienolate intermediate) is the key step of this reaction. The alkyl radical (R·) is generated from alkyl halide R-X by Ru(bpy)<sub>3</sub>(PF<sub>6</sub>)<sub>2</sub> catalyzed photocatalysis whereas intermediate **2.1.97A** is generated from enal by NHC catalysis (Scheme 52).

In summary, *N*-heterocyclic carbenes demonstrate high efficiency in asymmetric radical reactions. Even though involvement of an open-shell species is not always questioned, the area is still open to unraveling the black box nature of mechanistic details of this reaction.

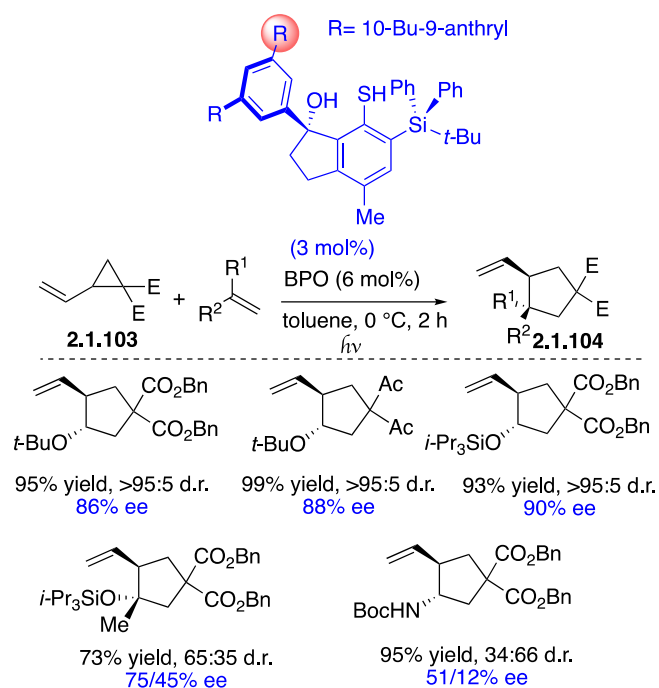
### 2.1.3 Asymmetric catalysis involving chiral thiyl and stannyl radicals

The first use of chiral organotin hydride to discriminate the prochiral faces in radical chemistry was independently reported by Curran and Metzger.<sup>118,119,120</sup> However, the chiral reducing agent was used in stoichiometric amount and only moderate stereoselectivity was observed.

Four decades later, to develop a successful catalytic variant, the Maruoka group proposed an enantioselective radical cyclization catalyzed by organotin hydride using stoichiometric Ph<sub>2</sub>SiH<sub>2</sub> as a reducing agent (Scheme 53).<sup>121</sup> Addition of chiral stannyl radical to aldehyde connected to an internal alkene **2.1.101** afforded heterocycle **2.1.02** in good yield albeit with moderate enantio- and diastereoselectivity (53% ee, 87:13 dr). Initiation step is assumed by AIBN, then addition of the chiral stannyl radical to aldehyde moiety generates *O*-stannyl ketyl radical **2.1.101A** which adds to pendant alkene giving the resulting heterocyclic radical **2.1.101B** possessing organotin alkoxide. In this stereoselective C-C bond formation, the temporarily installed organotin catalyst governs the approach of the olefin. A radical chain mechanism is maintained through hydrogen atom abstraction from chiral organotin hydride with intermediate **2.1.101B** with concomitant regeneration of the active catalyst. Protonation of organotin alkoxide **2.1.101C** furnishes the product and organotin ethoxide. The regeneration of the dormant catalyst is achieved by Ph<sub>2</sub>SiH<sub>2</sub> used in stoichiometric amount.



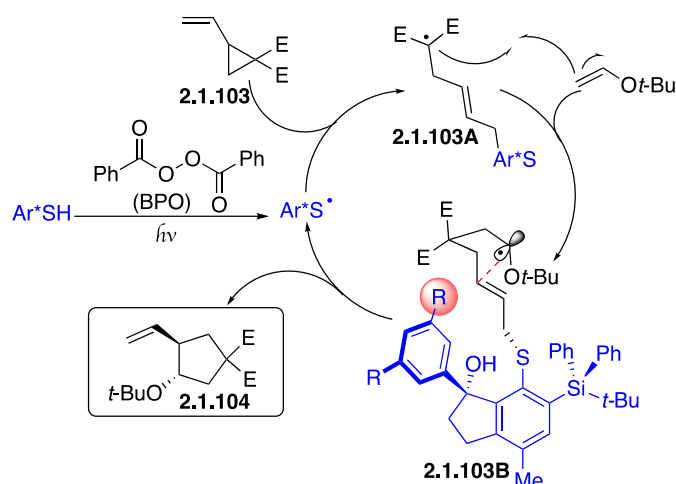
## Scheme 55 Chiral Thiols in the Synthesis of Vinylcyclopentanes



Chiral thiol used as an organocatalyst in the presence of light and benzoyl peroxide (BPO, 6 mol%) generates an aryl sulfanyl radical which reacts with vinyl cyclopropane generating the  $\alpha$ -cyclopropyl radical.  $\beta$ -scission opens the ring and affords the stabilized electrophilic radical **2.1.103A** (Scheme 56). Addition to electron rich olefin furnishes radical **2.1.803B** which is involved in a cyclization followed by  $\beta$ -fragmentation of the pendant chiral thiyl radical precursor allowing the turnover of the catalyst. This addition-elimination step is the stereocontrolling step and is assisted by the presence of a transient chiral template leading to high enantio- and diastereoselective cyclization (up to 95:5 dr and 90% ee). The rate of the addition step ( $10^6 \text{ M}^{-1} \text{ S}^{-1}$ ) and  $\beta$ -scission (under diffusion control) is critical for the success of the cascade. A well-designed chiral catalyst by introducing a bulky aryl group (shielding the *Si* face) at the stereocenter allows for a formal  $\text{S}_{\text{N}}2'$  approach from the *Re* face.

Enantioselective formation of cyclopentane derivatives was also reported by Miller using the same concept with disulfide-bridged peptide as a source of chiral thiyl radical.<sup>126</sup>

## Scheme 56 Mechanism for the use of Chiral Thiols for Cyclopentane Formation

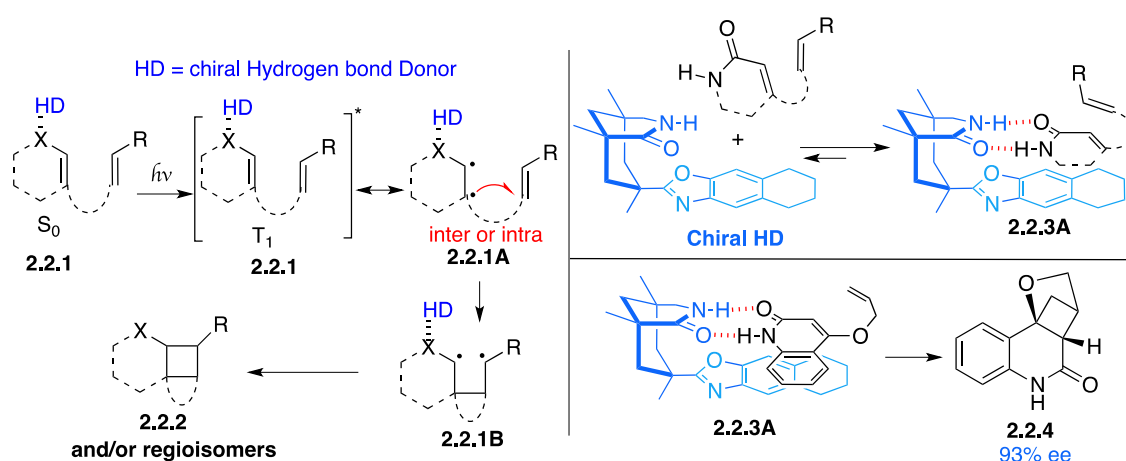


## 2.2. Non-covalent-based mode of activation

### 2.2.1. Hydrogen-bonding mediated organocatalyzed radical reactions

Weak hydrogen bonds are known to be involved in many processes in natural systems. Inspired by nature, organic chemists have used this phenomenon to design chiral catalysts to perform numerous asymmetric transformations.<sup>127</sup> Extending this concept to enantioselective radical reactions constitutes a major challenge given the weakness of hydrogen bond activation and the inherent reactivity of radical intermediates.<sup>128</sup>

## Scheme 57 Chiral Hydrogen Bond Donor in Enantioselective [2+2] Photocycloaddition



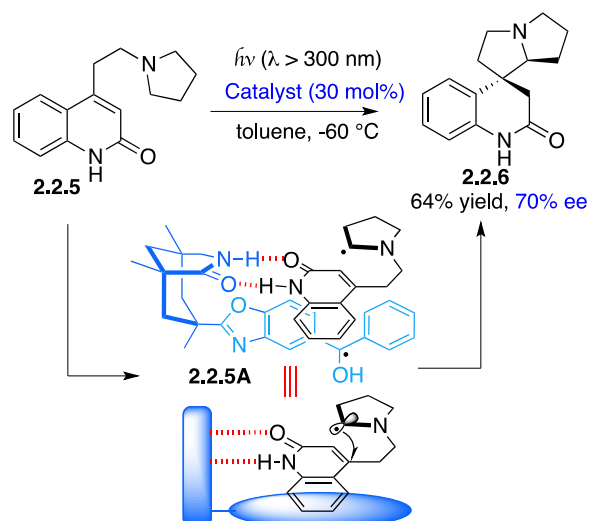
Owing to the known role of hydrogen bonding in the control of diastereoselectivity in cycloaddition reactions, Bach investigated the possibility of controlling enantioselectivity using chiral complexing agents when used in excess amounts (up to 2.5 equiv) (Scheme 57). The

Bach group designed a U-shape two-point interaction chiral template derived from Kemp's triacid for [2+2] photocycloadditions and radical cyclizations through direct excitation of the substrate **2.2.1**.

Total synthesis of (-)-pinolinone and (+)-meloscine were reported employing the lactam hydrogen bonding enantioselective [2+2] photocycloaddition as the key step.<sup>129,130</sup>

In their effort to develop catalytic enantioselective photochemical reactions, the Bach group focused on energy transfer (or SET) between the chiral catalyst and the substrate through catalyst sensitization. In addition to the sensitization aspects, the choice of the catalyst for enantioface differentiation of the olefin was also critical. The linkage via a rigid oxazole revealed a better ability to induce high stereocontrol. Indeed, the Bach's group achieved a major breakthrough, and the first asymmetric radical reaction based on this concept of hydrogen bond activation was reported in 2005.<sup>131</sup> After excitation ( $\lambda > 300$  nm) of the benzophenone catalyst and SET with quinolone substrate **2.2.5** (or alternative remote HAT<sup>132</sup>), enantioselective RCA of the resulting  $\alpha$ -amino alkyl radical to enone moiety affords spirocyclic product **2.2.6** in 64% yield and 70% ee as a single diastereomer (Scheme 58). The shielding from the quinolone of the *Si* face allows the upper *Re* face for radical addition. Back electron transfer from the catalyst to the substrate followed by a deprotonation makes catalytic turnover possible.

### Scheme 58 Chiral Hydrogen Bond Mediated Radical Conjugate Addition



When the catalyst loading was lowered to 5 mol%, the product was isolated in 61% yield and only 20% ee, an indication that uncatalyzed radical chain reaction operates. This observation limits the application of the methodology to reactions with radical chain mechanism.

The Bach group has also shown that a hydrogen-bonding catalyst is suitable for photocycloaddition reactions. In 2009, they reported enantioselective intramolecular [2+2] photocycloaddition using quinolone tethered alkenes.<sup>133</sup> After modification of the catalyst structure by introducing a xanthone photosensitizer and again due to the two-point hydrogen bonding at the lactam motif, excellent enantiocontrol was achieved using 10 mol% loading. Instead of SET (or HAT) mechanism, alternative mode of action through energy transfer from the xanthone to the substrate is illustrated in Scheme 59. The success of the strategy is based on the selective excitation of the xanthone moiety with a maximum of absorption at 350 nm. UV measurements showed that little spectral overlap at this region with the substrate. Therefore, irradiation at 366 nm will allow the excitation of the catalyst and not the substrate. Higher energy transfer ( $\sim 310 \text{ kJ mol}^{-1}$ ) for xanthone than for the quinolone substrate ( $\sim 280 \text{ kJ mol}^{-1}$ ) is also an important criterion. Finally, sensitization in the complex is found faster than intermolecular one, which guarantees an efficient asymmetric catalysis and prevents the detrimental non-enantioselective background reaction.

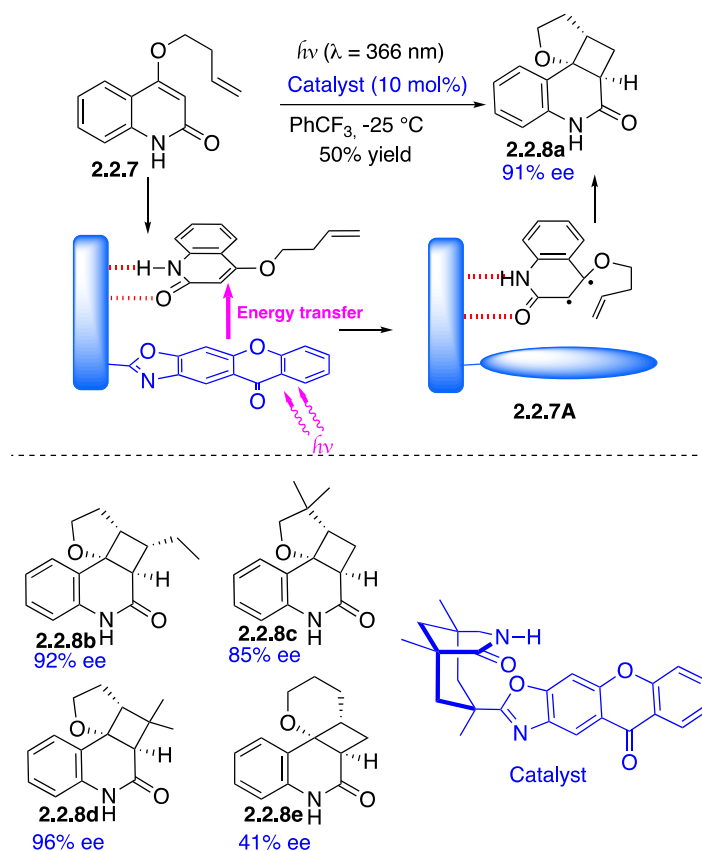
In the presence of the U-shape catalyst and 4h irradiation at 366 nm in trifluorotoluene, the tetracyclic compound was isolated in 50 % yield and 91% ee. At shorter irradiation times, the product was however isolated in the presence of an enantioenriched regioisomer. After absorption of UV light, the xanthone antenna transmits the energy through a Dexter triplet energy transfer giving the biradical species. Catalyst-Substrate association affords a chiral "sandwich" micro-environment providing enantioface differentiation in the addition to the pendant alkene giving chiral 1,4-biradical **2.2.7A** with high stereocontrol. Radical-radical

recombination gives the enantioenriched cycloadduct **2.2.8a** and releases the hydrogen bonding organocatalyst.

Bach's bifunctional photochemical catalyst showed great versatility in substrate scope either by changing the nature of the olefin or substitution of quinolone moiety giving good yields and ee's except for a tetrahydropyran derivatives **2.2.8a-e** which gave up to 96% ee (Scheme 59).<sup>134</sup>

### Scheme 59 Xanthone Incorporated Hydrogen Bonding Catalyst in [2+2]

#### Photocycloadditions

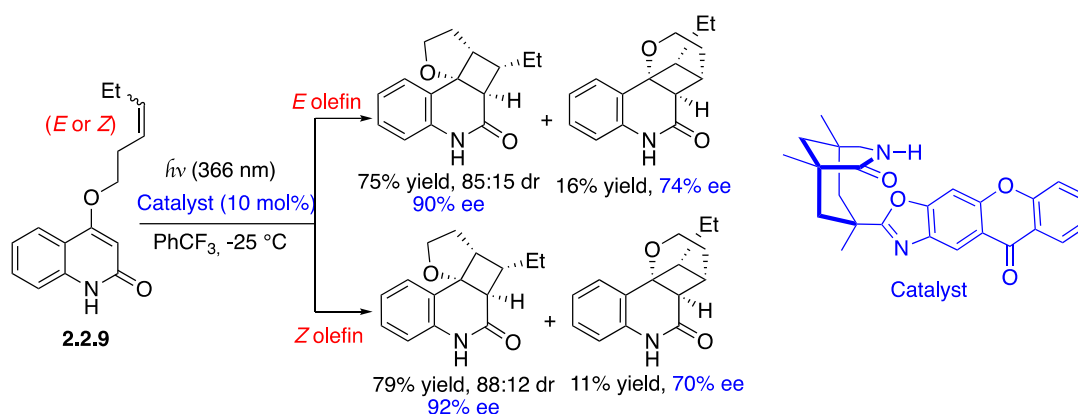


Interestingly, when *Z* and *E*-isomeric olefins **2.2.9** were investigated, the geometry of the olefin had only a slight influence on the regio- and enantioselectivity of the reaction (Scheme 60).<sup>135</sup>

Krische's attempt to induce enantioselective photocycloaddition received less success providing the cycloadduct *ent*-**2.2.8a** in 19% ee using a three-point binding hydrogen bonding sensitizer (Scheme 61). In contrast to Bach's rigid catalyst, the flexibility of the chiral complexing agent using amide linkages may explain the observed low enantioselectivity.

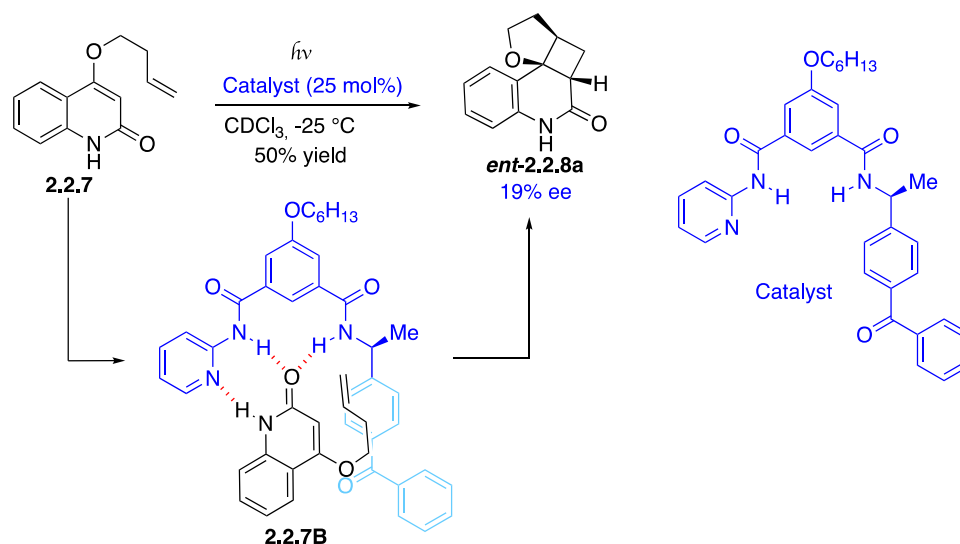


## Scheme 60 Influence of Alkene Geometry in [2+2] Photocycloadditions



## Scheme 61 Three-point Binding Hydrogen Bonding Sensitizer in [2+2] Photocycloaddition

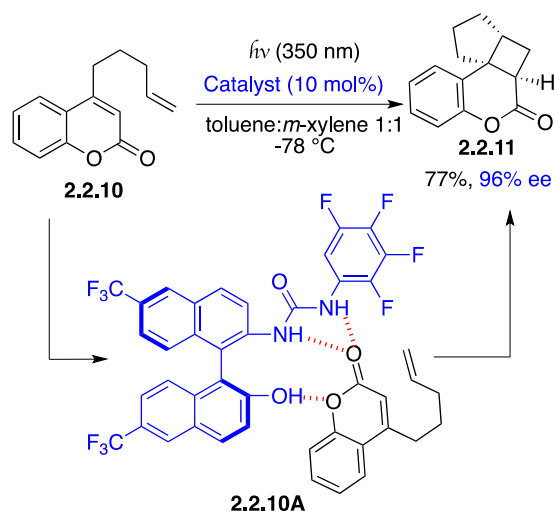
### Photocycloaddition



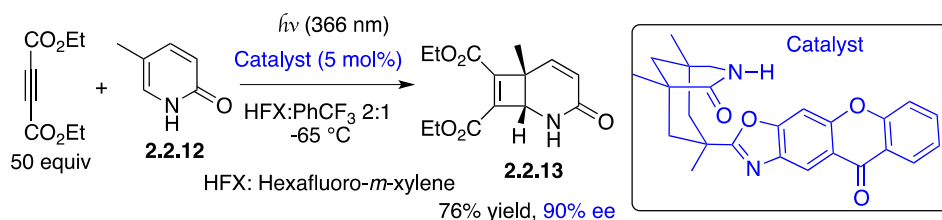
Sibi, Sivaguru and co-workers reported an efficient three-fold hydrogen bonding chiral catalyst possessing atropisomeric thiourea to promote cycloaddition of coumarin **2.2.10** (Scheme 62).<sup>136</sup> This rigid system offers higher enantiomeric control compared to Krische's catalyst. The stereodifferentiation arises from the binaphthyl motif while the substrate is maintained in a chiral microenvironment thanks to the anchoring by the hydrogen bond. Interestingly, when a methoxy group was incorporated on the aromatic ring of coumarin, a significant decrease of ee for the product **2.2.11** was observed (16%), a consequence of disruption of hydrogen bonding caused by the methoxy substituent. Under  $\text{O}_2$  which acts as a triplet quencher, the conversion

was only 12% confirming that under inert atmosphere the triplet excited state is engaged in this photocycloaddition. With additional experiments like fluorescence measurement, the authors affirmed that the photocatalytic cycle proceeds by energy sharing through exciplex formation (formation of both static and dynamic complexes). In 2016, thiourea catalyst was used by Bach to provide [2+2] photocycloadduct with only moderate results using 50 mol% of catalyst.<sup>137</sup>

### Scheme 62 Chiral Thiourea Catalyzed Intramolecular [2+2] Photocycloadditions



### Scheme 63 Intermolecular [2+2] Photocycloaddition using Hydrogen Bonding Catalyst

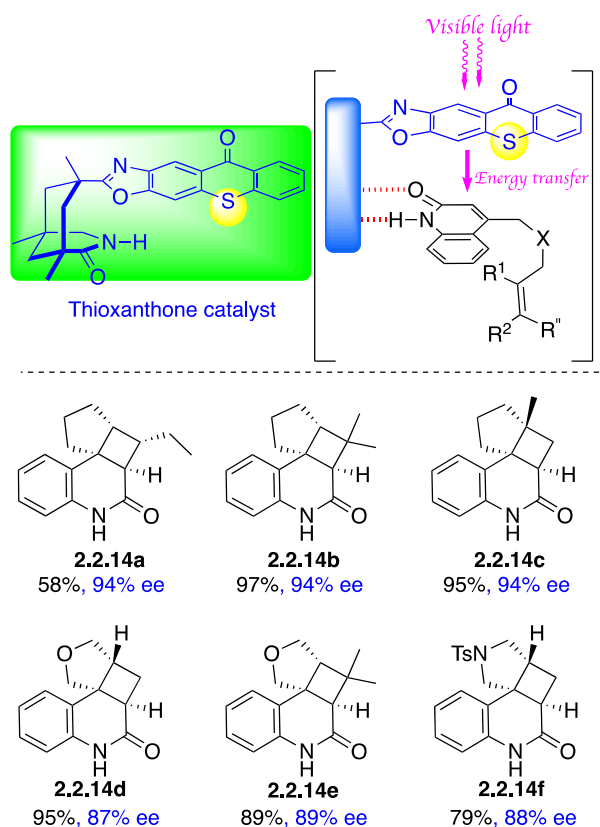


Reaction with Bach's catalyst was also extended to intermolecular cycloadditions demonstrating the real potential of this strategy in asymmetric radical reactions. 2-Pyridones and acetylenedicarboxylate in the presence of 5 mol% of xanthone catalyst enantiomer afforded cyclobutenes **2.2.13** as a single diastereoisomer.<sup>138</sup> High yields and excellent enantiomeric excesses were obtained in this enantioselective intermolecular [2+2] photocycloaddition. The reaction was performed with 50 equivalents of the alkyne which is the major drawback of the methodology (Scheme 63).

Study of spectral properties of thioxanthone derived catalyst showed a bathochromic shift in UV/Vis spectra when compared to xanthone. A significant absorption in the visible region was observed opening therefore an opportunity to use a low-energy consumption visible excitation.<sup>139</sup>

The thioxanthone linked Kemp's acid was competent in transferring light energy to quinolone substrates. Based on the same concept for stereocontrol and under irradiation at 419 nm, excellent yields and ee's were obtained in the formation of compounds **2.2.14a-f** (Scheme 64).

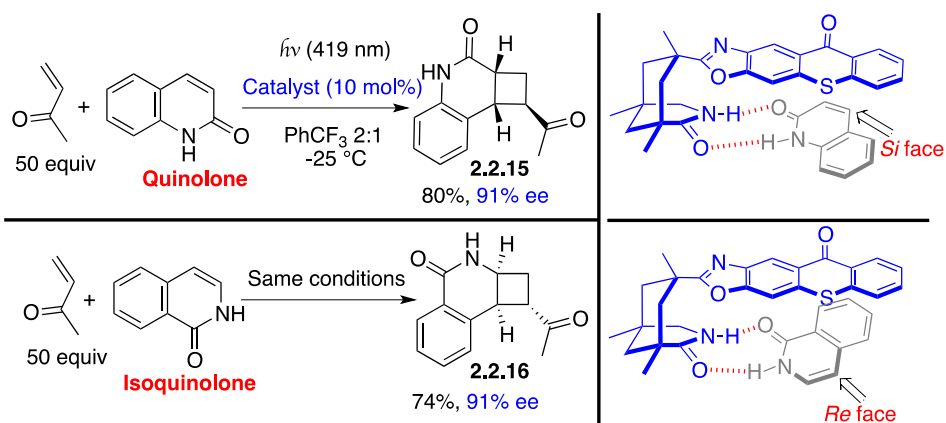
### Scheme 64 Intramolecular [2+2] Photocycloadditions of Quinolones using a Thioxanthone Catalyst



In the presence of the thioxanthone catalyst, intermolecular photocycloaddition of quinolone and electron deficient olefins was reported by Bach's group in 2016. Excellent regio-, diastereo- and enantioselectivity was observed in favor of the *exo* product **2.2.15**. When an acrylate was used instead of methylvinyl ketone, the reaction gave a mixture of endo and exo products. Isoquinolone was also a good substrate in this cycloaddition furnishing high ee, however the

authors showed the inverse absolute configurations when compared to the quinolone derivative.<sup>140</sup> This result may be explained by the opposite anchoring of the isoquinolone to fit the two-point hydrogen bonding motif delivering the enantiotopic face for the olefin addition giving the product **2.2.16** (Scheme 65).

### Scheme 65 Intermolecular [2+2] Photocycloadditions with Quinolone and Isoquinolone

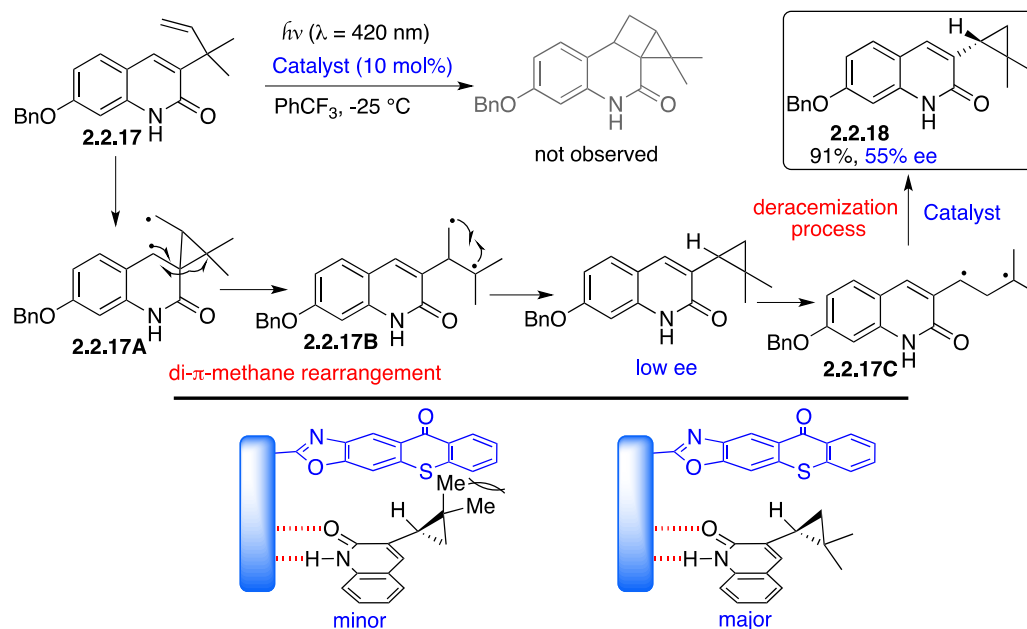


While the conversion of an achiral substrate to a chiral product and kinetic resolution of racemic starting materials are well documented, methods for achieving selective deracemization are rare. This concept consists of the conversion of a racemic mixture of a compound into its enantiopure form with no additional chemical transformation. This is a challenging strategy because both enantiomers are energetically identical. The passage through a planar prochiral intermediate (radical for instance) coupled with stereo-differentiation of the two enantiotopic faces by a catalyst which will recreate the stereocenter is an ideal approach. The deracemization can be achieved therefore if reverse and forward steps proceed through distinct mechanisms from the prochiral intermediate.

Very recently, using shorter alkenyl chain linked to a quinolone derived substrate, the constrained tetracyclic photoproduct was not observed, instead, product **2.2.18** obtained from a di- $\pi$ -methane rearrangement was isolated in 91% yield (Scheme 66).<sup>141</sup> A deracemization process takes place to ensure an enantio-enrichment through the cyclopropyl ring opening,

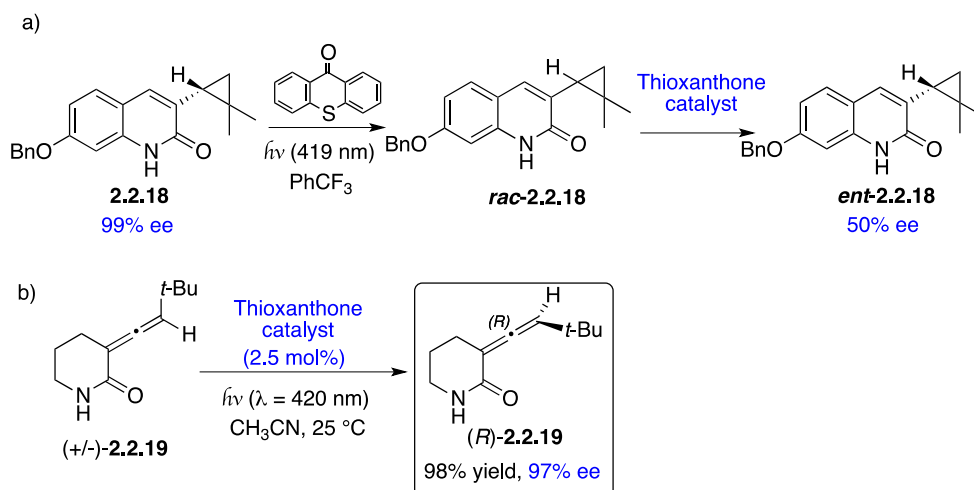
generating the 1,3-diradical **2.2.17C**. Ring closure of this short lifetime species within the complex, affording the cyclopropane with moderate stereocontrol.

### Scheme 66 Kinetic Resolution in [2+2] Photocycloadditions



In this study, it was demonstrated that the product ( $E_T = 270 \text{ kJ mol}^{-1}$ ) is sensitive to photosensitization which explains the cap value of 55% for ee. Independent experiment in which an enantiopure cyclopropane product (obtained by chiral HPLC purification) confirmed a rapid racemization upon exposure to visible light (420 nm) in the presence of achiral xanthone (Scheme 67a). The racemic product when subjected to irradiation in the presence of chiral thioxanthone catalyst, a photostationary state was reached in which the ee of the cyclopropane reached a maximum of 50%. It is reasonable to ascertain from these two experiments that the enantioenrichment is a consequence of deracemization process and not enantioselective di- $\pi$ -methane rearrangement. Using the same strategy, the authors have reported very recently the deracemization of spirocyclopropyl oxindoles.<sup>142</sup> The use of xanthone template catalyst for deracemization of allenes was more efficient, ee's of up to 97% was reached through the photosensitization facilitated by the two-point hydrogen bonding (Scheme 67b).<sup>143</sup>

## Scheme 67 Mechanism of Kinetic Resolution in [2+2] Photocycloaddition

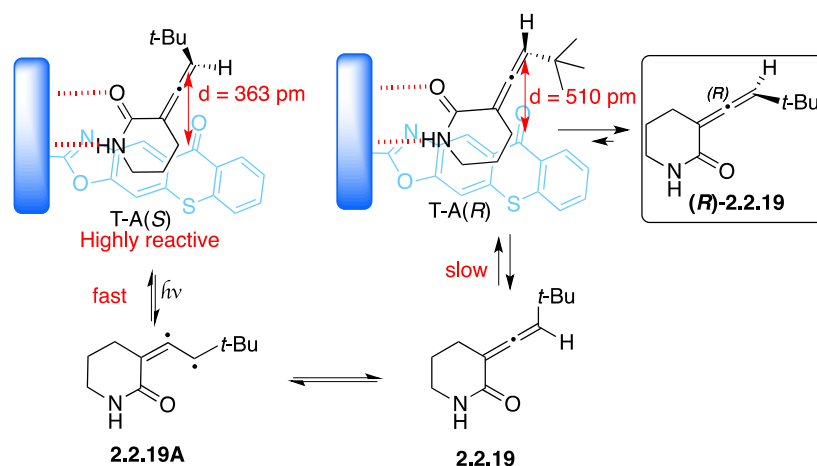


The binding of the allene substrate to the catalyst allows for the generation of two diastereomeric complexes, T-A(*R*) and T-A(*S*) (Scheme 68). Depending on the strength of the hydrogen-bond association of these diastereomeric complexes, the behavior of enantiomers will differ regarding the triplet excitation. The presence of *tert*-butyl group revealed a higher association between the chiral template and the *S*-allene **2.2.19** than with the *R*-allene. This scenario favors an energy transfer in complex T-A(*S*) rather than T-A(*R*). The thermodynamic preference of the template to *S*-allene in the ground state impacts therefore the rate of sensitization, indeed the formation of diradical **2.2.19A** from the *S*-allene is 10 times faster. In other words, both association constants and sensitization rates of diastereomeric intermediates are crucial for this concept.

DFT calculations supported this assumption and displayed a distance between the allene and the xanthone moieties of 363 and 510 pm for T-A(*S*) and T-A(*R*), respectively. This allows the enrichment of the *R*-allene while the *S*-enantiomer racemizes through the passage from the diradical form. The unfavorable thermodynamic process due to decrease in entropy is compensated by light energy.

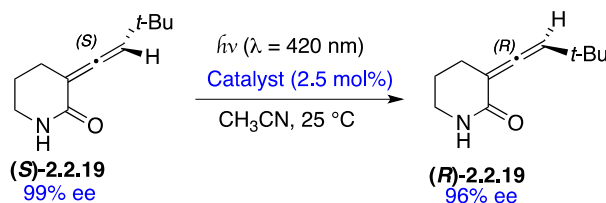
## Scheme 68 Kinetic Resolution of Allenes using Photochemically Derived Diradical Intermediates

### Intermediates



Impressively, Bach and co-workers realized a complete inversion from *S*-allene possessing 99% ee to *R*-allene **2.2.19** with 96% ee in only 40 minutes (Scheme 69). This finding accounts for a breakthrough in radical asymmetric synthesis.

### Scheme 69 Complete Inversion of Allene Stereochemistry using Photocatalyzed Reaction

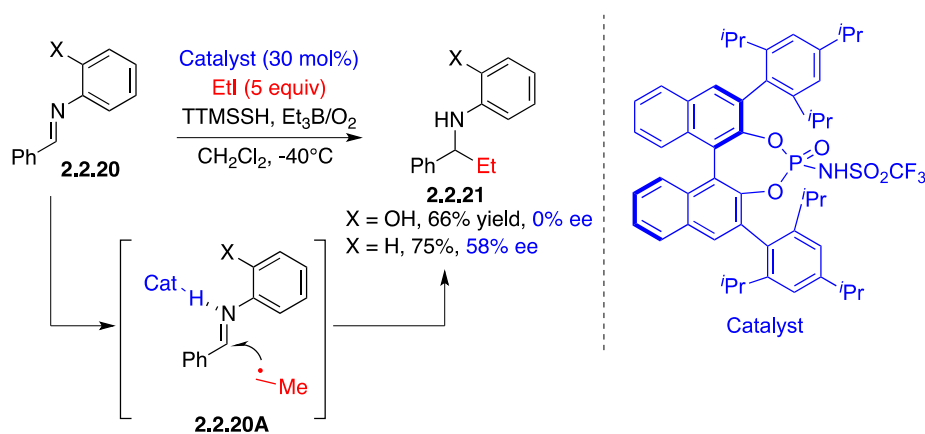


Chiral Brønsted acid organocatalysts derived from BINOL have been extensively employed in ionic asymmetric catalysis.<sup>144,145</sup> They have proven to be synthetically useful in numerous transformations offering high enantiocontrol.<sup>146</sup> Their use in radical chemistry is however not common. These eco-friendly catalysts are easy to handle and stable toward oxygen and water. In contrast to Lewis acids, chiral Brønsted acids exhibit intrinsic catalytic activity with no need of external activation (no association to a metal).

In 2009, Lee and Kim reported the use of catalytic amount of binaphthol-derived chiral phosphoric acid in enantioselective radical reactions (Scheme 70).<sup>147</sup> Using 30 mol% of chiral phosphoric acid, addition of ethyl radical to the imine **2.2.20** moiety resulted in the formation

of amine product **2.2.21** in 75% yield and 58% ee (X = H).<sup>148</sup> When the ortho position is substituted with a hydroxyl group, the product was isolated in racemic form. This substitution disrupts the hydrogen bonding with imine which prevents enantioface selective approach of the radical.

### Scheme 70 Chiral Brønsted Acid Mediated Radical Addition to Imines



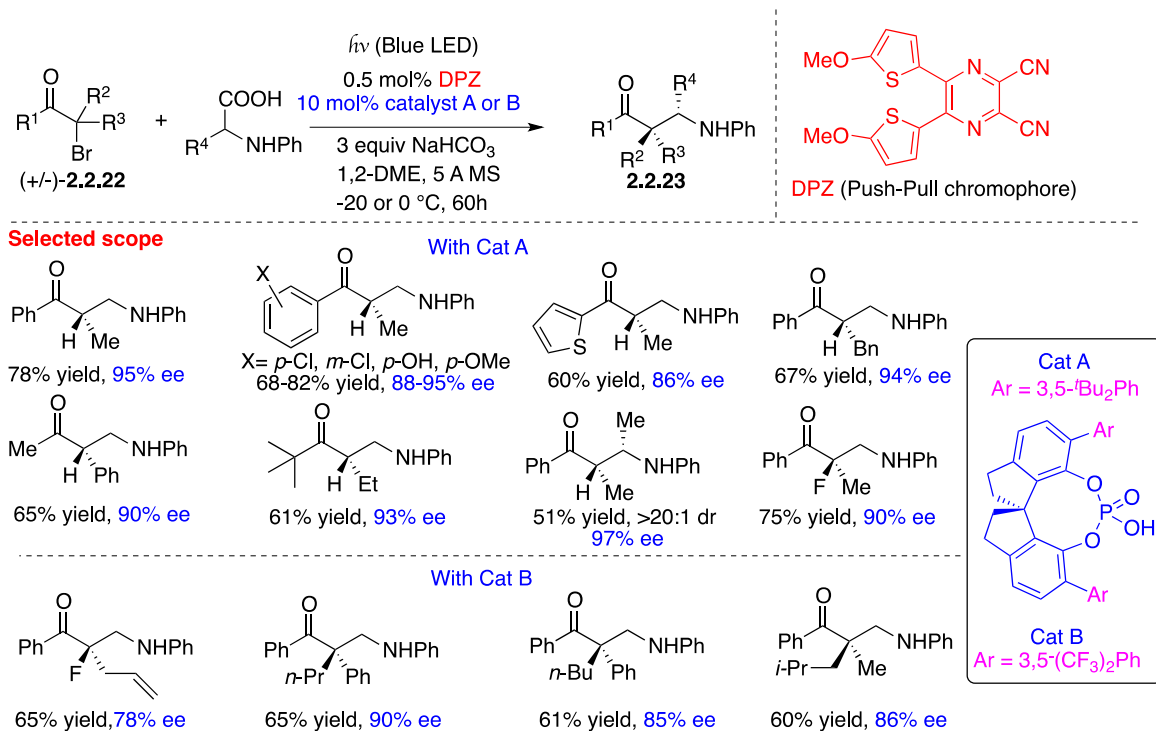
With the advent of organic photocatalysis to generate open shell species,<sup>149</sup> numerous applications using chiral Brønsted acid organocatalysts have been designed. In 2018, Jiang and co-workers reported a metal-free radical-radical coupling upon visible light irradiation through the dicyanopyrazine (DPZ)<sup>150</sup> photocatalyst relay.<sup>151</sup> Asymmetric reaction was driven by the use of chiral phosphoric acid derived from SPINOL as a hydrogen bonding catalyst.<sup>128</sup>

Impressive range of products were obtained in this asymmetric photoredox radical coupling strategy with high stereocontrol. Products containing fluorine atoms as well as quaternary carbons were efficiently synthesized using this methodology (Scheme 71). The synthetic utility of these products was demonstrated by conversion into  $\beta$ -amino alcohols and  $\beta$ -amino acids. This radical pathway involves the excitation of DPZ chromophore followed by the formation of electron rich radical **2.2.22B**, after CO<sub>2</sub> release (Scheme 72). The resulting DPZ radical anion engages in a SET with  $\alpha$ -bromoketone to form the corresponding electrophilic radical **2.2.22A** and the regeneration of the ground state DPZ making the overall photocatalytic cycle redox neutral. These reductive and oxidative quenching avoid the use of external oxidant or reductant

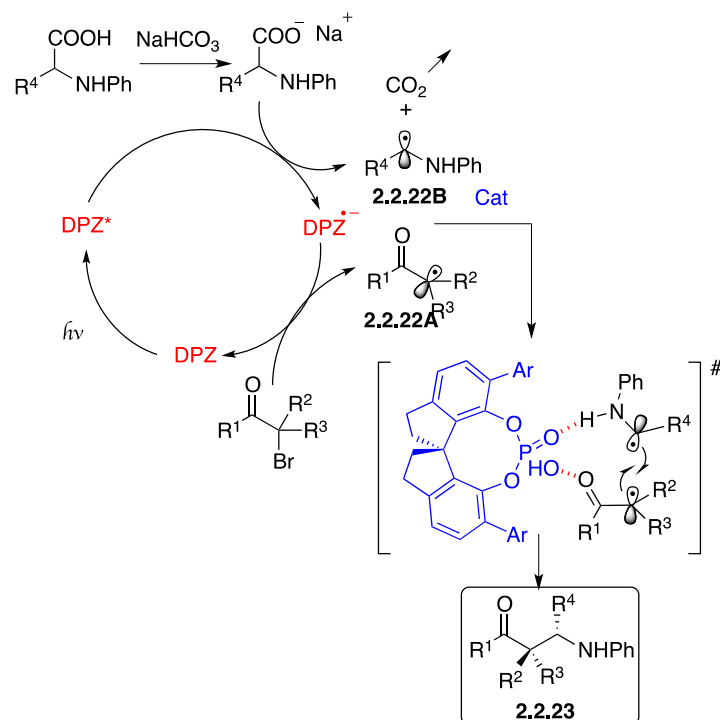


making the system eco-friendly. Cross coupling of the two radicals assisted by SPINOL catalyst affords the product amino ketone **2.2.23** with high enantiomeric excess.

### Scheme 71 SPINOL as a Hydrogen Bonding Catalyst in the Synthesis of $\beta$ -Amino Acids



### Scheme 72 Mechanism for SPINOL Mediated Radical Coupling



The same strategy has been used in coupling of ketyl radical derived from reduction of 1,2-diketone and  $\alpha$ -amino radical obtained by oxidation of *N*-aryl glycine derivative.<sup>152</sup> The redox potential of the photocatalyst is competent to allow redox neutral coupling reaction. Use of photoredox catalyst Ru<sup>2+</sup> or rose bengal instead of DPZ afforded lower yields.

The double binding of both radicals by the chiral SPINOL catalyst was again hypothesized, however, no support for such association was given in these studies. Given the basicity of the ketyl radical anion, deprotonation of the chiral phosphoric acid would generate neutral ketyl radical ready to couple with the *in situ* oxidative formation of  $\alpha$ -amino radical. Both isatins and acyclic diketones in the presence of the chiral catalyst, gives 1,2-amino tertiary alcohols with high enantioselectivity (Scheme 73). The suppression of hydrogen bonding in *N*-aryl glycine derivative by introduction of a methyl group had a detrimental impact on the enantiocontrol of the reaction and only 15% ee was observed in the formation of **2.2.24b** (Scheme 73b). The products were transformed to biologically relevant derivative **2.2.24c** (Scheme 73c), precursor of (+)-dioxibassinin without any loss of enantioselectivity.

### Scheme 73 Reductive $\alpha$ -Amino Alkylation using SPINOL and Photoredox Conditions

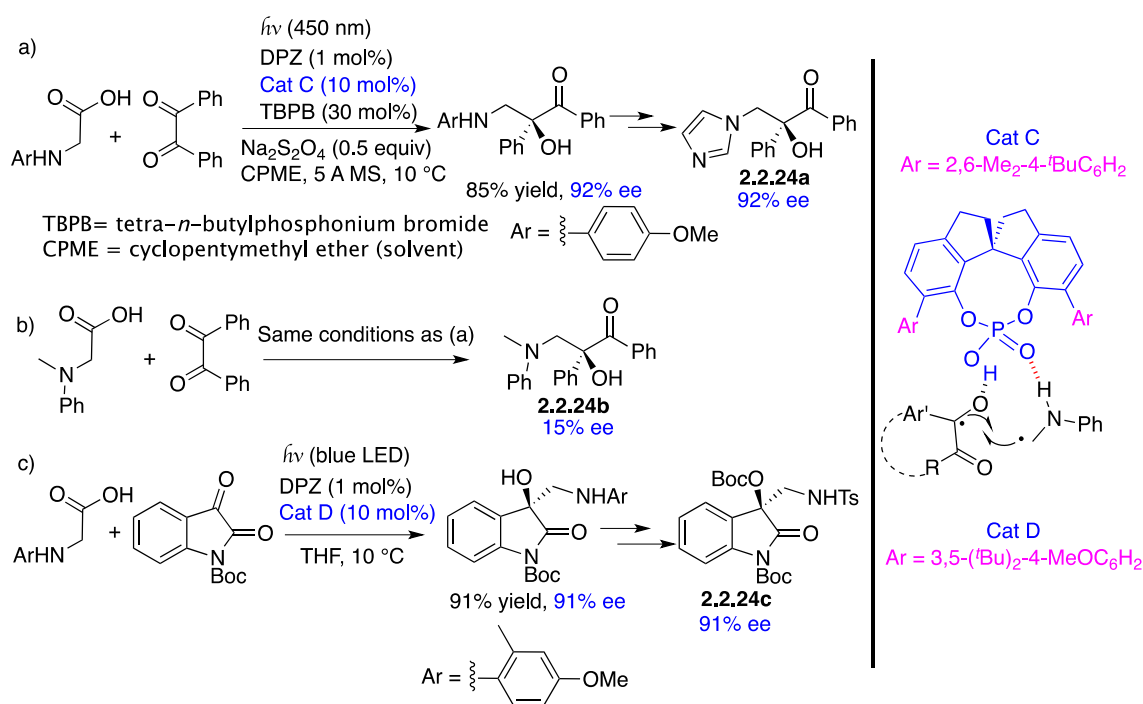
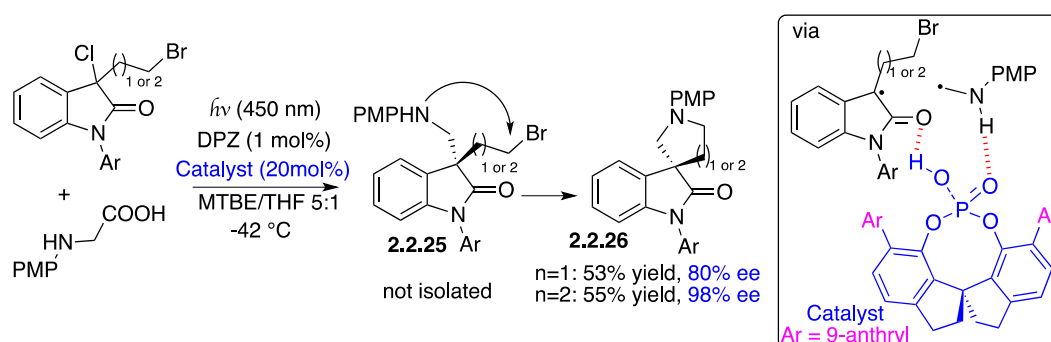


Photo-decarboxylative formation of a radical combined with dehalogenative generation of oxindolyl radical enabled an iterative radical cross coupling to synthesize valuable biorelevant heterocycles bearing quaternary stereocenters (Scheme 74).<sup>153</sup> The cooperative use of DPZ organophotoredox and H-bonding SPINOL phosphoric acid catalysts facilitated the enantioselective formation of the products.

### Scheme 74 Synthesis of Spirocyclic Oxindoles using SPINOL under Photoredox

#### Conditions



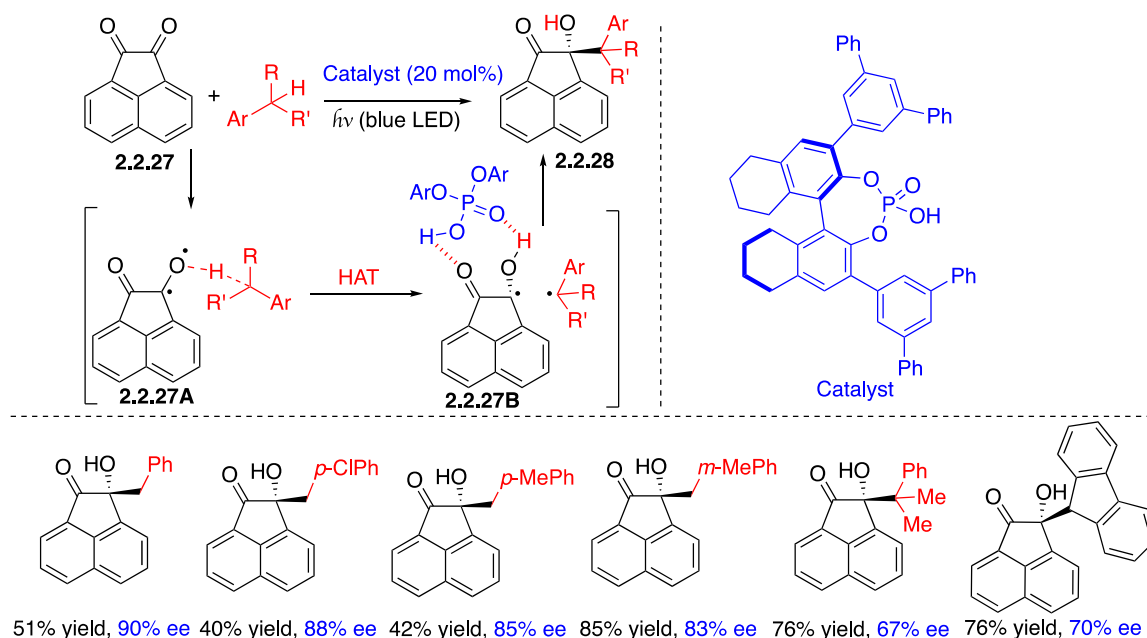
The DPZ showed a clear superiority over ruthenium in this photoredox system, the latter catalyst could not promote the same reaction. Rose Bengal organic dye could be used; however, the product was obtained in lower yield and ee than when using the DPZ catalyst. 3-Chlorooxindole showed higher reactivity than the bromo analog. A wide range of chiral oxindoles were synthesized using this strategy and excellent yields and ee's were obtained. Interestingly, the spirocyclization could be achieved in a one pot process using oxindole bearing bromoethyl or bromopropyl substituent leading to five- or six-membered spirocyclic indoles **2.2.26**, respectively (Scheme 74).

Following these developments, the same group replaced the amine fragment with toluene as the coupling partner. In contrast to Melchiorre work,<sup>91</sup> regarding the incompatibility of redox potentials of toluene and excited state of isatin **2.2.27**, a H-atom transfer is more likely to proceed between the two species rather than a SET mechanism. Radical coupling assisted by a hydrogen-bonding catalyst allowed an enantioselective functionalization of toluene derivatives

(Scheme 75). Reaction of acenaphthoquinones in the presence of BINOL catalyst afforded the tertiary alcohols **2.2.28** in moderate to good yields and good ee's.<sup>154</sup>

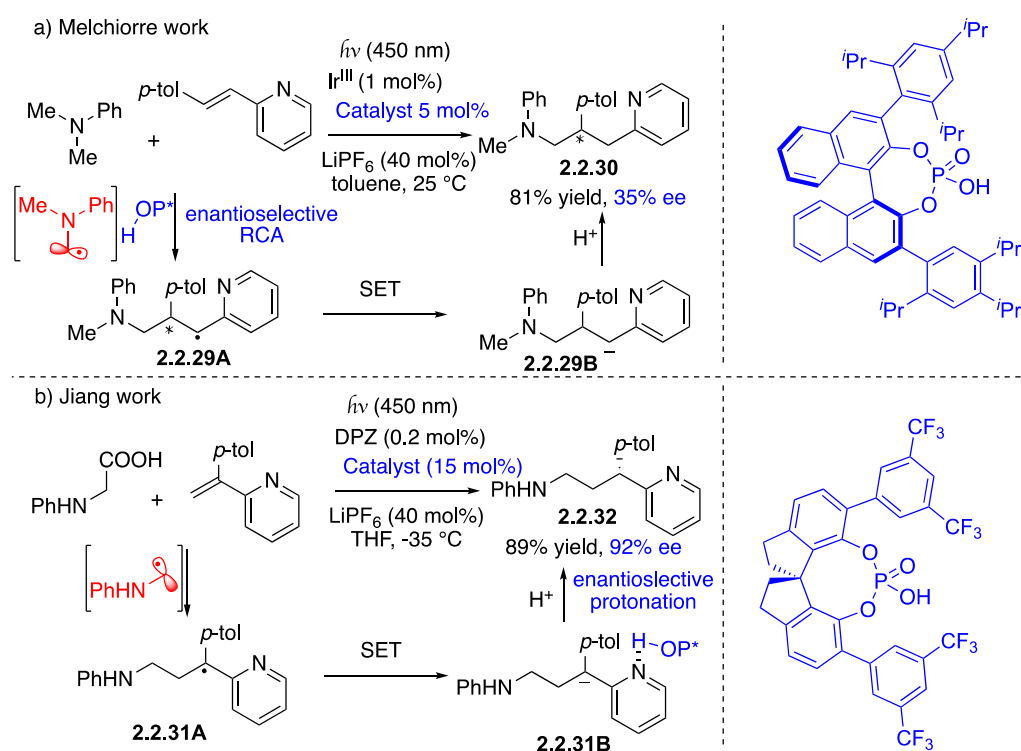
### Scheme 75 Radical Coupling using Chiral Phosphoric Acid under Photoredox

#### Conditions



### Scheme 76 Enantioselective Radical Additions to Vinyl Pyridines using Chiral

#### Phosphoric Acid

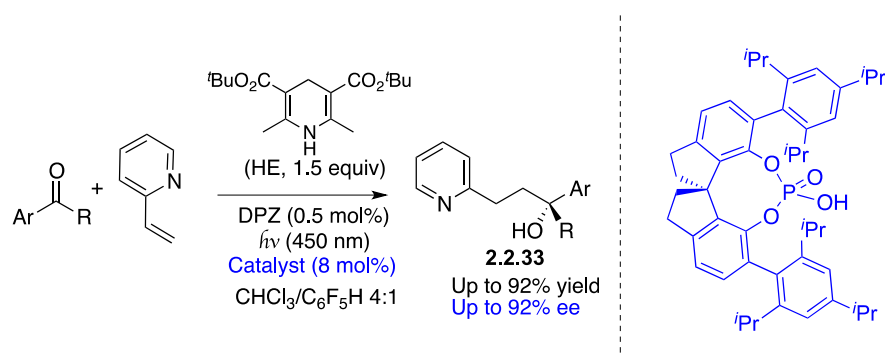


In addition to cross coupling of radicals, the Jiang's group studied the possibility to trigger conjugate addition reactions upon photoredox generation of radicals using DPZ catalyst.<sup>155</sup> Inspired by the iridium catalyzed reaction developed by Melchiorre, where a modest enantioselectivity was observed (Scheme 76a),<sup>156</sup> the authors started their study by the decarboxylative formation of  $\alpha$ -amino radical; subsequent addition onto 2-vinylpyridine affords highly stabilized radical (Scheme 76b). This reaction fits well with an enantioselective radical/polar mechanism in which intermediate **2.2.31B**, obtained after an SET, is protonated. Assistance of hydrogen bonding by SPINOL chiral catalyst allows for high control of stereochemistry in this strategy (Scheme 76a). The lower ee in Melchiorre's iridium catalyzed photoredox reaction can be explained by the differences in reaction conditions and that the stereodetermining step is the radical conjugate addition. Whereas in Jiang's work, the carbanion protonation is the stereocenter-forming step (Scheme 76b).

Jiang group has also used the same strategy to induce the stereochemistry in reduction of azaarene ketones to provide chiral alcohols.<sup>157</sup>

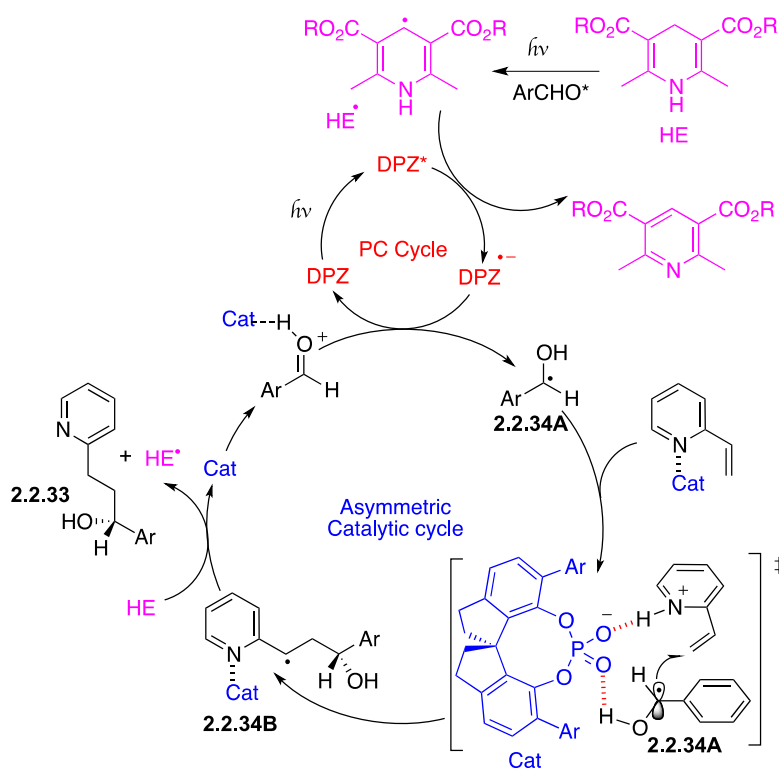
Later on, Jiang and co-workers demonstrated that it is possible to control enantioselectivity in the radical addition step by using ketyl radicals.<sup>158</sup> They combined carbonyl (or imines) substrates, DPZ, Hantzsch ester and chiral phosphoric acid under blue LED irradiation to obtain chiral  $\gamma$ -hydroxy (or amino) substituted pyridines **2.2.33** (Scheme 77).

### Scheme 77 Addition of Ketyl Radical to Vinyl Pyridine using Chiral Phosphoric Acid



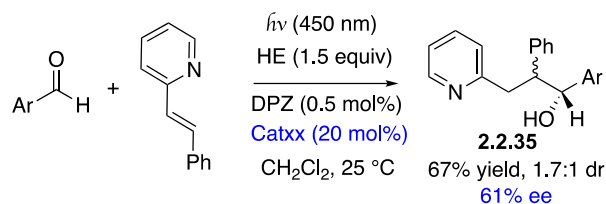
A non-asymmetric variant of this reaction has been previously reported by Ngai using Ru<sup>II</sup> as a photocatalyst and they proposed a mechanism in which the Hantzsch ester is crucial for the generation of ketyl radical.<sup>159</sup> The same observation was also made by Jiang's group and postulated the mechanism depicted in Scheme 78. The radical initiation step starts with the formation of Hantzsch ester radical (HE<sup>•</sup>) generated from the excitation of the carbonyl group. SET with excited DPZ\* and HE<sup>•</sup> generates DPZ<sup>•-</sup> that engages in another SET with ground state carbonyl substrate furnishing the ketyl radical **2.2.34A**. According to Knowles observations, the authors proposed a possible Proton Coupled Electron Transfer (PCET) mechanism for this transformation. DFT calculations showed 2.7 kcal/mol difference to reach the transition state in favor of the pro-*R* approach over the pro-*S*. This enantiocontrol is the result of the hydrogen bonding assistance from chiral phosphoric acid SPINOL in intermediate **2.2.34A**. Radical chain mechanism is assumed by HAT process from HE, regenerating the HE radical. This assumption is consistent with the fact that an excess amount of HE is necessary.

### Scheme 78 Mechanism of Radical Generation from Hantzsch Ester

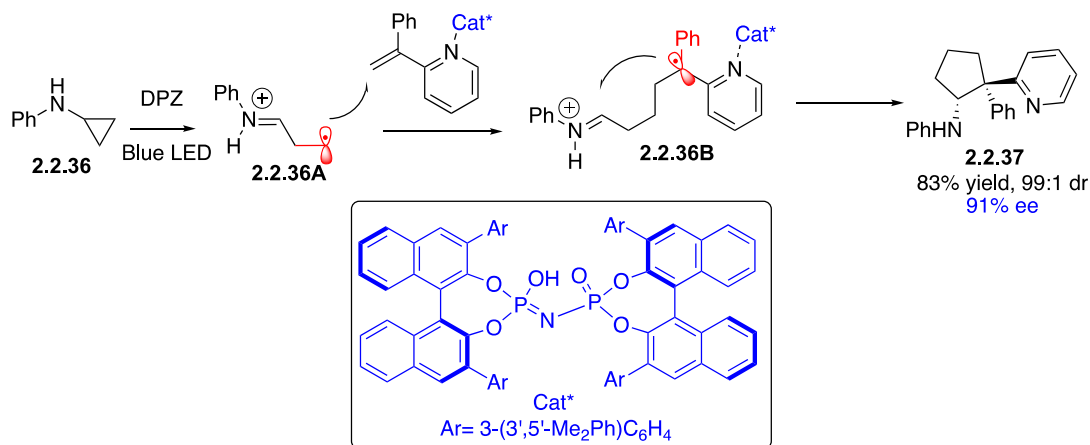


As also observed in Melchiorre's work, the facial approach of stereodefined olefin like **2.2.35** seems difficult to control, both diastereo- and enantioselectivities are moderate which constitutes a non-negligible limitation for the methodology (Scheme 79).

### Scheme 79 Synthesis of Chiral Tertiary Alcohols using Chiral Phosphoric Acids numbering



### Scheme 80 Addition of Radical Generated from Amino Cyclopropane to Vinyl Pyridine

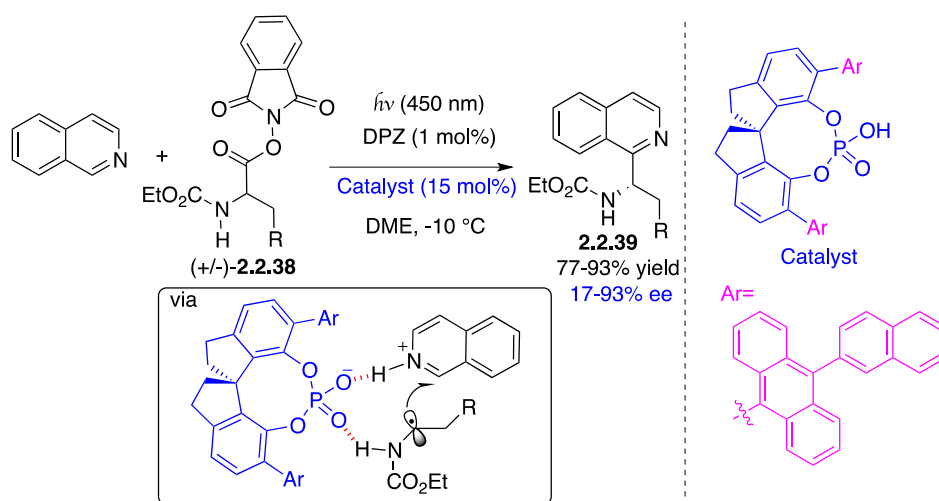


Based on a previous report by Zheng who developed ruthenium catalyzed intramolecular [3+2] annulation of *N*-cyclopropylanilines with alkenes,<sup>160</sup> a radical-based asymmetric radical cascade cyclization has been reported in 2020 by the Jiang group.<sup>161</sup> This strategy was based on oxidation of cyclopropylamine derivative through photoredox SET from excited DPZ. The ring opening of radical cation would give the alkyl radical **2.2.36A** that will engage in a radical addition to 2-vinylpyridine. Intramolecular radical addition of the resulting intermediate **2.2.36B** onto pendent iminium furnishes the cyclopentane skeleton **2.2.37** (Scheme 80). The H-bonding interactions with C<sub>2</sub>-symmetric imidodiphosphoric acid catalyst provides the chiral environment necessary for enantiocontrol in this cyclization elementary step. After a reduction

of the generated radical cation, the [3+2] cycloadduct possessing all-carbon stereocenter was isolated in good yield, high ee and excellent diastereocontrol.

Organocatalyzed and photoredox mediated enantioselective Minisci type reaction<sup>162,163</sup> has been reported recently by the Jiang group using DPZ and SPINOL-CPA strategy (Scheme 81).<sup>164</sup> The chiral phosphoric acid serves to activate the isoquinoline to facilitate the Minisci radical addition by lowering the energy of the LUMO orbital<sup>165</sup> and to induce chirality through the creation of a chiral environment around the two reactive protagonists enabled by hydrogen bonds. An iridium photoredox variant has also been developed recently in the presence of chiral phosphoric acid (*vide infra*). Under the same conditions, replacing DPZ by iridium photocatalyst gave a slight lowering of yield and stereocontrol. The scope of this Minisci reaction revealed a high tolerance for different racemic amino esters **2.2.38** (redox active esters) except for the alanine derived substrate that affords a low ee (17% ee). The use of only isoquinoline substrates accounts for a limitation for this study.

### Scheme 81 Enantioselective Minisci type reaction using Chiral Phosphoric Acid under Photoredox Conditions

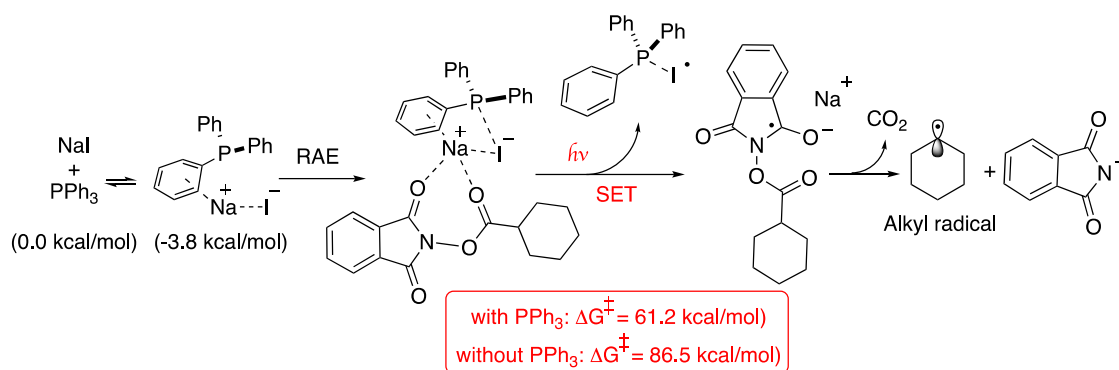


Very recently, Fu and co-workers reported an impressively simple and low-cost method for the photogeneration of radicals from phthalimide redox active esters (RAE) using catalytic amounts of sodium iodide and triphenylphosphine.<sup>166</sup>



## Scheme 82 Photogeneration of Radicals from Redox Active Esters using Catalytic

### Amounts of Sodium Iodide and Triphenylphosphine

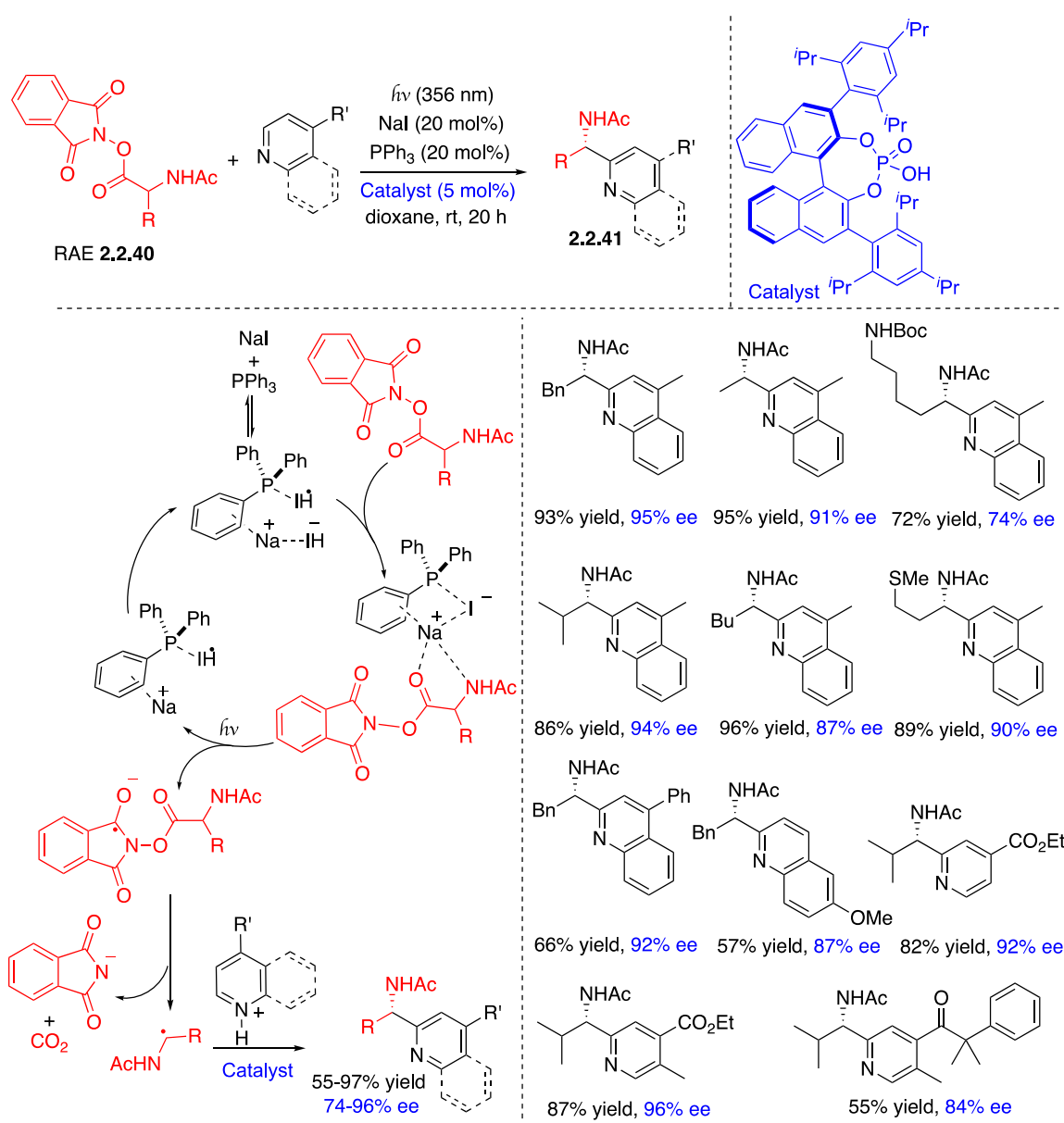


Under blue LED excitation, the energy barrier of the electron transfer process from iodide to the phthalimide was estimated to be 25 kcal/mol lower in the presence of triphenyl phosphine than in its absence. It appears that phosphine is crucial to allow intermolecular charge transfer and also to stabilize the iodine radical forming the persistent  $\text{Ph}_3\text{P-I}$  radical species (Scheme 82 and Scheme 83). After decarboxylation, formation of cyclohexyl radical was exploited in radical alkylation of silyl enol ethers, styrene derivatives and *N*-heteroarenes.

In the presence of chiral CPA and racemic RAE, the strategy allowed for excellent enantiocontrol in the Minisci reaction (Scheme 83). A larger substrate scope than in Jiang's report was found in this study. Different quinolines and pyridines groups possessing a variety of electron donating/withdrawing groups were tolerated. Redox active esters derived from racemic alanine, valine, methionine, phenylalanine and lysine amino acids were effectively introduced with good yields and high ee's.

## Scheme 83 Enantioselective Minisci Reaction using Redox Active Esters Derived from

### Racemic Amino Acids

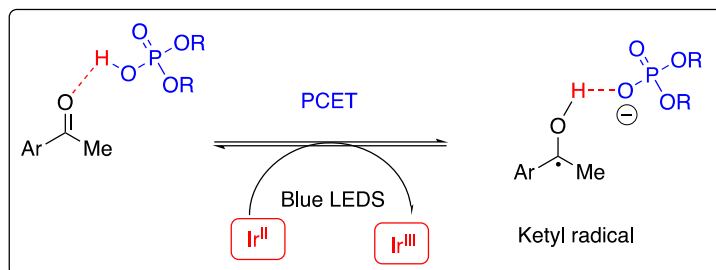


### 2.2.2. Merging Photoredox and chiral Brønsted acids

The use of chiral Brønsted acid responsible of chirality induction in the presence of a photocatalyst, that initiate the formation of a radical, is also a powerful method to perform enantioselective radical reactions. Interesting results could be obtained during the reductive coupling of ketones and hydrazones with the intermediate neutral ketyl radical remained bonded

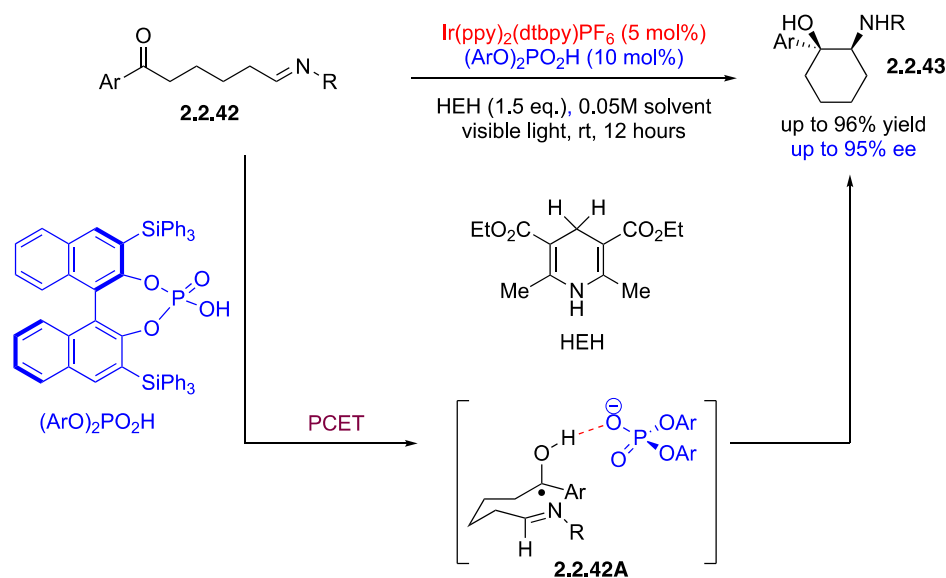
to the chiral catalyst during C-C bond formation, so that the final products could be obtained with an excellent level of diastereoselectivity and enantioselectivity.<sup>167</sup>

**Scheme 84 Proton Coupled Electron Transfer (PCET)**



Proton-Coupled Electron Transfer (PCET) concept has been introduced by Knowles in 2013 to facilitate the formation of radicals (Scheme 84).<sup>168,169</sup> Inspired by biological redox processes, he hypothesized that proton-exchange reactions can exert an effect on the kinetics and thermodynamics of electron transfer in the ketyl formation. Remarkably, the ketyl radical is involved in a H-bond to the phosphoric acid catalyst. This crucial arrangement provides key information for the development of asymmetric catalysis.

**Scheme 85 Use of PCET for the Enantioselective Synthesis of Amino Alcohols**

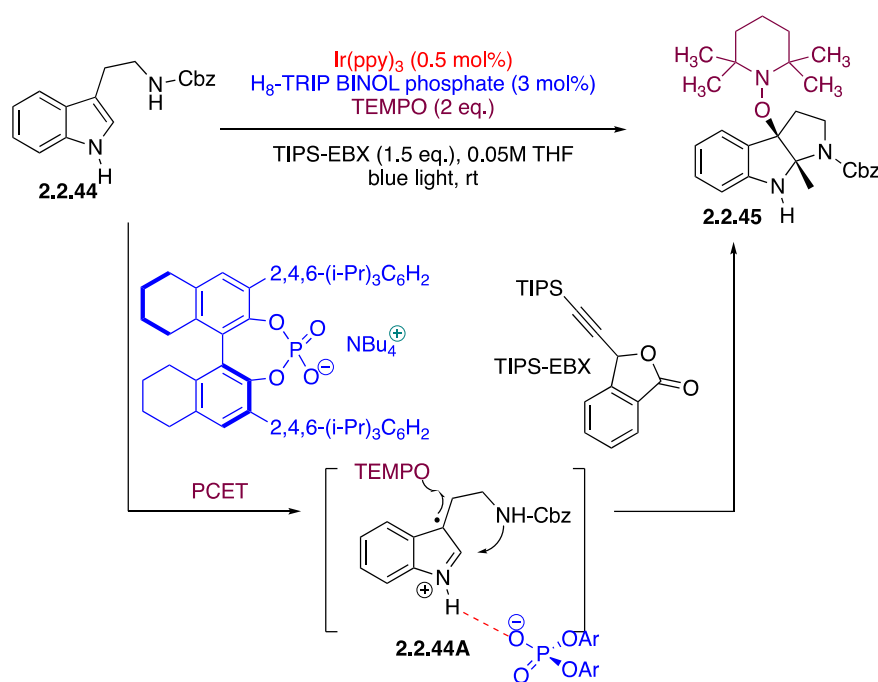


Indeed, Knowles and co-workers demonstrated the impact of this H-bonded organization in asymmetric catalysis through a PCET activation of tethered iminyl ketone **2.2.42**. Under visible light, the asymmetric aza-pinacol cyclization was determined as proceeding in first step via a

(PCET) process, providing the intermediate radical **2.2.42A** shown in Scheme 85.<sup>167</sup> Carbon-carbon bond formation provides enantioenriched cyclic 1,2-amino alcohols **2.2.43** in highly enantioselective manner.

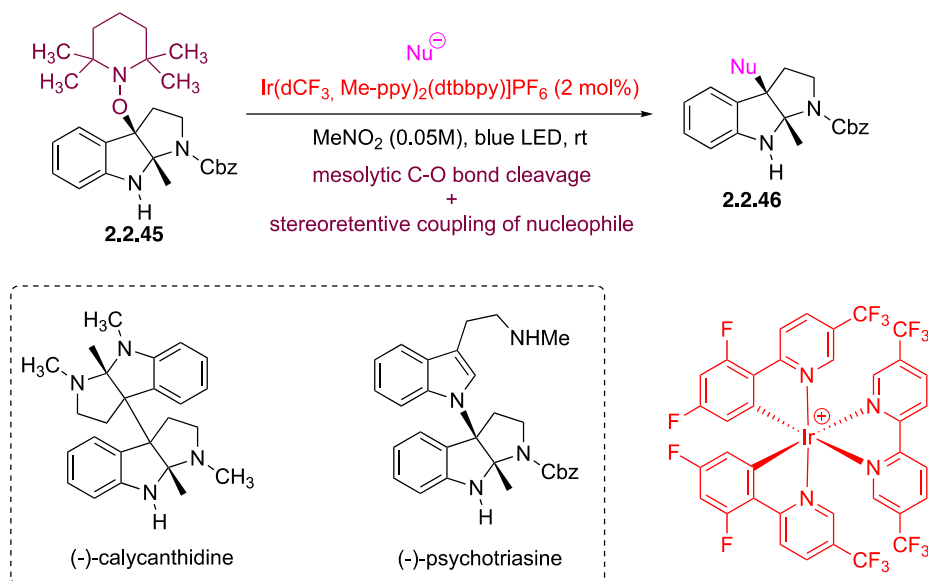
This dual photoredox hydrogen bonding catalysis was also applied to PCET reduction of indole derivatives followed by intercepting the intermediate radical **2.2.44A** by a nitroxyl radical such as TEMPO (Scheme 86). The optically enriched adducts could be achieved via a catalytic single-electron oxidation/mesolytic cleavage sequence to furnish transient carbocations that can react with a wide range of nucleophiles (like NHCbz in the present example).<sup>170</sup>

### Scheme 86 Synthesis of Heterocycles using PCET Conditions



By introducing TEMPO, the enantioselective coupling of nucleophile could be decomposed into a two-step reaction, enabling first to isolate the TEMPO adduct and second, following the mesolytic C-O bond cleavage, a stereoretentive coupling of different nucleophiles could be studied. Using this approach, several alkaloid natural products such as (-)-calycanthidine or (-)-psychotriasine could be efficiently conducted (Scheme 87).

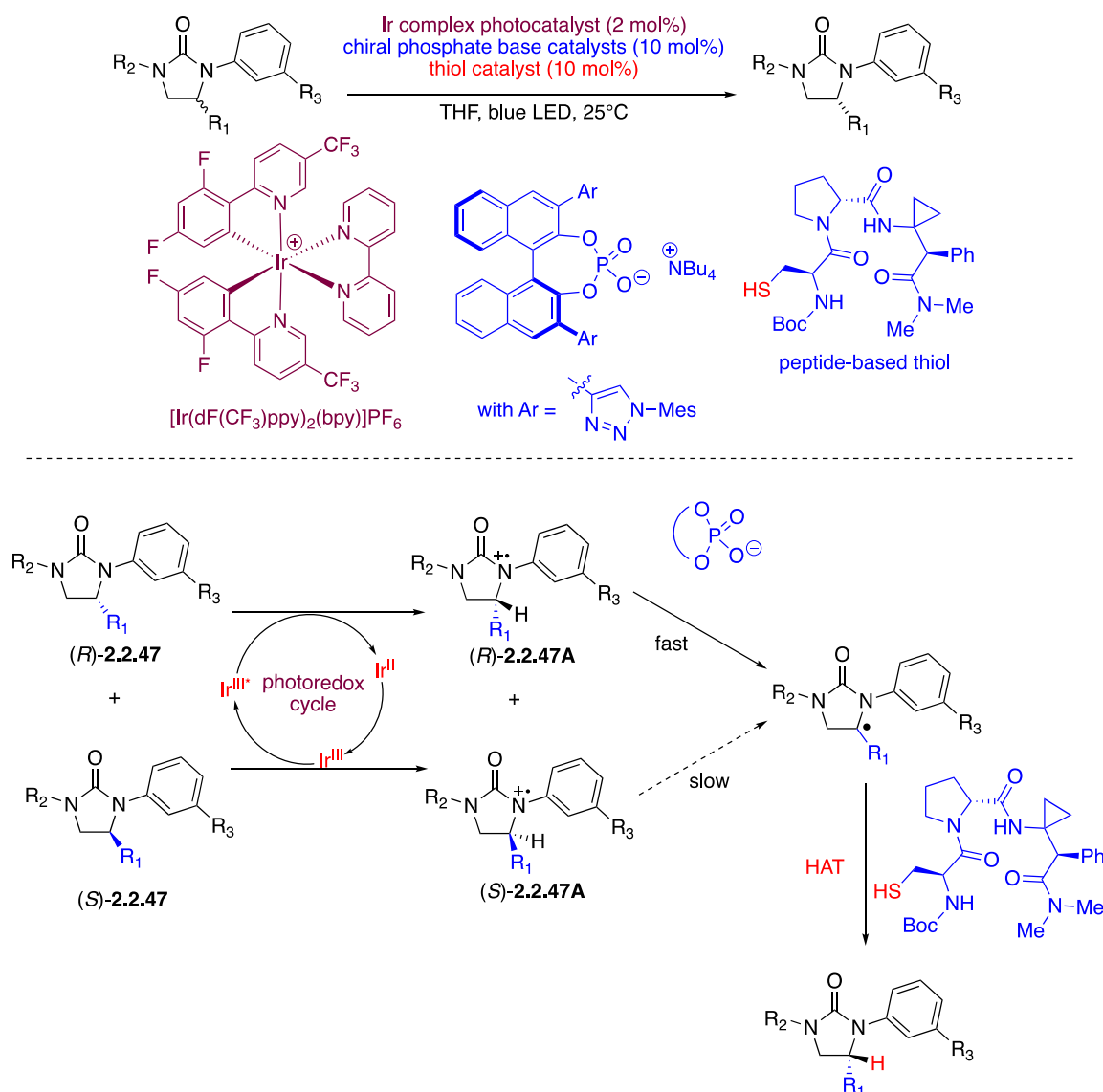
## Scheme 87 Transformation of Amino Alcohols Derived by PCET Reactions in the Synthesis of Alkaloids



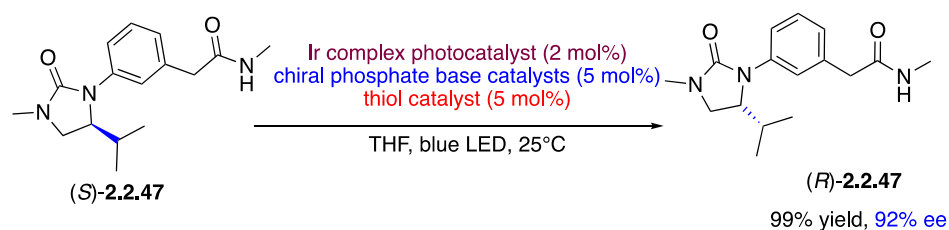
$[\text{Ir}(\text{dF}(\text{CF}_3)\text{ppy})_2(\text{bpy})]\text{PF}_6$  is a versatile photocatalyst that was recently used for asymmetric synthesis by deracemization (Scheme 88).<sup>171</sup> This multicatalytic reaction is likely to proceed by means of a sequential electron, proton and hydrogen-atom transfer sequence that could be used to break and reform C-H bonds. A proof of concept experiment was demonstrated with achiral thiophenol where a kinetic resolution take place with a moderate efficiency. The use of chiral peptide-based thiol catalyst, in cooperation with the chiral phosphate catalyst, provided a high enantiocontrol. The implication of potential hydrogen interaction between the substrate and catalyst has supported by specific experiments.

This cooperative catalytic system was also able to control the stereoinversion of (*S*)-**2.2.47** to (*R*)-**2.2.47** with 92% ee and 99% yield (Scheme 89).

### Scheme 88 Use of Iridium Photocatalyst in Asymmetric Deracemization



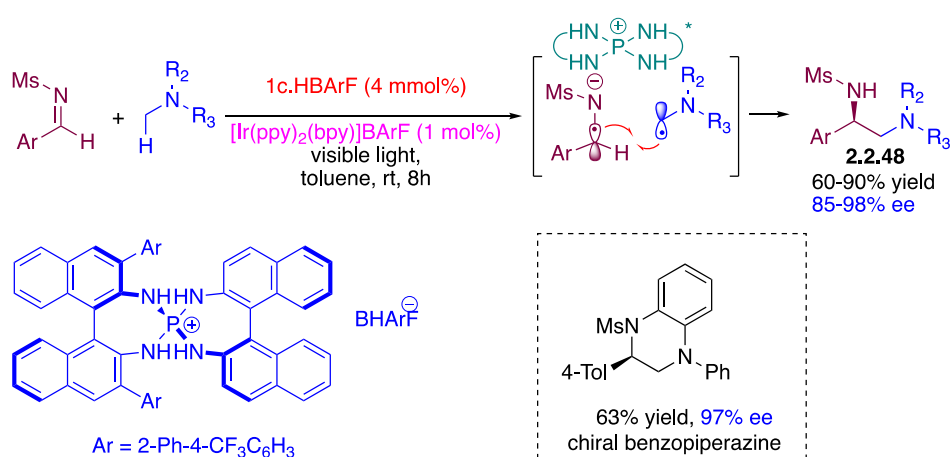
### Scheme 89 Multicatalytic Stereoconversion of Urea (S)-2.2.47



Ooi and co-workers opted for another strategy consisting of a dual catalytic system based on the combination of transition-metal photosensitizer and a stereocontroller.<sup>172</sup> By using this strategy, the visible-light activated and stereocontrolled radical anion–radical coupling of

*N*-aryl aminomethanes with *N*-sulfonyl aldimines using an iridium photosensitizer and a chiral arylaminophosphonium salt was proposed. To promote the radical anion–radical coupling, a careful selection of both the substrate and the reductant was important and [Ir(ppy)<sub>2</sub>(bpy)]BARF was selected as a strong and appropriate reductant [ $E_{\text{red}} = -1.40\text{V}$  vs. SCE] for the generation of radical anions of *N*-sulfonyl imines [ $E_{\text{red}} = -1.45\text{ V}$  vs. SCE). The chiral induction was achieved thanks to counter-ion strategy, chiral phosphonium and radical anion interaction would engage an enantiofacial approach of the aminomethyl radical delivering enantioenriched 1,2-diamine product. H-bond interaction could also be envisaged in this step. A wide range of aromatic *N*-sulfonyl imines could be efficiently coupled with various *N*-arylaminomethanes. In contrast, aliphatic imines remained inert as a result of low reduction potentials. The authors also demonstrated the utility of this reaction in the synthesis of a chiral benzopiperazine, structures known as cholesterol ester transfer protein (CETP) inhibitors. Starting from *N*-2-bromophenyl-*N*-phenylaminomethane, the desired chiral benzopiperazine was obtained in 63% for the two steps and 98% ee (Scheme 90).

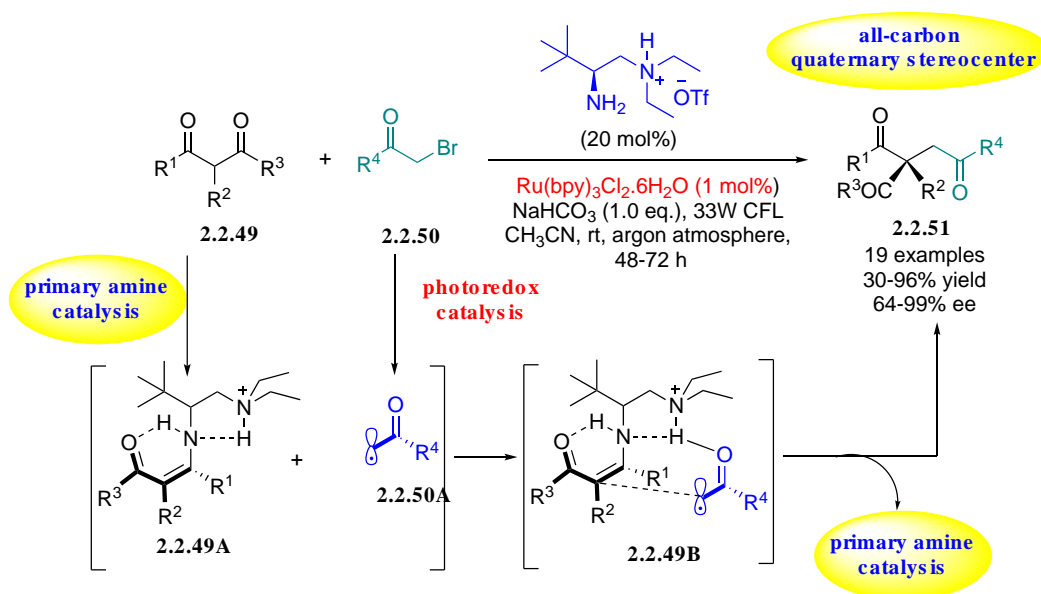
### Scheme 90 Radical Anion–Radical Coupling using a Transition-metal Photosensitizer and a Stereocontroller



Luo et al. described another methodology for  $\alpha$ -photoalkylation and  $\beta$ -ketocarboxyls by combining photoredox catalysis and primary amine catalysis for the construction of all-carbon quaternary stereocenters with excellent enantioselectivities.<sup>173</sup> When a wide range of  $\beta$ -

ketocarboxyls **2.2.49** were treated with  $\alpha$ -bromocarboxyls **2.2.50** in the presence of combined catalysis of 20 mol% primary amine catalyst and 1 mol% photoredox catalyst  $\text{Ru}(\text{bpy})_3\text{Cl}_2 \cdot 6\text{H}_2\text{O}$  in acetonitrile using inorganic base  $\text{NaHCO}_3$  ( $\text{NaHCO}_3$  is used to trap the *in situ* liberated  $\text{HBr}$ ) under light irradiation, the desired alkylation adducts **2.2.51** with all-carbon quaternary centers were obtained in 30-96% yield with 64-99% ee (Scheme 91). According to the proposed mechanism, the reaction proceeds through the formation of acyl radical **2.2.50A** via photoredox catalysis and with formation of enamine **2.2.49A** from **2.2.49** via primary amine catalysis. Subsequent formation of transition state **2.2.49B** from the combination of these two intermediates would generate the desired product **2.2.51** with the regeneration of catalyst.

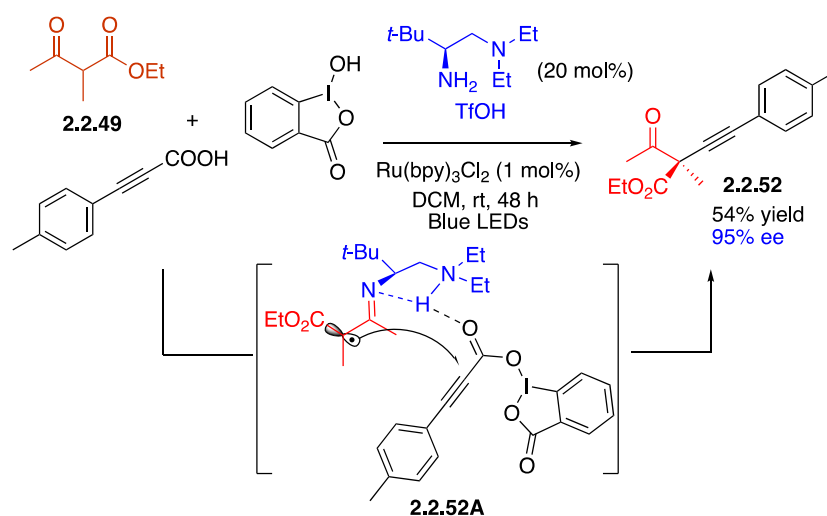
**Scheme 91 Enantioselective  $\alpha$ -Alkylation of  $\beta$ -Ketocarboxyls by Merging Photoredox Catalysis with Primary Amine Catalysis.**



Enantioselective  $\alpha$ -alkynylation of  $\beta$ -ketocarboxyls **2.2.49** by merging photoredox catalysis with primary amine catalysis has been reported by the same group.<sup>174</sup>  $\alpha$ -Iminyl radical generated from a photoredox Ru-catalyzed process and proton loss underwent radical addition to give the alkylation product **2.2.52** in high ee and moderate yield. As in the previous example, hydrogen bond assistance was proposed to support the high stereocontrol in the construction of quaternary carbon (Scheme 92).

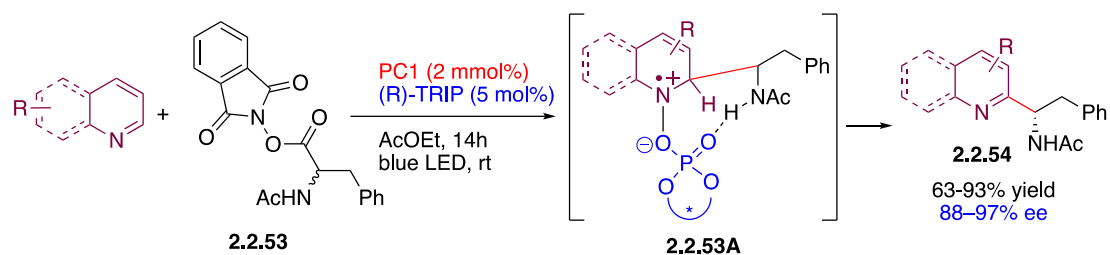


## Scheme 92 Enantioselective $\alpha$ -Alkynylation of $\beta$ -Ketocarboxyls



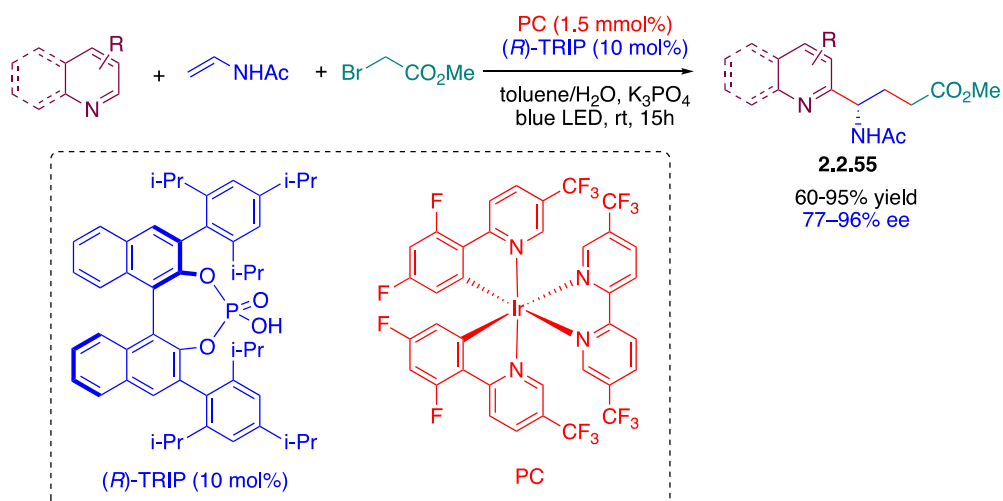
The development of carbon-carbon bond formation with nucleophilic radicals and electron-deficient heteroarenes was introduced by Minisci and co-workers in the 1960s. This class of reactions has been successfully used in visible-light-driven dual catalysis, opening therefore promising asymmetric reactions. This decarboxylative formation of amino-radical followed by addition to electron-deficient heteroarenes has been successfully applied using dual iridium/chiral phosphoric acid catalysis. Addition of prochiral radicals generated from amino acids to pyridine and quinoline derivatives was examined (Scheme 93).<sup>175</sup> An excellent control of both the enantioselectivity and the regioselectivity could be obtained. In this reaction, an enantiopure chiral Brønsted acid was advantageously used as a catalyst serving both to activate the substrate and induce the asymmetry. Parallel to this, the transition metal photocatalyst could mediate the electron transfer processes. Here again, the crucial role of hydrogen bonding was also demonstrated, a substrate such as L-proline delivering the product in good yield but with negligible enantioselectivity. Comparison of the enantiopurity of the catalyst and the product revealed a nonlinear relationship and the possible involvement of two phosphate molecules during the deprotonation step. Lastly, the scope of this reaction was extended to diazines such as pyrimidines and pyrazines, maintaining a similar efficiency.<sup>176</sup>

## Scheme 93 Enantioselective Addition of Prochiral Radicals Generated from Aminoacids to Pyridine and Quinoline Derivatives



In the different Minisci-type reactions mentioned above, only the mono functionalization of the substrate was evaluated. The catalytic asymmetric difunctionalization of double bonds by intermolecular three-component reactions was examined. It should be noticed that such reactions remain challenging at present and relevant examples have been reported with chiral copper complexes developed for the enantioselective difunctionalization of styrene or the dicarbofunctionalization of diarylalkenes.

## Scheme 94 Catalytic Asymmetric Difunctionalization of Double Bonds by Intermolecular Three-component Reactions

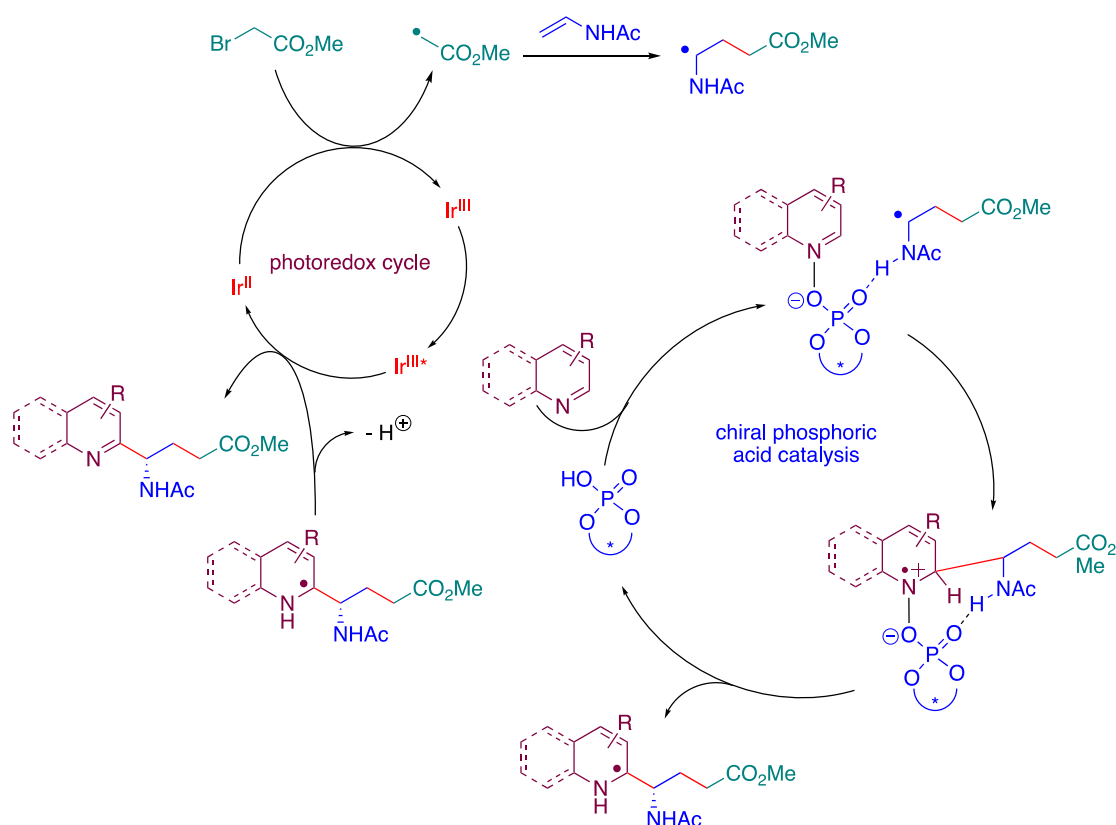


In 2019, Studer and co-workers proposed a three-component radical cascade for the preparation of  $\gamma$ -heteroaryl-substituted  $\gamma$ -amino-acids using a radical addition step to generate  $\alpha$ -amino-alkyl radicals.<sup>177</sup> To achieve this, PC was selected as the transition metal catalyst and the BINOL-phosphoric acid ligand (R)-TRIP as the stereocontroller (Scheme 94). In general,

a good tolerance to the substitution pattern of pyridine or quinoline substrates was found during the Minisci-type reaction. Besides, a reduced enantioselectivity was found for all substrates comprising electron-donating groups.

Elucidation of the mechanism also revealed an uncertainty concerning the reduction of **PC1** to Ir<sup>II</sup>. Notably, TRIP and its related phosphate anion have been previously reported as possible reductants capable of reducing Ir<sup>III\*</sup> to Ir<sup>II</sup>.<sup>175</sup> The low reaction yield and the negligible enantioselectivity obtained with *N*-methyl-*N*-vinylacetamide (33% yield, 52:48 er) also revealed the crucial role of hydrogen bonding and the ability of substrate was even determined as the key parameter governing both the enantioselectivity as well as the radical coupling efficiency (Scheme 95).

### Scheme 95 Mechanism for the Three Component Minisci Type Reactions



### 2.2.2 Lewis Acid Catalyzed Reactions

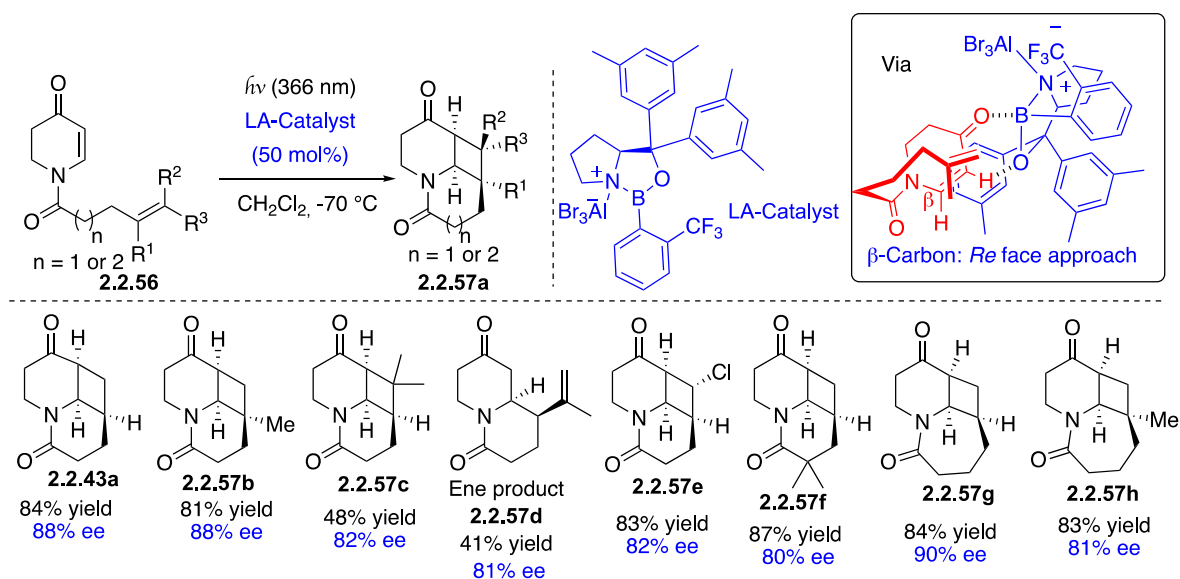
Historically, chiral Lewis acids (CLA) have been used to provide enantiocontrol through a transient chiral catalytic LA-substrate complex. This interaction has been well exploited in the

development of successful enantioselective radical reactions. The first application of chiral Lewis acid catalyzed RCA (radical conjugate addition) was reported by Sibi and Porter in 1996.<sup>99</sup> A book chapter on “stereoselective radical reactions” has covered the literature on this subject until 2010.<sup>178</sup>

Following their work on two-point hydrogen bond catalysts in photocycloaddition and facing the limit on the need for lactam substrates (*vide infra*), Bach's group was interested in Lewis-acid activated [2+2] photocycloaddition. Fortunately, as with the Kemp's acid derived catalyst, an extensive bathochromic absorption shift (> 50 nm) in UV-Visible spectrum of the complex enone substrate/Lewis acid allows a selective excitation, a condition required to develop a potential catalytic regime. This specificity is crucial to avoid detrimental non-asymmetric background reactions. Based on a previous observation on the effect of EtAlCl<sub>2</sub> on photodimerization,<sup>179</sup> preliminary study using AlBr<sub>3</sub>-oxazaborolidine catalyst showed that it is possible to induce enantiocontrol in [2+2] photocycloaddition of coumarin (Scheme 96) with moderate to good enantioselectivities.<sup>180,181</sup>

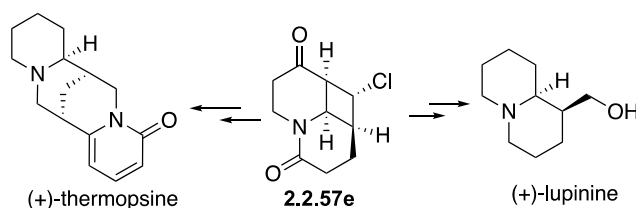
The enantioselective process was more efficacious in photocycloaddition of enones like 5,6-dihydro-4-pyridones **2.2.56**.<sup>182</sup> With irradiation at 366 nm, the chiral LA-substrate complex is excited through  $\pi$ - $\pi^*$  transition and photocycloaddition proceed enantioselectively. The enantioface approach of the tethered alkene relied on double linkage of the chiral Lewis acid and enone which yields the cyclobutane product as a single diastereoisomer with good to high ee's. This synthetically relevant method was applied to different enones with variations on the alkene moiety using chiral AlBr<sub>3</sub>-activated oxazaborolidines as the catalyst (Scheme 96). This type of super Lewis acid catalyst has been known to induce high enantiocontrol in ionic reactions but not yet used in radical chemistry.<sup>183</sup> Six and seven membered fused tricyclic compounds were obtained in good yield except for compound **2.2.57d** that was isolated in the presence of ene product. ee's up to 90% was obtained in these transformations.

## Scheme 96 Lewis Acid Activated Enantioselective [2+2] Photocycloaddition



This synergistic system allows preparation of natural products such as (+)-lupinine and formal synthesis (+)-thermopsine (Scheme 97) from cycloadduct **2.2.57e** with high enantiocontrol.

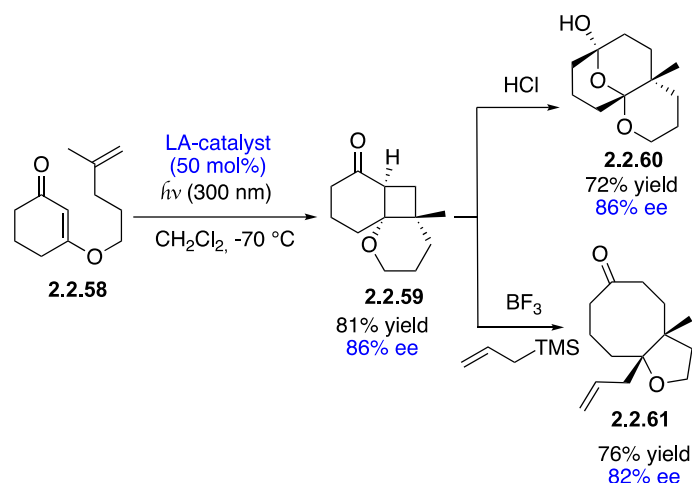
## Scheme 97 Synthesis of Alkaloid Natural Products



Mechanistic comparison between enone and coumarin substrates revealed that in the presence of Lewis acid, the reaction was accelerated with coumarins whereas a decrease of reaction rate was observed with enones but a high stereoselective reaction was operative due to the high extinction coefficient of the LA-enone complex.<sup>184</sup>

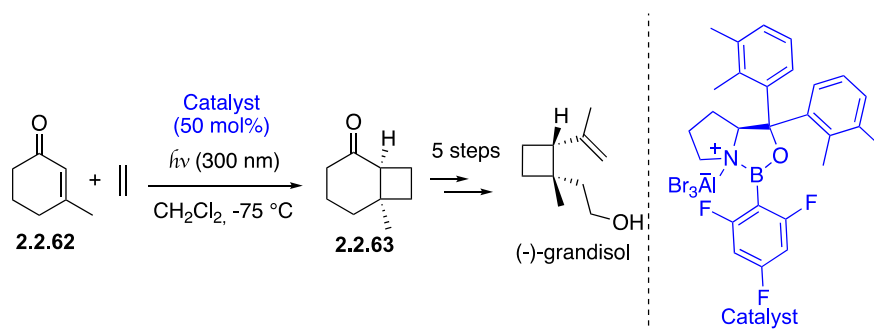
The enantioselective [2+2] photocycloaddition was also successfully applied to 3-alkenyloxy-2-cycloalkenones **2.2.58** with high enantioselectivity (Scheme 98).<sup>185</sup> Under acidic conditions it is possible to trigger cleavage of cyclobutane ring **2.2.59** delivering tricyclic compound **2.2.60** without erosion of ee. In the presence of  $\text{BF}_3$ , ring expansion combined with allylation allowed the formation of eight membered ring **2.2.61** with good yield and ee.

## Scheme 98 Enantioselective [2+2] Photocycloaddition of 3-Alkenyloxy-2-Cycloalkenones



Subsequent report by the same group has demonstrated the transposition of this strategy to intermolecular photocycloaddition. Refining the catalyst structure was necessary for the development of reaction with cyclic enones and alkenes.<sup>186</sup> The authors took advantage from the high efficiency of this methodology to design the enantioselective total synthesis of (-)-grandisol, which was accomplished in six steps with overall yield of 13% from cyclohexanone 2.2.62 (Scheme 99).

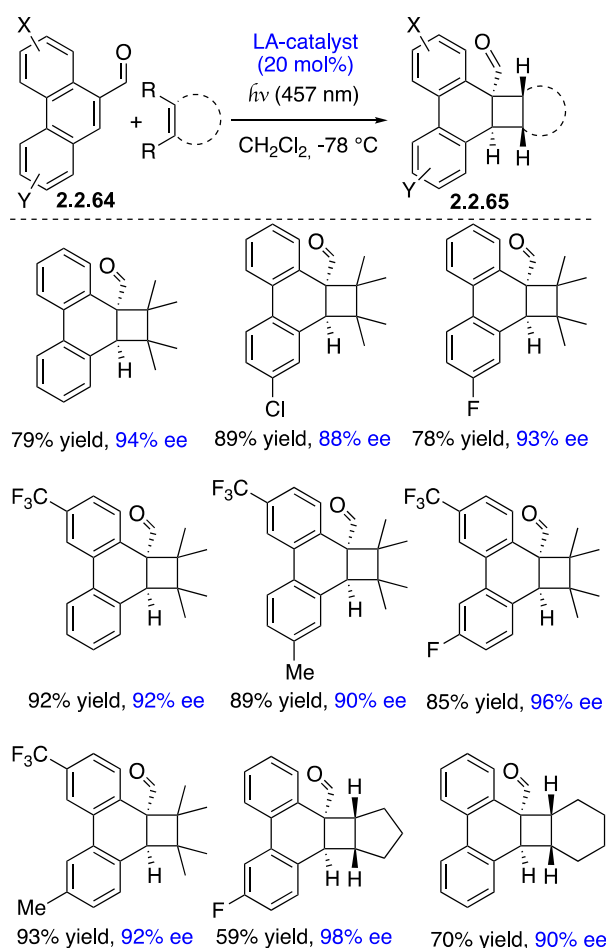
## Scheme 99 Intermolecular [2+2] Photocycloadditions using Chiral Lewis Acids



As mentioned before, excitation at this wavelength allowed the energy lowering of  $\pi\text{-}\pi^*$  in the complex, however it also affects the  $n\text{-}\pi^*$  of the non-complexed  $\alpha,\beta$ -unsaturated carbonyl compounds which undergoes a racemic background reaction. A high catalyst loading (50 mol%) was therefore necessary to limit this phenomenon.

To overcome this problem, the search for a substrate that will give a bathochromic shift beyond  $n-\pi^*$  absorption was required. Lewis acid complexed to phenanthrene-9-carboxaldehyde **2.2.64** was a good candidate for a selective excitation. Despite a maximum absorption at 387 nm, the complex showed a broad absorption wavelength region beyond 420 nm. Indeed, after optimization of experimental conditions, excitation at  $\lambda = 457$  nm allowed the decrease of the catalyst quantity to 20 mol% to induce good stereocontrol.<sup>187</sup> Different groups were tolerated except Lewis basic sites (like alkoxy and carbonyl groups) because of competitive binding to the catalyst. Products **2.2.65** were obtained in 59-93% yields and 82-98% ee's (Scheme 100).

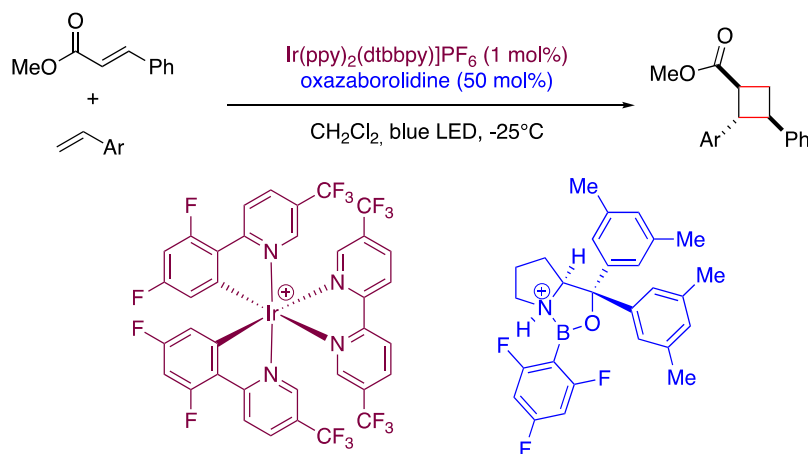
**Scheme 100 Intermolecular [2+2] Photocycloaddition to Phenanthrene-9-Carboxaldehyde**



Recently, [2+2] photocycloadditions of cinnamate esters in a highly enantioselective manner using chiral oxazaborolidine Lewis acids has been reported (Scheme 101).<sup>188</sup> Efficiency

of this cocatalytic system relies on the ability of the chiral Lewis acid to accelerate the Dexter energy transfer. Especially, oxazaborolidine was selected as the chiral Lewis acid due to its remarkable efficiency during the enantioselective syntheses of cyclobutanes reported by Bach. More precisely, the Lewis acid cocatalyst could lower the energies of the frontier orbitals of the substrate, enabling a more efficient electronic coupling between the photosensitizer and the substrate, facilitating the energy transfer from the excited iridium photocatalyst to the cinnamate ester.

### Scheme 101 Enantioselective Intermolecular [2+2] Photocycloadditions using Chiral Lewis Acids



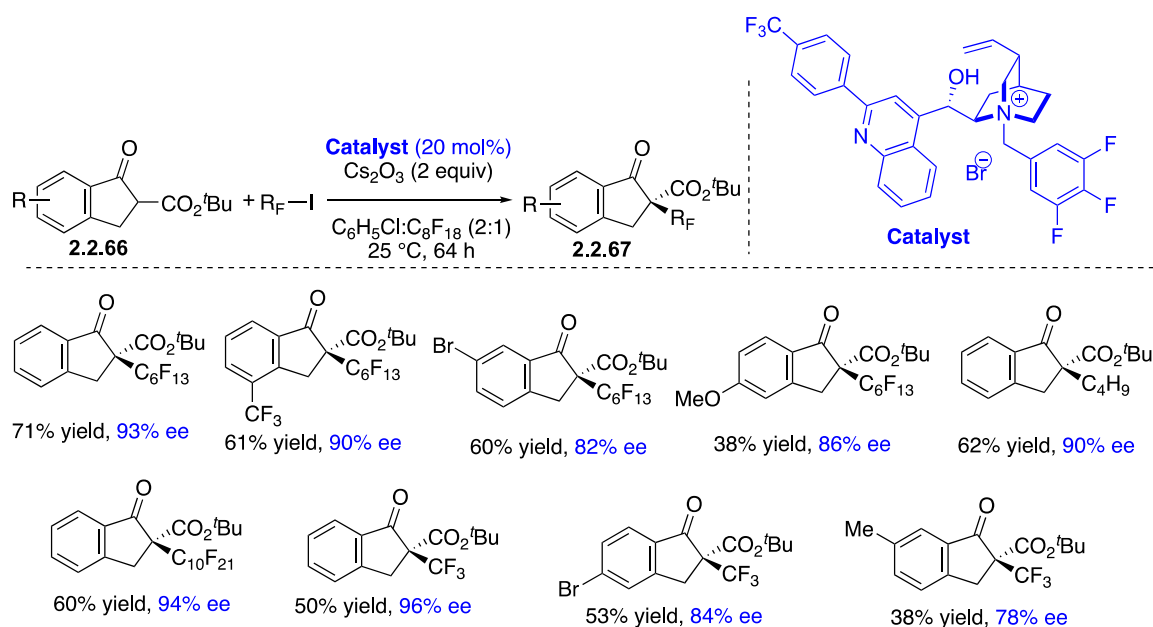
#### 2.2.3. Ion-pairing assisted radical transformations

Chiral phase transfer reagents (PTC) have been explored as catalysts to control stereochemistry of organic transformations considering that many intermediates in organic reactions are charged species. The success of this strategy relies on the electrostatic association between chiral anionic (or cationic) catalyst and cationic (or anionic) reactive intermediate. A wide range of reactions using this concept in ionic chemistry has been developed in the past three decades.<sup>189</sup> However, examples of control of enantioselectivity by ion-pairing catalysis in radical chemistry are scarce, and this strategy constitutes therefore an exciting challenge for the radical community. In continuation of their interest in photo-organocatalytic enantioselective alkylations, the Melchiorre group developed a visible-light-driven perfluoroalkylation and trifluoromethylation



of cyclic  $\beta$ -ketoesters **2.2.66** using EDA-complex activation strategy, in the presence of a chiral PTC catalyst.<sup>190</sup> The cinchonine catalyst was found to be better than the cinchonidine derivative in this stereoselective process, delivering perfluoroalkylated products **2.2.67** with ee's up to 96%. These indanones possessing quaternary stereocenters were synthesized in moderate yields (Scheme 102). Reactions with electron withdrawing groups on the aryl ring were superior to electron donating substituents which can be explained by a better stabilization of the enolate intermediate.

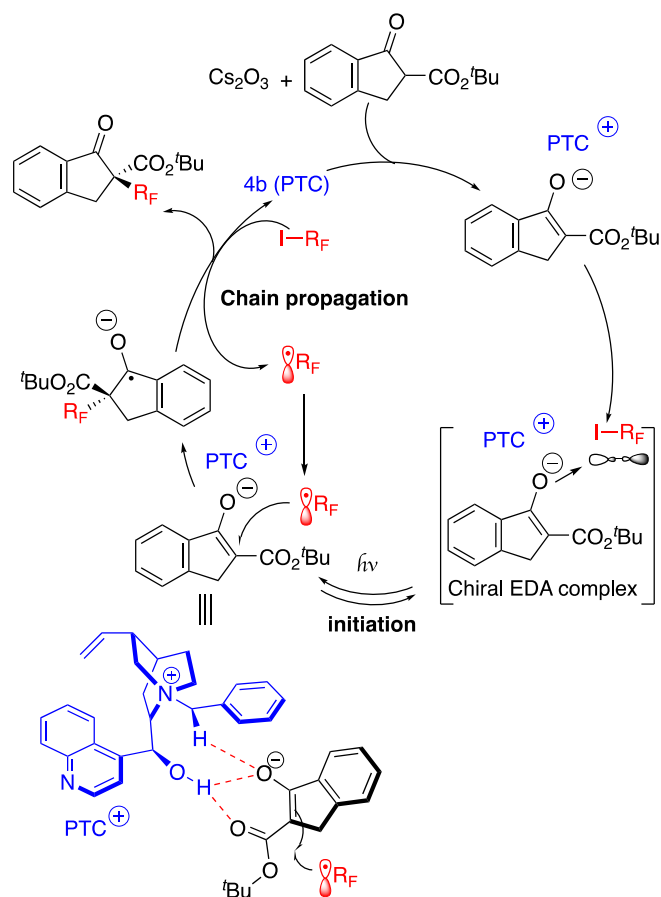
### Scheme 102 Ion-Pairing Catalysis: Enantioselective Perfluoroalkylation of $\beta$ -Keto Esters



The goal for this study was to take advantage of the *in-situ* generation of chiral pair between enolate and the PTC catalyst to induce the creation of a quaternary stereocenter. Upon deprotonation of the  $\beta$ -ketoester, the resulting enolate can act as an electron donor with respect to the electron acceptor perfluoroalkyl iodide through  $\pi$ - $\sigma^*$  orbitals (Scheme 103). The association of both species delivers a chiral EDA complex which facilitates a photoinduced SET. Thanks to matching polar considerations, the generated electrophilic perfluoroalkyl radical is a good candidate for radical addition to the chiral electron rich enolate transferring

the chiral information in this step. A radical chain propagation mechanism was anticipated in this reaction where the initiation step is assumed to result from the photoexcitation of the EDA complex.

### Scheme 103 Mechanism of Enantioselective Perfluoroalkylation of $\beta$ -Keto Esters via Ion-Pairing Catalysis

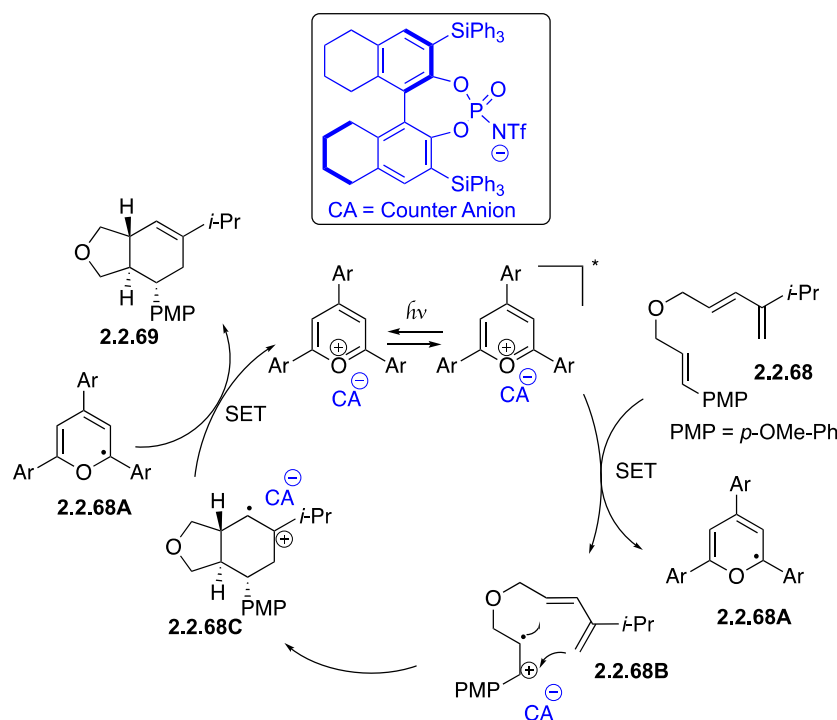


DFT calculations were conducted by another group to understand the source of the asymmetric induction, which suggests that multiple hydrogen-bonding interactions are the key factors for the observed high enantioselectivity.<sup>191</sup>

The Nicewicz group attempted to induce enantioselectivity in a formal Diels-Alder reaction using counter anion catalysis with moderate success. The authors combined pyrrylium salt, as a photooxidant catalyst able to generate a radical cation, and a chiral phosphonate as a counter anion catalyst to ensure stereo induction (Scheme 104).<sup>192</sup> An electron-rich dienophile is first oxidized generating the transient radical cation, which undergoes radical addition with the

electron-rich diene furnishing the cyclohexyl radical cation. Ion pair interaction between the two partners in this cyclization is anticipated as the key step for enantiocontrol. SET reduction of intermediate **2.2.68A** delivers the product **2.2.69** with 50% ee and 6:1 dr. Despite the modest enantioselectivity of this reaction, the proof of concept is interesting.

### Scheme 104 Formal Diels-Alder Reaction using Counter Anion Catalysis



### 3. Asymmetric radical processes with chiral transition metal-catalyzed

As already stated in the introduction, there is currently no clear-cut frontier between organometallic and radical chemistry. The coordination chemistry of radicals is manifold in view of the number of events that can happen when a radical reacts with a metal complex.<sup>193</sup> The two domains have established so strong and complex interplays, that numerous advances in one field have necessarily had an impact on the other. This is especially true of course for the top level reached by asymmetric transition metal catalysis. However, due to their sticky reputation of being highly reactive species difficult to control, enantioselective radical reactions have long remained a challenging field. The second part of this review aims to demonstrate how dominant enantioselective transition metal-catalyzed reactions proceeding via radical relay

have become. Progress due to additional merging of visible light photocatalysis are also covered. The atomic number of the metal has been selected to structure this section.

### 3.1 Titanocene and Chromium-catalyzed enantioselective radical reactions

#### 3.1.1 Titanocene asymmetric radical chemistry

Inner-sphere single electron transfer agents are key tools to promote redox radical reactions.

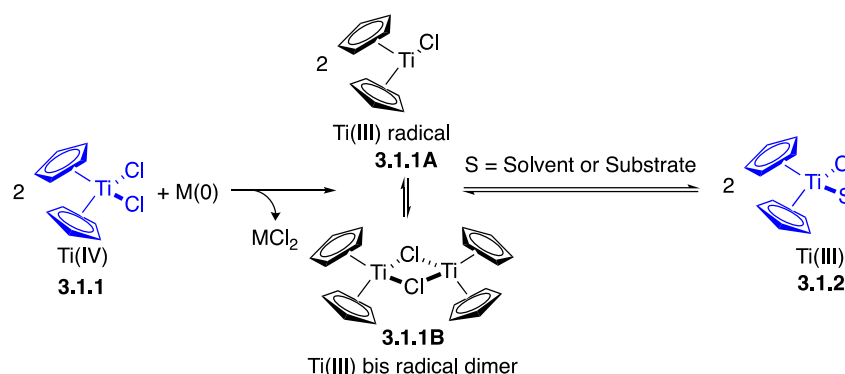
Among the latter, special attention has been devoted to Titanium (III) complexes, like  $\text{Cp}_2\text{TiCl}$

**3.1.1A**, universally known as the Nugent-RajanBabu reagent.<sup>194,195</sup>  $\text{Cp}_2\text{TiCl}$  is generally prepared by reducing the air-stable complex  $\text{Cp}_2\text{TiCl}_2$  with metal reductants like  $\text{Mn}(0)$ ,  $\text{Zn}(0)$

or  $\text{Mg}(0)$  (Scheme 105).  $\text{Cp}_2\text{TiCl}$  is in equilibrium with the corresponding dinuclear species

**3.1.1B**. Even though it is probably an oversimplified picture,<sup>196</sup> the dimer leads to the active complex by coordinating to the solvent and then to the substrate.

#### Scheme 105. Reduction of $\text{Cp}_2\text{Cl}_2$



Titanium-based reagents are attractive for numerous reasons: (i) catalytic titanium(III)-promoted redox transformations are readily accessible (vide infra); (ii) titanium is a rather inexpensive metal, among the most abundant transition metals on earth's crust; (iii) titanium derivatives are non-toxic and now widely accepted as green species.

Titanium(III) complexes possess an unpaired d electron, responsible for their reducing character. Although their reducing properties are mild,<sup>197,198,199</sup> the presence of a vacant site enables coordination with heteroatoms which increases their reactivity. Titanium has a Lewis acidic character and a strong oxophilicity, thus, carbonyl groups, oxiranes, oxetanes and

peroxides are substrates of choice. Titanium reagents also react with imines, Michael acceptors and some alkyl halides to mediate couplings, Barbier type and tandem radical reactions.<sup>200,201</sup> Recent studies merging Ti(IV)/Ti(III)-mediated transformations and photoredox catalysis as well as searches for new catalysts like cationic species will undoubtedly open routes to further developments.<sup>202,203</sup>

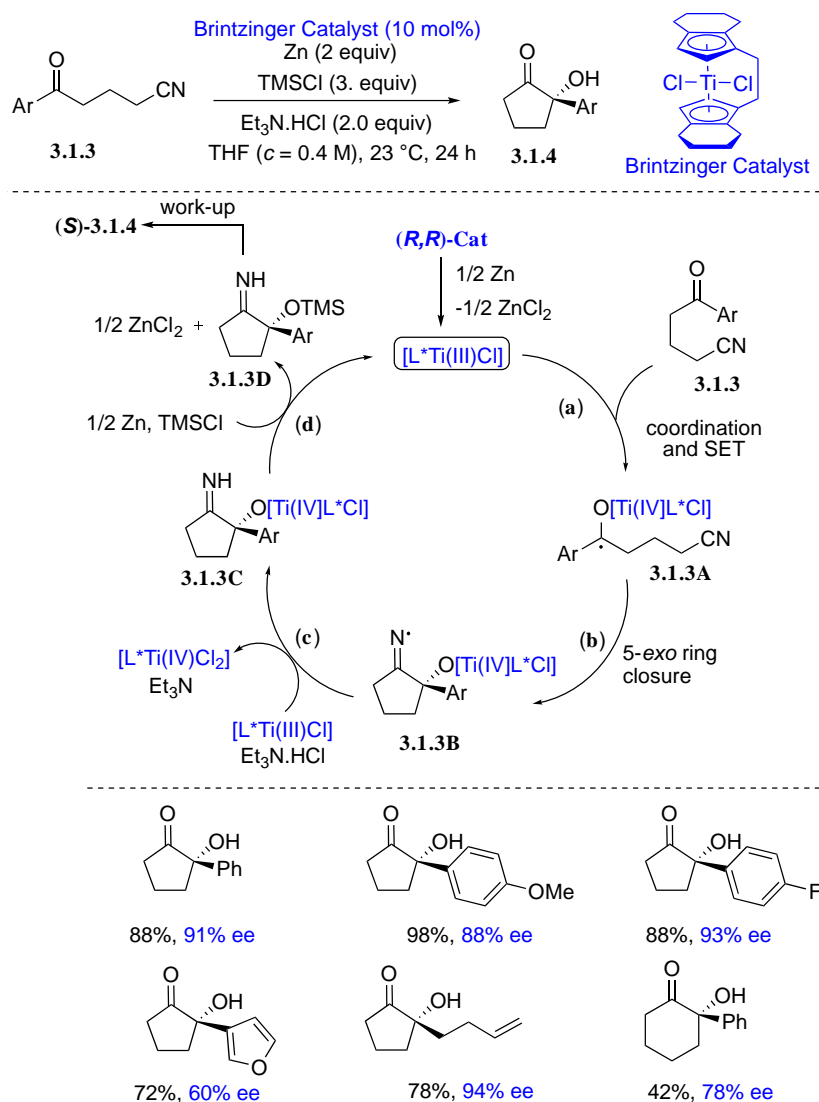
Although recall of historical background and mechanistic discussions are unavoidable, the following sections intend to focus on the most recent progresses in the use of chiral ligands for enantioselective catalysis in radical reactions.

### 3.1.1.2 Ketyl radicals coupling reactions

Ti(III) chiral catalysts are long known to promote highly enantioselective pinacol couplings.<sup>204,205</sup> After optimizing experimental conditions, chiral *ansa*-bis-tetrahydroindenyl titanium(IV) complex (Brintzinger's catalyst) was recently shown to efficiently catalyze the enantioselective reductive cyclization of  $\omega$ -ketonitriles **3.1.3** in the presence of zinc dust as stoichiometric reducing agent and additives that allow for catalytic turnover (Scheme 106).<sup>206</sup> The reaction leads to cyclic  $\alpha$ -hydroxyketones in good yield and high enantioselectivity. The proposed mechanism and selected results are exemplified in Scheme 106.<sup>207</sup> This protocol presents a precious advantage over the use of stoichiometric reducing agents like Sm(II). Once formed through the reductive initiation step, Ti(III) coordinates to the carbonyl group, simultaneous SET leads to ketyl radical **3.1.3A**. The latter undergoes 5-exo ring closure to form iminyl radical **3.1.3B**, which gives rise to imine **3.1.3C** via hydrogen atom transfer. The enantioselectivity is controlled in the cyclization step. The process works similarly with substrates prone to undergo 6-exo trig ring closure although with lower yields. The role of the trialkylammonium chloride in this redox step is crucial, as it allows hydrogen atom transfer to the nitrogen centered radical (the nature of the hydrogen atom donor in this type of reaction is still investigated and discussed, the process might also be viewed as a proton coupled electron

transfer (PCET)).<sup>208</sup> At the same stage, the Ti(IV) pre-catalyst is regenerated. The titanium(IV) alkoxide is quenched by TMSCl which also releases another Ti(IV) dichloride, reduced by Zn(0), to propagate the catalytic cycle by regenerating the Ti(III) active specie.

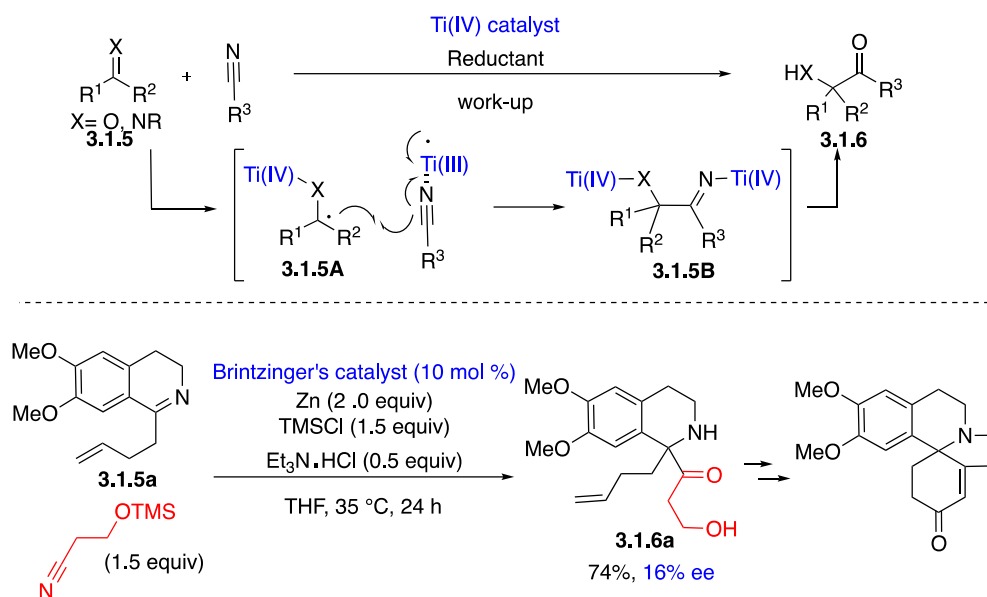
### Scheme 106. Intramolecular Addition of Ketyl Radicals to Nitriles



#### 3.1.1.3 Cross-coupling of imines and nitriles

Mechanistic studies point to the fact that these umpolung coupling reactions involve double activation of the radical precursor and of the radical acceptor.<sup>163</sup> As shown in Scheme 107, this is the case for intermolecular cross-coupling of carbonyls and imines (**3.1.5**) with nitriles. Attempts to perform the reductive coupling of imines with nitriles resulted in rather poor enantiomeric excesses.

## Scheme 107. Cross coupling of Imines and Nitriles

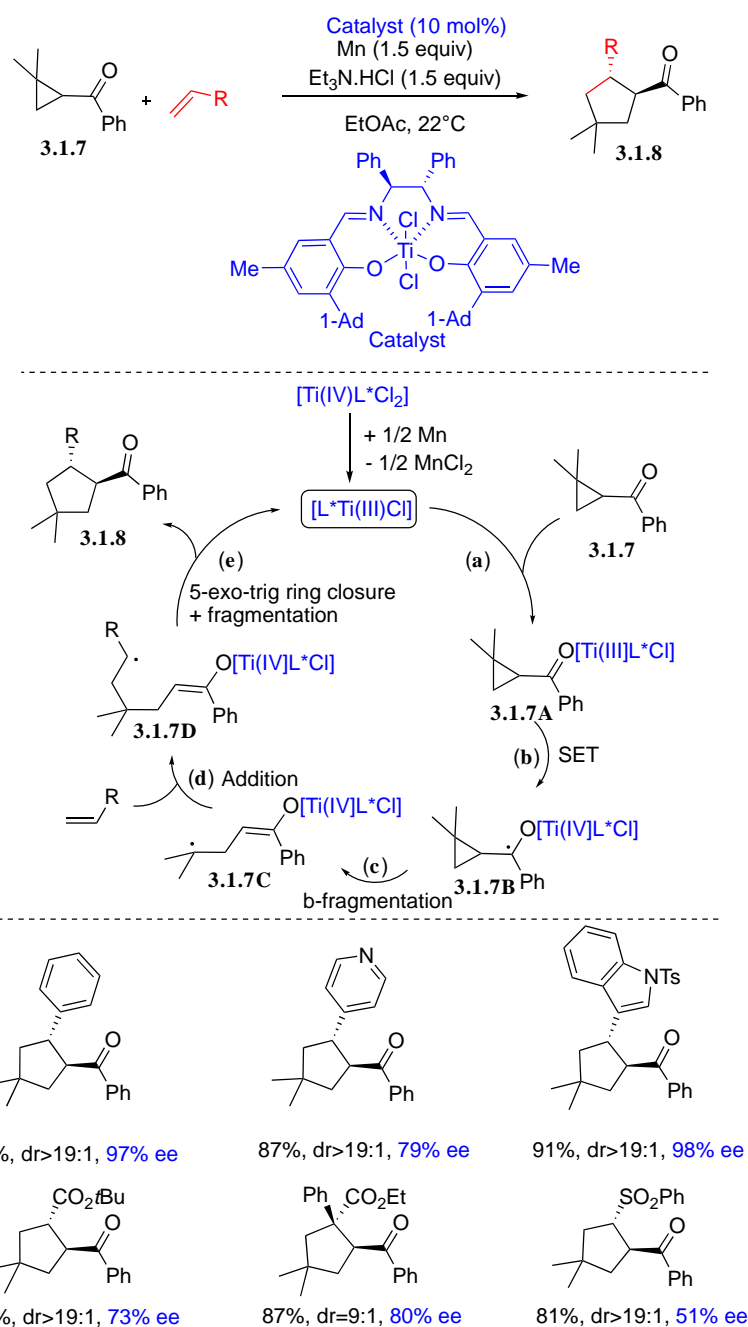


### 3.1.1.4 Redox relay to formal [3+2] cycloadditions

The intermolecular addition of homoallylic radicals **3.1.7C**, that can be formed either directly or through the opening of cyclopropylmethyl radical **3.1.7B**, to alkenes is a convenient route to five-membered rings **3.1.8**. This formal [3+2] cycloaddition has been applied to the Ti(III)-mediated reduction of cyclopropyl arylketones performed in the presence of alkenes (Scheme 108).<sup>209</sup>

The general mechanism is shown in Scheme 108. The tertiary homoallylic radical is generated through SET from Ti(III) to the carbonyl group followed by ring opening (the process can either be stepwise or concerted). Addition to styrene is followed by 5-exo trig ring closure onto the titanium-enolate double-bond. Subsequent or concerted fragmentation releases the Ti(III) catalyst which is the chain transfer agent. Formally the reaction should require a catalytic amount of reductant but decreasing the amount of Mn to 20 mol% resulted in lower yields. ESR evidence of the formation of the tertiary homoallylic radical was obtained by trapping it with DMPO. Enantioenriched cyclopentanes were obtained by using salen-supported Ti(IV) complex as catalyst. As exemplified in Scheme 108, diastereomeric ratios as high as 19:1 and enantiomeric excesses up to 98% were achieved.

## Scheme 108. [3+2]-Annulation of Cyclopropyl Arylketones



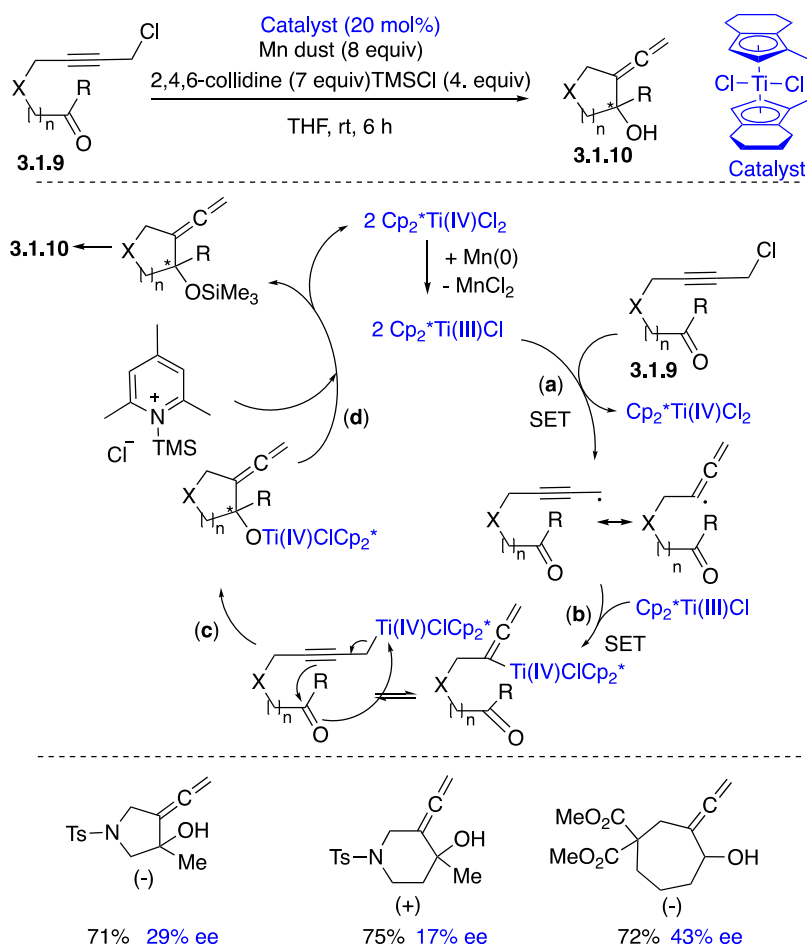
### 3.1.1.5 Barbier reactions

The synthesis of exocyclic allene can be achieved via the Ti(III)-mediated cyclization of propargyl chloride bearing an aldehyde or a ketone function located in a suitable position. The scope of the reaction was illustrated by the closure of 5- to 7-membered ring carbocycles and heterocycles.<sup>210</sup> According to the authors, the mechanism, supported by deuteration experiments, proceeds in three steps (Scheme 109). Upon coordination with Ti(III), the BDE



of O-H bond in water is weakened by about 60 kcal/mol, so that water becomes a good hydrogen atom donor. Theoretical calculations were performed in THF and this reactivity has been applied to radical deuteration.<sup>211</sup>

### Scheme 109. Enantioselective Formation of Exocyclic Allenes from the Cyclization of *O*-Ti(IV)-Ketyl Radicals

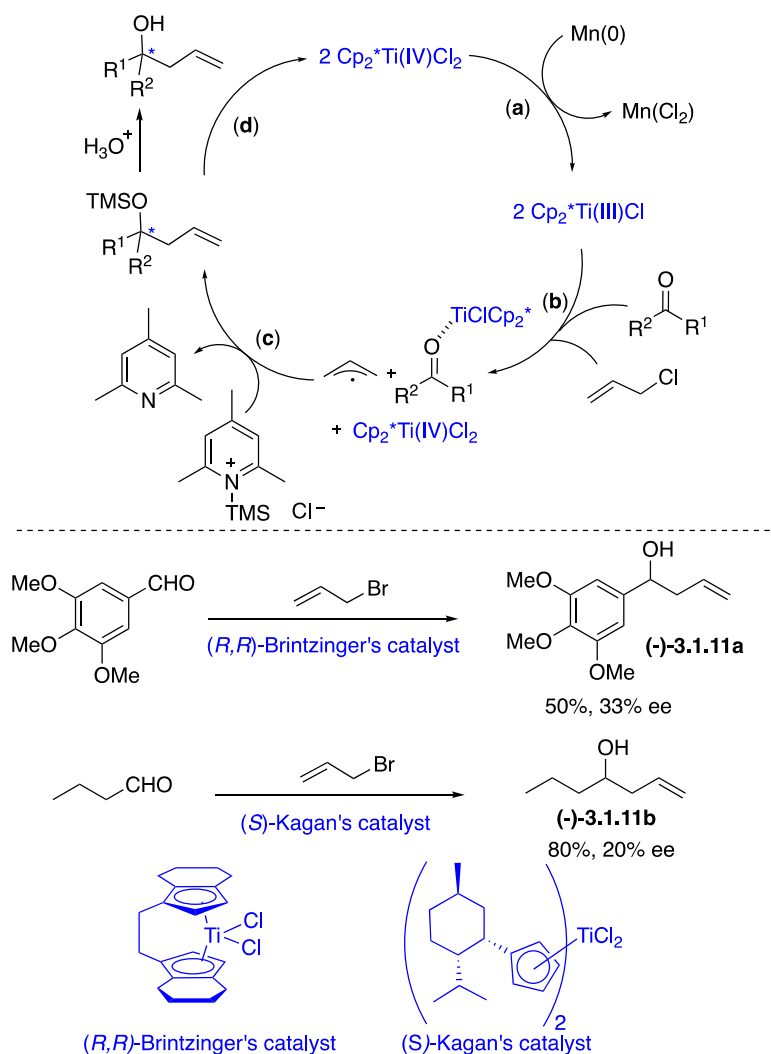


It is a typical radical-polar crossover process where a propargyl radical is reduced into a nucleophile by SET from the transition metal complex. The resulting nucleophile then reacts with the electrophile which can be a carbonyl or an imine.

The active catalyst is generated in situ by reducing Ti(IV) with Mn(0). The process starts with the formation of a propargyl radical (first SET event), then a second electron transfer generates the organometallic titanium(IV) intermediate which undergoes ring closure by nucleophilic addition to the carbonyl group. Ti(IV) dichloride is regenerated upon reaction with the *N*-SiMe<sub>3</sub>

pyridinium chloride formed in situ from  $\text{Me}_3\text{SiCl}$  and 2,4,6-collidine. The enantioselective synthesis was achieved by using the already mentioned Brintzinger's *ansa*-complex ((+)-dichloro(*R,R*)-ethylenebis(4,5,6,7-tetrahydro-1-indenyl)titanium(IV)) as a pre-catalyst. Low ee's, ranging from 15 to 43%, were obtained (Scheme 109). The use of  $\text{CpTiCl}_2$  (formed in situ via the reduction of  $\text{CpTiCl}_3$  by Mn dust), a catalyst which allows coordination with bidentate BOX ligands did not lead to higher ee's, however, this reagent increases the scope of enantiopure ligands that can be used.<sup>212</sup>

### Scheme 110. Barbier's Allylation Reactions

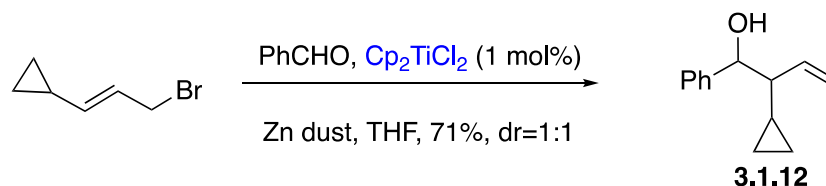


This reactivity of titanocene complexes also applies to Barbier type allylations, crotylations and prenylations of carbonyls.<sup>213</sup> These reactions take place under mild conditions at room

temperature. The proposed mechanism differs from those discussed above. It involves the addition of an allyl radical to an activated carbonyl group (Scheme 110). This addition would be fast and irreversible. The search for chiral complexes to afford enantiomerically enriched homoallylic alcohols led to rather tedious ee's. As exemplified in Scheme 110, the allylation of 3,4,5-trimethoxybenzaldehyde, catalyzed by (*R,R*)-Britzinger catalyst, gave a 50% yield of (*S*)-**3.1.11a** and 33% ee. (*S*)-Kagan's catalyst led to **3.1.11b** in 80% yield and 20% ee.

However, the allylation mechanism is extremely complex. Reactions with conjugated aldehydes would proceed through the coupling of a Ti(IV)-coordinated ketyl radical with an allyl radical, whereas a competitive nucleophilic addition of allyl metal is envisaged in the case of prenylation. The complexity of the mechanism, its multi-parameter sensitivity and thus, its speculative character, is well illustrated by a recent article of Fleury et al.<sup>214</sup> These authors have pointed out the cooperative effect of Cp<sub>2</sub>TiCl<sub>2</sub>/Zn and phosphine in the activation of C-X bond to form allyl metal derivatives. The use of a cyclopropylmethyl vinylogous radical clock and the absence of ring opened products in the reaction of the corresponding bromide with benzaldehyde, support a pathway involving two rapid single electron reductions of the bromide (Scheme 111). They even propose that an allylzinc specie resulting from transmetalation of an intermediate allyl titanium complex might be the nucleophilic specie in this case.

#### Scheme 111. Use of Radical Clock: Two Sequential Fast Single Electron Reductions



#### 3.1.1.6 Epoxides ring-opening

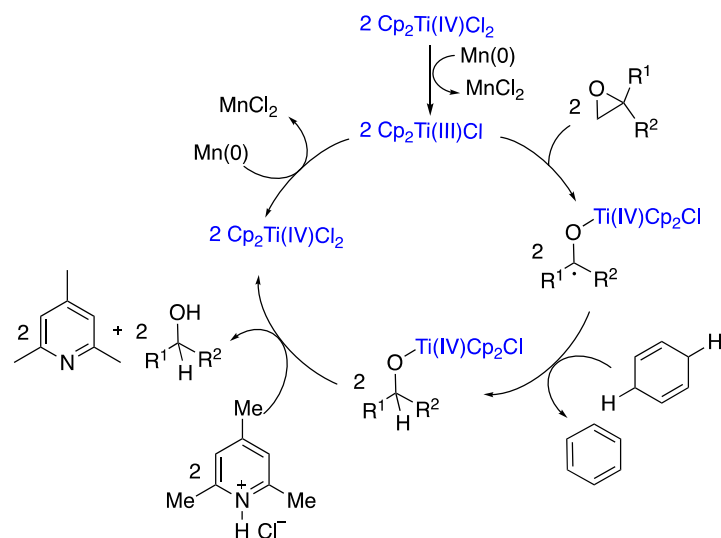
Since the seminal work of Nugent and RajanBabu,<sup>150,215</sup> the Ti(III)-promoted ring opening of epoxides has constantly expanded, mostly thanks to the impressive contributions from the Gansäuer's group.<sup>216,217,218</sup> Following on advances in the knowledge of its regio-and

stereoselectivity, this ring opening methodology became widespread due to the large array of available subsequent steps (reduction, elimination, cyclization to C=C, C≡C, C=O, C≡N bonds, conjugate addition, etc.). It constitutes probably the most important field of synthetic applications of Ti(III)/Ti(IV) redox system.

As already stated, the first decisive turning-point came from the design of procedures allowing for the catalytic use of titanium complexes.<sup>219</sup> Catalytic turn-over was accomplished thanks to the stoichiometric use of strong reducing metals like Zn or Mn (Mn appeared superior to Zn, probably because of the Lewis acidic character of ZnCl<sub>2</sub> formed during the process which can contribute to competitive polar epoxide ring-opening) capable of reducing in situ Ti(IV) into Ti(III) in the presence of weak acids. The suitable acids must not be acidic enough to protonate and open the epoxide ring but they must allow the titanium alkoxide to be protonated and regenerate the Ti(IV) pre-catalyst (Scheme 112). Substituted pyridine hydrochlorides and more particularly, collidine hydrochloride were shown to be mediators of choice. Ring-opening is regioselective. It leads to the more substituted radical (3° > 2° > 1°). Due to strain-release in the opening of the three-membered ring, this step is exothermic and thus has an early transition state. The preference for the formation of the more highly substituted radical should rather be connected to the steric strain introduced by the bulk of titanium complex rather than to the stabilization of the radical specie.<sup>220</sup> This is only true for electronically unbiased epoxides. Whenever a radical stabilizing substituent is attached to one of the epoxide carbon atoms, the stabilizing electronic effect governs the regioselectivity.<sup>171</sup>

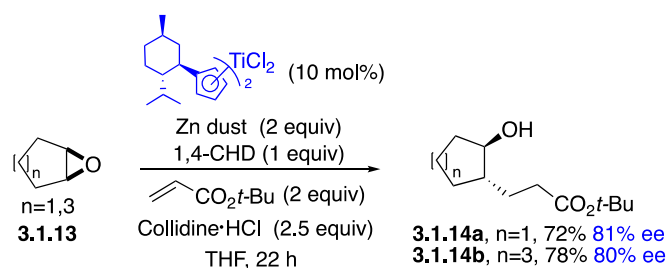
A catalytic cycle is exemplified in Scheme 112. Although efficient, the choice of 1,4-cyclohexadiene or even  $\gamma$ -terpinene as hydrogen atom donors (HAD) could not be considered as judicious in view of devising sustainable processes due to the formation of stoichiometric aromatic waste, particularly benzene. Other HAD were examined like water and methanol.<sup>221,222</sup>

### Scheme 112. General Catalytic Cycle for Epoxide Reduction



Dihydrogen was also an attractive HAD and the use of organometallic complexes like Vaska's<sup>223</sup> and Wilkinson's<sup>224</sup> homogeneous catalysts whose Metal-H bonds dissociation energies are rather low ( $\approx 59$  kcal/mol in the case of Rh-H) have been investigated. The latter methodologies could as well have been classified as bimetallic dual catalysis (vide infra). Early and late transition metal catalysts were shown to be compatible. The combination of  $\text{CpCr(CO)}_3\text{Na}$  and  $\text{CpCr(CO)}_3\text{H}$  catalysts with titanocene avoids the use of any stoichiometric reductant.<sup>225</sup>

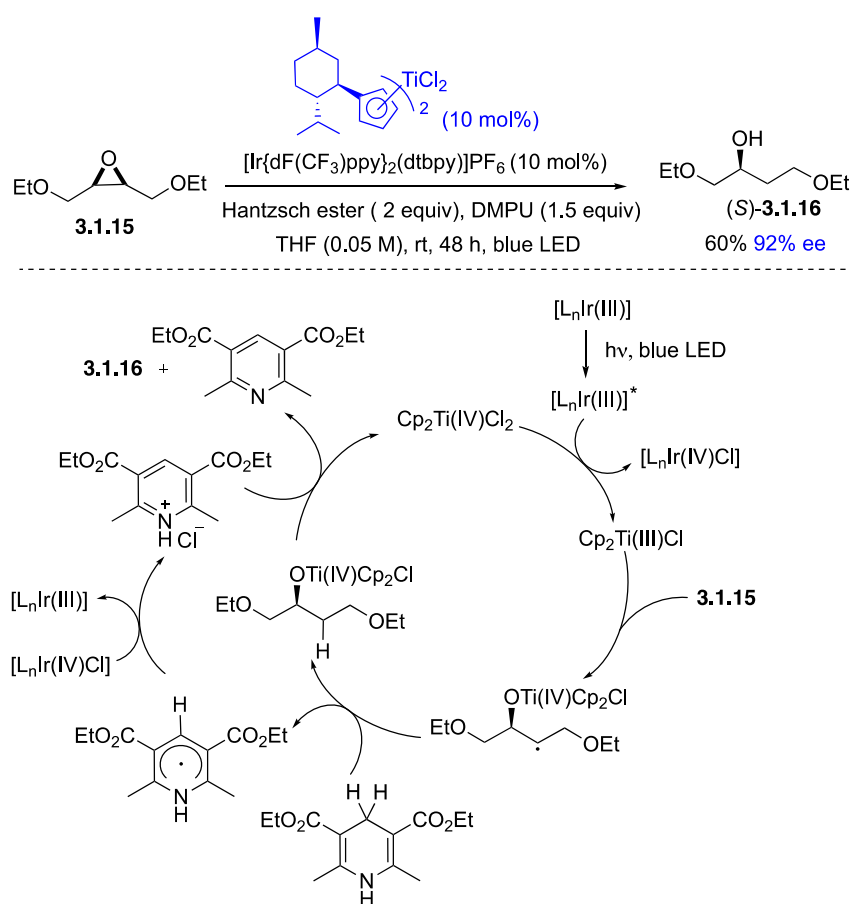
### Scheme 113. Desymmetrization of Meso-epoxides: Ring Opening Followed by Giese Addition



Investigations have naturally moved towards the pursuit of enantioselective processes. The ready availability of enantiopure epoxides from allylic alcohol using Sharpless' oxidation strategy has opened routes to enantioselective syntheses of natural products.<sup>226,227</sup> However, the

search of enantiopure ligands to perform regio- and enantioselective ring opening was the biggest challenge. The first developments arising from the desymmetrization of *meso*-epoxides.<sup>228</sup> The highest ee's were observed when using Kagan's catalyst (10 mol%), with Zn(0) as stoichiometric reductant, 1,4-cyclohexadiene as hydrogen atom donor and collidine hydrochloride. Examples of tandem ring-opening, radical-controlled *trans*-conjugate addition (d.r.>98:2) are shown in Scheme 113. It was noted that somewhat counterintuitively, the menthol-derived Kagan's complex led to enantiomeric excesses similar or even superior to those obtained with its phenylmenthol analog. Molecular modelling clearly showed that only steric interactions were responsible for the selectivity in ring opening.

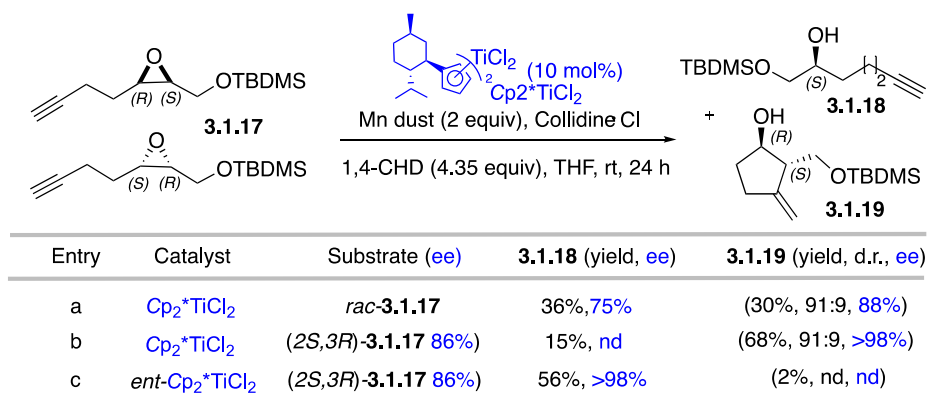
#### Scheme 114. Merging Ti(III)-mediated Enantioselective Epoxide Ring-opening and Ir Photoredox Catalysis



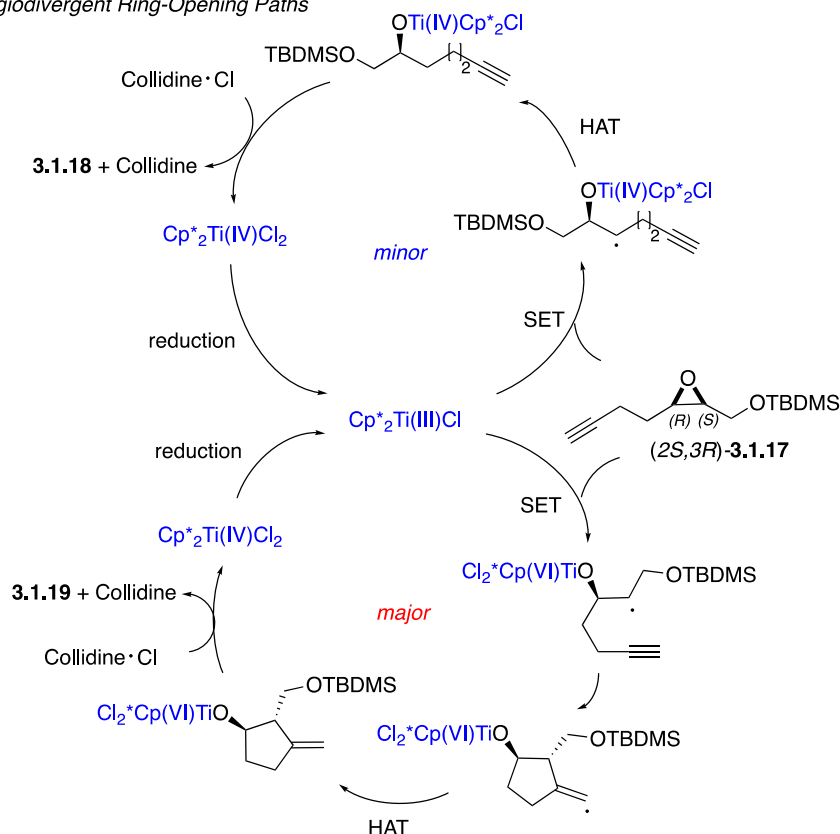
It has recently been shown that the association of Ti(III) catalysis with photoredox catalysis lead to experimental protocols that circumvent the need for metallic reductant and

stoichiometric acidic additives. In these reactions, Hantzsch-ester is the HAD and the resulting delocalized radical is oxidized into the corresponding hydrochloride by Ir(IV)-generated from Ir(III) in the light-induced initiation electron transfer step (Scheme 114).

### Scheme 115. Enantioselective 5-*exo-dig*-Cyclization from Regiodivergent Epoxide



#### Regiodivergent Ring-Opening Paths



In spite of the problem arising from regioselectivity, application to regiodivergent ring-opening afforded new resources.<sup>229,230,231</sup> The reaction was applied to unbiased *cis*-1,2-disubstituted epoxides (the latter can be viewed as “pseudo *meso*-epoxides” according to Gansäeur). In this case, the products resulting from the two-competitive enantioselective C-O bond cleavage are

constitutional isomers. Unless the substituents in position 1 and 2 are sterically and electronically very different, the two expected products are formed in similar yields from racemic starting material. As stated by the authors, the ring-opened products are formed in high enantiomeric excess from racemic substrates and in exceptionally high enantiomeric excess from enantioenriched substrates via a double asymmetric process. This is well illustrated by the case of Sharpless epoxide **1** (1-(tert-butyldimethylsilyl)oxy-2, 3-epoxy-hept-6-yne), (Scheme 115, entry a/b).

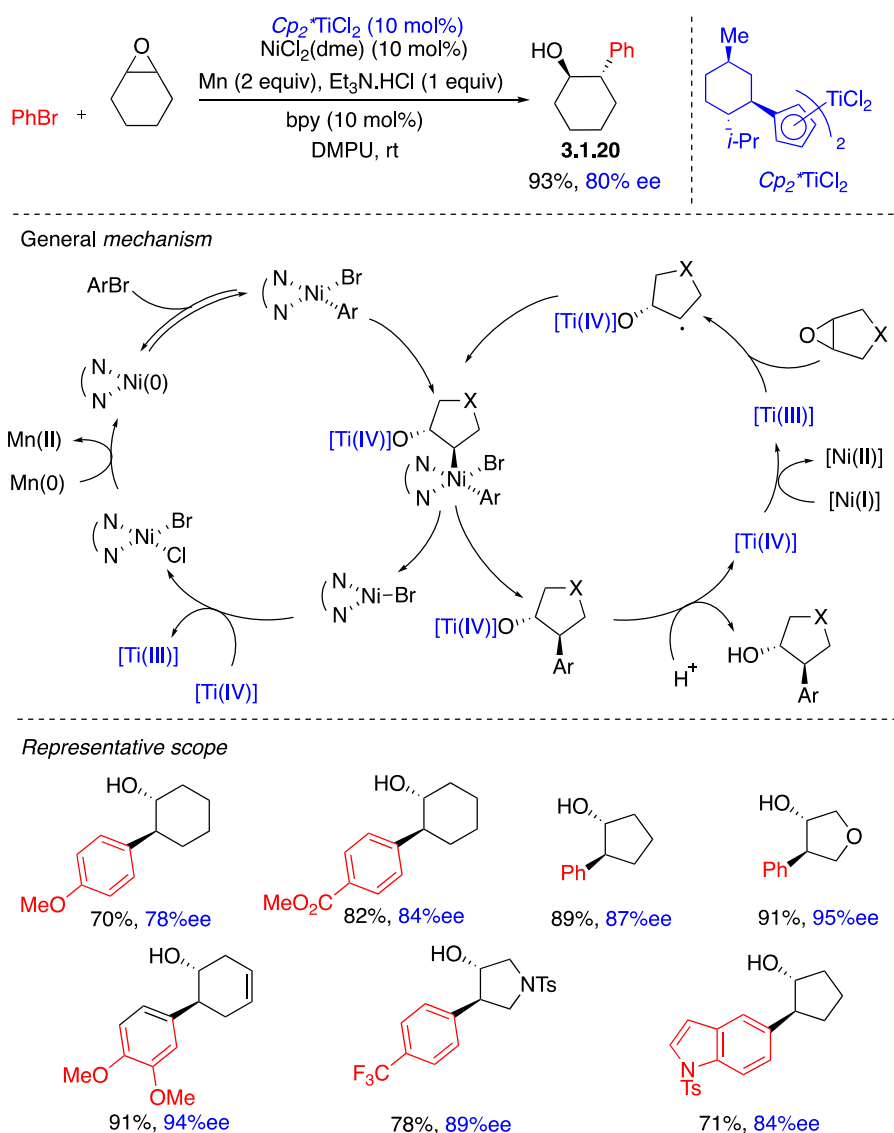
In this particular case, one route leads to a 5-hexynyl intermediate radical which undergoes a fast 5-*exo-dig* diastereoselective ring closure before the hydrogen atom is transferred (product **3.1.19**). Both routes for ring opening are enantioselective with selectivity determined in the SET step and it can be noted that the minor product is obtained with the highest ee. When the reaction is applied to enantiomerically enriched starting material, the enantiomeric purity of the major product is effectively higher than that of the substrate (entry b). The use of the enantiomeric catalyst results in the reversal of chemoselectivity (entry c).

#### 3.1.1.7 Dual radical redox relay catalysis

The enantioselective cross-coupling of *meso*-epoxides with aryl halides has been investigated by Zhao and Weix.<sup>232</sup> The reaction is catalyzed by associating (bpy)NiCl<sub>2</sub> to a chiral titanocene under reducing conditions (Mn(0)). Menthol-derived Kagan's complex again provided the best results. As shown in Scheme 116, the radical resulting from the homolytic cleavage of the C-O bond reacts with Ni(II) intermediate (*vide infra*, section 3.3). The resulting Ni(III) complex undergoes reductive elimination with retention of configuration to give the coupling product **3.1.20** in excellent yield and ee. A variety of functional groups (ether, ester, ketone, nitrile, ketal, trifluoromethyl group, sulfonamide, sulfonate ester) were compatible; both aryl and vinyl halides (or triflates), as well as five- to seven-membered rings were used.

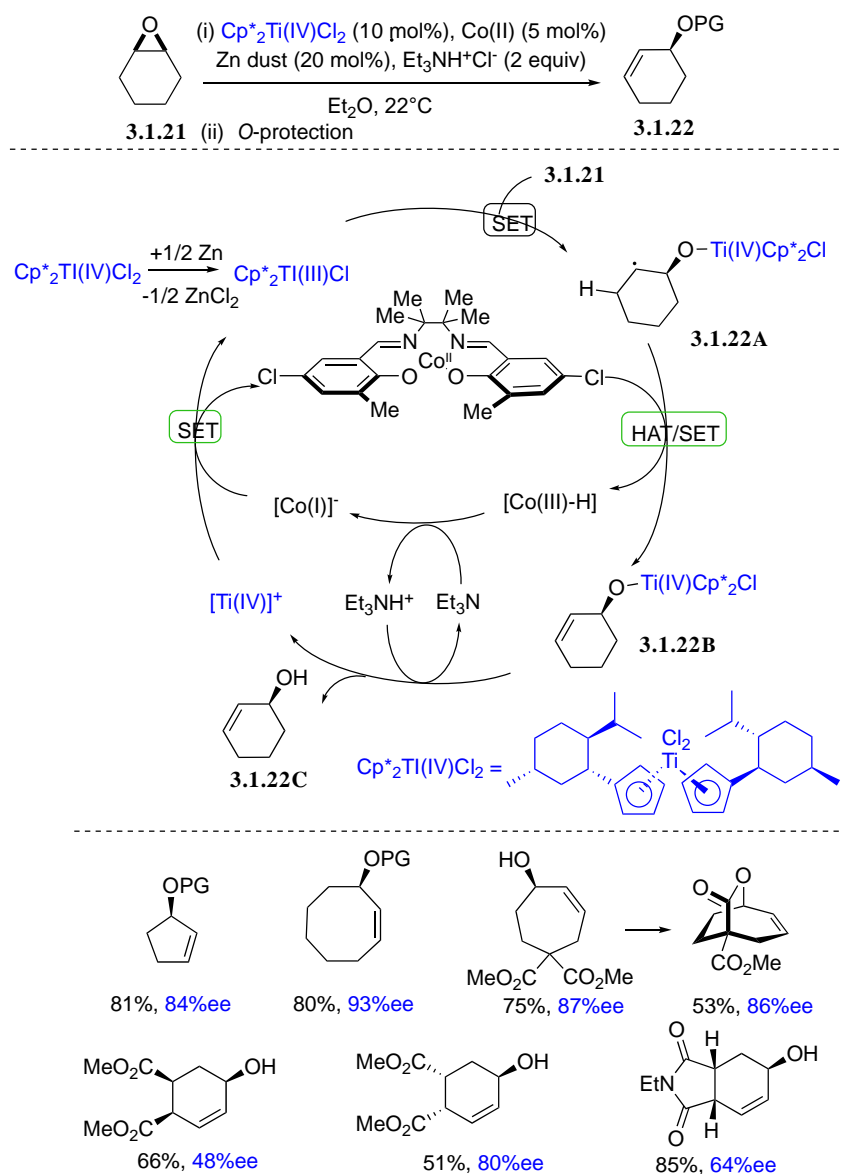


## Scheme 116. Dual Ti/Ni Catalysis for the Enantioselective Arylation of Epoxides



Recently, the cooperative use of Ti and Co as co-catalysts to promote the enantioselective transformation of *meso*-epoxides to allylic alcohols has been reported.<sup>233</sup> Yields were improved and chemoselectivity was shown to be complementary with respect to the methodology using  $\text{Cp}_2\text{TiCl}$  alone.<sup>234</sup> The proposed mechanism for the so-called *redox neutral* transformation and selected examples are given in Scheme 117. The results were optimized by using Kagan's complex and an electrophilic Co(II)-salen complex as catalysts. The latter was found to be a good compromise preventing the alcohol resulting from the reduction of the epoxide to be formed as side-product.

### Scheme 117. Dual Ti/Co Catalysis for the Enantioselective Formation of Allylic Alcohol



The formation of the active Ti(III) chiral complex is initiated by reduction of Ti(IV) pre-catalyst with a catalytic amount of zinc dust. The enantioselective reductive opening of the C-O bond generates an alkyl radical A which undergoes hydrogen atom transfer to the Co(II) co-catalyst to form the enantio-enriched allylic Ti(IV)-alkoxide B and a weakly acidic Co(III)-hydride.

Proton transfer to trimethylamine would serve as a relay to release the allylic alcohol **3.1.22C**, it generates at the same time as the anionic Co(I) specie. Subsequent electron-transfer between Co(I) and Ti(IV) regenerates the two active metallic species and allows for the two catalytic

cycles to proceed. It can be pointed out that the proposed mechanism should not necessitate a stoichiometric amount of  $\text{Et}_3\text{N}\cdot\text{HCl}$ . According to the authors, the latter, poorly soluble in the reaction medium, might play a critical role in activating zinc dust and stabilizing Ti(III) catalytic intermediates. The reaction can be applied to a series of *meso*-epoxides to provide products in high yields and good ee's. It is worth noting that in the given examples of polycyclic epoxides, they were converted into alcohols bearing three stereocenters.

As a concluding remark, one can forecast that this story is more than thirty years old and is far from being over due to the new impetus provided by the attractive cooperative use of photocatalysts<sup>152,153</sup> and the active search for more sustainable processes.<sup>235</sup>

### **3.1.2 Chromium-mediated enantioselective radical polar cross over reactions**

#### **3.1.2.1 Allylation from allyl halides.**

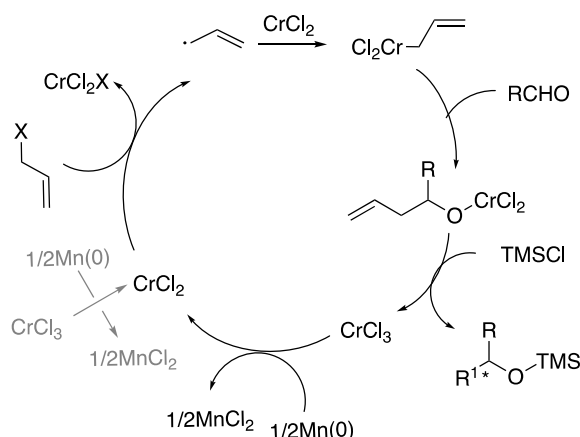
The historical back-ground of Cr(II)/Cr(III) redox reactions is extremely well related in a review published by Smith in 2006.<sup>236</sup> The activation of allyl halides by  $\text{CrCl}_2$  leads via allyl radical relay to allyl-Cr(III) species able to couple to aldehydes or ketones. The stoichiometric reaction was first improved by the addition of a catalytic amount of  $\text{NiCl}_2$  which once reduced in Ni(0) was able to activate less reactive organic halides and following on this modification, the new reaction became well known as the 'Nozaki-Hiyama-Kishi' (NHK) reaction. The problem to be solved to make the reaction catalytic in Cr was due to the strength of the Cr-O bond at the final stage. The solution came from Furstner and Shi who used  $\text{TMSCl}$  to cleave the Cr-O bond and Mn(0) as stoichiometric reductant to regenerate Cr(II) catalyst (these experimental conditions recall those of titanocene mediated Barbier allylations). As a consequence, sensitive  $\text{CrCl}_2$  could be replaced by in situ reduced, less expensive and air stable  $\text{CrCl}_3$ .

As summarized in Scheme 118, the activation of the halide proceeds in two steps. First, innersphere halogen atom transfer generates Cr(III) and an allyl radical. The latter adds to

another Cr(II) complex to form the reactive allyl Cr(III) specie. The sensitivity of the C-C bond formation creating a chiral carbon center to the presence of chiral ligands was then investigated. The first example of catalytic asymmetric NHK reaction was reported by the group of Cozzi and Umani-Ronchi who used a Cr(salen) complex.<sup>237</sup>

It is worth noting that pinacol coupling was a side reaction in nearly all cases and that several authors have reported asymmetric pinacol coupling mediated with Cr catalysts.<sup>238,239,240</sup>

### Scheme 118 Cr-Catalyzed Coupling of allyl Halides to Aldehydes

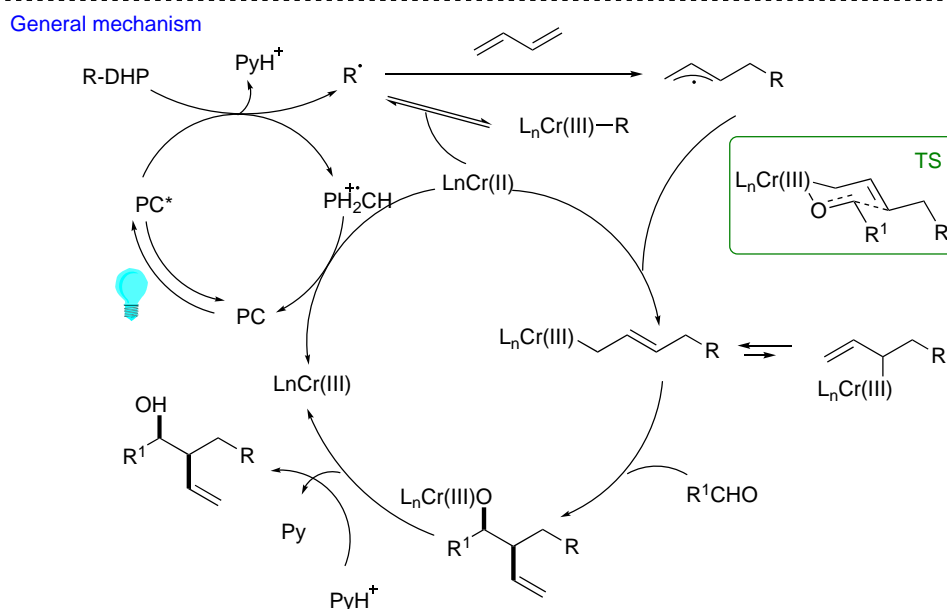
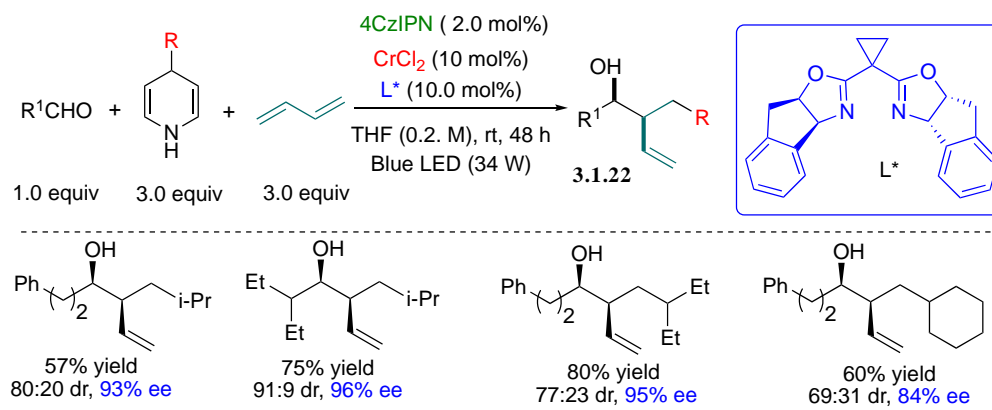


#### 3.1.2.2 Enantioselective allylation using dienes and alkenes as precursors

Several groups were interested recently in the use of photoredox catalysis to promote the formation of allylic radicals from alkenes or dienes. Starting from 1,3-conjugated dienes Glorius has reported the three-component enantioselective dialkylation of dienes involving Hantzsch esters as source of radical, and aldehydes as ultimate partners.<sup>241</sup> Optimization led to the use of 4CzIPN as organophotocatalyst rather than Ir based metallaphotocatalysts. As shown in Scheme 119, several difficulties had to be overcome. As the rate constant for the bimolecular trapping of the alkyl radical by Cr(II) is faster than that of radical addition to 1,3-diene, the trapping by Cr(II) had to be reversible to favor the formation of the stabilized allyl radical. A Bronsted acid was needed to cleave the Cr(III)-O bond but not acidic enough to cleave the Cr-C bond, PyH<sup>+</sup> cation was well suited. The diastereoselectivity of the process is explained on the

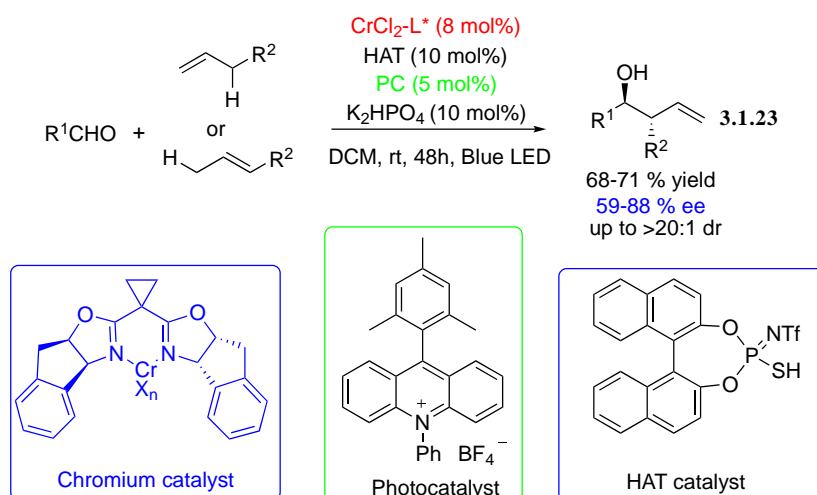
ground of Zimmerman-Traxler model. High enantioselectivity was reached by complexing Cr with bis-oxazoline ligands.

### Scheme 119. Example of Enantioselective Dual Photoredox Cr catalysis



Cr-catalyzed direct allylation of aldehydes from unactivated alkenes was accomplished by Kanai and Mitsunama.<sup>242,243</sup> Their system, catalyzed by  $CrCl_2$  in the presence of a chiral bisoxazoline ligand, includes an organophotoredox catalyst ( $9-Mes-10-PhAc^+ BF_4^-$ ), a HAT catalyst (thiophosphoric imide) which at the same time serves a source of proton to cleave in situ the O-Cr(III) bond (Scheme 120).

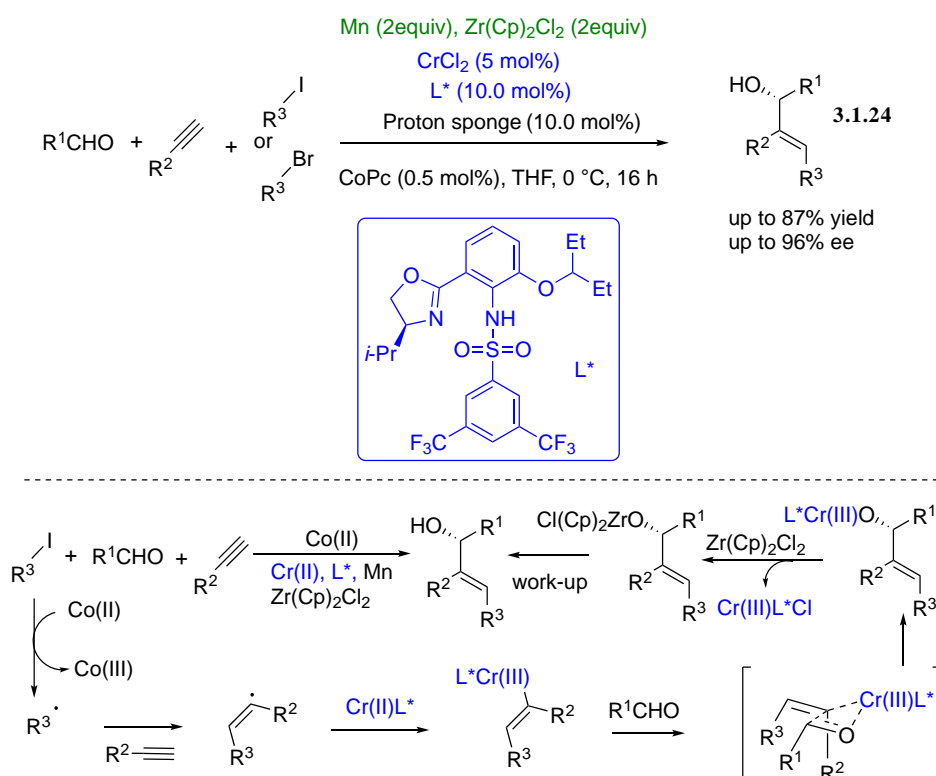
## Scheme 120 Cr-Catalyzed allylation of Aldehydes from Unactivated Alkenes



### 3.1.2.3 Vinylation

A complex three component reaction co-catalyzed by Cr and Co was designed by Zhand and coworkers,<sup>244</sup> that allows enantioselective vinylation of aldehydes (Scheme 121).

### Scheme 121 Cr-Catalyzed Vinylation of Aldehydes



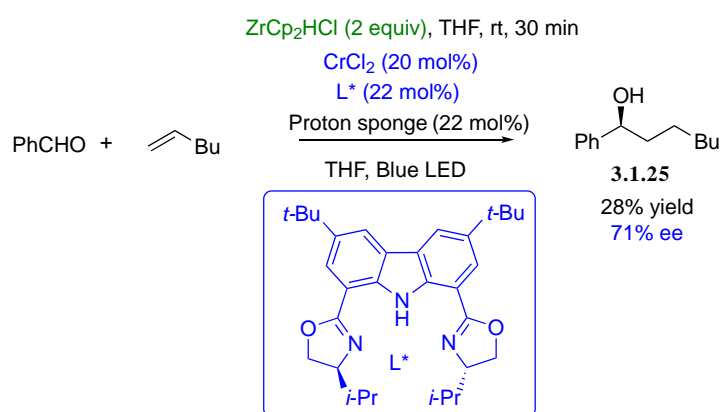
Based on TEMPO inhibition of the reaction, a mechanism involving the addition of a tertiary or a secondary radical or a perfluoroalkyl radical to the alkyne followed by trapping of

the resulting vinyl radical by Cr(II) to form the reactive nucleophilic specie is proposed. The Co(II) phthalocyanine (CoPc) catalyst would be necessary to form the alkyl or perfluoro alkyl radicals. The complex reaction medium involves 2 equivalents of Zr(IV) zirconocene to exchange the O-Co(III) bond by O-Zr(IV) bond and equal amount of Mn(0) to regenerate Cr(II) and Co(II) catalysts. Albeit ee as high as 96% could be reached with 70% yield, the process is far from meeting the requirements of sustainable chemistry.

### 3.1.2.4 Alkylation via hydrozirconation

Kanai and Mitsunuma<sup>245</sup> have recently developed a photostimulated radical relay linear alkylation of aldehydes (Scheme 122). After in situ hydrozirconation of terminal alkene, visible light irradiation cleaves the resulting linear alkylZr(IV) complex to form of an *n*-hexyl radical and Zr(III) specie. The radical intercepted by the Cr(II) complex provides the Cr(III) reactant that adds to the aldehyde. Metal exchange would then lead to Zr(IV) alkoxide and release Cr(III) that is reduced in situ by Zr(III). Two equivalents of the latter are necessary. Preliminary attempts to perform enantioselective reaction afford the expected alcohol **3.1.25** in 71% ee albeit in low yield (28%) in the presence of tridentate bis-oxazoline ligand.

#### Scheme 122. Photostimulated Linear Alkylation of aldehydes



### **3.2. Iron and Manganese-catalyzed enantioselective reactions**

Despite their performance in asymmetric synthesis, many transition metal catalysts suffer from the ever-growing concern for environment conservation and cost. Their high price and their toxicity are becoming a major barrier to the development of their industrial use.

Iron is the most abundant transition metal on earth crust being at the same time safe and very cheap. Moreover, it is involved in numerous biological systems as fundamental as cell oxygenation. In a very recent review, Rana et al. have detailed how rich is iron catalysis and how it has evolved since the 1940s to the most recent years.<sup>246</sup> Considering the ability of iron in different oxidation states to participate in a variety of elementary processes involving radicals, it is quite surprising that the use of iron in enantioselective catalysis of radical reactions has so far been very under developed.<sup>247,248</sup> The enantioselective organocatalytic photoredox alkylation of aldehyde was reported by Cozzi and coworkers where an iron(II) complex, i.e.,  $[\text{Fe}(\text{bpy})_3]\text{Br}_2$ , was used for the first time as photosensitizer.<sup>249</sup> In this process, visible light-excited Fe(II) complex initiates, via SET reduction of a C-Br bond, the formation of an alkyl radical but Fe is not involved in the catalytic cycle controlling enantioselectivity. In fact, very few articles were found where the Fe complex is the effective chirality transfer agent.

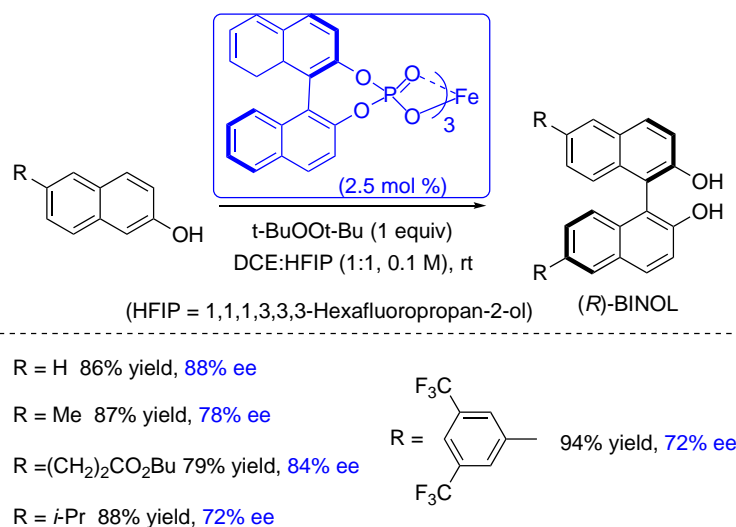
#### **3.2.1. Enantioselective homocoupling of 2-naphthols**

The first example is concerned with the enantioselective homocoupling (and even cross-coupling) of 2-naphthols catalyzed by iron(III) phosphate complexes.<sup>250</sup> As exemplified in Scheme 123



**Scheme 124. Mechanism for the Coupling of an Anion and a Radical**, chiral iron phosphate complexes were designed to perform the synthesis of  $C_2$  symmetrical chiral 1,1'-bi-2-naphthols with 3- and 3'- positions, potentially available for further chemical modification. The catalyst was prepared from ligand exchange between  $Fe(ClO_4)_3$  and the corresponding CPA conjugated base.

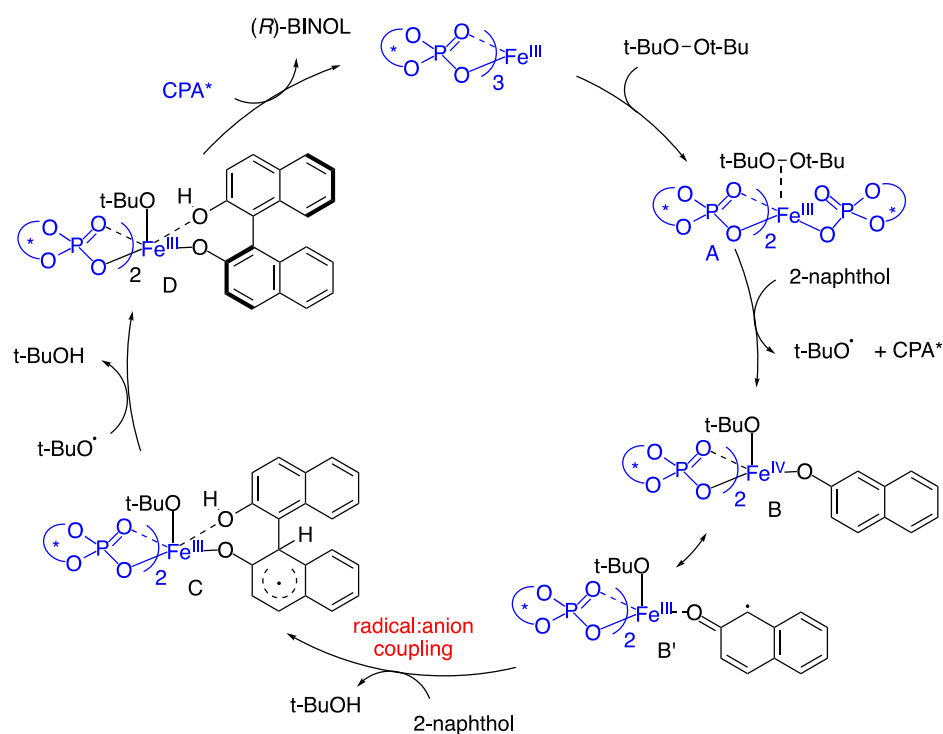
**Scheme 123. Iron Catalyzed Enantioselective Coupling of 2-Naphthols**



A kinetic study of the oxidative coupling of 2-naphthol is consistent with the radical/anion coupling mechanism proposed by the group of Katsuki.<sup>251</sup> After coordination of the peroxide to iron(III) (complex **A**, Scheme124), homolytic cleavage of the peroxidic bond generates a *tert*-butoxy radical and a high-valent Fe(IV) complex **B**, via ligand exchange between one of the phosphate ligands and a 2-naphtholate. Complexes **B** and **B'** can be viewed as mixed-valence isomers (internal SET). A radical/anion coupling step occurs after introducing another naphthol ligand which affords complex **C**. HAT (or electron transfer) from the complex to *tert*-butoxy radical rearomatizes the system (complex **D**). Eventually, a last ligand exchange releases (*R*)-BINOL. It is to be noted that an undesired SET process (reverse internal electron transfer in **D**) is likely to be responsible for the loss in optical purity of the product by allowing rotation around the C-C axis. These data show that the use of chiral phosphate anions as ligands might

provide a general platform for forthcoming applications of chiral iron catalysts in asymmetric synthesis.

### Scheme 124. Mechanism for the Coupling of an Anion and a Radical



### 3.2.2. Kumada and Suzuki-Miyaura enantioselective couplings

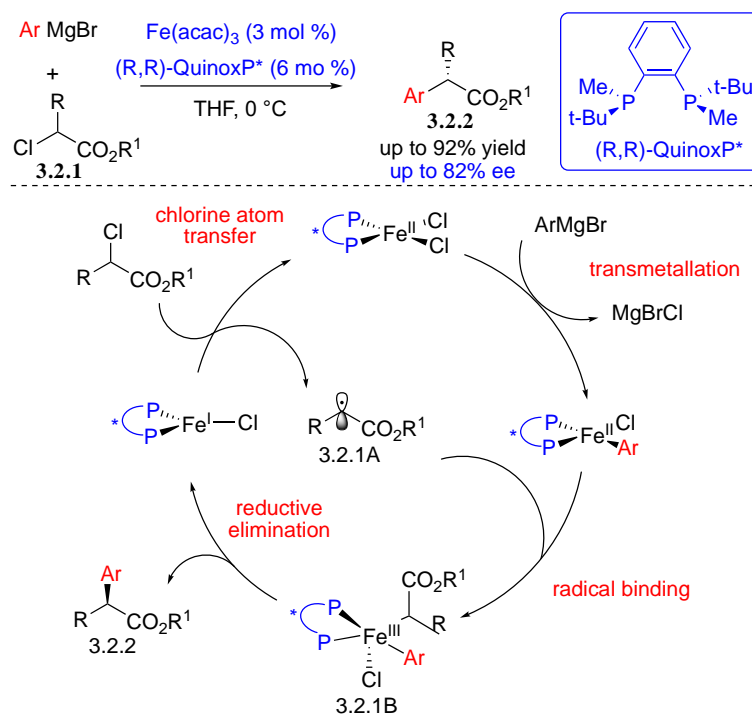
The enantioselective cross-coupling of  $\alpha$ -chloroesters with aryl Grignard reagents was achieved by Kumada and coworkers using  $\text{Fe}(\text{acac})_3$  as catalyst in the presence of chiral biphosphine ligands (Scheme 125). High yields and good ees were reported. The methodology is a route to  $\alpha$ -arylalkanoic acids **3.2.2** which are well known non-steroidal anti-inflammatories.<sup>252</sup>

Radical clocks of 5-hexenyl type were used as probe for the radical mechanism.<sup>252,253</sup> The reaction leads in this case to a mixture of enantioenriched acyclic arylated product and to cyclic

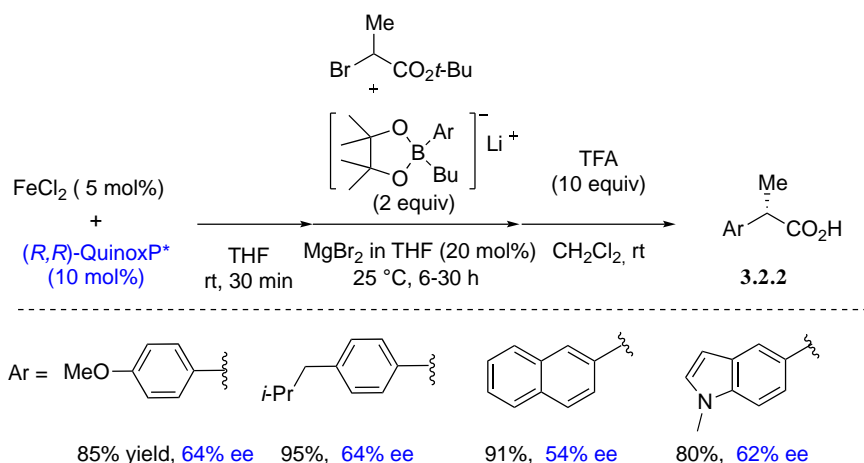
racemic cross-coupling products. Whereas similar Ni-catalyzed<sup>254</sup> enantioconvergent cross-coupling had already been reported, Fe had never been used before.

Theoretical calculations led the authors to select the mechanism depicted in Scheme 125 which involves Fe(III), Fe(II) and Fe(I) species.<sup>255</sup> Fe(I) chloride undergoes chlorine atom transfer to give Fe(II) chloride and release the carbon centered radical. Transmetalation of the latter Fe(II) intermediate with the organomagnesium reagent leads to a tetracoordinated aryl-Fe(II) complex that binds to the radical to form a Fe(III) complex. Reductive elimination of intermediate **3.2.1B** closes the catalytic cycle and regenerates the reactive Fe(I) specie (Scheme 125).

### Scheme 125. Fe-Catalyzed Kumada Enantioselective Cross-Coupling



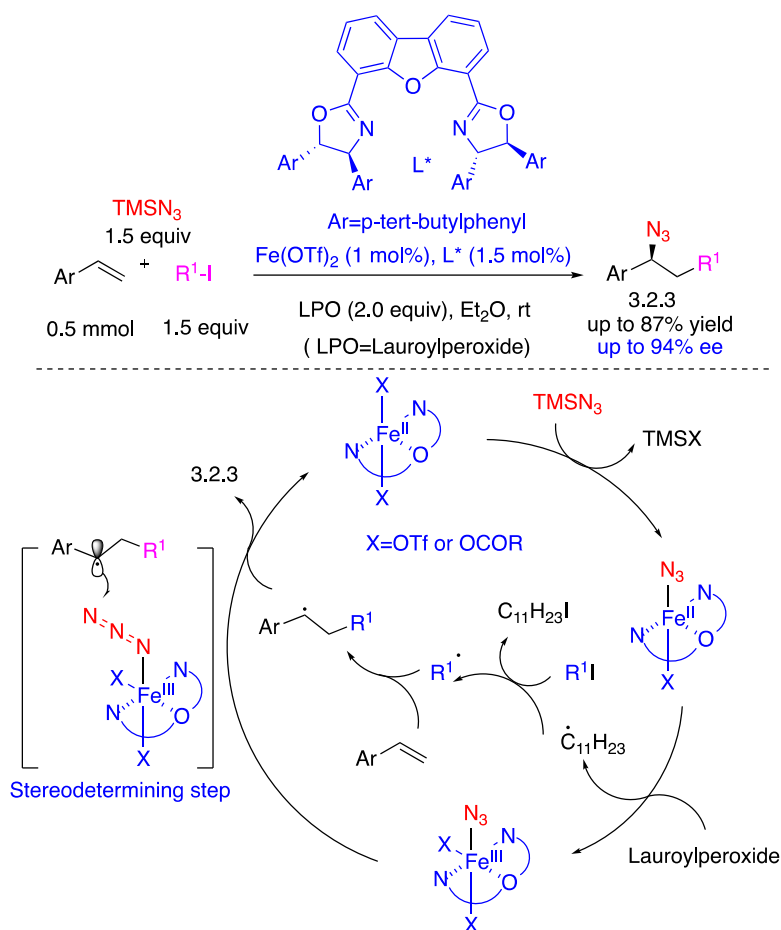
### Scheme 126. Iron-catalyzed Enantioselective Suzuki-Miyaura Coupling



Nakamura has also developed iron-catalyzed enantioconvergent Suzuki-Miyaura coupling of  $\alpha$ -haloesters.<sup>256</sup> The cross-coupling of lithium arylborates was accomplished by associating catalytic amounts of  $\text{FeCl}_2$  and the optimal chiral diphosphine derived from quinoxaline ((*R,R*)-QuinoxP\*). Yields ranging from 49 to 95% were recorded together with ee up to 64% (Scheme 126). Only the transmetallating agent differs from Kumada coupling; a mechanism similar to that discussed for Kumada cross-coupling is proposed.

Bao and co-workers have recently performed the enantioselective carboazidation of styrenes to reach products **3.2.3**,<sup>257</sup> aminoazidation and diazidation of styrenes.<sup>258</sup> As exemplified in Scheme 127, the carboazidation methodology is based on the use of  $\text{Fe(II)(OTf)}_2$  as catalyst in the presence of tridentate BOX ligand and  $\text{TMSN}_3$  as azide source. The  $\text{Fe-N}_3$  chiral complex enables the transfer of azide to the prochiral alkyl radical generated via X atom transfer. Based on theoretical investigations, the authors suggested a transition state through an outer-sphere pathway to explain the stereocontrol.

### Scheme 127. Iron Catalyzed Enantioselective Azide Transfer

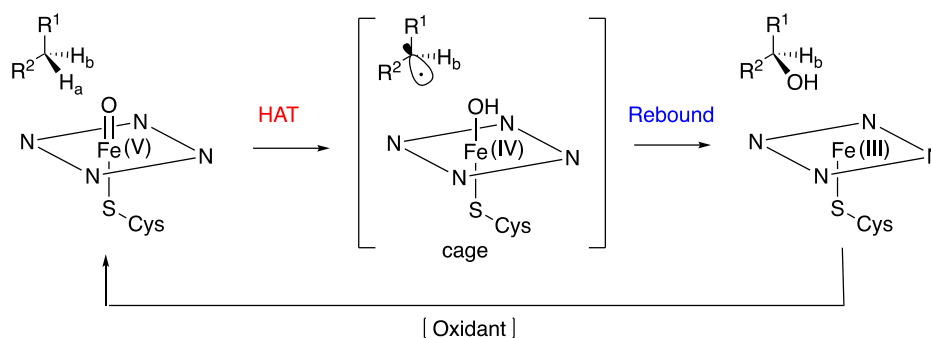


Taking into account the irreversible evolution of research towards the discovery of more and more sustainable processes in organic synthesis. The development of enantioselective iron-catalyzed radical methodologies remains a big challenge for the near future.

### 3.2.3. Iron and Manganese Bio-inspired Enantioselective Hydroxylation and Oxidation

The search for site selective non-activated C-H functionalization is a challenging field that still stimulates the creativity of synthetic chemists until at least half a century. The goal of this section is to illustrate how the understanding of Nature's metalloenzymes performance like cytochrome P-450s has inspired the design of complexes able to achieve bio-inspired enantioselective oxidations.<sup>259,260</sup> The mechanism of P450 hydroxylation and epoxidation is still an open subject of controversial debate.<sup>261,262</sup> Due to the wide extent and the complexity of this field the following report is restricted to selected recent examples illustrating enantioselective radical processes that mimic enzymatic C-H activation (Scheme 128).

### Scheme 128. A Simplified Mechanism of Cytochrome P450 HAT/Oxygen Rebound



A rather consensual mechanism for hydroxylation mediated by heme-iron(V)-oxo complexes is summarized in Scheme 128. It involves first a HAT step, immediately followed by oxygen rebound internal to the radical cage. Other mechanisms have been discussed for non-heme catalytic species notably those implying cage escape.<sup>263</sup> If the rebound mechanism (RM) is generally admitted for iron-oxo complexes, according to Nam and Pushkar,<sup>264</sup> the mechanism of C-H bond activation by manganese-oxo analogues is not fully elucidated yet. A recent proposal of

Theoretical examination of the occupancy of orbitals in the iron-oxo complex shows that the oxygen atom is close to an oxyl radical with a spin density of 1.0. The reaction starts with hydrogen atom abstraction that generates an alkyl radical in cage with the Fe(IV)-OH specie. The rebound of the carbon radical with the hydroxyl group leads to the formation of R-OH and release the Fe(III) complex which needs being reoxidized to close the catalytic cycle. The rate-determining step is the H-atom abstraction, the rebound step is very fast, its energy barrier ranging close to zero kcal mol<sup>-1</sup>. Thus, the alcohol is formed with a high degree of retention of stereochemistry.

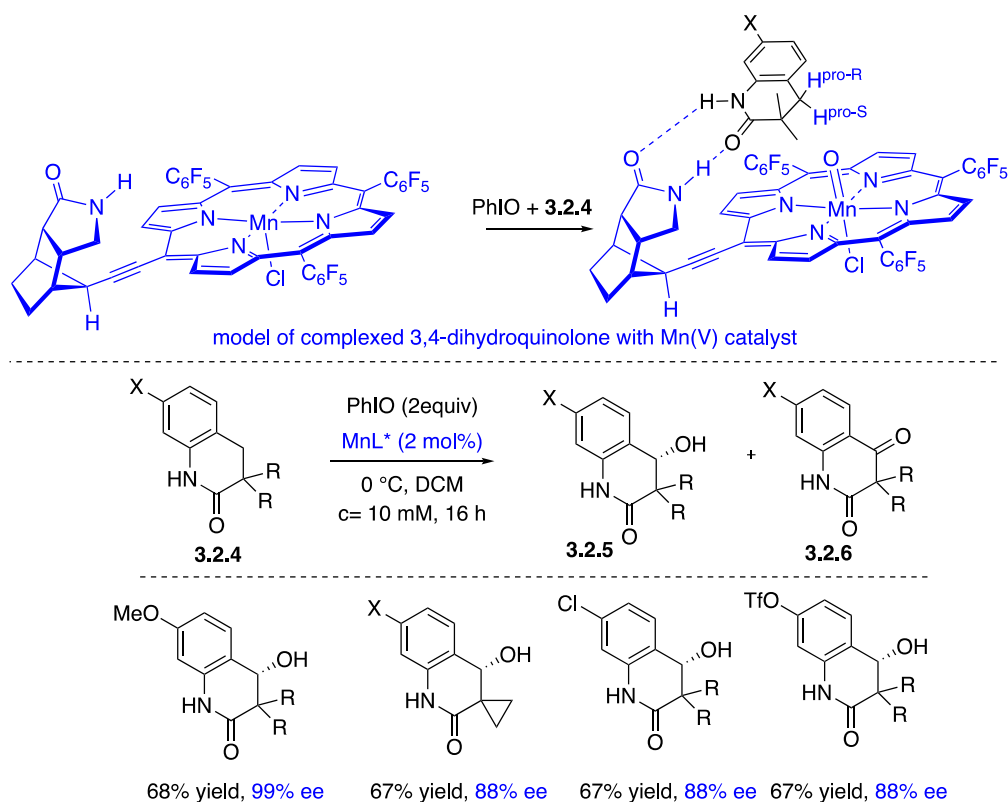
In nature, the host-guest interaction pre-positions the C-H bond to be submitted to the oxidant. Seminal attempts by Breslow to perform selective remote C-H functionalization introduced rigid linkers covalently attached to the substrate and the radical precursor.<sup>265</sup> Then, several groups inspired by Cram, Pedersen, Lehn (Nobel Prize 1987) and Rebek have demonstrated

that remote functionalization could get released from the harness of covalent linkage and benefit from double molecular recognition of the substrate by adequately designed enzyme mimics. This is notably the case of Breslow<sup>266</sup> (cyclodextrines), of Crabtree<sup>267</sup> (double anchoring by hydrogen bond based on Kemp's triacid) and Costas<sup>268</sup> (crown ethers). These pioneering data was the groundwork for the development of enantioselective bio-inspired oxidations.

As suspected early and now well exemplified in recent reviews, (renvoi??) the control of geometric rigidity of the substrate-complex governs the selectivity of the oxidation and overcome thermochemical barriers. The incidence of other parameters like medium influence, polar, electronic, torsional effects have been investigated. Most synthetic applications regarding enantioselective hydroxylation concern Mn catalysts rather than Fe catalysts.<sup>269</sup>

Bach and co-workers have designed a Mn porphyrin complex with a remote binding site giving rise to two-point hydrogen bonding interactions to oxidize 3,3-disubstituted 3,4-dihydroquinolones **3.2.4** (Scheme 129).<sup>270</sup> They used iodosobenzene as stoichiometric oxidant. The complexity of such process is that once formed, the enantioenriched secondary benzylic alcohol **3.2.5** can still be oxidized into the corresponding ketone **3.2.6**, leading to a significant loss of the optical purity. In fact, the C-H bond of the primary product is significantly weaker due to the vicinity of the oxygen atom. Thus, experimental conditions have to be optimized in order to minimize overoxidation. Ketone **3.2.6** and recovered starting material **3.2.4** can be readily separated. Under the optimized conditions, high conversion and excellent ee's could be achieved. It should be noted that the chlorine and triflate substituted starting materials led to low conversion but ee's remained very high.

### **Scheme 129. Enantioselective Oxygenation of 3,4-Dihydroquinolones**



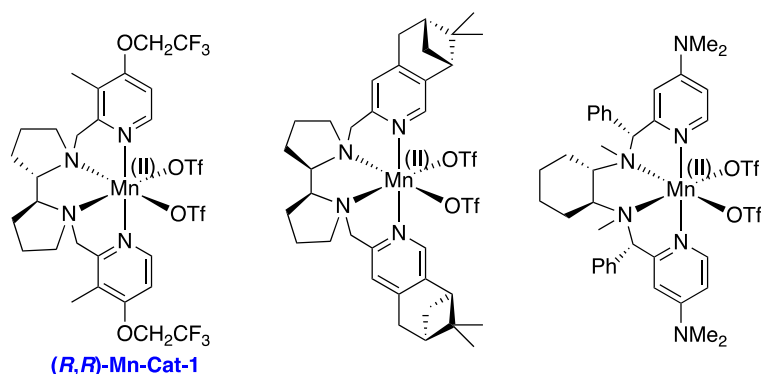
Reactions of the cyclopropane derivatives shown in Scheme 129 are mechanistically very informative. According to the authors, the absence of ring opening product resulting from the intermediate cyclopropyl methyl radical argues in favor of an oxygen rebound process, otherwise the very rapid ring opening ( $k \approx 10^8 \text{ s}^{-1}$ ) would have interfered.<sup>271</sup> In addition, the loss of one hydrogen bonding anchoring site, as a consequence of the replacement of the NH group by an NMe group, dramatically reduces the reactivity to 14% with nearly no differentiation of the enantiotopic hydrogen atoms (5% ee). An additional complexification of the process comes from overoxidation to ketone **3.2.6**. Kinetic resolution studies showed that the latter does not significantly alter the ee of the alcohol under optimized conditions ( $k_R/k_S = 4.2$  for X = OMe). Further developments showed that the scope of substrates could be extended to 3-alkyl-quinolones.<sup>272</sup>

Bryliakov and co-workers have provided a more general method avoiding any need of substrate chelation and supramolecular binding by designing a catalyst with a suitable chiral cavity. Inspired by Simonneaux's<sup>273</sup> report and Costas' iron catalyst<sup>274</sup>, they found that chiral



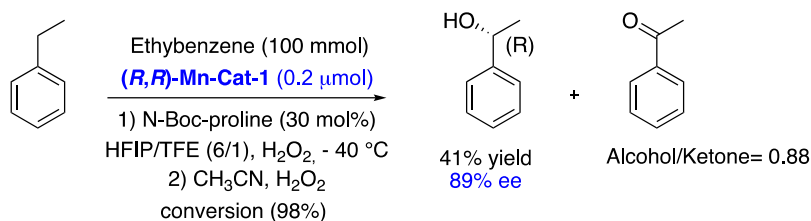
manganese aminopyridine complexes exhibited enantioselection in the oxidation of substituted ethylbenzenes with H<sub>2</sub>O<sub>2</sub> in the presence of carboxylic acid additives.<sup>275,276</sup> The catalyst was highly efficient (up to 250 TONs). The drawback for this process is again that significant amounts of ketones were formed, which required an excess of substrate to obtain the chiral alcohol as the major product. They have performed detailed kinetic studies of the oxidation of benzylic methylene groups by hydrogen peroxide catalyzed by chiral *bis*-amine-*bis*-pyridine manganese complexes [LMn(II)(OTf)<sub>2</sub>] where chirality is introduced by incorporation a 2,2'-bipyrrolidine moiety (Figure 4).

**Figure 4. Examples of Chiral Mn-catalysts Based on Tetradentate Aminopyridine Ligands**



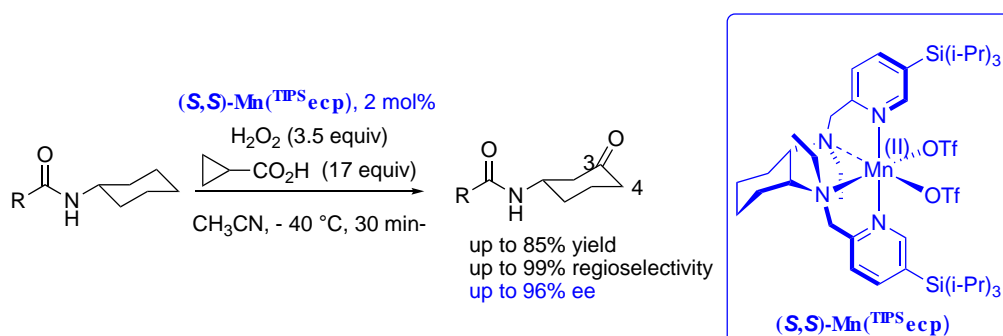
As suggested by Costas and Bietti,<sup>277</sup> in the presence of strong hydrogen bond donors like polyfluorinated alcohols, the alcohol reactivity could be efficiently lowered. Strong hydrogen bonding with the fluorinated alcohol reduces the nucleophilicity of the produced alcohol and reduces the rate of its further oxidation into the corresponding ketone. The benzylic C-H hydroxylation followed by oxidative kinetic resolution was optimized using ethylbenzene as substrate, 1-phenylethanol was obtained in 41% yield with up to 89% ee in the presence of 0.2-0.4 mol% catalyst loading (Scheme 130).<sup>275c</sup>

**Scheme 130. Optimization of Ethylbenzene Oxidation**



Costas and Bietti have made a highly important contribution to the understanding of the parameters that controls the aptitude of unactivated hydrogen atoms to be transferred. They started comparing the relative performance of H<sub>2</sub>O<sub>2</sub>-mediated oxidation catalyzed by Fe or Mn complexes to simple hydrogen abstraction by cumyloxy radical.<sup>269a</sup> This study provided evidence that both type of reactions involved HAT. In addition, the incidence of electronic effects of different functional groups led the authors to select amides as the most appropriate functional group to govern selectivity.

### Scheme 131. Desymmetrization of Mono-substituted Cyclohexanes



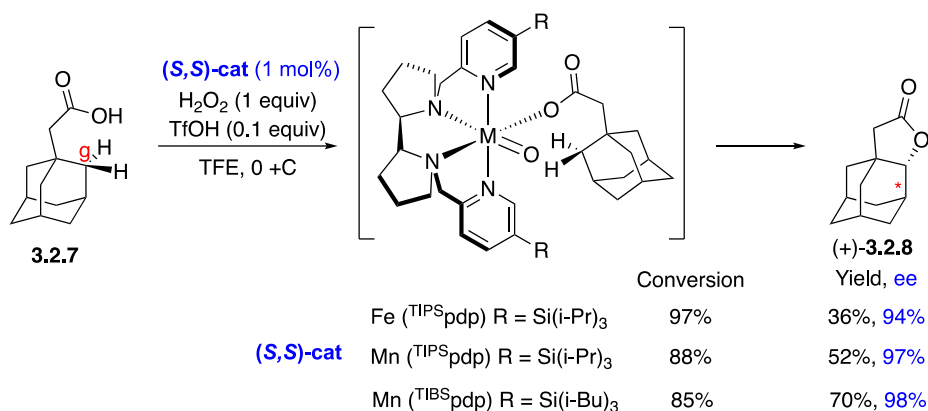
Bietti and Costas achieved the desymmetrization of monosubstituted cyclohexane derivatives (Scheme 131). In these substrates with particularly strong C-H bonds ( $\approx 95$  kcal/mol), the center  $\alpha$  to the functional group does not coincide with the reactive center. Over-oxidation up to the ketone avoids all the complexity introduced by the hydroxylation step.<sup>278</sup>

Oxidation can occur at C3 and C4 positions. The regioselectivity and the enantioselectivity depends on the nature of the substituent at C1. Bulky amide function proved again its superiority compared to non-polar or less hindered polar substituents. The C3/C4 ratio enhances up to >99 in the case of *t*-butylamide, providing C3 ketone in good yields (up to 85%) and good ee's (up to 96 %) in the presence of cyclopropanecarboxylic acid (Scheme 131). Carboxylic acids were

shown to bind to the metal center in position *cis* to the site where hydrogen peroxide is activated which improves the selectivity of the process. This clearly demonstrates the incidence of a directing functional group able to fix the location of the substrate in the active site of the enzyme mimic and rigidify the transition state for C-H abstraction. It is worth noting that no HAT occurs at C1 despite the lower BDEs. Torsional strain is likely to explain the deactivation.

The same authors have very recently reported the lactonization of unactivated methylenes directed by carboxylic groups (Scheme 132).<sup>279</sup> A rigid model, i.e., adamantylacetic acid **3.2.7** was selected as the substrate. Representative results are shown in Scheme 132.

### Scheme 132. Enantioselective Lactonization of Adamantylacetic Acid

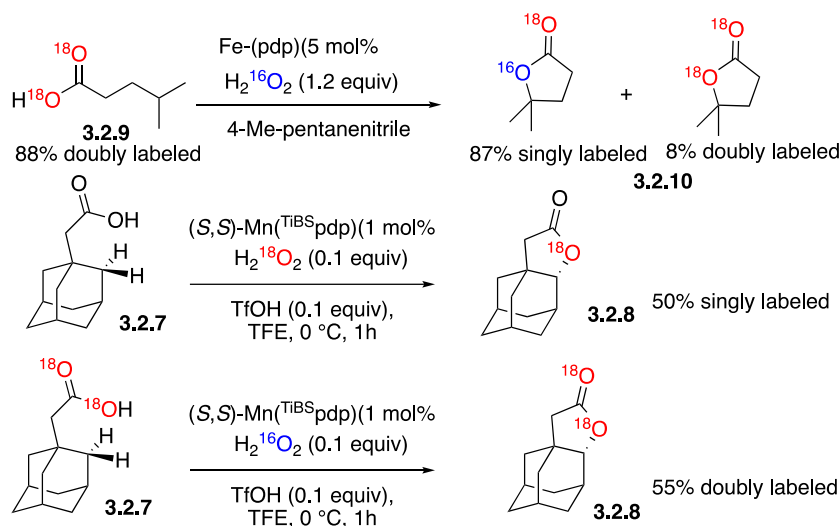


<sup>18</sup>O labeling experiments pointed to a significant difference in the behavior of Fe and Mn-oxo catalysts. White and coworkers had previously shown that, upon exposure of <sup>18</sup>O-doubly labeled acid **3.2.9** to Fe(dpd) (Scheme 133, R = H) and labeled hydrogen peroxide, the expected lactone **3.2.10**, singly labeled, was the major product (87% singly labeled, only 8% doubly labeled). These data suggested that lactonization proceeded via hydroxyl rebound and that carboxylate rebound was, a minor pathway.<sup>280</sup> Completely different data were obtained for Mn catalyst.<sup>279</sup> <sup>18</sup>O incorporation dropped down to 50% in the case adamantyl acetic acid oxidation with <sup>18</sup>O-labeled hydrogen peroxide catalyzed by Mn which showed that the remaining part of the lactone originated from the carboxylic group. In this case the carbon-centered radical also undergoes competitive rebound to either oxygen atom of the carboxylate ligand. When doubly

labeled **3.2.7** was oxidized with non-labeled hydrogen peroxide, doubly labeled **3.2.8** accounted for 55%.

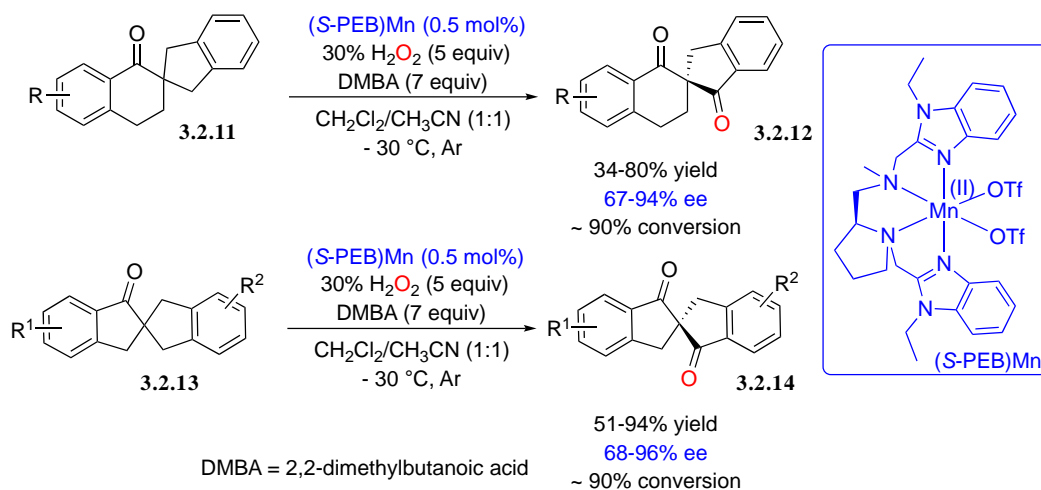
The reaction was extended to determine the HAT regioselectivity on an array of bridgehead substituted derivatives which can lead to three different products.<sup>279</sup>

### Scheme 133. Mechanistic Investigations of Lactone Formation via <sup>18</sup>O Labeling



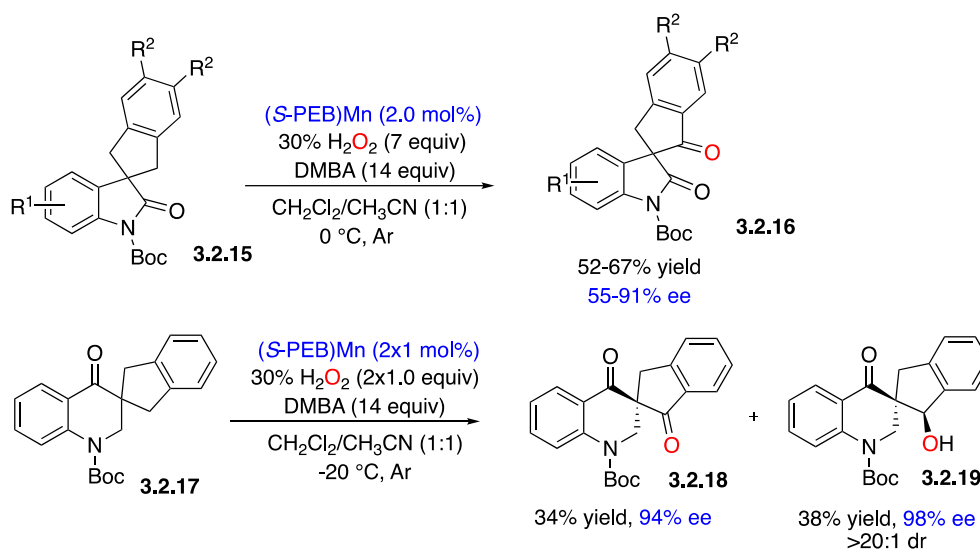
Sun and Nam investigated the asymmetric oxidation of spirocyclic hydrocarbons<sup>281</sup> and heterocycles.<sup>282</sup> As the targeted products are ketones resulting from overoxidation, the stereoselectivity of the primary hydroxylation step is not problematic. New *C1*-symmetrical Mn complexes with N4 ligands derived from L-proline and where the pyridine donor is replaced by a benzimidazole moiety proved to be very efficient. As exemplified in Scheme 134, tetralones **3.2.11** and indolones **3.2.13** could be converted into the corresponding enantioenriched diketones via a highly regioselective oxidation of enantiotopic benzylic methylene groups. Under optimized experimental conditions, an array of spirodiketones substituted at the aromatic ring were prepared in moderate to high yields and excellent ee's.

### Scheme 134. Mn-catalyzed Enantioselective Oxidation of Spirocyclic Hydrocarbons



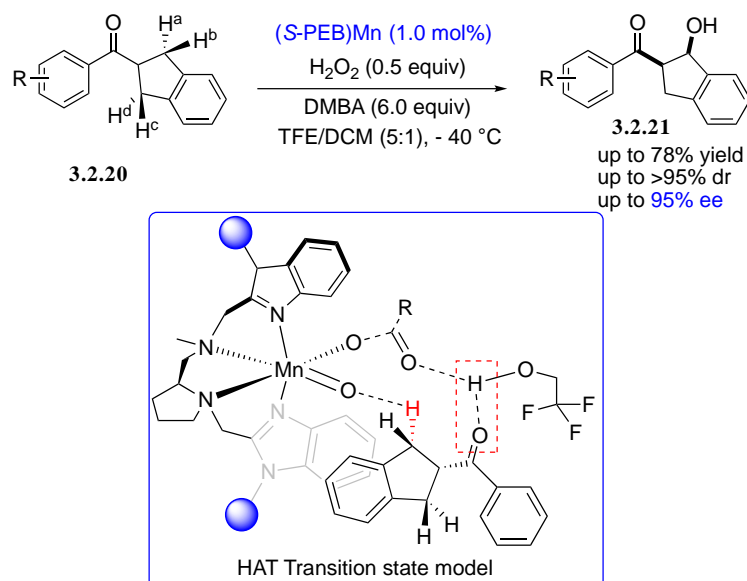
The process was then expanded to the enantioselective oxidation of spirocyclic oxindoles and dihydroquinolones still by aqueous hydrogen peroxide (Scheme 135).<sup>282</sup> Up to 67% yield and 91% ee could be reached in the case of oxindoles **3.2.15**. In the case of 2,3-dihydroquinolin-4-one **3.2.17**, at 63% conversion, both the alcohol **3.2.19** (26% yield, 97% ee) and the ketone **3.2.18** (34% yield and 94% ee) resulting from its further oxidation were isolated under the conditions applied to oxindoles. After optimizing the experimental protocol, the alcohol became the major product.<sup>283</sup>

### Scheme 135. Mn-catalyzed Enantioselective Oxidation of Spirocyclic Heterocycles



To close this section, it is worth mentioning that Sun's group was able to discriminate between enantiotopic and diastereotopic benzylic X-H bonds in the Mn-catalyzed hydroxylation of indane derived symmetrical ketones **3.2.20**.<sup>284</sup> As the result of its symmetrical structure, **2.2.20** exhibits two pairs of enantiotopic hydrogen atoms (Ha/Hd and Hc/Hb) and simultaneously two pairs of diastereotopic hydrogen atoms (Ha/Hb and Hc/Hd). In the presence of TFE as co-solvent (TFE/DCM, 5:1 ratio), as stated above, hydrogen bonding slows down the over oxidation of the alcohol (Scheme 136). Furthermore, the reaction benefits of DMA carboxylate at the metal center which not only increases steric crowding close to the reactive oxygen atom but also contributes to direct enantioselectivity of the HAT step by creating a hydrogen bonded network around the immobilized substrate. The authors proposed the model shown in Scheme 136. In the presence of  $(S\text{-PEB})\text{Mn}$  (1 mol%) alcohol **3.2.21** was isolated with good to excellent diastereomeric ratio (up to > 95:5), yield (up to 78%) excellent ee (up to 95%). Control experiments showed that neither the alcohol resulting from the reduction of **3.2.20** carbonyl group nor the corresponding hydrocarbon could be oxidized under the same experimental conditions. The carbonyl group in the substrate appears to be crucial in controlling the whole process.

### Scheme 136. Stereochemical Discrimination During Mn-Catalyzed Hydroxylation



### 3.3. Asymmetric cobalt-catalyzed radical reactions

#### 3.3.1 Cobalt metalloradical catalysis

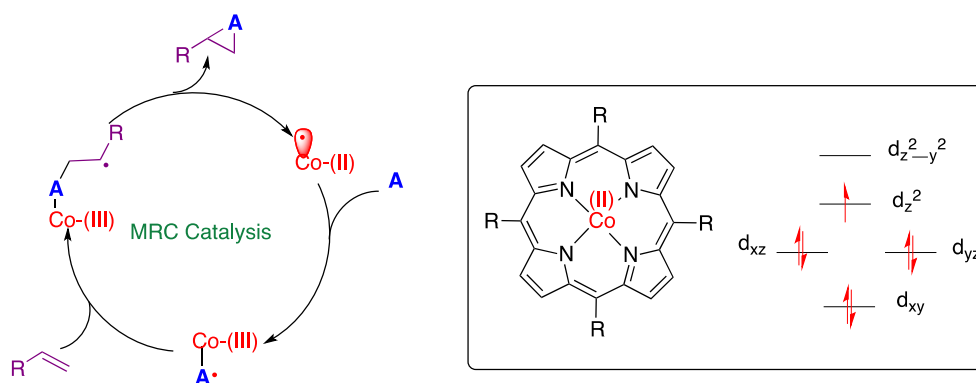
The persistent radical effect<sup>285,43</sup> is an essential concept to understand the radical chemistry of R-Co(III) compounds. C-Co(III) bonds are weak and vary with the nature of the Co ligand (acetylacetonate, porphyrin, glyoxime...) their homolysis is therefore very easy and the incorporation of electron-withdrawing ligands even more weakens the Co(III)–C bond.<sup>288</sup> Furthermore, as Co(II) centered radicals are persistent species recombination is particularly efficient, it allows to extend the lifetime of the alkyl radicals, and prevent self-coupling reactions which benefit to other types of evolution. In other word, the fate of transient carbon-centered generated from the cleavage of R-Co(III) is controlled by the Co(II) species. R-Co(III) species can undergo a large variety of subsequent evolutions: radical additions, H-atom abstractions, radical substitutions, which open route to a panel of transformations. These processes are attractive because excellent control of enantioselectivity can be reached when asymmetric Co catalysts are employed.

##### 3.3.1.1 Cyclopropanation reactions

Processes employing cobalt catalysts with close-shell electronic structures have been widely used. Among them, enantioselective cyclopropanation using chiral salen cobalt (III) catalyst

proceed via a polar reaction pathway.<sup>286</sup> Using open-shell paramagnetic cobalt complexes - having a single unpaired electron in its d orbital - as catalysts in radical cyclopropanations was challenging. A breakthrough in such reactions was made in 2004 by the Zhang group using *MetalloRadical Catalysis (MRC)* concept.<sup>287</sup> Schematic presentation of the catalytic cycle is outlined in Scheme 132. It is based on the use of a stable metal centered radical, namely cobalt, which is able to activate a molecule **A** through a radical process to generate a new radical species (Co(III)-A<sup>•</sup>) upon redox behavior. The nature of the activatable molecule **A** is crucial to start the system which gives a nice opportunity to generate a wide range of carbon-, nitrogen and oxygen-centered radicals (Co(III)-A<sup>•</sup>). Further trapping of the latter, like olefin addition, would generate a new radical that would evolve to cyclopropyl (or aziridiny) product regenerating the metalloradical<sup>288</sup> species and complete the catalytic cycle as shown in Scheme 137.

### Scheme 137. MetalloRadical Catalysis (MRC)

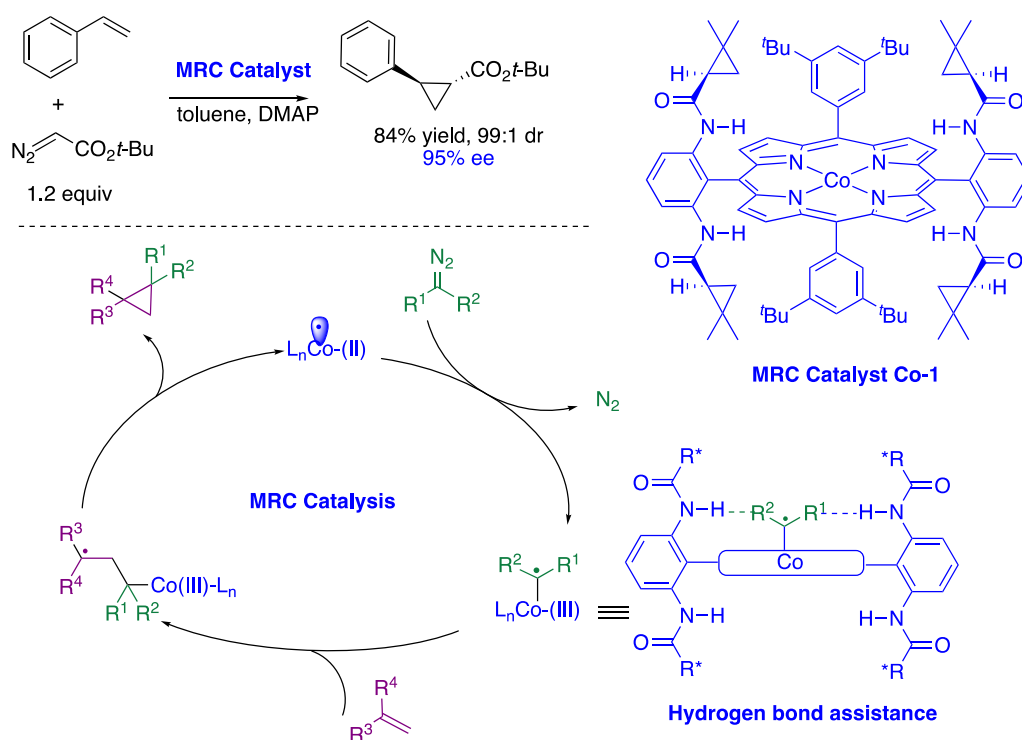


Inspired by the vitamin B<sub>12</sub> mechanism,<sup>289</sup> Zhang developed a series of chiral cobalt(II) D<sub>2</sub>-symmetric porphyrins and applied the MRC approach to control selectivity and reactivity of radical transformations.<sup>286</sup> Many asymmetric applications were developed using this concept like alkene and alkyne cyclopropanations, olefin aziridinations, alkylations, and C-H aminations. The Zhang group designed a porphyrin catalyst connected in an orthogonal fashion to chiral symmetrical amides (Scheme 138). This geometry has shown a particular efficiency in chiral recognition of activatable diazo substrate. The product alkyl radical is stabilized by the



metal and is able to react with olefin in radical addition reaction allowing the formation of  $\gamma$ -cobalt alkyl radical which proceeds by an *exo-tet* radical cyclization (intramolecular radical substitution releasing the persistent Co(II) centered radical) delivering the cyclopropane in good yields, high ee's and excellent diastereoselectivities. It was postulated that hydrogen bonding from the amide groups in the catalyst play a crucial role in the control of stereochemistry and enhancing reactivity.

### Scheme 138. Design of Porphyrin Catalysts for MRC



From mechanistic point of view, EPR spectroscopic investigations, DFT calculations, ESI-MS techniques and TEMPO radical trapping experiments have provided conclusive evidence for the existence of cobalt(III)-carbene radical intermediate supporting therefore that the metalloradical character of Co(II) is at the origin of a radical mechanism.<sup>290,291</sup>

This protocol was found to be a nice alternative for closed-shell metal (Rh and Cu) catalyzed cyclopropanation using metalcarbenes since it prevents the side diazo compounds dimerization and the use of excess olefin. Moreover, it permits the successful use of acceptor/acceptor-substituted diazo reagents as well as electron-deficient olefins. Interestingly,

this method surpassed the stereocontrol offered by copper, ruthenium and dirhodium catalysts since these latter ones only promote addition of simple and conjugated olefins. The notable feature of the MRC system in the use of a wide range of alkenes with different diazoesters that allows therefore elegant asymmetric radical cyclopropanations.

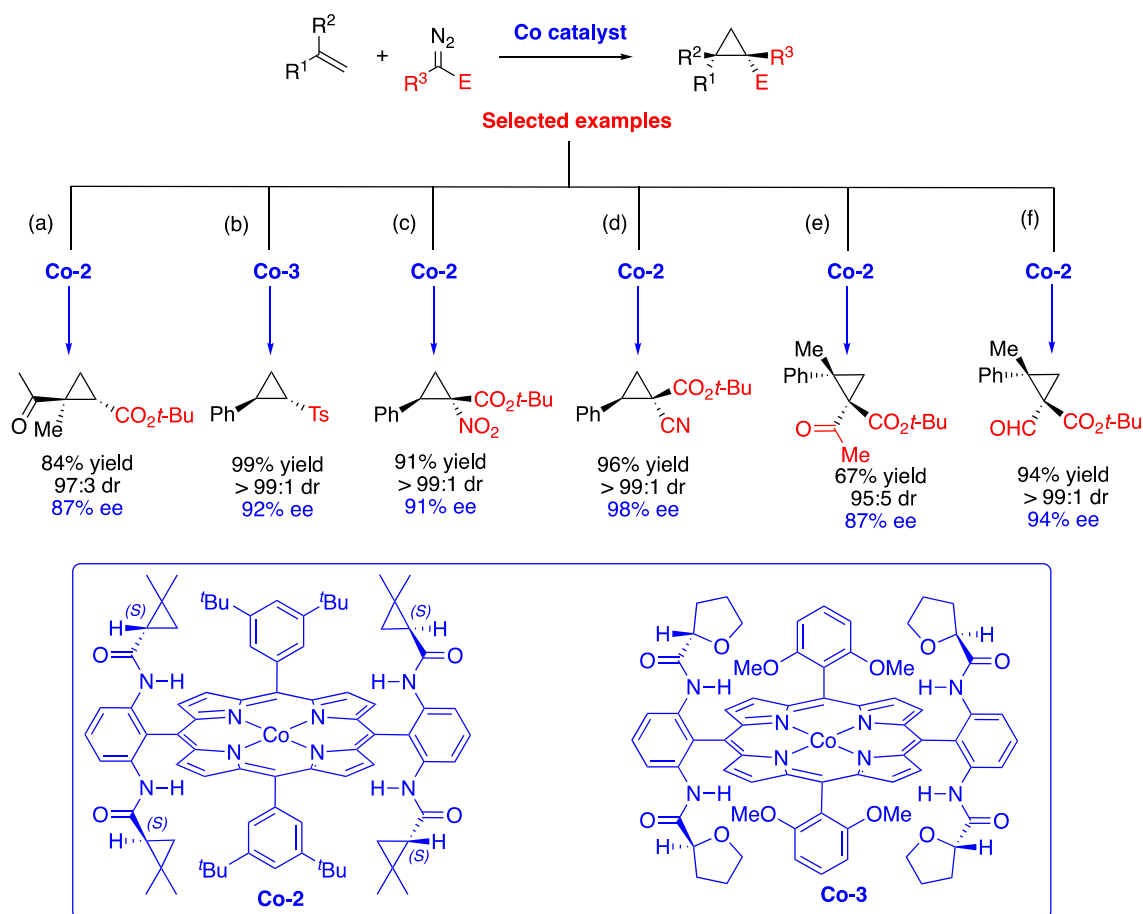
In 2007, Zhang and co-workers demonstrated that catalyst (Scheme 139), derived from a commercially available amide, is effective in controlling the enantioselective cyclopropanation of electron-deficient olefins under mild conditions forming in some cases cyclopropanes possessing a quaternary stereocenter (Scheme 139a).<sup>292</sup> It was found that the use of DMAP as an additive was beneficial to enhance the stereoselectivity.

Cyclopropanation of styrene with diazosulfone was achieved in 2008 with the cobalt *D*<sub>2</sub>-symmetric porphyrin **Co-3** in 99% yield, >99:1 diastereomeric ratio and 92% ee (Scheme 139b).<sup>293</sup> Although the previously developed catalyst did produce desirable level of stereocontrol, Zhang group designed a complex with a more sterically demanding ligand to achieve the highest enantiocontrol.

The authors continued their efforts on increasing the substrate scope and the cobalt **Co-2** was shown to be efficient in the use of acceptor/acceptor type diazo reagent.  $\alpha$ -Nitrodiazoacetate for instance afforded, in the presence of styrene, the desired product in 91% yield, >99:1 diastereoselectivity for the *trans* isomer (NO<sub>2</sub> and Ph) and 91% ee (Scheme 139c).<sup>294</sup> In addition to styrene, olefins bearing alkyl groups were also tolerated. However, olefins with ester and amide groups gave lower selectivity.

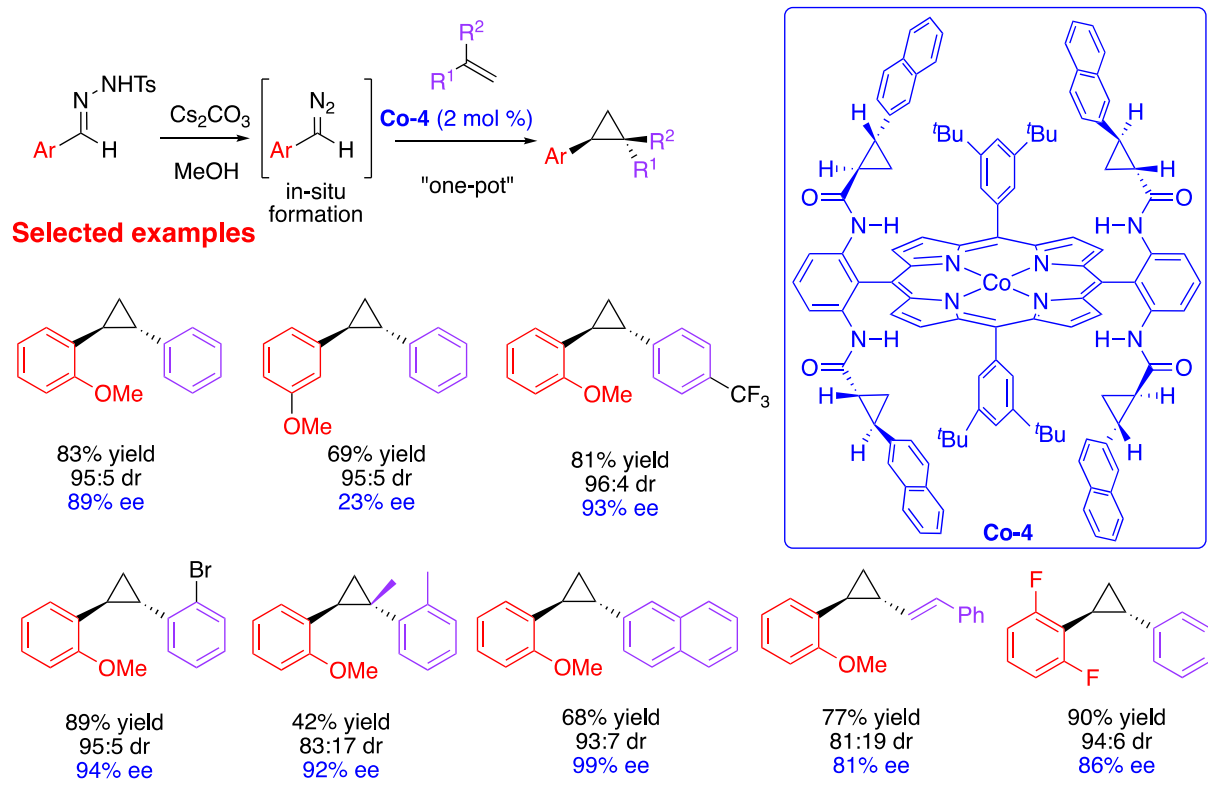
The latter limitation was circumvented by using  $\alpha$ -cyanodiazoacetates in the presence of a broad range of different alkenes possessing electron rich and poor aromatics, electron-deficient nonaromatics and simple aliphatics, with high stereocontrol.<sup>295</sup> As exemplified in Scheme 139d, the cyclopropane product was obtained in 96% yield, >99:1 diastereoselectivity for the *trans* isomer and 98% ee.

## Scheme 139. Cobalt-Mediated Enantioselective Cyclopropanation



Formation of cyclopropane with two contiguous quaternary stereocenters was achieved with high selectivity using the same catalyst (Scheme 139e).<sup>296</sup> This study was the first cyclopropanation using diazo reagent with two  $\alpha$ -carbonyl groups. An improvement was reported in 2017 using  $\alpha$ -formyldiazoacetates (Scheme 139f).<sup>297</sup>

## Scheme 140. Use of ortho-Substituted Hydrazones in Enantioselective Cyclopropanations

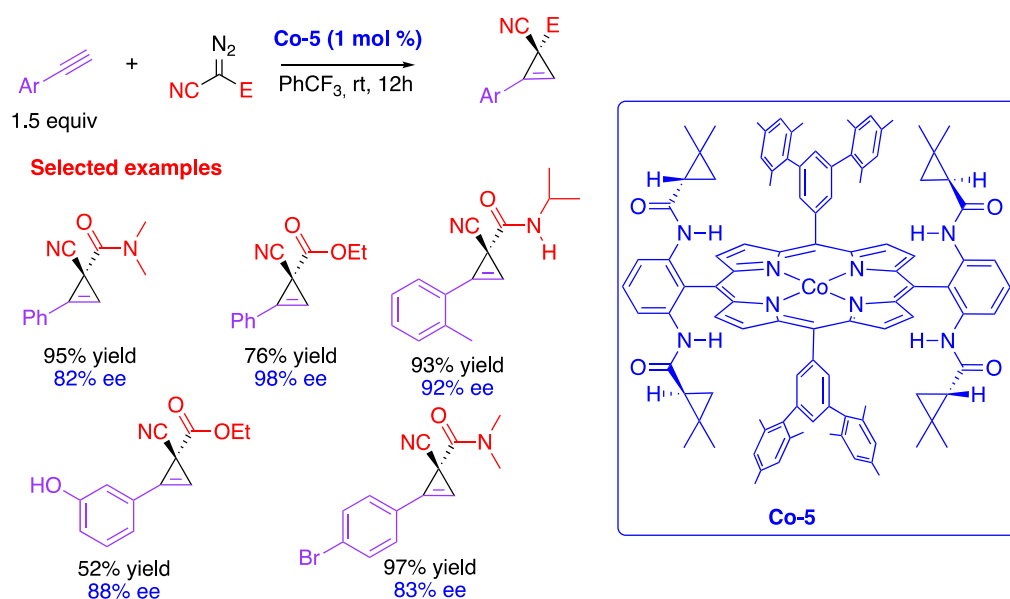


*In situ* formation of the donor-substituted diazo reagents is known to proceed from hydrazones in the presence of a base. Taking advantage of this opportunity, Zhang attempted the asymmetric cyclopropanation of sulfonyl hydrazones with slight modification of the catalyst. However, the lack of H-bonding partner in this case makes the cyclopropanation of aryl diazo compounds challenging. This difficulty has been overcome by using ortho-substituted arylhydrazones which are able to provide hydrogen bonding interactions (OMe and F) with amide moiety of the catalyst.<sup>298</sup> This was evidenced by comparing reactions with ortho and meta-substituted methoxy phenyl hydrazone. The ortho functionalized substrate afforded the product with 89% ee whereas the meta-substituted substrate gave only 23% ee (Scheme 140). 2-Naphthyl substituted catalyst **Co-4** was shown to be an effective metalloradical catalyst with various alkenes that afford good yields, high diastereomeric ratio and excellent ee's.

To further extend the MRC concept, the Zhang group envisioned a similar reactivity with alkynes. The catalytic process was applied for asymmetric cyclopropanation of  $\alpha$ -cyanodiazooacetates with terminal alkynes providing trisubstituted cyclopropenes in high yields

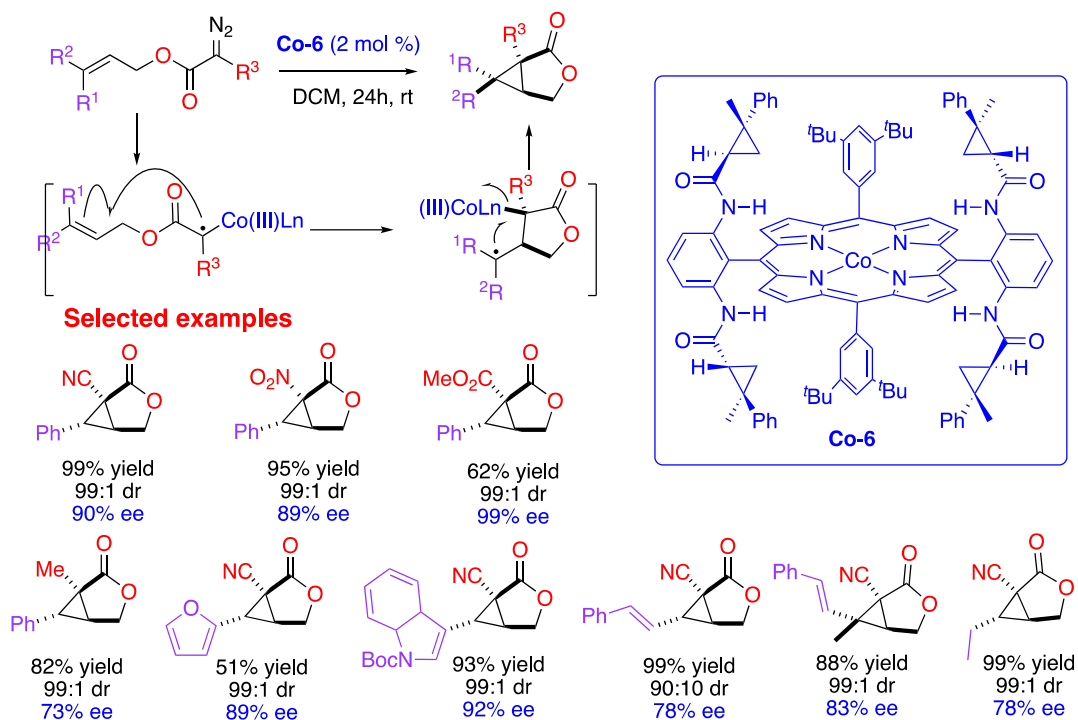
and excellent enantiocontrol of the newly created stereocenter (Scheme 141). Low catalyst loading, stoichiometric ratio of reactants and one-time protocol without slow addition were the highlights of this process, in addition to high control of the stereochemistry.<sup>299</sup> In this report, the incorporation of mesityl groups in the catalyst (**Co-5**) was necessary to reach higher conversions.

### Scheme 141. Enantioselective Cyclopropanation



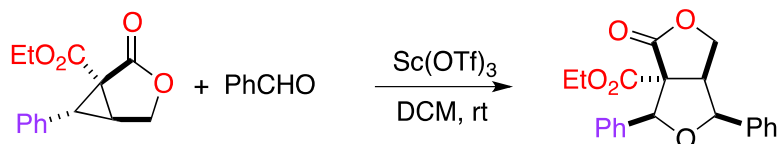
Zhang et al. elaborated by tuning the substrate in a way to form a fused bicycle. As shown in Scheme 142, the catalyst with two contiguous stereocenters on the amide moieties (**Co-6**) efficiently promotes this intramolecular cyclization for a range of diazoacetate tethered alkenes to provide highly functionalized 3-oxabicyclo[3.1.0]hexan-2-one derivatives bearing three contiguous stereocenters.<sup>300</sup> The mechanism involves a radical 5-exo trig cyclization followed by S<sub>H</sub>2 delivering cyclopropyl/butyrolactone fused system.

### Scheme 142. Intramolecular Enantioselective MRC Cyclopropanation



The product could be further transformed, through a [3+2] dipolar cycloaddition with benzaldehyde as dipolarophile, into a densely functionalized butyrolactone (Scheme 143).

### Scheme 143. Synthesis of Densely Functionalized Butyrolactone

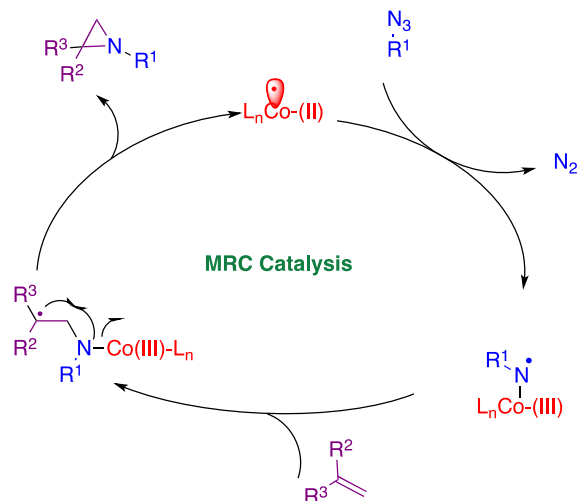


#### 3.3.1.2 Aziridination reactions

Aziridines represent fascinating precursors to access complex molecules. The aziridine ring possesses a high strain energy, ring cleavage can therefore provide a wide range of N-heterocyclic compounds. In order to demonstrate the versatility of their MRC approach, the Zhang group extended the methodology to aziridines. Analogous to cyclopropanation, addition of organoazide to Co(II), after nitrogen displacement, would allow the formation of new type of nitrogen centered radical. The aminyl radical nature of this intermediate was again evidenced using various spectroscopic techniques and DFT calculations.<sup>301,302</sup> The nitrogen centered radical can then undergo addition to C=C double bond to generate  $\gamma$ -Co(III)-alkyl radical

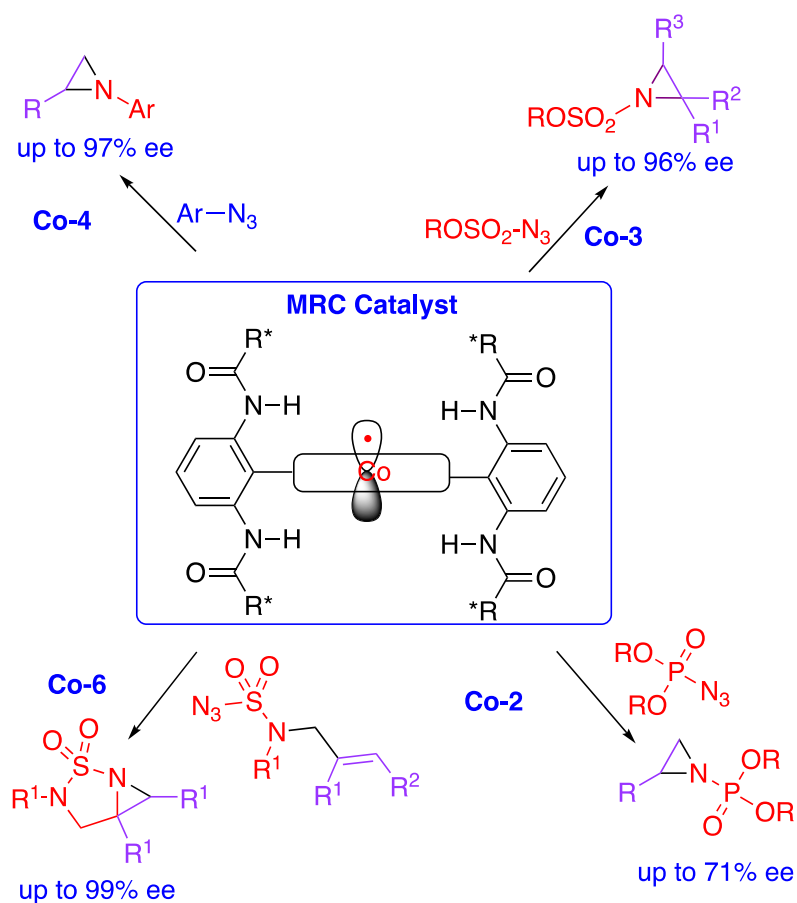
intermediates that evolve, after 3-*exo-tet* radical cyclization (intramolecular radical substitution releasing the persistent Co(II) complex), to provide the aziridine product (Scheme 144).

**Scheme 144. Enantioselective Aziridination using MRC**



This discovery has allowed the aziridination of alkenes using aromatic, phosphorous, sulfonyl azides as nitrene sources through inter- or- intramolecular process to produce aziridines. Metalloporphyrin complexes were capable of performing an asymmetric transformation with high level of enantiocontrol particularly when **Co-2**, **Co-3**, **Co-4** and **Co-6** were used (Scheme 145) with up to 99% ee. When the phosphoryl azide was used as nitrene source with 10 mol% of **Co-2**, only moderate yields and enantioselectivities could be obtained (up to 71% ee).<sup>303</sup> A higher enantioselectivity in the aziridination of trichloroethoxysulfonyl azide by using *D*<sub>2</sub>-symmetric cobalt catalyst **Co-3** gave products with up to 96% ee.<sup>304</sup> The scope of this MRC methodology could be extended for the construction of aziridine/oxazolidinone fused bicyclic derivatives with **Co-6**.<sup>305</sup> Analogous mechanism to intramolecular cyclopropanation (Scheme 138) was proposed for this cascade reaction involving enantioselective 5-*exo-trig* cyclization followed by diastereoselective 3-*exo-tet* 3-membered ring formation.

### Scheme 145. Enantioselective Formation of Aziridines

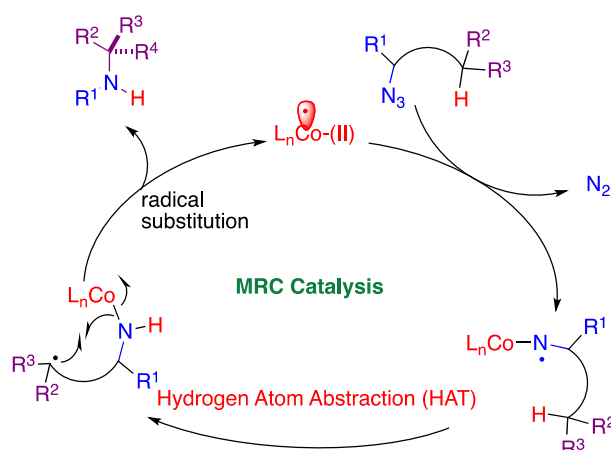


#### 3.3.1.3. Aminations via C–H activation

Development of catalytic asymmetric processes for direct C–H bond functionalization have gained a high-level interest in the last decade. It allows the construction of optically active architectures using atom-economy strategy. To this issue, Zhang and co-workers have elegantly devised asymmetric C–H amination using their MRC concept. Their idea was to exploit the  $\alpha$ -Co(III) aminyl radical to engage it in a H-atom transfer (HAT) process to generate new alkyl radical species. Breaking the weak  $N$ -cobalt bond releasing the Co(II) complex, that reenters the catalytic cycle, allows for the C-amination of the substrate (Scheme 146).



### Scheme 146. Direct Asymmetric C-H Functionalization leading to Amines



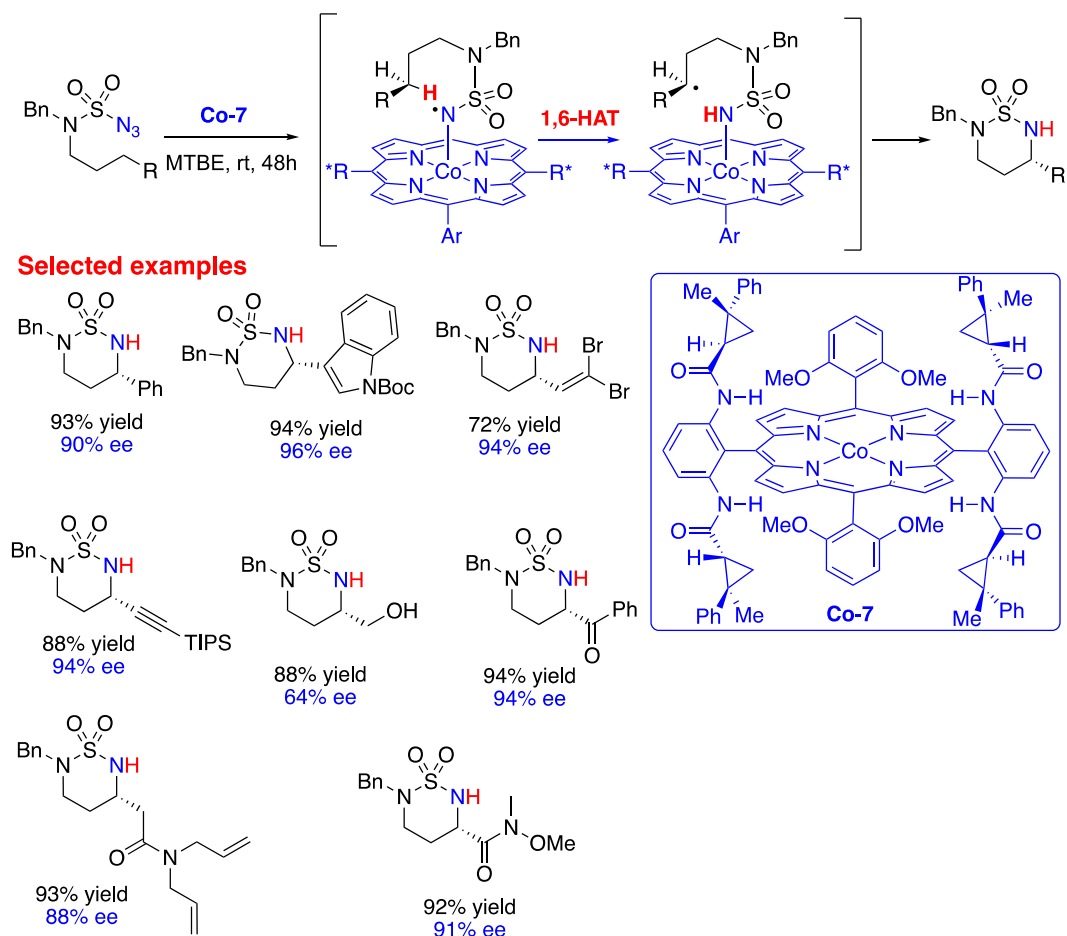
It is well established that 1,5- and 1,6-HAT are frequently encountered in radical chemistry.<sup>132</sup>

Taking this into account, Zhang was interested in developing an asymmetric MRC catalyzed cascade involving 1,6-HAT followed by 6-exo-tet radical cyclization. This last elementary step has been anticipated to control the stereochemistry, a well-designed substrate with sulfamoyl azide has been therefore used to adjust H-bonding interactions with the chiral complex. Indeed, the authors remarkably succeeded in the enantioselective construction of six-membered heterocycles (Scheme 147).<sup>306</sup> Amination of a broad range of C(sp<sup>3</sup>)-H bonds from benzyl, allyl, propargyl positions have been reported with high yields and enantioselectivities. Other functional groups (alcohol, indole, amide) are also tolerated in this reaction with no alteration of the selectivity. Moreover, it is important to highlight the remarkable regioselective 1,6-hydrogen abstraction over the 1,5-pathway. In the case of the substrate possessing a diallylamide moiety, a clean reaction toward C-N bond formation was favored despite the presence of a C=C bond.

It should also be noted that the optically active heterocycles can be transformed into chiral 1,3-diamines, upon desulfonylation.

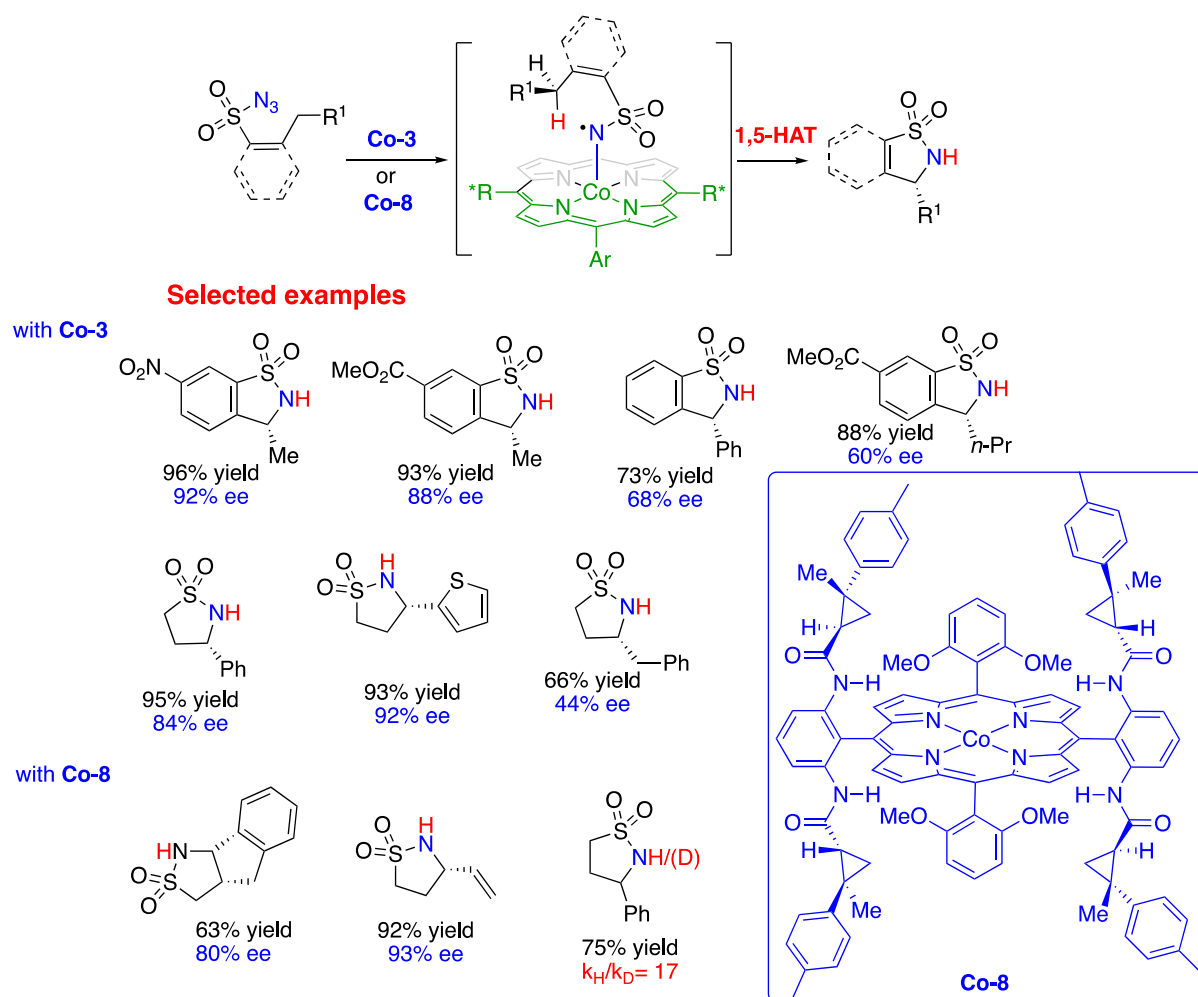
Enantioconvergent amination of racemic tertiary C-H bonds has been also reported.<sup>307</sup>

## Scheme 147. Intramolecular C-H Amination using MRC



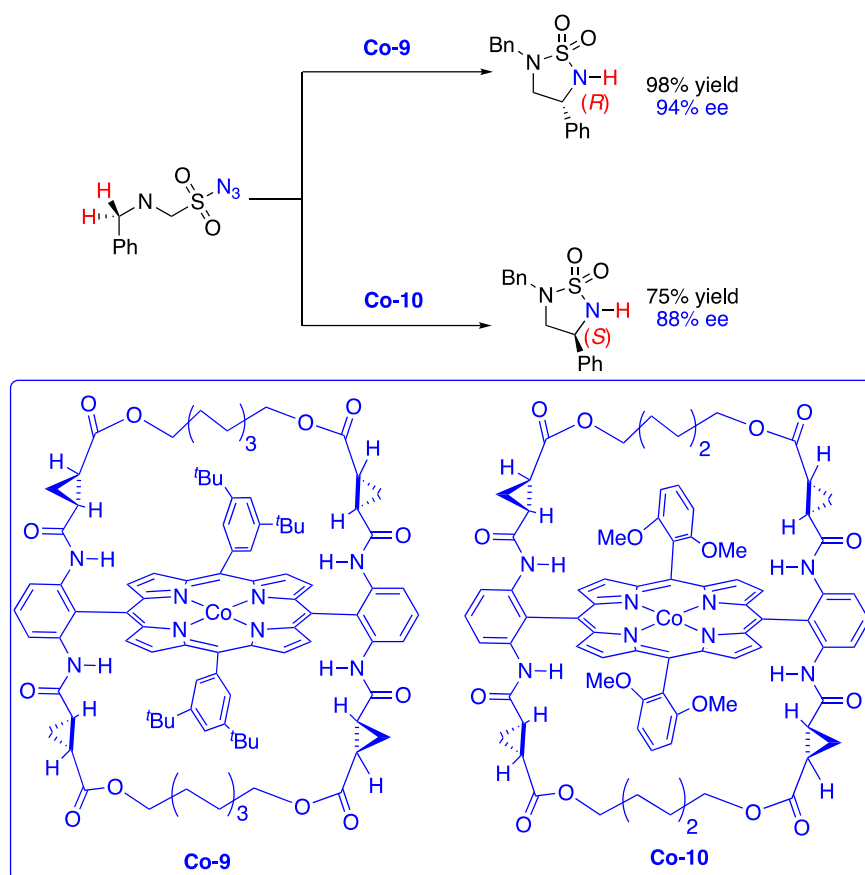
Subsequent to this work and pursuing their efforts to target a 1,5-hydrogen abstraction, Zhang and co-workers designed substrates lacking hydrogen at 1,6-position offering therefore 1,5-HAT as the only possibility. To this aim, the authors attempted radical cyclization of arylsulfonyl azides offering a benzylic hydrogen. Indeed, cobalt catalyst **Co-3** was the most efficient in this operation delivering fused benzene/cyclic sulfonamides through an enantioselective 1,5-C-H amination with good ee's (Scheme 148). Cyclization of aliphatic substrates possessing benzylic or allylic hydrogen revealed the necessity for the use of catalyst **Co-8**.<sup>308</sup> In addition to EPR trapping and mass spectrometry experiments, the authors demonstrated a stepwise radical mechanism by using a monodeuterated substrate with achiral catalyst that revealed kinetic isotopic effect of 17 (Scheme 148).

## Scheme 149. Enantioselective Intramolecular 1,5-C–H Amination

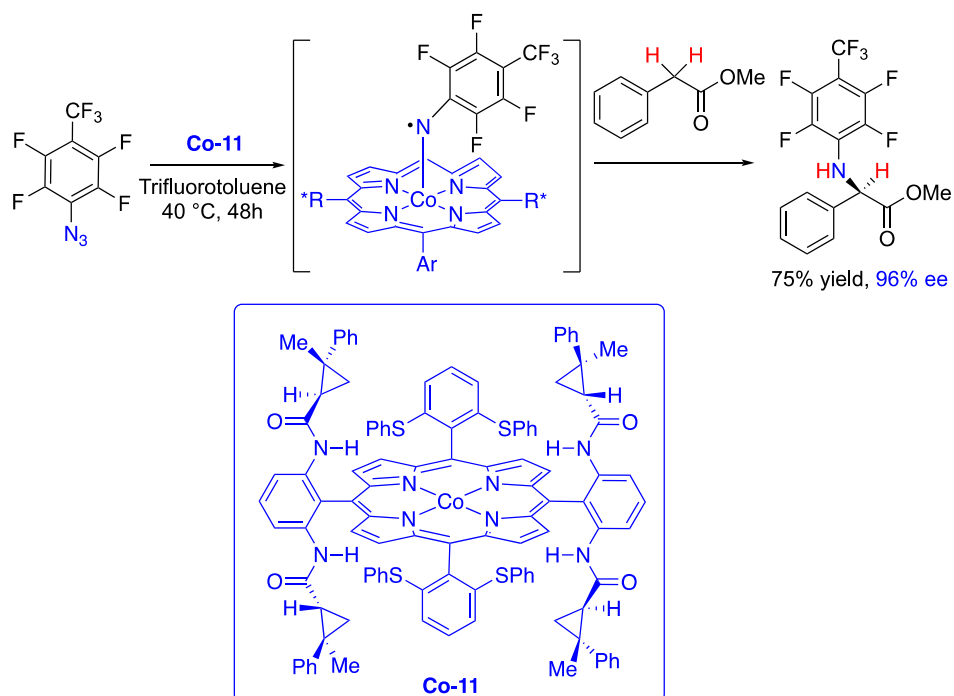


Parallel to these investigations in C–H amination, the Zhang group reported enantiodivergent MRC radical C–H 1,5-functionalization using a complex with fine-tuned cavity environment. Remarkably, the alkyl bridge length and the nature of the non-chiral aryl groups in the porphyrin affected the sense of the chiral induction. Enantio-discriminative H-atom abstraction and stereoselective radical substitution was directed by the tunable chiral cavity of the catalyst. The longest bridge ( $C_8$ ) in combination with 3,5-di-*tert*-butylphenyl group (**Co-9**) engaged *R*-selective cyclization whereas the smallest bridge ( $C_6$ ) with 2,6-dimethoxyphenyl group (**Co-10**) oriented toward the *S*-product (Scheme 150) obtained in high yields and ee's.<sup>309</sup> This enantiodivergent transformation closely resembles (*S*)-selective protease<sup>310</sup> and (*R*)-selective lipase<sup>311</sup> acylation of amines, whose active sites are mirror images.

### Scheme 150. Enantiodivergent Radical C–H 1,5-Functionalization using MRC



### Scheme 151. Enantioselective Intramolecular 1,5-C–H Amination



It is important to highlight that most examples deal with asymmetric intramolecular version of C–H amination has been reported. Enantioselective intermolecular C–H amination has very recently been reported by Zhang.<sup>312</sup> The  $\alpha$ -Co(III)-aminyl radical this time undergoes intermolecular HAT from activated benzylic positions (Scheme 151). Further intermolecular applications are expected.

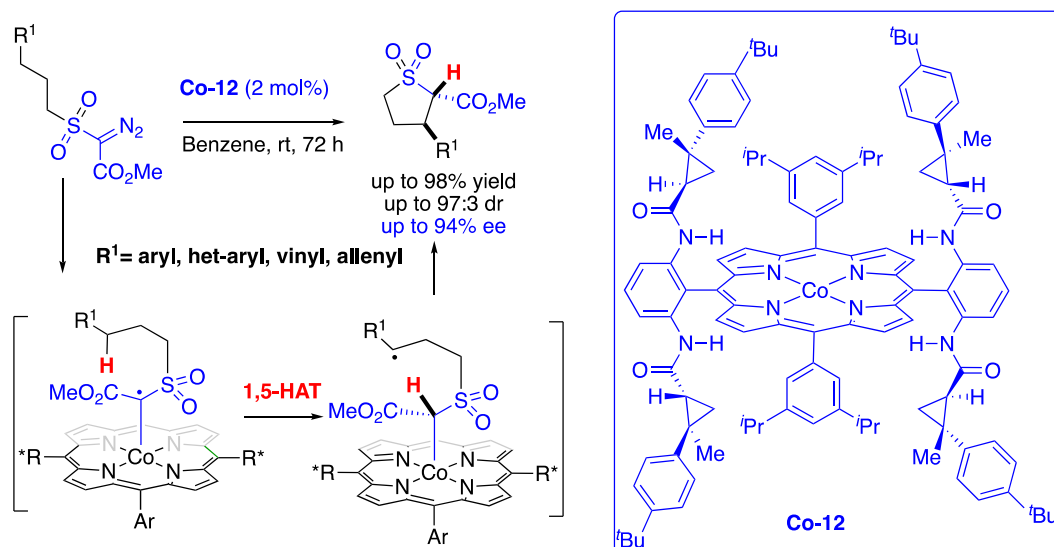
#### 3.3.1.4. Intramolecular C–H alkylation

Parallel to their work on C–H amination, Zhang and co-workers have been interested in C–H alkylation because it is also a topic of high interest in modern organic chemistry. The main advantage of using radical MRC chemistry over Fischer-type metallocarbene catalysis, is the higher reactivity we can expect with acceptor/acceptor substituted reagents and also the scope of the C–H partner. Indeed, the latter diazo reagents are too electrophilic to perform C–H insertion.

Based on the same mechanism denoted in Scheme 146, the use of tethered diazoesters triggering intramolecular HAT would offer the possibility of C–C bond formation delivering cyclic compounds.

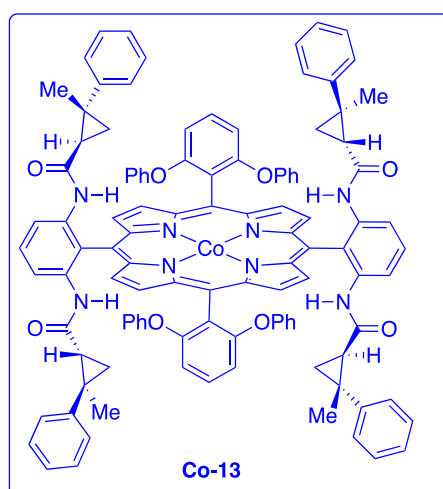
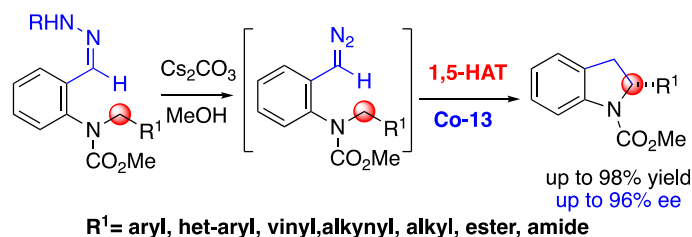
Activation of sulfonyl diazoacetate with co-catalyst gives a nice opportunity to construct five-membered sulfolane derivatives (Scheme 152).<sup>313</sup> **Co-12** was shown to be capable to induce high regio-, chemo-, diastereo- and enantioselectivity in alkylation of wide range of substrates including aryl, heteroaryl, vinyl and allenyl groups. It is also important to mention that the R<sup>1</sup>-aryl group tolerates unprotected functional groups like amine and alcohol. Thanks to X-ray structure of the TEMPO-trapped intermediate, the authors pointed out the presence of double H-bonding interactions between the two substrate-functional groups and amide groups of the catalyst.

### Scheme 152. Enantioselective Formation of Cyclic Sulfone using MRC



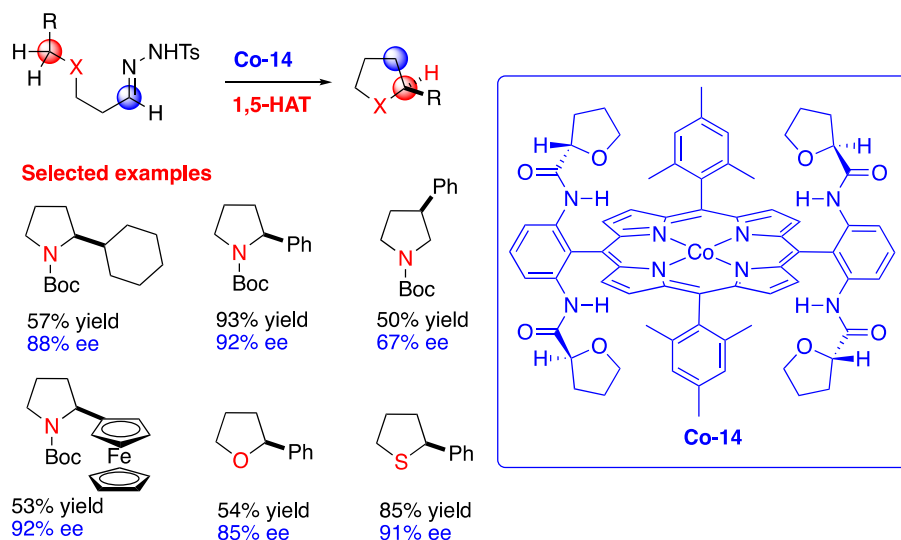
The scope of this C–H alkylation has been further extended to aryl diazo reagents generated in-situ from tosyl hydrazones. This new methodology affords chiral 2-substituted indolines. In addition to high functional group tolerance, excellent ee's were also obtained in this transformation (Scheme 153).<sup>314</sup>

### Scheme 153. Synthesis of Chiral 2-Substituted Indolines using MRC



Chiral pyrrolidines and their five-membered analogs could also be reached by the MRC catalysis. Zhang and co-workers described the use of challenging linear aliphatic tosyl hydrazone compounds as precursors of these valuable five-membered heterocycles (Scheme 154).<sup>315</sup>

**Scheme 154. Synthesis of Chiral Pyrrolidines and other 5-Membered Heterocycles**

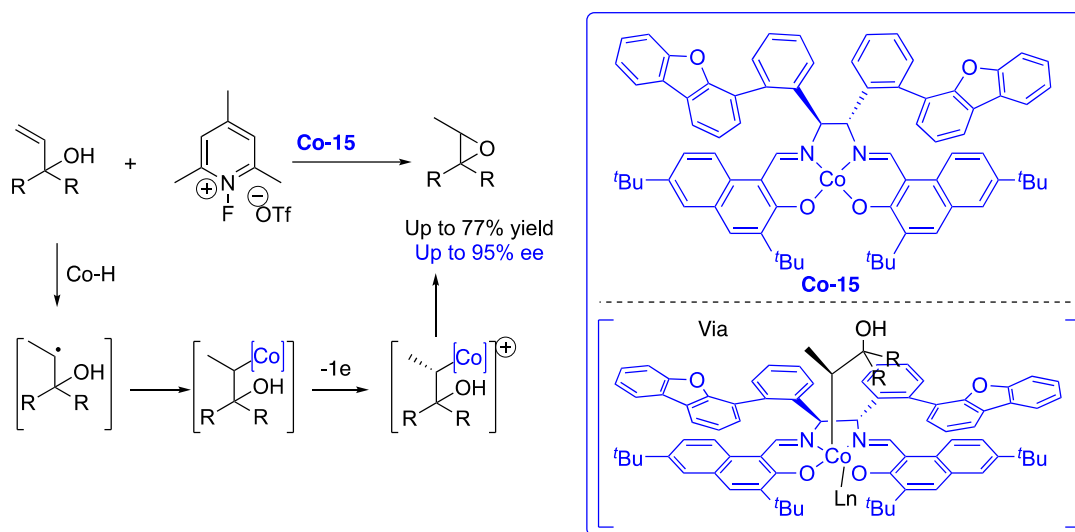


The same mechanism as above involving 1,5-HAT was operative to form the C–C bond in an enantioselective manner giving rise to pyrrolidines, thiophenes and furans with acceptable yields and high enantioselectivities. Interestingly, chiral  $\alpha$ -ferrocenylpyrrolidine, which can be useful in homogenous catalysis, has been synthesized with 92% ee and 53% yield.

### 3.3.2 Cobalt-Catalyzed Miscellaneous Reactions

In the last decade, Metal-Induced Hydrogen Atom Transfer (MHAT) processes provided new directions for radical chemistry through a hydrofunctionalization of alkenes.<sup>316,317</sup> An asymmetric intramolecular hydroalkoxylation of tertiary allylic alcohol was reported in 2019 by Pronin and co-workers using cobalt salen catalyst **Co-15**.<sup>318</sup> Even though radical pathway is involved in the mechanism, the stereodetermining step is polar in nature through cation- $\pi$  interactions (Scheme 155).

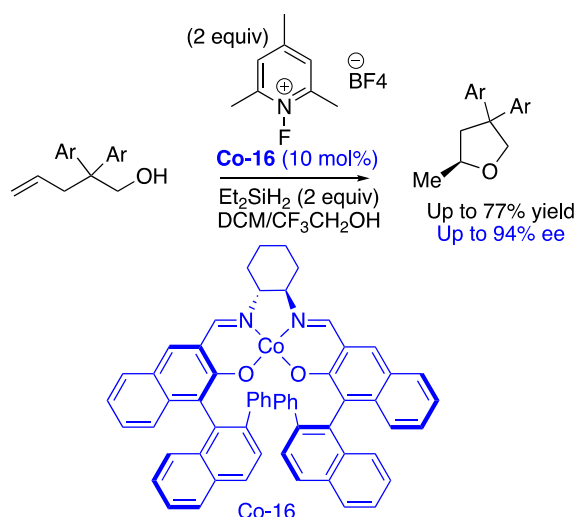
### Scheme 155. Asymmetric Intramolecular Hydroalkoxylation of Tertiary Allylic Alcohol



Asymmetric synthesis of THF derivatives has been reported by Shigehisa group using hydroalkoxylation of non-activated alkenes catalyzed by chiral cobalt-salen catalyst (Scheme 156).<sup>319</sup> As in the previous example, a radical-polar crossover mechanism is implicated in this reaction.

Lu reported regio- and enantioselective hydroamination of alkenes through MHAT catalyzed by  $\text{CoCl}_2$  in the presence of chiral imidazoline ligand.<sup>320</sup>

### Scheme 156. Asymmetric Synthesis of THF Derivatives

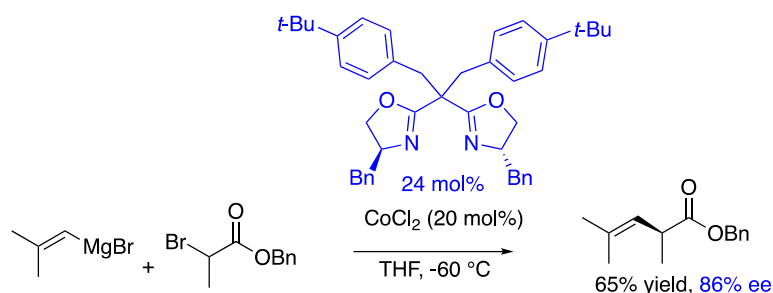


A few data concern the Co-catalyzed cross coupling reactions initiated by Oshima,<sup>321</sup> however, enantiomeric excesses were rather low in attempts to perform asymmetric coupling reactions.

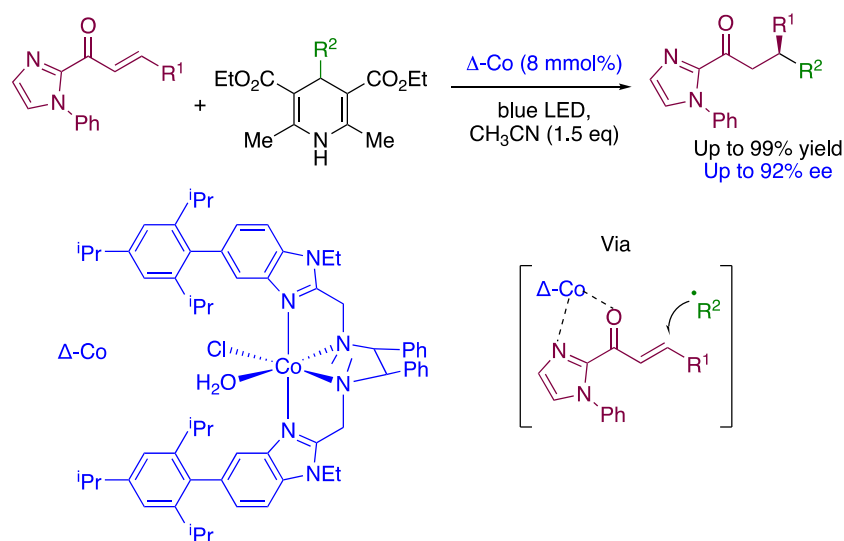


A recent review by Han et al. covers this field.<sup>322</sup> Enantioselective Kumada coupling of  $\alpha$ -bromoesters with alkenyl magnesium reagents was recently performed with  $\text{CoCl}_2$  as catalysts. In the presence of BOX ligands, ee's varying from 72 to 93% and yields from 50 to 80% were reported. Experiments performed with radical clocks supported a radical mechanism (Scheme 157).<sup>323</sup>

### Scheme 157. Cobalt-Catalyzed Kumada Cross-Coupling



### Scheme 158 Cobalt-Catalyzed Enantioselective Photo-Giese Addition



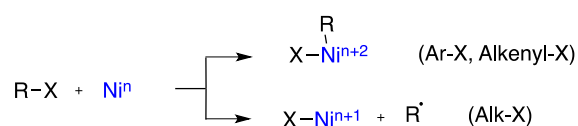
Visible light-induced enantioselective Giese addition<sup>95</sup> was recently achieved by Xiao by using chiral octahedral  $\text{Co(II)}$  complexes based on chiral  $\text{N}_4$  ligands and dihydropyridines as source of alkyl radical and Mesityl-Acrinium perchlorate ( $\text{Ms-AcrClO}_4$ ) as photocatalyst.<sup>324</sup> Yields varying from 54-90% and ees going from 92 to 83% were obtained in the presence of 8 mol% of the catalyst (Scheme 158). The mechanism is similar to the Meggers strategy with rhodium

(*vide infra*). Upon photorelease of alkyl radical from DHP, enantioselective addition assumed by the cobalt catalyst which acts as a chiral Lewis acid.

### 3.4. Nickel catalyzed radical reaction

According to Fu, the great propensity of earth abundant nickel to access to an array of oxidation states makes it the transition metal of choice to achieve radical-based metal catalyzed substitution reactions.<sup>325,326,327</sup> As detailed by Diao and co-workers in a very comprehensive review, Ni complexes are stable in oxidation states ranging from Ni(0) to Ni(IV). As compared to other group 10 metals, Ni is characterized by a small nuclear radius, a low electronegativity, a high electron-pairing energy and low redox potentials. Thus, Ni complexes easily adopt open-shell configurations. As a consequence, the activation of electrophiles by Ni can proceed either by two-electron oxidative addition to give organonickel intermediates (Csp<sup>2</sup>-X derivatives) or by single electron transfer to afford alkyl radicals (Csp<sup>3</sup>-X derivatives) (Scheme 159). The preferred route depends on the stabilization energy of the carbon-centered radical. Moreover, in contrast to Pd, Ni-alkyl complexes undergo slow β-H elimination which enables the use of a large variety of partners.

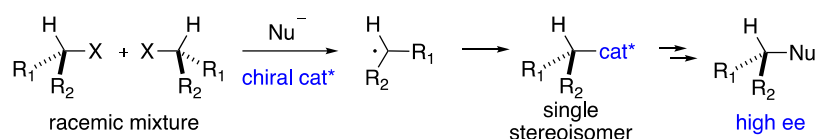
#### Scheme 159. One and Two-electron Redox Processes with Nickel



#### 3.4.1 Ni-Catalyzed enantioconvergent coupling of organic halides with stoichiometric organometallic nucleophiles

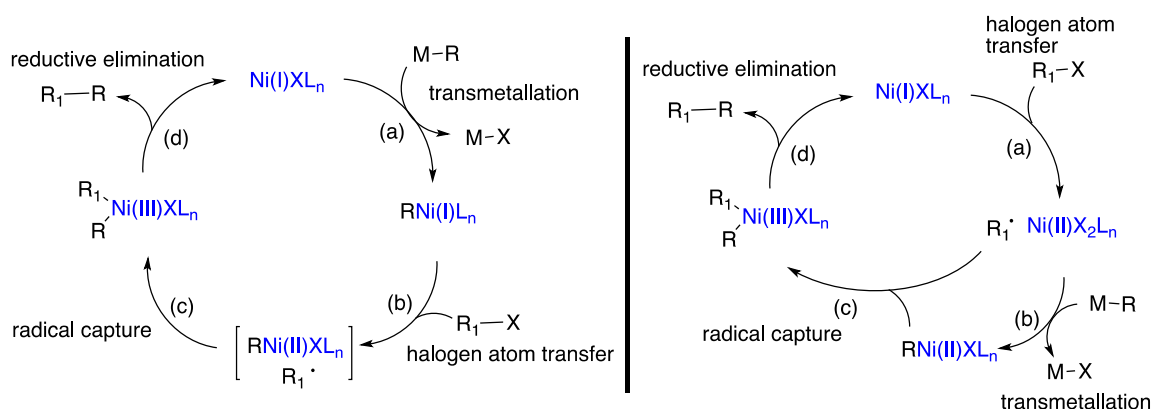
The pursuit by Fu of enantioconvergent substitution of racemic halides via radical intermediates (Scheme 160) through the use of chiral transition-metal catalysts has met every success thanks to the use of Ni catalyzed cross-coupling reactions that involve a large scope organometallic compounds as nucleophiles.<sup>218</sup> These reactions have been extended to coupling with olefins.<sup>326,328,329,330</sup>

**Scheme 160. Concept of Enantioconvergent Substitution of Racemic Halides by means of Chiral Transition Metal Catalyst**



From the very beginning of these studies, slight variants of the radical chain mechanism have been envisaged for the different types of coupling investigated (Negishi,<sup>331,332,333,334,335,336,337</sup> Suzuki,<sup>338,339</sup> Kumada,<sup>340</sup> organozirconium derivatives,<sup>341,342</sup> borylation,<sup>343</sup> etc.) (Scheme 161) depending on whether or not transmetalation precedes the oxidative halogen atom transfer. It is worth noting that enantiocontrol of quaternary centers creation has been successfully achieved. Other routes involving transient Ni(IV) species have also been discussed.

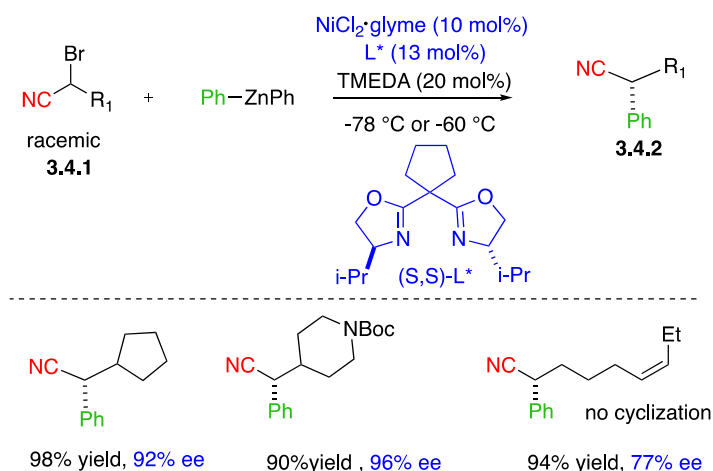
**Scheme 161. Possible Mechanisms (all elementary steps are considered as irreversible for clarity)**



The structural diversity of racemic electrophiles in Negishi type coupling reactions is wide. The reaction that was highlighted with halides activated by the vicinity of a  $\pi$ -system or a coordinating group has been expanded. It is worth mentioning that the use of 5-hexenyl radical clock resulted in the trapping of cyclized radical in the case of simple alkyl radicals, whereas no cyclization was observed in the case of an  $\alpha$ -cyano radical (Scheme 162).<sup>221</sup>

## Scheme 162. Examples of Enantioconvergent Negishi Coupling Involving an $\alpha$ -Cyano Radical

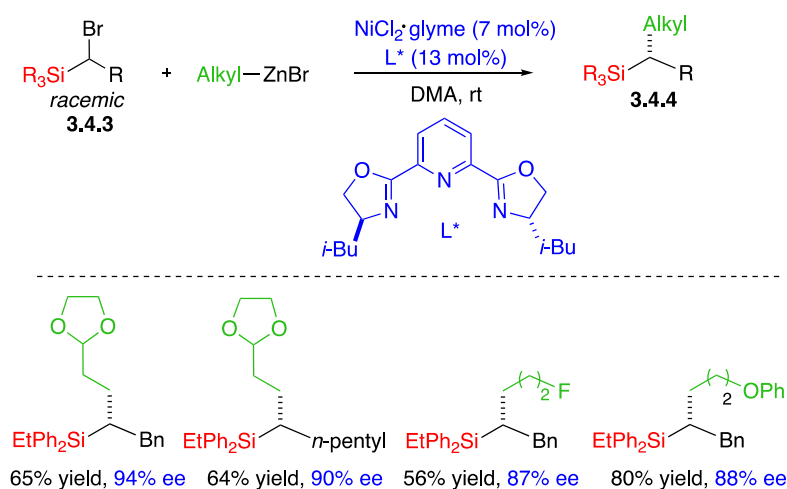
### Radical



In further studies, it was established that bidentate ligands were superior to tridentate ones like PyBox. Conversely, in the coupling of propargyl halides **3.4.3** with organozinc reagents, tridentate PyBox ligands gave the best results in terms of yields and ee (Scheme 163). It is worth noting that no trapping of the propargyl radical intermediate could be detected in the presence of TEMPO.<sup>225,344</sup> As shown in Scheme 163, PyBox ligands were also efficient in the recent application to  $\alpha$ -silyl radicals.<sup>216</sup>

## Scheme 163. Examples of Enantioconvergent Negishi Coupling Involving $\alpha$ -Silyl Radicals

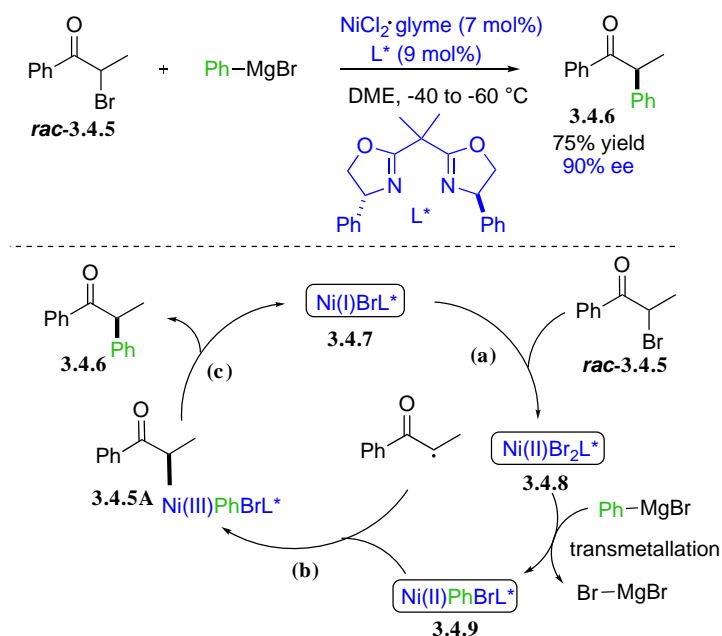
### Radicals



The proposed mechanism was similar to that investigated further for the coupling with organomagnesium derivatives (Scheme 164). Success was effectively met with Kumada coupling of racemic  $\alpha$ -bromoketones as exemplified in Scheme 155.<sup>230</sup> Based on a panel of mechanistic probes (UV-visible and ESR spectroscopies, inhibition by TEMPO, radical-clock, etc.), a mechanism involving Ni(I) as chain carrying radical has been confirmed (reactive species **3.4.7**, **3.4.8** and **3.4.9** were isolated).

Ni(I) would abstract a bromine atom from the bromo-ketone to produce the  $\alpha$ -keto radical and Ni(II) dibromide **3.4.8**. The latter would undergo transmetallation with phenylmagnesium bromide to give Ni(II) complex **3.4.9** that would react with the alkyl radical to produce Ni(III) complex **3.4.5A**. Inner-sphere reductive elimination from **3.4.5A** regenerates the chain carrier **3.4.7** and release the coupling product. Either step **b** or step **c** could control the stereochemistry; theoretical calculations are in favor of step **b**. Indeed, the detailed mechanism depends on the nature of all partners among which the nature of the chiral ligand.

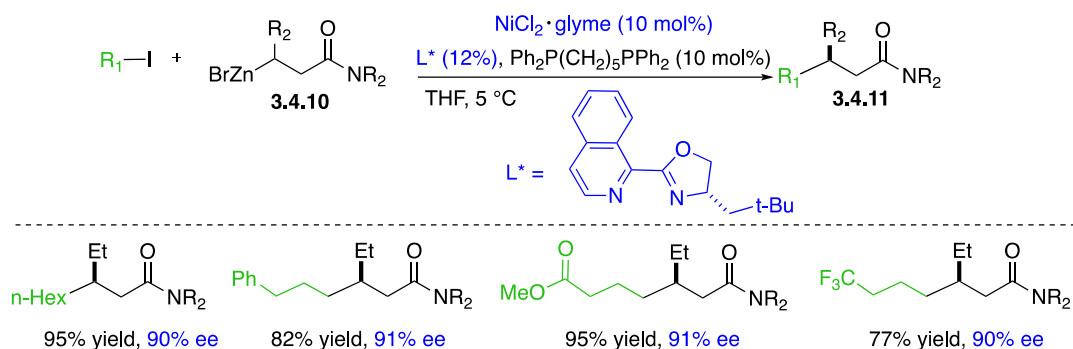
### Scheme 164. Enantioconvergent Kumada Coupling



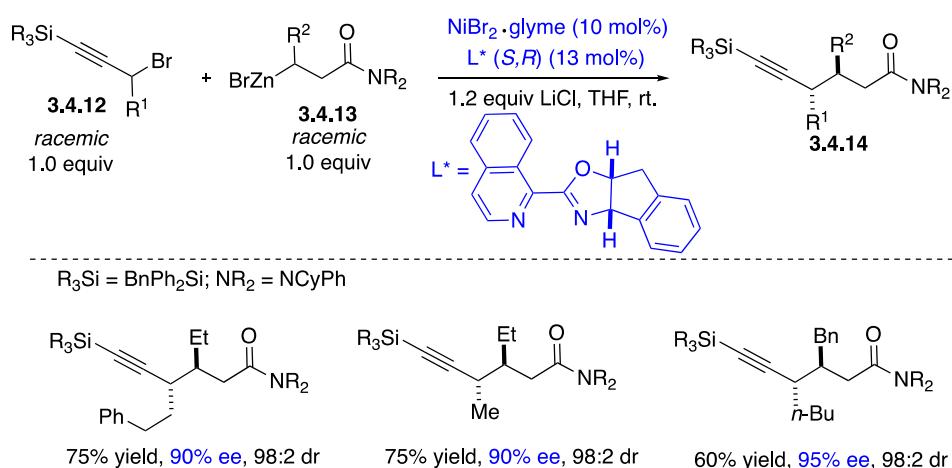
The methodology has been expanded to the synthesis of amines via the substitution racemic *N*-hydroxyphthalimides esters by organozinc iodides catalyzed by chiral Ni-catalysts, this procedure offers an alternative to the substitution of  $\alpha$ -phthalimido alkyl chlorides.<sup>345</sup>

Enantioconvergent substitution could also result from the use of racemic nucleophile and achiral electrophile, although the nature of the nucleophile is limited to date.<sup>346,347</sup> Optimized conditions enables  $\beta$ -zincated pentanamide to couple with a wide range of primary alkyl iodides in excellent yield and ee. A slight increase of the reaction temperature (5 °C instead of -5 °C) allows the coupling of achiral secondary iodides (Scheme 165).

### Scheme 165. Enantioconvergent Substitution of Racemic $\beta$ -Zincated Amides



### Scheme 166. Doubly Enantioconvergent Couplings Mediated by Nickel



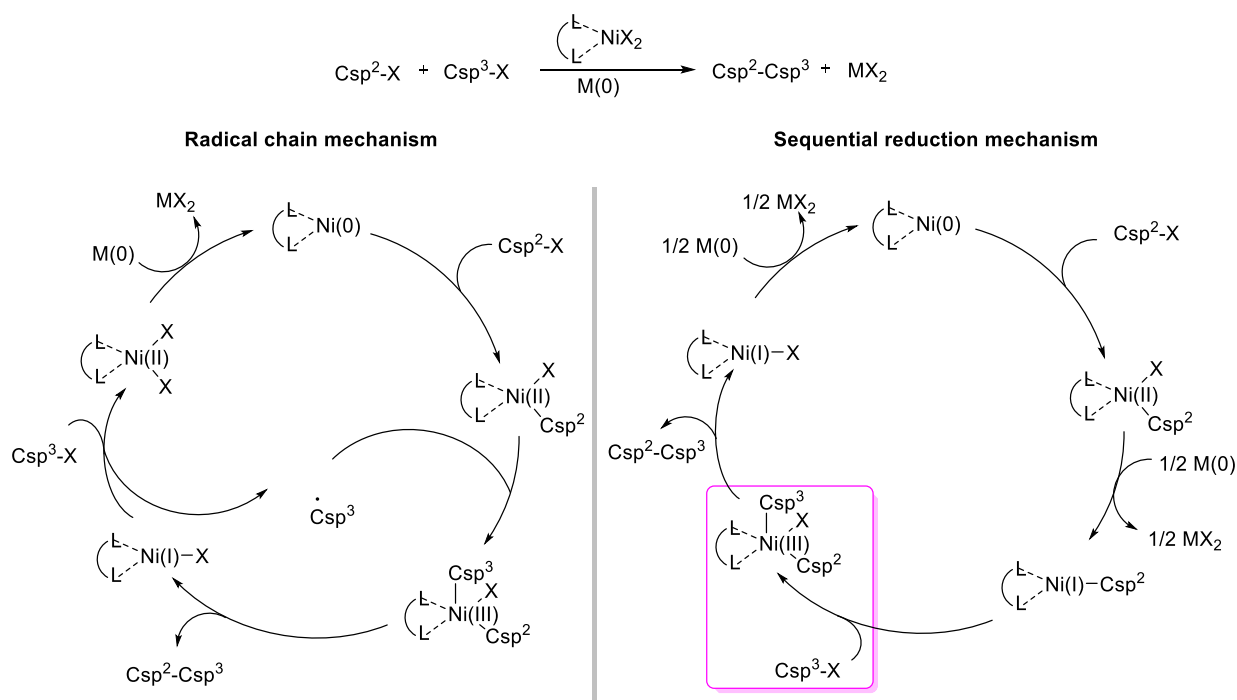
The system is so powerful that it not only allows the enantioconvergent coupling of achiral electrophiles with racemic prochiral nucleophilic organometallics but also a doubly

enantioconvergent coupling when both reagents are racemic.<sup>235</sup> As exemplified in Scheme 166 excellent yields, dr and ee's were obtained with propargylic electrophiles.

### 3.4.2 Reductive cross-coupling in the presence of stoichiometric reductant (Mn(0), Zn(0), TDAE)

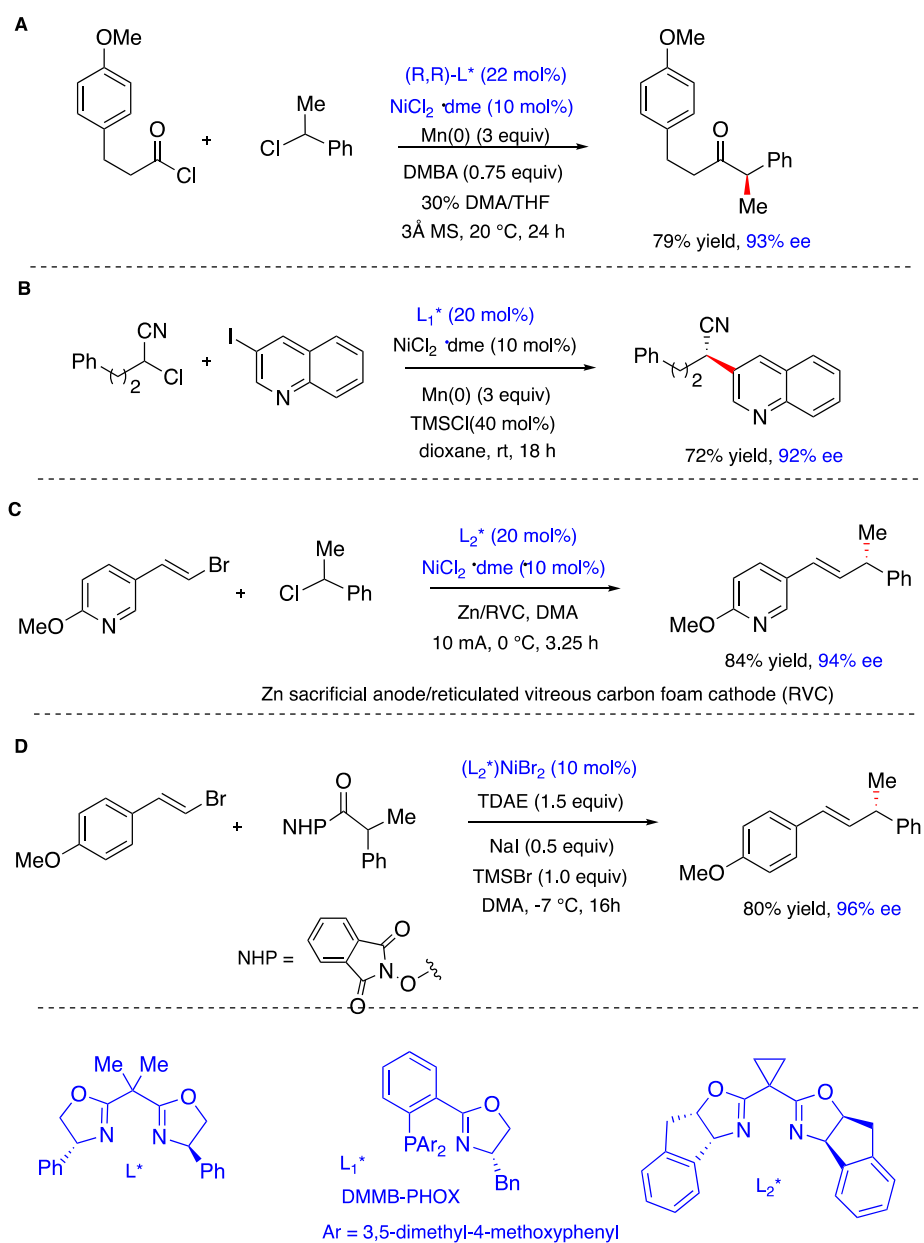
In this section are collected reactions where the Ni-catalyzed coupling does not necessitate to pre-form the nucleophile. However, the turn-over of the catalytic process implies the stoichiometric use a reducing agent. Mn(0), Zn(0) and the super electron donor organic agent tetrakis(dimethylamino)ethylene (TDAE)<sup>348,349</sup> have been used. These protocols have been applied to the coupling of aryl-, vinyl- and acyl halides to alkyl halides. To be chemoselective, the process must avoid the formation of homocoupling products, therefore one has to play with the reactivity difference between the electrophilic partners. Aryl-, vinyl- and acyl halides are more prone to undergo oxidative addition with Ni(0), whereas alkyl halides are more prone to generate alkyl radicals.

#### Scheme 167. Mechanisms envisaged for reductive cross-coupling



Two main mechanisms have been discussed by Weix<sup>350,351</sup> and Reisman<sup>352</sup>: (i) the sequential reduction mechanism that might involve the formation of alkyl radical which would not escape to the cage and instantaneously recombine to Ni and (ii) the radical chain mechanism that involves longer-lived radicals (Scheme 167). Arguments in favor of a chain radical mechanism follow from experiments performed with cyclopropylmethyl radical clocks, however, some inhibition experiments are not so conclusive, many parameters influence the reaction.

**Scheme 168. Examples (A<sup>353e</sup>, B<sup>353c</sup>, C<sup>354</sup>, D<sup>355</sup>) of enantioselective reductive couplings**





Reisman and co-workers have developed the enantioselective coupling of aryl and vinyl halides with alkyl halides in the presence of Mn(0)<sup>353</sup> or Zn(0).<sup>354</sup> TDAE was selected as reducing agent when the precursors of the prochiral alkyl radicals were *N*-hydroxy phthalimides (NHP) esters.<sup>355</sup> Representative examples are given in Scheme 168.

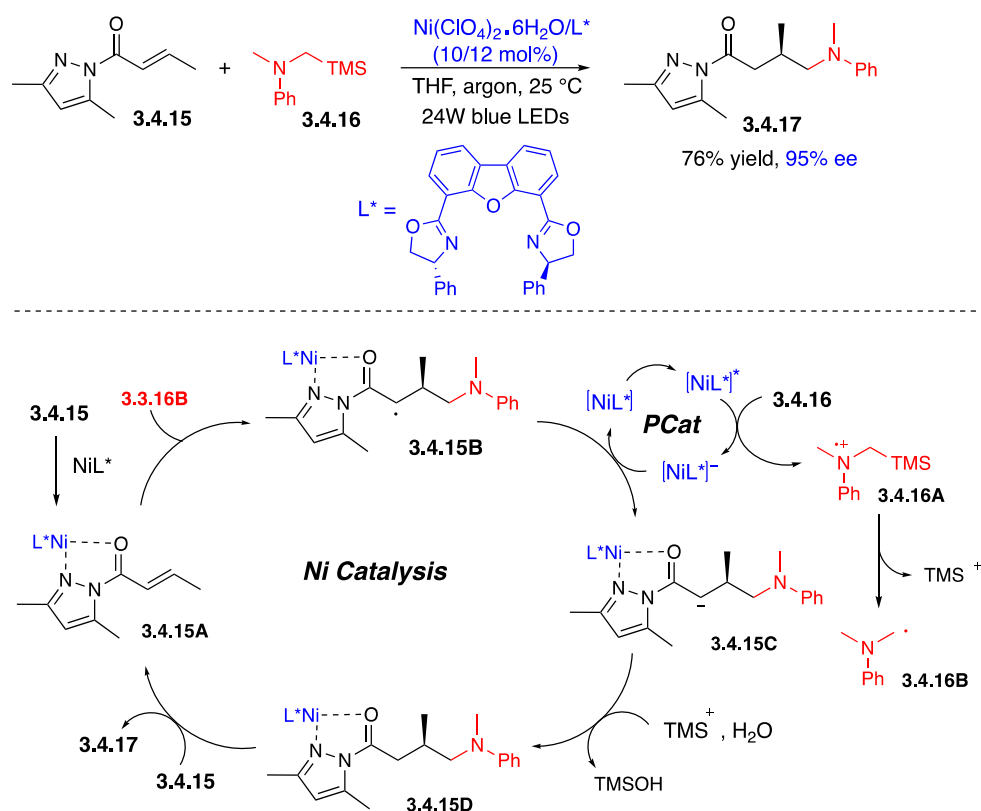
### **3.4.3 Processes involving photocatalytic generation of alkyl radicals, where chirality is controlled by chiral Ni-complexes templating effects**

In the above methodologies, no photocatalysis was needed to generate the radical specie. Conversely, in the following strategies, photoredox catalysis is mandatory for the key radical intermediate to be formed and a dual catalysis to operate.

Stereoselective addition to substrates chelated with chiral metal complexes, largely developed since the pioneering work of Sibi and Porter,<sup>356,357,358</sup> has recently been applied to the Ni-catalyzed conjugate addition of alpha amino radical.<sup>359</sup> In this reaction the Ni(II) complex plays a dual role, i.e., at the same time it acts as photocatalyst to generate the key radical intermediate and, in addition, as chiral Lewis acid it controls diastereofacial selection in the radical addition step. The complex formed from mixing Ni(ClO<sub>4</sub>)<sub>2</sub>·6H<sub>2</sub>O and DBFOX exhibits blue-green luminescence in THF, it was selected as redox active metal center. On the other hand, tertiary  $\alpha$ -silylamines are known, due to their low oxidation potential, to generate  $\alpha$ -amino radicals via SET oxidation followed by desilylation (Scheme 169). The selection of the proper radical acceptor is crucial so it can coordinate to Ni (complex **3.4.15A**) before the addition to the double bond proceeds. The resulting alpha carbonylated radical **3.4.15B** is reduced by Ni(0) to the corresponding anion (**3.3.15C**) according to the mechanism outlined in Scheme 158 that was proposed after a series of control experiments (inhibition, trapping, etc.). The protonation of **3.4.15D** releases product **3.4.17** and Ni(II)L\* to start a new catalytic cycle. Meanwhile radical **3.4.16B** is generated by SET from the silylamine to the photoexcited complex NiL\*. The reduced Ni complex acts as the reducing agent by transferring an electron to radical **3.4.15A**.

## Scheme 169. Dual Role of Ni Complex in Photocatalyzed Enantioselective Conjugate Addition

### Addition

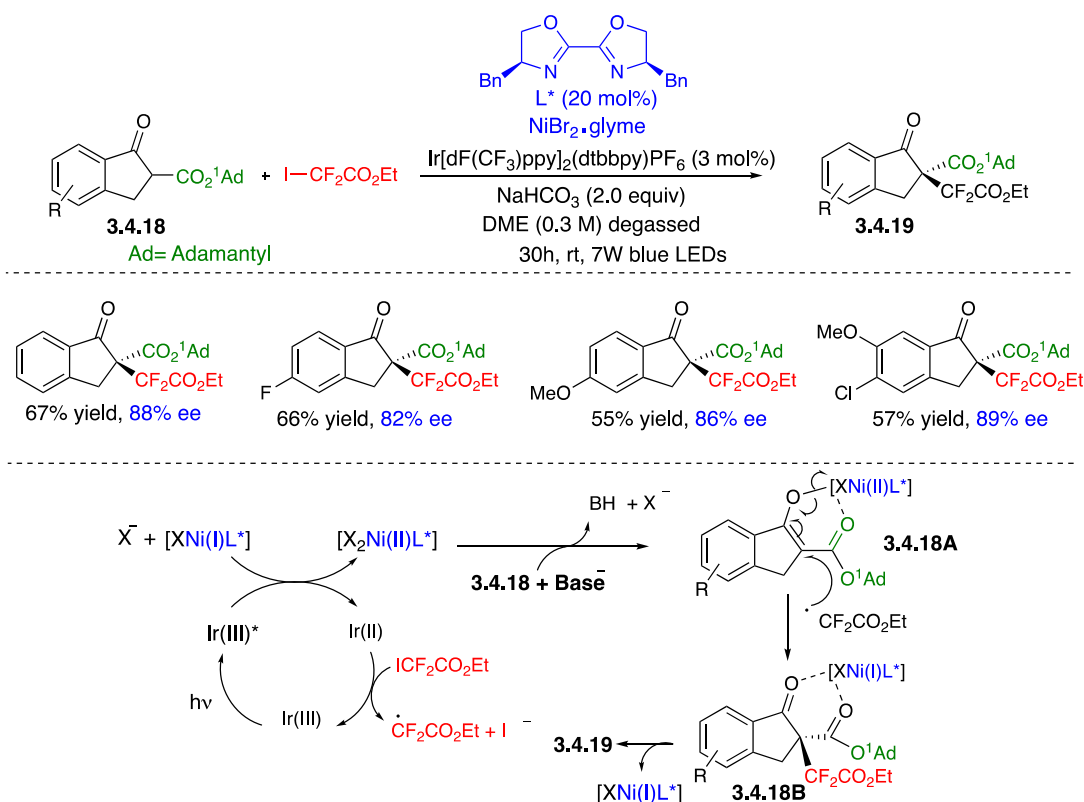


Transition metal polypyridyl complexes that, upon excitation by visible light, promote single-electron transfer (SET) with common electron accepting functional groups have undergone spectacular development.<sup>360,361,362</sup> More specifically, the merge of photoredox catalysis, using transition metal or organic photo-catalysts, with Ni-catalyzed cross-coupling of carbon-centered radical with alkyl or aryl halides is currently undergoing a remarkable growth.

Indeed, by substituting the bipyridyl ligand with fluoro and trifluoromethyl groups, a number of more oxidizing photocatalysts have been prepared. The latter are capable of performing SET oxidations on numerous functionalities. Different types of precursors have been used to generate alkyl radicals via SET oxidation event, among which, carboxylates, alkyltrifluoroborates, alkylsilicates, alkyldihydropyridines. Hydrogen Atom Transfer (HAT) from unactivated C–H bonds have also been exploited.<sup>363,364,365</sup>

The difluoroalkylation of  $\beta$ -ketoesters that has been reported by Lu and Xiao is singular.<sup>366</sup> In this process, Ir(III)-based photocatalyst and chiral Ni(II) complex are proposed as cooperative catalysts in the visible light triggered formation of chiral difluorinated alkylation product **3.3.19** containing a quaternary center. As exemplified in Scheme 170, under optimized conditions satisfying yields and good ee's could be reached for a series of adamantyl esters. Control experiments revealed that both the irradiation and the photocatalyst were necessary for the reaction to proceed.

### Scheme 170. Enantioselective Addition of Difluorinated Radicals to Ni-Enolates



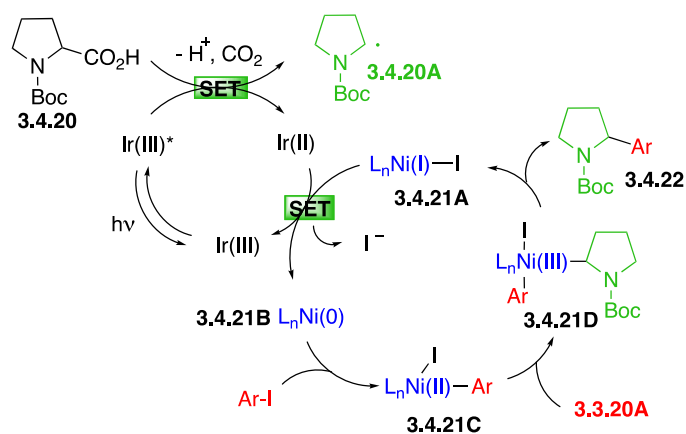
In the presence of the base, the chiral Ni(II)-ate complex would be formed. Its templating effect controls the diastereoselective addition of the difluorinated radical. This addition step would lead to the concomitant reduction of Ni(II) to Ni(I). The latter is being reoxidized by Ir(III) in the photocatalytic cycle. The singularity resides in the fact that Ir(II) would therefore reduce the iodo-fluoroester to produce the reactive radical specie, this SET event may not be necessary to promote the homolysis of the C-I bond. The latter SET event regenerates the Ir(III)-complex

whose photoexcitation is necessary to complete the Ni catalytic cycle by reoxidizing Ni(I) to Ni(II).

### 3.4.4 Dual Ni/Metallaphotoredox catalysis

Metalla-photoredox catalysis coupled to Ni catalysis opens route to cascades reactions leading to a variety of new bonds formation.<sup>367</sup> Notably, in asymmetric synthesis, it enables the decarboxylative  $sp^3$ - $sp^2$  cross-coupling of amino acids.<sup>368</sup> The general mechanism of these reactions that involve Ir(III) complexes as photocatalysts, is outlined below on the selected example of *Boc*-proline **3.4.20** (Scheme 171). Alpha amino radicals like **3.4.20A** can also be generated via SET directly from dimethylanilines and the process can be expanded to O- or phenyl-substituted carboxylic acids leading to stabilized alkyl radicals. It must be underlined that this widespread scenario is completely different from the previous one as the radical precursor is oxidized by Ir(III) conversely to the above example where the precursor was reduced by Ir(II) to generate the radical.

#### Scheme 171. Mechanism of Decarboxylative Metalla-Photoredox Catalysis Coupled to Ni-Catalyzed Cross-coupling Leading to Benzylic Amines

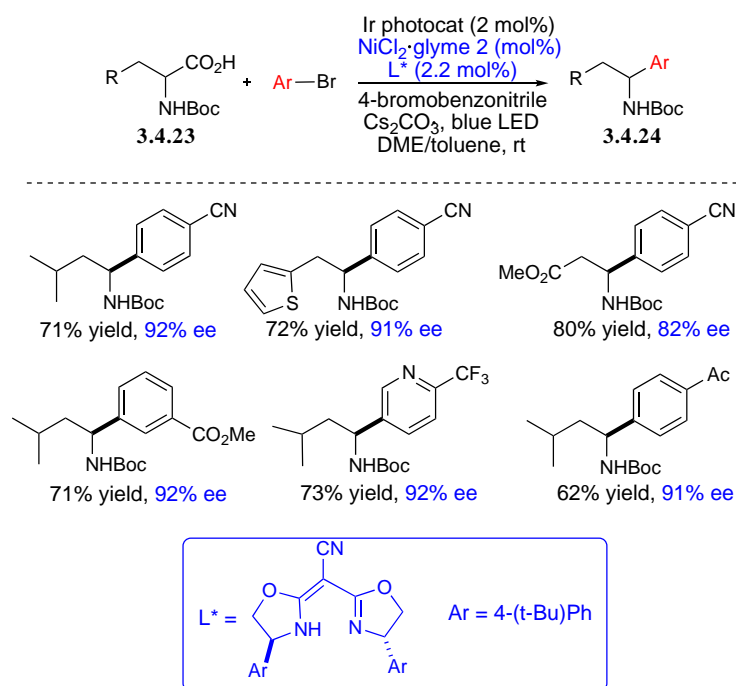


Ni catalytic cycle proceeds via oxidative addition of the aryl halide to Ni(0) (**3.4.21B**) which leads to the Ni(II) complex **3.4.21C**. Reaction with the alkyl radical **3.4.20A** leads to the Ni(III) specie **3.4.21D**. This electron deficient specie undergoes fast reductive elimination to form the coupling product **3.4.22** and the Ni(I) halide **3.4.21A**. The Ir catalyst plays a dual role. First as

an oxidant, it generates the alpha-amino radical **3.4.20A**. Even though most authors represent these two steps in that order, according to theoretical calculations, due to its lower activation energy, addition of the carbon-centered radical to Ni(0) would precede oxidative addition of the aryl iodide that would therefore involve a Ni(I) specie.<sup>369</sup> The light induced oxidative decarboxylation of protected proline conjugated base is promoted via SET towards the Ir(III) polypyridyl complex. Second, the so-formed Ir(II) complex is able to reduce Ni(I) **3.4.21A** to regenerate the Ni(0) active specie **3.4.21B** via a second SET event.

### Scheme 172. Enantioselective Synthesis of Benzylic Amines via Decarboxylative Arylation

#### Arylation

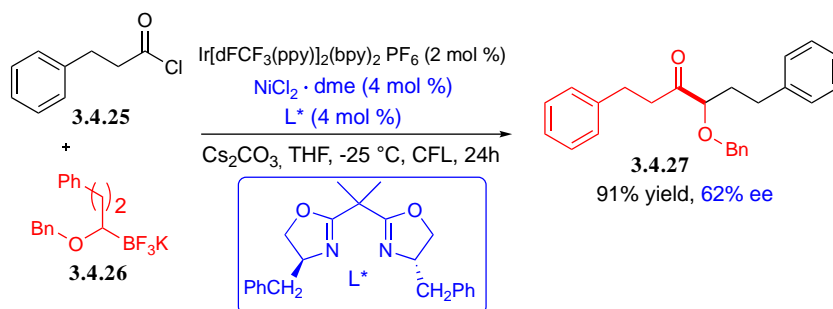


The association of nickel-catalyzed cross-coupling and the above decarboxylative arylation, enabled the enantioselective synthesis of benzyl amines by using chiral nickel-catalysts formed with bidentate BOX ligands. Ni(II) complex, would control facial stereoselectivity in the reductive elimination step. Representative examples are given in Scheme 172.<sup>370</sup>

Other precursors like trifluoroborates can also be employed with efficiency in metallaphotoredox catalysis coupled with Ni cross-coupling.<sup>371</sup> As exemplified in Scheme 173,

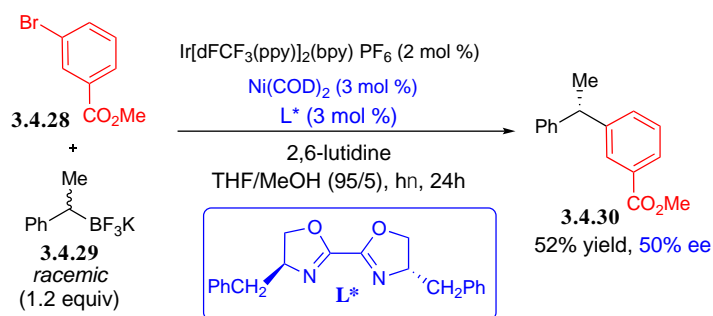
prochiral  $\alpha$ -alkoxy radical generated from the corresponding trifluoroborate was acylated with 62% ee using a BOX ligand.

### Scheme 173. Enantioselective Acylation of $\alpha$ -Alkoxy Alkyl Radicals Generated from Alkyl Trifluoroborates



It is worth noting that the same Ir photocatalyst enabled the enantioselective coupling of a racemic secondary alkyltrifluoroborate with an aryl bromide by using a BOX type chiral ligand in the Ni cross-coupling catalytic cycle. However, both the yield (52%) and the ee (50%) were relatively modest (Scheme 174).<sup>369</sup>

### Scheme 174. Enantioconvergent Coupling of a Secondary Alkyl Trifluoroborate



Alkyltrifluoroborates were efficient source of radicals in the three-component enantioselective arylation of activated alkenes. In the presence of BOX ligand dual Ni/Ir photocatalysis led to ee's up to 97% in average to excellent yields.<sup>372</sup>

Amines constitute a special class of hydrogen atom donors as they are good electron donors and the generation of  $\alpha$ -aminoradicals therefore occurs via direct SET event with the photocatalyst.<sup>373</sup> This leads to a radical cation whose deprotonation generates the required carbon-centered radical (PCET could as well be involved<sup>374</sup>). It is worth mentioning, that direct

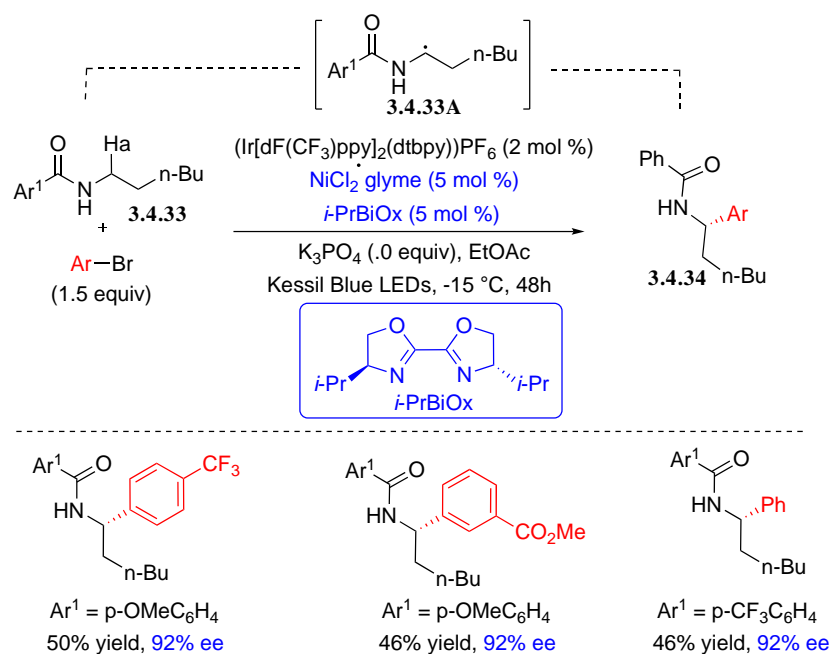
arylation of *N*-phenyl pyrrolidine **3.4.31** and related cyclic and acyclic substrates was achieved by Doyle under closely related conditions using aryl iodides as electrophiles (Scheme 175).<sup>375</sup> The reaction is likely to proceed in this case via indirect HAT (SET concerted with or followed by proton transfer). Although the enantioselectivity was moderate, the asymmetric synthesis of 2-phenyl-*N*-phenylpyrrolidine **3.4.32** was performed by using *S,S*-Bn-BiOx as the ligand.

**Scheme 175. Asymmetric Synthesis of 2-Phenyl-*N*-Phenylpyrrolidine**



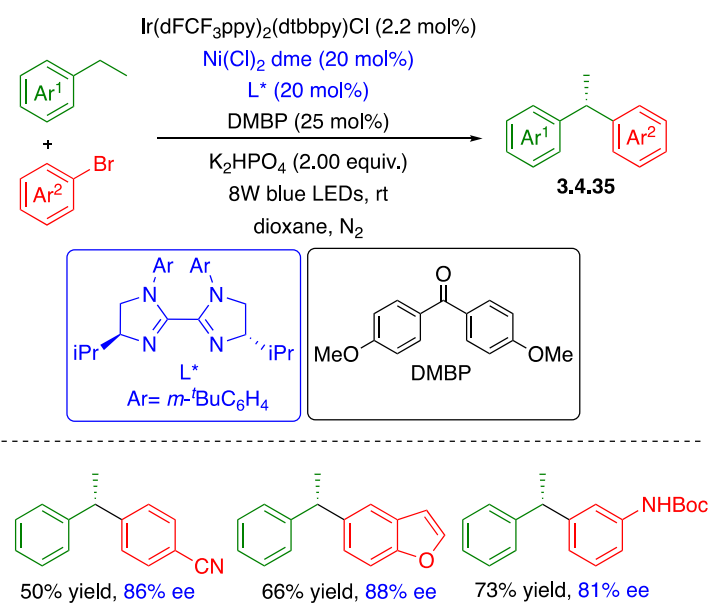
Martin and co-workers have recently disclosed the chemo- and enantioselective C-sp<sup>3</sup>  $\alpha$ -arylation of benzamides **3.4.33** (Scheme 176).<sup>376</sup> The fate of the generic reaction is highly sensitive to the nature of the base and the solvent. Under optimal experimental conditions, high enantiomeric ratios are reported whatever the substituent on the aryl bromide. The mechanism is not yet elucidated, however, isotopic labeling points to the fact that the homolytic cleavage of the  $\alpha$  C-H bond occurs in the rate determining step. The formation of the  $\alpha$ -amido radical key intermediate **3.4.33A** might result from HAT to bromine atom. The latter, resulting from the homolysis of photo-excited Ni-Br bond, would be the chain carrier of the radical process. Such a scenario had already been suggested for related reactions (vide infra).<sup>377,378,379</sup> It is worth noting that selective regiodivergent activation of the  $\delta$  C-H bond can be observed depending on the nature of amide skeleton, the nature of the Ir catalyst and the base.<sup>375</sup> The photo-induced Ir-promoted HAT from *N*-alkylbenzamides was used to perform Ni-mediated cross-coupling acylation catalyzed leading to  $\alpha$ -aminoketone precursors. Acylating electrophiles were in situ generated mixed anhydrides.<sup>380</sup>

### Scheme 176. Enantioselective $\alpha$ -arylation of benzamides



### 3.4.5 Dual photocatalytic reactions involving organic photocatalysts

#### Scheme 177. Enantioselective Synthesis of 1,1-Biaryl Alkyl Derivatives



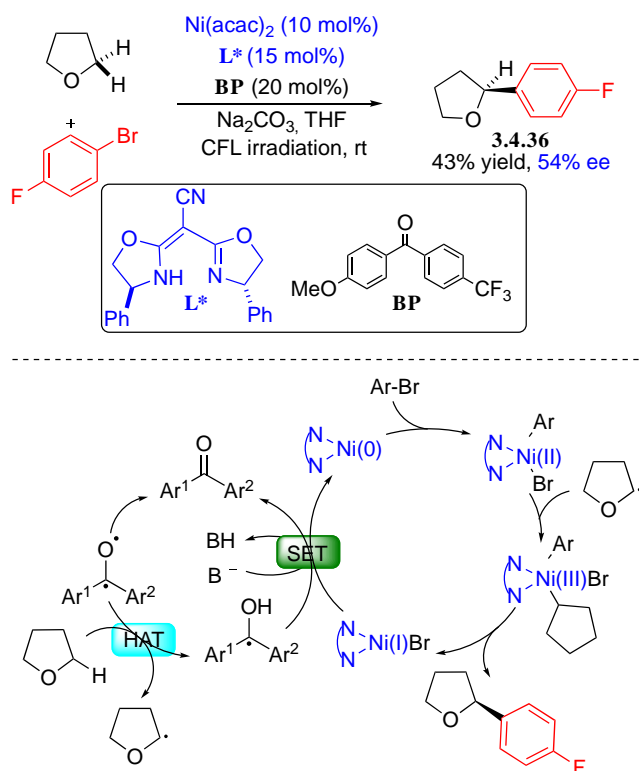
The cooperative effect of two photocatalysts, i.e., Ir(III) and benzophenones in the presence of a base has been investigated by Molander.<sup>381,382</sup> Dimethoxybenzophenone (DMBP) led to the best experimental results. Although the mechanism is still under debate, the scenario



according to which the triplet excited state of DMBP would act as HAT reagent is highly plausible (the alternative scenario, among others, is an energy transfer to the Ni(II) complex resulting from oxidative addition of the aryl bromide that would release a bromine atom as the effective HAT agent). The methodology was recently successfully applied to the synthesis of enantioenriched 1,1-biaryl derivatives by using BiIM ligands **3.4.35** (Scheme 177).<sup>383</sup>

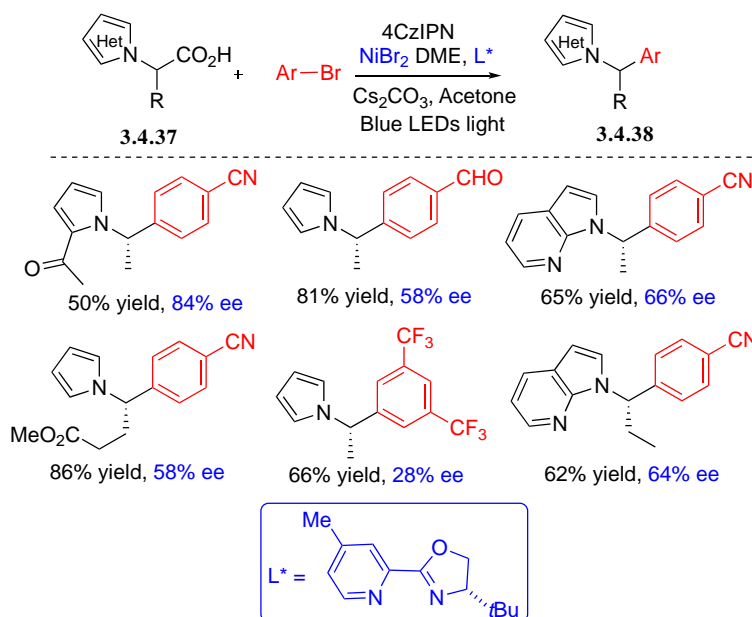
An isolated example of enantioselective coupling of a prochiral radical involving an organophotocatalyst has been reported by Martin.<sup>384</sup> In contrast to the above results, the originality of this report resides in the dual role of benzophenone used as the single redox photocatalyst (Scheme 178). The triplet state excited benzophenone acts first as hydrogen atom abstractor. In the presence of a base the resulting ketyl radical is able to reduce Ni(I) and thus regenerate the active Ni(0) catalyst.

### Scheme 178. Ni-mediated Cross Coupling of Prochiral Radical Generated by HAT Promoted by Benzophenone Dual Catalyst



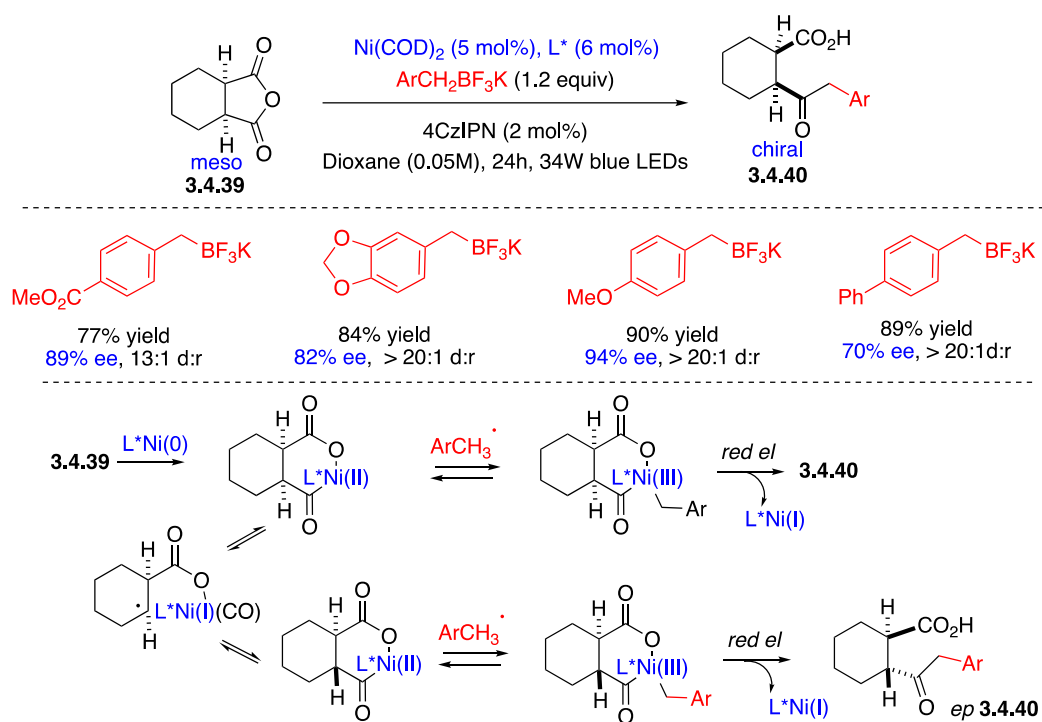
Based on a decarboxylative strategy, the enantioselective formation of *N*-benzylic heterocycles has recently been reported.<sup>385</sup>  $\alpha$ -Heterocyclic carboxylic acids **3.4.37** have been successfully coupled to aryl bromides, in this case the authors used pyridine–oxazoline (PyOx) chiral ligands. Like in the preceding example, a metal-free photocatalytic system operated. An organic SET agent, 1,2,3,5-tetrakis(carbazol-9-yl)-4,6-dicyanobenzene (4CzIPN),<sup>363</sup> was used. Selected examples are shown in Scheme 179.

### Scheme 179. Enantioselective Formation of *N*-Benzylic Heterocycles



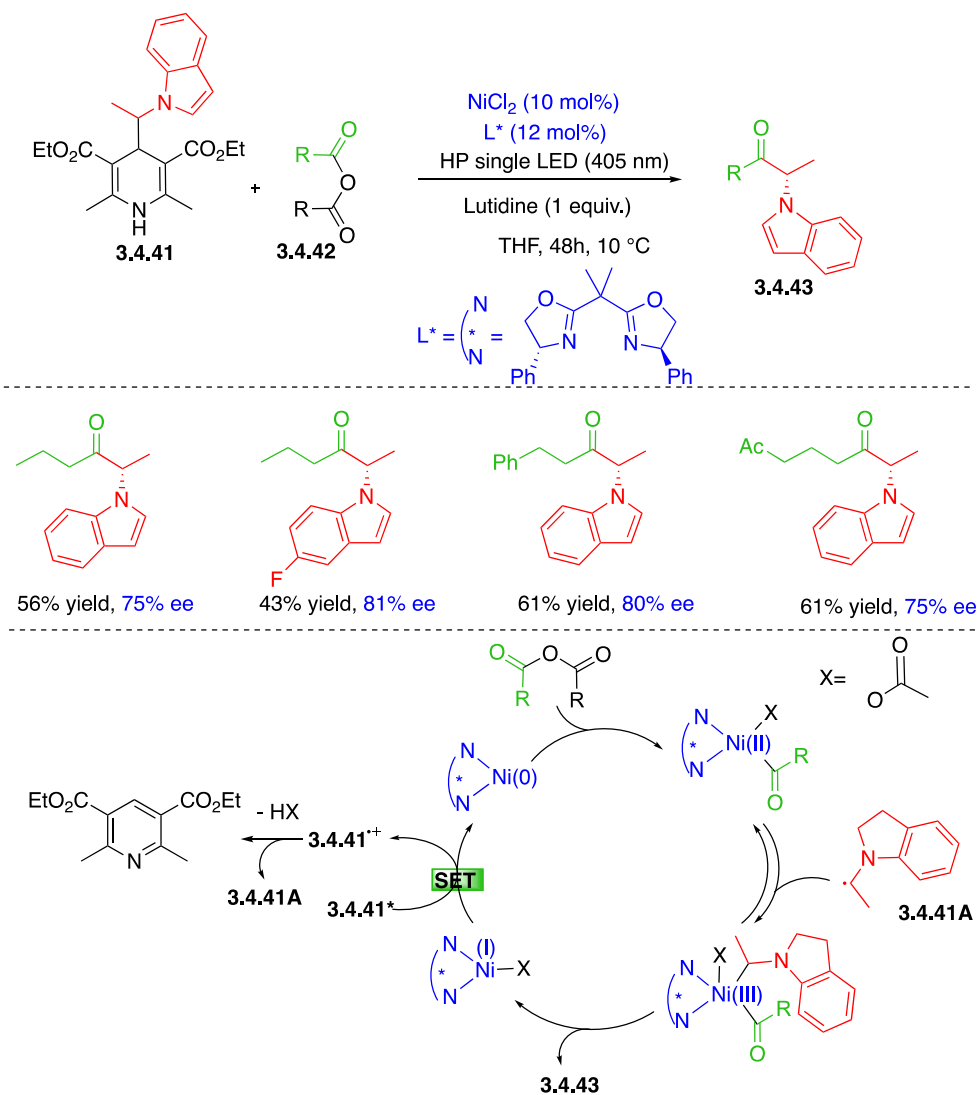
The photoredox-catalyzed desymmetrization of meso anhydride **3.4.39** reported by Stache *et al* is also based on the use of 4CzIPN as photo-reducing agent to generate benzylic radicals from the corresponding benzyltrifluoroborates and its merger with Ni cross-coupling catalysis.<sup>386</sup> According to the authors, the ee determining step, i.e., the oxidative addition to Ni(0) precedes the formation of Ni(III) species by reaction with the benzylic radical. The small amount of epimerized product *epi*-**3.4.40** would be best explained on the ground of the coordinatively unsaturated Ni(II) intermediate. Representative data are given in Scheme 180.

## Scheme 180. Photoredox Desymmetrization of Meso Anhydrides



Hantzsch esters constitute a useful class of electron donors and proton sources in photo-redox catalyzed processes.<sup>387</sup> In a recent expansion on the use of 4-alkyl-1,4-dihydropyridines **3.4.41** (DHPs), Gandolfo *et al.* have shown that they could be used at the same time as precursor for carbon-centered radical via direct photo-excitation and as SET reducing agent, which interplays with the Ni cross-coupling catalytic cycle to insure its turn-over.<sup>388</sup> As exemplified in Scheme 181, the enantioselective acylation of indole derivatives bearing a stereocenter in position  $\alpha$  to the heterocyclic nitrogen was achieved using chiral BOX ligands. The same procedure was applied to the synthesis of  $\alpha$ -aryl ketones.

### Scheme 181. Dual Role of DHP in Ni-Catalyzed Acylation



Ir photocatalysts are expensive. It is not unlikely that the potentiality of classical cheap organic photocatalysts could lead to significant expansion of their use in organic synthesis.

### 3.5. Enantioselective copper-catalyzed radical reactions

One has to go back to the second half of the twentieth century to remind the reader of copper salts catalyzed Kharasch addition (ATRA) of perhalogenated compounds<sup>389,390,391</sup> and even much earlier for the discovery of reactions involving the reduction of aryldiazonium salts like Pschorr cyclization, Sandmeyer and Meerwein reactions.<sup>392</sup> Copper catalyzed enantioselective reactions using suitable chiral ligands came about much later.<sup>393,394</sup> The low cost and low toxicity of copper makes it very attractive to develop catalytic transformations.

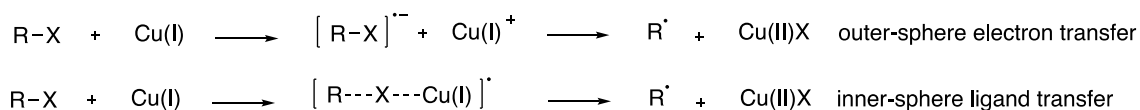
As a matter of fact, attempts to mediate asymmetric radical processes with copper catalysts can be divided into two sections: (i) the first one relies exclusively on the Lewis acidic properties of Cu(II) complexes to chelate either the radical or the radical acceptor; (ii) the second one takes additional advantage of redox properties of Cu(I)/Cu(II) couple to generate and functionalize radicals.

As summarized in Scheme 170, Cu(I) is an excellent electron donor to initiate the formation of alkyl (or even heteroatom-centered) radicals from suitable precursors. The formation of the carbon-centered radical can be viewed as one electron transfer from the metal to the precursor (outer sphere mechanism) or as atom or group transfer from the precursor to the metal (inner-sphere electron transfer mechanism).

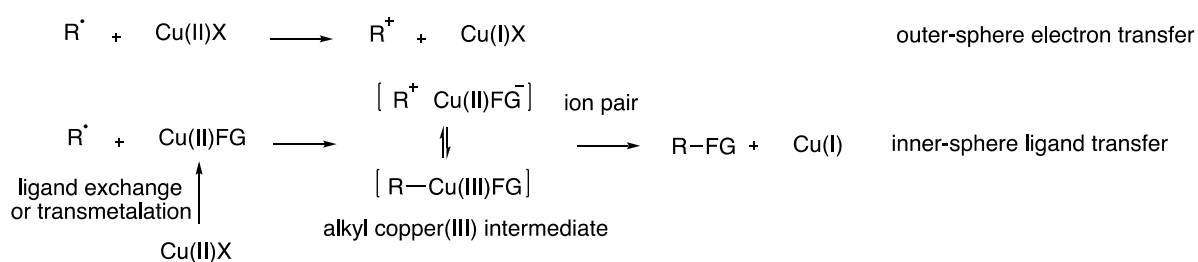
### Scheme 182. Mechanisms for the Formation and the Functionalization of Alkyl (aryl)

#### Radicals by Cu(I)/Cu(II) Couple

##### Generation of alkyl radicals via Cu(I)-mediated electron transfer



##### Oxidation of alkyl radicals by Cu(II)



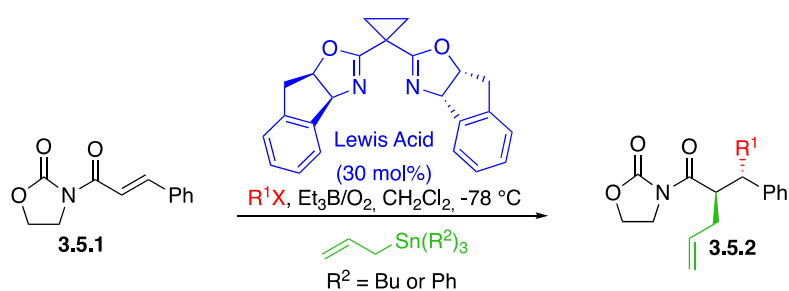
Similarly, the oxidative trapping of the alkyl (aryl) radical by Cu(II) can be viewed as one electron transfer from the radical to the metal generating a carbocation that further reacts with a nucleophilic specie (outer sphere mechanism) or a ligand transfer from the Cu(II)-complex to the radical via a cage mechanism involving an ion pair or an intermediate Cu(III) complex that undergoes reductive elimination. It is very difficult to distinguish between the last two paths. It

must be noted that these reactions need the presence of a complexing agent (initially bipyridine was mostly used) which solubilizes and modifies the redox potential of the metal. It is easy to infer that only the second type of mechanism can result in chirality transfer from appropriate ligands. Ligand exchange or transmetalation allows the introduction of nucleophilic new functionalities. *In the following discussion, data are not reported chronologically but rather classified as much as possible by the type of reaction.*

### 3.5.1 Chiral Lewis acidic Cu(II) complexes-mediated radical reactions

Enantioselective conjugate additions have been extensively investigated, essentially by Porter and Sibi.<sup>357,395</sup>

#### Scheme 183. Lewis Acid Mediated Enantioselective Tandem Conjugate Addition/Allylation



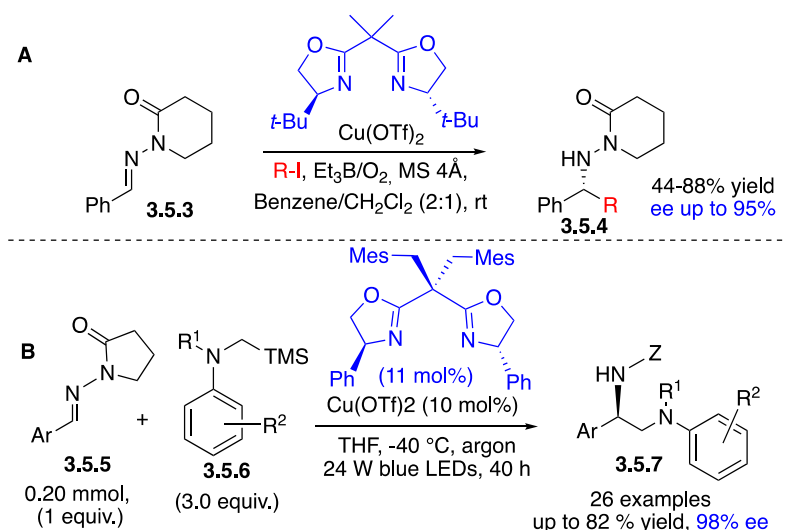
Entry	R <sup>1</sup> X	LA	Yield (%)	dr	ee (%)
1	<i>i</i> -PrI	MgI <sub>2</sub>	93	37:1	93
2	<i>t</i> -BuI	MgI <sub>2</sub>	84	99:1	97
3	<i>i</i> -PrI	Cu(OTf) <sub>2</sub>	93	30:1	-79
4	<i>t</i> -BuI	Cu(OTf) <sub>2</sub>	90	99:1	-96

All parameters like the structure of the bidentate structural element incorporated into the radical or the radical acceptor, the structural parameters of additional chiral ligand and the nature of the Lewis acid that controls the geometry of the reactive complex and enhance reactivity have been scrutinized. Moreover, the difficulty to make the reaction catalytic has been overcome. As regards to the nature of the metal salts, copper(II) salts proved to be poor partners in radical conjugate additions,<sup>396,397</sup> except in the case of tandem addition/allylation (Scheme 183).<sup>398</sup> It

is worth noting that opposite enantioselectivity were observed when replacing  $\text{MgI}_2$  by  $\text{Cu}(\text{OTf})_2$ .

Good facial discrimination was also observed in the addition of radicals to C=N bond of *N*-acyl hydrazones **3.5.3** investigated by Friestad (Scheme 184, A).<sup>399</sup> The aminoalkylation of acyclic imine performed by Han et al.<sup>400</sup> must be brought close to Friestad report due to similarity, even though this reaction implies photoredox catalysis the use of which will be exemplified later on. In this reaction, the  $\alpha$ -aminoradical is generated by the irradiation of an  $\alpha$ -silylamine **3.5.6** that undergoes SET to Cu(II). The reaction leads to chiral vicinal diamines **3.5.7** (Scheme 184, B).

### Scheme 184. Cu(II) Chiral Lewis Acid-controlled Addition to Hydrazones



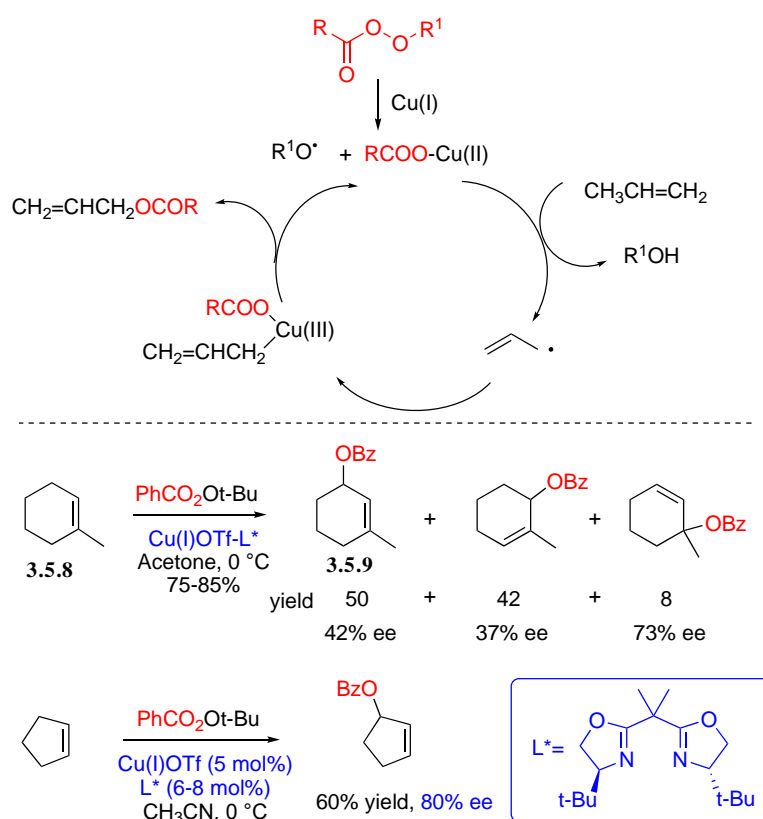
The chiral bis-oxazoline copper(II) catalyst plays several roles in the photochemical reaction, including initiation of the single electron transfer (SET) to generate the  $\alpha$ -aminoalkyl radical. This step generates a visible-light activatable copper(I) specie capable to reduce the *N*-acyl hydrazinyl radical that results from the addition step. As a chiral Lewis acid, it increases the electrophilicity of the imine substrate and controls chirality transfer in the radical addition process.

### 3.5.2 Cu-mediated enantioselective functionalization of alkyl radicals

#### 3.5.2.1 Radicals generated via intermolecular HAT

The very first attempts to perform copper-catalyzed enantioselective reactions followed from the investigation of Kharasch-Sosnovsky allylic oxidation.<sup>401,402,403</sup> Interesting ee's were obtained when using bidentate chiral  $C_2$ -symmetrical ligands like bisoxazolines. However, the reaction is restricted with respect to the type of alkene due to the lack of regioselectivity of the first step which implies hydrogen atom abstraction by an alkoxy radical (the latter is generated via reduction of a peroxide by Cu(I)) (Scheme 185). This reaction has been a source of inspiration for recent expansion of copper-catalyzed asymmetric reactions.

#### Scheme 185. Enantioselective Kharash-Sosnovsky Allylic Oxidation

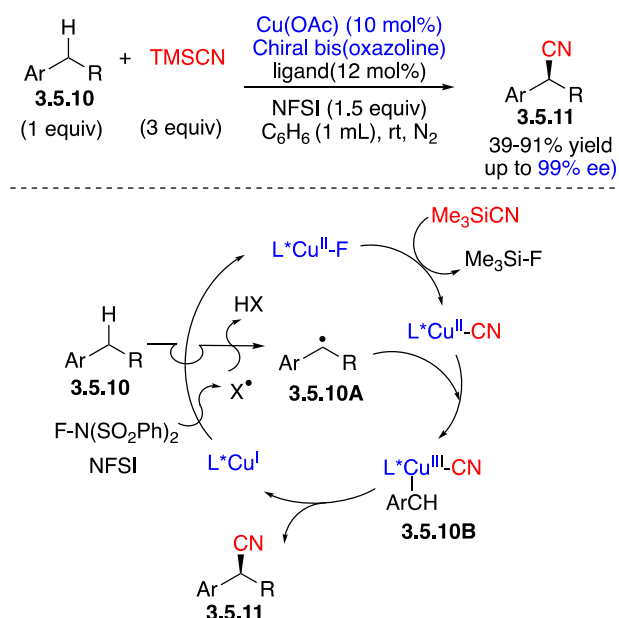


Liu *et al.* disclosed a copper-catalyzed enantioselective cyanation of benzylic C-H bonds in which the organic radical, is also produced by hydrogen atom abstraction (Scheme 186).<sup>404</sup> In this case, bissulfonimidyl radical generated from copper(I)-mediated reduction of NFSI, was used to abstract the benzylic hydrogen atom. It proved to be effective where oxygen-



centered radicals were not. According to the mechanistic scheme, supported by DFT studies, the prochiral benzylic radical **3.5.10A** is rapidly trapped by a chiral (Box)Cu<sup>II</sup>-CN species formed via ligand exchange with TMSCN. The resulting copper(III) complex intermediate **3.5.10B** would be formed reversibly. It evolves via reductive elimination to the expected nitrile **3.5.1A** with high enantioselectivity. This suggests the close proximity between the benzylic carbon and the Cu atom in the enantioselectivity-determining step, *i.e.*, the reductive elimination.

### Scheme 186. Copper-catalyzed Enantioselective Benzylic Cyanation

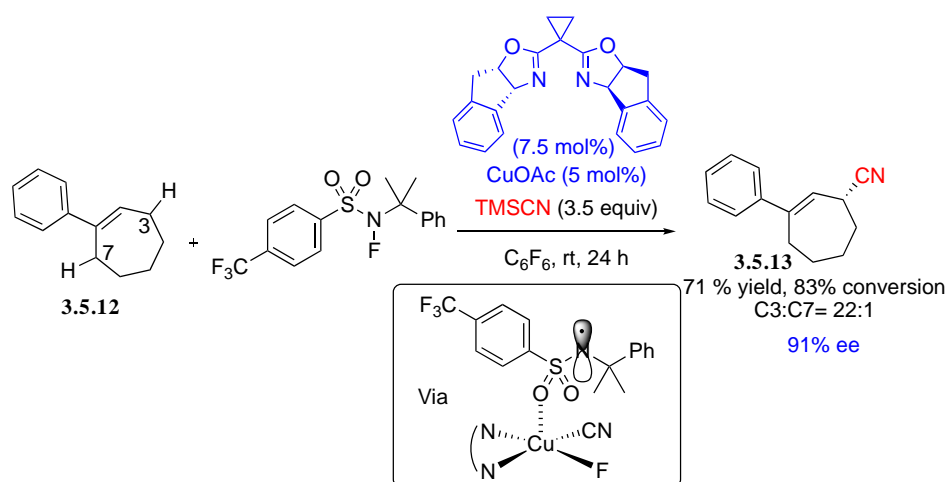


A closely related methodology has been applied to the regio- and enantioselective allylic cyanation of alkenes.<sup>405</sup> The basic idea of the authors was to modulate the structure of the abstracting *N*-centered radical so as to improve the site selectivity of the allylic hydrogen atom transfer. This was achieved by modifying the bulkiness of the alkyl group at nitrogen and the electronic properties of the substituent on the aromatic part of the arene sulfonyl group.

The authors observed high ee's for the formation of **3.5.13** which proved that the enantioselective radical trapping by Cu(II)-cyanide was independent of the HAT step (Scheme 187). The most original observation was that the site-selectivity, as high as 22:1, was much higher than the selectivity observed for xanthylation performed under typical radical conditions

by irradiating *N*-xanthyl sulfonylaminides (3.4:1). This meant that H-abstraction was not achieved by a free sulfonimidyl radical but rather by a copper-bound nitrogen-centered radical. Mechanistic investigation performed on an acyclic alkene was successfully extended to a series of other acyclic and cyclic alkenes. It should be noted that the challenge of directly replacing a benzylic C-H by a trifluoromethyl group in a catalytic process was demonstrated by Xiao et al.<sup>406</sup> The originality of this work resides in the use of (bpy)Zn(CF<sub>3</sub>)<sub>2</sub> complex as source of trifluoromethyl anion equivalent merged with copper(I) catalyzed initiation of a radical chain process by the reduction of NFSI. No examples of enantioselective reaction in the presence of chiral ligand to exchange bpy has been disclosed yet.

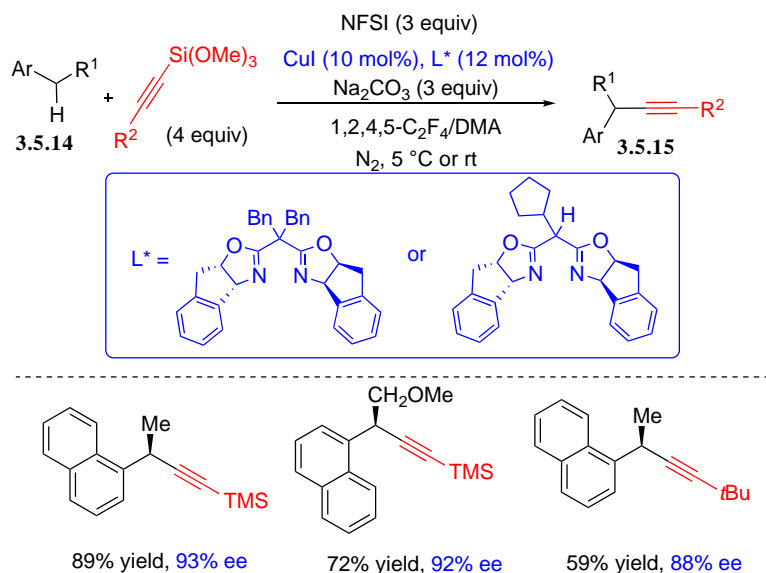
### Scheme 187. Regio- and Enantioselective Allylic Cyanation of Alkenes



Fu et al. have achieved the copper catalyzed enantioselective alkylation of benzylic radicals based on the fundamental role of bisulfonimidyl radical to generate the prochiral radical from a large array of alkyl aromatic substrates **3.5.14** (Scheme 188).<sup>407</sup> After examination of different plausible mechanisms, substantiated by control experiments and computational data, the authors propose the involvement of the following steps: (i) the reactive amidyl radical HAT reagent remains complexed to Cu(II) when reacting with the substrate; (ii) exchange between Cu(II)F (generated via CuI-mediated reduction of NFSI) and

trimethoxyalkynylsilanes leads to the Cu(II)-alkynyl intermediate that reacts with the benzylic radical via a Cu(III) intermediate to eventually give rise to the enantioenriched product **3.5.15**.

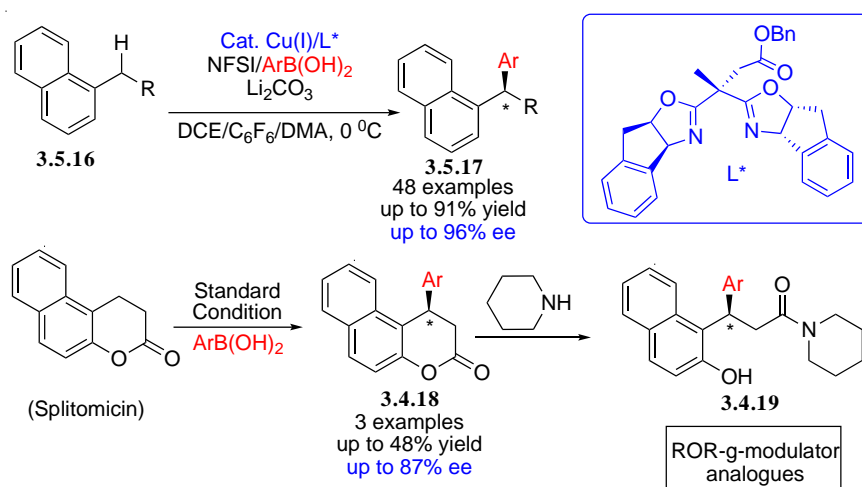
### Scheme 188. Representative Examples of Enantioselective Alkynylation of Benzylic Radicals



Liu et al. have extended their methodology using NFSI to asymmetric benzylic C-H arylation. In this case, the catalytic cycle involves transmetalation with a boron “ate” specie to generate the active L\*ArCu(II) complex that reacts with the benzylic radical, formed as above via HAT to bisulfonimidyl radical. The protocol uses the alkylarene **3.5.16** as limiting reagent and leads to chiral 1,1-diarylalkanes **3.5.17** with good to excellent enantioselectivities (Scheme 189).<sup>408,409</sup> The incorporation of a benzyl ester moiety into the box ligand plays a crucial role for the enhancement of both chemo- and enantioselectivity of the process. Possibly, the interaction between the (L\*)Cu(II) species and ArB(OH)<sub>2</sub> accelerates the transmetalation which is the rate limiting step. This leads to higher concentration of (L\*)Cu<sup>II</sup>Ar species which efficiently capture the benzylic radicals and prohibit the side reactions leading to undesired fluorinated and aminated products. This standard methodology has also been applied to the synthesis of ROR- $\gamma$ -modulator analogues **3.5.19** from Splitomicin.

## Scheme 189. Synthesis of Chiral 1,1-Diarylalkanes by Asymmetric Benzylic C-H

### Arylation via Copper-catalyzed Radical Relay Strategy

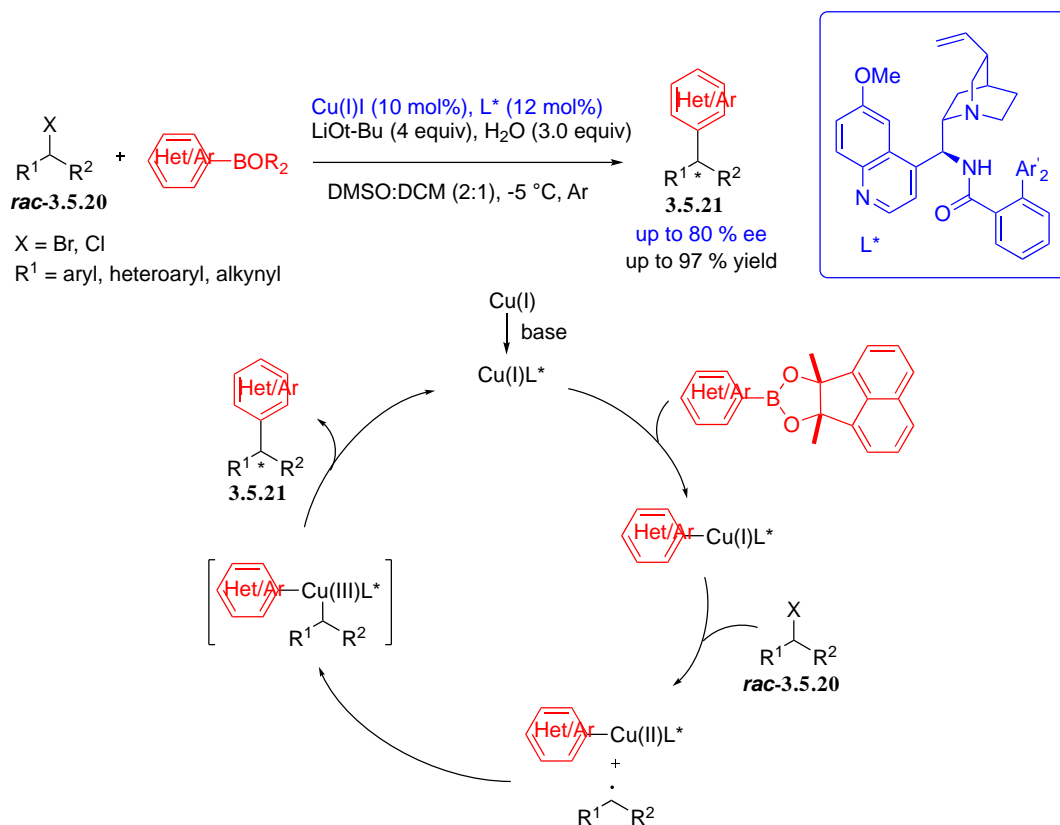


#### 3.5.2.2. Radicals generated via direct reduction of organic radical precursor

The enantioconvergent copper-catalyzed radical Suzuki–Miyaura C(sp<sup>3</sup>)–C(sp<sup>2</sup>) cross-coupling of alkyl halides **3.5.20** with organoboronates has been recently reported by Li, Liu and co-workers.<sup>410</sup> In this procedure, the alkyl radical is directly generated via the reduction of the corresponding chloride or bromide by Cu(I)-iodide. This reaction should be related to Ni-mediated couplings (see: § 3.4.) A wide array of 1,1-diarylalkanes, 1-aryl-1-heteroarylalkanes and (hetero)benzyl alkynes were prepared in good yields and high ee's (Scheme 190). In these processes, the alkyl radical results from halogen atom transfer to Cu(I) in the presence of a chiral *N,N,P*-cinchona alkaloid-derived ligand that enhances the reducing capacity of Cu(I). At the same time, ortho-substitution of the ligand was expected to increase steric strain and enhance enantioselectivity. In the proposed mechanism, transmetalation proceeds at the stage of the chiral Cu(I) complex by reaction of the alkylboronate, it is promoted by LiOt-Bu. The optimized solvent mixture is a 2:1 mixture of DMSO and DCM (3 equiv of H<sub>2</sub>O is necessary to solubilize the base), water is also known to accelerate the transmetalation step. Ligand transfer to Cu(I) induces the formation of the prochiral radical and the reactive Cu(II)-complex. The latter are likely to release the product, via reductive elimination from a Cu(III) intermediate,

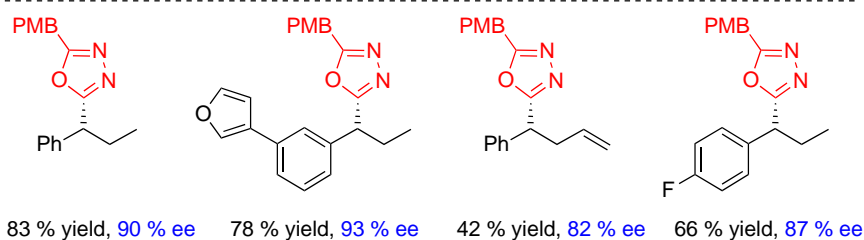
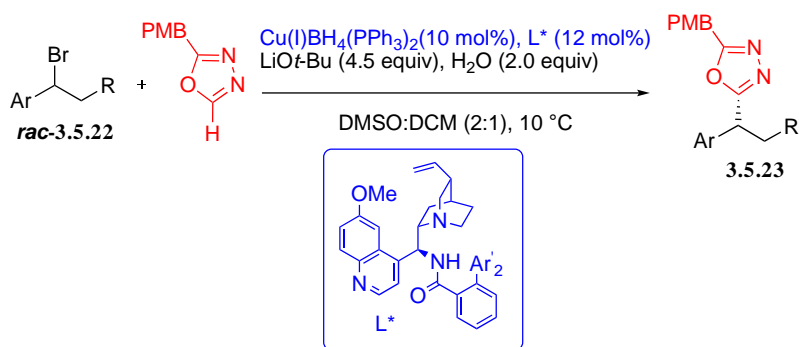
which regenerates Cu(I). The radical mechanism was proved by control experiments using TEMPO as an inhibitor and a radical clock.

**Scheme 190. Enantioconvergent Cu-mediated Cross-coupling of Racemic Alkyl Halides with Organoboronates**



The enantioconvergent coupling of racemic alkyl bromides **3.5.22** with azole C(*sp*<sup>2</sup>)-H bonds was achieved by Su et al. by using the same type of *N,N,P* alkaloids derived ligands.<sup>411</sup> Azoles are easily deprotonated by LiOt-Bu at 10 °C under inert atmosphere. Cu(I)-borohydride bis-triphenylphosphine was used as the catalyst (10 mol%). As above, the formal mechanism involves ligand exchange with azole conjugated base, the resulting C(*sp*<sup>2</sup>)-Cu(I) complex promotes the reduction of the alkyl bromide and thus the generation of the prochiral radical and Cu(II). Subsequent reaction between the radical and Cu(II) complete the catalytic cycle. Representative examples **3.5.23** are given in Scheme 191.

**Scheme 191. Enantioconvergent Cross-coupling of Racemic Alkyl Bromides and Azoles**



### 3.5.3 Enantioselective functionalization of radicals necessitating dual Cu/photocatalysis

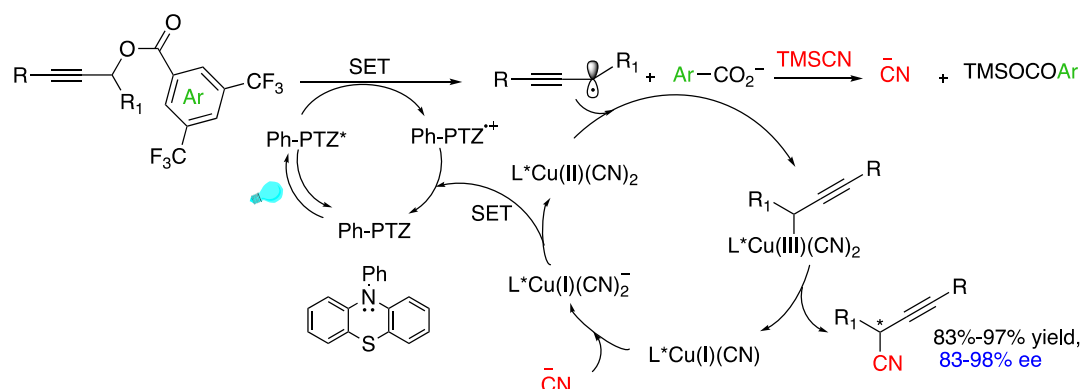
There are cases where Cu(I) alone is not reducing enough to generate the active radical species from the suitable radical precursor. Photocatalysts (organometallic complexes or organic compounds) supply solution to the failure of non-photochemical strategy. They absorb light efficiently and at longer wavelength than do most simple organic compounds. In the excited state photocatalysts can easily react by energy transfer, electron transfer or hydrogen atom abstraction.<sup>412,413,414,415,416</sup> Moreover, visible light is a safe and sustainable source of energy in line with the increasing attention given to green chemistry.

#### 3.5.3.1 Enantioselective copper-mediated photocatalyzed cyanation

Lu et al. have developed the asymmetric propargylic radical cyanation (APRC) of propargyl esters via a synergistic organophotoredox/copper catalysis strategy.<sup>417</sup> Upon optimized reaction conditions, when propargyl *bis*-trifluorobenzoates ( $\text{LG} = 3,5\text{-(CF}_3\text{)}_2\text{PhC(=O)O}$ ) and  $\text{TMSCN}$  (3 equiv) were irradiated in anhydrous THF with visible light (2x3W, purple LEDs, 390 nm) for 24 h at 30 °C, in the presence of Ph-PTZ as organic photocatalyst (*N*-phenylphenothiazine, 5 mol%),  $\text{Cu(I)(CH}_3\text{CN)}_4\text{BF}_4$  (2.5 mol%) and chiral BOX ligand (5 mol%), enantio-enriched propargyl cyanides were obtained in good yields (83%-97%) with ee's varying from 83 to 98% (Scheme 180). In all likelihood, SET reduction of the electron accepting benzoate promotes the

homolysis of the propargylic C-O bond. A propargylic radical is formed concomitantly to a carboxylate anion which reacts with TMS-CN to release CN<sup>-</sup>. The Cu(I)-cyanide so-generated is oxidized by transferring an electron to the phenothiazine radical cation. Reaction of Cu(II) cyanide with the prochiral propargylic radical completes the redox-copper catalytic cycle and releases the enantioenriched alkyne.

**Scheme 192. Asymmetric Cyanation of Propargyl Radicals via Dual Organophotoredox/ Copper Catalysis**

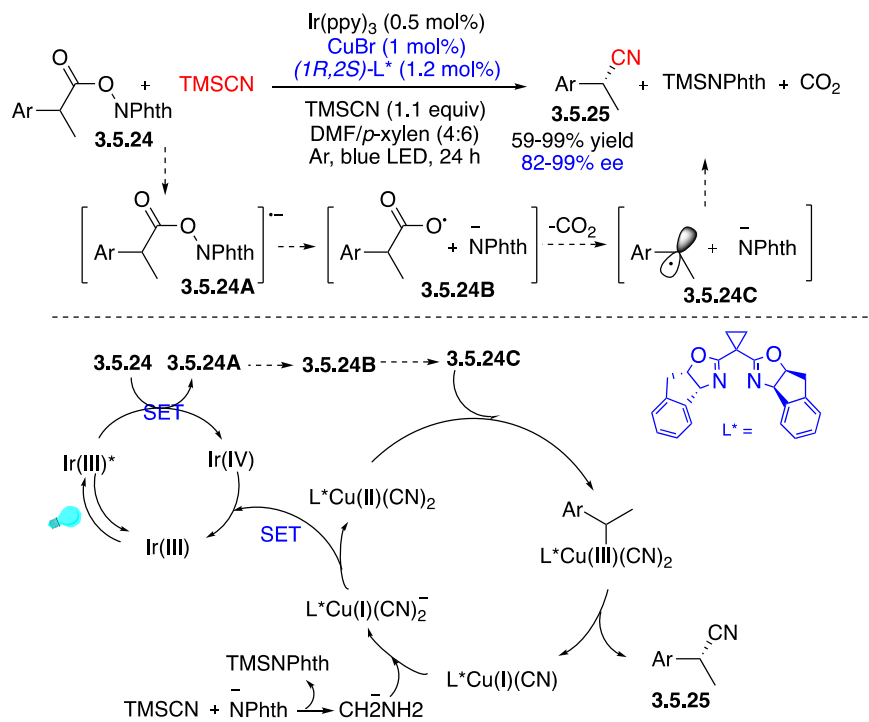


Wang et al. reported the enantioselective cyanation of benzylic radical generated via the reductive cleavage of *N*-hydroxy-phthalimide (NHP) esters followed by decarboxylation of the resulting acyloxy radical (Scheme 193).<sup>418</sup> The phthalimide anion reacts with TMS-CN to form in situ CN<sup>-</sup> anion. Cu(I) is introduced as CuBr in the reaction medium. In this protocol, Cu catalysis is merged with metallaphotoredox catalysis. On the basis of redox potentials, the authors propose that Ir(III)(ppy)<sub>3</sub> is an efficient electron donor to reduce the NHP ester **3.5.24**. This leads to an Ir(IV) complex that oxidizes Cu(I) cyanide into Cu(II) cyanide. Again, a C<sub>2</sub>-symmetrical optically active BOX ligand reveals to be the best ligand to promote chirality transfer in the reductive elimination step. The reaction failed to give a good enantioselective ratio in the case of non-benzylic radicals

### 3.5.3.2 Copper as photocatalyst in visible light-assisted enantioselective C(sp<sup>3</sup>)-

#### N(sp<sup>3</sup>) coupling

#### Scheme 193. Dual Cu/photocatalytic Decarboxylative Cyanation numbering



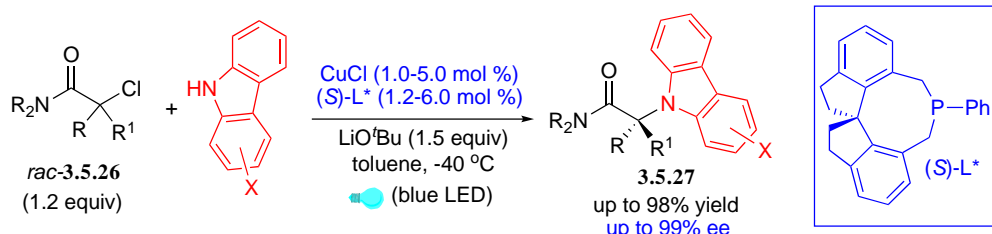
Fu and Peters have reported the enantioconvergent synthesis of carbazole-derived tertiary amines via visible light-induced copper-catalyzed substitution of racemic tertiary alkyl halides activated by the vicinity of an amide carbonyl group that probably coordinates to copper.<sup>419</sup> The use of copper as photocatalyst is not widespread yet.<sup>420,421</sup> It must be emphasized that, unlike most dual photoredox/metal-catalysis methods, in this case, copper alone plays a dual role. Photoactivated Cu(I) is a strong reductant; it undergoes electron transfer to the organic halide to generate the prochiral radical after which event, the classical mechanism, i.e., radical rebound leading to Cu(III) species and ligand exchange (or alternative ligand exchange followed by ligand transfer to the carbon-centered radical) promotes the formation of the C-N bond. In summary, Cu is used for both the photoactivation of the redox process and the chiral ligand-assisted enantioselective bond construction. Irradiation of carbazole derivatives and racemic tertiary alkyl halides at -40 °C for 16 hours in the presence of CuCl, a chiral phosphine (L\*),



and a Brønsted base (LiO<sup>t</sup>Bu) provides the C-N cross-coupling products in good to excellent yields and enantioselectivities (Scheme 194).

### Scheme 194. Asymmetric Copper-catalyzed C-N Cross-couplings Induced by Visible

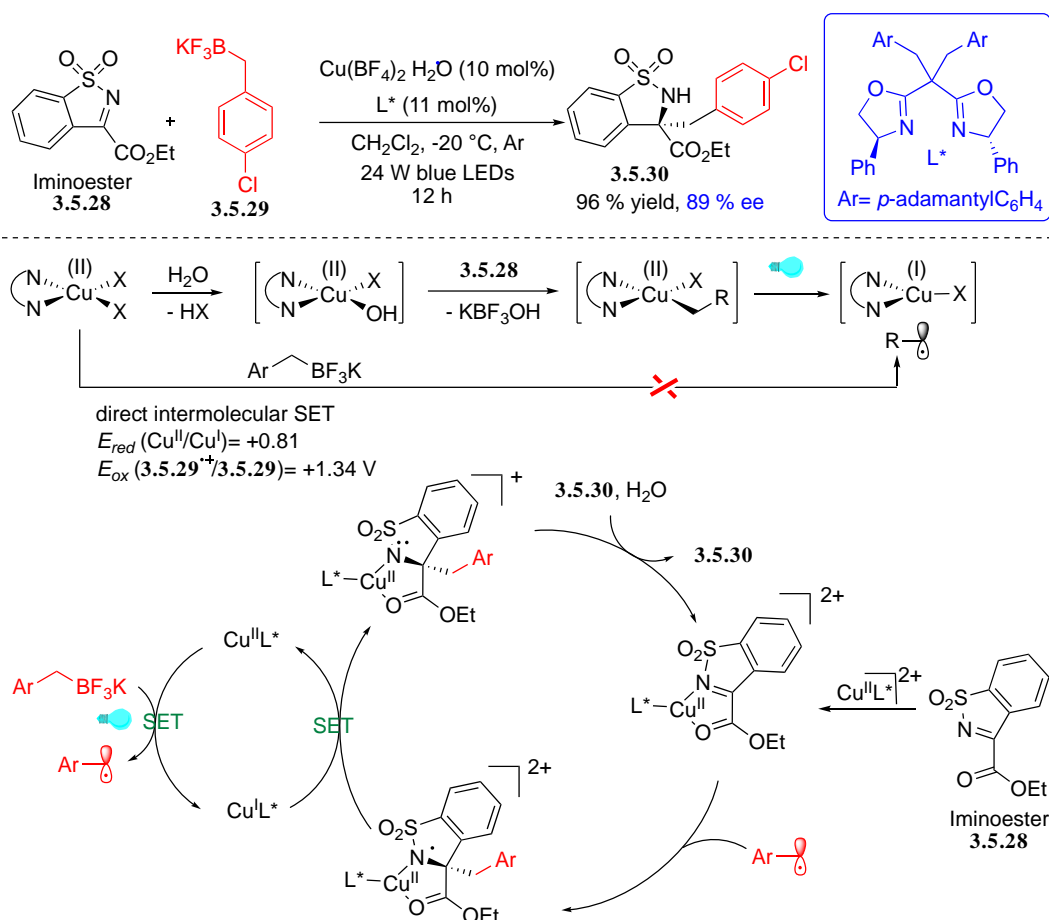
#### Light



#### 3.5.3.3 Visible light driven enantioselective alkylation of $\alpha$ -iminoesters

The enantioselective addition of alkyl radicals to an imino group designed by Li et al. could as well have been included in section 2.2.2 in the sense that Cu(II) chiral Box complex is coordinated to the bidentate substrate and controls chirality transfer in the radical addition step by discriminating the two faces to the C=N double bond. However, like in the addition reported in Scheme 172B, the originality of the methodology is based on the photoactivation and oxidizing properties of Cu(II). It is a typical case of Lewis acid dual functional photocatalysis.<sup>422</sup> Whereas silylamines are very easily oxidized to generate  $\alpha$ -aminoradicals, the direct oxidation of benzyltetrafluoroborate by Cu(II) complex is thermodynamically unfavorable as suggested by cyclic voltammetry studies (Scheme 195). According to the authors, a plausible mechanism involves ligand exchange introducing Cu(II)-OH bond before transmetalation with the tetrafluoroborate occurs. Blue LEDs irradiation would accelerate the formation of the intermediate benzyl radical that adds stereoselectively to the C=N bond activated by coordination to Cu(II).

## Scheme 195. Visible Light Driven Enantioselective Alkylation of $\alpha$ -Iminoesters



Evidence for the formation of the benzylic radical was obtained from radical trapping experiments. The chelating properties of the substrate are essential for the reaction to proceed. The latter leads to chiral amines bearing a quaternary stereogenic center. High yields and with ee's up to 98% were obtained from cyclic sulfonylimines and isatin-derived ketimines.

### 3.5.4 Enantioselective Copper-catalyzed radical functionalization after intercalation of radical addition, ring-opening or 1,5-HAT rearrangement

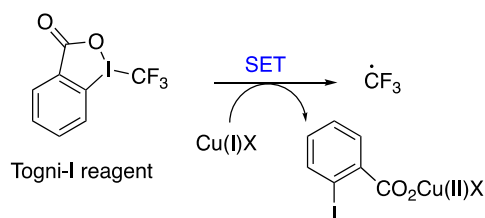
#### 3.5.4.1 Intercalation of addition to alkenes<sup>423</sup> and arylcyclopropanes

Trifluoromethylated groups play a profound role in the field of pharmaceuticals and agrochemicals as it has excellent metabolic stability, lipophilicity, permeability and electrostatic interactions with targets.<sup>424</sup> In particular, enantiopure CF<sub>3</sub>-containing molecules are at the forefront of innovation in modern organic and medicinal chemistry because the effect

of stereochemistry on biological activity is of prime importance for medicinal application. Therefore, the incorporation of trifluoromethyl groups into organic molecules has received much attention and thereby significant progress has been achieved in recent times.

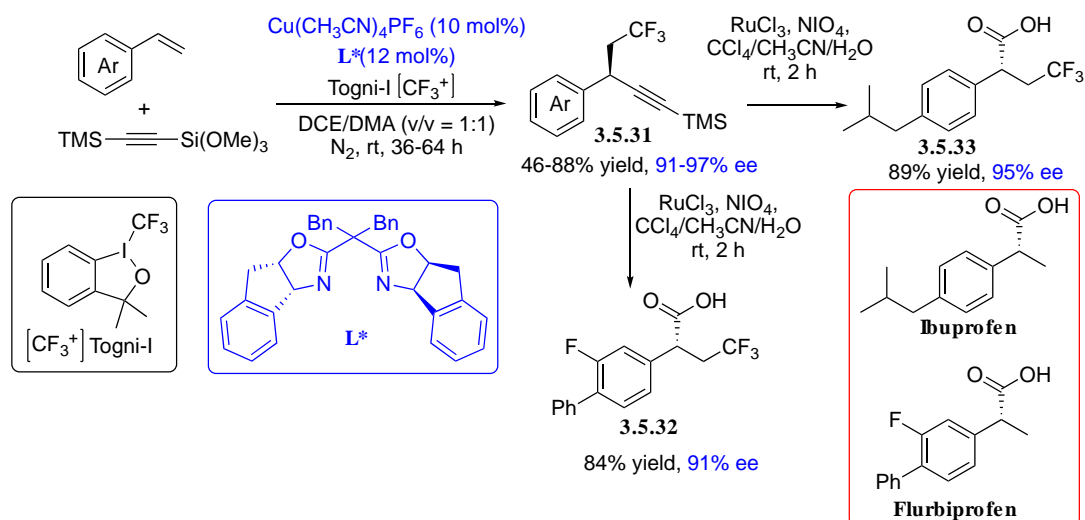
In 2018, Fu et al. developed the enantioselective copper-catalyzed trifluoromethylalkynylation of styrene via a radical relay process, which provides an easy access to the structurally diverse and enantiomerically enriched CF<sub>3</sub>-containing propargylic compounds.<sup>425,426</sup> Trifluoromethyl radical is easily available from the reduction of electrophilic trifluoromethyl reagents,<sup>427</sup> Togni-I reagent revealed itself to be very efficient (Scheme 196).

### Scheme 196. Copper(I) Assisted Generation of Trifluoromethyl Radical from Togni-I



### Scheme 197. Enantioselective Copper-catalyzed Trifluoromethylalkynylation of Styrenes

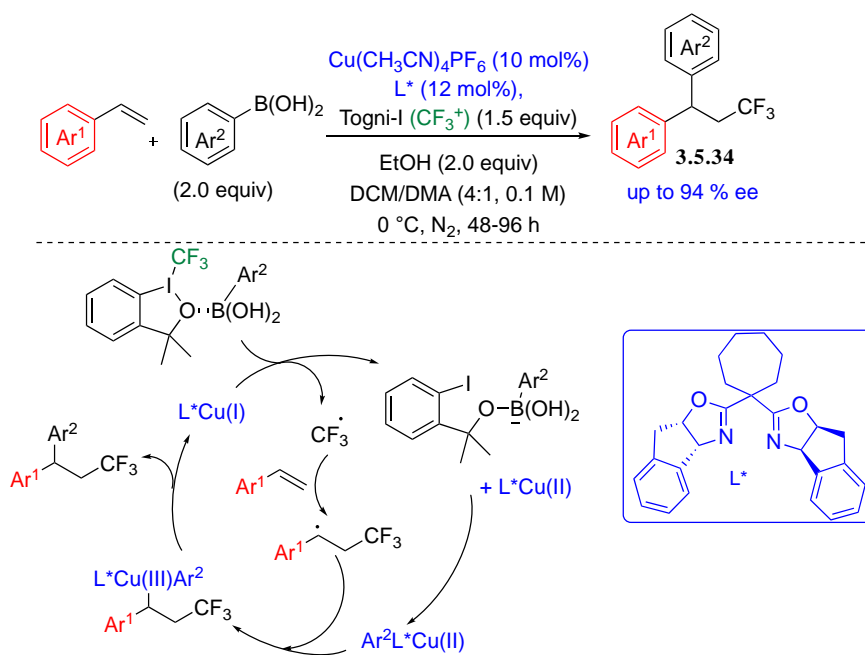
#### Reagent



When styrene was reacted with trimethylsilyl alkynylsiloxane, Togni-I reagent in DCE/DMA in presence of Cu(CH<sub>3</sub>CN)<sub>4</sub>PF<sub>6</sub> as catalyst (10 mol%) and bisoxazoline as a chiral ligand (L\*, 12 mol%), the 1,2-trifluoromethylalkynylated adduct was obtained in good yield with high

enantioselectivity (Scheme 197). The enantiomeric excesses were improved by using bulkier ligands and lesser amount of DMA. The trifluoromethylalkynylation reaction was significantly inhibited in the presence of TEMPO, a radical scavenger, which argues in favor of the radical pathway. Further oxidation of the C≡C triple bond of products **3.5.32** and **3.5.33** gave the enantiomerically enriched CF<sub>3</sub>-modified nonsteroidal anti-inflammatory drugs Ibuprofen and Flurbiprofen.

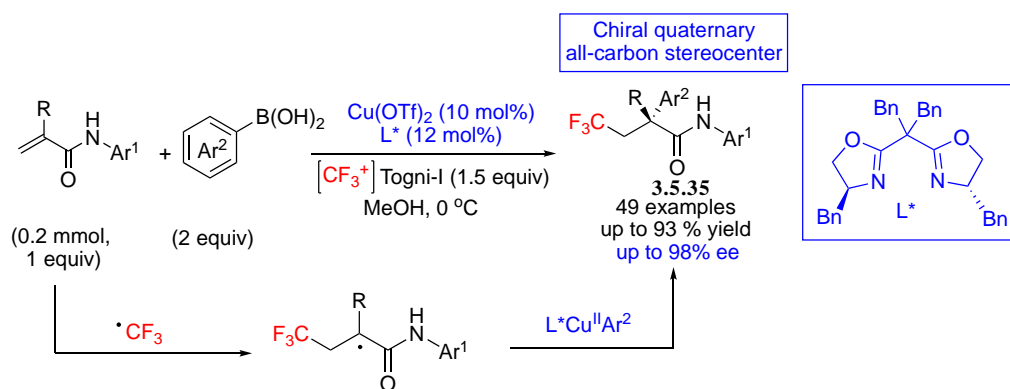
### Scheme 198. Trifluoromethylarylation of Alkenes Reagent numbering



A similar strategy had previously been reported for copper-catalyzed asymmetric radical trifluoromethylarylation of alkenes to synthesize chiral CF<sub>3</sub> containing diarylalkane derivatives **3.5.34** with good to excellent enantioselectivities.<sup>428</sup> Trifluoromethyl asymmetric arylation was performed using transmetalation with boronic acid derived nucleophiles. Various vinyl arenes and aryl boronic acids are compatible with the implemented experimental conditions. The utility of the method was demonstrated in tailoring modified bioactive molecules.<sup>429</sup> In the plausible mechanism, the interesting point is the proposal of the mutual activation of arylboronic acid and CF<sub>3</sub><sup>+</sup> reagent, as shown in Scheme 198 (other proposals are discussed by the authors) closely related to the mechanism (vide infra).

The construction of chiral quaternary all-carbon stereocenters was achieved by Wu et al. from  $\alpha$ -substituted acrylamides.<sup>430</sup> The tertiary carbon-centered radicals were produced by the addition of trifluoromethyl radical to the double bond. It was subsequently captured by the chiral aryl copper(II) species to form products with all-carbon chiral quaternary stereocenter in excellent enantioselectivity. It is important to note that the acylamidyl (CONHAr) group, adjacent to the tertiary radical carbon, is essential to assist the asymmetric radical coupling (Scheme 199).

**Scheme 199. Copper-catalyzed Enantioselective Construction of Chiral Quaternary All-Carbon Stereocenters Reagent**

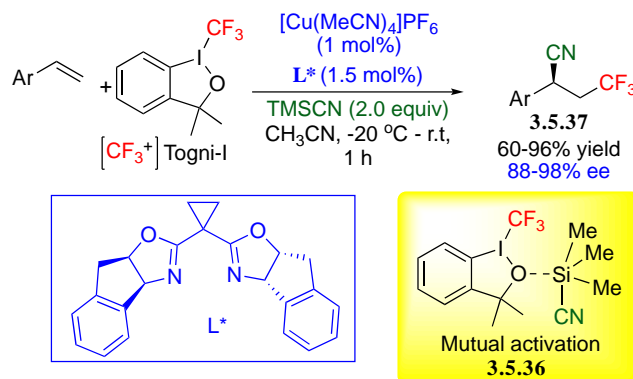


Liu and co-workers developed an innovative enantioselective copper-catalyzed intermolecular cyanotrifluoromethylation of alkenes that affords a variety of  $\text{CF}_3$ -containing alkyl nitriles with high enantioselectivity.<sup>431,432</sup> The experimental conditions depicted in Scheme 200 were applied to a series of styrene analogs.<sup>303</sup> The cyanotrifluoromethylation of styrenes failed to provide the desired product **3.5.37** in presence of inorganic cyanides, such as NaCN and KCN indicating that the mutual activation of TMS-CN and Togni's  $[\text{CF}_3^+]$  reagent i.e. complex **3.5.36** is very important to activate cyanide transfer. A low concentration of cyanide anion is crucial to obtain high enantiocontrol. At the same time, it avoids dissociation of Cu from the chiral ligand and allows the interaction between TMS-CN and Togni's  $[\text{CF}_3^+]$

reagent. The involvement of trifluoromethyl radical and the intermediate benzylic radical in the process was confirmed using radical scavengers.

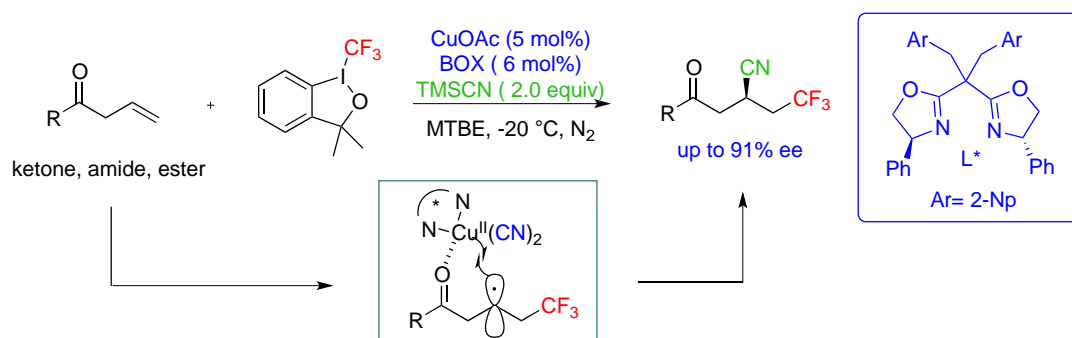
### Scheme 200. Copper-catalyzed Asymmetric Cyanotrifluoromethylation of Alkenes

#### Reagent



### Scheme 201. Asymmetric Trifluoromethylcyanation of Alkenes via Carbonyl-assisted

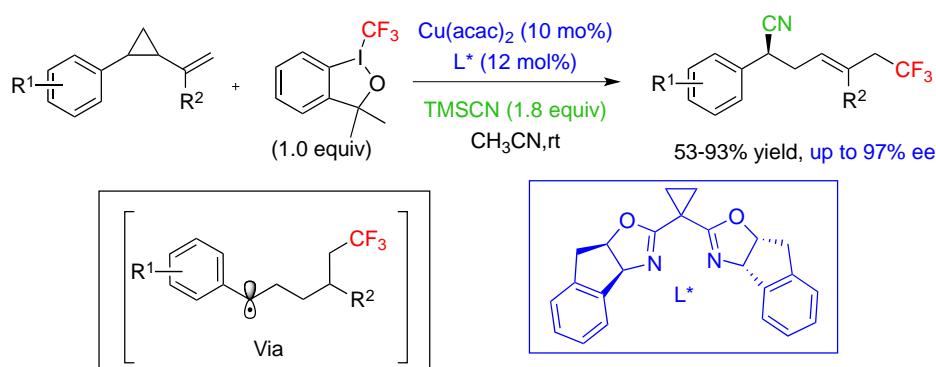
#### Coupling of Carbon-centered Radicals



Liu transposed the methodology to the functionalization of alkyl-substituted alkenes.<sup>304</sup> They gave evidence that the non-stabilized prochiral radical intermediate could be effectively trapped by copper(II) thanks to the assistance of a carbonyl group (Scheme 201). The carbonyl group of ketones, amides and esters provided optimal assistance when located in the  $\beta$ -position. Other basic functional groups like sulfones were much less efficient.

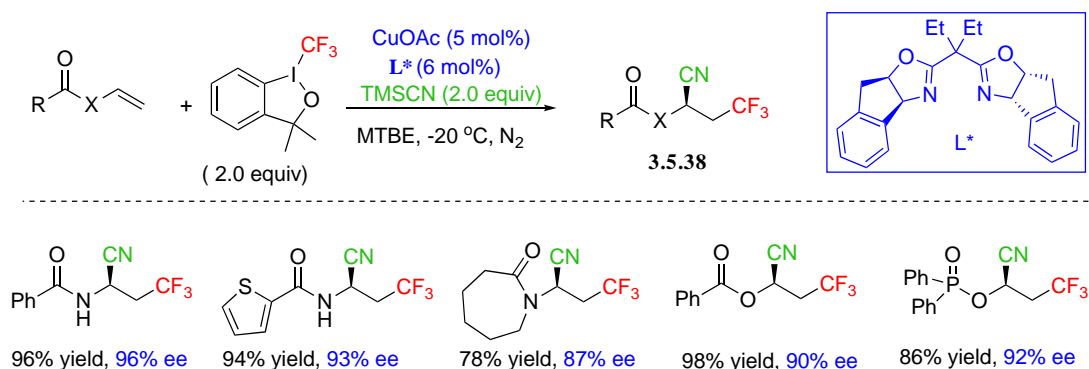
When the methodology was applied to vinyl cyclopropane, products resulting from the fast opening of the intermediate cyclopropylmethyl radical were isolated with excellent ee's (Scheme 202).<sup>433</sup>

## Scheme 202. Enantioselective Copper-Catalyzed 1,5-Cyanotrifluoromethylation of Vinylcyclopropanes



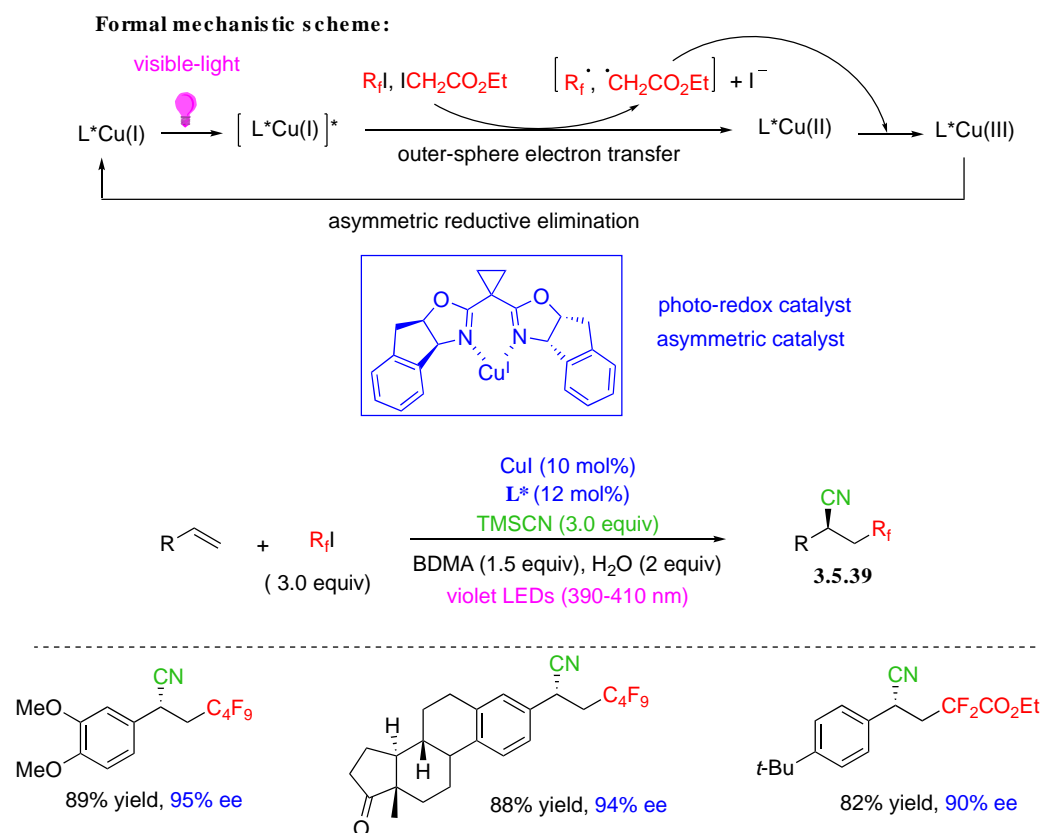
The copper catalyzed trifluorocyanation of enamides proceeds similarly in good yields and high ee's, this time via an alkyl radical adjacent to nitrogen (Scheme 203).<sup>434</sup> The synthesis of  $\alpha$ -cyanoamides can easily evolve towards the synthesis of  $\alpha$ -cyanoethers and hemiaminals by changing the nature of the substrate or by replacing TMSCN by an alcohol.

## Scheme 203. Trifluorocyanation of Enamides Reagent numbering



The use of Togni's reagent limit the reactions to the introduction of trifluoromethyl radical. Guo et al. also designed a methodology allowing for the synthesis of a variety of chiral perfluoroalkyl-nitriles. The peculiarity of their process is that Cu(I)-complex plays a dual role, i.e., photosensitizer and at the same time catalyst for asymmetric cross-coupling (Scheme 192).<sup>435</sup> The introduction of a series of fluorinated groups proceeds in good yields and high ee's.

## Scheme 204. Visible Light Photocatalytic Assistance to the Synthesis of Chiral Perfluoroalkylnitriles



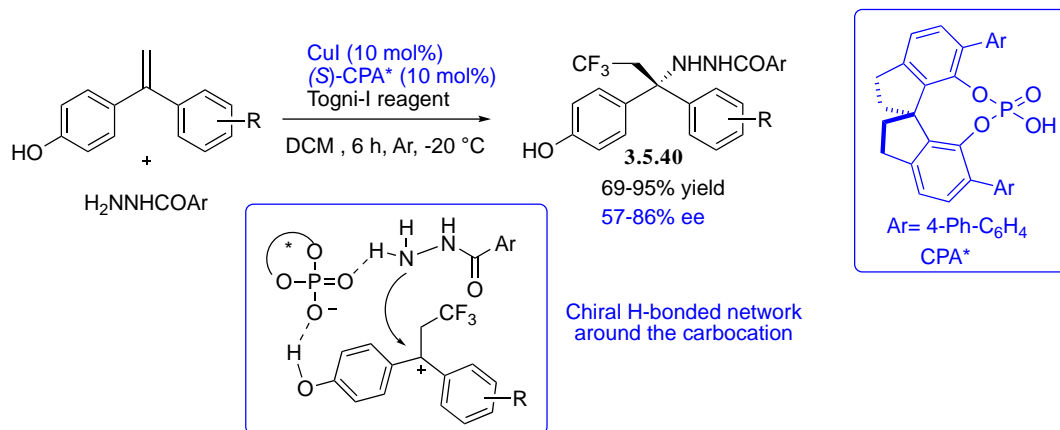
A complementary method has been recently disclosed by Bao and co-workers.<sup>436</sup> The authors used the primary radical obtained from the reduction of lauroyl peroxide by CuTc (copper thiophene-2-carboxylate) as relay to produce the perfluoroalkyl radical via iodine atom transfer from the corresponding iodide in association with TMSCN and the same chiral BOX ligand.

The enantioselective trifluoroamination of alkenes bearing different aryl groups was achieved by means of Cu(I)/chiral phosphoric acid (CPA) cooperative catalysis, using hydrazides and Togni-I reagent (Scheme 205). A mechanism implying an outer-sphere oxidation of the intermediate alkyl radical is proposed. The joint action of Cu(I) and CPA implies the generation of a carbocation. The microenvironment of the latter and, as a consequence, the formation of the C-N bond, is controlled by the hydrogen-bonded network around the chiral phosphate pocket. It is worth noting that the presence of an electron rich



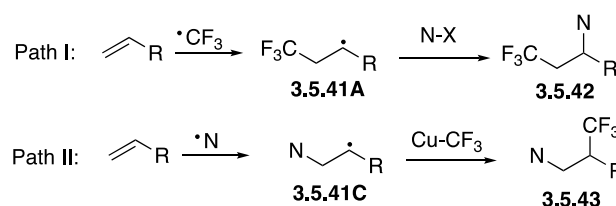
aromatic (para hydroxyl-substituted) is needed to favor both the radical oxidation step and hydrogen bonding.

### Scheme 205. Trifluoroamination of gem Diaryl Alkenes



As already discussed in the previous section, aminotrifluoromethylation of alkenes often start with addition of  $\text{CF}_3^\bullet$  to alkenes to form the adduct radicals **3.5.41A** which are then trapped by *N*-nucleophiles such as amines to form compounds **3.5.42**. Therefore, in most aminotrifluoromethylation products  $\text{CF}_3$  is present in the terminal position. But there is another possibility of aminotrifluoromethylation reaction when nitrogen-centered radical first adds to the alkene to form radical **3.5.41C**. Then trifluoromethylation provides products **3.5.43** with the reverse regioselectivity (Scheme 206).<sup>437</sup>

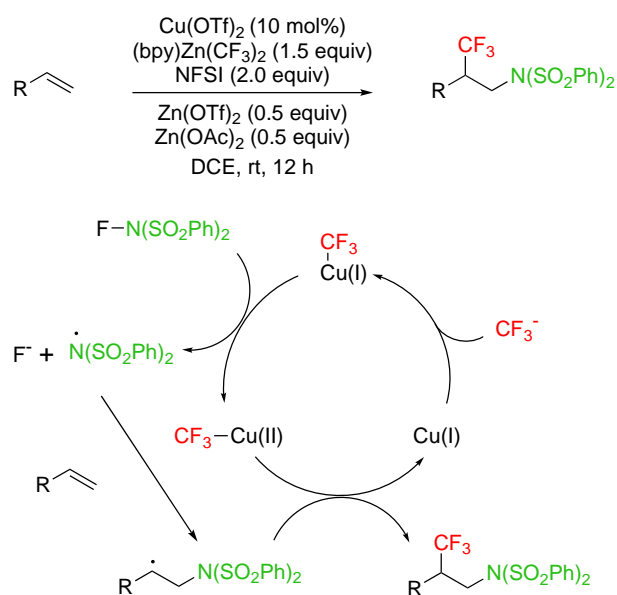
### Scheme 206. Different strategies for Aminotrifluoromethylation Reactions



Li, Zhu and co-workers have developed an unprecedented protocol for aminotrifluoromethylation reaction of both activated and unactivated alkenes which is driven by *N*-centered radical addition to the double bond.<sup>438</sup> According to this protocol, when alkenes were treated with 10 mol%  $\text{Cu}(\text{OTf})_2$  as the catalyst,  $(\text{bpy})\text{Zn}(\text{CF}_3)_2$  (1.5 equiv.) as the  $\text{CF}_3^-$

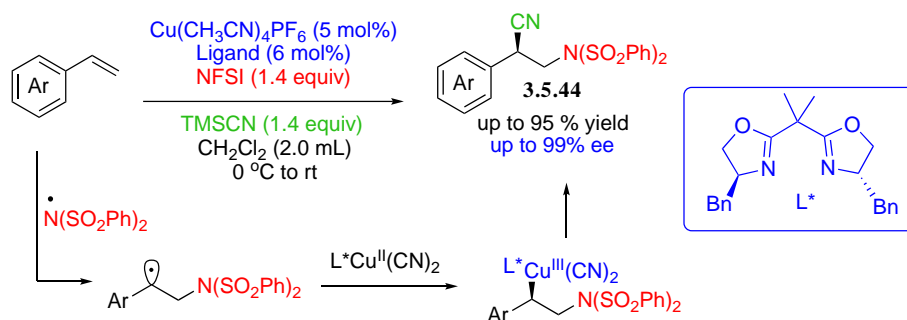
source, in the presence of  $\text{Zn}(\text{OTf})_2$  (50 mol%) and  $\text{Zn}(\text{OAc})_2$  (50 mol%) as additives together with *N*-fluorobis(benzenesulfonyl)imide (NFSI: source of bis sulfonimidyl radical) at room temperature for 12-24 h, the expected aminotrifluoromethylation products were obtained in satisfactory yields with high regioselectivity in agreement with the simplified mechanism shown in Scheme 207.

**Scheme 207. Aminotrifluoromethylation Reaction of Alkene Driven by *N*-Centered Radical Alkene Addition**



Liu and Lin also developed the copper-catalyzed enantioselective aminocyanation reaction of styrenes using NFSI as the imidyl radical precursor via reaction with Cu(I) catalyst. As above, the *N*-centered radical adds to styrenes to generate a benzylic radical intermediate which is enantioselectively trapped by a chiral Box/Cu(II) cyanide complex to deliver highly functionalized  $\beta$ -amino nitriles **3.5.44** in good yields with good to excellent enantioselectivity (Scheme 196).<sup>439</sup>

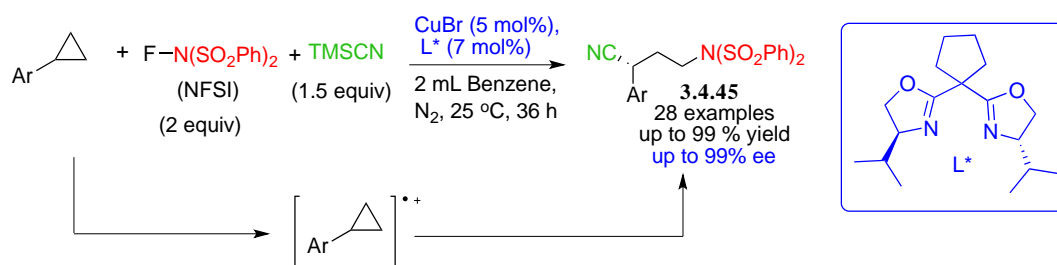
### Scheme 208. Copper-catalyzed Asymmetric Synthesis of $\beta$ -Amino Nitriles



A non-asymmetric azidocyanation had been previously reported using diacetoxyiodobenzene and  $\text{TMSN}_3$ .<sup>440</sup> Changing the oxidizing agent to  $\text{Phi}(\text{O}_2\text{CET})_2$  in the presence of chiral Box ligand, Liu and Lin have performed the azido cyanation of styrenes in good yields with excellent ee's (it is to be noted that the side diazidation was difficult to avoid, but it could be reduced to less than 10% by optimization of the reaction).<sup>312</sup>

Due to their bent bonds, cyclopropanes have a high ring strain enhanced by torsional strain of the attached C-H bonds and their C atoms have stronger  $\pi$  character than those of other aliphatic compounds. Even though the following mechanism slightly differs from straightforward addition to double bonds, this paragraph concerning ring opening of aryl cyclopropanes is included hereafter. Zhang, Li and co-workers expanded the aminocyanation of alkenes to the highly enantioselective synthesis of  $\gamma$ -amino nitriles via copper-catalyzed ring-opening of arylcyclopropanes (Scheme 209).<sup>441</sup>

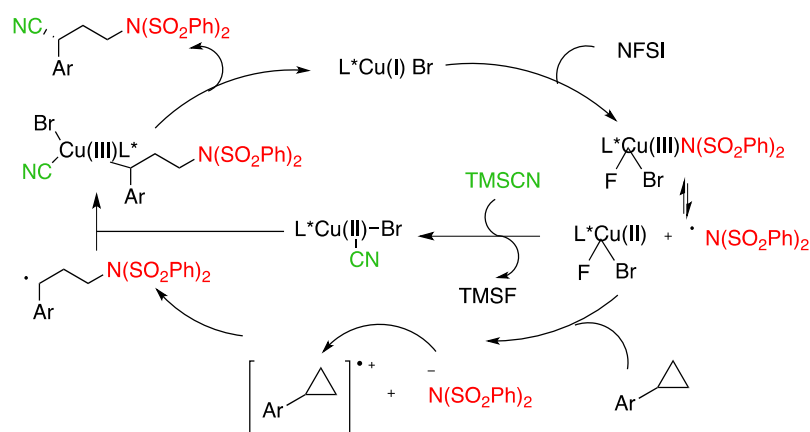
### Scheme 209. Copper-catalyzed Asymmetric Aminocyanation of Arylcyclopropanes



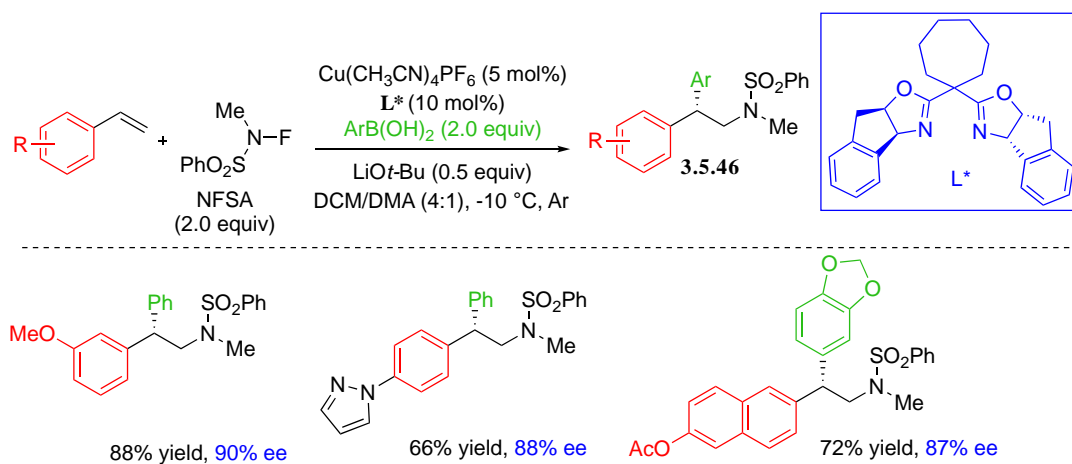
The main difference with all the mechanistic proposals reported above is that NFSI would first undergo a two-electron reduction via oxidative addition to  $\text{Cu}(\text{I})$  and only at that stage, the

intermediate Cu(III) intermediate would release bisulfonimidyl radical (Scheme 210). The *N*-centered radical would then react via SET with the phenylcyclopropane to give rise to a *N*-centered nucleophilic species and a radical cation where the C-C bond of the cyclopropane ring is strongly weakened. Nucleophile-assisted ring opening affords the intermediate benzylic radical which is functionalized via copper(II) redox chemistry.

### Scheme 210. Proposed Mechanism for the Asymmetric Synthesis of $\gamma$ -Amino Nitriles



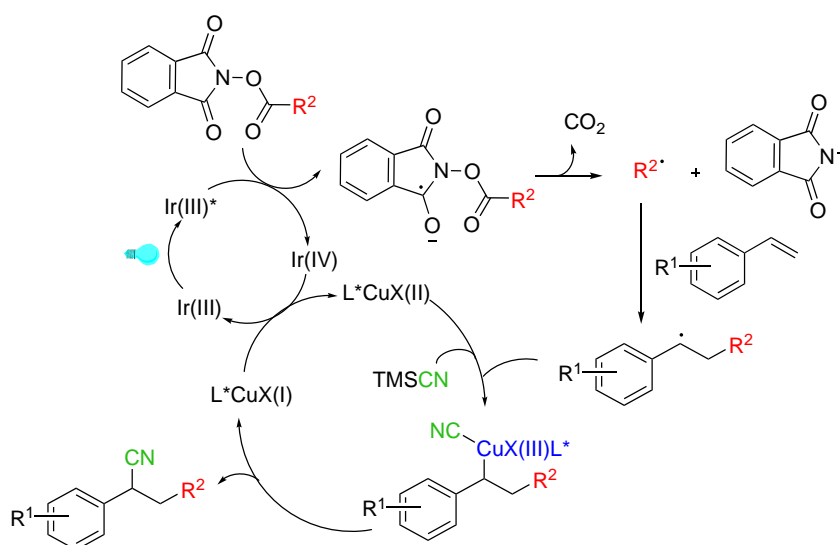
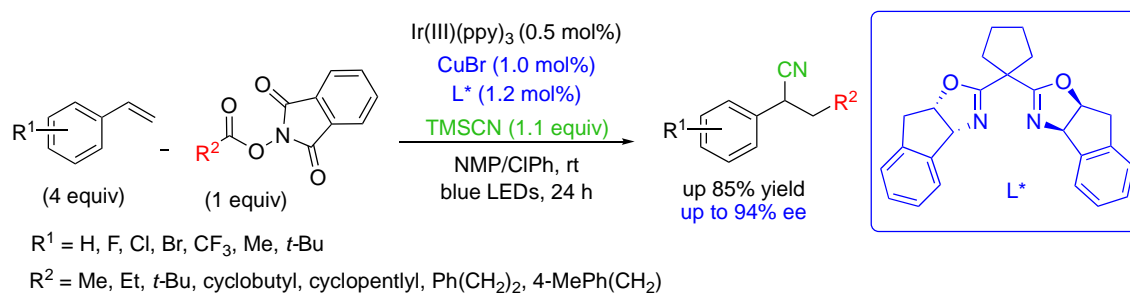
### Scheme 211. Enantioselective Aminoarylation of Styrenes



Wang et al. achieved an enantioselective aminoarylation of styrenes to synthesize various enantioenriched 2,2-diarylethylamine derivatives using novel reactants, *N*-fluoro-*N*-alkylsulfonamides (NFAS), as the key amination reagents and various arylboronic acids (Scheme 211).<sup>442</sup>

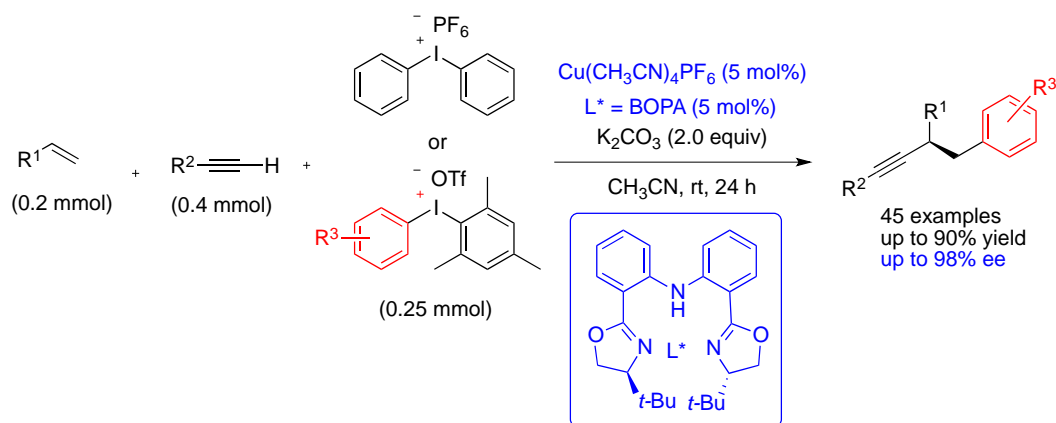
A dual photoredox/copper catalyzed asymmetric cyanoalkylation reaction of alkenes has been developed, which uses alkyl *N*-hydroxyphthalimide esters as alkyl radical precursors. Control experiments showed that the metal, visible-light and the photocatalyst were all essential for the reaction to proceed. The reaction was inhibited by TEMPO. In this radical cyanoalkylation reaction, the Ir(III) photoredox catalyst induces the formation of the alkyl radical. SET to the phthalimide carbonyl group induces a double homolytic fragmentation to afford the reactive alkyl radical that adds to styrene. The resulting benzylic radical couples with a chiral Box/Cu(II) cyanide complex, formed via transmetalation with TMSCN, to achieve the enantioselective cyanation (Scheme 212). This asymmetric radical difunctionalization of alkenes is characterized by mild reaction conditions, simple implementation and it is applicable to a large array of aromatic derivatives. It leads to high yields, and high enantioselectivities.<sup>443</sup>

### Scheme 212. Dual Ir-photoredox/Copper Catalysis for the Cyanoalkylation of Alkenes



An arylocyanation procedure involving diazonium salts, generated in situ from anilines and *t*-butyl nitrite, as source of aryl radicals has been developed by Liu and Chen. In the presence of Box ligand, the reaction affords 2,3-diarylpropionitriles with yields up 85% and ee's up to 90%.<sup>444</sup>

### Scheme 213. Enantioselective Three-component Arylalkynylation of Alkenes

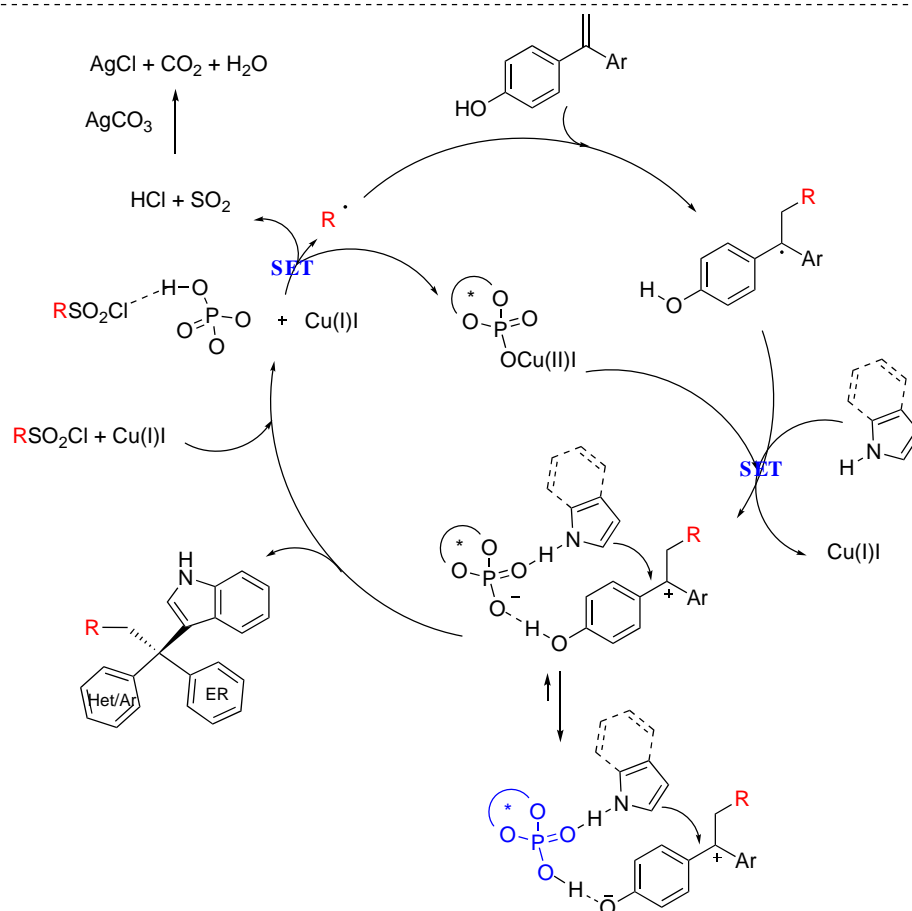
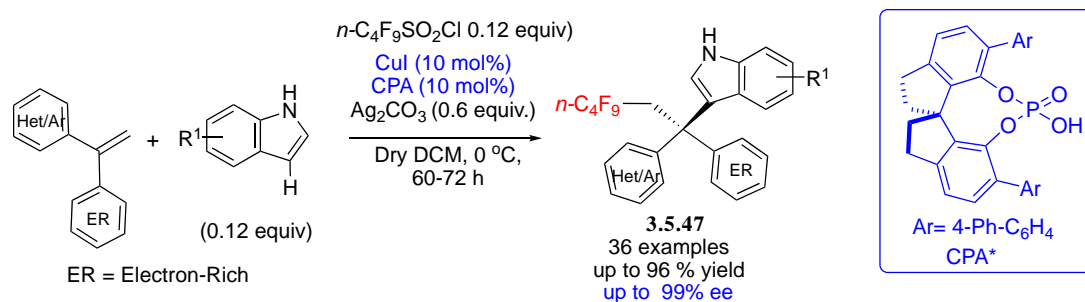


The copper-catalyzed enantioselective arylalkynylation of alkenes has recently been reported. The proposed mechanism is supposed to proceed via the addition of an aryl radical to the alkene. The resulting alkyl radical would react further with the alkynyl-Cu(II) chiral complex, itself formed during the reduction of the aryliodonium salt by the alkynyl-Cu(I) complex. The source of aryl radical in this three-component procedure is a diaryliodonium salt. The reaction leads to chiral 1,2-diaryl-3-butynes in good yields and high ee's (Scheme 213). The success relies on the use of chiral phenylaniline derived bisoxazoline as ligand.

Lin et al. described an asymmetric intermolecular three-component radical-initiated dicarbofunctionalization of 1,1-diarylalkenes involving sulfonyl chlorides as carbon-centered radical precursors (perfluoro or perchlorosulfonyl chlorides) and substituted indoles as carbon-centered nucleophiles. Cu(I)/chiral phosphoric acid (CPA), i.e., dual redox/chiral Bronsted acid catalysis enables access to chiral triarylmethanes **3.5.47** bearing all-carbon quaternary stereocenters with excellent chemo- and enantioselectivity (Scheme 214).<sup>445</sup>

**Scheme 214. Asymmetric Three-component Radical-initiated**

**Dicarbofunctionalization of Alkenes**

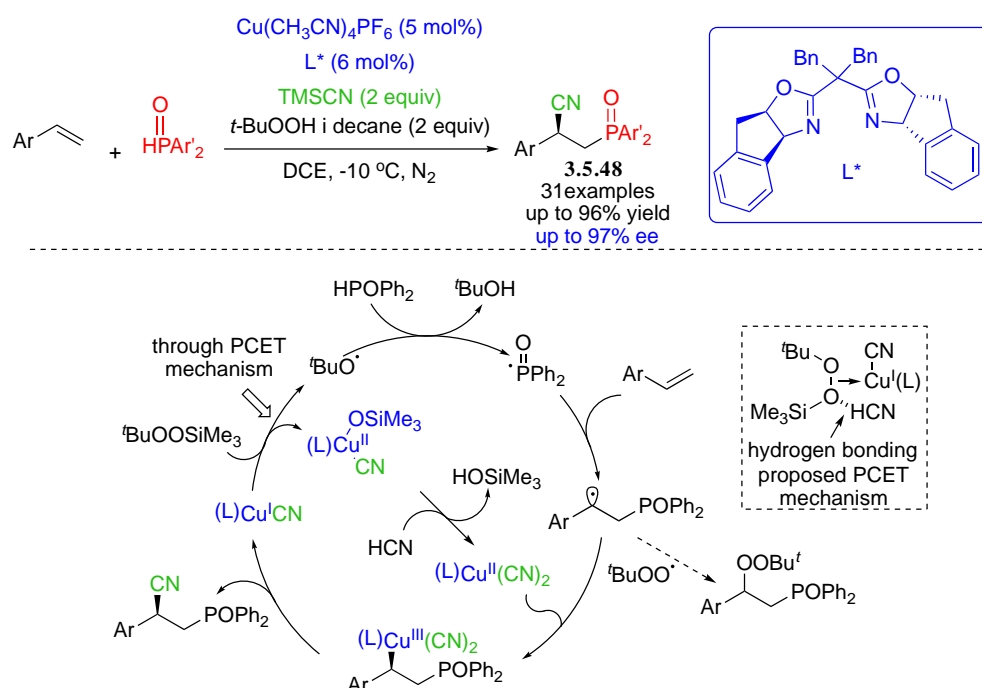


This method represents a mechanistically distinct approach to achieve rapid asymmetric difunctionalization of olefins via the intermediacy of a carbocation specie produced through single-electron oxidation. The SET event is facilitated by the presence of the electron rich aromatic (OR group in para position). It is to be noted that when the electron-donating group is OH, the carbocation is in equilibrium with a quinonemethide via proton transfer. Density functional theory calculations helped in visualizing the critical chiral environment created by

hydrogen-bonding interactions between the ion-pair, the chiral phosphoric acid catalyst and the nucleophile which controls the enantioselective C–C bond formation. The additive  $\text{Ag}_2\text{CO}_3$  acts as a HCl scavenger via the formation of insoluble  $\text{AgCl}$  in organic solution

Liu and co-workers also developed a Cu(I)-catalyzed asymmetric phosphinoylcyanation of styrene to synthesize various  $\beta$ -phosphino nitriles **3.5.48** in good yields and excellent enantioselectivities (Scheme 215).<sup>446</sup>

### Scheme 215. Asymmetric Copper-catalyzed Phosphinoylcyanation of Styrenes. Proposed Mechanism



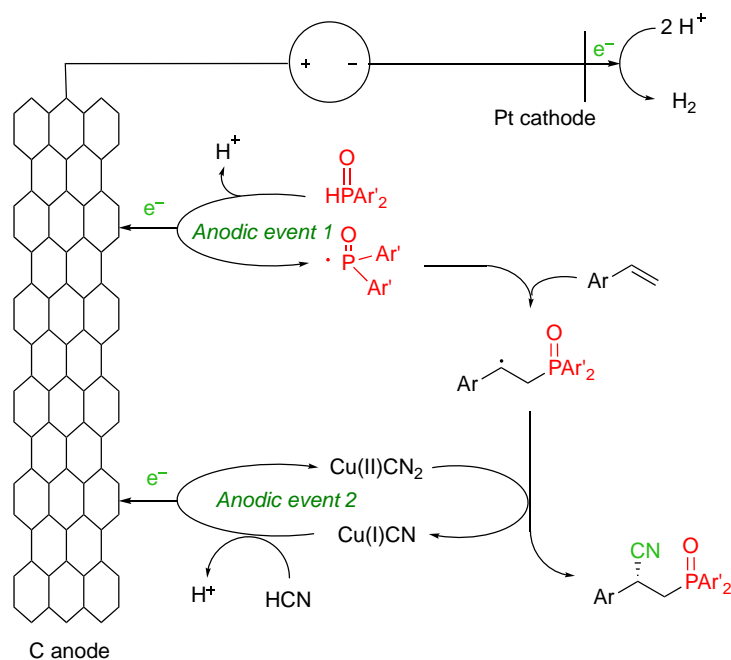
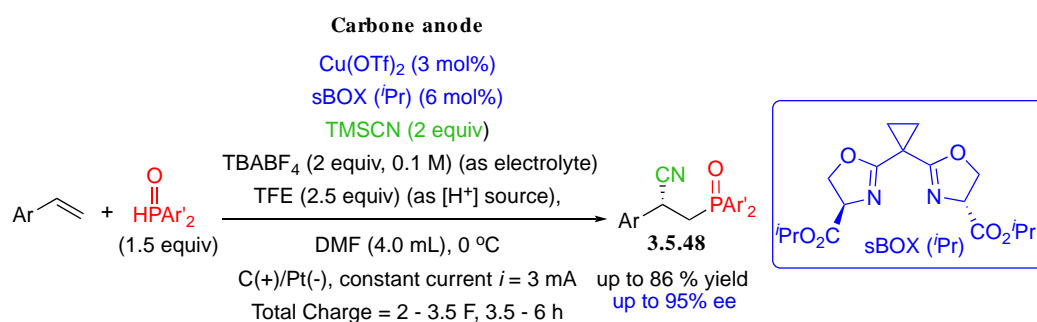
According to the mechanism depicted in Scheme 215, a proton-coupled-electron transfer (PCET) pathway generates *tert*-butoxy radical from *tert*-butylperoxytrimethylsilane (TBPS) (TBHP reacted with TMSCN to generate TBPS and HCN). The generation of phosphinoyl radicals results from subsequent HAT between the alkoxy radical and  $\text{Ar}'_2\text{P}(\text{O})\text{H}$ . This phosphinoyl radical then adds to styrene to afford benzylic radical. Subsequently, Cu(II) species reacts with HCN to generate the  $(\text{L}^*)\text{Cu}^\text{II}(\text{CN})_2$  active specie that enantioselectively traps the benzylic radical to give the phosphinoylcyanation products **3.4.48**. It is worth mentioning that, the ratio of TBHP to TMSCN was essential for the reaction, employing an equimolar or more



TMSCN than TBHP led to the desired product and HCN rather than TMS-CN acted as a real cyanide source to participate in the cyanation of benzylic radicals.

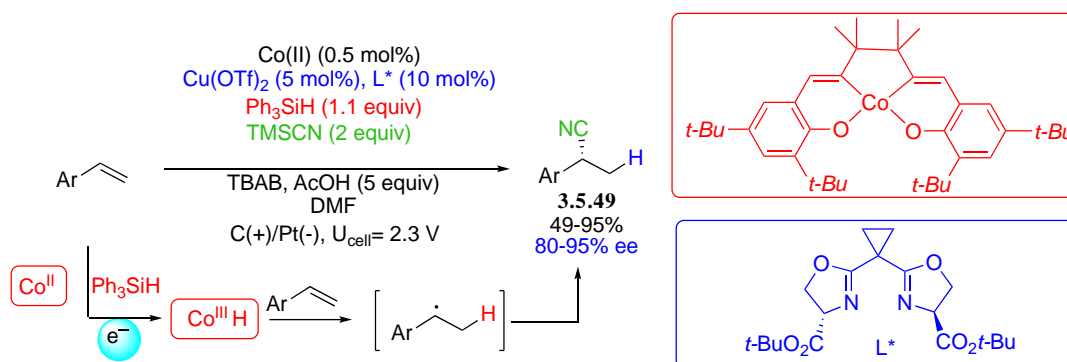
Lin and co-workers also developed enantioselective phosphinoylcyanation of vinylarenes powered by electrochemistry (Scheme 216).<sup>447</sup> When vinylarenes were reacted with TMSCN and diarylphosphine oxide as the phosphorous source in the presence of catalytic amount of  $\text{Cu}(\text{OTf})_2$  and chiral ligand sBOX(<sup>i</sup>Pr) in DMF in an electrochemical cell, the enantiomerically enriched phosphinoylcyanation products **3.5.48** is obtained in good yields. In this reaction  $\text{TBABF}_4$  was used as electrolyte and trifluoroethanol (TFE) as the proton source. In the prospect of green chemistry development, this method is very attractive as there is no need for any conventional chemical oxidant.

### Scheme 216. Asymmetric Electrocatalytic Phosphinoylcyanation of Vinylarenes



A related approach using anodic oxidation in lieu of common oxidant was designed to achieve chiral hydrocyanation of styrenes. The process used dual Co/Cu catalysis. In the proposed catalytic cycle, Co(III)–H (formally),<sup>193</sup> generated from a Co(III) precursor and a hydrosilane, reacts with the double bond via hydrogen-atom transfer (HAT) to produce a carbon-centered benzylic radical (Scheme 217). The latter subsequently enters the cyanation cycle by adding electron to Cu(II) cyanide to form Cu(III) intermediate. In the presence of serine-derived BOX ligand, the subsequent reductive elimination completes the enantioselective hydrocyanation reaction. Like in the previous example, anodic oxidation promotes two events, i.e., reoxidation of Co(II) to Co(III) and of Cu(I) to Cu(II).

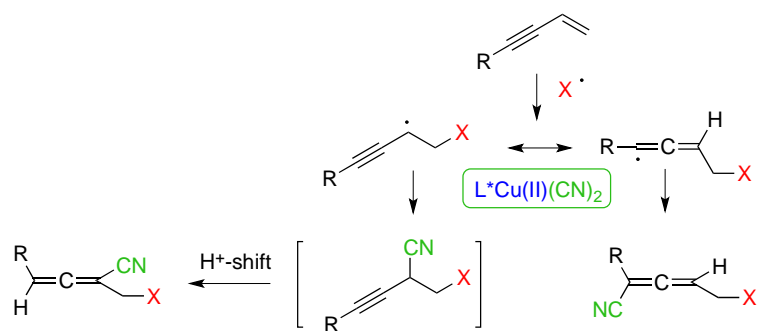
### Scheme 217. Electrochemical Enantioselective Hydrocyanation



#### 3.5.4.2 Intercalation of addition to enynes: synthesis of axially chiral allenes

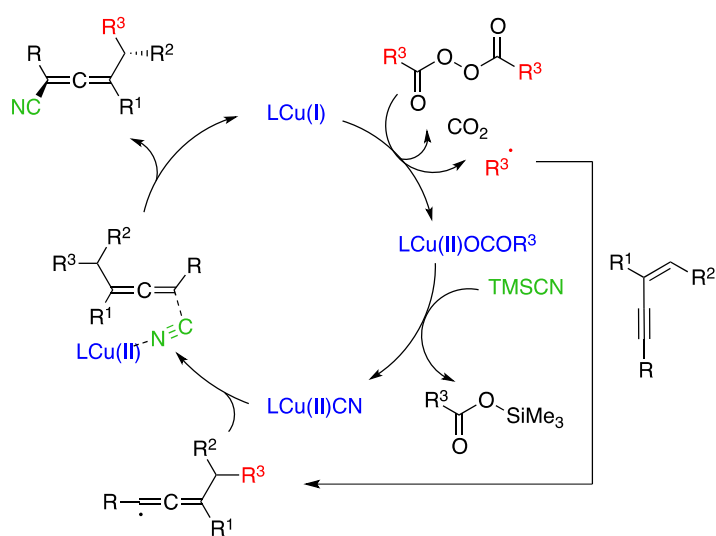
The conjugate addition to the double bond of 1,3-enynes can formally evolve towards 1,2- or 1,4- adducts via the two mesomeric form of the intermediate radical that can be trapped by either at the propargylic or the allenic position. The copper-catalyzed trifluorocyanation of conjugated enynes has been investigated by Lin, Liu and co-workers.<sup>448</sup> As shown in Scheme 218, the 1,2-adduct also affords an allene through 1,3-proton shift. The regioselectivity could be tuned by the nature of the ligand.

### Scheme 218. Regiodivergent Radical Addition to 1,3-Enynes



In spite of progress discussed above, asymmetric trapping of allenyl radical (likely to be due to its linear geometry) in the presence of chiral ligand remained a challenge. The reactivity of 1,3-enynes was further investigated by Zhang, Bao and co-workers who reported the regio- and highly diastereoselective synthesis of tetrasubstituted allenes by 1,4-alkylarylation promoted by the reaction of Cu(I)-catalyst (CuTc) in the presence of a diacylperoxide as the source of radical, TMSCN, an arylboronic acid as transmetalation agent and N,N-diisopropylethylamine. The most original point is that the authors concluded that the cyanation step would in fact proceed according to a group transfer mechanism involving an isocyanocopper(II) intermediate instead of a copper(II) cyanide (Scheme 219).

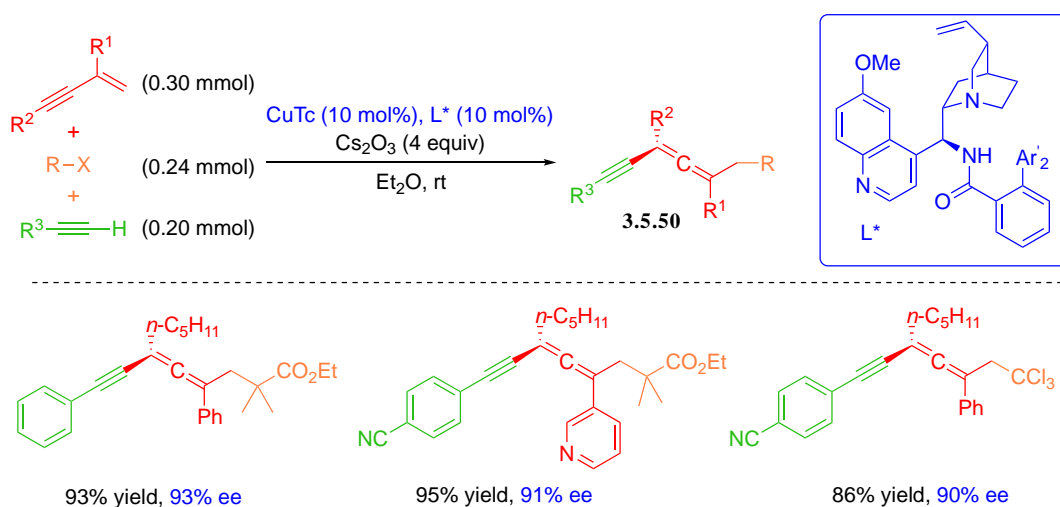
### Scheme 219. Revised Mechanistic Proposal for 1,4-Alkylcyanation of 1,3-Enynes



Bao's group performed the enantioselective benzyloxycyanation and carbocyanation of 1,3-enynes using copper(II) acetate as catalyst in the presence of TMSCN and diacylperoxides, R<sub>F</sub>-

I as source of radical.<sup>449</sup> Meanwhile, the asymmetric coupling of terminal alkynes with allenyl radicals was achieved by Liu. The authors were in search of stereo-differentiation based on motifs remote from the radical reactive site and they demonstrate that the use of chiral *N,N,P*-ligand was crucial for the enantiocontrol.<sup>450</sup> The scope of allenes **3.5.50** in this procedure is summarized in Scheme 220.

### Scheme 220. Enantioselective Synthesis of Tetrasubstituted Allenes



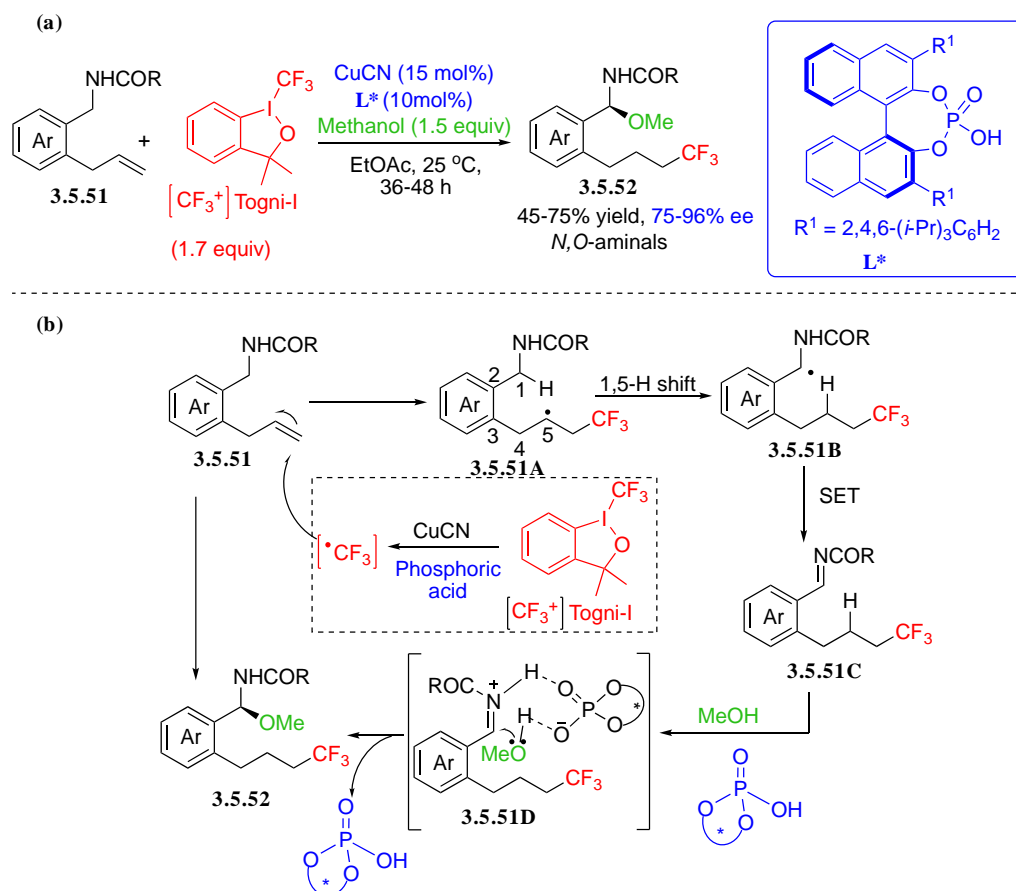
#### 3.5.4.3 Intercalation of 1,5-hydrogen atom transfer

Liu and coworkers described an excellent pathway for the formation of enantioenriched trifluoromethylated *N,O*-aminals by radical trifluoromethylalkoxylation of unactivated alkenes.<sup>451</sup> The reaction involves successive formation C-CF<sub>3</sub> bond/1,5-H shift/C-H functionalization in the presence of a copper/Brønsted acid catalytic system. When the alkene **3.5.51** was treated with Togni-I reagent and methanol in the presence of 15 mol% of CuCN and 10 mol% substituted enantioenriched phosphoric acid in EtOAc at room temperature for 36-48 h, the trifluoromethylated *N,O*-aminal (**3.4.52**) was isolated in 45-75% yield with 75-96% ee (Scheme 221a).

The authors established via control experiments that the chiral phosphoric acid not only plays a vital role in controlling the last stage of the asymmetric nucleophilic attack, but also as an acid successfully co-activates Togni's reagent together with copper catalyst. Mechanistically,

CF<sub>3</sub> enantioselective copper-catalyzed radical is generated from the reaction of Togni-I reagent with Cu(I). It adds to the alkene to form the nascent α-CF<sub>3</sub>-alkyl radical intermediate **3.5.51A**. The reaction then proceeds through activation of the benzylic position by 1,5-hydride shift followed by single-electron oxidation concomitant to proton transfer to form the imine intermediate **3.5.51C** (Scheme 221b). Finally, nucleophilic addition of the alcohol to the imine intermediate via a zwitterionic intermediate **3.4.51D** involving chiral phosphoric acid (CPA) affords the enantioenriched trifluoromethylated *N,O*-aminals **3.5.52** (Scheme 221b). This reaction reaches the limits defined for this section as the enantioselectivity determining step does not involve the copper catalyst. The reaction was expanded to the synthesis of indole derivatives by slightly modifying the experimental conditions.<sup>329</sup>

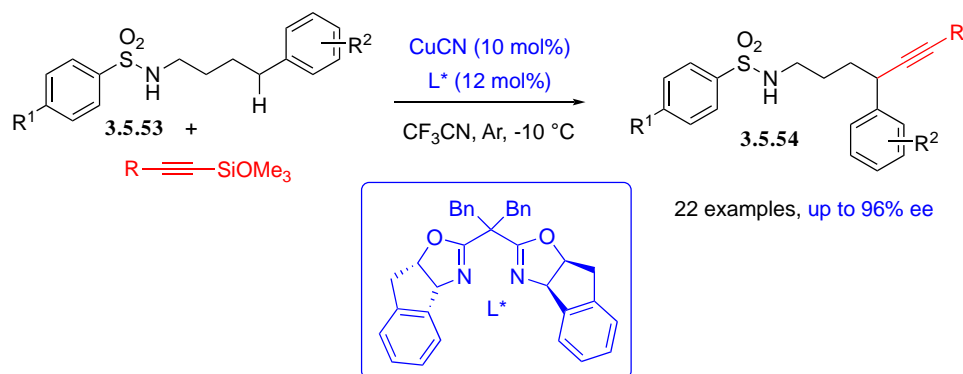
**Scheme 221. (a) Enantioselective Copper-catalyzed Trifluoromethylalkynylation of Unactivated alkenes to synthesize *N,O*-aminals. (b) Mechanistic proposal**



It is worth mentioning that 1,5-HAT has recently been shown to be involved in performing interesting copper-catalyzed remote trifluoromethylation and azidation of amidyl radicals, but an enantioselective variant has not been described yet. Closely related dual photoredox/copper catalysis has also been used to promote the formation of azido-alcohols through the intermediacy of 1,5-HAT rearrangement of alkoxy radicals.

However, the successful enantioselective alkylation of linear primary sulfonamides **3.5.53** has recently been reported by Wang and co-workers. The use of radical clocks confirmed a radical mechanism (Scheme 222). The same group also achieved via 1,5-HAT the remote asymmetric cyanation of the same type of substrates by using TMS-CN as the reagent. A closely related methodology was applied to the synthesis of enantioenriched piperidines via deprotection and reductive cyclization of the  $\delta$ -cyano tosylamides resulting from copper-catalyzed remote cyanation.

### Scheme 222. Remote Asymmetric Alkylation of Linear Sulfonamides

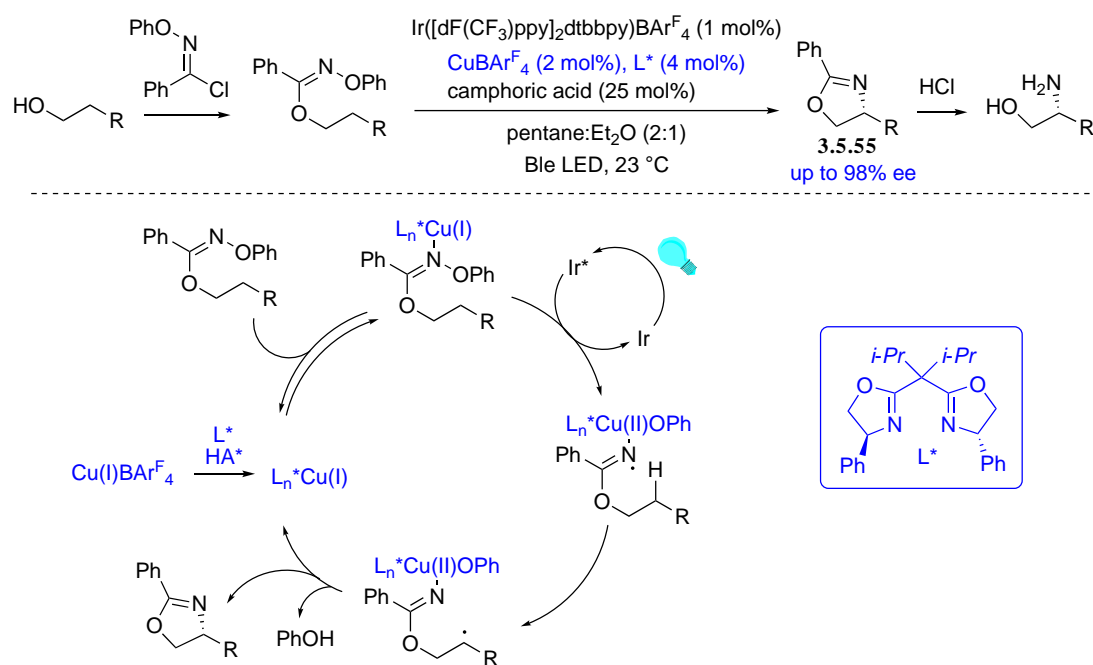


The enantioselective synthesis of  $\beta$ -amino alcohols was recently disclosed by Nagib and co-workers and it relies on the merging of Ir-metallaphoto-catalysis and copper redox process (Scheme 223).<sup>452</sup> It involves a radical cascade by the successive generation of iminyl radical, 1,5-HAT, enantioselective 5-endo ring closure followed by hydrolytic work-up of **3.5.55**.

The authors propose an original strategy for direct C-H amination that applies to an array of sterically and electronically different alcohols. To this end, the alcohol was first temporarily transformed into an oxime imidate that coordinated to a Cu(I) catalyst. This complex is the

source of the corresponding *N*-centered radical; photocatalytic energy transfer from visible-light excited Ir catalyst leads to triplet sensitization and subsequent homolytic cleavage of the N-O bond (Scheme 223). The whole process implies a radical cascade involving sequential 1,5-HAT, enantioselective 5-endo ring closure, C-oxidation and concomitant Cu(II)-reduction regenerating Cu(I) followed by hydrolytic work-up. It is worth noting that a screening showed that the acid co-catalyst plays a crucial role in controlling efficiency and selectivity. A bulky albeit not necessarily chiral acid is required.

### Scheme 223. Enantioselective C-H Amination Leading to $\beta$ -Amino-Alcohols



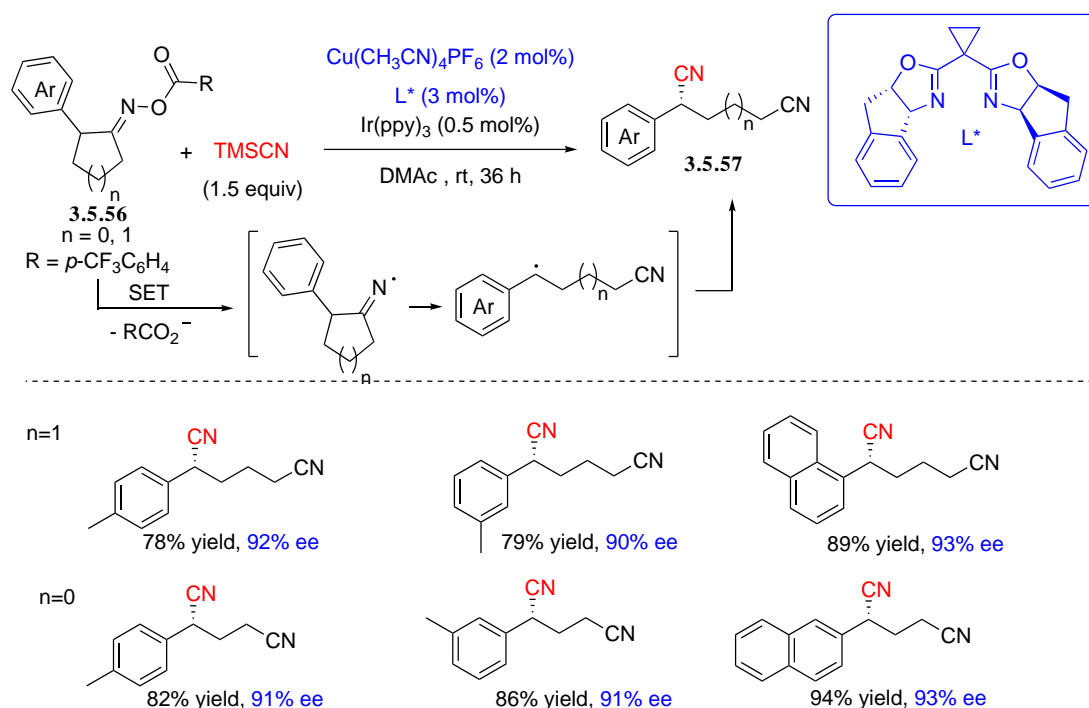
Dual Ir-photoredox/Copper catalysis has also been implemented to functionalize the ortho-side chain of aryl carboxamides. The enantioselective synthesis of chiral benzylic nitriles was optimized to obtain high yields and high ee's in the presence of chiral BOX ligands.<sup>453</sup>

#### 3.5.4.4 Intercalation of ring fragmentation

The ring-opening of iminyl radicals has been implemented to promote the formation of optically active dinitriles in the presence of TMSCN.<sup>454</sup> Different experimental conditions merging Cu-catalysis with photoredox catalysis have been tested.

As summarized in Scheme 224, Wang and co-workers used metallaphotoredox catalysis. Electron transfer from activated Ir(III) complex to cyclic oxime esters results in the formation of the targeted iminyl radical while releasing an aryl carboxylate that reacts with TMS-CN to release cyanide anion. Homolytic ring opening affords a prochiral radical bearing the first nitrile group that enters the Cu catalytic cycle by reacting with copper(II) cyanide. The enantio-enriched dinitrile results from reductive elimination from the Cu(III) intermediate.

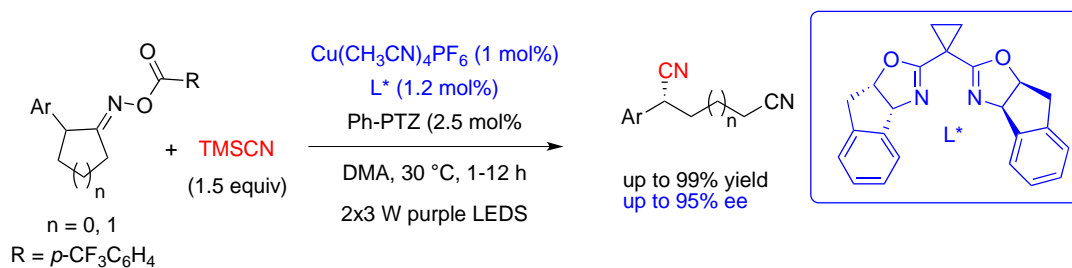
### Scheme 224. Enantioselective Synthesis of $\omega$ -Dinitriles via Dual Metallaphotoredox and Cu Catalysis



The alternative use of an organophotocatalyst (phenyl-phenothiazine, Ph-PTZ) was selected by Xiao and co-workers (Scheme 225). Under mild conditions a wide range of dinitriles was prepared with high yields and excellent ee's. The two catalytic cycles are similar to that discussed in Scheme 180. It is worth noting that non-asymmetric synthesis of  $\omega$ -trifluoronitriles from cycloalkanone oximes has been reported using  $\text{Cu}(\text{OAc})_2$  as catalyst and  $(\text{DMPU})_2\text{Zn}(\text{CF}_3)_2$  as source of nucleophilic  $\text{CF}_3$ .

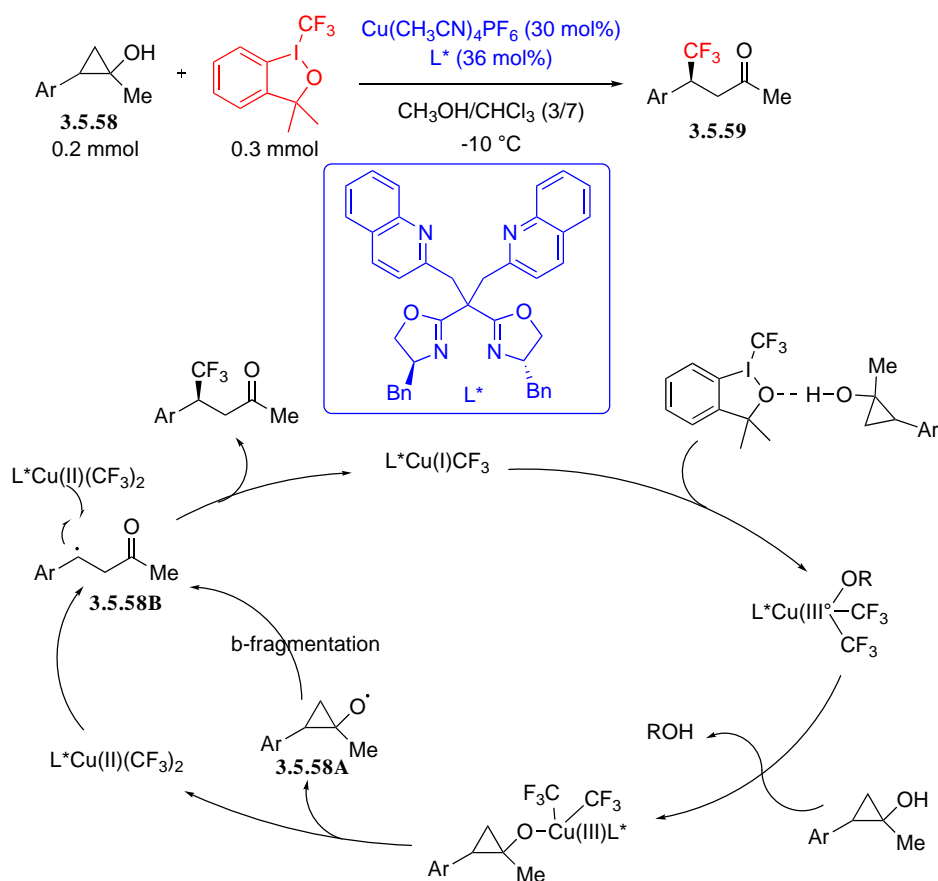


## Scheme 225. Enantioselective Synthesis of $\omega$ -Dinitriles via Dual Organophotoredox and Cu Catalysis



Copper-catalyzed ring opening of  $\beta$ -arylcyclopropanol **3.5.58** via  $\beta$ -fragmentation of the corresponding alkoxy radical **3.5.59** offers an interesting route to enantioenriched  $\beta,\beta$ -aryl, trifluoromethyl ketones. The authors used a new quinolinyln-containing bisoxazoline ligand which played a significant role in improving the selectivity of the benzylic radical trifluoromethylation step (Scheme 226).

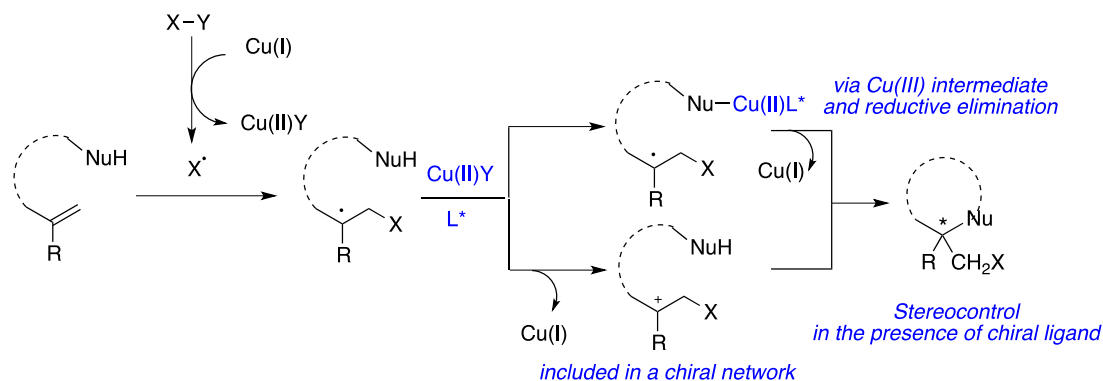
## Scheme 226. Trifluoromethylation of Benzylic Radical via Ring Opening of Cyclopropanols



Classical anionic  $\text{CF}_3$  reagents failed to give the expected product and what is more, excess of  $\text{CF}_3$  anion in the medium proved to be deleterious to the yield. Rather surprisingly, the authors reached their objective in promoting the reaction with Togni-I reagent which is a source of electrophilic  $\text{CF}_3$  (Scheme 226). A  $\text{L}^*\text{Cu(II)(CF}_3)_2$  complex was proposed as the key intermediate that couples with the benzylic radical before regenerating  $\text{Cu(I)}$  via reductive elimination. It would result from the homolysis of a  $\text{Cu(III)}$  alkoxide that would be the source of the alkoxy radical. Evidence for the formation of the benzylic radical was provided by ESR spin trapping experiments. A closely related study discloses optimized experimental conditions to perform ring-opening cyanation of the same aryl cyclopropanols using benzoylperoxide or NFSI as oxidants. When applied to the corresponding acetals the method leads to  $\beta$ -cyano esters with a high level of enantiocontrol.<sup>455</sup>

### 3.5.5 Synthesis of heterocyclic compounds through polar/radical cyclization

#### Scheme 227. General Pattern for Cu-catalyzed Heterocyclization

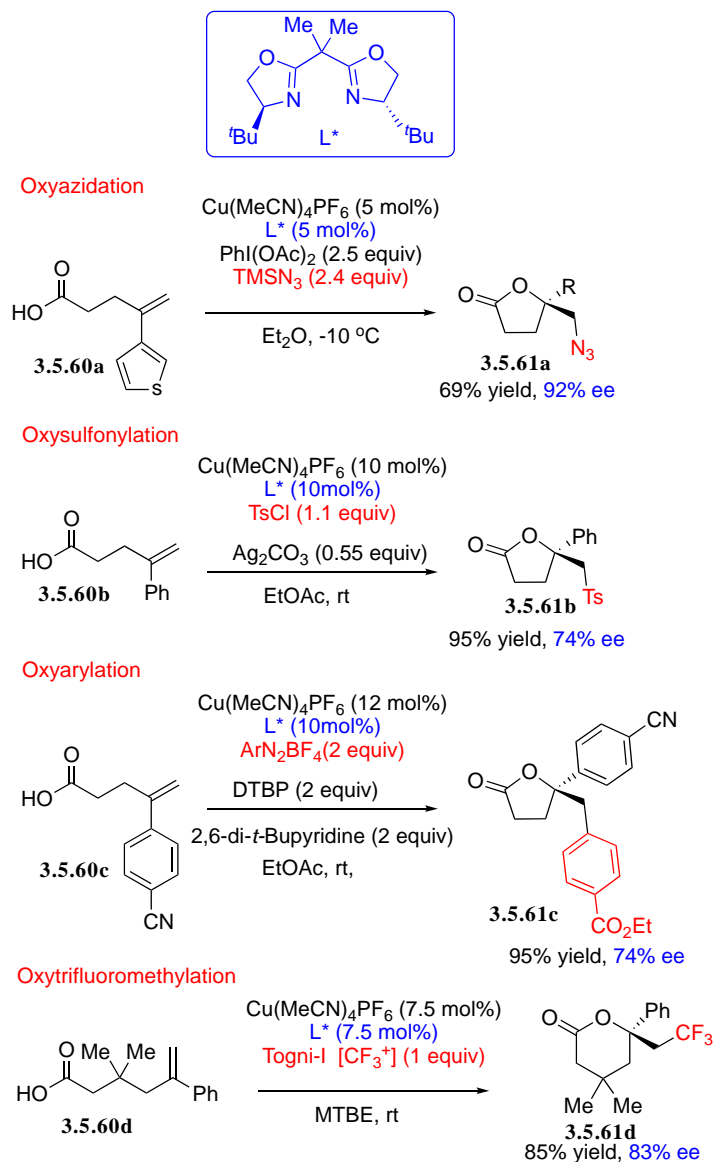


The formation of heterocyclic compounds is a special case of alkene difunctionalization. It can be promoted by the initial addition of several types of radicals to alkenes suitably tethered to nucleophiles (Scheme 227). The mechanism of the subsequent ring-closure via the C-heteroatom bond formation depends on the nature of the catalyst and the chiral co-catalyst, the key intermediate being either a chiral  $\text{Cu(III)}$  intermediate or a solvated ion-pair in a well-defined chiral environment. Three families of ligands have proven their efficiency in these

processes: neutral BOX ligands, anionic CPA conjugated base or chinchona alkaloids derived dual neutral/anionic ligands.

### 3.5.5.1 Ring closure via C-O bond formation

**Scheme 228. Selected Examples of Buchwald's Enantioselective Lactonization**

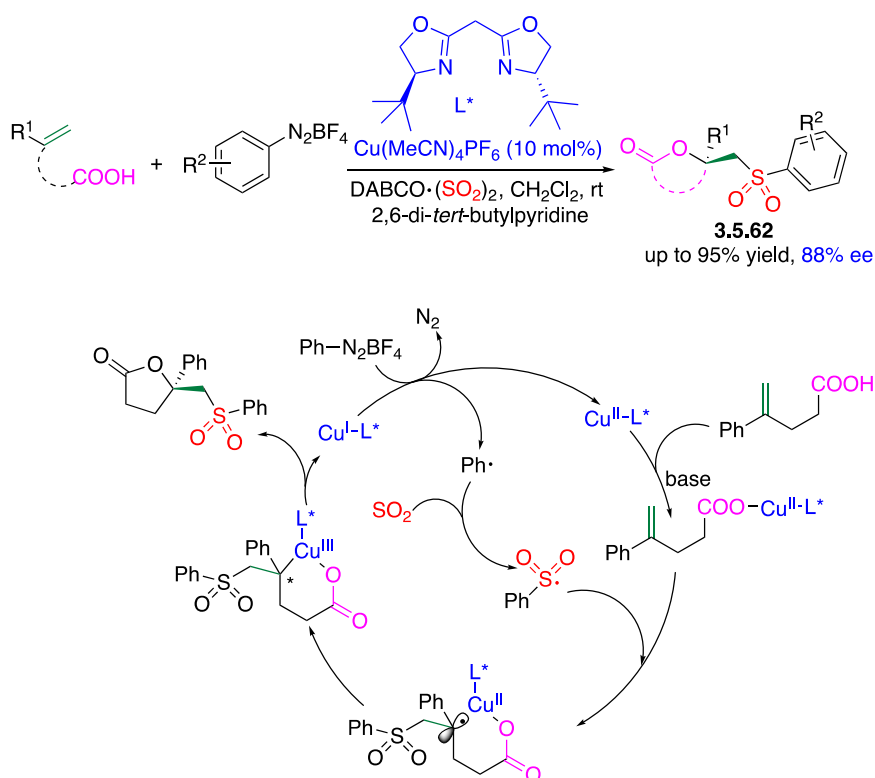


Buchwald and Zhu developed a general Cu-mediated catalytic methodology for the synthesis of enantiomerically-enriched lactones **3.5.61a**. This method is based on enantioselective difunctionalization of the double bond of  $\omega$ -ethylenic carboxylic acids **3.5.60**. It leads to a large array of functionalized lactones. Depending on the nature of the added radical, oxyazidation, oxysulfonylation, oxyarylation, oxytrifluoromethylation. Even diacyloxylation can be achieved

using benzoyl peroxide as source of radical and Mn(0) as co-reductant, however, the latter reaction gives rise to side arylation product due to competitive decarboxylation of benzoyloxy radical. Chirality is introduced thanks to the catalytic amount of BOX ligands. Selected examples are given in Scheme 228.

Applying a similar methodology, Wang et al. also prepared chiral arylsulfonyl lactones. The originality of the procedure resides in the use of  $\text{DABCO}\cdot(\text{SO}_2)_2$  as the source of  $\text{SO}_2$  able to react with the aryl radicals generated via the reduction of diazonium salts to produce arylsulfonyl radicals (Scheme 229).

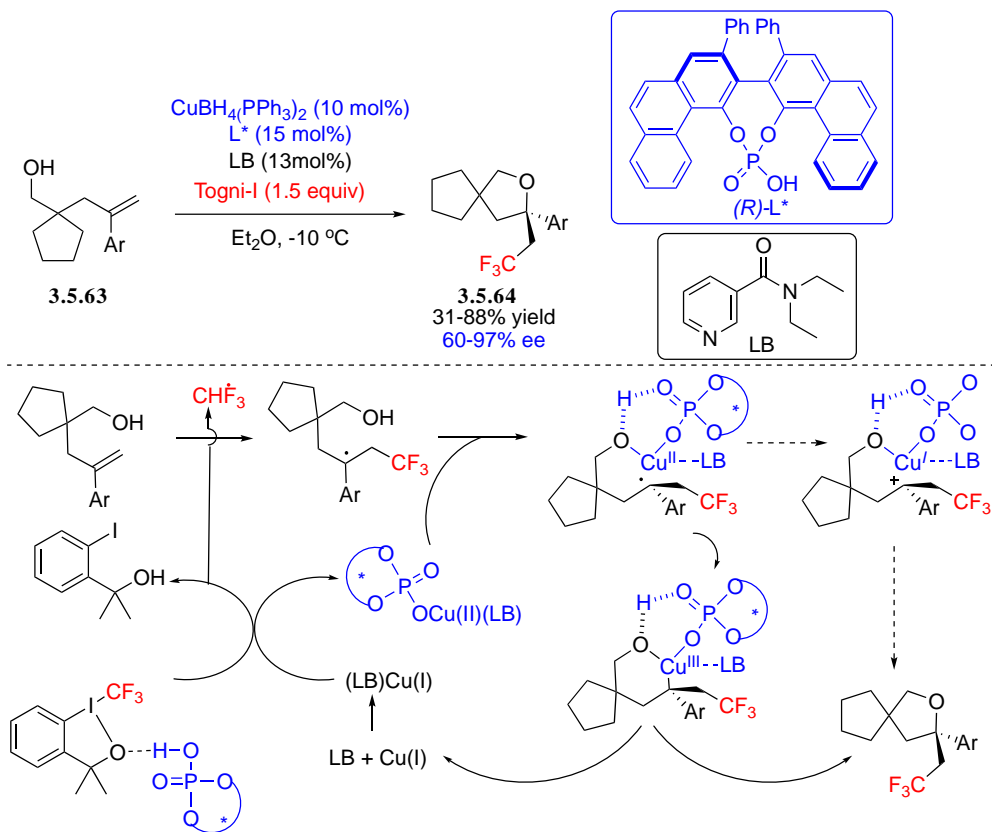
**Scheme 229. Copper-catalyzed Radical Enantioselective Oxysulfonylation using  $\text{DABCO}(\text{SO}_2)_2$  and Arene Diazonium Salts as Precursors of Sulfonyl Radicals**



Alcohols were found to be unsuccessful precursors of chiral ethers with the copper-BOX catalytic system developed by Buchwald. Liu and co-workers have further investigated the ability of the hydroxyl group to associate to CPA-ligated copper to form a chiral network.<sup>456</sup>

Possibly, the hydroxyl group alone would be too weakly acidic, and poor stereoinduction resulted (Scheme 230).

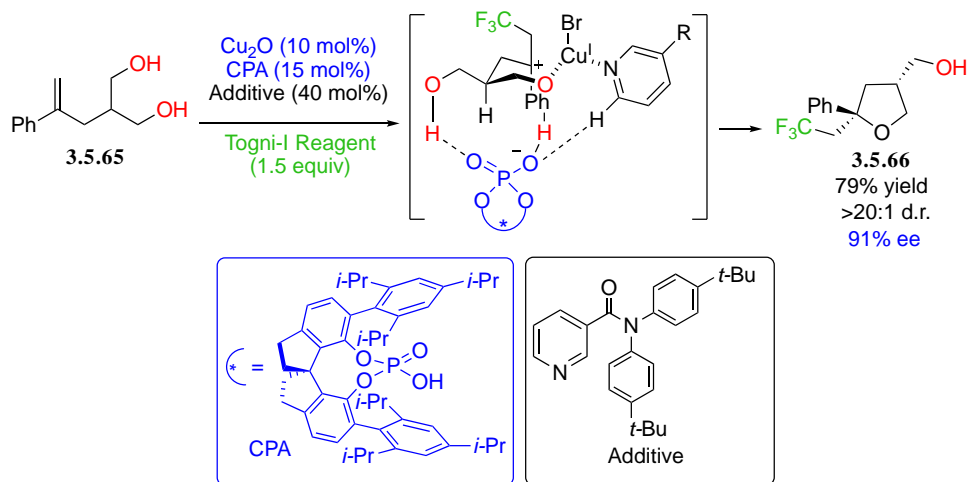
### Scheme 230. Enantioselective Oxytrifluoromethylation of $\delta$ -Ethylenic Alcohols



The problem was solved by adding a Lewis base (LB = *N,N*-diethyl nicotinamide) to the catalytic system as an ancillary achiral ligand able to stabilize the key Cu(II) and Cu(III) intermediates supposed to be involved in the stereoinduction process. According to a study on the impact of pKa, performed by varying the nature of the pyridine ligand, the latter would not play the role of proton shuttle. As exemplified in Scheme 230 chiral THF **3.5.64** bearing a  $\alpha$ -tertiary stereogenic carbon were isolated in most cases in good yields and high ee's. For all given examples, the cyclization step benefits from Thorpe-Ingold effect. A mechanism involving H-bond assisted cleavage of Togni's reagent and the key formation of Cu (II)- and Cu(III)-phosphate complexes is suggested. However, the pathway involving a carbocation intermediate could not be excluded.

The above methodology was artfully applied to the desymmetrizing functionalization of alkenes tethered by 1,3-diols.<sup>457</sup> These reactions enable in one step the formation of two stereocenters with a high level of enantio- and diastereocontrol. As shown in Scheme 231, in the case of meso-diols **3.5.65**, two stereocenters including tetrasubstituted carbon were successfully controlled. Among three mechanistic hypotheses, i.e., intramolecular radical substitution, inner-sphere electron transfer (Cu(III) intermediate) and outer-sphere SET (carbocation intermediate), computational studies support an outer-sphere C-O bond creation. They enable to modelize the synergistic impact of hydrogen-bonding network around the CPA anion and p-stacking interactions with the pyridine ligand on stereocontrol. These theoretical studies and all the previously discussed mechanisms of enantioselective reactions implying CPA as Cu(I) co-catalyst illustrate how complex might be the origin of stereoinduction in such systems.

**Scheme 231. Desymmetrizing Functionalization of Ethylenic 1,3-Diols. Computed Model for the Zwitterionic Intermediate**



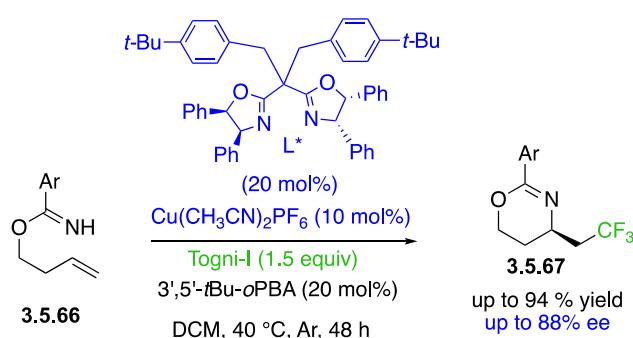
Chinchona-alkaloid-based sulfonamides are bidentate ligands that provide both a neutral tertiary amine and an anionic deprotonated N-atom (Liu and co-workers have proved that the sulfonamide N-H bond is essential to control asymmetric induction in the process). Associated to copper catalyst, they enable the highly enantioselective synthesis of isoxazolines from alkenyl ketoximes via radical trifluoromethylation<sup>458</sup> oxysulfonylation.<sup>459</sup>

### 3.5.5.2 Ring closure via C-N bond formation

Intramolecular aminotrifluoromethylation of non-activated alkenes was achieved with a panel of nitrogen-based nucleophiles varying from sulfonamides,<sup>460</sup> ureas, benzimidates to *N*-tosylhydrazones.

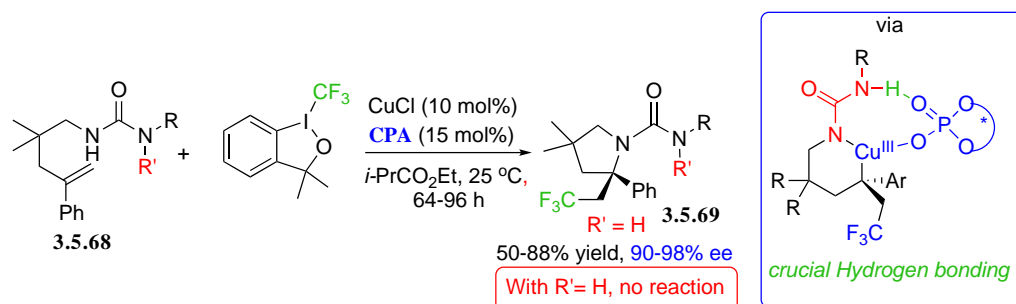
He, Chen and co-workers recently showcased the synthesis of CF<sub>3</sub>-containing enantioenriched 1,3-oxazines via Cu(I)-catalyzed intramolecular aminotrifluoromethylation of *O*-homoallyl benzimidates in the presence of a chiral BOX ligand using Togni's reagent-I as source of trifluoromethyl radical (Scheme 232). Chiral 1,3-oxazines **3.5.67** resulting from cyclization according to the 6-exo-trig mode were isolated in yields going up to 94% and ee's as high as 88%. A mechanism involving the reductive elimination of a chiral Cu(III) complex is proposed in the first case to explain stereoinduction, whereas outer-sphere electron transfer leading to a stabilized carbocation would operate in the second case. It is worth mentioning that when *O*-allyl benzimidates were used as substrates, they preferentially undergo Overman rearrangement under the reaction conditions and therefore no intramolecular aminotrifluoromethylation occurred.

#### Scheme 232. Intramolecular Aminotrifluoromethylation



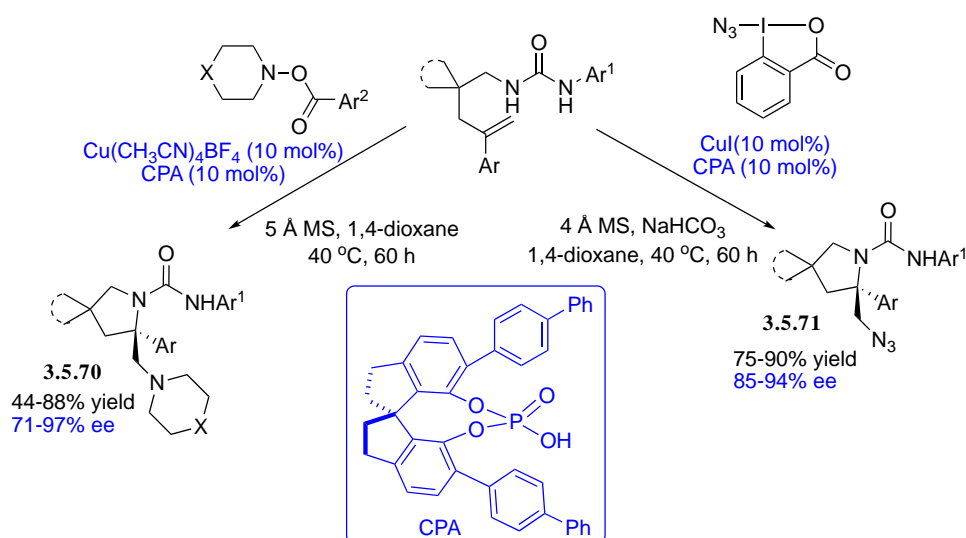
In contrast to the preceding report,<sup>350</sup> the dual-catalytic system associating Cu(I) and CPA, enabled the catalytic asymmetric radical aminotrifluoromethylation of  $\delta$ -ethylenic ureas **3.5.68**. The reaction leads to functionalized CF<sub>3</sub>-containing chiral pyrrolidines **3.5.69** bearing an  $\alpha$ -quaternary stereocenter with good enantioselectivities (Scheme 233).

**Scheme 233. Enantioselective Synthesis of Pyrrolidines via Cu(I) and Chiral Phosphoric Acid Co-catalyzed Trifluoromethylamination of Ethylenic Ureas**



The reaction failed to produce the desired product when methyl protected urea derivative was used as substrate clearly indicating that urea with two acidic N-H plays a crucial role in this asymmetric synthesis as both the nucleophile and directing group involved in the chiral hydrogen-bonds network. The same group further explored the methodology by replacing Togni-I reagent by trifluoromethanesulfonyl chloride as the  $\text{CF}_3$  source. The reaction necessitates the addition of silver carbonate to suppress side hydroamination reaction caused by the in-situ generation of stoichiometric amount of  $\text{HCl}$ .<sup>461</sup>

**Scheme 234. Radical Diamination of Alkenes**



Liu et al. described an asymmetric radical diamination of alkenes triggered by intramolecular addition of dialkylaminyl radical to the alkene via Cu(I)/chiral phosphoric acid (CPA) dual catalysis to access a wide range of highly enantio-enriched  $\alpha$ -dialkylaminomethyl pyrrolidines

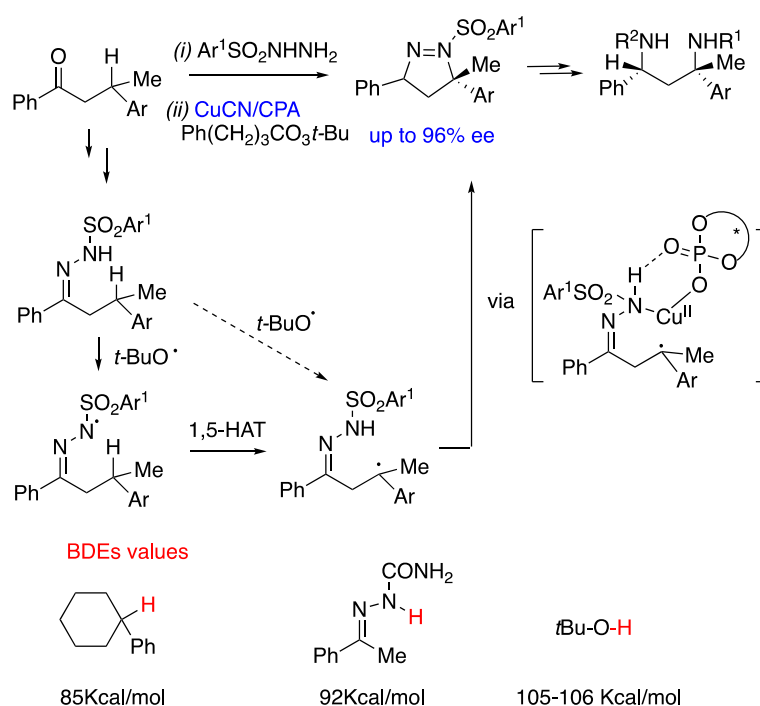


**3.5.70** and **3.5.71** (Scheme 234).<sup>462</sup> The aminyl radical was generated through Cu(I)-mediated reductive homolytic cleavage of *O*-acyl hydroxylamines.

Finally, the following last example might have been included in the paragraph devoted to intercalation of 1,5-HAT. The intramolecular enantioconvergent amination of racemic ketones bearing a tertiary benzylic stereogenic center in position  $\beta$  was achieved via their conversion into sulfonyl hydrazones (Scheme 235).<sup>463</sup> It leads to chiral dihydropyrazoles that, as exemplified by the authors can be converted in a few steps to chiral 1,3-diamines or to chiral congested cyclopropanes without significant erosion of enantiopurity.

The dual Cu(I)/CPA-catalyzed cascade process is supposed to involve successively: (i) N-H abstraction by *t*-butoxy radical, rearrangement of the resulting hydrazinyl radical via 1,5-HAT, (iii) Cu(II)-catalyzed oxidative ring closure through enantioselective formation of the C-N bond. It can be noticed that the alternative mechanism implying direct abstraction of the benzylic hydrogen atom by *t*-butoxy radical is not envisaged although, as shown in Scheme 235 the BDEs are quite favorable.

### Scheme 235. Enantioconvergent Amination of Racemic Ketones

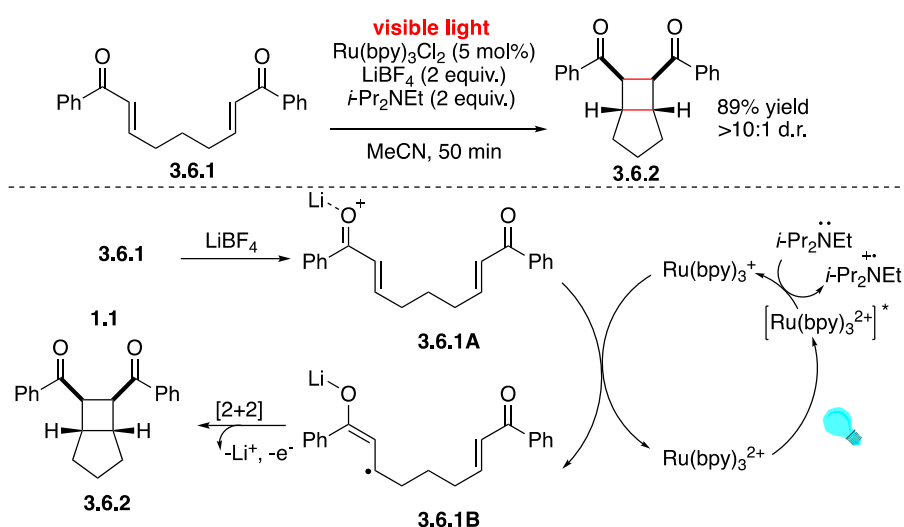


### 3.6. Photoredox Reactions using Chiral Lewis Acids

#### 3.6.1 Merging Photoredox Catalysts with Rare Earth Elements

We highlighted in section 2 that photo-cycloaddition reactions in the presence of organocatalysts provide a distinctive ability to give high regio- and stereoncontrol. Transition metal photocatalyst ruthenium is also used in the photoredox-chiral Lewis acid dual catalysis for performing highly enantioselective catalytic photoreactions.<sup>412</sup> In most of the cases, ruthenium shows its activity as a visible-light absorbing photoredox catalyst<sup>464</sup> This dual catalysis strategy has been successfully applied to perform several photochemical enantiocontrolled reactions which include [2+2] cycloadditions, [3+2] cycloadditions, and radical conjugate addition reactions.

#### Scheme 236. Ru-catalyzed [2+2] Cycloaddition of Enone.

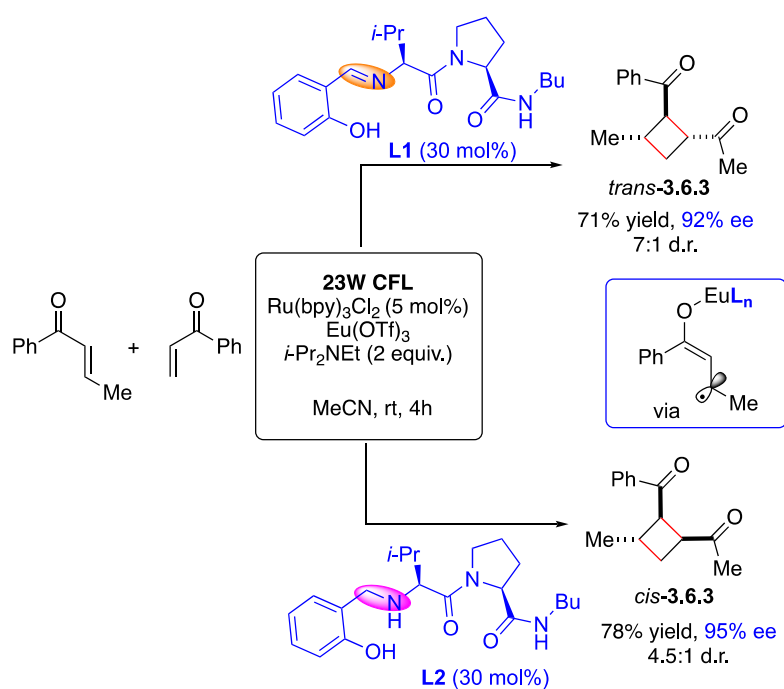


In preliminary study for developing catalytic system for such transformations, Yoon et al. focused on reactivity-selectivity principle before developing enantioselective reactions. They synthesized compound **3.6.2** by intramolecular [2+2] photocycloaddition reaction of *bis*(enone) **3.6.1** upon visible light irradiation (275 W floodlight at a distance of 20 cm) using 5% Ru(bpy)<sub>3</sub>Cl<sub>2</sub> as photocatalyst in combination with LiBF<sub>4</sub> and *i*-Pr<sub>2</sub>NEt as additives (Scheme 236). According to the established mechanism, photoactivated [Ru(bpy)<sub>3</sub><sup>2+</sup>]<sup>\*</sup> undergoes reductive quenching by *i*-Pr<sub>2</sub>NEt to form the strong reducing agent Ru(bpy)<sub>3</sub><sup>3+</sup> that transfers an

electron to the lithium-activated enone **3.6.1A** resulting in the formation of radical anion **3.6.1B**. This anion radical initiates the [2+2] cycloaddition with the regeneration of the Ru<sup>2+</sup> photocatalyst. Inter- as well as intramolecular cycloadditions were reported.<sup>464</sup>

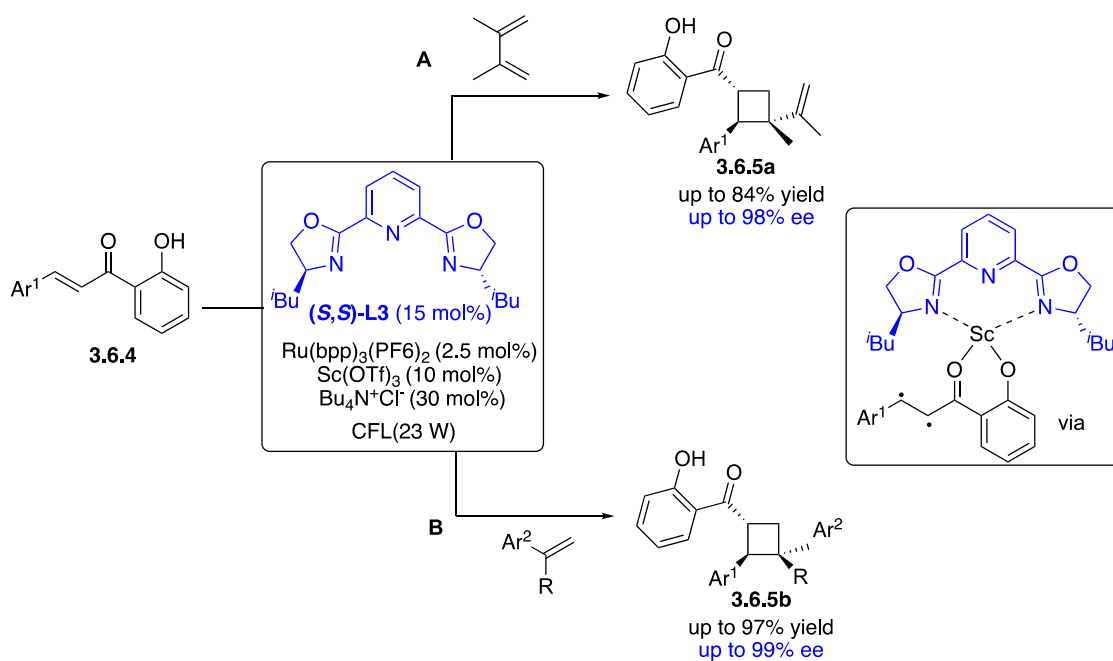
In order to overcome the competing background racemic photoreactions, many researchers relied on the difference absorption capacity of colorless substrates in the visible region and ruthenium chromophores that absorb intensely. This difference is a key for developing efficient asymmetric reactions. However, another Lewis acid catalyst is needed for the stereocontrol. Based on this principle, the Yoon group screened several chiral lanthanide Lewis acids in the presence of ruthenium photocatalyst to suppress the racemic background cycloaddition. They succeeded to synthesize a wide range of enantiomerically pure cyclobutane derivatives using Eu(OTf)<sub>3</sub> and proline-valine Schiff base ligand. Interestingly, using the imine of this dipeptide (**L1**) allows a *trans*-selective cycloaddition, whereas the amine ligand (**L2**) affords the *cis*-cycloadduct **3.6.3**. This asymmetric [2+2] photocycloadditions of  $\alpha,\beta$ -unsaturated ketones provides good yields and enantioselectivities (Scheme 237).<sup>465</sup>

**Scheme 237. Synthesis of cyclobutane derivatives via enantioselective [2+2] photocycloadditions.**



Moreover, cyclobutanes **3.6.5a** were synthesized with good yields and enantioselectivities by asymmetric [2+2] photocycloadditions of 2'-hydroxychalcones **3.6.4** using Scandium chiral Lewis acid complex catalyzed triplet energy transfer from an electronically excited photosensitizer (Scheme 238A).<sup>466</sup> Extension of this strategy to 2'-hydroxychalcones with a range of styrene coupling partners giving **3.6.5b** was also reported by the same group (Scheme 238b).<sup>467</sup>

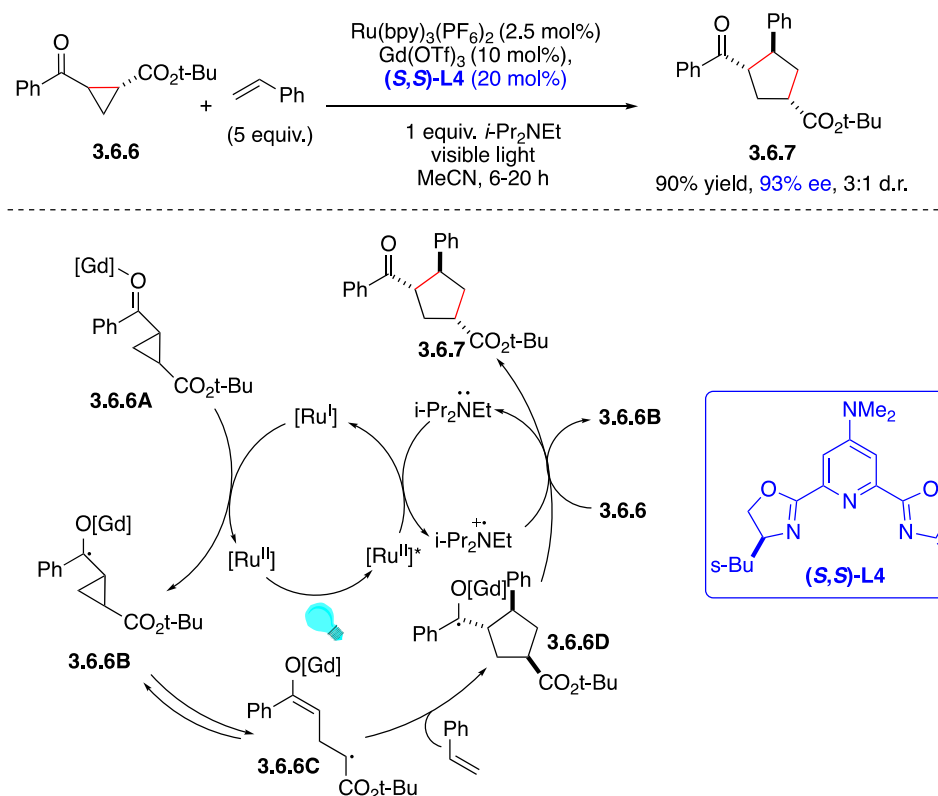
**Scheme 238. Synthesis of cyclobutane derivatives via enantioselective [2+2] photocycloadditions of chalcones.**



Besides [2+2] photocycloadditions of enones, the Yoon group also developed catalytic asymmetric [3+2] photocycloaddition of aryl cyclopropyl ketones **3.6.6** with alkene substrates that successfully gave enantioenriched densely substituted cyclopentanes **3.6.7** with good yields and enantioselectivities. When phenyl ketone was reacted with styrene employing 2.5 mol% Ru(bpy)<sub>3</sub><sup>2+</sup> as the photocatalyst, 10 mol% Gd(OTf)<sub>3</sub> as the Lewis acid cocatalyst, 20 mol% *s*-Bu-substituted pybox ligand **L4**, and *i*-Pr<sub>2</sub>NEt as the reductive quencher in acetonitrile solvent under irradiating with a 23 W CFL for 6 h, afforded the corresponding cyclopentane derivative

**3.6.7** in 90% yield with 93% ee (Scheme 239). According to the proposed mechanism, SET reduction of chiral Gd(III) Lewis acid activated phenyl ketone (**3.6.6A**) generates ketyl radical (**3.6.6B**) which undergoes reversible ring opening (**3.6.6C**) followed by cycloaddition with styrene affords the product ketyl radical (**3.6.6D**). Then the neutral product **3.6.7** could form either by electron transfer to another equivalent of substrate or by reduction of the amine radical cation (Scheme 239).

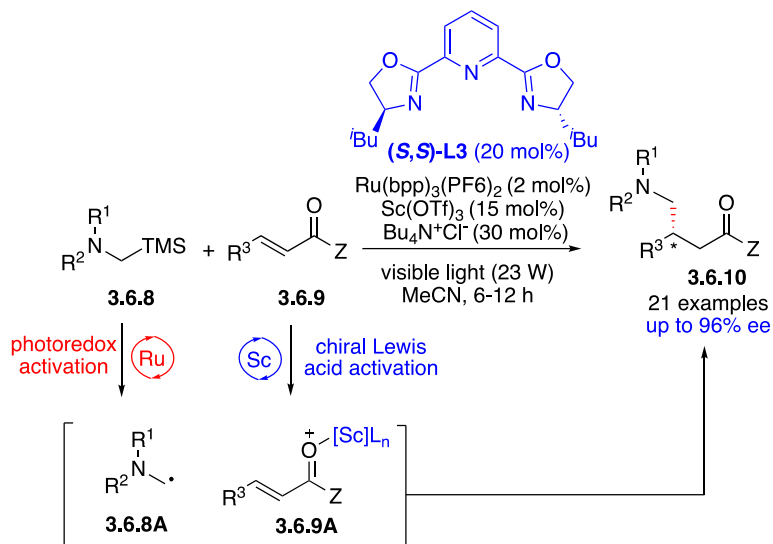
**Scheme 239. Ru-catalyzed Enantioselective [3+2] Photocycloaddition of Aryl Cyclopropyl Ketones.**



In 2015, Yoon et al. developed enantioselective addition of  $\alpha$ -amino radicals **3.6.8A** to the activated Michael acceptors **3.6.9** for the formation of radical conjugate addition product **3.6.10** in good yields with high enantioselectivities (Scheme 240). The  $\alpha$ -amino radical **3.6.8A** was photogenerated from  $\alpha$ -silyl amines **3.6.8** under visible light irradiation in the presence of photocatalyst Ru(bpy)<sub>3</sub>Cl<sub>2</sub> whereas the activated Michael acceptor **3.6.9A** was formed from Michael acceptors **3.6.9** by Lewis acid catalysis. This dual catalysis is very efficient to generate

and control the reactivity of reactive intermediates and the role of  $\text{Bu}_4\text{N}^+\text{Cl}^-$  is to increase the rate of formation of product **3.6.10** by interacting intimately with the Lewis acid.

**Scheme 240. Ru-catalyzed Enantioselective Conjugate Additions of  $\alpha$ -Amino Radicals.**



**3.6.2 Photoredox reactions using chiral-at-metal complexes as Lewis acid catalyst**

The photoredox-chiral Lewis acid dual catalysis by Rhodium is a long-standing and challenging goal to the synthetic chemist for performing highly enantioselective catalytic photoreactions. Although research in this field has been ongoing for several past decades, there are a limited number of examples reported on successful photochemical enantiocontrolled reactions. The success of this dual catalysis includes highly enantioselective photocatalytic  $\alpha$ - and  $\beta$ -alkylations,  $\alpha$ - and  $\beta$ -aminations,  $\beta$ -C-H functionalization, [3+2]-, [2+2]- and [2+3] photocycloadditions, etc.

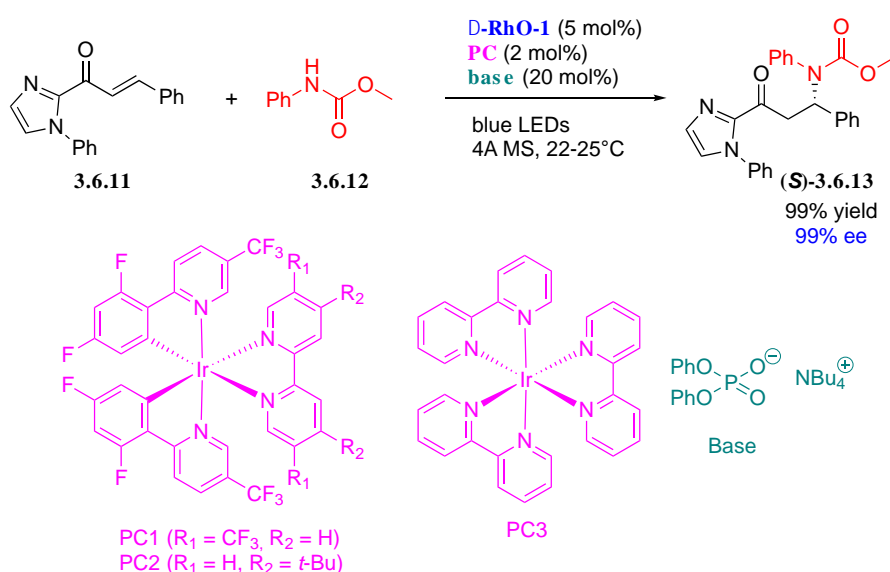
Meggers et al. designed and synthesized very reactive photoactivatable chiral catalysts, bis-cyclometalated rhodium (III) complexes (**Rh-1**), for asymmetric photocatalysis (Scheme 241).<sup>468</sup> These chiral catalysts contain two inert cyclometalating 5-(*tert*-butyl)-2-phenylbenzo[*d*]oxazole (RhO)<sup>469</sup> or 5-(*tert*-butyl)-2-phenylbenzo[*d*]thiazole (RhS)<sup>470</sup> ligands along with two labile acetonitriles and one hexafluorophosphate counteranion which provided helical chirality with a left-handed ( $\Lambda$ -enantiomer,  $\Lambda$ -**RhS-1** and  $\Lambda$ -**RhO-1** or right-handed ( $\Delta$ -



The asymmetric construction of C–N bonds is of particular interest as the presence of stereogenic carbon connected to nitrogen-containing groups can be found in numerous natural products and compounds of biological interest.<sup>472</sup> In 2014, Knowles introduced the concept of proton-coupled electron transfer (PCET) to convert N-H groups into nitrogen-centered radicals (cf section 2.2.2).<sup>169,473</sup> These species can be formed under mild conditions, by means of a weak base and PCET can also be promoted under visible light using a photoredox mediator (PRM).<sup>72</sup> Besides, nitrogen-centered radicals often lack reactivity due to their inherent electron-deficiency for the direct radical  $\beta$ -amination of unsaturated carbonyl compounds. In 2017, this issue was addressed with the Lewis acid  $\Delta$ -**RhO-1** enabling the coupling of *N*-aryl carbamates with  $\alpha,\beta$ -unsaturated 2-acyl imidazoles.<sup>474</sup> In dichloromethane, (**S**)-**3.6.13** could be obtained in quantitative yield with a 98% ee using **PC1** as the mediator (Scheme 242). Examination of other chiral-at-metal catalysts such as  $\Delta$ -**RhS** or  $\Delta$ -**IrO** revealed these catalysts to be less promising in terms of ee and reaction yields. To support the high ee obtained with the chiral-at-rhodium Lewis acid  $\Delta$ -**RhO**, the mechanism shown in the Scheme 243 was proposed.

### Scheme 242. Conjugate Addition N-Centered Radicals to Enones using Chiral at Metal

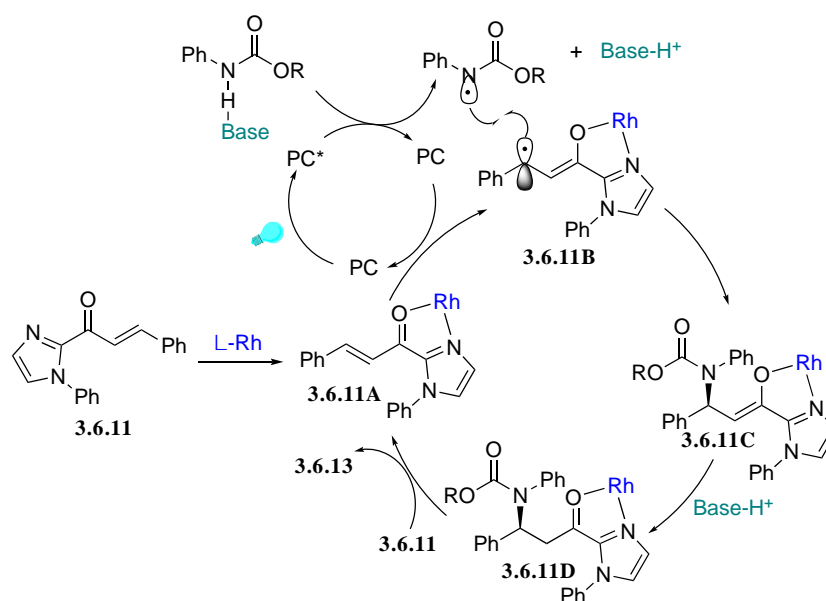
#### Lewis Acids





The photoredox mediator is an important element of the mechanism by first promoting the PCET generating the nitrogen-centered radicals and second by promoting a single electron transfer to the carbamate to the Rh-bound substrate (Scheme 243). Following the radical-radical coupling and protonation by the protonated base, (*S*)-**3.5.13** can be obtained. Role of the rhodium catalyst in this mechanism is also twofold. Indeed, the *N,O*-bidentate coordination of the rhodium catalyst facilitates the reduction of the substrate and second, the chiral Lewis acid controls the stereochemistry of the radical–radical coupling by providing an asymmetric environment. A great tolerance of the aryl substituents of the  $\alpha,\beta$ -unsaturated 2-acyl imidazole.

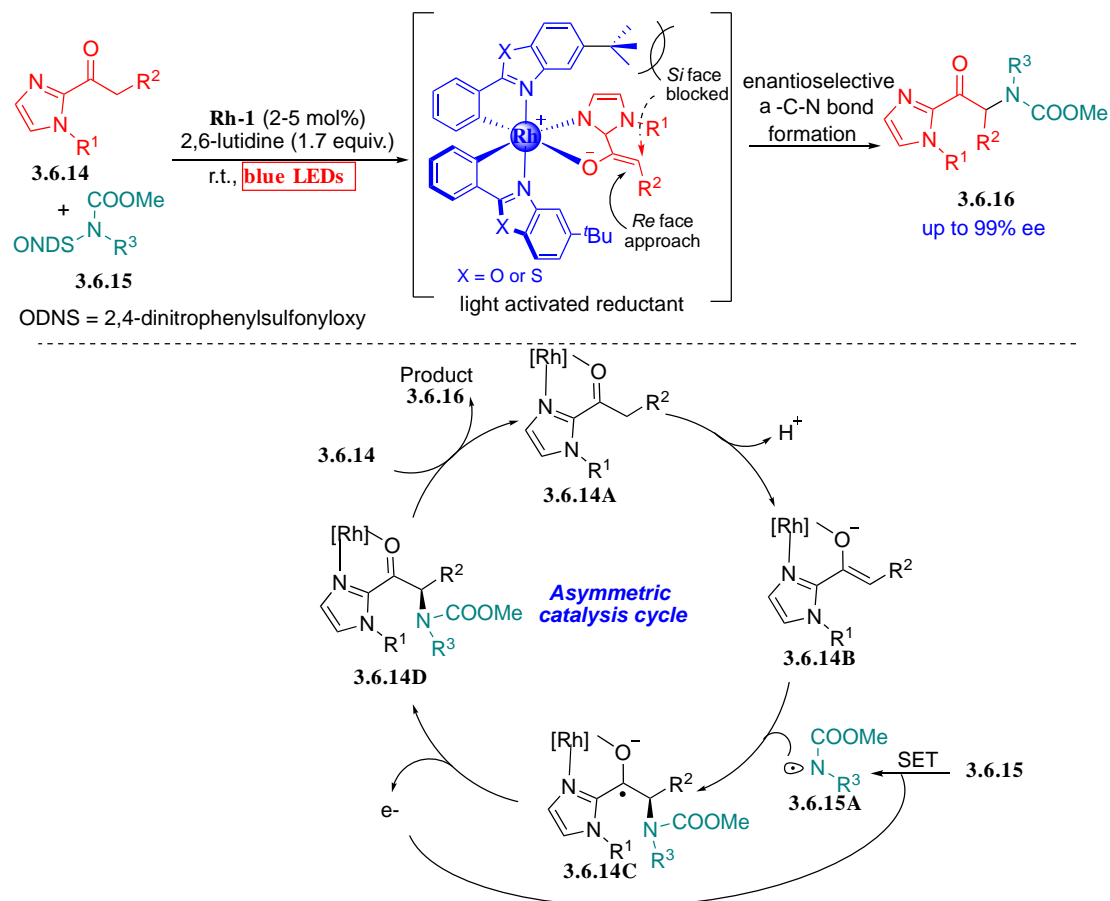
**Scheme 243. Mechanism Involved in the Radical Amination of  $\alpha,\beta$ -Unsaturated 2-Acyl Imidazole**



This proof of concept has opened access to various radical reactions. For example, when 2-acyl imidazoles **3.6.11** were reacted with (ODN)-*N*-functionalized carbamates **3.6.15** in presence of 2-5% Rh-1, the enantioselective  $\alpha$ -C-N bond formation occurred to result in the formation of products **3.6.16** with high enantioselectivities through enantioselective secondary photocatalysis. Mechanistically, substrate coordination followed by deprotonation gave the key rhodium enolate intermediate **3.6.14B**. An electron deficient radical **3.6.15A** which was

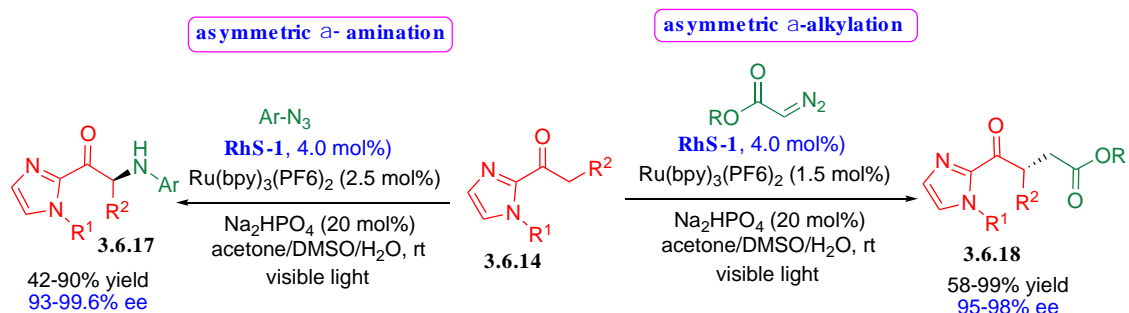
generated from carbamate **3.6.16** by visible-light-induced SET reduction, then attacked the electron rich enolate intermediate **3.6.14B** to form a ketyl radical intermediate **3.6.14C**. Finally, the product-coordinated rhodium intermediate **3.6.15D** was formed via SET oxidation of ketyl radical intermediate **3.6.14C** which delivered product **3.6.16** with recoordination of new substrate to start a new catalytic cycle (Scheme 244). By a similar mechanism, Xu et al. also successfully synthesized fluorine-containing  $\gamma$ -keto acid derivatives in high yields and excellent enantioselectivities by difluoroalkylation of 2-acylimidazoles via merging  $\Delta$ -RhS catalyzed Lewis acid catalysis and Ir(ppy)<sub>2</sub>(dtbbpy)(PF<sub>6</sub>)-catalyzed visible-light photocatalysis.<sup>475</sup> Here it is worth mentioning that Houk et al. established through computational study that the distortion of the Rh enolate and its benzothiazole ligand are responsible for enforcing enantioselectivity in the transition states.<sup>476</sup>

### Scheme 244. Bis-cyclometalated Rhodium (III) Complex Catalyzed Enantioselective $\alpha$ -C-N Bond Formation.



The same group also extended their work for visible-light-activated asymmetric  $\alpha$ -amination and  $\alpha$ -alkylation of 2-acyl imidazoles **3.6.14** with aryl azides and  $\alpha$ -diazo carboxylic esters respectively by the combination of  $\Delta$ -RhS-**1** with a photoredox sensitizer  $[\text{Ru}(\text{bpy})_3](\text{PF}_6)_2$ .<sup>477</sup> A variety of aryl azides and  $\alpha$ -diazo carboxylic esters were used for the amination and alkylation of 2-acyl imidazoles with 20 mol%  $\text{Na}_2\text{HPO}_4$  as base in the presence of chiral rhodium-based Lewis acid catalyst  $\Delta$ -RhS-**1** (4.0 mol%) and 1.5-2.5 mol% of photoredox sensitizer  $[\text{Ru}(\text{bpy})_3](\text{PF}_6)_2$  in mixed solvents acetone/DMSO/ $\text{H}_2\text{O}$  at rt (Scheme 245). The respective aminated product **3.6.17** and alkylated product **3.6.18** were obtained with high yields and enantioselectivities. Detailed mechanistic studies showed that the reactions were gone through a radical pathway as similar as shown in Scheme 244 instead of a carbene/nitrene pathway.

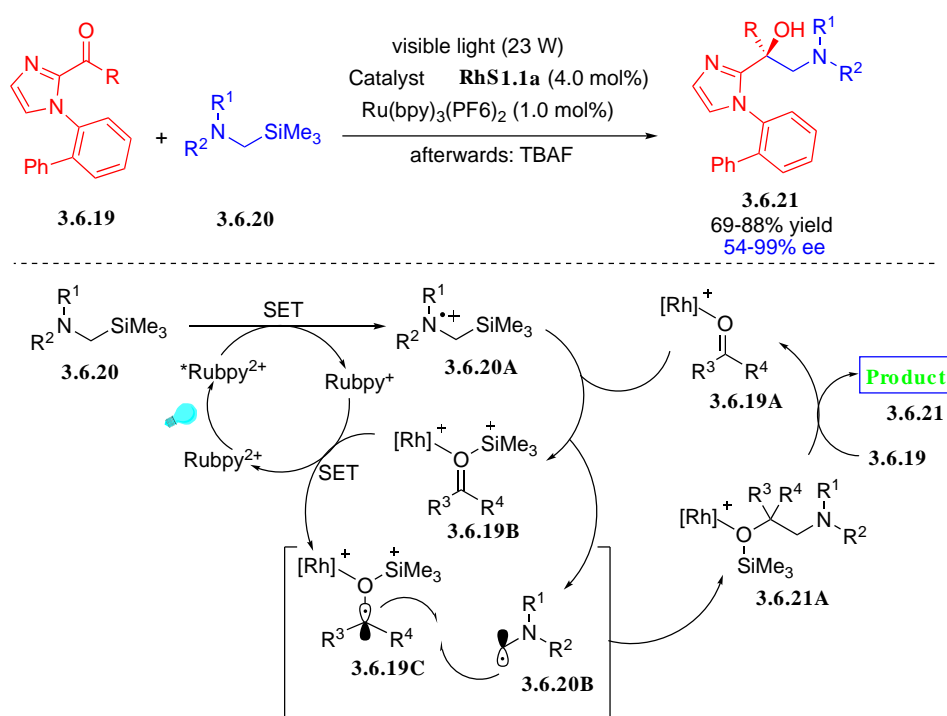
**Scheme 245. Bis-cyclometalated Rhodium (III) Complex Catalyzed Enantioselective  $\alpha$ -Amination and  $\alpha$ -Alkylation.**



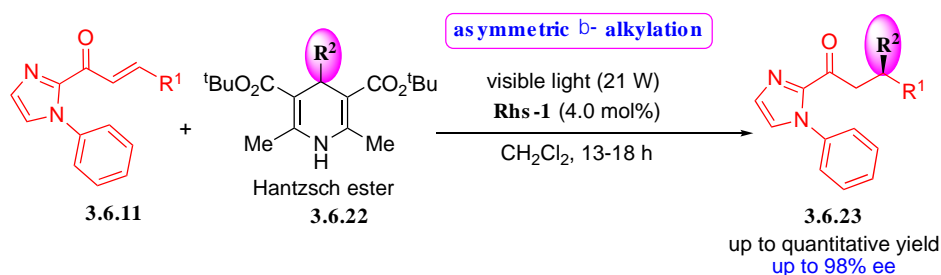
Meggers et al. also synthesized chiral 1,2-aminoalcohols **3.6.21** in good yields and high enantioselectivities by visible-light-activated redox coupling of  $\alpha$ -silylamines **4.6.20** with 2-acyl imidazoles **4.6.19** followed by desilylation promoted by the rhodium-based chiral Lewis acid catalyst  $\Delta$ -RhS-**1** in combination with photoredox sensitizer  $[\text{Ru}(\text{bpy})_3](\text{PF}_6)_2$  (Scheme 246).<sup>478</sup> According to the proposed mechanism, the visible light activated  $[\text{Ru}(\text{bpy})_3]^{2+}$  first oxidizes  $\alpha$ -silylamines **4.6.20** to generate the corresponding radical cation **4.6.20A** which subsequently transforms into  $\alpha$ -aminomethyl radical **4.6.20B** by rapid desilylation. On the other hand, this released trimethylsilyl group is captured by rhodium-coordinated substrate **4.6.19A** to afford intermediate **4.6** which readily converts to silylated ketyl intermediate **4.6.19C**

through an electron transfer from the reduced sensitizer. Then radical-radical recombination occurs between two radical intermediates **4.6.19C** and **4.6.20B** to generate a new intermediate **4.6.21A** which delivered product **4.6.21** by the replacement of a new substrate **4.1** to start a new catalytic cycle.

### Scheme 246. Bis-cyclometalated Rhodium (III) Complex Catalyzed Synthesis of 1,2-Aminoalcohols.



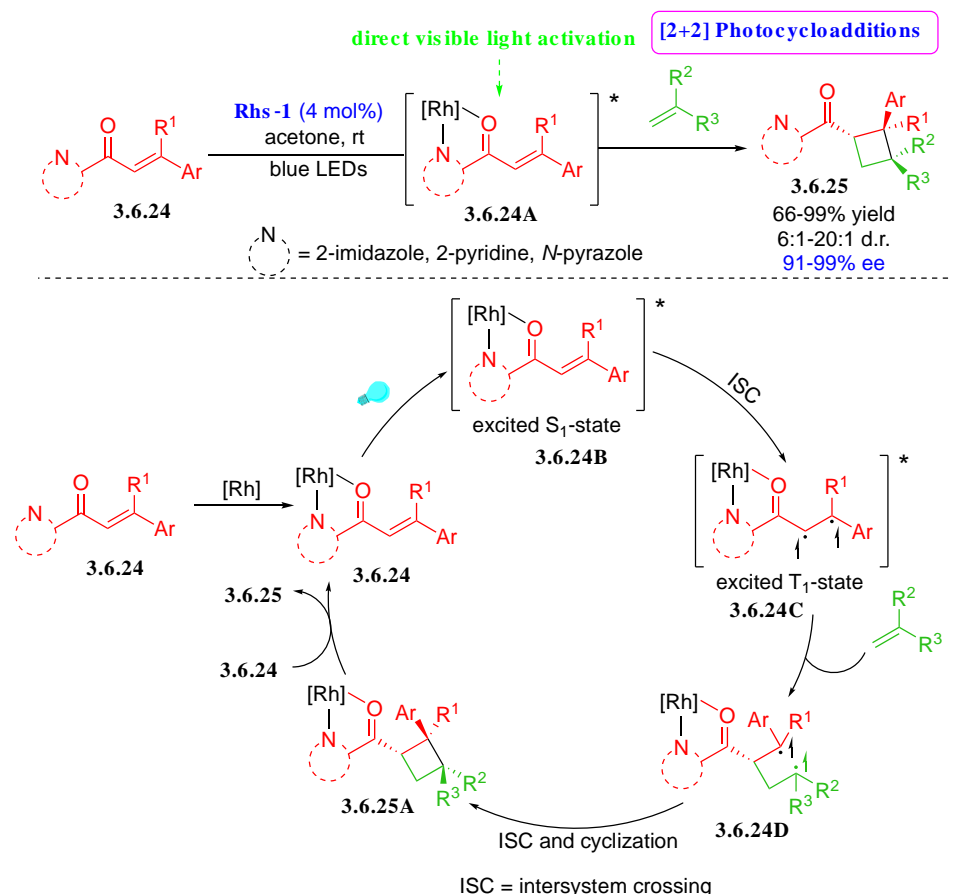
### Scheme 247. Bis-cyclometalated Rhodium (III) Complex Catalyzed $\beta$ -Alkylation of $\alpha,\beta$ -Unsaturated 2-Acyl Imidazoles.



Meggers et al. further developed visible-light-activated asymmetric  $\beta$ -alkylation of  $\alpha,\beta$ -unsaturated 2-acyl imidazoles **3.6.11** using Hantzsch esters **3.6.22** as the alkyl radicals source in the presence of rhodium-based chiral Lewis acid catalyst  $\Lambda$ -RhS-1 (Scheme 247).<sup>479</sup> The

advantage of this method is that there is no further need of photoredox sensitizer which was essential for the previously described method. Here,  $\Delta$ -RhS-1) plays the dual role as the visible-light-absorbing unit upon substrate binding and also as the asymmetric catalyst.

**Scheme 248. Bis-cyclometalated Rhodium (III) Complex Catalyzed Intermolecular [2+2] Photocycloadditions.**

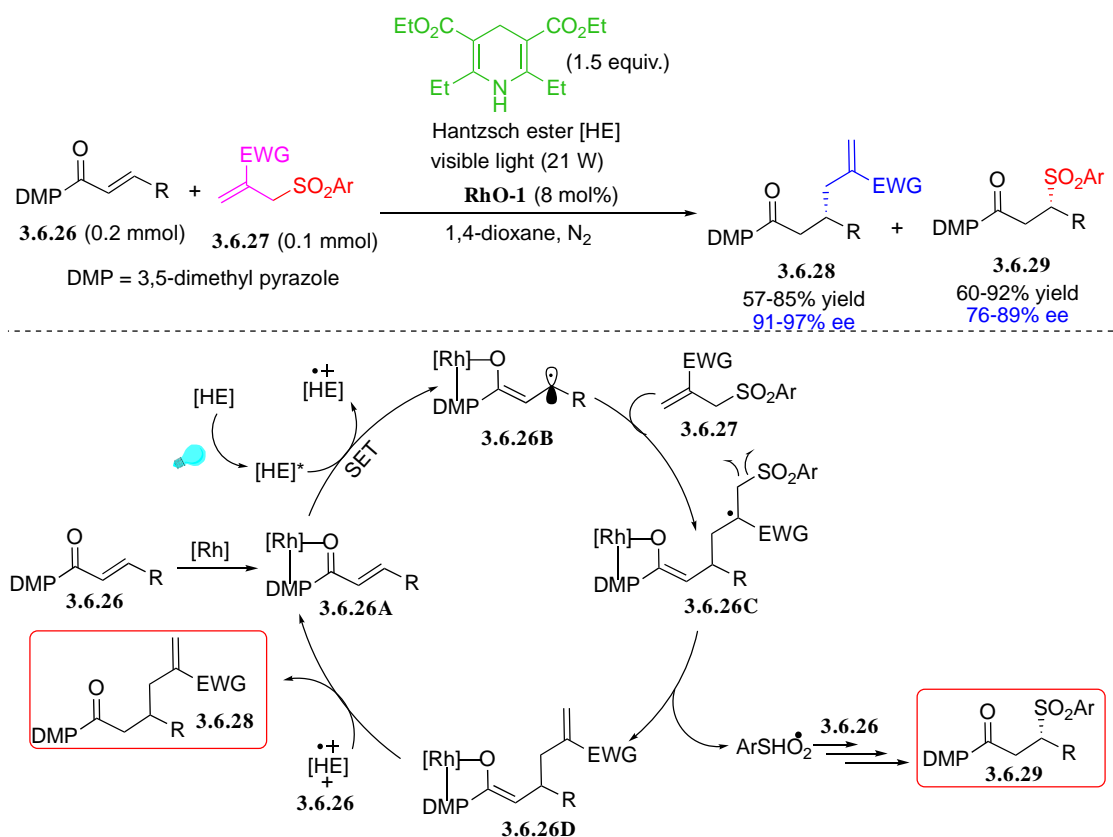


Meggens and co-workers successfully synthesized a wide range of cyclobutanes **3.6.25** with high enantio- and diastereoselectivities via  $\Delta$ -RhS-1-catalyzed, visible-light-activated intermolecular [2+2] cycloadditions of the  $\alpha,\beta$ -unsaturated nitrogen heterocycles **3.6.24** with an alkene (Scheme 248).<sup>480</sup> Mechanistically, the reaction proceeds through the coordination of substrate **3.6.24** to rhodium catalyst to form intermediate **3.6.24A** which becomes excited by visible light to its lowest excited state ( $S_1$ ) to afford intermediate **3.6.24B**. After intersystem crossing (ISC), this intermediate is converted to the triplet state to form intermediate **3.6.24C** which reacts with the olefin under control of stereochemistry by the chiral rhodium catalyst to

afford 1,4-diradical intermediate **3.6.24D**. By recombination of this diradicals, Rh-coordinated cycloadduct **3.6.25A** is formed which delivered product **3.6.25** by the replacement of a new substrate **3.6.24** to start a new catalytic cycle.

In 2017, Meggers et al. reported an unusual radical allylation reaction of  $\alpha,\beta$ -unsaturated *N*-acylpyrazole **3.6.26** with allyl sulfones **3.6.27** using Hantzsch ester as the photoredox mediator and reductant and chiral bis-cyclometalated rhodium (III) complex  $\Delta$ -RhO-1) as catalyst under visible light irradiation.<sup>481</sup> The advantages of this method was that beside providing the radical allylation products **3.6.28** with up to 97% ee, the generated sulfonyl radical by-product was trapped by electron deficient alkenes to provide enantioenriched *S*-containing building blocks **3.6.29** with up to 89% ee (Scheme 249).

### Scheme 249. Bis-cyclometalated Rhodium (III) Complex Catalyzed Radical Allylation Reaction.

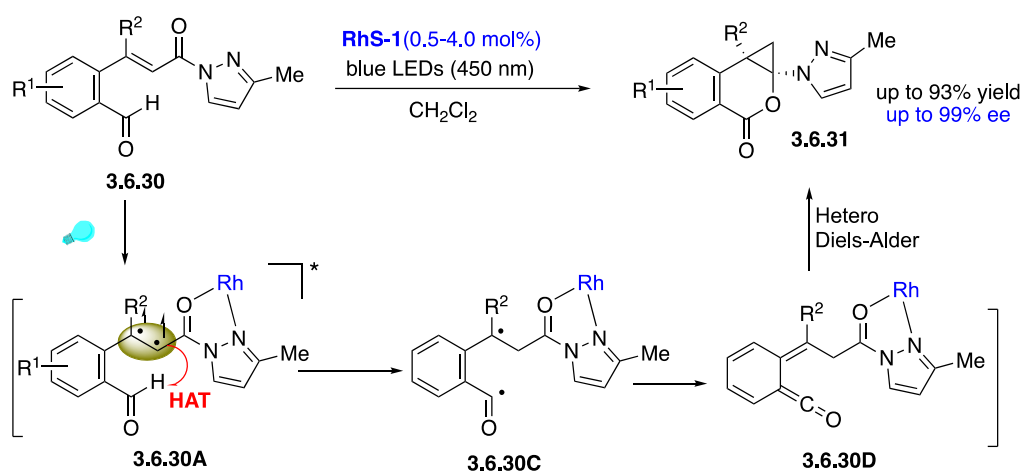


According to the proposed mechanism, substrate coordinated rhodium complex **3.6.26A**, which is much better electron acceptor than free substrate **3.6.26**, was reduced by the visible-light-

excited HE to form radical intermediate **3.6.26B**. This radical is readily trapped by the electron deficient allyl sulfone **3.6.27** to afford secondary radical intermediate **3.6.2C** which provides the sulfonyl radical and enolate intermediate **3.6.26D**. This enolate intermediate then gives the allylation product **3.6.28** upon protonation and sulfonyl radical is trapped by another molecule of complexed alkene **3.6.26A** which provides additional enantioenriched product **3.6.29** by HAT followed by ligand exchange process.

Furthermore, Meggers et al. reported a rhodium ( $\Delta$ -RhS-1)-catalyzed asymmetric photoreaction of substrate **3.6.30** which proceeds through a 1,5-hydrogen-atom transfer (HAT) from a photoexcited catalyst-substrate complex **3.6.30A** followed by a highly stereocontrolled hetero-Diels-Alder reaction that afforded benzo[*d*]cyclopropana[*b*]pyranones **3.6.31** with up to >99% ee (Scheme 250).<sup>482</sup> The stereo-determining step is the Diels-Alder cycloaddition rather than radical step. Mechanistic studies and DFT calculations supported the proposed mechanism.

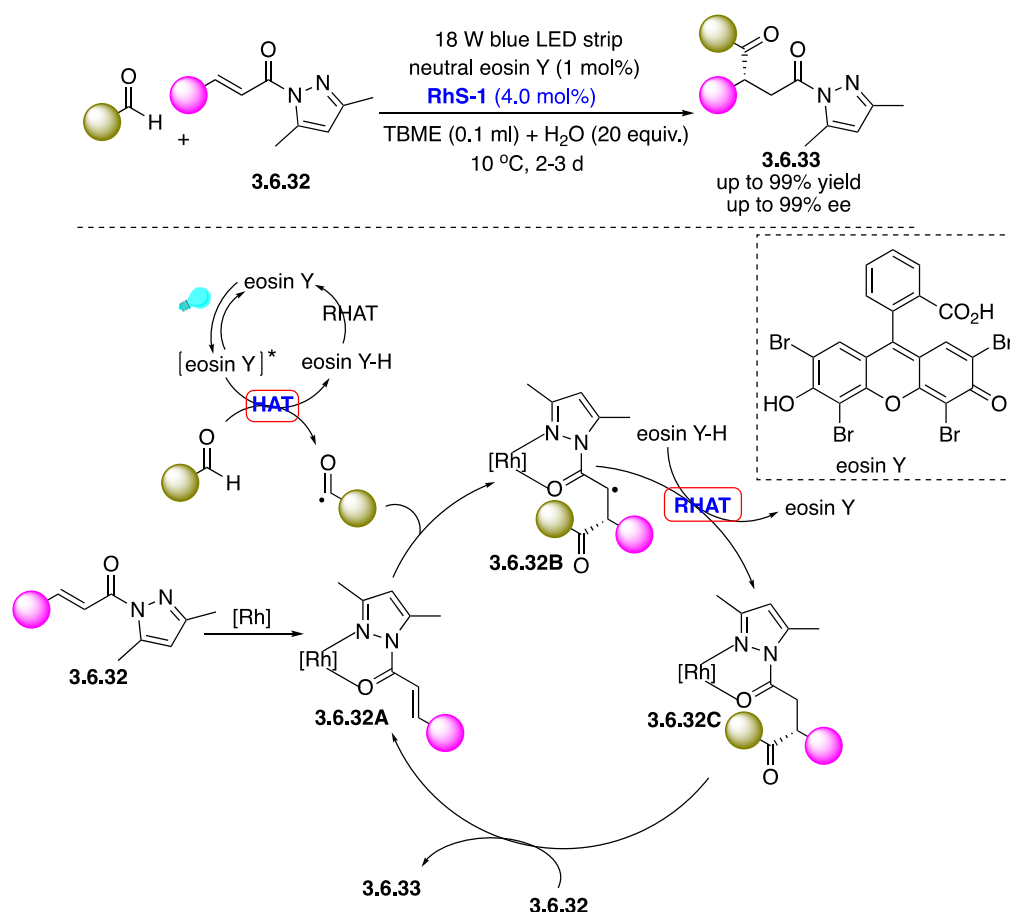
**Scheme 250. Bis-cyclometalated Rhodium (III) Complex Catalyzed Asymmetric Photocatalysis by HAT in Photoexcited Catalyst-substrate Complex.**



In 2019, Wu et al. demonstrated that aldehydes can be directly used as acyl radical precursors for catalytic enantioselective addition to  $\alpha,\beta$ -unsaturated *N*-acyl-3,5-dimethylpyrazoles **3.6.32** for enantioselective synthesis of 1,4-dicarbonyl compounds **3.6.33** with good yield and enantioselectivity through the synergistic combination of a neutral eosin Y hydrogen atom

transfer photocatalyst and a chiral bis-cyclometalated rhodium (III) complex  **$\Lambda$ -RhS-1** (Scheme 251).<sup>483</sup> According to the proposed mechanism, the acyl radical generated from aldehyde adds to the rhodium coordinated complex **3.6.32A** to form secondary radical intermediate **3.6.32B**. Intermediate **3.6.32C** which is generated from intermediate **3.6.32B** by reverse HAT then undergoes ligand exchange with starting **3.6.32** to deliver asymmetric 1,4-dicarbonyl products **3.6.33** with the regeneration of active complex **3.6.32A**.

**Scheme 251. Bis-cyclometalated Rhodium (III) Complex Catalyzed Asymmetric Synthesis of 1,4-Dicarbonyl Compounds.**

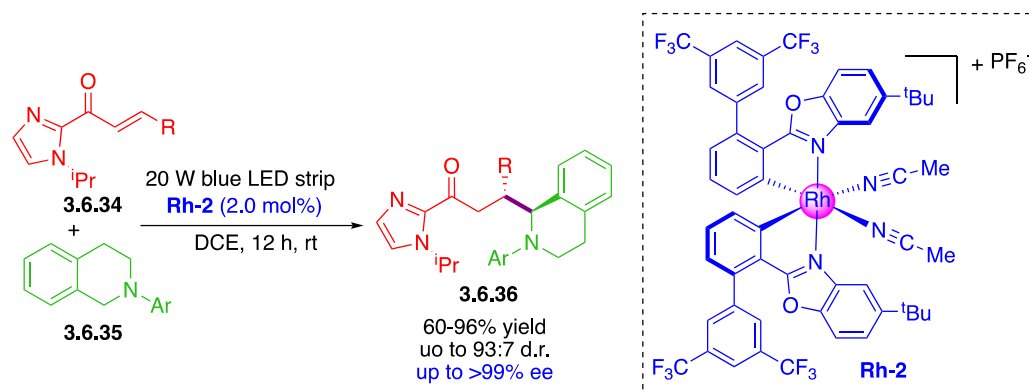


Kang and co-workers described an enantioselective intermolecular Michael addition of photogenerated  $\alpha$ -amino radicals which was generated from *N*-aryl tetrahydroisoquinolines **3.6.35** to Michael acceptors **3.6.34** catalyzed by a chiral-at-metal rhodium complex  **$\Lambda$ -Rh-2**, affording the Michael adducts **3.6.36** in good yields with excellent enantioselectivities (Scheme



239).<sup>484</sup> the rhodium complex  $\Lambda$ -Rh acts as the visible-light-activated photoredox catalyst to control the enantioselectivity during bond formation and also as an excellent chiral Lewis acid which accelerates the radical addition to the Michael acceptors.

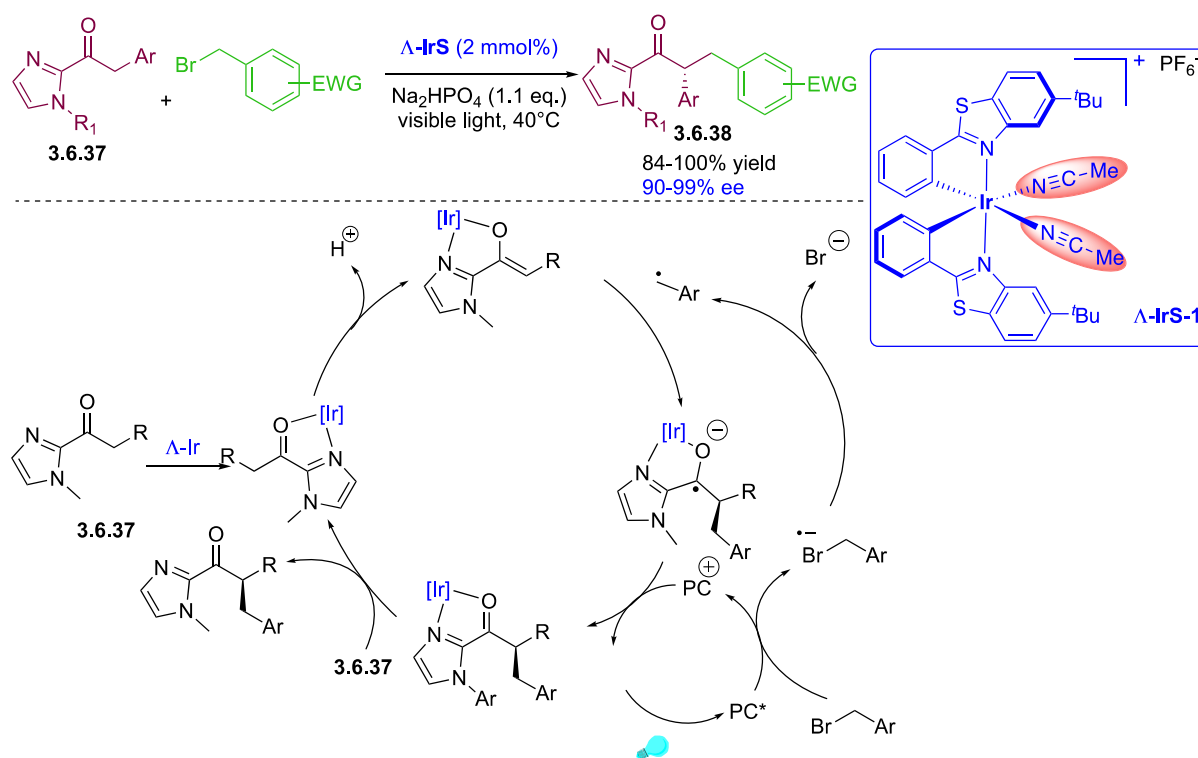
**Scheme 252. Rhodium-catalyzed Asymmetric Conjugate Addition of  $\alpha$ -Amino Radicals with Michael Acceptors**



An iridium photosensitizer could also activate the production of radicals efficiently. Several reviews have summarized emerging strategies of photoredox processes where iridium is involved.<sup>412,485</sup> Analogous mechanism to rhodium and ruthenium could be involved, upon photoexcitation depending on the nature of the quencher, oxidative or reduction radical transformation could then be triggered in the catalytic cycle.

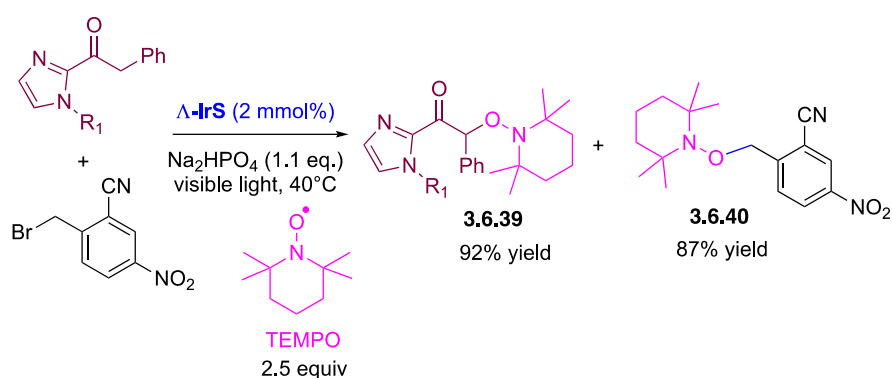
Before reporting rhodium catalysts, Meggers has developed configurationally stable (chiral at metal) iridium catalysts possessing two bidentate benzoxazoles in 2014.<sup>486</sup>  $\Delta$ -configured catalysts with right-handed propeller and  $\Lambda$ -configured ones with the opposite configuration were synthesized in enantiomerically pure form. They provided excellent catalytic asymmetric  $\alpha$ -alkylations of ketones. Interestingly, this strategy allows enantioselective alkylation of acylimidazole by benzyl bromide derivatives. Upon photoredox formation of benzyl radical, addition of the latter into the in situ formed enolate is the stereo-determining step. The chiral iridium is therefore playing a double role, as a photocatalyst for the reduction of benzyl bromide and as a Lewis acid that activates the asymmetric addition (Scheme 253).

### Scheme 253. Chiral at Iridium Catalysts for $\alpha$ -Benzylation of Ketones



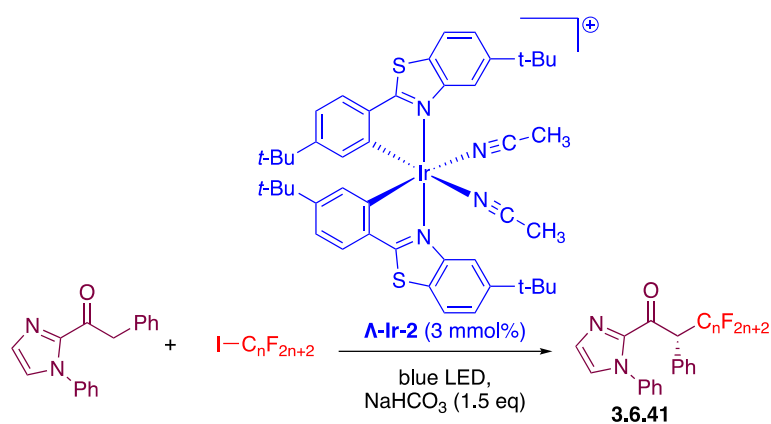
Presence of a radical mechanism was proved by spin-trapping experiments with tetramethylpiperidine-1-oxyl (TEMPO), enabling to identify the two adducts **3.6.39** and **3.6.40** (Scheme 254).

### Scheme 254. Mechanism of $\alpha$ -Alkylation using Iridium Catalysts



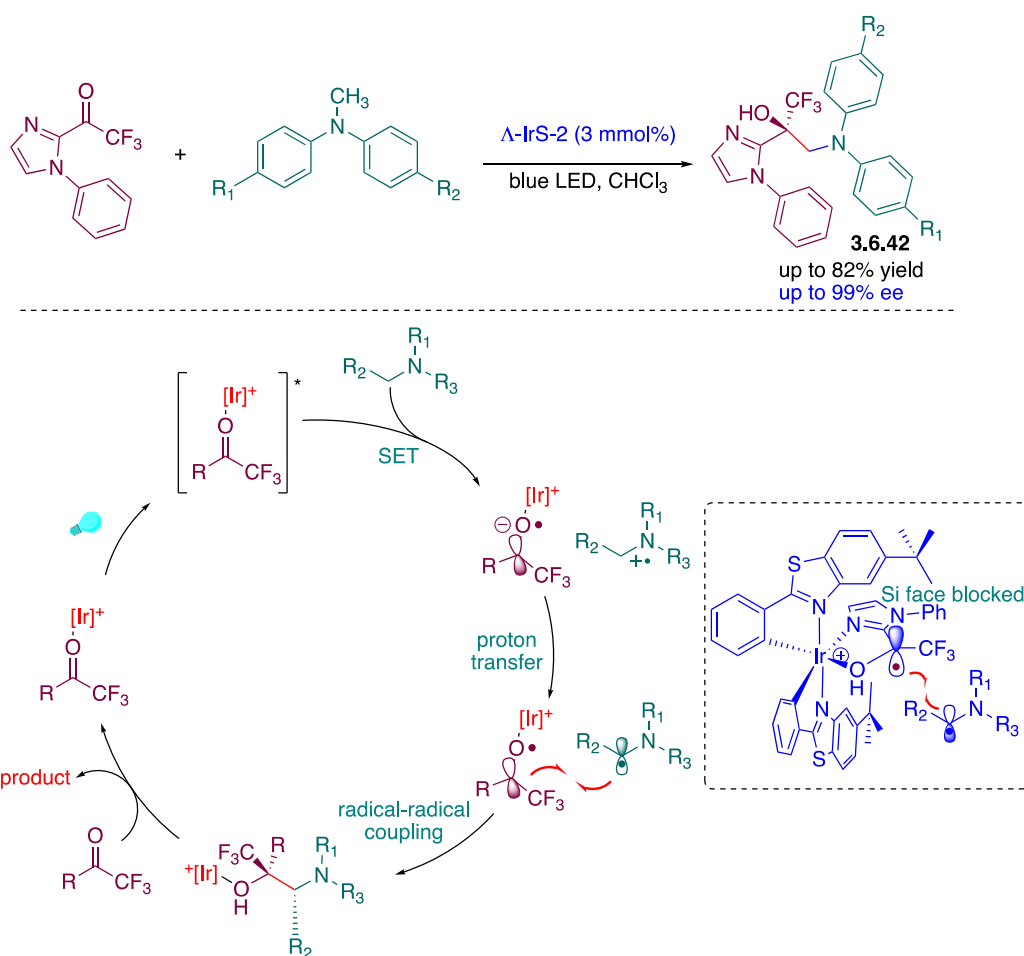
Enantioselective perfluoroalkylation of acylimidazole was also examined by the same authors, providing the products with ee up to 99.5%. In this case, the reaction could still proceed via the combination of a photoredox and electron-catalyzed reaction enabling the formation of the intermediate perfluoroalkyl radicals (Scheme 255).<sup>487</sup>

### Scheme 255. Alkylation of Ketones with Perfluoroalkyl Radicals



In 2016, Meggers and coworkers developed a stereocontrolled radical-radical cross-coupling reaction promoted by visible light and involving a SET between two substrates.<sup>488</sup> Especially, Meggers focused on the radical coupling of trifluoromethyl ketones acting as electron acceptors with tertiary amines acting as electron donors, furnishing 1,2-aminoalcohols. Enantioselectivity is strongly controlled by the chiral environment generated by the iridium complexes and the different experiments revealed  $\Lambda$ -IrS to provide higher reaction yields and enantioselectivities than  $\Lambda$ -IrO. Control experiments also revealed the weak influence of the solvents on stereoselectivity. Satisfactory yields and high enantioselectivities were obtained for the aminoalkylation of trifluoromethyl ketones with various *N*-methyl diarylamines (Scheme 256). Interestingly, the mechanism is related to the use of a photoredox catalysts  $\Lambda$ -IrS that is capable upon photoexcitation of directing a single electron transfer from the electron-rich diarylamine to the catalyst-bound electron-deficient trifluoromethyl ketones. Following the SET, an enantioselective radical-radical cross-coupling controlled by the chiral environment of the propeller-type iridium complex can occur, furnishing the 1,2-aminoalcohol product. To support the excellent stereochemical control of the reaction, steric hindrance of the prochiral Si face of the iridium-coordinated ketyl radical provided by the *tert*-butyl group was suggested, offering a unique opportunity for stereoselectivity.

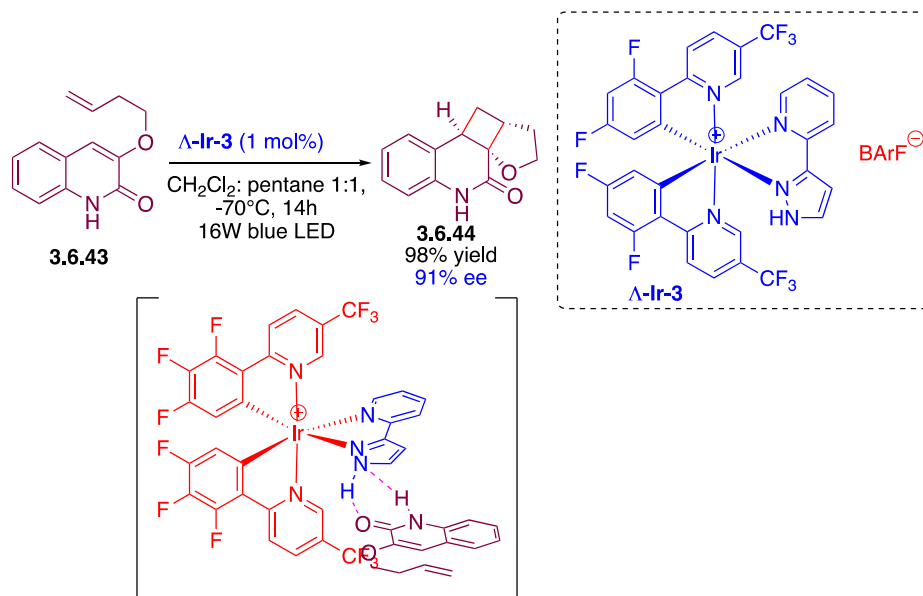
**Scheme 256. Stereocontrolled Radical-radical Cross-coupling Reaction Promoted by Visible Light**



To close this section, we will discuss the two last examples sealing with cycloaddition reaction using a chiral organometallic triplet sensitizer. Stereocontrol in catalytic systems is a longstanding issue and one of the easiest ways to accomplish this is to combine a photoredox catalyst with a stereocontroller or to use a chiral organometallic triplet sensitizer with prochiral substrates. This strategy was notably developed for the [2 + 2] photocycloaddition of quinolones **3.6.43** capable of efficiently binding to **PC1.BArF** by means of hydrogen bonds.<sup>489</sup> By optimizing the design of the triplet sensitizer, an enantiomerically pure iridium complex could be obtained and act as an efficient sensitizer. Careful selection of the ligands also enabled **PC1.BArF** to efficiently bind to the quinolone substrate via hydrogen bonds but also to orient the substrates, ensuring high enantioselectivities in the formation of **3.6.44** (Scheme 257). High

enantioselectivities could be obtained for loading as low as 0.1 mol% for the chiral triplet sensitizer. This is an original strategy considering that  $\pi$ - $\pi$  interactions and hydrogen bond formation is exploited for getting the desired enantioselectivity rather than a direct inner-sphere substrate-catalyst association. Therefore, in this strategy, **PC1.BArF** plays a dual role as both chiral Lewis acid and photoredox catalyst. Examination of various ligands also revealed the pyridylpyrazole ligand by its NH group to be sufficient for inducing enantioselectivity. Hydrogen bonding between **PC1.BArF** and the substrates was integral to obtain selectivity, and an improvement of the enantioselectivity while reducing the hydrogen-bonding ability of the solvent was also demonstrated. A Dexter energy transfer mechanism between the photocatalyst and the substrate was also determined as the photoactivation pathway, therefore requiring a proximity between the catalyst and the substrate.

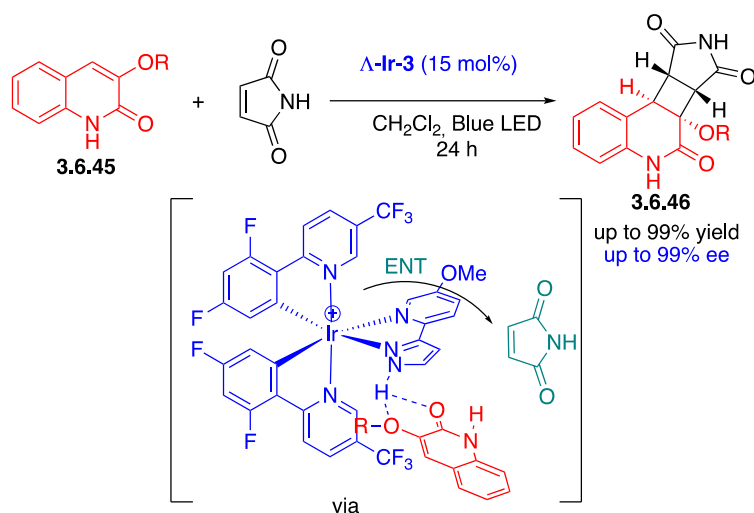
#### Scheme 257. [2+2] Cycloaddition using Chiral at Metal Lewis Acid



Recently, the concept of substrate sensitization by a triplet sensitizer capable of forming hydrogen bonds with the substrate, was extended to the enantioselective intermolecular [2 + 2] cycloaddition of 3-alkoxyquinolones **3.6.45** and maleimides.<sup>490</sup> By a preferred sensitization of maleimide, the excited maleimide could react with the hydrogen-bonded quinolone, enabling the formation of the enantioenriched cycloadduct **3.6.46** (Scheme 258). Enantioselectivities as

high as 99% ee were obtained for reactions involving a wide range of maleimides and electron-deficient alkenes. Especially, bidentate hydrogen-bonding interaction prevents quinolones to initiate a direct inner-sphere substrate–catalyst association and enforce the Dexter energy transfer between the coordinated quinolones and maleimides to occur.

#### Scheme 258. Intermolecular [2+2] Photocycloaddition using Chiral at Metal Lewis Acid



Lewis acid catalyzed conjugate addition of  $\alpha$ -amino radicals has been reported by Yoon and co-workers by using ruthenium as a photocatalyst and chiral scandium used as Lewis acid (Scheme 101, section 2.2.2).<sup>188</sup> Such radicals, when formed with iridium photocatalyst in the presence of Michael acceptor and chiral oxazaborolidium, affords enantioselective 1,2-addition instead of 1,4-addition. In this latest work from the Ryu group, visible-light dual catalysis provides enantioenriched  $\beta$ -amino functionalized alcohols.<sup>491</sup>

## 4. Enzyme-Catalyzed Radical Reactions

After a long period of lack of interest from organic chemists, biocatalyzed organic transformations have gained increasing applications since enzymes present several advantages.<sup>492</sup> A better understanding of mechanisms in addition to enzyme engineering which offers a broad range of applications, has finally convinced chemists that this area of research is promising.

One of the under-explored topics is the association of radicals with biocatalysts even though numerous radical processes play a major role in living organisms.<sup>493</sup> Biocatalyzed reactions involving radical species are even scarce. The advent of photoradical chemistry opened a route for developing photoenzymatic catalysis with an enormous potential.<sup>494</sup>

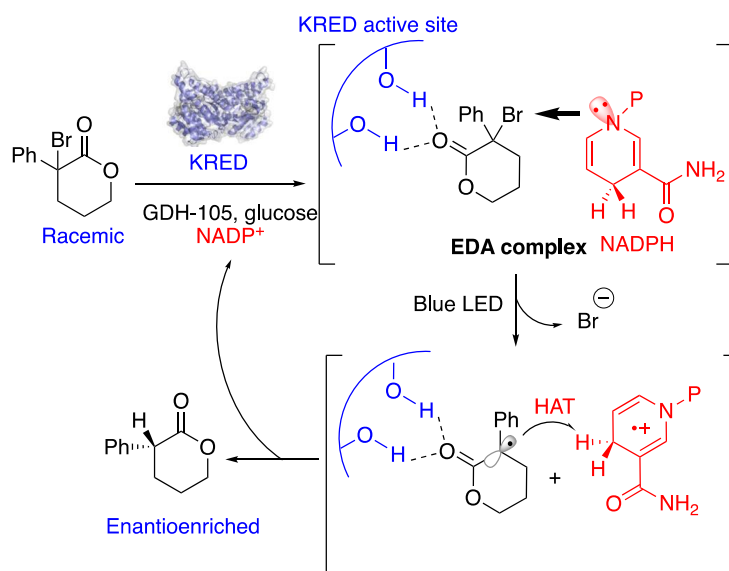
One of the first report on the association of enzymes and radicals was on dynamic kinetic resolution of amines by Gil and Bertrand.<sup>495</sup> They reached (*R*)-enantioenriched amines with photogenerated thyl radical mediated racemization combined with CAL-B lipase. The (*S*)-enantioenriched amines could be accessed with proteases using analogous racemization.<sup>310</sup>

In 2016, Hyster reported a new process for enantioselective radical dehalogenation of lactones assisted by light.<sup>496</sup> The originality of this strategy is the non-natural SET induced in the active site thus opening up new windows for radical reactions. Photoexcited nicotinamide adenine dinucleotide phosphate (NADPH, generated in the enzyme active site from NADP<sup>+</sup>) serves as a single electron reductant ( $E^*_{\text{ox}} = -2.6 \text{ V}$ ) and also as a HAT source (Scheme 246). The idea was to take advantage from the promiscuity of the enzyme active site and the photoreductant co-factor in order to induce enantioselective HAT from the organic substrate. NADPH, the active cofactor, could be regenerated from glucose dehydrogenase (GDH-105) and glucose, thereby rendering the reaction catalytic both in enzyme and NADP<sup>+</sup>.

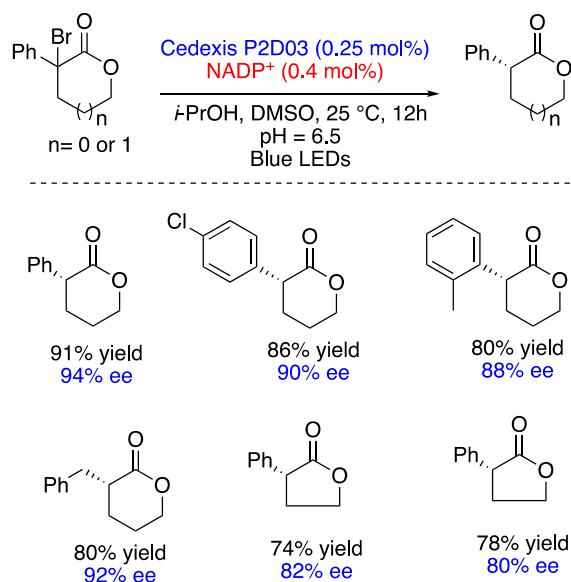
The Hyster group started their investigations using racemic  $\alpha$ -bromo- $\alpha$ -aryl lactones using commercially available ketoreductase (KRED). Interestingly, a mixture of the substrate/KRED/NADPH is responsible for the formation of colored EDA complex that is able to absorb blue light. Irradiation of the EDA complex within the enzyme active site results in charge transfer excitation followed by mesolytic cleavage of the C—Br bond (Scheme 259). Hydrogen atom transfer inside the active site (assisted by hydrogen bond interactions) from the prochiral radical evolves enantioselectively to product with high control of stereochemistry. Modeling studies confirmed the existence of hydrogen bonding interactions between tyrosine

and serine residues of the active site and the lactone moiety. These interactions are not only crucial for stereocontrol but they also alter redox potential. The authors have also demonstrated that the bromolactone substrate is not involved in a kinetic resolution process.

### Scheme 259. Photoexcited NADPH in Enantioselective Radical Reductions



### Scheme 260. Stereodivergent Reduction with Different Enzymes

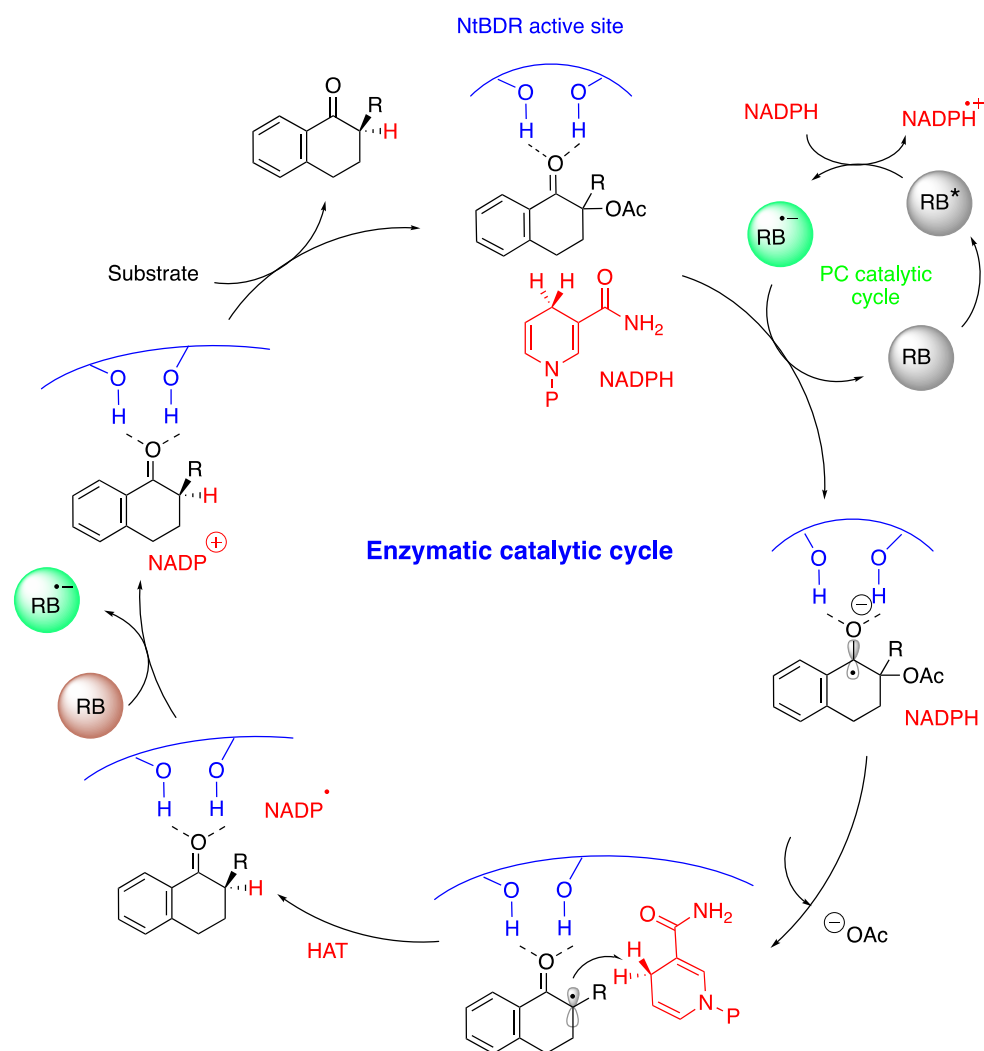


The authors demonstrated the stereodivergency of the process depending on the nature of the reductase used. Codexis KRED-12 delivers the (*R*)-enantiomer (81% yield and 96% ee) whereas LKADH variant dehydrogenase led to the formation of the (*S*)-enantiomer (76% yield



and 92% ee) (Scheme 260). The substrate scope of this reaction was demonstrated by varying the structure of  $\alpha$ -halo- $\alpha$ -aryl lactones. Using chloro- or bromolactones afforded similar yields and selectivities for different lactones. A variety of  $\delta$ -valerolactones and  $\gamma$ -butyrolactones were obtained in good yields and high ee's.

### Scheme 261. Redox Activation for Biocatalyzed Deacetoxylation

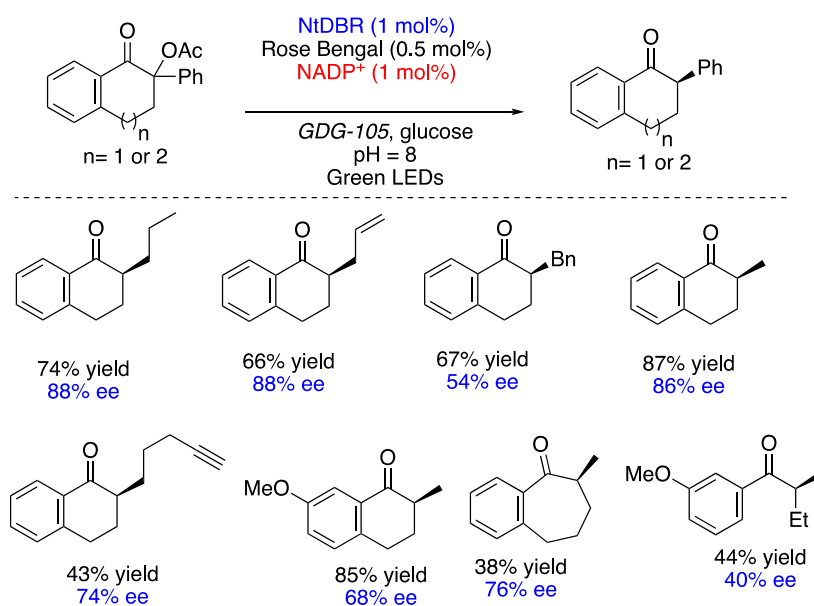


Subsequent to this work, the same group devised a redox activation for biocatalyzed radical deacetoxylation of tetralones.<sup>497</sup> Again, the hydrogen bonding association in the nicotinamide-dependent double bond reductase (DBR) enzyme is responsible for activation of the system. In this report, the addition of organic dye, Rose Bengal (RB) photocatalyst, is compulsory to

engage, after photoexcitation, a SET with NADPH to afford  $RB^{\bullet-}$  (Scheme 261). This radical anion can reduce the tetralone substrate generating a ketyl radical. The loss of acetate delivers the substrate derived prochiral radical that evolves to the product after hydrogen atom abstraction from NADPH in a way analogous to KRED mechanism discussed above.

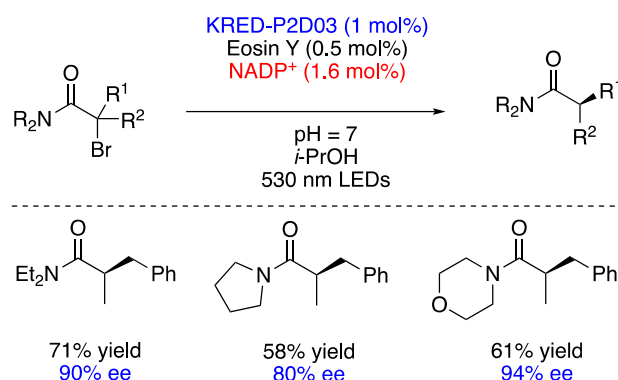
Examination of the substrate scope revealed that this enantioselective radical deacetoxylation is effective with variously substituted tetralones including allyl, alkyl, benzyl, as well as bulky isopropyl group. However, switching from six to seven-membered substrate diminished both reactivity and stereoselectivity. Another limitation resides in the use of acyclic ketone substrates where low yields and ee's were obtained (Scheme 262).

### Scheme 262. Substrate Scope in Enantioselective Radical Deacetoxylation



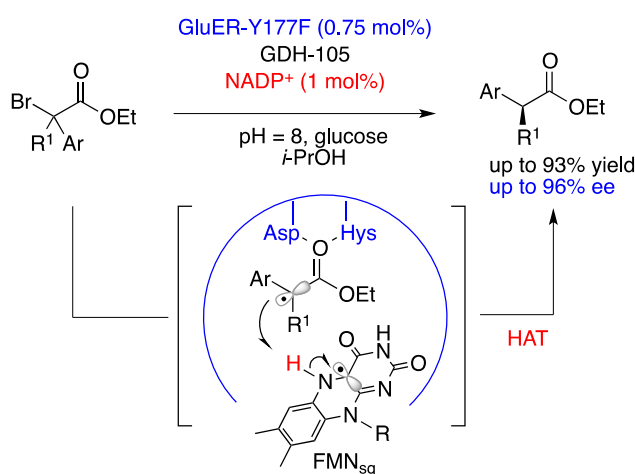
Limitation to the methodology is that  $\alpha$ -bromo esters are not reactive under the previously discussed KRED-conditions, they need to be converted to  $\alpha$ -bromo amides in the presence of Eosin Y to give acceptable yields and ee's (Scheme 250).

### Scheme 263. Reduction of $\alpha$ -Bromo Amides using Eosin Y and a Biocatalyst



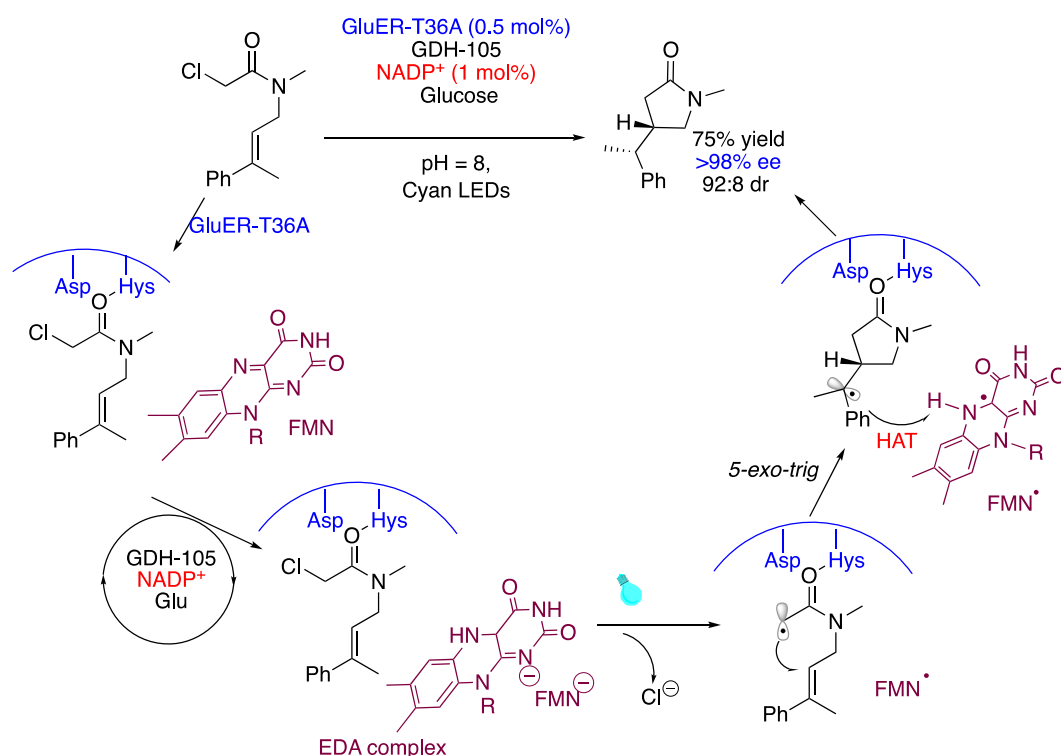
In contrast to lactones, acyclic esters do not form the EDA complex required for SET to occur and the reason on their non-reactivity. To address this limitation, Hyster group selected flavin-dependent ‘ene’-reductases. The flavin would then act as a single electron reductant and ultimately as a hydrogen atom source. They developed a novel protocol using flavin hydroquinone (FMN<sub>hq</sub>) as the co-factor and *Gluconobacter* mutant (GluER-Y177F) that is capable of directly reducing  $\alpha$ -bromo esters with no more requirement for photoactivation (Scheme 264). After a redox pathway and mesolytic cleavage of the C–Br bond, hydrogen atom abstraction occurs from the *Si* face from the resulting semiquinone (FMN<sub>sq</sub>). This enantiocontrol is once again governed by H-bonding from amino acids residues: asparagine and histidine in this case; in the HAT process H atom is delivered opposite to these residues.<sup>498</sup>

### Scheme 264. Reduction of $\alpha$ -Bromo Esters using Flavin-dependent Ene Reductases



Extension of this strategy to stereoselective radical cyclization was disclosed in 2019.<sup>499</sup> The flavin-dependent ‘ene’-reductase under cyan LEDs irradiation enables the construction of five-, six-, seven- and eight-membered heterocyclic lactams in an enantioselective cyclization and diastereoselective HAT. Although the cyclization of  $\alpha$ -chloroamides is well documented, their catalyzed enantioselective reactions are scarce. This challenging transformation was achieved by exciting the FMN<sub>hq</sub> that is able to accomplish SET with  $\alpha$ -chloroamides releasing the electron-deficient  $\alpha$ -amidyl radical (Scheme 265). Subsequent cyclization assisted stereochemically by H-bonding interaction with enzyme active site allows the enantioselective construction of the heterocycle. Contiguous stereocenters are established during the hydrogen atom abstraction step favored by the enzymatic H-Bonding.

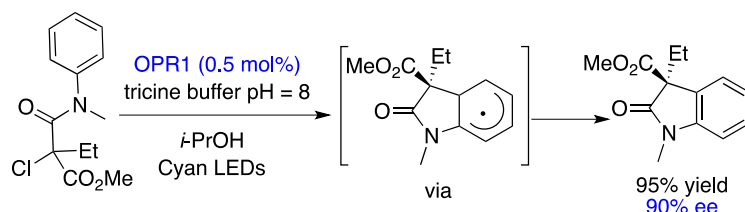
### Scheme 265. Enantioselective Radical Cyclization using $\alpha$ -Chloroamides



The Hyster applied this strategy to access chiral oxindoles from racemic  $\alpha$ -chloroamide using OPR1 enzyme. In this case, benzene is the radical acceptor (Scheme 266).<sup>500</sup>

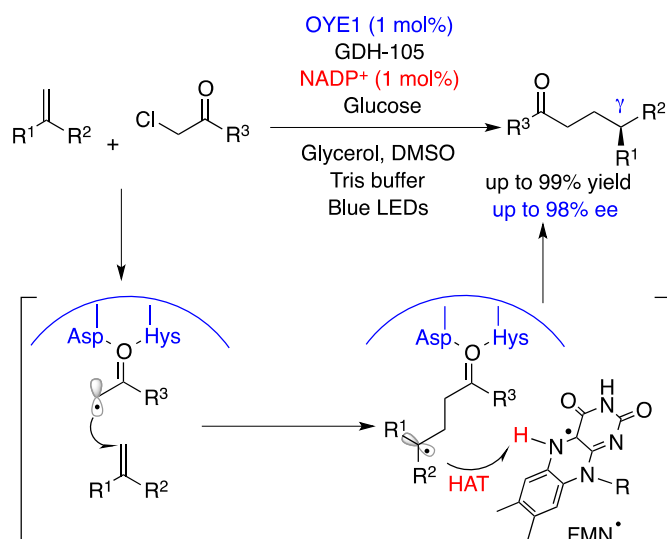
## Scheme 266. Synthesis of Chiral Oxindoles from Racemic $\alpha$ -Chloroamide using OPR1

### Enzyme



Challenging intermolecular version of this reaction was reported recently by another group.<sup>501</sup> Photoinduced enzyme catalyzed radical addition was achieved by Zhao and co-workers. The remote stereocontrol that offers the enzymatic amino-acids residues is particularly efficient in the formation of chiral ketones and amides with 'ene'-reductase OYE1 (Scheme 267). Terminal alkyls possessing aryl, heteroaryl and propargyl groups were mandatory for the formation of stabilized radical upon radical addition of  $\alpha$ -halocarbonyl radical. The latter is formed through a photoredox process identical to the one proposed in Hyster's work. When achiral  $\alpha$ -halocarbonyl substrates were used, excellent yields and ee's were observed. However, when racemic chiral substrates were engaged, the diastereoselectivity was poor.

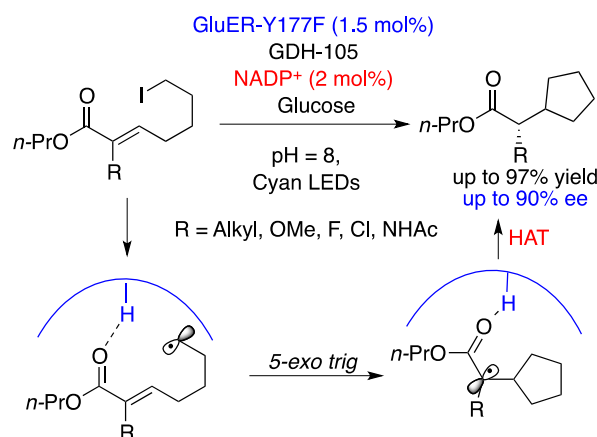
## Scheme 267. Synthesis of Amino Acids by Biocatalysis



In the previous example, the generation of stabilized  $\alpha$ -acyl radical was the driving force for the enzymatic photoreduction of the substrate. However, the formation of unstabilized radicals

using the same protocol seems more challenging. Intramolecular Giese radical cyclization was attempted by exploring alkyl iodide bearing radical Michael acceptor. These substrates were found to be excellent candidates for forming charge transfer complex within the enzyme cavity.<sup>502</sup> This allows for photo-induced reduction of alkyl iodide delivering nucleophilic radical that is trapped intramolecularly by the tethered electrophilic alkene (Scheme 268). The stereodetermining step remains the HAT from FMN inside the chiral cavity of the EREDs enzyme. While *5-exo-trig* cyclization afforded good yields and ee's, the *6-exo-trig* pathway gave modest enantiocontrol.

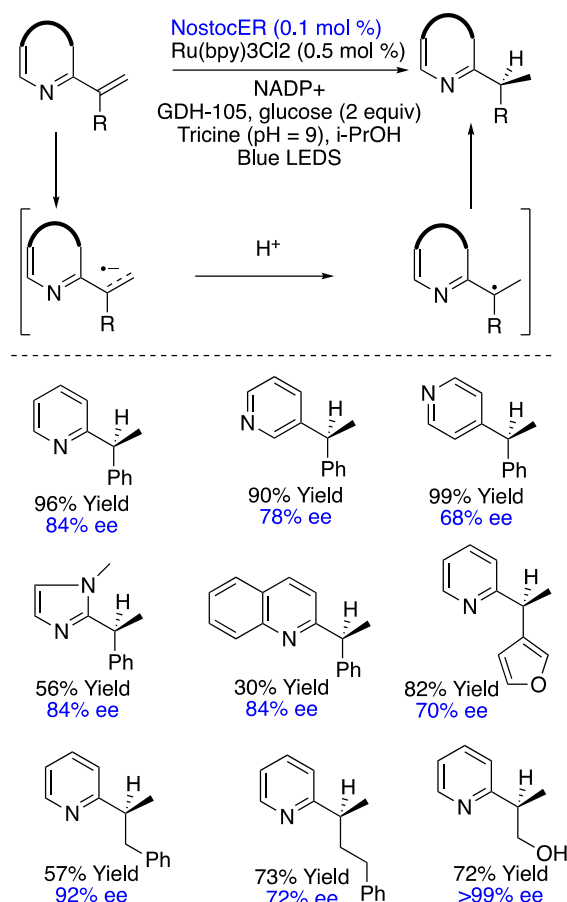
### Scheme 268. Intramolecular Giese Reaction using Biocatalysis



It was previously discussed that photo-organocatalysis is able to initiate the formation of radical anion, however, with modest enantioselectivity.<sup>149</sup> In 2020, Hyster group succeeded in this task using EREDs enzymes through a reductive generation of such species followed by protonation and enantioselective HAT.<sup>503</sup> The use of ortho-substituted vinyl pyridine motif was essential for the stereocontrol since it offers a H-bonding possibility. This merging photoredox and enzyme catalysis is a promising method for reduction of heteroaromatic olefins since a broad range of disubstituted groups are tolerated yielding the hydrogenated products with good to excellent enantioselectivities. In the optimized reaction conditions, Ru(bpy)<sub>3</sub>Cl<sub>2</sub> was used as a photocatalyst and NostocER as a biocatalyst (Scheme 269). Mechanistic experiments, including

deuterium labeling, DFT docking and radical clock reactions, suggest that radical pathway occurs via HAT from flavin within the enzyme active site.

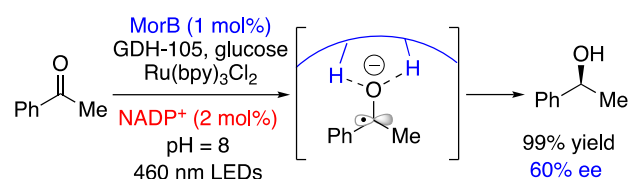
### Scheme 269. Merging Photoredox and Enzyme Catalysis for Reduction of Heteroaromatic Olefins



In 2018, Hartwig and co-workers reported a cooperative photocatalyzed isomerization of alkenes followed by their 'ene'-reductase reduction to obtain enantioenriched compound. However, the mechanism for this transformation has not been discussed.<sup>504</sup>

Flavin-dependent EREDs using light activation with Ru(bpy)<sub>3</sub>Cl<sub>2</sub> was also the method of choice developed by Hyster group to access enantioenriched alcohols.<sup>505</sup> Photoenzymatic reduction of acetophenone, upon formation of ketyl radical and HAT process, was achieved performing the reaction in the presence of MoRB enzyme and NAD<sup>+</sup> cofactor delivering benzylic alcohol with modest ee (Scheme 270). The synergistic catalysis of Ru and EREDs under light irradiation was essential for the reaction to proceed.

### Scheme 270. Photoenzymatic Reduction of Acetophenone



Enantioselective synthesis of mercapto-functionalized secondary alcohols was reported by Castagnolo and co-workers through a photo-biocatalytic approach.<sup>506</sup> Under visible light, photogeneration of thyl radical, thanks to ruthenium photocatalyst, allows a 1,4-addition a Michael acceptor delivering  $\alpha$ -carbonyl radical. A subsequent reduction of the latter followed by KRED ketone reduction delivers the enantiopure alcohol. The *R*- and *S*-selectivity could be reached by KRED-311 and KRED-349, respectively (Scheme 271).

### Scheme 271. Enantioselective synthesis of mercapto-functionalized alcohols

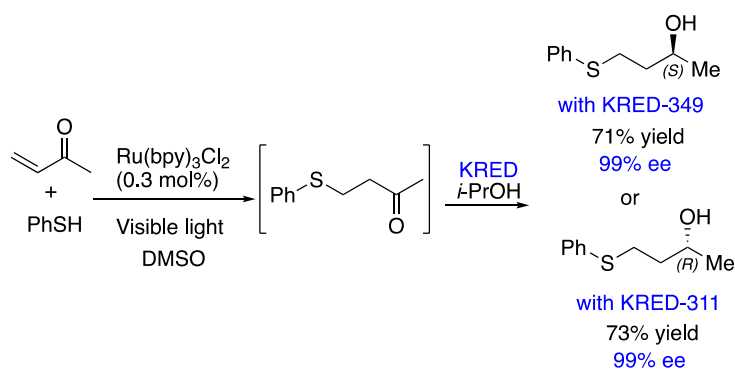


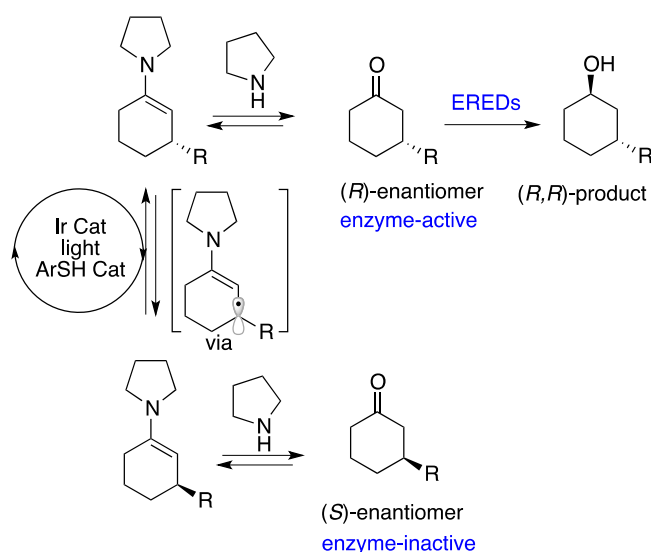
Photo-decarboxylative hydroxylation of carboxylic acid to reach chiral benzylic alcohols has been reported by Wu using sodium anthraquinone sulfonate as a photocatalyst and carbonyl reductase.<sup>507</sup>

In 2013, MacMillan reported a direct  $\beta$ -coupling of cyclic ketones through a merged photoredox catalysis and organocatalysis. In this formal  $\beta$ -Mannich reaction, only racemic compounds were investigated.<sup>57</sup> The mechanism involves a transient  $\beta$ -enaminy radical. An asymmetric version of this strategy is challenging with organocatalyst because of the distal stereocontrol limitation. MacMillan and Hyster groups have combined their expertise to introduce an elegant Dynamic Kinetic Resolution of such substrates when subjected to EREDs reduction (Scheme 272).<sup>508</sup>



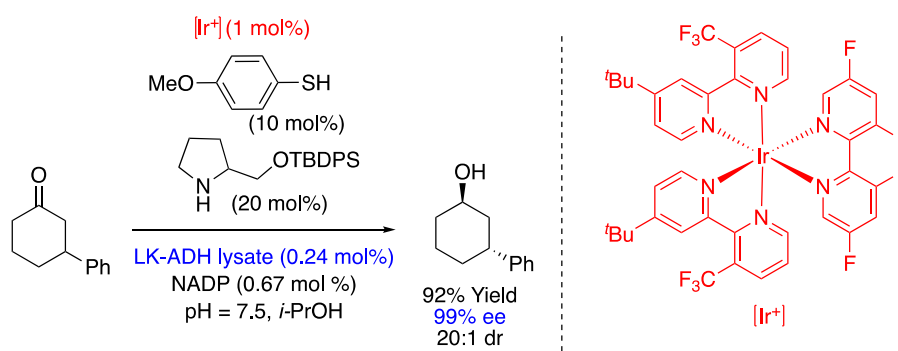
The thought was to explore the formation of prochiral  $\beta$ -enaminyll radical from racemic  $\beta$ -substituted cyclic ketones and amine catalyst in the presence of iridium photocatalyst. The presence of thiol catalyst would allow the regeneration of the substrate through HAT. This photoredox catalyzed stereo-ablative process will act as a permanent dynamic racemization of the substrate while associated to a chemoenzymatic reductive kinetic resolution of  $\beta$ -substituted cyclic ketone to furnish  $\beta$ -substituted alcohol.

### Scheme 272. Enantioselective Functionalization of the $\beta$ -Carbon of Ketones



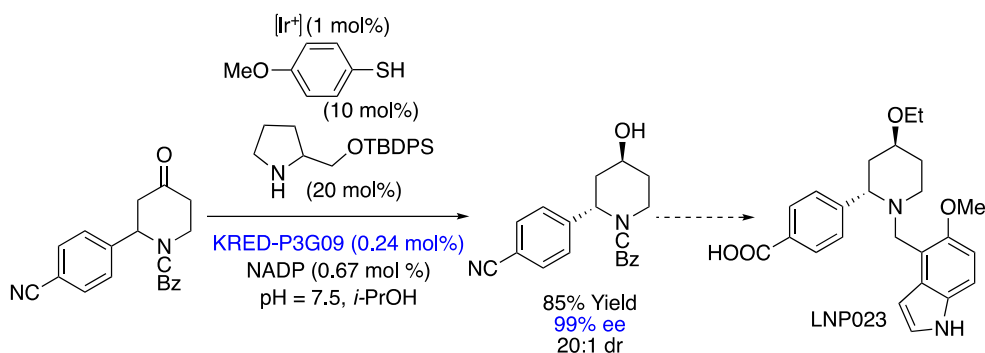
It is important to mention that the product is inert to these racemization conditions which makes this route viable to furnish enantioenriched products. Indeed, this sophisticated protocol utilizes four catalysts including the enzyme in a synergetic manner delivering the desired product in high yield, excellent enantio- and diastereoselectivity (Scheme 259).

### Scheme 272. Four Catalysts in Action. Functionalization of $\beta$ -Carbon of Ketones



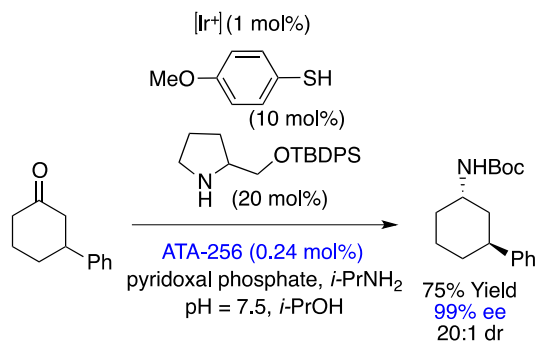
The authors have shown the utility of their strategy by developing a formal synthesis of Novartis drug candidate LNP023. The precursor was obtained with 99% ee and 20:1 dr using KRED-P3G09 enzyme (Scheme 274).

#### Scheme 274. Formal Synthesis of Novartis Drug Candidate LNP023



Replacing the EREDs by aminotransferase in the presence of pyridoxyl phosphate, the Hyster group also developed the synthesis of enantioenriched amines demonstrating the versatility of this methodology (Scheme 275).

#### Scheme 275. Synthesis of 1,3-Disubstituted Cyclohexanes by a Biocatalytic Strategy



## 5. Conclusion and outlook

This review detailed enantioselective radical chemistry from its exciting beginning to where we are today, a very hot area of science. Enantioselective radical chemistry has seen spectacular growth. This review has comprehensively covered progress made in the past two decades. The exponential growth in enantioselective radical reactions can be attributed to the development of new chiral activators and the use of photochemistry. The early phase of enantioselective

radical chemistry relied heavily on the use of tin reagents and only a modest number of radical initiators. The current surge in enantioselective radical chemistry has significantly benefited from new methods for generating radicals. Chiral Lewis acids played an important role in the early development of radical reactions. In the past two decades, a variety of organocatalysts including H-bond activators have been widely utilized. Transition metal mediated radical processes have also been investigated extensively. The impact of photoredox on radical chemistry, especially, the combination of photoredox and organocatalysis continues to make a huge impact on the development of enantioselective radical reactions.

A variety of transformations have been discovered during the past two decades and a majority of them involve functionalization of aldehydes and ketones using aminocatalysis. Thus, these reactions are complementary to enolate functionalization. However, radical reactions allow for reaction partners such as alkenes which are not generally compatible with enolate intermediates. Enantioselective radical reactions which allow for the formation of C-C and C-X bonds have been developed and extended to the synthesis of carbo- and heterocycles. Several of these transformations allow for the establishment of hindered chiral centers, a distinctive feature of radical reactions. Many of the radical reactions developed in the early part of this journey required metal additives. The development of metal-free reactions required a proper combination of organocatalysts and photoinitiators. Similar to enantioselective radical reactions discovered in the 1990's, many of the metal-free reactions proceed via a chain mechanism. Another unique transformation discussed in this review is the direct functionalization of the  $\beta$ -carbon of ketones. This has been achieved by a clever combination of light and an organocatalyst. In the early development of enantioselective radical reactions, conjugate radical addition, a.k.a. the Giese reaction, was investigated extensively. Several variants of organocatalyst mediated Giese reactions have been developed including transformations which

provide access to all carbon quaternary centers. This type of transformation has been extended to the synthesis of acetate aldols and the formation of contiguous chiral centers.

The discovery and development of H-Bonding catalysts has had a significant impact on asymmetric synthesis. In the arena of enantioselective radical chemistry, weak H-bonding compounds such as imides derived from Kemp's triacid, chiral thioureas, and strong H-bonding chiral phosphoric acids (Brønstead acids) have had a significant impact on the development of enantioselective radical reactions. Control of absolute stereochemistry during photochemical cycloadditions has been challenging. A variety of enantioselective inter- and intramolecular cycloadditions proceeding via radical intermediates have been developed using H-bonding catalysts. The review also details chiral Lewis acid mediated photochemical [2+2] cycloadditions and cycloadditions using a combination of photoredox and chiral Lewis acid catalysts.

Chiral Brønstead acids are now considered as a privileged class of catalysts for a variety of asymmetric transformations. They have also played an important role in the development of enantioselective radical reactions. The review includes several reactions in which the  $\alpha$ -carbon of carbonyl compounds are functionalized using chiral Brønstead acid activators. Examples of enantioselective Minisci reactions by a merger of photoredox and chiral Brønstead acids are also included.

The successful and creative use of transition metals to carry out radical reactions can be considered as a major advance in the field of asymmetric synthesis. The review details the use of several transition metals in the development of a variety of useful transformations. It is interesting to note that a particular transition metal is well suited to carry out a certain type of reaction more efficiently than another metal. Furthermore, the chiral ligands associated with these metals are also different. The number of enantioselective radical reactions which use iron,

chromium or manganese is rather small. A majority of these reactions are oxidations. The use of titanium in radical reactions is well explored. A main feature of radical chemistry with titanium involves ring opening reactions of three membered rings, epoxides and cyclopropanes. The concept of Metalloradical Catalysis has been introduced using cobalt. In contrast to titanium, reactions using cobalt centered radical are mainly for the formation of cyclopropanes and aziridines. Thus, these reactions are complimentary to the synthesis of three-membered ring using carbenes or nitrenes. Metalloradical catalysis has also been used in C-H activation reactions leading to the formation of heterocycles where a new C-N is formed. Two metals which have found extensive use in radical chemistry are earth-abundant nickel and copper, a step in the right direction with respect to sustainable chemistry. The activation of electrophiles by Ni can proceed either by two-electron oxidative addition to give organonickel intermediates ( $Csp^2$ -X derivatives) or by single electron transfer to afford alkyl radicals ( $Csp^3$ -X derivatives). These nickel intermediates are well-suited for a variety of enantioselective cross-coupling reactions and several examples have been discussed in the review. Nickel catalysts as chiral Lewis acids in combination with photoredox initiators have been investigated for the development of enantioselective radical reactions. Copper has played an important role in the evolution of radical chemistry since the 1950's. Early enantioselective radical chemistry took advantage of the Lewis acidic properties of Cu(II) complexes. Another property of copper which has been extensively utilized in the recent past is the redox properties of Cu(I)/Cu(II) couple to generate and functionalize radicals. Copper catalysts have been used to generate allylic or benzylic radicals by either H-atom or halogen abstraction and subsequent enantioselective trapping of the radical intermediate. An alternate way of generating intermediate radicals is by addition of an electrophilic radical to a terminal alkene. This is followed by trapping with a variety of reagents and several examples of these types of enantioselective radical reaction were discussed. Chiral-at metal Lewis acid catalysts with

rhodium and iridium as the metal are interesting dual catalysts and can be considered as a significant discovery. These catalysts activate the substrate as well have the ability to generate the required radical under photoredox conditions. A variety of enantioselective reactions have been developed using these catalysts including  $\alpha$ - and  $\beta$ -alkylations,  $\alpha$ - and  $\beta$ -aminations, conjugate additions,  $\beta$ -C-H functionalization, and photocycloadditions demonstrating the broad utility of dual catalysis. For majority of the transformations discussed in this review we have provided mechanistic details as well information on the catalytic cycle such that the reader can appreciate the level of complexity involved as well as how the scientists have used their ingenuity to develop these interesting reactions.

Numerous radical processes play a major role in living organisms. Reports on enantioselective radical reactions mediated by enzymes have been sparse. There has been increased interest recently and several examples of enzyme-mediated enantioselective reactions have been reported. The final section of the review describes how enzymes in combination with light or photoredox catalysts can be cleverly used to develop a variety of enantioselective radical transformations.

In the past two decades we have seen an exponential growth in the development of enantioselective radical reactions. However, there are still many unmet challenges. The catalyst loading of the chiral activator in most of the reported reactions are still high and the reaction times are relatively long. Thus, the discovery of reactions which can be carried out using low catalyst loading together with a significant increase in both TON and TOF are important. The stereo determining step in majority of the reactions are with electron poor acceptors and nucleophilic radicals. It will be of significance if one can reverse this combination and develop reactions where stereochemistry is established during the addition of an electrophilic radical to an electron rich acceptor. Currently, only a limited number of H-atom or proton donors are efficient and compatible in photoredox reactions and identification of other alternates will be

highly beneficial. Of the different types of chiral activators investigated thus far, NHC carbenes and thioureas have seen limited use and development of new radical reactions using them will be worthy of pursuit. It is evident from the large number of examples presented in this review that the field of enantioselective radical chemistry is maturing rapidly and can now effectively compete with ionic chemistry for installation of stereochemistry. In general, radical chemistry complements ionic chemistry and at times has its own unique qualities. The future looks very bright for new and useful discoveries in asymmetric radical chemistry and achieve indispensability as a technique for bond construction in organic synthesis.

---

<sup>1</sup> Luo, Y.-R. *Comprehensive Handbook of Chemical Bond Energies*, 1st ed.; CRC Press, 2007. <https://doi.org/10.1201/9781420007282>.

<sup>2</sup> For silicon-centered radicals, see: Tumanskii, B.; Karni, M.; Apeloig, Y. *Encyclopedia of Radicals in Chemistry, Biology, and Materials*; Chatgililoglu, C., Studer, A., Eds.; John Wiley & Sons: Chichester, West Sussex; Hoboken, N.J, 2012.

<sup>3</sup> For boryl radicals, see: Rosenthal, A.; Mallet-Ladeira, S.; Bouhadir, G.; Bourissou, D. Persistent P-Stabilized Boryl Radicals with Bulky Substituents at Boron. *Synthesis* **2018**, 50 (18), 3671–3678. <https://doi.org/10.1055/s-0037-1610151>.

<sup>4</sup> Griller, D.; Ingold, K. U. Persistent carbon-centered radicals. *Acc. Chem. Res.* **1976**, 9, 13–19. <https://doi.org/10.1021/ar50097a003>.

<sup>5</sup> Hicks, R. G. What's new in stable radical chemistry? *Org. Biomol. Chem.* **2007**, 5, 1321–1338. <https://doi.org/10.1039/B617142G>

<sup>6</sup> Chen, Z. X.; Li, Y.; Huang, E. Persistent and Stable Organic Radicals: Design, Synthesis, and Applications. *CHEM* **2021**, 7, 288–332. <https://doi.org/10.1016/j.chempr.2020.09.024>

<sup>7</sup> Curran, D. P.; Porter, N. A.; Giese, B. *Stereochemistry of Radical Reactions: Concepts, Guidelines, and Synthetic Applications*, 1st ed.; Wiley, 1995. <https://doi.org/10.1002/9783527615230>.

<sup>8</sup> Amos, S. G. E.; Garreau, M.; Buzzetti, L.; Waser, J. Photocatalysis with organic dyes: facile access to reactive intermediates for synthesis. *Beilstein J. Org. Chem.* **2020**, 16, 1163–1187. <https://doi.org/10.3762/bjoc.16.103>.

---

<sup>9</sup> Vega-PeÇaloza, A.; Mateos, J.; Companyl, X.; Escudero-Casao, M.; Dell'Amico, L. A Rational Approach to Organo-Photocatalysis: Novel Designs and Structure-Property Relationships. *Angew. Chem. Int. Ed.* **2021**, *60*, 1082–1097.

<https://doi.org/10.1002/anie.202006416>.

<sup>10</sup> Marzo, L.; Pagire, S. K.; Reiser, O.; König, B. Visible-Light Photocatalysis: Does It Make a Difference in Organic Synthesis? *Angew. Chem. Int. Ed.* **2018**, *57*, 10034–10072.

<https://doi.org/10.1002/anie.201709766>

<sup>11</sup> Twilton, J.; Le, C.; Zhang, P.; Shaw, M. H.; Evans, R. W.; MacMillan, D. W. C. The merger of transition metal and photocatalysis. *Nature Rev. Chem.* **2017**, *1*, 0052.

<https://doi.org/10.1038/s41570-017-0052>

<sup>12</sup> For a rapid overview, see: Poli, R. Radical Coordination Chemistry and its Relevance to Metal-Mediated Radical Polymerization. *Eur. J. Inorg. Chem.* **2011**, 1513–1530.

<https://doi.org/10.1002/ejic.201001364>

<sup>13</sup> *Comprehensive Enantioselective Organocatalysis: Catalysts, Reactions, and Applications*; Dalco, P. I., Ed.; Wiley-VCH Verlag GmbH & Co. KGaA: Weinheim, Germany, 2013.

<https://doi.org/10.1002/9783527658862>.

<sup>14</sup> Mukherjee, S.; Yang, J. W.; Hoffmann, S.; List, B. Asymmetric Enamine Catalysis. *Chem. Rev.* **2007**, *107* (12), 5471–5569. <https://doi.org/10.1021/cr0684016>.

<sup>15</sup> Vega-Peñaloza, A.; Paria, S.; Bonchio, M.; Dell'Amico, L.; Companyó, X. Profiling the Privileges of Pyrrolidine-Based Catalysts in Asymmetric Synthesis: From Polar to Light-Driven Radical Chemistry. *ACS Catal.* **2019**, *9* (7), 6058–6072.

<https://doi.org/10.1021/acscatal.9b01556>.

<sup>16</sup> Noncovalent Interactions in Catalysis: Mahmudov, K. T., Kopylovich, M. N., Guedes da Silva, M. F. C., Pombeiro, A. J. L., Eds.; Catalysis Series; Royal Society of Chemistry: Cambridge, 2019. <https://doi.org/10.1039/9781788016490>.

<sup>17</sup> Zhu, L.; Wang, D.; Jia, Z.; Lin, Q.; Huang, M.; Luo, S. Catalytic Asymmetric Oxidative Enamine Transformations. *ACS Catal.* **2018**, *8* (6), 5466–5484.

<https://doi.org/10.1021/acscatal.8b01263>.

<sup>18</sup> Beeson, T. D.; Mastracchio, A.; Hong, J.-B.; Ashton, K.; MacMillan, D. W. C. Enantioselective Organocatalysis Using SOMO Activation. *Science* **2007**, *316* (5824), 582.

<https://doi.org/10.1126/science>.



- 
- <sup>19</sup> Macmillan, D. W. C.; Rendler, S. Enantioselective Organo-SOMO Catalysis: A Novel Activation Mode for Asymmetric Synthesis. In *Asymmetric Synthesis II*; Christmann, M., Bräse, S., Eds.; Wiley-VCH Verlag GmbH & Co. KGaA: Weinheim, Germany, 2013; pp 87–94. <https://doi.org/10.1002/9783527652235.ch12>.
- <sup>20</sup> Mečiarová, M.; Tisovský, P.; Šebesta, R. Enantioselective Organocatalysis Using SOMO Activation. *New J. Chem.* **2016**, *40* (6), 4855–4864. <https://doi.org/10.1039/C6NJ00079G>.
- <sup>21</sup> Sibi, M. P.; Hasegawa, M. Organocatalysis in Radical Chemistry. Enantioselective  $\alpha$ -Oxyamination of Aldehydes. *J. Am. Chem. Soc.* **2007**, *129* (14), 4124–4125. <https://doi.org/10.1021/ja069245n>.
- <sup>22</sup> Mastracchio, A.; Warkentin, A. A.; Walji, A. M.; MacMillan, D. W. C. Direct and Enantioselective  $\alpha$ -Allylation of Ketones via Singly Occupied Molecular Orbital (SOMO) Catalysis. *Proc. Natl. Acad. Sci.* **2010**, *107* (48), 20648–20651. <https://doi.org/10.1073/pnas.1002845107>.
- <sup>23</sup> Van Humbeck, J. F.; Simonovich, S. P.; Knowles, R. R.; MacMillan, D. W. C. Concerning the Mechanism of the  $\text{FeCl}_3$ -Catalyzed  $\alpha$ -Oxyamination of Aldehydes: Evidence for a Non-SOMO Activation Pathway. *J. Am. Chem. Soc.* **2010**, *132* (29), 10012–10014. <https://doi.org/10.1021/ja1043006>.
- <sup>24</sup> Pham, P. V.; Ashton, K.; MacMillan, D. W. C. The Intramolecular Asymmetric Allylation of Aldehydes via Organo-SOMO Catalysis: A Novel Approach to Ring Construction. *Chem. Sci.* **2011**, *2* (8), 1470. <https://doi.org/10.1039/c1sc00176k>.
- <sup>25</sup> Rendler, S.; MacMillan, D. W. C. Enantioselective Polyene Cyclization via Organo-SOMO Catalysis. *J. Am. Chem. Soc.* **2010**, *132* (14), 5027–5029. <https://doi.org/10.1021/ja100185p>.
- <sup>26</sup> Nicolaou, K. C.; Reingruber, R.; Sarlah, D.; Bräse, S. Enantioselective Intramolecular Friedel–Crafts-Type  $\alpha$ -Arylation of Aldehydes. *J. Am. Chem. Soc.* **2009**, *131* (6), 2086–2087. <https://doi.org/10.1021/ja809405c>.
- <sup>27</sup> Conrad, J. C.; Kong, J.; Laforteza, B. N.; MacMillan, D. W. C. Enantioselective  $\alpha$ -Arylation of Aldehydes via Organo-SOMO Catalysis. An Ortho-Selective Arylation Reaction Based on an Open-Shell Pathway. *J. Am. Chem. Soc.* **2009**, *131* (33), 11640–11641. <https://doi.org/10.1021/ja9026902>.

- 
- <sup>28</sup> Um, J. M.; Gutierrez, O.; Schoenebeck, F.; Houk, K. N.; MacMillan, D. W. C. Nature of Intermediates in Organo-SOMO Catalysis of  $\alpha$ -Arylation of Aldehydes. *J. Am. Chem. Soc.* **2010**, *132* (17), 6001–6005. <https://doi.org/10.1021/ja9063074>.
- <sup>29</sup> Jui, N. T.; Garber, J. A. O.; Finelli, F. G.; MacMillan, D. W. C. Enantioselective Organo-SOMO Cycloadditions: A Catalytic Approach to Complex Pyrrolidines from Olefins and Aldehydes. *J. Am. Chem. Soc.* **2012**, *134* (28), 11400–11403. <https://doi.org/10.1021/ja305076b>.
- <sup>30</sup> Jui, N. T.; Lee, E. C. Y.; MacMillan, D. W. C. Enantioselective Organo-SOMO Cascade Cycloadditions: A Rapid Approach to Molecular Complexity from Simple Aldehydes and Olefins. *J. Am. Chem. Soc.* **2010**, *132* (29), 10015–10017. <https://doi.org/10.1021/ja104313x>.
- <sup>31</sup> García-Fortanet, J.; Buchwald, S. L. Asymmetric Palladium-Catalyzed Intramolecular  $\alpha$ -Arylation of Aldehydes. *Angew. Chem. Int. Ed.* **2008**, *47* (42), 8108–8111. <https://doi.org/10.1002/anie.200803809>.
- <sup>32</sup> Comito, R. J.; Finelli, F. G.; MacMillan, D. W. C. Enantioselective Intramolecular Aldehyde  $\alpha$ -Alkylation with Simple Olefins: Direct Access to Homo-Ene Products. *J. Am. Chem. Soc.* **2013**, *135* (25), 9358–9361. <https://doi.org/10.1021/ja4047312>.
- <sup>33</sup> Kim, H.; MacMillan, D. W. C. Enantioselective Organo-SOMO Catalysis: The  $\alpha$ -Vinylolation of Aldehydes. *J. Am. Chem. Soc.* **2008**, *130* (2), 398–399. <https://doi.org/10.1021/ja077212h>.
- <sup>34</sup> Jang, H.-Y.; Hong, J.-B.; MacMillan, D. W. C. Enantioselective Organocatalytic Singly Occupied Molecular Orbital Activation: The Enantioselective  $\alpha$ -Enolation of Aldehydes. *J. Am. Chem. Soc.* **2007**, *129* (22), 7004–7005. <https://doi.org/10.1021/ja0719428>.
- <sup>35</sup> Tisovský, P.; Mečiarová, M.; Šebesta, R. Asymmetric Organocatalytic SOMO Reactions of Enol Silanes and Silyl Ketene (Thio)Acetals. *Org. Biomol. Chem.* **2014**, *12* (46), 9446–9452. <https://doi.org/10.1039/C4OB01385A>.
- <sup>36</sup> Graham, T. H.; Jones, C. M.; Jui, N. T.; MacMillan, D. W. C. Enantioselective Organo-Singly Occupied Molecular Orbital Catalysis: The Carbo-Oxidation of Styrenes. *J. Am. Chem. Soc.* **2008**, *130* (49), 16494–16495. <https://doi.org/10.1021/ja8075633>.
- <sup>37</sup> Wilson, J. E.; Casarez, A. D.; MacMillan, D. W. C. Enantioselective Aldehyde  $\alpha$ -Nitroalkylation via Oxidative Organocatalysis. *J. Am. Chem. Soc.* **2009**, *131* (32), 11332–11334. <https://doi.org/10.1021/ja904504j>.

- 
- <sup>38</sup> Amatore, M.; Beeson, T. D.; Brown, S. P.; MacMillan, D. W. C. Enantioselective Linchpin Catalysis by SOMO Catalysis: An Approach to the Asymmetric  $\alpha$ -Chlorination of Aldehydes and Terminal Epoxide Formation. *Angew. Chem. Int. Ed.* **2009**, *48* (28), 5121–5124. <https://doi.org/10.1002/anie.200901855>.
- <sup>39</sup> Naesborg, L.; Corti, V.; Leth, L. A.; Poulsen, P. H.; Jørgensen, K. A. Catalytic Asymmetric Oxidative  $\gamma$ -Coupling of  $\alpha,\beta$ -Unsaturated Aldehydes with Air as the Terminal Oxidant. *Angew. Chem. Int. Ed.* **2018**, *57* (6), 1606–1610.
- <sup>40</sup> Naesborg, L.; Leth, L. A.; Reyes-Rodríguez, G. J.; Palazzo, T. A.; Corti, V.; Jørgensen, K. A. Direct Enantio- and Diastereoselective Oxidative Homocoupling of Aldehydes. *Chem. - Eur. J.* **2018**, *24* (55), 14844–14848. <https://doi.org/10.1002/chem.201803506>.
- <sup>41</sup> Li, Y.; Wang, D.; Zhang, L.; Luo, S. Redox Property of Enamines. *J. Org. Chem.* **2019**, *84* (18), 12071–12090. <https://doi.org/10.1021/acs.joc.9b02003>.
- <sup>42</sup> Roth, H.; Romero, N.; Nicewicz, D. Experimental and Calculated Electrochemical Potentials of Common Organic Molecules for Applications to Single-Electron Redox Chemistry. *Synlett* **2015**, *27* (05), 714–723. <https://doi.org/10.1055/s-0035-1561297>.
- <sup>43</sup> Leifert, D.; Studer, A. The Persistent Radical Effect in Organic Synthesis. *Angew. Chem. Int. Ed.* **2019**. <https://doi.org/10.1002/anie.201903726>.
- <sup>44</sup> Leth, L. A.; Næsberg, L.; Reyes-Rodríguez, G. J.; Tobiesen, H. N.; Iversen, M. V.; Jørgensen, K. A. Enantioselective Oxidative Coupling of Carboxylic Acids to  $\alpha$ -Branched Aldehydes. *J. Am. Chem. Soc.* **2018**, *140* (40), 12687–12690. <https://doi.org/10.1021/jacs.8b07394>.
- <sup>45</sup> Blom, J.; Reyes-Rodríguez, G. J.; Tobiesen, H. N.; Lamhauge, J. N.; Iversen, M. V.; Barløse, C. L.; Hammer, N.; Rusbjerg, M.; Jørgensen, K. A. Umpolung Strategy for  $\alpha$ -Functionalization of Aldehydes for the Addition of Thiols and Other Nucleophiles. *Angew. Chem. Int. Ed.* **2019**. <https://doi.org/10.1002/anie.201911793>.
- <sup>46</sup> Rezayee, N. M.; Lauridsen, V. H.; Næsberg, L.; Nguyen, T. V. Q.; Tobiesen, H. N.; Jørgensen, K. A. Oxidative Organocatalysed Enantioselective Coupling of Indoles with Aldehydes That Forms Quaternary Carbon Stereocentres. *Chem. Sci.* **2019**, *10* (12), 3586–3591. <https://doi.org/10.1039/C9SC00196D>.
- <sup>47</sup> Cano-Yelo, H.; Deronzier, A. Photocatalysis of the Pschorr Reaction by Tris-(2,2'-Bipyridyl)Ruthenium(II) in the Phenanthrene Series. *J. Chem. Soc. Perkin Trans. 2* **1984**, No. 6, 1093–1098. <https://doi.org/10.1039/P29840001093>.

- 
- <sup>48</sup> Cano-Yelo, H.; Deronzier, A. Photo-Oxidation of Some Carbinols by the Ru(II) Polypyridyl Complex-Aryl Diazonium Salt System. *Tetrahedron Lett.* **1984**, *25* (48), 5517–5520. [https://doi.org/10.1016/S0040-4039\(01\)81614-2](https://doi.org/10.1016/S0040-4039(01)81614-2).
- <sup>49</sup> Nicewicz, D. A.; MacMillan, D. W. C. Merging Photoredox Catalysis with Organocatalysis: The Direct Asymmetric Alkylation of Aldehydes. *Science* **2008**, *322* (5898), 77–80. <https://doi.org/10.1126/science.1161976>.
- <sup>50</sup> Welin, E. R.; Warkentin, A. A.; Conrad, J. C.; MacMillan, D. W. C. Enantioselective  $\alpha$ -Alkylation of Aldehydes by Photoredox Organocatalysis: Rapid Access to Pharmacophore Fragments from  $\beta$ -Cyanoaldehydes. *Angew. Chem. Int. Ed.* **2015**, *54* (33), 9668–9672. <https://doi.org/10.1002/anie.201503789>.
- <sup>51</sup> Li, M.; Sang, Y.; Xue, X.-S.; Cheng, J.-P. Origin of Stereocontrol in Photoredox Organocatalysis of Asymmetric  $\alpha$ -Functionalizations of Aldehydes. *J. Org. Chem.* **2018**, *83* (6), 3333–3338. <https://doi.org/10.1021/acs.joc.8b00469>.
- <sup>52</sup> Nagib, D. A.; Scott, M. E.; MacMillan, D. W. C. Enantioselective  $\alpha$ -Trifluoromethylation of Aldehydes via Photoredox Organocatalysis. *J. Am. Chem. Soc.* **2009**, *131* (31), 10875–10877. <https://doi.org/10.1021/ja9053338>.
- <sup>53</sup> Shih, H.-W.; Vander Wal, M. N.; Grange, R. L.; MacMillan, D. W. C. Enantioselective  $\alpha$ -Benzoylation of Aldehydes via Photoredox Organocatalysis. *J. Am. Chem. Soc.* **2010**, *132* (39), 13600–13603. <https://doi.org/10.1021/ja106593m>.
- <sup>54</sup> Nacsa, E. D.; MacMillan, D. W. C. Spin-Center Shift-Enabled Direct Enantioselective  $\alpha$ -Benzoylation of Aldehydes with Alcohols. *J. Am. Chem. Soc.* **2018**, *140* (9), 3322–3330. <https://doi.org/10.1021/jacs.7b12768>.
- <sup>55</sup> Capacci, A. G.; Malinowski, J. T.; McAlpine, N. J.; Kuhne, J.; MacMillan, D. W. C. Direct, Enantioselective  $\alpha$ -Alkylation of Aldehydes Using Simple Olefins. *Nat. Chem.* **2017**, *9* (11), 1073–1077. <https://doi.org/10.1038/nchem.2797>.
- <sup>56</sup> Huang, Z.; Dong, G. Catalytic C-C Bond Forming Transformations via Direct  $\beta$ -CH Functionalization of Carbonyl Compounds. *Tetrahedron Lett.* **2014**, *55* (43), 5869–5889. <https://doi.org/10.1016/j.tetlet.2014.09.005>.
- <sup>57</sup> Pirnot, M. T.; Rankic, D. A.; Martin, D. B. C.; MacMillan, D. W. C. Photoredox Activation for the Direct  $\alpha$ -Arylation of Ketones and Aldehydes. *Science* **2013**, *339* (6127), 1593–1596. <https://doi.org/10.1126/science.1232993>.

- 
- <sup>58</sup> Murphy, J. J.; Bastida, D.; Paria, S.; Fagnoni, M.; Melchiorre, P. Asymmetric Catalytic Formation of Quaternary Carbons by Iminium Ion Trapping of Radicals. *Nature* **2016**, *532* (7598), 218–222. <https://doi.org/10.1038/nature17438>.
- <sup>59</sup> Zhao, J.-J.; Zhang, H.-H.; Shen, X.; Yu, S. Enantioselective Radical Hydroacylation of Enals with  $\alpha$ -Ketoacids Enabled by Photoredox/Amine Cocatalysis. *Org. Lett.* **2019**, *21* (4), 913–916. <https://doi.org/10.1021/acs.orglett.8b03840>
- <sup>60</sup> Yoon, H.-S.; Ho, X.-H.; Jang, J.; Lee, H.-J.; Kim, S.-J.; Jang, H.-Y. N719 Dye-Sensitized Organophotocatalysis: Enantioselective Tandem Michael Addition/Oxyamination of Aldehydes. *Org. Lett.* **2012**, *14* (13), 3272–3275. <https://doi.org/10.1021/ol3011858>
- <sup>61</sup> Hörmann, F. M.; Kerzig, C.; Chung, T. S.; Bauer, A.; Wenger, O. S.; Bach, T. Triplet Energy Transfer from Ruthenium Complexes to Chiral Eniminium Ions: Enantioselective Synthesis of Cyclobutanecarbaldehydes by [2+2] Photocycloaddition. *Angew. Chem. Int. Ed.* **2020**, *59* (24), 9659–9668. <https://doi.org/10.1002/anie.202001634>
- <sup>62</sup> Zou, Y.-Q.; Hörmann, F. M.; Bach, T. Iminium and Enamine Catalysis in Enantioselective Photochemical Reactions. *Chem. Soc. Rev.* **2018**, *47* (2), 278–290. <https://doi.org/10.1039/C7CS00509A>.
- <sup>63</sup> Neumann, M.; Földner, S.; König, B.; Zeitler, K. Metal-Free, Cooperative Asymmetric Organophotoredox Catalysis with Visible Light. *Angew. Chem. Int. Ed.* **2011**, *50* (4), 951–954. <https://doi.org/10.1002/anie.201002992>.
- <sup>64</sup> Srivastava, V.; Singh, P. P. Eosin Y Catalysed Photoredox Synthesis: A Review. *RSC Adv.* **2017**, *7* (50), 31377–31392. <https://doi.org/10.1039/C7RA05444K>.
- <sup>65</sup> Cismesia, M. A.; Yoon, T. P. Characterizing Chain Processes in Visible Light Photoredox Catalysis. *Chem. Sci.* **2015**, *6* (10), 5426–5434. <https://doi.org/10.1039/C5SC02185E>.
- <sup>66</sup> Studer, A.; Curran, D. P. Catalysis of Radical Reactions: A Radical Chemistry Perspective. *Angew. Chem. Int. Ed.* **2016**, *55* (1), 58–102. <https://doi.org/10.1002/anie.201505090>.
- <sup>67</sup> Cherevatskaya, M.; Neumann, M.; Földner, S.; Harlander, C.; Kümmel, S.; Dankesreiter, S.; Pfitzner, A.; Zeitler, K.; König, B. Visible-Light-Promoted Stereoselective Alkylation by Combining Heterogeneous Photocatalysis with Organocatalysis. *Angew. Chem. Int. Ed.* **2012**, *51* (17), 4062–4066. <https://doi.org/10.1002/anie.201108721>.

- 
- <sup>68</sup> Fidaly, K.; Ceballos, C.; Falguières, A.; Veitia, M. S.-I.; Guy, A.; Ferroud, C. Visible Light Photoredox Organocatalysis: A Fully Transition Metal-Free Direct Asymmetric  $\alpha$ -Alkylation of Aldehydes. *Green Chem.* **2012**, *14* (5), 1293. <https://doi.org/10.1039/c2gc35118h>.
- <sup>69</sup> Rigotti, T.; Casado-Sánchez, A.; Cabrera, S.; Pérez-Ruiz, R.; Liras, M.; de la Peña O'Shea, V. A.; Alemán, J. A Bifunctional Photoaminocatalyst for the Alkylation of Aldehydes: Design, Analysis, and Mechanistic Studies. *ACS Catal.* **2018**, *8* (7), 5928–5940. <https://doi.org/10.1021/acscatal.8b01331>.
- <sup>70</sup> Tagami, T.; Arakawa, Y.; Minagawa, K.; Imada, Y. Efficient Use of Photons in Photoredox/Enamine Dual Catalysis with a Peptide-Bridged Flavin–Amine Hybrid. *Org. Lett.* **2019**, *21* (17), 6978–6982. <https://doi.org/10.1021/acs.orglett.9b02567>.
- <sup>71</sup> Cecere, G.; König, C. M.; Alleva, J. L.; MacMillan, D. W. C. Enantioselective Direct  $\alpha$ -Amination of Aldehydes via a Photoredox Mechanism: A Strategy for Asymmetric Amine Fragment Coupling. *J. Am. Chem. Soc.* **2013**, *135* (31), 11521–11524. <https://doi.org/10.1021/ja406181e>.
- <sup>72</sup> Kärkäs, M. D. Photochemical Generation of Nitrogen-Centered Amidyl, Hydrazonyl, and Imidyl Radicals: Methodology Developments and Catalytic Applications. *ACS Catal.* **2017**, *7* (8), 4999–5022. <https://doi.org/10.1021/acscatal.7b01385>.
- <sup>73</sup> Chen, J.-R.; Hu, X.-Q.; Lu, L.-Q.; Xiao, W.-J. Visible Light Photoredox-Controlled Reactions of N-Radicals and Radical Ions. *Chem. Soc. Rev.* **2016**, *45* (8), 2044–2056. <https://doi.org/10.1039/C5CS00655D>.
- <sup>74</sup> Arceo, E.; Jurberg, I. D.; Álvarez-Fernández, A.; Melchiorre, P. Photochemical Activity of a Key Donor–Acceptor Complex Can Drive Stereoselective Catalytic  $\alpha$ -Alkylation of Aldehydes. *Nat. Chem.* **2013**, *5* (9), 750–756. <https://doi.org/10.138/nchem.1727>.
- <sup>75</sup> Holden, C. M.; Melchiorre, P. Photochemistry and Excited-State Reactivity of Organocatalytic Intermediates. In *Photochemistry*; Albini, A., Protti, S., Eds.; Royal Society of Chemistry: Cambridge, 2019; Vol. 47, pp 344–378. <https://doi.org/10.1039/9781788016520-00344>.
- <sup>76</sup> Russell, G. A.; Wang, K. Electron Transfer Processes. 53. Homolytic Alkylation of Enamines by Electrophilic Radicals. *J. Org. Chem.* **1991**, *56* (11), 3475–3479. <https://doi.org/10.1021/jo00011a007>.

- 
- <sup>77</sup> Bahamonde, A.; Melchiorre, P. Mechanism of the Stereoselective  $\alpha$ -Alkylation of Aldehydes Driven by the Photochemical Activity of Enamines. *J. Am. Chem. Soc.* **2016**, *138* (25), 8019–8030. <https://doi.org/10.1021/jacs.6b04871>.
- <sup>78</sup> Arceo, E.; Bahamonde, A.; Bergonzini, G.; Melchiorre, P. Enantioselective Direct  $\alpha$ -Alkylation of Cyclic Ketones by Means of Photo-Organocatalysis. *Chem. Sci.* **2014**, *5* (6), 2438. <https://doi.org/10.1039/c4sc00315b>.
- <sup>79</sup> Silvi, M.; Arceo, E.; Jurberg, I. D.; Cassani, C.; Melchiorre, P. Enantioselective Organocatalytic Alkylation of Aldehydes and Enals Driven by the Direct Photoexcitation of Enamines. *J. Am. Chem. Soc.* **2015**, *137* (19), 6120–6123. <https://doi.org/10.1021/jacs.5b01662>.
- <sup>80</sup> Filippini, G.; Silvi, M.; Melchiorre, P. Enantioselective Formal  $\alpha$ -Methylation and  $\alpha$ -Benzoylation of Aldehydes by Means of Photo-Organocatalysis. *Angew. Chem. Int. Ed.* **2017**, *56* (16), 4447–4451. <https://doi.org/10.1002/anie.201612045>.
- <sup>81</sup> Schweitzer-Chaput, B.; Horwitz, M. A.; de Pedro Beato, E.; Melchiorre, P. Photochemical Generation of Radicals from Alkyl Electrophiles Using a Nucleophilic Organic Catalyst. *Nat. Chem.* **2019**, *11* (2), 129–135. <https://doi.org/10.1038/s41557-018-0173-x>.
- <sup>82</sup> Spinnato, D.; Schweitzer-Chaput, B.; Goti, G.; Ošeka, M.; Melchiorre, P. A Photochemical Organocatalytic Strategy for the  $\alpha$ -Alkylation of Ketones by Using Radicals. *Angew. Chem. Int. Ed.* **2020**, *59* (24), 9485–9490. <https://doi.org/10.1002/anie.201915814>.
- <sup>83</sup> Silvi, M.; Verrier, C.; Rey, Y. P.; Buzzetti, L.; Melchiorre, P. Visible-Light Excitation of Iminium Ions Enables the Enantioselective Catalytic  $\beta$ -Alkylation of Enals. *Nat. Chem.* **2017**, *9* (9), 868–873. <https://doi.org/10.1038/nchem.2748>.
- <sup>84</sup> Zhang, N.; Samanta, S. R.; Rosen, B. M.; Percec, V. Single Electron Transfer in Radical Ion and Radical-Mediated Organic, Materials and Polymer Synthesis. *Chem. Rev.* **2014**, *114* (11), 5848–5958. <https://doi.org/10.1021/cr400689s>.
- <sup>85</sup> Kulinkovich, O. G. The Chemistry of Cyclopropanols. *Chem. Rev.* **2003**, *103* (7), 2597–2632. <https://doi.org/10.1021/cr010012i>.
- <sup>86</sup> Woźniak, Ł.; Magagnano, G.; Melchiorre, P. Enantioselective Photochemical Organocascade Catalysis. *Angew. Chem. Int. Ed.* **2018**, *57* (4), 1068–1072. <https://doi.org/10.1002/anie.201711397>.

- 
- <sup>87</sup> Mondal, S.; Bertrand, M. P.; Nechab, M. Enantioselective Synthesis of Carbocycles and Heterocycles by Radical/Polar and Polar/Radical Cascades. *Angew. Chem. Int. Ed.* **2013**, *52* (3), 809–811. <https://doi.org/10.1002/anie.201207518>.
- <sup>88</sup> Bonilla, P.; Rey, Y. P.; Holden, C. M.; Melchiorre, P. Photo-Organocatalytic Enantioselective Radical Cascade Reactions of Unactivated Olefins. *Angew. Chem. Int. Ed.* **2018**, *57* (39), 12819–12823. <https://doi.org/10.1002/anie.201808183>.
- <sup>89</sup> Margrey, K. A.; Nicewicz, D. A. A General Approach to Catalytic Alkene Anti-Markovnikov Hydrofunctionalization Reactions via Acridinium Photoredox Catalysis. *Acc. Chem. Res.* **2016**, *49* (9), 1997–2006. <https://doi.org/10.1021/acs.accounts.6b00304>.
- <sup>90</sup> Perego, L. A.; Bonilla, P.; Melchiorre, P. Photo-Organocatalytic Enantioselective Radical Cascade Enabled by Single-Electron Transfer Activation of Allenes. *Adv. Synth. Catal.* **2019**, *adsc.201900973*. <https://doi.org/10.1002/adsc.201900973>.
- <sup>91</sup> Mazzarella, D.; Crisenza, G. E. M.; Melchiorre, P. Asymmetric Photocatalytic C–H Functionalization of Toluene and Derivatives. *J. Am. Chem. Soc.* **2018**, *140* (27), 8439–8443. <https://doi.org/10.1021/jacs.8b05240>.
- <sup>92</sup> Buzzetti, L.; Prieto, A.; Roy, S. R.; Melchiorre, P. Radical-Based C–C Bond-Forming Processes Enabled by the Photoexcitation of 4-Alkyl-1,4-Dihydropyridines. *Angew. Chem. Int. Ed.* **2017**, *56* (47), 15039–15043. <https://doi.org/10.1002/anie.201709571>.
- <sup>93</sup> Huang, W.; Cheng, X. Hantzsch Esters as Multifunctional Reagents in Visible-Light Photoredox Catalysis. *Synlett* **2016**, *28* (02), 148–158. <https://doi.org/10.1055/s-0036-1588129>.
- <sup>94</sup> Goti, G.; Bieszczad, B.; Vega-Peñaloza, A.; Melchiorre, P. Stereocontrolled Synthesis of 1,4-Dicarbonyl Compounds by Photochemical Organocatalytic Acyl Radical Addition to Enals. *Angew. Chem. Int. Ed.* **2019**, *58* (4), 1213–1217. <https://doi.org/10.1002/anie.201810798>.
- <sup>95</sup> Chen, L.; Hu, L.; Du, Y.; Su, W.; Kang, Q. Asymmetric Photoinduced Giese Radical Addition Enabled by a Single Chiral-at-Metal Rhodium Complex. *Chin. J. Org. Chem.* **2020**, *40* (11), 3944. <https://doi.org/10.6023/cjoc202004041>.
- <sup>96</sup> Verrier, C.; Alandini, N.; Pezzetta, C.; Moliterno, M.; Buzzetti, L.; Hepburn, H. B.; Vega-Peñaloza, A.; Silvi, M.; Melchiorre, P. Direct Stereoselective Installation of Alkyl Fragments at the  $\beta$ -Carbon of Enals via Excited Iminium Ion Catalysis. *ACS Catal.* **2018**, *8* (2), 1062–1066. <https://doi.org/10.1021/acscatal.7b03788>.



- 
- <sup>97</sup> Nechab, M.; Campolo, D.; Maury, J.; Perfetti, P.; Vanthuyne, N.; Siri, D.; Bertrand, M. P. Memory of Chirality in Cascade Rearrangements of Eneidyne. *J. Am. Chem. Soc.* **2010**, *132* (42), 14742–14744. <https://doi.org/10.1021/ja106668d>.
- <sup>98</sup> Mondal, S.; Nechab, M.; Campolo, D.; Vanthuyne, N.; Bertrand, M. P. Copper Carbenoid, Reactant and Catalyst for One-Pot Diazo Ester Coupling Cascade Rearrangement of Eneidyne: Formation of Two Contiguous Tetrasubstituted Stereocenters. *Adv. Synth. Catal.* **2012**, *354* (10), 1987–2000. <https://doi.org/10.1002/adsc.201200045>.
- <sup>99</sup> Sibi, M. P.; Ji, J.; Wu, J. H.; Gürtler, S.; Porter, N. A. Chiral Lewis Acid Catalysis in Radical Reactions: Enantioselective Conjugate Radical Additions. *J. Am. Chem. Soc.* **1996**, *118* (38), 9200–9201. <https://doi.org/10.1021/ja9623929>.
- <sup>100</sup> Bahamonde, A.; Murphy, J. J.; Savarese, M.; Brémond, É.; Cavalli, A.; Melchiorre, P. Studies on the Enantioselective Iminium Ion Trapping of Radicals Triggered by an Electron-Relay Mechanism. *J. Am. Chem. Soc.* **2017**, *139* (12), 4559–4567. <https://doi.org/10.1021/jacs.7b01446>.
- <sup>101</sup> Cao, Z.-Y.; Ghosh, T.; Melchiorre, P. Enantioselective Radical Conjugate Additions Driven by a Photoactive Intramolecular Iminium-Ion-Based EDA Complex. *Nat. Commun.* **2018**, *9* (1), 3274. <https://doi.org/10.1038/s41467-018-05375-2>.
- <sup>102</sup> Le Saux, E.; Ma, D.; Bonilla, P.; Holden, C. M.; Lustosa, D.; Melchiorre, P. A General Organocatalytic System for Enantioselective Radical Conjugate Additions to Enals. *Angew. Chem. Int. Ed.* **2021**, *60* (10), 5357.
- <sup>103</sup> Biju, A. T.; Breslow, R. *N-Heterocyclic Carbenes in Organocatalysis*; 2019.
- <sup>104</sup> Guin, J.; De Sarkar, S.; Grimme, S.; Studer, A. Biomimetic Carbene-Catalyzed Oxidations of Aldehydes Using TEMPO. *Angew. Chem. Int. Ed.* **2008**, *47* (45), 8727–8730. <https://doi.org/10.1002/anie.200802735>.
- <sup>105</sup> White, N. A.; Rovis, T. Enantioselective N-Heterocyclic Carbene-Catalyzed  $\beta$ -Hydroxylation of Enals Using Nitroarenes: An Atom Transfer Reaction That Proceeds via Single Electron Transfer. *J. Am. Chem. Soc.* **2014**, *136* (42), 14674–14677. <https://doi.org/10.1021/ja5080739>.
- <sup>106</sup> Regnier, V.; Romero, E. A.; Molton, F.; Jazzar, R.; Bertrand, G.; Martin, D. What Are the Radical Intermediates in Oxidative N-Heterocyclic Carbene Organocatalysis? *J. Am. Chem. Soc.* **2019**, *141* (2), 1109–1117. <https://doi.org/10.1021/jacs.8b11824>.

- 
- <sup>107</sup> Zhang, Y.; Du, Y.; Huang, Z.; Xu, J.; Wu, X.; Wang, Y.; Wang, M.; Yang, S.; Webster, R. D.; Chi, Y. R. N-Heterocyclic Carbene-Catalyzed Radical Reactions for Highly Enantioselective  $\beta$ -Hydroxylation of Enals. *J. Am. Chem. Soc.* **2015**, *137* (7), 2416–2419. <https://doi.org/10.1021/ja511371a>.
- <sup>108</sup> Wang, H.; Wang, Y.; Chen, X.; Mou, C.; Yu, S.; Chai, H.; Jin, Z.; Chi, Y. R. Chiral Nitroarenes as Enantioselective Single-Electron-Transfer Oxidants for Carbene-Catalyzed Radical Reactions. *Org. Lett.* **2019**, *21* (18), 7440–7444. <https://doi.org/10.1021/acs.orglett.9b02736>.
- <sup>109</sup> White, N. A.; Rovis, T. Oxidatively Initiated NHC-Catalyzed Enantioselective Synthesis of 3,4-Disubstituted Cyclopentanones from Enals. *J. Am. Chem. Soc.* **2015**, *137* (32), 10112–10115. <https://doi.org/10.1021/jacs.5b06390>.
- <sup>110</sup> Wu, X.; Zhang, Y.; Wang, Y.; Ke, J.; Jeret, M.; Reddi, R. N.; Yang, S.; Song, B.-A.; Chi, Y. R. Polyhalides as Efficient and Mild Oxidants for Oxidative Carbene Organocatalysis by Radical Processes. *Angew. Chem. Int. Ed.* **2017**, *56* (11), 2942–2946. <https://doi.org/10.1002/anie.201611692>.
- <sup>111</sup> De Sarkar, S.; Studer, A. NHC-Catalyzed Michael Addition to  $\alpha,\beta$ -Unsaturated Aldehydes by Redox Activation. *Angew. Chem. Int. Ed.* **2010**, *49* (48), 9266–9269. <https://doi.org/10.1002/anie.201004593>.
- <sup>112</sup> Zhu, Z.-Q.; Zheng, X.-L.; Jiang, N.-F.; Wan, X.; Xiao, J.-C. Chiral N-Heterocyclic Carbene Catalyzed Annulation of  $\alpha,\beta$ -Unsaturated Aldehydes with 1,3-Dicarbonyls. *Chem. Commun.* **2011**, *47* (30), 8670. <https://doi.org/10.1039/c1cc12778k>.
- <sup>113</sup> Chen, X.-Y.; Chen, K.-Q.; Sun, D.-Q.; Ye, S. N-Heterocyclic Carbene-Catalyzed Oxidative [3 + 2] Annulation of Dioxindoles and Enals: Cross Coupling of Homo-enolate and Enolate. *Chem. Sci.* **2017**, *8* (3), 1936–1941. <https://doi.org/10.1039/C6SC04135C>.
- <sup>114</sup> Sun, L.-H.; Shen, L.-T.; Ye, S. Highly Diastereo- and Enantioselective NHC-Catalyzed [3+2] Annulation of Enals and Isatins. *Chem. Commun.* **2011**, *47* (36), 10136. <https://doi.org/10.1039/c1cc13860j>.
- <sup>115</sup> Song, Z.-Y.; Chen, K.-Q.; Chen, X.-Y.; Ye, S. Diastereo- and Enantioselective Synthesis of Spirooxindoles with Contiguous Tetrasubstituted Stereocenters via Catalytic Coupling of Two Tertiary Radicals. *J. Org. Chem.* **2018**, *83* (5), 2966–2970. <https://doi.org/10.1021/acs.joc.7b03161>.

- 
- <sup>116</sup> Chen, Q.; Zhu, T.; Majhi, P. K.; Mou, C.; Chai, H.; Zhang, J.; Zhuo, S.; Chi, Y. R. Carbene-Catalyzed Enantioselective Oxidative Coupling of Enals and Di(Hetero)Arylmethanes. *Chem. Sci.* **2018**, *9* (46), 8711–8715. <https://doi.org/10.1039/C8SC03480J>.
- <sup>117</sup> Dai, L.; Xia, Z.; Gao, Y.; Gao, Z.; Ye, S. Visible-Light-Driven N-Heterocyclic Carbene Catalyzed  $\Gamma$ - and  $\epsilon$ -Alkylation with Alkyl Radicals. *Angew. Chem. Int. Ed.* **2019**, *58* (50), 18124–18130. <https://doi.org/10.1002/anie.201909017>.
- <sup>118</sup> Nanni, D.; Curran, D. P. Synthesis and Some Reactions of the First Chiral Tin Hydride Containing a C2-Symmetric Binaphthyl Substituent. *Tetrahedron Asymmetry* **1996**, *7* (8), 2417–2422. [https://doi.org/10.1016/0957-4166\(96\)00300-X](https://doi.org/10.1016/0957-4166(96)00300-X).
- <sup>119</sup> Blumenstein, M.; Schwarzkopf, K.; Metzger, J. O. Enantioselective Hydrogen Transfer from a Chiral Tin Hydride to a Prochiral Carbon-Centered Radical. *Angew. Chem. Int. Ed. Engl.* **1997**, *36* (3), 235–236. <https://doi.org/10.1002/anie.199702351>.
- <sup>120</sup> Dang, H.-S.; Roberts, B. P. Radical-Chain Addition of Aldehydes to Alkenes Catalysed by Thiols. *J. Chem. Soc. Perkin I* **1998**, No. 1, 67–76. <https://doi.org/10.1039/a704878>.
- <sup>121</sup> Shirakawa, S.; Usui, A.; Kan, S. B. J.; Maruoka, K. Chiral Organotin Hydride Catalyzed Enantioselective Radical Cyclization of Aldehydes. *Asian J. Org. Chem.* **2013**, *2* (11), 916–919. <https://doi.org/10.1002/ajoc.201300138>.
- <sup>122</sup> Dénès, F.; Pichowicz, M.; Povie, G.; Renaud, P. Thiyl Radicals in Organic Synthesis. *Chem. Rev.* **2014**, *114* (5), 2587–2693. <https://doi.org/10.1021/cr400441m>.
- <sup>123</sup> Cai, Y.; Roberts, B. P.; Tocher, D. A. Carbohydrate-Derived Thiols as Protic Polarity-Reversal Catalysts for Enantioselective Radical-Chain Reactions. *J. Chem. Soc. Perkin I* **2002**, No. 11, 1376–1386. <https://doi.org/10.1039/b202022j>
- <sup>124</sup> Roberts, B. P. Polarity-Reversal Catalysis of Hydrogen-Atom Abstraction Reactions: Concepts and Applications in Organic Chemistry. *Chem. Soc. Rev.* **1999**, *28* (1), 25–35. <https://doi.org/10.1039/a804291h>.
- <sup>125</sup> Hashimoto, T.; Kawamata, Y.; Maruoka, K. An Organic Thiyl Radical Catalyst for Enantioselective Cyclization. *Nat. Chem.* **2014**, *6* (8), 702–705. <https://doi.org/10.1038/nchem.1998>.
- <sup>126</sup> Ryss, J. M.; Turek, A. K.; Miller, S. J. Disulfide-Bridged Peptides That Mediate Enantioselective Cycloadditions through Thiyl Radical Catalysis. *Org. Lett.* **2018**, *20* (6), 1621–1625. <https://doi.org/10.1021/acs.orglett.8b00364>.

- 
- <sup>127</sup> Doyle, A. G.; Jacobsen, E. N. Small-Molecule H-Bond Donors in Asymmetric Catalysis. *Chem. Rev.* **2007**, *107* (12), 5713–5743. <https://doi.org/10.1021/cr068373r>.
- <sup>128</sup> Yin, Y.; Zhao, X.; Qiao, B.; Jiang, Z. Cooperative Photoredox and Chiral Hydrogen-Bonding Catalysis. *Org. Chem. Front.* **2020**, *7* (10), 1283–1296. <https://doi.org/10.1039/D0QO00276C>.
- <sup>129</sup> Mayr, F.; Wiegand, C.; Bach, T. Enantioselective, Intermolecular [2+2] Photocycloaddition Reactions of 3-Acetoxyquinolone: Total Synthesis of (–)-Pinolinone. *Chem Commun* **2014**, *50* (25), 3353–3355. <https://doi.org/10.1039/C3CC49469A>.
- <sup>130</sup> Selig, P.; Bach, T. Enantioselective Total Synthesis of the *Melodinus* Alkaloid (+)-Meloscine. *Angew. Chem. Int. Ed.* **2008**, *47* (27), 5082–5084. <https://doi.org/10.1002/anie.200800693>.
- <sup>131</sup> Bauer, A.; Westkämper, F.; Grimme, S.; Bach, T. Catalytic Enantioselective Reactions Driven by Photoinduced Electron Transfer. *Nature* **2005**, *436* (7054), 1139–1140. <https://doi.org/10.1038/nature03955>.
- <sup>132</sup> Nechab, M.; Mondal, S.; Bertrand, M. P. 1, *n*-Hydrogen-Atom Transfer (HAT) Reactions in Which *n* ≠ 5: An Updated Inventory. *Chem. - Eur. J.* **2014**, *20* (49), 16034–16059. <https://doi.org/10.1002/chem.201403951>.
- <sup>133</sup> Müller, C.; Bauer, A.; Bach, T. Light-Driven Enantioselective Organocatalysis. *Angew. Chem. Int. Ed.* **2009**, *48* (36), 6640–6642. <https://doi.org/10.1002/anie.200901603>.
- <sup>134</sup> Müller, C.; Bauer, A.; Maturi, M. M.; Cuquerella, M. C.; Miranda, M. A.; Bach, T. Enantioselective Intramolecular [2 + 2]-Photocycloaddition Reactions of 4-Substituted Quinolones Catalyzed by a Chiral Sensitizer with a Hydrogen-Bonding Motif. *J. Am. Chem. Soc.* **2011**, *133* (41), 16689–16697. <https://doi.org/10.1021/ja207480q>.
- <sup>135</sup> Maturi, M. M.; Wenninger, M.; Alonso, R.; Bauer, A.; Pöthig, A.; Riedle, E.; Bach, T. Intramolecular [2+2] Photocycloaddition of 3- and 4-(But-3-Enyl)Oxyquinolones: Influence of the Alkene Substitution Pattern, Photophysical Studies, and Enantioselective Catalysis by a Chiral Sensitizer. *Chem. - Eur. J.* **2013**, *19* (23), 7461–7472. <https://doi.org/10.1002/chem.201300203>.
- <sup>136</sup> Vallavoju, N.; Selvakumar, S.; Jockusch, S.; Sibi, M. P.; Sivaguru, J. Enantioselective Organo-Photocatalysis Mediated by Atropisomeric Thiourea Derivatives. *Angew. Chem. Int. Ed.* **2014**, *53* (22), 5604–5608. <https://doi.org/10.1002/anie.201310940>.

- 
- <sup>137</sup> Mayr, F.; Brimiouille, R.; Bach, T. A Chiral Thiourea as a Template for Enantioselective Intramolecular [2 + 2] Photocycloaddition Reactions. *J. Org. Chem.* **2016**, *81* (16), 6965–6971. <https://doi.org/10.1021/acs.joc.6b01039>.
- <sup>138</sup> Maturi, M. M.; Bach, T. Enantioselective Catalysis of the Intermolecular [2+2] Photocycloaddition between 2-Pyridones and Acetylenedicarboxylates. *Angew. Chem. Int. Ed.* **2014**, *53* (29), 7661–7664. <https://doi.org/10.1002/anie.201403885>.
- <sup>139</sup> Alonso, R.; Bach, T. A Chiral Thioxanthone as an Organocatalyst for Enantioselective [2+2] Photocycloaddition Reactions Induced by Visible Light. *Angew. Chem. Int. Ed.* **2014**, *53* (17), 4368–4371. <https://doi.org/10.1002/anie.201310997>.
- <sup>140</sup> Tröster, A.; Alonso, R.; Bauer, A.; Bach, T. Enantioselective Intermolecular [2 + 2] Photocycloaddition Reactions of 2(1 *H*)-Quinolones Induced by Visible Light Irradiation. *J. Am. Chem. Soc.* **2016**, *138* (25), 7808–7811. <https://doi.org/10.1021/jacs.6b03221>.
- <sup>141</sup> Tröster, A.; Bauer, A.; Jandl, C.; Bach, T. Enantioselective Visible-Light-Mediated Formation of 3-Cyclopropylquinolones by Triplet-Sensitized Deracemization. *Angew. Chem. Int. Ed.* **2019**, *58* (11), 3538–3541. <https://doi.org/10.1002/anie.201814193>.
- <sup>142</sup> Li, X.; Kutta, R. J.; Jandl, C.; Bauer, A.; Nuernberger, P.; Bach, T. Photochemically Induced Ring Opening of Spirocyclopropyl Oxindoles: Evidence for a Triplet 1,3-Diradical Intermediate and Deracemization by a Chiral Sensitizer. *Angew. Chem. Int. Ed.* **2020**, *59* (48), 21640–21647. <https://doi.org/10.1002/anie.202008384>.
- <sup>143</sup> Hölzl-Hobmeier, A.; Bauer, A.; Silva, A. V.; Huber, S. M.; Bannwarth, C.; Bach, T. Catalytic Deracemization of Chiral Allenes by Sensitized Excitation with Visible Light. *Nature* **2018**, *564* (7735), 240–243. <https://doi.org/10.1038/s41586-018-0755-1>.
- <sup>144</sup> Akiyama, T. Stronger Brønsted Acids. *Chem. Rev.* **2007**, *107* (12), 5744–5758. <https://doi.org/10.1021/cr068374j>.
- <sup>145</sup> Rueping, M.; Parmar, D.; Sugiono, E. *Asymmetric Brønsted Acid Catalysis: Rueping/Asymmetric Brønsted Acid Catalysis*; Wiley-VCH Verlag GmbH & Co. KGaA: Weinheim, Germany, 2015. <https://doi.org/10.1002/9783527694785>.
- <sup>146</sup> Parmar, D.; Sugiono, E.; Raja, S.; Rueping, M. Complete Field Guide to Asymmetric BINOL-Phosphate Derived Brønsted Acid and Metal Catalysis: History and Classification by Mode of Activation; Brønsted Acidity, Hydrogen Bonding, Ion Pairing, and Metal Phosphates. *Chem. Rev.* **2014**, *114* (18), 9047–9153. <https://doi.org/10.1021/cr5001496>.

- 
- <sup>147</sup> Lee, S.; Kim, S. Enantioselective Radical Addition Reactions to Imines Using Binaphthol-Derived Chiral N-Triflyl Phosphoramides. *Tetrahedron Lett.* **2009**, *50* (26), 3345–3348. <https://doi.org/10.1016/j.tetlet.2009.02.136>.
- <sup>148</sup> Friestad, G. K. Control of Asymmetry in the Radical Addition Approach to Chiral Amine Synthesis. In *Stereoselective Formation of Amines*; Li, W., Zhang, X., Eds.; Springer Berlin Heidelberg: Berlin, Heidelberg, 2013; Vol. 343, pp 1–32. [https://doi.org/10.1007/128\\_2013\\_481](https://doi.org/10.1007/128_2013_481).
- <sup>149</sup> Romero, N. A.; Nicewicz, D. A. Organic Photoredox Catalysis. *Chem. Rev.* **2016**, *116* (17), 10075–10166. <https://doi.org/10.1021/acs.chemrev.6b00057>.
- <sup>150</sup> Zhao, Y.; Zhang, C.; Chin, K. F.; Pytela, O.; Wei, G.; Liu, H.; Bureš, F.; Jiang, Z. Dicyanopyrazine-Derived Push–Pull Chromophores for Highly Efficient Photoredox Catalysis. *RSC Adv* **2014**, *4* (57), 30062–30067. <https://doi.org/10.1039/C4RA05525J>.
- <sup>151</sup> Li, J.; Kong, M.; Qiao, B.; Lee, R.; Zhao, X.; Jiang, Z. Formal Enantioconvergent Substitution of Alkyl Halides via Catalytic Asymmetric Photoredox Radical Coupling. *Nat. Commun.* **2018**, *9* (1), 2445. <https://doi.org/10.1038/s41467-018-04885-3>.
- <sup>152</sup> Liu, Y.; Liu, X.; Li, J.; Zhao, X.; Qiao, B.; Jiang, Z. Catalytic Enantioselective Radical Coupling of Activated Ketones with *N*-Aryl Glycines. *Chem. Sci.* **2018**, *9* (42), 8094–8098. <https://doi.org/10.1039/C8SC02948B>.
- <sup>153</sup> Zeng, G.; Li, Y.; Qiao, B.; Zhao, X.; Jiang, Z. Photoredox Asymmetric Catalytic Enantioconvergent Substitution of 3-Chlorooxindoles. *Chem. Commun.* **2019**, *55* (76), 11362. Y.; Qiao, B.; Zhao, X.; Jiang, Z. Photore
- <sup>154</sup> Li, F.; Tian, D.; Fan, Y.; Lee, R.; Lu, G.; Yin, Y.; Qiao, B.; Zhao, X.; Xiao, Z.; Jiang, Z. Chiral Acid-Catalysed Enantioselective C–H Functionalization of Toluene and Its Derivatives Driven by Visible Light. *Nat. Commun.* **2019**, *10* (1), 1774. <https://doi.org/10.1038/s41467-019-09857-9>.
- <sup>155</sup> Yin, Y.; Dai, Y.; Jia, H.; Li, J.; Bu, L.; Qiao, B.; Zhao, X.; Jiang, Z. Conjugate Addition–Enantioselective Protonation of *N*-Aryl Glycines to  $\alpha$ -Branched 2-Vinylazaarenes via Cooperative Photoredox and Asymmetric Catalysis. *J. Am. Chem. Soc.* **2018**, *140* (19), 6083–6087. <https://doi.org/10.1021/jacs.8b01575>.

- 
- <sup>156</sup> Hepburn, H. B.; Melchiorre, P. Brønsted Acid-Catalysed Conjugate Addition of Photochemically Generated  $\alpha$ -Amino Radicals to Alkenylpyridines. *Chem. Commun.* **2016**, 52 (17), 3520–3523. <https://doi.org/10.1039/C5CC10401G>.
- <sup>157</sup> Qiao, B.; Li, C.; Zhao, X.; Yin, Y.; Jiang, Z. Enantioselective Reduction of Azaarene-Based Ketones via Visible Light-Driven Photoredox Asymmetric Catalysis. *Chem. Commun.* **2019**, 55 (52), 7534–7537. <https://doi.org/10.1039/C9CC03661J>.
- <sup>158</sup> Cao, K.; Tan, S. M.; Lee, R.; Yang, S.; Jia, H.; Zhao, X.; Qiao, B.; Jiang, Z. Catalytic Enantioselective Addition of Prochiral Radicals to Vinylpyridines. *J. Am. Chem. Soc.* **2019**, 141 (13), 5437–5443. <https://doi.org/10.1021/jacs.9b00286>.
- <sup>159</sup> Lee, K. N.; Lei, Z.; Ngai, M.-Y.  $\beta$ -Selective Reductive Coupling of Alkenylpyridines with Aldehydes and Imines via Synergistic Lewis Acid/Photoredox Catalysis. *J. Am. Chem. Soc.* **2017**, 139 (14), 5003–5006. <https://doi.org/10.1021/jacs.7b01373>.
- <sup>160</sup> Maity, S.; Zhu, M.; Shinabery, R. S.; Zheng, N. Intermolecular [3+2] Cycloaddition of Cyclopropylamines with Olefins by Visible-Light Photocatalysis. *Angew. Chem. Int. Ed.* **2012**, 51 (1), 222em. Int. Ed.hinabery, R. S.; Zheng, N. Interm
- <sup>161</sup> Yin, Y.; Li, Y.; Gonçalves, T. P.; Zhan, Q.; Wang, G.; Zhao, X.; Qiao, B.; Huang, K.-W.; Jiang, Z. All-Carbon Quaternary Stereocenters  $\alpha$  to Azaarenes via Radical-Based Asymmetric Olefin Difunctionalization. *J. Am. Chem. Soc.* **2020**, 142 (46), 19451–19456. <https://doi.org/10.1021/jacs.0c08329>.
- <sup>162</sup> Proctor, R. S. J.; Phipps, R. J. Recent Advances in Minisci-Type Reactions. *Angew. Chem. Int. Ed.* **2019**, 58 (39), 13666–13699. <https://doi.org/10.1002/anie.201900977>
- <sup>163</sup> Ermanis, K.; Colgan, A. C.; Proctor, R. S. J.; Hadrys, B. W.; Phipps, R. J.; Goodman, J. M. A Computational and Experimental Investigation of the Origin of Selectivity in the Chiral Phosphoric Acid Catalyzed Enantioselective Minisci Reaction. *J. Am. Chem. Soc.* **2020**, 142 (50), 21091–21101. <https://doi.org/10.1021/jacs.0c09668>.
- <sup>164</sup> Liu, X.; Liu, Y.; Chai, G.; Qiao, B.; Zhao, X.; Jiang, Z. Organocatalytic Enantioselective Addition of  $\alpha$ -Aminoalkyl Radicals to Isoquinolines. *Org. Lett.* **2018**, 20 (19), 6298–6301. <https://doi.org/10.1021/acs.orglett.8b02791>.
- <sup>165</sup> Tauber, J.; Imbri, D.; Opatz, T. Radical Addition to Iminium Ions and Cationic Heterocycles. *Molecules* **2014**, 19 (10), 16190–16222 [10.3390/molecules191016190](https://doi.org/10.3390/molecules191016190).

- 
- <sup>166</sup> Fu, M.-C.; Shang, R.; Zhao, B.; Wang, B.; Fu, Y. Photocatalytic Decarboxylative Alkylations Mediated by Triphenylphosphine and Sodium Iodide. *Science* **2019**, *363* (6434), 1429–1434. <https://doi.org/10.1126/science.aav3200>.
- <sup>167</sup> Rono, L. J.; Yayla, H. G.; Wang, D. Y.; Armstrong, M. F.; Knowles, R. R. Enantioselective Photoredox Catalysis Enabled by Proton-Coupled Electron Transfer: Development of an Asymmetric Aza-Pinacol Cyclization. *J. Am. Chem. Soc.* **2013**, *135* (47), 17735–17738. <https://doi.org/10.1021/ja4100595>.
- <sup>168</sup> Tarantino, K. T.; Liu, P.; Knowles, R. R. Catalytic Ketyl-Olefin Cyclizations Enabled by Proton-Coupled Electron Transfer. *J. Am. Chem. Soc.* **2013**, *135* (27), 10022–10025. <https://doi.org/10.1021/ja404342j>.
- <sup>169</sup> Gentry, E. C.; Knowles, R. R. Synthetic Applications of Proton-Coupled Electron Transfer. *Acc. Chem. Res.* **2016**, *49* (8), 1546–1556. <https://doi.org/10.1021/acs.accounts.6b00272>.
- <sup>170</sup> Gentry, E. C.; Rono, L. J.; Hale, M. E.; Matsuura, R.; Knowles, R. R. Enantioselective Synthesis of Pyrroloindolines via Noncovalent Stabilization of Indole Radical Cations and Applications to the Synthesis of Alkaloid Natural Products. *J. Am. Chem. Soc.* **2018**, *140* (9), 3394–3402. <https://doi.org/10.1021/jacs.7b13616>.
- <sup>171</sup> Shin, N. Y.; Ryss, J. M.; Zhang, X.; Miller, S. J.; Knowles, R. R. Light - Driven Deracemization Enabled by Excited - State Electron Transfer. *Science* **2019**, *366* (6463), 364–369. <https://doi.org/10.1126/science.aay2204>.
- <sup>172</sup> Uraguchi, D.; Kinoshita, N.; Kizu, T.; Ooi, T. Synergistic Catalysis of Ionic Brønsted Acid and Photosensitizer for a Redox Neutral Asymmetric  $\alpha$ -Coupling of *N*-Arylaminoethanes with Aldimines. *J. Am. Chem. Soc.* **2015**, *137* (43), 13768–13771. <https://doi.org/10.1021/jacs.5b09329>.
- <sup>173</sup> Zhu, Y.; Zhang, L.; Luo, S. Asymmetric  $\alpha$ -Photoalkylation of  $\beta$ -Ketocarboxyls by Primary Amine Catalysis: Facile Access to Acyclic All-Carbon Quaternary Stereocenters. *J. Am. Chem. Soc.* **2014**, *136* (42), 14642–14645. <https://doi.org/10.1021/ja508605a>.
- <sup>174</sup> Wang, D.; Zhang, L.; Luo, S. Enantioselective Decarboxylative  $\alpha$ -Alkynylation of  $\beta$ -Ketocarboxyls via a Catalytic  $\alpha$ -Imino Radical Intermediate. *Org. Lett.* **2017**, *19* (18), 4924–4927. <https://doi.org/10.1021/acs.orglett.7b02386>.
- <sup>175</sup> Proctor, R. S. J.; Davis, H. J.; Phipps, R. J. Catalytic Enantioselective Minisci-Type Addition to Heteroarenes. *Science* **2018**, *360* (6387), 419–422. <https://doi.org/10.1126/science.aar6376>.



- 
- <sup>176</sup> Reid, J. P.; Proctor, R. S. J.; Sigman, M. S.; Phipps, R. J. Predictive Multivariate Linear Regression Analysis Guides Successful Catalytic Enantioselective Minisci Reactions of Diazines. *J. Am. Chem. Soc.* **2019**, *141* (48), 19178–19185. <https://doi.org/10.1021/jacs.9b11658>.
- <sup>177</sup> Zheng, D.; Studer, A. Asymmetric Synthesis of Heterocyclic  $\Gamma$ -Amino-Acid and Diamine Derivatives by Three-Component Radical Cascade Reactions. *Angew. Chem. Int. Ed.* **2019**, *58* (44), 15803–15807. <https://doi.org/10.1002/anie.201908987>.
- <sup>178</sup> Yang, Y.-H.; Sibi, M. P. Stereoselective Radical Reactions. In *Encyclopedia of Radicals in Chemistry, Biology and Materials*; Chatgililoglu, C., Studer, A., Eds.; John Wiley & Sons, Ltd: Chichester, UK, 2012; p rad019. <https://doi.org/10.1002/9781119953678.rad019>.
- <sup>179</sup> Lewis, F. D.; Barancyk, S. V. Lewis Acid Catalysis of Photochemical Reactions. 8. Photodimerization and Cross-Cycloaddition of Coumarin. *J. Am. Chem. Soc.* **1989**, *111* (23), 8653–8661. <https://doi.org/10.1021/ja00205a015>.
- <sup>180</sup> Guo, H.; Herdtweck, E.; Bach, T. Enantioselective Lewis Acid Catalysis in Intramolecular [2+2] Photocycloaddition Reactions of Coumarins. *Angew. Chem. Int. Ed.* **2010**, *49* (42), 7782–7785. <https://doi.org/10.1002/anie.201003619>.
- <sup>181</sup> Brimiouille, R.; Guo, H.; Bach, T. Enantioselective Intramolecular [2+2] Photocycloaddition Reactions of 4-Substituted Coumarins Catalyzed by a Chiral Lewis Acid. *Chem. - Eur. J.* **2012**, *18* (24), 7552–7560. <https://doi.org/10.1002/chem.201104032>.
- <sup>182</sup> Brimiouille, R.; Bach, T. Enantioselective Lewis Acid Catalysis of Intramolecular Enone [2+2] Photocycloaddition Reactions. *Science* **2013**, *342* (6160), 840–843. <https://doi.org/10.1126/science.1244809>.
- <sup>183</sup> Corey, E. J. Enantioselective Catalysis Based on Cationic Oxazaborolidines. *Angew. Chem. Int. Ed.* **2009**, *48* (12), 2100–2117. <https://doi.org/10.1002/anie.200805374>.
- <sup>184</sup> Brimiouille, R.; Bauer, A.; Bach, T. Enantioselective Lewis Acid Catalysis in Intramolecular [2 + 2] Photocycloaddition Reactions: A Mechanistic Comparison between Representative Coumarin and Enone Substrates. *J. Am. Chem. Soc.* **2015**, *137* (15), 5170–5176. <https://doi.org/10.1021/jacs.5b01740>.
- <sup>185</sup> Brimiouille, R.; Bach, T. [2+2] Photocycloaddition of 3-Alkenyloxy-2-Cycloalkenones: Enantioselective Lewis Acid Catalysis and Ring Expansion. *Angew. Chem. Int. Ed.* **2014**, *53* (47), 12921–12924. <https://doi.org/10.1002/anie.201407832>.

- 
- <sup>186</sup> Poplata, S.; Bach, T. Enantioselective Intermolecular [2+2] Photocycloaddition Reaction of Cyclic Enones and Its Application in a Synthesis of (-)-Grandisol. *J. Am. Chem. Soc.* **2018**, *140* (9), 3228–3231. <https://doi.org/10.1021/jacs.8b01011>.
- <sup>187</sup> Stegbauer, S.; Jandl, C.; Bach, T. Enantioselective Lewis Acid Catalyzed *Ortho* Photocycloaddition of Olefins to Phenanthrene-9-Carboxaldehydes. *Angew. Chem. Int. Ed.* **2018**, *57* (44), 14593–14596. <https://doi.org/10.1002/anie.201808919>.
- <sup>188</sup> Daub, M. E.; Jung, H.; Lee, B. J.; Won, J.; Baik, M.-H.; Yoon, T. P. Enantioselective [2+2] Cycloadditions of Cinnamate Esters: Generalizing Lewis Acid Catalysis of Triplet Energy Transfer. *J. Am. Chem. Soc.* **2019**, *141* (24), 9543–9547. <https://doi.org/10.1021/jacs.9b04643>.
- <sup>189</sup> Brak, K.; Jacobsen, E. N. Asymmetric Ion-Pairing Catalysis. *Angew. Chem. Int. Ed.* **2013**, *52* (2), 534–561. <https://doi.org/10.1002/anie.201205449>.
- <sup>190</sup> Woźniak, Ł.; Murphy, J. J.; Melchiorre, P. Photo-Organocatalytic Enantioselective Perfluoroalkylation of  $\beta$ -Ketoesters. *J. Am. Chem. Soc.* **2015**, *137* (17), 5678–5681. <https://doi.org/10.1021/jacs.5b03243>.
- <sup>191</sup> Yang, C.; Zhang, W.; Li, Y.-H.; Xue, X.-S.; Li, X.; Cheng, J.-P. Origin of Stereoselectivity of the Photoinduced Asymmetric Phase-Transfer-Catalyzed Perfluoroalkylation of  $\beta$ -Ketoesters. *J. Org. Chem.* **2017**, *82* (18), 9321–9327. <https://doi.org/10.1021/acs.joc.7b01130>.
- <sup>192</sup> Morse, P. D.; Nguyen, T. M.; Cruz, C. L.; Nicewicz, D. A. Enantioselective Counter-Anions in Photoredox Catalysis: The Asymmetric Cation Radical Diels-Alder Reaction. *Tetrahedron* **2018**, *74* (26), 3266–3272. <https://doi.org/10.1016/j.tet.2018.03.052>.
- <sup>193</sup> Poli, R. Radical Coordination Chemistry and its Relevance to Metal-Mediated Radical Polymerization. *Eur. J. Inorg. Chem.* **2011**, 1513–1530. <https://doi.org/10.1002/ejic.201001364>.
- <sup>194</sup> RajanBabu, T. V.; Nugent, W. A. Selective Generation of Free Radicals from Epoxides Using a Transition-Metal Radical. A Powerful New Tool for Organic Synthesis. *J. Am. Chem. Soc.* **1994**, *116* (3), 986–997. <https://doi.org/10.1021/ja00082a021>.
- <sup>195</sup> Gansäuer, A.; Bluhm, H. Reagent-Controlled Transition-Metal-Catalyzed Radical Reactions. *Chem. Rev.* **2000**, *100* (8), 2771–2788. <https://doi.org/10.1021/cr9902648>.
- <sup>196</sup> Enemærke, R. J.; Larsen, J.; Skrydstrup, T.; Daasbjerg, K. Revelation of the Nature of the Reducing Species in Titanocene Halide-Promoted Reductions. *J. Am. Chem. Soc.* **2004**, *126* (25), 7853–7864. <https://doi.org/10.1021/ja0491230>.

- 
- <sup>197</sup> Richrath, R. B.; Olyschläger, T.; Hildebrandt, S.; Enny, D. G.; Fianu, G. D.; Flowers, R. A.; Gansäuer, A. Cp<sub>2</sub>TiX Complexes for Sustainable Catalysis in Single-Electron Steps. *Chem. - Eur. J.* **2018**, *24* (24), 6371–6379. <https://doi.org/10.1002/chem.201705707>.
- <sup>198</sup> Kuhn, A.; Conradie, J. Orbital Control over the Metal vs. Ligand Reduction in a Series of Neutral and Cationic Bis(Cyclopentadienyl) Ti(IV) Complexes. *New J. Chem.* **2018**, *42* (1), 662–670. <https://doi.org/10.1039/C7NJ03746E>.
- <sup>199</sup> Liedtke, T.; Hilche, T.; Klare, S.; Gansäuer, A. Condition Screening for Sustainable Catalysis in Single-Electron Steps by Cyclic Voltammetry: Additives and Solvents. *ChemSusChem* **2019**, *12* (13), 3166–3171. <https://doi.org/10.1002/cssc.201900344>.
- <sup>200</sup> McCallum, T.; Wu, X.; Lin, S. Recent Advances in Titanium Radical Redox Catalysis. *J. Org. Chem.* **2019**, *84* (22), 14369–14380. <https://doi.org/10.1021/acs.joc.9b02465>.
- <sup>201</sup> Manßen, M.; Schafer, L. L. Titanium Catalysis for the Synthesis of Fine Chemicals – Development and Trends. *Chem. Soc. Rev.* **2020**, *49* (19), 6947–6994. <https://doi.org/10.1039/D0CS00229A>.
- <sup>202</sup> Zhang, Z.; Richrath, R. B.; Gansäuer, A. Merging Catalysis in Single Electron Steps with Photoredox Catalysis—Efficient and Sustainable Radical Chemistry. *ACS Catal.* **2019**, *9* (4), 3208–3212. <https://doi.org/10.1021/acscatal.9b00787>.
- <sup>203</sup> Lin, S.; Chen, Y.; Li, F.; Shi, C.; Shi, L. Visible-Light-Driven Spirocyclization of Epoxides via Dual Titanocene and Photoredox Catalysis. *Chem. Sci.* **2020**, *11* (3), 839–844. <https://doi.org/10.1039/C9SC05601G>.
- <sup>204</sup> Bensari, A.; Renaud, J.-L.; Riant, O. Enantioselective Pinacol Coupling of Aldehydes Mediated and Catalyzed by Chiral Titanium Complexes. *Org. Lett.* **2001**, *3* (24), 3863–3865. <https://doi.org/10.1021/ol016664a>.
- <sup>205</sup> Frey, G.; Hausmann, J. N.; Streuff, J. Titanium-Catalyzed Reductive Umpolung Reactions with a Metal-Free Terminal Reducing Agent. *Chem. - Eur. J.* **2015**, *21* (15), 5693–5696. <https://doi.org/10.1002/chem.201500102>.
- <sup>206</sup> Streuff, J.; Feurer, M.; Bichovski, P.; Frey, G.; Gellrich, U. Enantioselective Titanium(III)-Catalyzed Reductive Cyclization of Ketonitriles. *Angew. Chem. Int. Ed.* **2012**, *51* (34), 8661–8664. <https://doi.org/10.1002/anie.201204469>.
- <sup>207</sup> Streuff, J.; Feurer, M.; Frey, G.; Steffani, A.; Kacprzak, S.; Weweler, J.; Leijendekker, L. H.; Kratzert, D.; Plattner, D. A. Mechanism of the Ti<sup>III</sup>-Catalyzed Acyloin-Type Umpolung:

---

A Catalyst-Controlled Radical Reaction. *J. Am. Chem. Soc.* **2015**, *137* (45), 14396–14405. <https://doi.org/10.1021/jacs.5b09223>.

<sup>208</sup> Gordon, J.; Hildebrandt, S.; Dewese, K. R.; Klare, S.; Gansäuer, A.; RajanBabu, T. V.; Nugent, W. A. Demystifying Cp<sub>2</sub>Ti(H)Cl and Its Enigmatic Role in the Reactions of Epoxides with Cp<sub>2</sub>TiCl. *Organometallics* **2018**, *37* (24), 4801–4809. <https://doi.org/10.1021/acs.organomet.8b00793>.

<sup>209</sup> Hao, W.; Harenberg, J. H.; Wu, X.; MacMillan, S. N.; Lin, S. Diastereo- and Enantioselective Formal [3 + 2] Cycloaddition of Cyclopropyl Ketones and Alkenes via Ti-Catalyzed Radical Redox Relay. *J. Am. Chem. Soc.* **2018**, *140* (10), 3514–3517. <https://doi.org/10.1021/jacs.7b13710>.

<sup>210</sup> Muñoz-Bascón, J.; Hernández-Cervantes, C.; Padial, N. M.; Álvarez-Corral, M.; Rosales, A.; Rodríguez-García, I.; Oltra, J. E. Ti-Catalyzed Straightforward Synthesis of Exocyclic Allenes. *Chem. - Eur. J.* **2014**, *20* (3), 801–810. <https://doi.org/10.1002/chem.201304033>.

<sup>211</sup> Gansäuer, A.; Behlendorf, M.; Cangönül, A.; Kube, C.; Cuerva, J. M.; Friedrich, J.; van Gastel, M. H<sub>2</sub>O Activation for Hydrogen-Atom Transfer: Correct Structures and Revised Mechanisms. *Angew. Chem. Int. Ed.* **2012**, *51* (13), 3266–3270. <https://doi.org/10.1002/anie.201107556>.

<sup>212</sup> Roldan-Molina, E.; Padial, N. M.; Lezama, L.; Oltra, J. E. CpTiCl<sub>2</sub>, an Improved Titanocene(III) Catalyst in Organic Synthesis: CpTiCl<sub>2</sub>, an Improved Titanocene(III) Catalyst in Organic Synthesis. *Eur. J. Org. Chem.* **2018**, *2018* (43), 5997–6001. <https://doi.org/10.1002/ejoc.201801120>.

<sup>213</sup> Estévez, R. E.; Justicia, J.; Bazdi, B.; Fuentes, N.; Paradas, M.; Choquesillo-Lazarte, D.; García-Ruiz, J. M.; Robles, R.; Gansäuer, A.; Cuerva, J. M.; Oltra, J. E. Ti-Catalyzed Barbier-Type Allylations and Related Reactions. *Chem. - Eur. J.* **2009**, *15* (12), 2774–2791. <https://doi.org/10.1002/chem.200802180>.

<sup>214</sup> Fleury, L. M.; Kosal, A. D.; Masters, J. T.; Ashfeld, B. L. Cooperative Titanocene and Phosphine Catalysis: Accelerated C–X Activation for the Generation of Reactive Organometallics. *J. Org. Chem.* **2013**, *78* (2), 253–269. <https://doi.org/10.1021/jo301726v>.

<sup>215</sup> Klare, S.; Gordon, J. P.; Gansäuer, A.; RajanBabu, T. V.; Nugent, W. A. The Reaction of β-epoxy Alcohols with Titanium(III) Reagents. A Proposed Role for Intramolecular

<sup>216</sup> Gansäuer, A.; Justicia, J.; Fan, C.-A.; Worgull, D.; Piestert, F. Reductive C–C Bond Formation after Epoxide Opening via Electron Transfer. In *Metal Catalyzed Reductive C–C Bond Formation*; Krische, M. J., Ed.; Topics in Current Chemistry; Springer Berlin Heidelberg: Berlin, Heidelberg, 2007; Vol. 279, pp 25–52. [https://doi.org/10.1007/128\\_2007\\_130](https://doi.org/10.1007/128_2007_130).

<sup>217</sup> Gansäuer, A.; Fleckhaus, A.; Lafont, M. A.; Okkel, A.; Kotsis, K.; Anoop, A.; Neese, F. Catalysis via Homolytic Substitutions with C–O and Ti–O Bonds: Oxidative Additions and Reductive Eliminations in Single Electron Steps. *J. Am. Chem. Soc.* **2009**, *131* (46), 16989–16999. <https://doi.org/10.1021/ja907817y>.

<sup>218</sup> Daasbjerg, K.; Svith, H.; Grimme, S.; Gerenkamp, M.; Mück-Lichtenfeld, C.; Gansäuer, A.; Barchuk, A.; Keller, F. Elucidation of the Mechanism of Titanocene-Mediated Epoxide Opening by a Combined Experimental and Theoretical Approach. *Angew. Chem. Int. Ed.* **2006**, *45* (13), 2041–2044. <https://doi.org/10.1002/anie.200504176>.

<sup>219</sup> Gansäuer, A.; Bluhm, H.; Pierobon, M. Emergence of a Novel Catalytic Radical Reaction: Titanocene-Catalyzed Reductive Opening of Epoxides. *J. Am. Chem. Soc.* **1998**, *120* (49), 12849–12859. <https://doi.org/10.1021/ja981635p>.

<sup>220</sup> Gansäuer, A.; Fleckhaus, A. Epoxides in Titanocene-Mediated and -Catalyzed Radical Reactions. In *Encyclopedia of Radicals in Chemistry, Biology and Materials*; Chatgililoglu, C., Studer, A., Eds.; John Wiley & Sons, Ltd: Chichester, UK, 2012; p rad029. <https://doi.org/10.1002/9781119953678.rad029>.

<sup>221</sup> Cuerva, J. M.; Campaña, A. G.; Justicia, J.; Rosales, A.; Oller-López, J. L.; Robles, R.; Cárdenas, D. J.; Buñuel, E.; Oltra, J. E. Water: The Ideal Hydrogen-Atom Source in Free-Radical Chemistry Mediated by Ti<sup>III</sup> and Other Single-Electron-Transfer Metals? *Angew. Chem. Int. Ed.* **2006**, *45* (33), 5522–5526. <https://doi.org/10.1002/anie.200600831>.

<sup>222</sup> Paradas, M.; Campaña, A. G.; Jiménez, T.; Robles, R.; Oltra, J. E.; Buñuel, E.; Justicia, J.; Cárdenas, D. J.; Cuerva, J. M. Understanding the Exceptional Hydrogen-Atom Donor Characteristics of Water in Ti<sup>III</sup>-Mediated Free-Radical Chemistry. *J. Am. Chem. Soc.* **2010**, *132* (36), 12748–12756. <https://doi.org/10.1021/ja105670h>.

<sup>223</sup> Gansäuer, A.; Otte, M.; Shi, L. Radical Cyclizations Terminated by Ir-Catalyzed Hydrogen Atom Transfer. *J. Am. Chem. Soc.* **2011**, *133* (3), 416–417. <https://doi.org/10.1021/ja109362m>.

- 
- <sup>224</sup> Gansäuer, A.; Fan, C.-A.; Piestert, F. Sustainable Radical Reduction through Catalytic Hydrogen Atom Transfer. *J. Am. Chem. Soc.* **2008**, *130* (22), 6916–6917. <https://doi.org/10.1021/ja801232t>.
- <sup>225</sup> Yao, C.; Dahmen, T.; Gansäuer, A.; Norton, J. Anti-Markovnikov Alcohols via Epoxide Hydrogenation through Cooperative Catalysis. *Science* **2019**, *364* (6442), 764–767. <https://doi.org/10.1126/science.aaw3913>.
- <sup>226</sup> Quílez del Moral, J. F.; Pérez, Á.; Herrador, M. del M.; Barrero, A. F. Access to Natural Valparanes and Daucanes: Enantioselective Synthesis of (–)-Valpara-2,15-Diene and (+)-Isodaucene. *J. Nat. Prod.* **2019**, *82* (1), 9–15.
- <sup>227</sup> Sun, Y.; Meng, Z.; Chen, P.; Zhang, D.; Baunach, M.; Hertweck, C.; Li, A. A Concise Total Synthesis of Sespenine, a Structurally Unusual Indole Terpenoid from *Streptomyces*. *Org. Chem. Front.* **2016**, *3* (3), 368–374. <https://doi.org/10.1039/C5QO00416K>.
- <sup>228</sup> Funken, N.; Zhang, Y.-Q.; Gansäuer, A. Regiodivergent Catalysis: A Powerful Tool for Selective Catalysis. *Chem. - Eur. J.* **2017**, *23* (1), 19–32. <https://doi.org/10.1002/chem.201603993>.
- <sup>229</sup> Gansäuer, A. From Enantioselective to Regiodivergent Epoxide Opening and Radical Arylation – Useful or Just Interesting? *Synlett* **2020**, *32* (5), 447–456. <https://doi.org/10.1055/s-0040-1706407>.
- <sup>230</sup> Gansäuer, A.; Shi, L.; Otte, M. Catalytic Enantioselective Radical Cyclization via Regiodivergent Epoxide Opening. *J. Am. Chem. Soc.* **2010**, *132* (34), 11858–11859. <https://doi.org/10.1021/ja105023y>.
- <sup>231</sup> For reactions starting from entioenriched epoxide, see: Mülhaus, F.; Weissbarth, H.; Dahmen, T.; Schenkenburg, G.; Gansäuer, A. Merging Regiodivergent Catalysis with Atom-Economical Radical Arylation. *Angew. Chem. Int. Ed.* **2019**, *58*, 14208–14212. <https://doi.org/10.1002/anie.201908860>.
- <sup>232</sup> Zhao, Y.; Weix, D. J. Enantioselective Cross-Coupling of *Meso* -Epoxides with Aryl Halides. *J. Am. Chem. Soc.* **2015**, *137* (9), 3237–3240. <https://doi.org/10.1021/jacs.5b01909>.
- <sup>233</sup> Ye, K.-Y.; McCallum, T.; Lin, S. Bimetallic Radical Redox-Relay Catalysis for the Isomerization of Epoxides to Allylic Alcohols. *J. Am. Chem. Soc.* **2019**, *141* (24), 9548–9554. <https://doi.org/10.1021/jacs.9b04993>.

- 
- <sup>234</sup> Fernández-Mateos, A.; Herrero Teijón, P.; Rubio González, R. Titanocene-Promoted Stereoselective Eliminations on Epoxy Alcohols Derived from R-(–)-Carvone. *Tetrahedron* **2013**, *69* (5), 1611–1616. <https://doi.org/10.1016/j.tet.2012.11.093>.
- <sup>235</sup> Mühlhaus, F.; Weißbarth, H.; Dahmen, T.; Schnakenburg, G.; Gansäuer, A. Merging Regiodivergent Catalysis with Atom-Economical Radical Arylation. *Angew. Chem. Int. Ed.* **2019**, *58* (40), 14208–14212. <https://doi.org/10.1002/anie.201908860>.
- <sup>236</sup> Smith, K. M. Paramagnetic organometallic Cr(II)/Cr(III) redox-active catalysts. *Coord. Chem. Rev.* **2006**, *250*, 1023–1031. <https://doi.org/10.1016/j.ccr.2005.11.019>.
- <sup>237</sup> Bandini, M.; Cozzi, P. G.; Melchiorre, P.; Umani-Ronchi, A. The First catalytic Enantioselective Nozaki-Hiyama Reaction. *Angew. Chem. Int. Ed.* **1999**, *38*, 3357–3359. [https://doi.org/10.1002/\(SICI\)1521-3773\(19991115\)38:22<3357::AID-ANIE3357>3.0.CO;2-W](https://doi.org/10.1002/(SICI)1521-3773(19991115)38:22<3357::AID-ANIE3357>3.0.CO;2-W).
- <sup>238</sup> For attempts to perform asymmetric pinacol type reactions, see: Groth, U.; Jung, M.; Till Vogel, T. Chromium-Catalyzed Pinacol-Type Cross-Coupling: Studies on Stereoselectivity. *Chem. Eur. J.* **2005**, *11*, 3127–3135. <https://doi.org/10.1002/chem.200400304>
- <sup>239</sup> Takenaka, N.; Xia, G.; Yamamoto, H. Catalytic, Highly Enantio- and Diastereoselective Pinacol Coupling Reaction with a New Tethered Bis(8-quinolinolato) Ligand. *J. Am. Chem. Soc.* **2004**, *126*, 13198–13199. <https://doi.org/10.1021/ja045430u>.
- <sup>240</sup> For a review, see: Yamamoto, H.; Xia, G. Asymmetric Catalytic Redox System: Tethered Bis(8-quinolinolato) (TBOx) Chromium(III/II) Complexes. *Chem. Letters* **2007**, *36*, 1082–1087. <https://doi.org/10.1246/cl.2007.1082>
- <sup>241</sup> Schwarz, J. L.; Huang, H.-M.; Paulisch, T. O.; Glorius, F. Dialkylation of 1,3-dienes by Dual Photoredox and Chromium Catalysis. *ACS Catal.* **2020**, *10*, 1621–1627. <https://doi.org/10.1021/acscatal.9b04222>.
- <sup>242</sup> Tanabe, S.; Mitsunuma, H.; Kanai, M. Catalytic Allylation of Aldehydes using Unactivated Alkenes. *J. Am. Chem. Soc.* **2020**, *142*, 12374–12381. <https://doi.org/10.1021/jacs.0c04735>.
- <sup>243</sup> For preliminary work, see: Mitsunuma, H.; Tanabe, S.; Fuse, H.; Ohkubo, K.; Kanai, M. Catalytic asymmetric allylation of aldehydes with alkenes through allylic C(sp<sup>3</sup>)–H functionalization mediated by organophotoredox and chiral chromium hybrid catalysis. *Chem. Sci.* **2019**, *10*, 3459–3465. <https://doi.org/10.1039/C8SC05677C>.

- 
- <sup>244</sup> Zhang, H.; Chen, B.; Zhang, G. Enantioselective 1,2-Alkylhydroxymethylation of Alkynes via Chromium/Cobalt Cocatalysis. *Org. Lett.* **2020**, *22*, 656–660. <https://doi.org/10.1021/acs.orglett.9b04430>.
- <sup>245</sup> Hirao, H.; Katayama, Y.; Mitsunuma, H.; Kanai, M. Chromium-Catalyzed Linear-Selective Alkylation of Aldehydes with Alkenes. *Org. Lett.* **2020**, *22*, 8584–8588. <https://doi.org/10.1021/acs.orglett.0c03180>.
- <sup>246</sup> Rana, S.; Biswas, J. P.; Paul, S.; Aniruddha Paika, A.; Maiti, D. Organic synthesis with the most abundant transition metal–iron: from rust to multitasking catalysts. *Chem. Soc. Rev.* **2021**, *50*, 243–472. <https://doi.org/10.1039/D0CS00688B>.
- <sup>247</sup> For a general review covering radical reactivity of groups 8 and 9 elements, see: Jahn, U. Radicals in Transition Metal Catalyzed Reactions? Transition Metal Catalyzed Radical Reactions? – A Fruitful Interplay Anyway. In *Radicals in Synthesis III*; Heinrich, M., Gansäuer, A., Eds.; Topics in Current Chemistry; Springer Berlin Heidelberg: Berlin, Heidelberg, 2011; Vol. 320, pp 191–322. [https://doi.org/10.1007/128\\_2011\\_285](https://doi.org/10.1007/128_2011_285).
- <sup>248</sup> For a coverage of the latest advances in iron-mediated asymmetric synthesis, see: (a) Casnati, A.; Lanzi, M.; Cera, G. Recent Advances in Asymmetric Iron Catalysis. *Molecules* **2020**, *25* (17), 3889. <https://doi.org/10.3390/molecules25173889>. (b) Pellissier, H. Recent developments in enantioselective iron-catalyzed transformations. *Coord. Chem. Rev.* **2019**, *386*, 1–31. <https://doi.org/10.1016/j.ccr.2019.01.011>.
- <sup>249</sup> Gualandi, A.; Marchini, M.; Mengozzi, L.; Natali, M.; Lucarini, M.; Ceroni, P.; Cozzi, P. G. Organocatalytic Enantioselective Alkylation of Aldehydes with [Fe(Bpy)<sub>3</sub>]Br<sub>2</sub> Catalyst and Visible Light. *ACS Catal.* **2015**, *5* (10), 5927–5931. <https://doi.org/10.1021/acscatal.5b01573>.
- <sup>250</sup> Narute, S.; Regev Parnes, R.; F. Dean Toste, F. D.; Pappo, D. D Enantioselective Oxidative Homocoupling and Cross-Coupling of 2-Naphthols Catalyzed by Chiral Iron Phosphate Complexes. *J. Am. Chem. Soc.* **2016**, *138*, 16553–16560. <https://doi.org/10.1021/jacs.6b11198>.
- <sup>251</sup> Egami, H.; Matsumoto, K.; Oguma, T.; Kunisu, T.; Katsuki, T. Enantioenriched Synthesis of C-1-Symmetric BINOLs: Iron-Catalyzed Cross-Coupling of 2-Naphthols and Some Mechanistic Insight. *J. Am. Chem. Soc.* **2010**, *132*, 13633–13635. DOI: 10.1021/ja105442m
- <sup>252</sup> Jin, M.; Adak, L.; Nakamura, M. Iron-Catalyzed Enantioselective Cross-Coupling Reactions of  $\alpha$ -Chloroesters with Aryl Grignard Reagents. *J. Am. Chem. Soc.* **2015**, *137*, 7128–7134. <https://doi.org/10.1021/jacs.5b02277>.



- 
- <sup>253</sup> For additional mechanistic investigation, see: Liu, L.; Lee, W.; Zhou, J.; Bandyopadhyay, S.; Gutierrez, O. Radical-clock  $\alpha$ -halo-esters as mechanistic probes for biphosphine iron-catalyzed cross-coupling reactions. *Tetrahedron* **2019**, *75*, 129–136. <https://doi.org/10.1016/j.tet.2018.11.043>
- <sup>254</sup> Lou, S.; Fu, G. C. Nickel/Bis(oxazoline)-Catalyzed Asymmetric Kumada Reactions of Alkyl Electrophiles: Cross-Couplings of Racemic  $\alpha$ -Bromoketones. *J. Am. Chem. Soc.* **2010**, *132*, 1264–1266. <https://doi.org/10.1021/ja909689t>
- <sup>255</sup> Sharma, A. K.; Sameera, W. M. C.; Jin, M.; Adak, L.; Okuzono, C.; Iwamoto, T.; Kato, M.; Nakamura, M.; Morokuma, K. DFT and AFIR Study on the Mechanism and the Origin of Enantioselectivity in Iron-Catalyzed Cross-Coupling Reactions. *J. Am. Chem. Soc.*, **2017**, *139*, 16117–13125.
- <sup>256</sup> Iwamoto, T.; Okuzono, C.; Adak, L.; Jinc, M.; Nakamura, M. Iron-catalyzed enantioselective Suzuki–Miyaura coupling of racemic alkyl bromides. *Chem. Commun.* **2019**, *55*, 1128–1131.
- <sup>257</sup> Ge, L.; Zhou, H.; Chiou, M.-F.; Jiang, H.; Jian, W.; Ye, C.; Li, X.; Zhu, X.; Xiong, H.; Li, Y.; Song, L.; Zhang, X.; Bao, H. Iron-catalysed asymmetric carboazidation of styrenes. *Nature Catal.* **2021**, *4*, 28–35. <https://doi.org/10.1038/s41929-020-00551-4>
- <sup>258</sup> Lv, D.; Sun, Q.; Zhou, H.; Ge, L.; Qu, Y.; Li, T.; Ma, X.; Li, Y.; Bao, H. Iron-Catalyzed Radical Asymmetric Aminoazidation and Diazidation of Styrenes. *Angew. Chem. Int. Ed.* **2021**, *60*, 12455–12460. <https://doi.org/10.1002/anie.202017175>
- <sup>259</sup> For a general review, see: Poulos, T. L. Heme Enzyme Structure and Function. *Chem. Rev.* **2014**, *114*, 3919–3962. <https://doi.org/10.1021/cr400415k>
- <sup>260</sup> For a review on mechanism, see: Huang, X.; Groves, J. T. Beyond ferryl-mediated hydroxylation: 40 years of the rebound mechanism and C–H activation. *J. Biol. Inorg. Chem.* **2017**, *22*, 185–207. <https://doi.org/10.1007/s00775-016-1414-3>
- <sup>261</sup> For recent discussion, see: Coleman, T.; Kirk, A. M.; Chao, R. R.; Podgorski, M. N.; Harbort, J. S.; Churchman, L. R.; Bruning, J. B.; Bernhardt, P. V.; Harmer, J. R.; Krenske, E. H.; De Voss, J. J.; Bell, S. G. Understanding the Mechanistic Requirements for Efficient and Stereoselective Alkene Epoxidation by a Cytochrome P450 Enzyme. *ACS Catal.* **2021**, *11*, 1995–2010. <https://doi.org/10.1021/acscatal.0c04872>

---

<sup>262</sup> See also: Lee, Y.-M.; Kim, S.; Ohkubo, K.; Kim, K.-H.; Nam, W.; Fukuzumi, S. Unified Mechanism of Oxygen Atom Transfer and Hydrogen Atom Transfer Reactions with a Triflic Acid-Bound Nonheme Manganese(IV)-Oxo Complex via Outer-Sphere Electron Transfer. *J. Am. Chem. Soc.* **2019**, *141*, 2614–2622. <https://doi.org/10.1021/jacs.8b12935>

<sup>263</sup> For a tutorial review, see: Cho, K.-B.; Hirao, H.; Sason Shaik, S.; Nam, W. To rebound or dissociate? This is the mechanistic question in C–H hydroxylation by heme and non-heme metal–oxo complexes. *Chem. Soc. Rev.* **2016**, *45*, 1197–1210. <https://doi.org/10.1039/C5CS00566C>

<sup>264</sup> Wu, X.; Seo, M. S.; Davis, K. M.; Lee, Y.-M.; Chen, J.; Cho, K.-B.; Pushkar, Y. N.; Nam, W. A highly Reactive Mononuclear Non-Heme Manganese(IV)-Oxo Complex That Can Activate the Strong C-H Bonds of Alkanes. *J. Am. Chem. Soc.* **2011**, *133*, 20088–20091. <https://doi.org/10.1021/ja208523u>

<sup>265</sup> (a) Breslow, R.; Winnik, M. A. Remote oxidation of unactivated methylene groups. *J. Am. Chem. Soc.* **1969**, *91*, 3083–3084. <https://doi.org/10.1021/ja01039a043>. (b) Breslow, R.; Rothbard, J.; Herman, F.; Rodriguez, M. L. Remote Functionalization Reactions as Conformational Probes for Flexible Alkyl Chains. *J. Am. Chem. Soc.* **1978**, *100*, 1213–1218. <https://doi.org/10.1021/ja00472a030>. (c) Breslow, R.; Maitra, U.; Heyer, D. Remote Functionalization On The Steroid B-Face: Attack On An Angular Methyl Group, And Into The Sidechain. *Tetrahedron Lett.* **1984**, *25*, 1123–1126. [https://doi.org/10.1016/S0040-4039\(01\)91539-4](https://doi.org/10.1016/S0040-4039(01)91539-4).

<sup>266</sup> (a) Breslow, R. Biomimetic Chemistry and Artificial Enzymes: Catalysis by Design. *Acc. Chem. Res.* **1995**, *28*, 146–153. <https://doi.org/10.1021/ar00051a008>. (b) Breslow R. Biomimetic Selectivity. *Chem. Rec.* **2001**, *1*, 3–11. [https://doi.org/10.1002/1528-0691\(2001\)1:1<3::AID-TCR3>3.0.CO;2-B](https://doi.org/10.1002/1528-0691(2001)1:1<3::AID-TCR3>3.0.CO;2-B).

<sup>267</sup> Das, S.; Brudvig, G. W.; Crabtree, R. H. Molecular recognition in homogeneous transition metal catalysis: a biomimetic strategy for high selectivity. *Chem. Commun.* **2008**, 413–424. <https://doi.org/10.1039/B710355G>

<sup>268</sup> Giorgio Olivo, G.; Giulio Farinelli, G.; Alessia Barbieri, A.; Osvaldo Lanzalunga, O.; Stefano Di Stefano, S.; Costas, M. Supramolecular Recognition Allows Remote, Site-Selective C-H Oxidation of Methylene Sites in Linear Amines. *Angew. Chem. Int. Ed.* **2017**, *56*, 16347–16351. <https://doi.org/10.1002/anie.201709280>

- 
- <sup>269</sup> (a) Milan, M.; Salamone, M.; Costas, M.; Bietti, M. The Quest for Selectivity in Hydrogen Atom Transfer Based Aliphatic C-H Oxidations. *Acc. Chem. Res.* **2018**, *51*, 1984–1995. <https://doi.org/10.1021/acs.accounts.8b00231> (b) Vidal, D.; Olivo, G.; Costas, M. Controlling selectivity in Aliphatic C-H oxidation through Supramolecular Recognition. *Chem. Eur. J.* **2018**, *24*, 5042–5054. <https://doi.org/10.1002/chem.201704852> (c) Sun, W.; Sun, Q. Bioinspired Manganese and Iron Complexes for Enantioselective Oxidation Reactions; Ligand Design, Catalytic Activity, and Beyond. *Acc. Chem. Res.* **2019**, *52*, 2370–2381. <https://doi.org/10.1021/acs.accounts.9b00285>
- <sup>270</sup> Burg, F.; Gicquel, M.; Breitenlechner, S.; Pöthig, A.; Bach, T. Site- and Enantioselective C-H Oxygenation Catalyzed by a Chiral Manganese Porphyrin Complex with a Remote Binding Site. *Angew. Chem. Int. Ed.* **2018**, *57*, 2953–2957. <https://doi.org/10.1002/anie.201712340>
- <sup>271</sup> The design of hypersensitive extremely fast radical clock led Newcomb to question the RM mechanism and has led to controversial debate on the cytochrome P450 mechanism of action. For representative reports, see: (a) Newcomb, M.; Toy, P. H. Hypersensitive Radical Probes and the Mechanisms of Cytochrome P450-Catalyzed Hydroxylation Reactions. *Acc. Chem. Res.* **2000**, *33*, 449–455. <https://doi.org/10.1021/ar960058b> (b) Austin, R. N.; Deng, D.; Jiang, Y.; Luddy, K.; van Beilen, J. B.; Ortiz de Montellano, P. R.; Groves, J. T. The Diagnostic Substrate Bicyclohexane Reveals a Radical Mechanism for Bacterial Cytochrome P450 in Whole Cells. *Angew. Chem. Int. Ed.* **2006**, *45*, 8192–8194. <https://doi.org/10.1002/anie.200603282>
- <sup>272</sup> Burg, F.; Breitenlechner, S.; Jandl, C.; Bach, T. Enantioselective oxygenation of exocyclic methylene groups by a manganese porphyrin catalyst with a chiral recognition site. *Chem. Sci.* **2020**, *11*, 2121–2129. [10.1039/C9SC06089H](https://doi.org/10.1039/C9SC06089H)
- <sup>273</sup> Srour, H.; Le Maux, P.; Simonneaux, G. Enantioselective Manganese-Porphyrin-Catalyzed Epoxidation and C–H Hydroxylation with Hydrogen Peroxide in Water/Methanol Solutions. *Inorg. Chem.* **2012**, *51*, 5850–5856. <https://doi.org/10.1021/ic300457z>
- <sup>274</sup> Gomez, L.; Garcia-Bosch, I.; Company, A.; J. Benet-Buchholz, J.; Sala, A. P.; Ribas, X.; Costas, M. Stereospecific CH Oxidation with H<sub>2</sub>O<sub>2</sub> Catalyzed by a Chemically Robust Site-Isolated Iron Catalyst. *Angew. Chem. Int. Ed.* **2009**, *48*, 5720–5723. <https://doi.org/10.1002/anie.200901865>
- <sup>275</sup> (a) Talsi, E. P.; Samsonenko, D. G.; Ottenbacher, R. V.; Bryliakov, K. P. Highly Enantioselective C-H Oxidation of Arylalkanes with H<sub>2</sub>O<sub>2</sub> in the Presence of Chiral Mn-

---

Aminopyridine. *Chem. Cat. Chem.* **2017**, *9*, 4580–4586. <https://doi.org/10.1002/cctc.201701169>. (b) Ottenbacher, R. V.; Talsi, E. P.; Rybalova, T. V.; Bryliakov, K. P. Enantioselective Benzylic Oxidation of Arylalkanes with H<sub>2</sub>O<sub>2</sub> in Fluorinated Alcohols in the Presence of Chiral Mn-Aminopyridine Complexes. *Chem. Cat. Chem.* **2018**, *10*, 5323–5330. <https://doi.org/10.1002/cctc.201801476>. (c) For recent extension, see: Ottenbacher, R. V.; Talsi, E. P.; Bryliakov, K. P. Highly enantioselective undirected catalytic hydroxylation of benzylic CH<sub>2</sub> groups with H<sub>2</sub>O<sub>2</sub>. *J. Catal.* **2020**, *390*, 170–177. <https://doi.org/10.1016/j.jcat.2020.08.005>. (d) Ottenbacher, R. V.; Talsi, E. P.; Konstantin P. Bryliakov, K. P. Chiral Manganese Aminopyridine Complexes: the Versatile Catalysts of Chemo- and Stereoselective Oxidations with H<sub>2</sub>O<sub>2</sub>. *Chem. Rec.* **2018**, DOI: 10.1002/tcr.201700032.

<sup>276</sup> For pioneering investigation of ethylbenzene oxidation with chiral iron-porphyrins, see: Groves, J. T.; Viski, P. Asymmetric Hydroxylation by a Chiral Iron Porphyrin. *J. Am. Chem. Soc.* **1989**, *111*, 8537–8538. <https://doi.org/10.1021/ja00204a047>.

<sup>277</sup> Dantignana, V.; Milan, M.; Cusso, O.; Company, A.; Bietti, M.; Costas, M. Chemoselective Aliphatic C–H Bond Oxidation Enabled by Polarity Reversal. *ACS Cent. Sci.* **2017**, *3*, 1350–1358. <https://doi.org/10.1021/acscentsci.7b00532>.

<sup>278</sup> Milan, M.; Bietti, M.; Costas, M. Highly Enantioselective Oxidation of Nonactivated C–H Bonds with Hydrogen Peroxide Catalyzed by Manganese Complexes. *ACS Cent. Sci.* **2017**, *3*, 196–204. <https://doi.org/10.1021/acscentsci.6b00368>.

<sup>279</sup> Cianfanelli, M.; Olivo, G.; Milan, M.; Klein Gebbink, R. J. M.; Ribas, X.; Bietti, M.; Costas, M. Enantioselective C–H Lactonization of Unactivated Methylenes Directed by Carboxylic Acids. *J. Am. Chem. Soc.* **2020**, *142*, 1584–1593. <https://doi.org/10.1021/jacs.9b12239>.

<sup>280</sup> Bigi, M. A.; Reed, S. A.; White, C. Directed Metal (Oxo) Aliphatic C–H Hydroxylations: Overriding Substrate Bias. *J. Am. Chem. Soc.* **2012**, *134*, 9721–9726. <https://doi.org/10.1021/ja301685r>.

<sup>281</sup> Qiu, B.; Xu, D.; Sun, Q.; Miao, C.; Lee, Y.-M.; Li, X.-X.; Nam, W.; Sun, W. Highly Enantioselective Oxidation of Spirocyclic Hydrocarbons by Bioinspired Manganese Catalysts and Hydrogen Peroxide. *ACS Catal.* **2018**, *8*, 2479–2487. <https://doi.org/10.1021/acscatal.7b03601>.

- 
- <sup>282</sup> Qiu, B.; Xu, D.; Sun, Q.; Lin, J.; Sun, S. Manganese-Catalyzed Asymmetric Oxidation of Methylene C–H of Spirocyclic Oxindoles and Dihydroquinolinones with Hydrogen Peroxide. *Org. Lett.* **2019**, *21*, 618–622. <https://doi.org/10.1021/acs.orglett.8b03652>.
- <sup>283</sup> For enantioselective oxygenation of spirocyclic oxindoles upon catalysis by a chiral ruthenium porphyrin complex see: Frost, J. R.; Huber, S. M.; Breitenlechner, S.; Bannwarth, C.; Bach, T. Enantiotopos-Selective CH Oxygenation Catalyzed by a Supramolecular Ruthenium Complex. *Angew. Chem., Int. Ed.* **2015**, *54*, 691–695. <https://doi.org/10.1002/anie.201409224>.
- <sup>284</sup> Sun, Q.; Sun, W. Catalytic Enantioselective Methylene C(sp<sup>3</sup>)–H Hydroxylation Using a Chiral Manganese Complex/Carboxylic Acid System. *Org. Lett.* **2020**, *22*, 9529–9533. <https://doi.org/10.1021/acs.orglett.0c03585>.
- <sup>285</sup> Fischer, H. The persistent radical effect: A principle for selective radical reactions and living radical polymerizations *Chem. Rev.* **2001**, *101*, 3581–3610. <https://doi.org/10.1021/cr990124y>.
- <sup>286</sup> Pellissier, H.; Clavier, H. Enantioselective Cobalt-Catalyzed Transformations. *Chem. Rev.* **2014**, *114* (5), 2775–2823. <https://doi.org/10.1021/cr4004055>.
- <sup>287</sup> Chen, Y.; Fields, K. B.; Zhang, X. P. Bromoporphyrins as Versatile Synthons for Modular Construction of Chiral Porphyrins: Cobalt-Catalyzed Highly Enantioselective and Diastereoselective Cyclopropanation. *J. Am. Chem. Soc.* **2004**, *126* (45), 14718–14719. <https://doi.org/10.1021/ja044889l>.
- <sup>288</sup> Demarteau, J.; Debuigne, A.; Detrembleur, C. Organocobalt Complexes as Sources of Carbon-Centered Radicals for Organic and Polymer Chemistries. *Chem. Rev.* **2019**, *119* (12), 6906–6955. <https://doi.org/10.1021/acs.chemrev.8b00715>.
- <sup>289</sup> Huang, L.; Chen, Y.; Gao, G.-Y.; Zhang, X. P. Diastereoselective and Enantioselective Cyclopropanation of Alkenes Catalyzed by Cobalt Porphyrins. *J. Org. Chem.* **2003**, *68* (21), 8179–8184. <https://doi.org/10.1021/jo035088o>.
- <sup>290</sup> Lu, H.; Dzik, W. I.; Xu, X.; Wojtas, L.; de Bruin, B.; Zhang, X. P. Experimental Evidence for Cobalt(III)-Carbene Radicals: Key Intermediates in Cobalt(II)-Based Metalloradical Cyclopropanation. *J. Am. Chem. Soc.* **2011**, *133* (22), 8518–8521. <https://doi.org/10.1021/ja203434c>.

- 
- <sup>291</sup> Dzik, W. I.; Xu, X.; Zhang, X. P.; Reek, J. N. H.; de Bruin, B. ‘Carbene Radicals’ in Co<sup>II</sup> (Por)-Catalyzed Olefin Cyclopropanation. *J. Am. Chem. Soc.* **2010**, *132* (31), 10891–10902. <https://doi.org/10.1021/ja103768r>.
- <sup>292</sup> Chen, Y.; Ruppel, J. V.; Zhang, X. P. Cobalt-Catalyzed Asymmetric Cyclopropanation of Electron-Deficient Olefins. *J. Am. Chem. Soc.* **2007**, *129* (40), 12074–12075. <https://doi.org/10.1021/ja074613o>.
- <sup>293</sup> Zhu, S.; Ruppel, J. V.; Lu, H.; Wojtas, L.; Zhang, X. P. Cobalt-Catalyzed Asymmetric Cyclopropanation with Diazosulfones: Rigidification and Polarization of Ligand Chiral Environment via Hydrogen Bonding and Cyclization. *J. Am. Chem. Soc.* **2008**, *130* (15), 5042–5043. <https://doi.org/10.1021/ja7106838>.
- <sup>294</sup> Zhu, S.; Perman, J. A.; Zhang, X. P. Acceptor/Acceptor-Substituted Diazo Reagents for Carbene Transfers: Cobalt-Catalyzed Asymmetric Z- Cyclopropanation of Alkenes with  $\alpha$ -Nitrodiazoacetates. *Angew. Chem. Int. Ed.* **2008**, *47* (44), 8460–8463. <https://doi.org/10.1002/anie.200803857>.
- <sup>295</sup> Zhu, S.; Xu, X.; Perman, J. A.; Zhang, X. P. A General and Efficient Cobalt(II)-Based Catalytic System for Highly Stereoselective Cyclopropanation of Alkenes with  $\alpha$ -Cyanodiazoacetates. *J. Am. Chem. Soc.* **2010**, *132* (37), 12796–12799. <https://doi.org/10.1021/ja1056246>.
- <sup>296</sup> Xu, X.; Zhu, S.; Cui, X.; Wojtas, L.; Zhang, X. P. Cobalt(II)-Catalyzed Asymmetric Olefin Cyclopropanation with  $\alpha$ -Ketodiazoacetates. *Angew. Chem. Int. Ed.* **2013**, *52* (45), 11857–11861. <https://doi.org/10.1002/anie.201305883>.
- <sup>297</sup> Xu, X.; Wang, Y.; Cui, X.; Wojtas, L.; Zhang, X. P. Metalloradical Activation of  $\alpha$ -Formyldiazoacetates for the Catalytic Asymmetric Radical Cyclopropanation of Alkenes. *Chem. Sci.* **2017**, *8* (6), 4347–4351. <https://doi.org/10.1039/C7SC00658F>.
- <sup>298</sup> Wang, Y.; Wen, X.; Cui, X.; Wojtas, L.; Zhang, X. P. Asymmetric Radical Cyclopropanation of Alkenes with In Situ-Generated Donor-Substituted Diazo Reagents via Co(II)-Based Metalloradical Catalysis. *J. Am. Chem. Soc.* **2017**, *139* (3), 1049–1052. <https://doi.org/10.1021/jacs.6b11336>.
- <sup>299</sup> Cui, X.; Xu, X.; Lu, H.; Zhu, S.; Wojtas, L.; Zhang, X. P. Enantioselective Cyclopropanation of Alkynes with Acceptor/Acceptor-Substituted Diazo Reagents via Co(II)-Based

---

Metalloradical Catalysis. *J. Am. Chem. Soc.* **2011**, *133* (10), 3304–3307. <https://doi.org/10.1021/ja111334j>.

<sup>300</sup> Xu, X.; Lu, H.; Ruppel, J. V.; Cui, X.; Lopez de Mesa, S.; Wojtas, L.; Zhang, X. P. Highly Asymmetric Intramolecular Cyclopropanation of Acceptor-Substituted Diazoacetates by Co(II)-Based Metalloradical Catalysis: Iterative Approach for Development of New-Generation Catalysts. *J. Am. Chem. Soc.* **2011**, *133* (39), 15292–15295. <https://doi.org/10.1021/ja2062506>.

<sup>301</sup> Goswami, M.; Lyaskovskyy, V.; Domingos, S. R.; Buma, W. J.; Woutersen, S.; Troeppner, O.; Ivanović-Burmazović, I.; Lu, H.; Cui, X.; Zhang, X. P.; Reijerse, E. J.; DeBeer, S.; van Schooneveld, M. M.; Pfaff, F. F.; Ray, K.; de Bruin, B. Characterization of Porphyrin-Co(III)-‘Nitrene Radical’ Species Relevant in Catalytic Nitrene Transfer Reactions. *J. Am. Chem. Soc.* **2015**, *137* (16), 5468–5479.

<sup>302</sup> Lyaskovskyy, V.; Suarez, A. I. O.; Lu, H.; Jiang, H.; Zhang, X. P.; de Bruin, B. Mechanism of Cobalt(II) Porphyrin-Catalyzed C–H Amination with Organic Azides: Radical Nature and H-Atom Abstraction Ability of the Key Cobalt(III)–Nitrene Intermediates. *J. Am. Chem. Soc.* **2011**, *133* (31), 12264–12273. <https://doi.org/10.1021/ja204800a>.

<sup>303</sup> Jones, J. E.; Ruppel, J. V.; Gao, G.-Y.; Moore, T. M.; Zhang, X. P. Cobalt-Catalyzed Asymmetric Olefin Aziridination with Diphenylphosphoryl Azide. *J. Org. Chem.* **2008**, *73* (18), 7260–7265. <https://doi.org/10.1021/jo801151x>.

<sup>304</sup> Subbarayan, V.; Ruppel, J. V.; Zhu, S.; Perman, J. A.; Zhang, X. P. Highly Asymmetric Cobalt-Catalyzed Aziridination of Alkenes with Trichloroethoxysulfonyl Azide (TcesN<sub>3</sub>). *Chem. Commun.* **2009**, No. 28, 4266. <https://doi.org/10.1039/b905727g>.

<sup>305</sup> Jiang, H.; Lang, K.; Lu, H.; Wojtas, L.; Zhang, X. P. Asymmetric Radical Bicyclization of Allyl Azidoformates via Cobalt(II)-Based Metalloradical Catalysis. *J. Am. Chem. Soc.* **2017**, *139* (27), 9164–9167. <https://doi.org/10.1021/jacs.7b05778>.

<sup>306</sup> Li, C.; Lang, K.; Lu, H.; Hu, Y.; Cui, X.; Wojtas, L.; Zhang, X. P. Catalytic Radical Process for Enantioselective Amination of C(Sp<sup>3</sup>)–H Bonds. *Angew. Chem. Int. Ed.* **2018**, *57* (51), 16837–16841. <https://doi.org/10.1002/anie.201808923>.

<sup>307</sup> Lang, K.; Li, C.; Kim, I.; Zhang, X. P. Enantioconvergent Amination of Racemic Tertiary C–H Bonds. *J. Am. Chem. Soc.* **2020**, *142* (49), 20902–20911. <https://doi.org/10.1021/jacs.0c11110>.

- 
- <sup>308</sup> Hu, Y.; Lang, K.; Li, C.; Gill, J. B.; Kim, I.; Lu, H.; Fields, K. B.; Marshall, M.; Cheng, Q.; Cui, X.; Wojtas, L.; Zhang, X. P. Enantioselective Radical Construction of 5-Membered Cyclic Sulfonamides by Metalloradical C–H Amination. *J. Am. Chem. Soc.* **2019**, *141* (45), 18160–18169. <https://doi.org/10.1021/jacs.9b08894>.
- <sup>309</sup> Lang, K.; Torker, S.; Wojtas, L.; Zhang, X. P. Asymmetric Induction and Enantiodivergence in Catalytic Radical C–H Amination via Enantiodifferentiative H-Atom Abstraction and Stereoretentive Radical Substitution. *J. Am. Chem. Soc.* **2019**, *141* (31), 12388–12396. <https://doi.org/10.1021/jacs.9b05850>.
- <sup>310</sup> Nechab, M.; El Blidi, L.; Vanthuyne, N.; Gastaldi, S.; Bertrand, M. P.; Gil, G. N-Acyl Glycinates as Acyl Donors in Serine Protease-Catalyzed Kinetic Resolution of Amines. Improvement of Selectivity and Reaction Rate. *Org. Biomol. Chem.* **2008**, *6* (21), 3917. <https://doi.org/10.1039/b812089g>.
- <sup>311</sup> Nechab, M.; Azzi, N.; Vanthuyne, N.; Bertrand, M.; Gastaldi, S.; Gil, G. Highly Selective Enzymatic Kinetic Resolution of Primary Amines at 80 °C: A Comparative Study of Carboxylic Acids and Their Ethyl Esters as Acyl Donors. *J. Org. Chem.* **2007**, *72* (18), 6918–6923. <https://doi.org/10.1021/jo071069t>.
- <sup>312</sup> Jin, L.-M.; Xu, P.; Xie, J.; Zhang, X. P. Enantioselective Intermolecular Radical C–H Amination. *J. Am. Chem. Soc.* **2020**, *142* (49), 20828–20836. <https://doi.org/10.1021/jacs.0c10415>.
- <sup>313</sup> Cui, X.; Xu, X.; Jin, L.-M.; Wojtas, L.; Zhang, X. P. Stereoselective Radical C–H Alkylation with Acceptor/Acceptor-Substituted Diazo Reagents via Co(Ii)-Based Metalloradical Catalysis. *Chem. Sci.* **2015**, *6* (2), 1219–1224. <https://doi.org/10.1039/C4SC02610A>.
- <sup>314</sup> Wen, X.; Wang, Y.; Zhang, X. P. Enantioselective Radical Process for Synthesis of Chiral Indolines by Metalloradical Alkylation of Diverse C(Sp<sup>3</sup>)–H Bonds. *Chem. Sci.* **2018**, *9* (22), 5082–5086. <https://doi.org/10.1039/C8SC01476K>.
- <sup>315</sup> Wang, Y.; Wen, X.; Cui, X.; Zhang, X. P. Enantioselective Radical Cyclization for Construction of 5-Membered Ring Structures by Metalloradical C–H Alkylation. *J. Am. Chem. Soc.* **2018**, *140* (14), 4792–4796. <https://doi.org/10.1021/jacs.8b01662>.
- <sup>316</sup> Crossley, S. W. M.; Obradors, C.; Martinez, R. M.; Shenvi, R. A. Mn-, Fe-, and Co-Catalyzed Radical Hydrofunctionalizations of Olefins. *Chem. Rev.* **2016**, *116* (15), 8912–9000. <https://doi.org/10.1021/acs.chemrev.6b00334>.



- 
- <sup>317</sup> Kyne, S. H.; Lefèvre, G.; Ollivier, C.; Petit, M.; Ramis Cladera, V.-A.; Fensterbank, L. Iron and Cobalt Catalysis: New Perspectives in Synthetic Radical Chemistry. *Chem. Soc. Rev.* **2020**, *49* (23), 8501–8542. <https://doi.org/10.1039/D0CS00969E>.
- <sup>318</sup> Discolo, C. A.; Touney, E. E.; Pronin, S. V. Catalytic Asymmetric Radical–Polar Crossover Hydroalkoxylation. *J. Am. Chem. Soc.* **2019**, *141* (44), 17527–17532. <https://doi.org/10.1021/jacs.9b10645>.
- <sup>319</sup> Ebisawa, K.; Izumi, K.; Ooka, Y.; Kato, H.; Kanazawa, S.; Komatsu, S.; Nishi, E.; Shigehisa, H. Catalyst- and Silane-Controlled Enantioselective Hydrofunctionalization of Alkenes by Cobalt-Catalyzed Hydrogen Atom Transfer and Radical-Polar Crossover. *J. Am. Chem. Soc.* **2020**, *142* (31), 13481–13490. <https://doi.org/10.1021/jacs.0c05017>.
- <sup>320</sup> Shen, X.; Chen, X.; Chen, J.; Sun, Y.; Cheng, Z.; Lu, Z. Ligand-Promoted Cobalt-Catalyzed Radical Hydroamination of Alkenes. *Nat. Commun.* **2020**, *11* (1), 783. <https://doi.org/10.1038/s41467-020-14459-x>.
- <sup>321</sup> Ohmiya, H.; Tsuji, T.; Yorimitsu, H.; Oshima, K. Cobalt-Catalyzed Cross-Coupling Reactions of Alkyl Halides with Allylic and Benzylic Grignard Reagents and Their Application to Tandem Radical Cyclization/Cross-Coupling Reactions. *Chem. - Eur. J.* **2004**, *10* (22), 5640–5648. <https://doi.org/10.1002/chem.200400545>.
- <sup>322</sup> Han, J.-F.; Guo, P.; Zhang, X.-G.; Liao, J.-B.; Ye, K.-Y. Recent Advances in Cobalt-Catalyzed Allylic Functionalization. *Org. Biomol. Chem.* **2020**, *18* (39), 7740–7750. <https://doi.org/10.1039/D0OB01581D>.
- <sup>323</sup> Zhou, Y.; Wang, L.; Yuan, G.; Liu, S.; Sun, X.; Yuan, C.; Yang, Y.; Bian, Q.; Wang, M.; Zhong, J. Cobalt-Bisoxazoline-Catalyzed Enantioselective Cross-Coupling of  $\alpha$ -Bromo Esters with Alkenyl Grignard Reagents. *Org. Lett.* **2020**, *22* (11), 4532–4536. <https://doi.org/10.1021/acs.orglett.0c01557>.
- <sup>324</sup> Zhang, K.; Lu, L.-Q.; Jia, Y.; Wang, Y.; Lu, F.-D.; Pan, F.; Xiao, W.-J. Exploration of a Chiral Cobalt Catalyst for Visible-Light-Induced Enantioselective Radical Conjugate Addition. *Angew. Chem. Int. Ed.* **2019**, *58* (38), 13375–13379. <https://doi.org/10.1002/anie.201907478>.
- <sup>325</sup> Fu, G. C. Transition-Metal Catalysis of Nucleophilic Substitution Reactions: A Radical Alternative to  $S_N1$  and  $S_N2$  Processes. *ACS Cent. Sci.* **2017**, *3* (7), 692–700. <https://doi.org/10.1021/acscentsci.7b00212>.

- 
- <sup>326</sup> Wang, Z.; Yin, H.; Fu, G. C. Catalytic Enantioconvergent Coupling of Secondary and Tertiary Electrophiles with Olefins. *Nature* **2018**, *563* (7731), 379–383. <https://doi.org/10.1038/s41586-018-0669-y>.
- <sup>327</sup> Diccianni, J.; Lin, Q.; Diao, T. Mechanisms of Nickel-Catalyzed Coupling Reactions and Applications in Alkene Functionalization. *Acc. Chem. Res.* **2020**, *53* (4), 906–919. <https://doi.org/10.1021/acs.accounts.0c00032>.
- <sup>328</sup> Wei, X.; Shu, W.; García-Domínguez, A.; Merino, E.; Nevado, C. Asymmetric Ni-Catalyzed Radical Relayed Reductive Coupling. *J. Am. Chem. Soc.* **2020**, *142* (31), 13515–13522. <https://doi.org/10.1021/jacs.0c05254>.
- <sup>329</sup> Qi, X.; Diao, T. Nickel-Catalyzed Dicarbofunctionalization of Alkenes. *ACS Catal.* **2020**, *10* (15), 8542–8556. <https://doi.org/10.1021/acscatal.0c02115>.
- <sup>330</sup> For a complementary general review, see: uo, Y.; Xu, C.; Zhang, X. Nickel-Catalyzed Dicarbofunctionalization of Alkenes. *Chin. J. Chem.* **2020**, *38* (11), 1371–1394. <https://doi.org/10.1002/cjoc.202000224>.
- <sup>331</sup> Choi, J.; Fu, G. C. Catalytic Asymmetric Synthesis of Secondary Nitriles via Stereoconvergent Negishi Arylations and Alkenylations of Racemic  $\alpha$ -Bromonitriles. *J. Am. Chem. Soc.* **2012**, *134* (22), 9102–9105. <https://doi.org/10.1021/ja303442q>.
- <sup>332</sup> Liang, Y.; Fu, G. C. Catalytic Asymmetric Synthesis of Tertiary Alkyl Fluorides: Negishi Cross-Couplings of Racemic  $\alpha,\alpha$ -Dihaloketones. *J. Am. Chem. Soc.* **2014**, *136* (14), 5520–5524. <https://doi.org/10.1021/ja501815p>.
- <sup>333</sup> Schwarzwald, G. M.; Matier, C. D.; Fu, G. C. Enantioconvergent Cross-Couplings of Alkyl Electrophiles: The Catalytic Asymmetric Synthesis of Organosilanes. *Angew. Chem. Int. Ed.* **2019**, *58* (11), 3571–3574. <https://doi.org/10.1002/anie.201814208>.
- <sup>334</sup> Do, H.-Q.; Chandrashekar, E. R. R.; Fu, G. C. Nickel/Bis(Oxazoline)-Catalyzed Asymmetric Negishi Arylations of Racemic Secondary Benzylic Electrophiles to Generate Enantioenriched 1,1-Diarylalkanes. *J. Am. Chem. Soc.* **2013**, *135* (44), 16288–16291. <https://doi.org/10.1021/ja408561b>.
- <sup>335</sup> Oelke, A. J.; Sun, J.; Fu, G. C. Nickel-Catalyzed Enantioselective Cross-Couplings of Racemic Secondary Electrophiles That Bear an Oxygen Leaving Group. *J. Am. Chem. Soc.* **2012**, *134* (6), 2966–2969. <https://doi.org/10.1021/ja300031w>.

- 
- <sup>336</sup> Choi, J.; Martín-Gago, P.; Fu, G. C. Stereoconvergent Arylations and Alkenylations of Unactivated Alkyl Electrophiles: Catalytic Enantioselective Synthesis of Secondary Sulfonamides and Sulfones. *J. Am. Chem. Soc.* **2014**, *136* (34), 12161–12165. <https://doi.org/10.1021/ja506885s>.
- <sup>337</sup> Chu, C. K.; Liang, Y.; Fu, G. C. Silicon–Carbon Bond Formation via Nickel-Catalyzed Cross-Coupling of Silicon Nucleophiles with Unactivated Secondary and Tertiary Alkyl Electrophiles. *J. Am. Chem. Soc.* **2016**, *138* (20), 6404–6407. <https://doi.org/10.1021/jacs.6b03465>.
- <sup>338</sup> Lundin, P. M.; Fu, G. C. Asymmetric Suzuki Cross-Couplings of Activated Secondary Alkyl Electrophiles: Arylations of Racemic  $\alpha$ -Chloroamides. *J. Am. Chem. Soc.* **2010**, *132* (32), 11027–11029. <https://doi.org/10.1021/ja105148g>.
- <sup>339</sup> Zultanski, S. L.; Fu, G. C. Catalytic Asymmetric  $\gamma$ -Alkylation of Carbonyl Compounds via Stereoconvergent Suzuki Cross-Couplings. *J. Am. Chem. Soc.* **2011**, *133* (39), 15362–15364. <https://doi.org/10.1021/ja2079515>.
- <sup>340</sup> Yin, H.; Fu, G. C. Mechanistic Investigation of Enantioconvergent Kumada Reactions of Racemic  $\alpha$ -Bromoketones Catalyzed by a Nickel/Bis(Oxazoline) Complex. *J. Am. Chem. Soc.* **2019**, *141* (38), 15433–15440. <https://doi.org/10.1021/jacs.9b08185>.
- <sup>341</sup> Lou, S.; Fu, G. C. Enantioselective Alkenylation via Nickel-Catalyzed Cross-Coupling with Organozirconium Reagents. *J. Am. Chem. Soc.* **2010**, *132* (14), 5010–5011. <https://doi.org/10.1021/ja1017046>.
- <sup>342</sup> Wang, Z.; Yang, Z.-P.; Fu, G. C. Quaternary Stereocentres via Catalytic Enantioconvergent Nucleophilic Substitution Reactions of Tertiary Alkyl Halides. *Nat. Chem.* **2021**, *13* (3), 236–242. <https://doi.org/10.1038/s41557-020-00609-7>.
- <sup>343</sup> Wang, Z.; Bachman, S.; Dudnik, A. S.; Fu, G. C. Nickel-Catalyzed Enantioconvergent Borylation of Racemic Secondary Benzylic Electrophiles. *Angew. Chem. Int. Ed.* **2018**, *57* (44), 14529–14532. <https://doi.org/10.1002/anie.201806015>.
- <sup>344</sup> Schley, N. D.; Fu, G. C. Nickel-Catalyzed Negishi Arylations of Propargylic Bromides: A Mechanistic Investigation. *J. Am. Chem. Soc.* **2014**, *136* (47), 16588–16593. <https://doi.org/10.1021/ja508718m>.

- 
- <sup>345</sup> Yang, Z.-P.; Freas, D. J.; Fu, G. C. The Asymmetric Synthesis of Amines via Nickel-Catalyzed Enantioconvergent Substitution Reactions. *J. Am. Chem. Soc.* **2021**, *143*, 2930–2937.
- <sup>346</sup> Cordier, C. J.; Lundgren, R. J.; Fu, G. C. Enantioconvergent Cross-Couplings of Racemic Alkylmetal Reagents with Unactivated Secondary Alkyl Electrophiles: Catalytic Asymmetric Negishi  $\alpha$ -Alkylations of *N*-Boc-Pyrrolidine. *J. Am. Chem. Soc.* **2013**, *135* (30), 10946–10949. <https://doi.org/10.1021/ja4054114>.
- <sup>347</sup> Mu, X.; Shibata, Y.; Makida, Y.; Fu, G. C. Control of Vicinal Stereocenters through Nickel-Catalyzed Alkyl-Alkyl Cross-Coupling. *Angew. Chem. Int. Ed.* **2017**, *56* (21), 5821–5824. <https://doi.org/10.1002/anie.201702402>.
- <sup>348</sup> Murphy, J. A. Discovery and Development of Organic Super-Electron-Donors. *J. Org. Chem.* **2014**, *79*, 3731–3746. <https://doi.org/10.1021/jo500071u>.
- <sup>349</sup> Broggi, J.; Terme, T.; Vanelle, P. Organic Electron Donors as Powerful Single-Electron Reducing Agents in Organic Synthesis. *Angew. Chem. Int. Ed.* **2014**, *53*, 384–413. <https://doi.org/10.1002/anie.201209060>.
- <sup>350</sup> Weix, D. J. Methods and Mechanisms for Cross-Electrophile Coupling of  $\text{Csp}^2$  Halides with Alkyl Electrophiles. *Acc. Chem. Res.* **2015**, *48*, 1767–1775. <https://doi.org/10.1021/acs.accounts.5b00057>
- <sup>351</sup> Everson, D. A.; Weix, D. J. Cross-Electrophile Coupling: Principles of Reactivity and Selectivity. *J. Org. Chem.* **2014**, *79*, 4793–4798. <https://doi.org/10.1021/jo500507s>
- <sup>352</sup> For a review, see: Poremba, K. E.; Dibrell, S. E.; Reisman, S. E. Nickel-Catalyzed Enantioselective Reductive Cross-Coupling Reactions. *ACS Catal.* **2020**, *10*, 8237–8246. <https://doi.org/10.1021/acscatal.0c01842>
- <sup>353</sup> (a) Hofstra, J. L.; Cherney, A. H.; Ordner, C. M.; Reisman, S. E. Synthesis of Enantioenriched Allylic Silanes via Nickel-Catalyzed Reductive Cross-Coupling. *J. Am. Chem. Soc.* **2018**, *140*, 139–142. <https://doi.org/10.1021/jacs.7b11707> (b) Poremba, K. E.; Kadunce, N. T.; Suzuki, N.; Cherney, A. H.; Reisman, S. E. Nickel-Catalyzed Asymmetric Reductive Cross-Coupling to Access 1,1-Diarylalkanes. *J. Am. Chem. Soc.* **2017**, *139*, 5684–5687. <https://doi.org/10.1021/jacs.7b01705> (c) Kadunce, N. T.; Reisman, S. E. Nickel-Catalyzed Asymmetric Reductive Cross-Coupling between Heteroaryl Iodides and  $\alpha$ -Chloronitriles. *J. Am. Chem. Soc.* **2015**, *137*, 10480–10483. <https://doi.org/10.1021/jacs.5b06466>

- 
- (d) Cherney, A. H.; Reisman, S. E. Nickel-Catalyzed Asymmetric Reductive Cross-Coupling Between Vinyl and Benzyl Electrophiles. *J. Am. Chem. Soc.* **2014**, *136*, 14365–14368. <https://doi.org/10.1021/ja508067c>. (e) Cherney, A. H.; Kadunce, N. T.; Reisman S. E. Catalytic Asymmetric Reductive Acyl Cross-Coupling: Synthesis of Enantioenriched Acyclic  $\alpha,\alpha$ -Disubstituted Ketones. *J. Am. Chem. Soc.* **2013**, *135*, 7442–7445. <https://doi.org/10.1021/ja402922w>
- <sup>354</sup> DeLano, T. J.; Reisman, S. E. Enantioselective Electroreductive Coupling of Alkenyl and Benzyl Halides via Nickel Catalysis. *ACS Catal.* **2019**, *9*, 6751–6754. <https://doi.org/10.1021/acscatal.9b01785>
- <sup>355</sup> Suzuki, N.; Hofstra, J. L.; Poremba, K. E.; Reisman, S. E. Nickel-Catalyzed Enantioselective Cross-Coupling of N-Hydroxyphthalimide Esters with Vinyl Bromides. *Org. Lett.* **2017**, *19*, 2150–2153. <https://doi.org/10.1021/acs.orglett.7b00793>
- <sup>356</sup> Sibi, M. P.; Porter, N. A. Enantioselective Free Radical Reactions. *Acc. Chem. Res.* **1999**, *32* (2), 163–171. <https://doi.org/10.1021/ar9600547>.
- <sup>357</sup> Sibi, M. P.; Manyem, S.; Zimmerman, J. Enantioselective Radical Processes. *Chem. Rev.* **2003**, *103* (8), 3263–3296. <https://doi.org/10.1021/cr020044l>.
- <sup>358</sup> Zimmerman, J.; Sibi, M. P. Enantioselective Radical Reactions. In *Radicals in Synthesis I*; Gansäuer, A., Ed.; Topics in Current Chemistry; Springer-Verlag: Berlin/Heidelberg, 2006; Vol. 263, pp 107–162. [https://doi.org/10.1007/128\\_027](https://doi.org/10.1007/128_027).
- <sup>359</sup> Shen, X.; Li, Y.; Wen, Z.; Cao, S.; Hou, X.; Gong, L. A Chiral Nickel DBFOX Complex as a Bifunctional Catalyst for Visible-Light-Promoted Asymmetric Photoredox Reactions. *Chem. Sci.* **2018**, *9* (20), 4562–4568. <https://doi.org/10.1039/C8SC01219A>.
- <sup>360</sup> Tucker, J. W.; Stephenson, C. R. J. Shining Light on Photoredox Catalysis: Theory and Synthetic Applications. *J. Org. Chem.* **2012**, *77* (4), 1617–1622. <https://doi.org/10.1021/jo202538x>.
- <sup>361</sup> Prier, C. K.; Rankic, D. A.; MacMillan, D. W. C. Visible Light Photoredox Catalysis with Transition Metal Complexes: Applications in Organic Synthesis. *Chem. Rev.* **2013**, *113* (7), 5322–5363. <https://doi.org/10.1021/cr300503r>.
- <sup>362</sup> Schultz, D. M.; Yoon, T. P. Solar Synthesis: Prospects in Visible Light Photocatalysis. *Science* **2014**, *343* (6174), 1239176–1239176. <https://doi.org/10.1126/science.1239176>.

- 
- <sup>363</sup> Shang, T.-Y.; Lu, L.-H.; Cao, Z.; Liu, Y.; He, W.-M.; Yu, B. Recent Advances of 1,2,3,5-Tetrakis(Carbazol-9-Yl)-4,6-Dicyanobenzene (4CzIPN) in Photocatalytic Transformations. *Chem. Commun.* **2019**, 55 (38), 5408–5419. <https://doi.org/10.1039/C9CC01047E>.
- <sup>364</sup> Tellis, J. C.; Primer, D. N.; Molander, G. A. Single-Electron Transmetalation in Organoboron Cross-Coupling by Photoredox/Nickel Dual Catalysis. *Science* **2014**, 345 (6195), 433–436. <https://doi.org/10.1126/science.1253647>.
- <sup>365</sup> Lin, K.; Wiles, R. J.; Kelly, C. B.; Davies, G. H. M.; Molander, G. A. Haloselective Cross-Coupling via Ni/Photoredox Dual Catalysis. *ACS Catal.* **2017**, 7 (8), 5129–5133. <https://doi.org/10.1021/acscatal.7b01773>.
- <sup>366</sup> Liu, J.; Ding, W.; Zhou, Q.-Q.; Liu, D.; Lu, L.-Q.; Xiao, W.-J. Enantioselective Di-/Perfluoroalkylation of  $\beta$ -Ketoesters Enabled by Cooperative Photoredox/Nickel Catalysis. *Org. Lett.* **2018**, 20 (2), 461–464. <https://doi.org/10.1021/acs.orglett.7b03826>.
- <sup>367</sup> Zhu, C.; Yue, H.; Chu, L.; Rueping, M. Recent Advances in Photoredox and Nickel Dual Catalyzed Cascade reactions: Pushing the Boundaries of Complexity. *Chem. Sci.* **2020**, 11, 4051–5064. <https://doi.org/10.1039/D0SC00712A>
- <sup>368</sup> Zuo, Z.; Ahneman, D. T.; Chu, L.; Terrett, J. A.; Doyle, A. G.; MacMillan, D. W. C. Merging Photoredox with Nickel Catalysis: Coupling of  $\alpha$ -Carboxyl  $sp^3$ -Carbons with Aryl Halides. *Science* **2014**, 345 (6195), 437–440. <https://doi.org/10.1126/science.1255525>.
- <sup>369</sup> Tellis, J. C.; Kelly, C. B.; Primer, D. N.; Jouffroy, M.; Patel, N. R.; Molander, G. A. Single-Electron Transmetalation via Photoredox/Nickel Dual Catalysis: Unlocking a New Paradigm for  $sp^3$ – $sp^2$  Cross-Coupling. *Acc. Chem. Res.* **2016**, 49 (7), 1429–1439. <https://doi.org/10.1021/acs.accounts.6b00214>.
- <sup>370</sup> Zuo, Z.; Cong, H.; Li, W.; Choi, J.; Fu, G. C.; MacMillan, D. W. C. Enantioselective Decarboxylative Arylation of  $\alpha$ -Amino Acids via the Merger of Photoredox and Nickel Catalysis. *J. Am. Chem. Soc.* **2016**, 138 (6), 1832–1835. <https://doi.org/10.1021/jacs.5b13211>.
- <sup>371</sup> Amani, J.; Sodagar, E.; Molander, G. A. Visible Light Photoredox Cross-Coupling of Acyl Chlorides with Potassium Alkoxyethyltrifluoroborates: Synthesis of  $\alpha$ -Alkoxyketones. *Org. Lett.* **2016**, 18 (4), 732–735. <https://doi.org/10.1021/acs.orglett.5b03705>.
- <sup>372</sup> Guo, L.; Yuan, M.; Zhang, Y.; Wang, F.; Zhu, S.; Gutierrez, O.; Chu, L. General Method for Enantioselective Three-Component carbonylation of Alkenes Enabled by Visible-Light

---

Dual Photoredox/Nickel Catalysis. *J. Am. Chem. Soc.* **2020**, *142*, 20390–20399. <https://doi.org/10.1021/jacs.0c08823>

<sup>373</sup> Hoffmann, N. Proton-Coupled Electron Transfer in Photoredox Catalytic Reactions: Proton-Coupled Electron Transfer in Photoredox Catalytic Reactions. *Eur. J. Org. Chem.* **2017**, *2017* (15), 1982–1992. <https://doi.org/10.1002/ejoc.201601445>.

<sup>374</sup> Hoffmann, N. Photochemical Electron and Hydrogen Transfer in Organic Synthesis: The Control of Selectivity. *Synthesis* **2016**, *48* (12), 1782–1802. <https://doi.org/10.1055/s-0035-1561425>.

<sup>375</sup> Ahneman, D. T.; Doyle, A. G. C–H Functionalization of Amines with Aryl Halides by Nickel-Photoredox Catalysis. *Chem Sci* **2016**, *7* (12), 7002–7006. <https://doi.org/10.1039/C6SC02815B>.

<sup>376</sup> Rand, A. W.; Yin, H.; Xu, L.; Giacoboni, J.; Martin-Montero, R.; Romano, C.; Montgomery, J.; Martin, R. Dual Catalytic Platform for Enabling  $sp^3$   $\alpha$  C–H Arylation and Alkylation of Benzamides. *ACS Catal.* **2020**, *10*, 4671–4676. <https://doi.org/10.1021/acscatal.0c01318>

<sup>377</sup> (a) Dewanji, A.; Krach, P. E.; Rueping, M. The Dual Role of Benzophenone in Visible-Light/Nickel Photoredox-Catalyzed C–H Arylations: Hydrogen-Atom Transfer and Energy Transfer. *Angew. Chem. Int. Ed.* **2019**, *58*, 3566–3570.

<https://doi.org/10.1002/anie.201901327> (b) Huang, L.; Rueping, M. Direct Cross-Coupling of Allylic C( $sp^3$ )–H Bonds with Aryl- and Vinylbromides by Combined Nickel and Visible-Light Catalysis. *Angew. Chem. Int. Ed.* **2018**, *57*, 10333–10337. <https://doi.org/10.1002/anie.201805118>.

<sup>378</sup> (a) Heitz, D. R.; Tellis, J. C.; Molander, G. A. Photochemical Nickel-Catalyzed C–H Arylation: Synthetic Scope and Mechanistic Investigations. *J. Am. Chem. Soc.* **2016**, *138*, 12715–12718. <https://doi.org/10.1021/jacs.6b04789>. (b) Matsui, J.; Lang, S. B.; Heitz, D. R.; Molander, G. A. Photoredox-Mediated Routes to Radicals: The Value of Catalytic Radical Generation in Synthetic Methods Development. *ACS Catal.* **2017**, *7*, 2563–2575. <https://doi.org/10.1021/acscatal.7b00094>

<sup>379</sup> Cheng, X.; Lu, H.; Lu, Z. Enantioselective Benzylic C–H Arylation via Photoredox and Nickel Dual Catalysis. *Nat. Commun.* **2019**, *10*:3549. <https://doi.org/10.1038/s41467-019-11392-6>.

- 
- <sup>380</sup> Shu, X.; Huan, L.; Huang, Q.; Huo, H. Direct Enantioselective C(sp<sup>3</sup>-H) for the Synthesis of  $\alpha$ -Amino Ketones. *J. Am. Chem. Soc.* **2020**, *142*, 19058-19064. <https://doi.org/10.1021/jacs.0c10471>.
- <sup>381</sup> Matsui, J. K.; Lang, S. B.; Heitz, D. R.; Molander, G. A. Photoredox-Mediated Routes to Radicals: The Value of Catalytic Radical Generation in Synthetic Methods Development. *ACS Catal.* **2017**, *7* (4), 2563–2575. <https://doi.org/10.1021/acscatal.7b00094>.
- <sup>382</sup> Heitz, D. R.; Tellis, J. C.; Molander, G. A. Photochemical Nickel-Catalyzed C–H Arylation: Synthetic Scope and Mechanistic Investigations. *J. Am. Chem. Soc.* **2016**, *138* (39), 12715–12718. <https://doi.org/10.1021/jacs.6b04789>.
- <sup>383</sup> Cheng, X.; Lu, H.; Lu, Z. Enantioselective Benzylic C-H Arylation via Photoredox and Nickel Dual Catalysis. *Nat. Commun.* **2019**, *10* (1), 3549–3549. <https://doi.org/10.1038/s41467-019-11392-6>.
- <sup>384</sup> Shen, Y.; Gu, Y.; Martin, R. Sp<sup>3</sup> C–H Arylation and Alkylation Enabled by the Synergy of Triplet Excited Ketones and Nickel Catalysts. *J. Am. Chem. Soc.* **2018**, *140* (38), 12200–12209. <https://doi.org/10.1021/jacs.8b07405>.
- <sup>385</sup> Pezzetta, C.; Bonifazi, D.; Davidson, R. W. M. Enantioselective Synthesis of N-Benzylic Heterocycles: A Nickel and Photoredox Dual Catalysis Approach. *Org. Lett.* **2019**, *21* (22), 8957–8961. <https://doi.org/10.1021/acs.orglett.9b03338>.
- <sup>386</sup> Stache, E. E.; Rovis, T.; Doyle, A. G. Dual Nickel- and Photoredox-Catalyzed Enantioselective Desymmetrization of Cyclic *Meso*-Anhydrides. *Angew. Chem. Int. Ed.* **2017**, *56* (13), 3679–3683. <https://doi.org/10.1002/anie.201700097>.
- <sup>387</sup> Wang, P.-Z.; Chen, J.-R.; Xiao, W.-J. Hantzsch Esters: An Emerging Versatile Class of Reagents in Photoredox Catalyzed Organic Synthesis. *Org. Biomol. Chem.* **2019**, *17* (29), 6936–6951. <https://doi.org/10.1039/C9OB01289C>.
- <sup>388</sup> Gandolfo, E.; Tang, X.; Raha Roy, S.; Melchiorre, P. Photochemical Asymmetric Nickel-Catalyzed Acyl Cross-Coupling. *Angew. Chem. Int. Ed.* **2019**, *58* (47), 16854–16858. <https://doi.org/10.1002/anie.201910168>.
- <sup>389</sup> Bellus, D. Copper-Catalyzed Additions of Organic Polyhalides to Olefins: A Versatile Synthetic Tool. *Pure Appl. Chem.* **1985**, *57* (12), 1827–1838. <https://doi.org/10.1351/pac198557121827>.



- 
- <sup>390</sup> Clark, A. J. Atom Transfer Radical Cyclisation Reactions Mediated by Copper Complexes. *Chem. Soc. Rev.* **2002**, *31* (1), 1–11. <https://doi.org/10.1039/b107811a>.
- <sup>391</sup> Eckenhoff, W. T.; Pintauer, T. Copper Catalyzed Atom Transfer Radical Addition (ATRA) and Cyclization (ATRC) Reactions in the Presence of Reducing Agents. *Catal. Rev.* **2010**, *52* (1), 1–59. <https://doi.org/10.1080/01614940903238759>.
- <sup>392</sup> *Organometallic Mechanisms and Catalysis*; Elsevier, 1978. <https://doi.org/10.1016/B978-0-12-418250-9.X5001-3>.
- <sup>393</sup> Wang, F.; Chen, P.; Liu, G. Copper-Catalyzed Radical Relay for Asymmetric Radical Transformations. *Acc. Chem. Res.* **2018**, *51* (9), 2036–2046. <https://doi.org/10.1021/acs.accounts.8b00265>.
- <sup>394</sup> Gu, Q.-S.; Li, Z.-L.; Liu, X.-Y. Copper(I)-Catalyzed Asymmetric Reactions Involving Radicals. *Acc. Chem. Res.* **2020**, *53* (1), 170–181. <https://doi.org/10.1021/acs.accounts.9b00381>.
- <sup>395</sup> Adachi, S.; Moorthy, R.; Sibi, M. P. Chiral Copper Lewis Acids in Asymmetric Transformations. In *Copper-Catalyzed Asymmetric Synthesis*; Alexakis, A., Krause, N., Woodward, S., Eds.; Wiley-VCH Verlag GmbH & Co. KGaA: Weinheim, Germany, 2014; pp 283–324. <https://doi.org/10.1002/9783527664573.ch11>.
- <sup>396</sup> Lee, S.; Lim, C. J.; Kim, S.; Subramaniam, R.; Zimmerman, J.; Sibi, M. P. Enantioselective Conjugate Radical Addition to  $\alpha'$ -Hydroxy Enones. *Org. Lett.* **2006**, *8* (19), 4311–4313. <https://doi.org/10.1021/ol061634z>.
- <sup>397</sup> Sibi, M.; Yang, Y.-H. Chiral Lewis Acid Catalyzed Enantioselective Conjugate Radical Additions to  $\alpha,\beta$ -Unsaturated 2-Pyridyl Ketones. *Synlett* **2008**, *2008* (1), 83–88. <https://doi.org/10.1055/s-2007-992386>.
- <sup>398</sup> Sibi, M. P.; Chen, J. Enantioselective Tandem Radical Reactions: Vicinal Difunctionalization in Acyclic Systems with Control over Relative and Absolute Stereochemistry. *J. Am. Chem. Soc.* **2001**, *123* (38), 9472–9473. <https://doi.org/10.1021/ja016633a>.
- <sup>399</sup> Friestad, G. K.; Shen, Y.; Ruggles, E. L. Enantioselective Radical Addition ToN-Acyl Hydrazones Mediated by Chiral Lewis Acids. *Angew. Chem. Int. Ed.* **2003**, *42* (41), 5061–5063. <https://doi.org/10.1002/anie.200352104>.

- 
- <sup>400</sup> Han, B.; Li, Y.; Yu, Y.; Gong, L. Photocatalytic Enantioselective  $\alpha$ -Aminoalkylation of Acyclic Imine Derivatives by a Chiral Copper Catalyst. *Nat. Commun.* **2019**, *10* (1), 3804. <https://doi.org/10.1038/s41467-019-11688-7>.
- <sup>401</sup> Gao, D.-W.; Zheng, J.; Ye, K.-Y.; Zheng, C.; You, S.-L. CHAPTER 5. Asymmetric Functionalization of C–H Bonds via a Transient Carbon–Metal (C–M) Species. In *Catalysis Series*; You, S.-L., Ed.; Royal Society of Chemistry: Cambridge, 2015; pp 141–213. <https://doi.org/10.1039/9781782621966-00141>.
- <sup>402</sup> Andrus, M. B.; Lashley, J. C. Copper Catalyzed Allylic Oxidation with Peresters. *Tetrahedron* **2002**, *58* (5), 845–866. [https://doi.org/10.1016/S0040-4020\(01\)01172-3](https://doi.org/10.1016/S0040-4020(01)01172-3). Andrus, M. B.; Lashley, J. C. Copper Catalyzed Allylic Oxidation with Peresters. *Tetrahedron* **2002**, *58* (5), 845–866. [https://doi.org/10.1016/S0040-4020\(01\)01172-3](https://doi.org/10.1016/S0040-4020(01)01172-3).
- <sup>403</sup> Eames, J.; Watkinson, M. Catalytic Allylic Oxidation of Alkenes Using an Asymmetric Kharasch–Sosnovsky Reaction. *Angew. Chem. Int. Ed.* **2001**, *40* (19), 3567–3571. [https://doi.org/10.1002/1521-3773\(20011001\)40:19<3567::AID-ANIE3567>3.0.CO;2-C](https://doi.org/10.1002/1521-3773(20011001)40:19<3567::AID-ANIE3567>3.0.CO;2-C).
- <sup>404</sup> Zhang, W.; Wang, F.; McCann, S. D.; Wang, D.; Chen, P.; Stahl, S. S.; Liu, G. Enantioselective Cyanation of Benzylic C–H Bonds via Copper-Catalyzed Radical Relay. *Science* **2016**, *353* (6303), 1014–1018. <https://doi.org/10.1126/science.aaf7783>.
- <sup>405</sup> Li, J.; Zhang, Z.; Wu, L.; Zhang, W.; Chen, P.; Lin, Z.; Liu, G. Site-Specific Allylic C–H Bond Functionalization with a Copper-Bound N-Centred Radical. *Nature* **2019**, *574* (7779), 516–521. <https://doi.org/10.1038/s41586-019-1655-8>.
- <sup>406</sup> Xiao, H.; Liu, Z.; Shen, H.; Zhang, B.; Zhu, L.; Li, C. Copper-Catalyzed Late-Stage Benzylic C(Sp<sup>3</sup>)–H Trifluoromethylation. *Chem* **2019**, *5* (4), 940–949. <https://doi.org/10.1016/j.chempr.2019.02.006>.
- <sup>407</sup> Fu, L.; Zhang, Z.; Chen, P.; Lin, Z.; Liu, G. Enantioselective Copper-Catalyzed Alkynylation of Benzylic C–H Bonds via Radical Relay. *J. Am. Chem. Soc.* **2020**, *142* (28), 12493–12500. <https://doi.org/10.1021/jacs.0c05373>.
- <sup>408</sup> Zhang, W.; Chen, P.; Liu, G. Copper-Catalyzed Arylation of Benzylic C–H Bonds with Alkylarenes as the Limiting Reagents. *J. Am. Chem. Soc.* **2017**, *139* (23), 7709–7712. <https://doi.org/10.1021/jacs.7b03781>.

- 
- <sup>409</sup> Zhang, W.; Wu, L.; Chen, P.; Liu, G. Enantioselective Arylation of Benzylic C–H Bonds by Copper-Catalyzed Radical Relay. *Angew. Chem. Int. Ed.* **2019**, *58* (19), 6425–6429. <https://doi.org/10.1002/anie.201902191>.
- <sup>410</sup> Jiang, S.-P.; Dong, X.-Y.; Gu, Q.-S.; Ye, L.; Li, Z.-L.; Liu, X.-Y. Copper-Catalyzed Enantioconvergent Radical Suzuki–Miyaura C(Sp<sup>3</sup>)–C(Sp<sup>2</sup>) Cross-Coupling. *J. Am. Chem. Soc.* **2020**, *142* (46), 19652–19659. <https://doi.org/10.1021/jacs.0c09125>.
- <sup>411</sup> Su, X.; Ye, L.; Chen, J.; Liu, X.; Jiang, S.; Wang, F.; Liu, L.; Yang, C.; Chang, X.; Li, Z.; Gu, Q.; Liu, X. Copper-Catalyzed Enantioconvergent Cross-Coupling of Racemic Alkyl Bromides with Azole C(Sp<sup>2</sup>)–H Bonds. *Angew. Chem. Int. Ed.* **2021**, *60* (1), 380–384. <https://doi.org/10.1002/anie.20200952>.
- <sup>412</sup> Skubi, K. L.; Blum, T. R.; Yoon, T. P. Dual Catalysis Strategies in Photochemical Synthesis. *Chem. Rev.* **2016**, *116* (17), 10035–10074. <https://doi.org/10.1021/acs.chemrev.6b00018>.
- <sup>413</sup> Goddard, J.-P.; Ollivier, C.; Fensterbank, L. Photoredox Catalysis for the Generation of Carbon Centered Radicals. *Acc. Chem. Res.* **2016**, *49* (9), 1924–1936. <https://doi.org/10.1021/acs.accounts.6b00288>.
- <sup>414</sup> Crespi, S.; Fagnoni, M. Generation of Alkyl Radicals: From the Tyranny of Tin to the Photon Democracy. *Chem. Rev.* **2020**, *120* (17), 9790–9833. <https://doi.org/10.1021/acs.chemrev.0c00278>.
- <sup>415</sup> Hong, B.-C. Enantioselective Synthesis Enabled by Visible Light Photocatalysis. *Org. Biomol. Chem.* **2020**, *18* (23), 4298–4353. <https://doi.org/10.1039/D0OB00759E>.
- <sup>416</sup> Lipp, A.; Badir, S. O.; Molander, G. A. Stereoinduction in Metallaphotoredox Catalysis. *Angew. Chem. Int. Ed.* **2020**, anie.202007668. <https://doi.org/10.1002/anie.202007668>.
- <sup>417</sup> Lu, F.-D.; Liu, D.; Zhu, L.; Lu, L.-Q.; Yang, Q.; Zhou, Q.-Q.; Wei, Y.; Lan, Y.; Xiao, W.-J. Asymmetric Propargylic Radical Cyanation Enabled by Dual Organophotoredox and Copper Catalysis. *J. Am. Chem. Soc.* **2019**, *141* (15), 6167–6172. <https://doi.org/10.1021/jacs.9b02338>.
- <sup>418</sup> Wang, D.; Zhu, N.; Chen, P.; Lin, Z.; Liu, G. Enantioselective Decarboxylative Cyanation Employing Cooperative Photoredox Catalysis and Copper Catalysis. *J. Am. Chem. Soc.* **2017**, *139* (44), 15632–15635. <https://doi.org/10.1021/jacs.7b09802>.
- <sup>419</sup> Kainz, Q. M.; Matier, C. D.; Bartoszewicz, A.; Zultanski, S. L.; Peters, J. C.; Fu, G. C. Asymmetric Copper-Catalyzed C–N Cross-Couplings Induced by Visible Light. *Science* **2016**, *351* (6274), 681–684. <https://doi.org/10.1126/science.aad8313>.

- 
- <sup>420</sup> Reiser, O. Shining Light on Copper: Unique Opportunities for Visible-Light-Catalyzed Atom Transfer Radical Addition Reactions and Related Processes. *Acc. Chem. Res.* **2016**, *49* (9), 1990–1996. <https://doi.org/10.1021/acs.accounts.6b00296>.
- <sup>421</sup> Hossain, A.; Bhattacharyya, A.; Reiser, O. Copper's Rapid Ascent in Visible-Light Photoredox Catalysis. *Science* **2019**, *364* (6439), eaav9713. <https://doi.org/10.1126/science.aav9713>.
- <sup>422</sup> Li, Y.; Zhou, K.; Wen, Z.; Cao, S.; Shen, X.; Lei, M.; Gong, L. Copper(II)-Catalyzed Asymmetric Photoredox Reactions: Enantioselective Alkylation of Imines Driven by Visible Light. *J. Am. Chem. Soc.* **2018**, *140* (46), 15850–15858. <https://doi.org/10.1021/jacs.8b09251>.
- <sup>423</sup> For a very recent general review, see: Li, Z.-L.; Fang, G.-C.; Gu, Q.-S.; Liu, X.-Y. Recent advances in copper-catalysed radical involved asymmetric 1,2-difunctionalization of alkenes. *Chem. Soc. Rev.* **2020**, *49*, 32–48. <https://doi.org/10.1039/C9CS00681H>.
- <sup>424</sup> Muller, K.; Faeh, C.; Diederich, F. Fluorine in Pharmaceuticals: Looking Beyond Intuition. *Science* **2007**, *317* (5846), 1881–1886. <https://doi.org/10.1126/science.1131943>.
- <sup>425</sup> Fu, L.; Zhou, S.; Wan, X.; Chen, P.; Liu, G. Enantioselective Trifluoromethylalkynylation of Alkenes via Copper-Catalyzed Radical Relay. *J. Am. Chem. Soc.* **2018**, *140* (35), 10965–10969. <https://doi.org/10.1021/jacs.8b07436>.
- <sup>426</sup> Li, Z.-L.; Fang, G.-C.; Gu, Q.-S.; Liu, X.-Y. Recent Advances in Copper-Catalysed Radical-Involved Asymmetric 1,2-Difunctionalization of Alkenes. *Chem. Soc. Rev.* **2020**, *49* (1), 32–48. <https://doi.org/10.1039/C9CS00681H>.
- <sup>427</sup> Charpentier, J.; Früh, N.; Togni, A. Electrophilic Trifluoromethylation by Use of Hypervalent Iodine Reagents. *Chem. Rev.* **2015**, *115* (2), 650–682. <https://doi.org/10.1021/cr500223h>.
- <sup>428</sup> Wu, L.; Wang, F.; Wan, X.; Wang, D.; Chen, P.; Liu, G. Asymmetric Cu-Catalyzed Intermolecular Trifluoromethylarylation of Styrenes: Enantioselective Arylation of Benzylic Radicals. *J. Am. Chem. Soc.* **2017**, *139* (8), 2904–2907. <https://doi.org/10.1021/jacs.6b13299>.
- <sup>429</sup> Wang, F.; Wang, D.; Mu, X.; Chen, P.; Liu, G. Copper-Catalyzed Intermolecular Trifluoromethylarylation of Alkenes: Mutual Activation of Arylboronic Acid and  $\text{CF}_3^+$  Reagent. *J. Am. Chem. Soc.* **2014**, *136* (29), 10202–10205. <https://doi.org/10.1021/ja504458j>.

- 
- <sup>430</sup> Wu, L.; Wang, F.; Chen, P.; Liu, G. Enantioselective Construction of Quaternary All-Carbon Centers via Copper-Catalyzed Arylation of Tertiary Carbon-Centered Radicals. *J. Am. Chem. Soc.* **2019**, *141* (5), 1887–1892. <https://doi.org/10.1021/jacs.8b13052>.
- <sup>431</sup> Wang, F.; Wang, D.; Wan, X.; Wu, L.; Chen, P.; Liu, G. Enantioselective Copper-Catalyzed Intermolecular Cyanotrifluoromethylation of Alkenes via Radical Process. *J. Am. Chem. Soc.* **2016**, *138* (48), 15547–15550. <https://doi.org/10.1021/jacs.6b10468>.
- <sup>432</sup> Zhou, S.; Zhang, G.; Fu, L.; Chen, P.; Li, Y.; Liu, G. Copper-Catalyzed Asymmetric Cyanation of Alkenes via Carbonyl-Assisted Coupling of Alkyl-Substituted Carbon-Centered Radicals. *Org. Lett.* **2020**, *22* (16), 6299–6303. <https://doi.org/10.1021/acs.orglett.0c02085>.
- <sup>433</sup> Zhang, Z.-Q.; Meng, X.-Y.; Sheng, J.; Lan, Q.; Wang, X.-S. Enantioselective Copper-Catalyzed 1,5-Cyanotrifluoromethylation of Vinylcyclopropanes. *Org. Lett.* **2019**, *21* (20), 8256–8260. <https://doi.org/10.1021/acs.orglett.9b03012>.
- <sup>434</sup> Zhang, G.; Zhou, S.; Fu, L.; Chen, P.; Li, Y.; Zou, J.; Liu, G. Asymmetric Coupling of Carbon-Centered Radicals Adjacent to Nitrogen: Copper-Catalyzed Cyanation and Etherification of Enamides. *Angew. Chem. Int. Ed.* **2020**, *59* (46), 20439–20444. <https://doi.org/10.1002/anie.202008338>.
- <sup>435</sup> Guo, Q.; Wang, M.; Peng, Q.; Huo, Y.; Liu, Q.; Wang, R.; Xu, Z. Dual-Functional Chiral Cu-Catalyst-Induced Photoredox Asymmetric Cyanofluoroalkylation of Alkenes. *ACS Catal.* **2019**, *9* (5), 4470–4476. <https://doi.org/10.1021/acscatal.9b00209>.
- <sup>436</sup> Israr, M.; Xiong, H.; Li, Y.; Bao, H. Copper-Catalyzed Enantioselective Cyano(Fluoro)Alkylation of Alkenes. *Adv. Synth. Catal.* **2020**, *362* (11), 2211–2215. <https://doi.org/10.1002/adsc.202000230>
- <sup>437</sup> Muñoz-Molina, J. M.; Belderrain, T. R.; Pérez, P. J. Copper-Catalysed Radical Reactions of Alkenes, Alkynes and Cyclopropanes with N–F Reagents. *Org. Biomol. Chem.* **2020**, *18* (43), 8757–8770. <https://doi.org/10.1039/D0OB01743D>.
- <sup>438</sup> Xiao, H.; Shen, H.; Zhu, L.; Li, C. Copper-Catalyzed Radical Aminotrifluoromethylation of Alkenes. *J. Am. Chem. Soc.* **2019**, *141* (29), 11440–11445. <https://doi.org/10.1021/jacs.9b06141>.
- <sup>439</sup> Wang, D.; Wang, F.; Chen, P.; Lin, Z.; Liu, G. Enantioselective Copper-Catalyzed Intermolecular Amino- and Azidocyanation of Alkenes in a Radical Process. *Angew. Chem. Int. Ed.* **2017**, *56* (8), 2054–2058. <https://doi.org/10.1002/anie.201611850>.

- 
- <sup>440</sup> Xu, L.; Mou, X.-Q.; Chen, Z.-M.; Wang, S.-H. Copper-Catalyzed Intermolecular Azidocyanation of Aryl Alkenes. *Chem Commun* **2014**, *50* (73), 10676–10679. <https://doi.org/10.1039/C4CC04640D>.
- <sup>441</sup> Yang, S.; Wang, L.; Zhang, H.; Liu, C.; Zhang, L.; Wang, X.; Zhang, G.; Li, Y.; Zhang, Q. Copper-Catalyzed Asymmetric Aminocyanation of Arylcyclopropanes for Synthesis of  $\gamma$ -Amino Nitriles. *ACS Catal.* **2019**, *9* (1), 716–721. <https://doi.org/10.1021/acscatal.8b03768>.
- <sup>442</sup> Wang, D.; Wu, L.; Wang, F.; Wan, X.; Chen, P.; Lin, Z.; Liu, G. Asymmetric Copper-Catalyzed Intermolecular Aminoarylation of Styrenes: Efficient Access to Optical 2,2-Diarylethylamines. *J. Am. Chem. Soc.* **2017**, *139* (20), 6811–6814. <https://doi.org/10.1021/jacs.7b02455>.
- <sup>443</sup> Sha, W.; Deng, L.; Ni, S.; Mei, H.; Han, J.; Pan, Y. Merging Photoredox and Copper Catalysis: Enantioselective Radical Cyanoalkylation of Styrenes. *ACS Catal.* **2018**, *8* (8), 7489–7494. <https://doi.org/10.1021/acscatal.8b01863>.
- <sup>444</sup> Zhuang, W.; Chen, P.; Liu, G. Enantioselective Arylcyanation of Styrenes *via* COPPER-CATALYZED Radical Relay. *Chin. J. Chem.* **2021**, *39* (1), 50–54. <https://doi.org/10.1002/cjoc.202000494>.
- <sup>445</sup> Lin, J.-S.; Li, T.-T.; Liu, J.-R.; Jiao, G.-Y.; Gu, Q.-S.; Cheng, J.-T.; Guo, Y.-L.; Hong, X.; Liu, X.-Y. Cu/Chiral Phosphoric Acid-Catalyzed Asymmetric Three-Component Radical-Initiated 1,2-Dicarbofunctionalization of Alkenes. *J. Am. Chem. Soc.* **2019**, *141* (2), 1074–1083. <https://doi.org/10.1021/jacs.8b11736>.
- <sup>446</sup> Zhang, G.; Fu, L.; Chen, P.; Zou, J.; Liu, G. Proton-Coupled Electron Transfer Enables Tandem Radical Relay for Asymmetric Copper-Catalyzed Phosphinoylcyanation of Styrenes. *Org. Lett.* **2019**, *21* (13), 5015–5020. <https://doi.org/10.1021/acs.orglett.9b01607>.
- <sup>447</sup> Fu, N.; Song, L.; Liu, J.; Shen, Y.; Siu, J. C.; Lin, S. New Bisoxazoline Ligands Enable Enantioselective Electrocatalytic Cyanofunctionalization of Vinylarenes. *J. Am. Chem. Soc.* **2019**, *141* (37), 14480–14485. <https://doi.org/10.1021/jacs.9b03296>.
- <sup>448</sup> Wang, F.; Wang, D.; Zhou, Y.; Liang, L.; Lu, R.; Chen, P.; Lin, Z.; Liu, G. Divergent Synthesis of CF<sub>3</sub>-Substituted Allenyl Nitriles by Ligand-Controlled Radical 1,2- and 1,4-Addition to 1,3-Enynes. *Angew. Chem. Int. Ed.* **2018**, *57* (24), 7140–7145. <https://doi.org/10.1002/anie.201803668>.
- <sup>449</sup> Zeng, Y.; Chiou, M.-F.; Zhu, X.; Cao, J.; Lv, D.; Jian, W.; Li, Y.; Zhang, X.; Bao, H. Copper-

---

Catalyzed Enantioselective Radical 1,4-Difunctionalization of 1,3-Enynes. *J. Am. Chem. Soc.* **2020**, *142* (42), 18014 Soc.M.-F.; Zhu, X.; Cao, J.; Lv, D.; Jian, W

<sup>450</sup> Dong, X.-Y.; Zhan, T.-Y.; Jiang, S.-P.; Liu, X.-D.; Ye, L.; Li, Z.-L.; Gu, Q.-S.; Liu, X.-Y. Copper-Catalyzed Asymmetric Coupling of Allenyl Radicals with Terminal Alkynes to Access Tetrasubstituted Allenes. *Angew. Chem. Int. Ed.* **2021**, *60* (4), 2160–2164. <https://doi.org/10.1002/anie.202013022>.

<sup>451</sup> Yu, P.; Lin, J. S., Li, L.; Zheng, S. C.; Xiong, Y. P.; Zhao, L. J.; Tan, B.; Liu, X. Y. Enantioselective CH Bond Functionalization Triggered by Radical Trifluoromethylation of Unactivated Alkene. *Angew. Chem.* **2014**, *126*, 12084–12088. <https://doi.org/10.1002/anie.201405401>.

<sup>452</sup> Nakafuku, K. M.; Zhang, Z.; Wappes, E. A.; Stateman, L. M.; Chen, A. D.; Nagib, D. A. Enantioselective Radical C–H Amination for the Synthesis of  $\beta$ -Amino Alcohols. *Nat. Chem.* **2020**, *12* (8), 697–704. <https://doi.org/10.1038/s41557-020-0482-8>.

<sup>453</sup> Chen, H.; Jin, W.; Yu, S. Enantioselective Remote C(Sp<sup>3</sup>)–H Cyanation via Dual Photoredox and Copper Catalysis. *Org. Lett.* **2020**, *22* (15), 5910–5914. <https://doi.org/10.1021/acs.orglett.0c02008>.

<sup>454</sup> Wang, T.; Wang, Y.-N.; Wang, R.; Zhang, B.-C.; Yang, C.; Li, Y.-L.; Wang, X.-S. Enantioselective Cyanation via Radical-Mediated C–C Single Bond Cleavage for Synthesis of Chiral Dinitriles. *Nat. Commun.* **2019**, *10* (1), 5373. <https://doi.org/10.1038/s41467-019-13369-x>.

<sup>455</sup> Wu, L.; Wang, L.; Chen, P.; Guo, Y.-L.; Liu, G. Enantioselective Copper-Catalyzed Radical Ring-Opening Cyanation of Cyclopropanols and Cyclopropanone Acetals. *Adv. Synth. Catal.* **2020**, *362* (11), 2189 Catal.Chen, P.; Guo, Y.-L.; Liu, G. Enantiose

<sup>456</sup> Cheng, Y.-F.; Dong, X.-Y.; Gu, Q.-S.; Yu, Z.-L.; Liu, X.-Y. Achiral Pyridine Ligand-Enabled Enantioselective Radical Oxytrifluoromethylation of Alkenes with Alcohols. *Angew. Chem. Int. Ed.* **2017**, *56* (30), 8883–8886. <https://doi.org/10.1002/anie.201702925>.

<sup>457</sup> Cheng, Y.-F.; Liu, J.-R.; Gu, Q.-S.; Yu, Z.-L.; Wang, J.; Li, Z.-L.; Bian, J.-Q.; Wen, H.-T.; Wang, X.-J.; Hong, X.; Liu, X.-Y. Catalytic enantioselective desymmetrizing functionalization of alkyl radicals via Cu(I)/CPA cooperative catalysis. *Nat. Catal.* **2020**, *3*, 401–410. <https://doi.org/10.1038/s41929-020-0439-8>.

- 
- <sup>458</sup> Li, X.-T.; Gu, Q.-S.; Dong, X.-Y.; Meng, X.; Liu, X.-Y. A Copper Catalyst with a Cinchona-Alkaloid-Based Sulfonamide Ligand for Asymmetric Radical Oxytrifluoromethylation of Alkenyl Oximes. *Angew. Chem. Int. Ed.* **2018**, *57* (26), 7668–7672. <https://doi.org/10.1002/anie.201804315>.
- <sup>459</sup> Li, X.-T.; Lv, L.; Wang, T.; Gu, Q.-S.; Xu, G.-X.; Li, Z.-L.; Ye, L.; Zhang, X.; Cheng, G.-J.; Liu, X.-Y. Diastereo- and Enantioselective Catalytic Radical Oxysulfonylation of Alkenes in  $\beta,\gamma$ -Unsaturated Ketoximes. *Chem* **2020**, *6* (7), 1692–1706. <https://doi.org/10.1016/j.chempr.2020.03.024>.
- <sup>460</sup> Lin, J.-S.; Xiong, Y.-P.; Ma, C.-L.; Zhao, L.-J.; Tan, B.; Liu, X.-Y. Efficient Copper-Catalyzed Direct Intramolecular Aminotrifluoromethylation of Unactivated Alkenes with Diverse Nitrogen-Based Nucleophiles. *Chem. – Eur. J.* **2014**, *20* (5), 1332–1340. <https://doi.org/10.1002/chem.201303387>.
- <sup>461</sup> Lin, J.-S.; Wang, F.-L.; Dong, X.-Y.; He, W.-W.; Yuan, Y.; Chen, S.; Liu, X.-Y. Catalytic Asymmetric Radical Aminoperfluoroalkylation and Aminodifluoromethylation of Alkenes to Versatile Enantioenriched-Fluoroalkyl Amines. *Nat. Commun.* **2017**, *8* (1), 14841. <https://doi.org/10.1038/ncomms14841>.
- <sup>462</sup> Wang, F.-L.; Dong, X.-Y.; Lin, J.-S.; Zeng, Y.; Jiao, G.-Y.; Gu, Q.-S.; Guo, X.-Q.; Ma, C.-L.; Liu, X.-Y. Catalytic Asymmetric Radical Diamination of Alkenes. *Chem* **2017**, *3* (6), 979–990. <https://doi.org/10.1016/j.chempr.2017.10.008>.
- <sup>463</sup> Yang, C.-J.; Zhang, C.; Gu, Q.-S.; Fang, J.-H.; Su, X.-L.; Ye, L.; Sun, Y.; Tian, Y.; Li, Z.-L.; Liu, X.-Y. Cu-Catalysed Intramolecular Radical Enantioconvergent Tertiary  $\beta$ -C(Sp<sup>3</sup>)-H Amination of Racemic Ketones. *Nat. Catal.* **2020**, *3* (7), 5391.; Zhang, C.; Gu, Q.-S.; Fang, J.-H.;20-0460-y.
- <sup>464</sup> Yoon, T. P. Photochemical Stereocontrol Using Tandem Photoredox–Chiral Lewis Acid Catalysis. *Acc. Chem. Res.* **2016**, *49* (10), 2307–2315. <https://doi.org/10.1021/acs.accounts.6b00280>
- <sup>465</sup> Du, J.; Skubi, K. L.; Schultz, D. M.; Yoon, T. P. A Dual-Catalysis Approach to Enantioselective [2 + 2] Photocycloadditions Using Visible Light. *Science* **2014**, *344* (6182), 392–396. <https://doi.org/10.1126/science.1251511>.



- 
- <sup>466</sup> Blum, T. R.; Miller, Z. D.; Bates, D. M.; Guzei, I. A.; Yoon, T. P. Enantioselective Photochemistry through Lewis Acid–Catalyzed Triplet Energy Transfer. *Science* **2016**, *354* (6318), 1391–1395. <https://doi.org/10.1126/science.aai8228>.
- <sup>467</sup> Miller, Z. D.; Lee, B. J.; Yoon, T. P. Enantioselective Crossed Photocycloadditions of Styrenic Olefins by Lewis Acid Catalyzed Triplet Sensitization. *Angew. Chem. Int. Ed.* **2017**, *56* (39), 11891–11895. <https://doi.org/10.1002/anie.201706975>.
- <sup>468</sup> Huang, X.; Meggers, E. Asymmetric Photocatalysis with Bis-Cyclometalated Rhodium Complexes. *Acc. Chem. Res.* **2019**, *52* (3), 833–847. <https://doi.org/10.1021/acs.accounts.9b00028>.
- <sup>469</sup> Wang, C.; Chen, L.-A.; Huo, H.; Shen, X.; Harms, K.; Gong, L.; Meggers, E. Asymmetric Lewis Acid Catalysis Directed by Octahedral Rhodium Centrochirality. *Chem. Sci.* **2015**, *6* (2), 1094–1100. <https://doi.org/10.1039/C4SC03101F>.
- <sup>470</sup> Ma, J.; Shen, X.; Harms, K.; Meggers, E. Expanding the Family of Bis-Cyclometalated Chiral-at-Metal Rhodium(III) Catalysts with a Benzothiazole Derivative. *Dalton Trans.* **2016**, *45* (20), 8320–8323. <https://doi.org/10.1039/C6DT01063F>.
- <sup>471</sup> Ma, J.; Zhang, X.; Huang, X.; Luo, S.; Meggers, E. Preparation of Chiral-at-Metal Catalysts and Their Use in Asymmetric Photoredox Chemistry. *Nat. Protoc.* **2018**, *13* (4), 605–632. <https://doi.org/10.1038/nprot.2017.138>.
- <sup>472</sup> Mailyan, A. K.; Eickhoff, J. A.; Minakova, A. S.; Gu, Z.; Lu, P.; Zakarian, A. Cutting-Edge and Time-Honored Strategies for Stereoselective Construction of C–N Bonds in Total Synthesis. *Chem. Rev.* **2016**, *116* (7), 4441–4557. <https://doi.org/10.1021/acs.chemrev.5b00712>.
- <sup>473</sup> Nguyen, L. Q.; Knowles, R. R. Catalytic C–N Bond-Forming Reactions Enabled by Proton-Coupled Electron Transfer Activation of Amide N–H Bonds. *ACS Catal.* **2016**, *6* (5), 2894–2903. <https://doi.org/10.1021/acscatal.6b00486>.
- <sup>474</sup> Zhou, Z.; Li, Y.; Han, B.; Gong, L.; Meggers, E. Enantioselective Catalytic  $\beta$ -Amination through Proton-Coupled Electron Transfer Followed by Stereocontrolled Radical–Radical Coupling. *Chem. Sci.* **2017**, *8* (8), 5757–5763. <https://doi.org/10.1039/C7SC02031G>.
- <sup>475</sup> Liang, H.; Xu, G.-Q.; Feng, Z.-T.; Wang, Z.-Y.; Xu, P.-F. Dual Catalytic Switchable Divergent Synthesis: An Asymmetric Visible-Light Photocatalytic Approach to Fluorine-

---

Containing  $\gamma$ -Keto Acid Frameworks. *J. Org. Chem.* **2019**, *84* (1), 60–72. <https://doi.org/10.1021/acs.joc.8b02316>.

<sup>476</sup> Chen, S.; Huang, X.; Meggers, E.; Houk, K. N. Origins of Enantioselectivity in Asymmetric Radical Additions to Octahedral Chiral-at-Rhodium Enolates: A Computational Study. *J. Am. Chem. Soc.* **2017**, *139* (49), 17902–17907. <https://doi.org/10.1021/jacs.7b08650>.

<sup>477</sup> Huang, X.; Webster, R. D.; Harms, K.; Meggers, E. Asymmetric Catalysis with Organic Azides and Diazo Compounds Initiated by Photoinduced Electron Transfer. *J. Am. Chem. Soc.* **2016**, *138* (38), 12636–12642. <https://doi.org/10.1021/jacs.6b07692>.

<sup>478</sup> Ma, J.; Harms, K.; Meggers, E. Enantioselective Rhodium/Ruthenium Photoredox Catalysis En Route to Chiral 1,2-Aminoalcohols. *Chem. Commun.* **2016**, *52* (66), 10183–10186. <https://doi.org/10.1039/C6CC04397F>.

<sup>479</sup> de Assis, F. F.; Huang, X.; Akiyama, M.; Pilli, R. A.; Meggers, E. Visible-Light-Activated Catalytic Enantioselective  $\beta$ -Alkylation of  $\alpha,\beta$ -Unsaturated 2-Acyl Imidazoles Using Hantzsch Esters as Radical Reservoirs. *J. Org. Chem.* **2018**, *83* (18), 10922–10932. <https://doi.org/10.1021/acs.joc.8b01588>.

<sup>480</sup> Huang, X.; Quinn, T. R.; Harms, K.; Webster, R. D.; Zhang, L.; Wiest, O.; Meggers, E. Direct Visible-Light-Excited Asymmetric Lewis Acid Catalysis of Intermolecular [2+2] Photocycloadditions. *J. Am. Chem. Soc.* **2017**, *139* (27), 9120–9123. <https://doi.org/10.1021/jacs.7b04363>.

<sup>481</sup> Huang, X.; Luo, S.; Burghaus, O.; Webster, R. D.; Harms, K.; Meggers, E. Combining the Catalytic Enantioselective Reaction of Visible-Light-Generated Radicals with a by-Product Utilization System. *Chem. Sci.* **2017**, *8* (10), 7126–7131. <https://doi.org/10.1039/C7SC02621H>.

<sup>482</sup> Zhang, C.; Chen, S.; Ye, C.; Harms, K.; Zhang, L.; Houk, K. N.; Meggers, E. Asymmetric Photocatalysis by Intramolecular Hydrogen-Atom Transfer in Photoexcited Catalyst–Substrate Complex. *Angew. Chem. Int. Ed.* **2019**, *58* (41), 14462–14466. <https://doi.org/10.1002/anie.201905647>.

<sup>483</sup> Kuang, Y.; Wang, K.; Shi, X.; Huang, X.; Meggers, E.; Wu, J. Asymmetric Synthesis of 1,4-Dicarbonyl Compounds from Aldehydes by Hydrogen Atom Transfer Photocatalysis and Chiral Lewis Acid Catalysis. *Angew. Chem. Int. Ed.* **2019**, *58* (47), 16859–16863. <https://doi.org/10.1002/anie.201910414>.

- 
- <sup>484</sup> Lin, S.-X.; Sun, G.-J.; Kang, Q. A Visible-Light-Activated Rhodium Complex in Enantioselective Conjugate Addition of  $\alpha$ -Amino Radicals with Michael Acceptors. *Chem. Commun.* **2017**, *53* (54), 7665–7668. <https://doi.org/10.1039/C7CC03650G>.
- <sup>485</sup> Shaw, M. H.; Twilton, J.; MacMillan, D. W. C. Photoredox Catalysis in Organic Chemistry. *J. Org. Chem.* **2016**, *81* (16), 6898–6926. <https://doi.org/10.1021/acs.joc.6b01449>.
- <sup>486</sup> (a) Huo, H.; Shen, X.; Wang, C.; Zhang, L.; Röse, P.; Chen, L.-A.; Harms, K.; Marsch, M.; Hilt, G.; Meggers, E. Asymmetric Photoredox Transition-Metal Catalysis Activated by Visible Light. *Nature* **2014**, *515* (7525), 100–103. <https://doi.org/10.1038/nature13892>. (b) Huo, H.; Fu, C.; Harms, K.; Meggers, E. Asymmetric Catalysis with Substitutionally Labile yet Stereochemically Stable Chiral-at-Metal Iridium(III) Complex. *J. Am. Chem. Soc.* **2014**, *136* (8), 2990–2993. <https://doi.org/10.1021/ja4132505>.
- <sup>487</sup> Huo, H.; Huang, X.; Shen, X.; Harms, K.; Meggers, E. Visible- Light-Activated Enantioselective Perfluoroalkylation with a Chiral Iridium Photoredox Catalyst. *Synlett* **2016**, *27*, 749–753. [10.1055/s-0035-1561284](https://doi.org/10.1055/s-0035-1561284)
- <sup>488</sup> Wang, C.; Qin, J.; Shen, X.; Riedel, R.; Harms, K.; Meggers, E. Asymmetric Radical-Radical Cross-Coupling through Visible-Light-Activated Iridium Catalysis. *Angew. Chem. Int. Ed.* **2016**, *55* (2), 685–688. <https://doi.org/10.1002/anie.201509524>.
- <sup>489</sup> Skubi, K. L.; Kidd, J. B.; Jung, H.; Guzei, I. A.; Baik, M.-H.; Yoon, T. P. Enantioselective Excited-State Photoreactions Controlled by a Chiral Hydrogen-Bonding Iridium Sensitizer. *J. Am. Chem. Soc.* **2017**, *139* (47), 17186–17192. <https://doi.org/10.1021/jacs.7b10586>.
- <sup>490</sup> Zheng, J.; Swords, W. B.; Jung, H.; Skubi, K. L.; Kidd, J. B.; Meyer, G. J.; Baik, M.-H.; Yoon, T. P. Enantioselective Intermolecular Excited-State Photoreactions Using a Chiral Ir Triplet Sensitizer: Separating Association from Energy Transfer in Asymmetric Photocatalysis. *J. Am. Chem. Soc.* **2019**, *141* (34), 13625–13634. <https://doi.org/10.1021/jacs.9b06244>.
- <sup>491</sup> Kim, J. Y.; Lee, Y. S.; Choi, Y.; Ryu, D. H. Enantioselective 1,2-Addition of  $\alpha$ -Aminoalkyl Radical to Aldehydes via Visible-Light Photoredox Initiated Chiral Oxazaborolidinium Ion Catalysis. *ACS Catal.* **2020**, *10* (18), 10585–10591. <https://doi.org/10.1021/acscatal.0c02443>.
- <sup>492</sup> (a) Winkler, C. K.; Schrittwieser, J. H.; Kroutil, W. Power of Biocatalysis for Organic Synthesis. *ACS Cent. Sci.* **2021**, *7* (1), 55–71. <https://doi.org/10.1021/acscentsci.0c01496>, (b) Bommarius, A. S.; Riebel-Bommarius, B. R. *Biocatalysis Fundamentals and Applications*; 2007.

- 
- <sup>493</sup> Frey, P. A. Radical Mechanisms of Enzymatic Catalysis. *Annu. Rev. Biochem.* **2001**, *70* (1), 121–148. <https://doi.org/10.1146/annurev.biochem.70.1.121>.
- <sup>494</sup> Chen, J.; Guan, Z.; He, Y. Photoenzymatic Approaches in Organic Synthesis. *Asian J. Org. Chem.* **2019**, *8* (10), 1775–1790. <https://doi.org/10.1002/ajoc.201900427>.
- <sup>495</sup> Gastaldi, S.; Escoubet, S.; Vanthuynne, N.; Gil, G.; Bertrand, M. P. Dynamic Kinetic Resolution of Amines Involving Biocatalysis and in Situ Free Radical Mediated Racemization. *Org. Lett.* **2007**, *9* (5), 837–839. <https://doi.org/10.1021/ol063062o>
- <sup>496</sup> Emmanuel, M. A.; Greenberg, N. R.; Oblinsky, D. G.; Hyster, T. K. Accessing Non-Natural Reactivity by Irradiating Nicotinamide-Dependent Enzymes with Light. *Nature* **2016**, *540* (7633), 414–417. <https://doi.org/10.1038/nature20569>.
- <sup>497</sup> Biegasiewicz, K. F.; Cooper, S. J.; Emmanuel, M. A.; Miller, D. C.; Hyster, T. K. Catalytic Promiscuity Enabled by Photoredox Catalysis in Nicotinamide-Dependent Oxidoreductases. *Nat. Chem.* **2018**, *10* (7), 770–775. <https://doi.org/10.1038/s41557-018-0059-y>.
- <sup>498</sup> Sandoval, B. A.; Meichan, A. J.; Hyster, T. K. Enantioselective Hydrogen Atom Transfer: Discovery of Catalytic Promiscuity in Flavin-Dependent ‘Ene’-Reductases. *J. Am. Chem. Soc.* **2017**, *139* (33), 11313–11316. <https://doi.org/10.1021/jacs.7b05468>.
- <sup>499</sup> Biegasiewicz, K. F.; Cooper, S. J.; Gao, X.; Oblinsky, D. G.; Kim, J. H.; Garfinkle, S. E.; Joyce, L. A.; Sandoval, B. A.; Scholes, G. D.; Hyster, T. K. Photoexcitation of Flavoenzymes Enables a Stereoselective Radical Cyclization. *Science* **2019**, *364* (6446), 1166. <https://doi.org/10.1126/science.aaw1143>.
- <sup>500</sup> Black, M. J.; Biegasiewicz, K. F.; Meichan, A. J.; Oblinsky, D. G.; Kudisch, B.; Scholes, G. D.; Hyster, T. K. Asymmetric Redox-Neutral Radical Cyclization Catalysed by Flavin-Dependent ‘Ene’-Reductases. *Nat. Chem.* **2020**, *12* (1), 71–75. <https://doi.org/10.1038/s41557-019-0370-2>.
- <sup>501</sup> Huang, X.; Wang, B.; Wang, Y.; Jiang, G.; Feng, J.; Zhao, H. Photoenzymatic Enantioselective Intermolecular Radical Hydroalkylation. *Nature* **2020**, *584* (7819), 69–74. <https://doi.org/10.1038/s41586-020-2406-6>.
- <sup>502</sup> Clayman, P. D.; Hyster, T. K. Photoenzymatic Generation of Unstabilized Alkyl Radicals: An Asymmetric Reductive Cyclization. *J. Am. Chem. Soc.* **2020**, *142* (37), 15673–15677. <https://doi.org/10.1021/jacs.0c07918>.

- 
- <sup>503</sup> Nakano, Y.; Black, M. J.; Meichan, A. J.; Sandoval, B. A.; Chung, M. M.; Biegasiewicz, K. F.; Zhu, T.; Hyster, T. K. Photoenzymatic Hydrogenation of Heteroaromatic Olefins Using ‘Ene’-Reductases with Photoredox Catalysts. *Angew. Chem. Int. Ed.* **2020**, *59* (26), 10484–10488. <https://doi.org/10.1002/anie.202003125>.
- <sup>504</sup> Litman, Z. C.; Wang, Y.; Zhao, H.; Hartwig, J. F. Cooperative Asymmetric Reactions Combining Photocatalysis and Enzymatic Catalysis. *Nature* **2018**, *560* (7718), 355–359. <https://doi.org/10.1038/s41586-018-0413-7>.
- <sup>505</sup> Sandoval, B. A.; Kurtoic, S. I.; Chung, M. M.; Biegasiewicz, K. F.; Hyster, T. K. Photoenzymatic Catalysis Enables Radical-Mediated Ketone Reduction in Ene-Reductases. *Angew. Chem. Int. Ed.* **2019**, *58* (26), 8714–8718. <https://doi.org/10.1002/anie.201902005>.
- <sup>506</sup> Lauder, K.; Toscani, A.; Qi, Y.; Lim, J.; Charnock, S. J.; Korah, K.; Castagnolo, D. Photo-Biocatalytic One-Pot Cascades for the Enantioselective Synthesis of 1,3-Mercaptoalkanol Volatile Sulfur Compounds. *Angew. Chem. Int. Ed.* **2018**, *57* (20), 5803–5807. <https://doi.org/10.1002/anie.201802135>.
- <sup>507</sup> Xu, J.; Arkin, M.; Peng, Y.; Xu, W.; Yu, H.; Lin, X.; Wu, Q. Enantiocomplementary Decarboxylative Hydroxylation Combining Photocatalysis and Whole-Cell Biocatalysis in a One-Pot Cascade Process. *Green Chem.* **2019**, *21* (8), 1907–1911. <https://doi.org/10.1039/C9GC00098D>.
- <sup>508</sup> DeHovitz, J. S.; Loh, Y. Y.; Kautzky, J. A.; Nagao, K.; Meichan, A. J.; Yamauchi, M.; MacMillan, D. W. C.; Hyster, T. K. Static to Inducibly Dynamic Stereocontrol: The Convergent Use of Racemic  $\beta$ -Substituted Ketones. *Science* **2020**, *369* (6507), 1113–1118. <https://doi.org/10.1126/science.abc9909>.